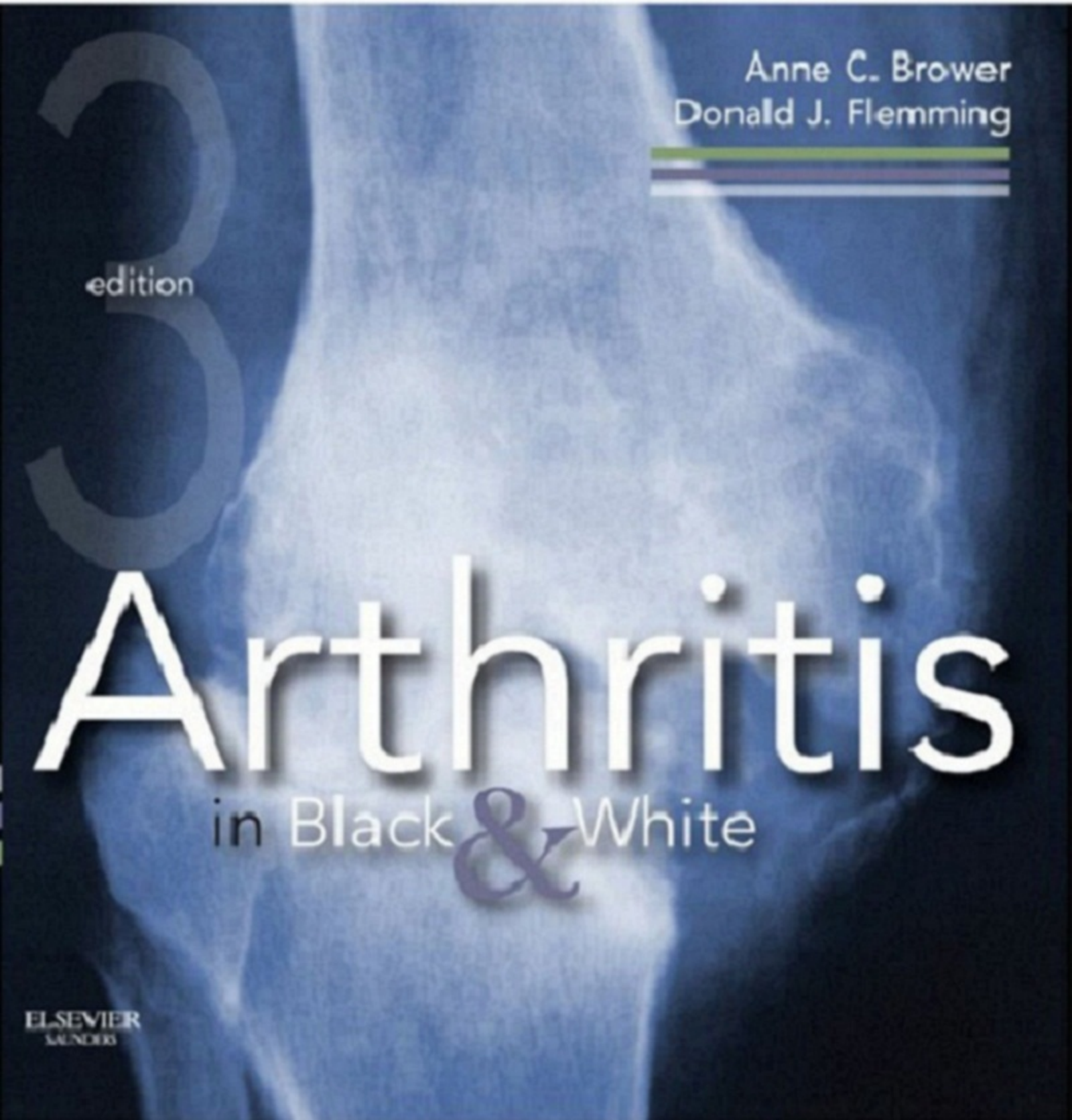

Anne C. Brower
Donald J. Flemming

3 edition

Arthritis in Black & White

ELSEVIER
SAUNDERS

ARTHRITIS

in Black and White

Third Edition

ANNE C. BROWER, MD
Teacher, Consultant, and Patient Advocate
Former Chief Radiologist and Director of Medical Imaging
Eastern Virginia Medical School
Norfolk, Virginia

DONALD J. FLEMMING, MD
Radiologist
G. Victor Rohrer Professor of Radiology Education
Vice Chair for Education
Professor of Radiology and Orthopedics
Milton S. Hershey Penn State Medical Center
Hershey, Pennsylvania

Associate Editor

STEPHANIE A. BERNARD, MD
Assistant Professor of Radiology
Milton S. Hershey Penn State Medical Center
Hershey, Pennsylvania

ELSEVIER
SAUNDERS

ELSEVIER
SAUNDERS

1600 John F. Kennedy Blvd.
Ste 1800
Philadelphia, PA 19103-2899

ARTHRITIS IN BLACK AND WHITE ISBN: 978-1-4160-5595-2

Notices

Knowledge and best practice in this field are constantly changing. As new research and experience broaden our understanding, changes in research methods, professional practices, or medical treatment may become necessary. Practitioners and researchers must always rely on their own experience and knowledge in evaluating and using any information, methods, compounds, or experiments described herein. In using such information or methods they should be mindful of their own safety and the safety of others, including parties for whom they have a professional responsibility.

With respect to any drug or pharmaceutical products identified, readers are advised to check the most current information provided (i) on procedures featured or (ii) by the manufacturer of each product to be administered, to verify the recommended dose or formula, the method and duration of administration, and contraindications. It is the responsibility of practitioners, relying on their own experience and knowledge of their patients, to make diagnoses, to determine dosages and the best treatment for each individual patient, and to take all appropriate safety precautions.

To the fullest extent of the law, neither the Publisher nor the authors, contributors, or editors, assume any liability for any injury and/or damage to persons or property as a matter of products liability, negligence or otherwise, or from any use or operation of any methods, products, instructions, or ideas contained in the material herein.

Library of Congress Cataloging-in-Publication Data
Brower, Anne C.
Arthritis in black and white / Anne C. Brower. – 3rd ed.
p. ; cm.
Includes bibliographical references and index.
ISBN 978-1-4160-5595-2 (hardback : alk. paper)
I. Title.
[DNLM: 1. Arthritis–radiography. 2. Arthritis–physiopathology. WE 344]
616.7'220757–dc22

Content Strategist: Don Scholz
Content Development Specialist: Rachel Miller
Publishing Services Manager: Julie Eddy
Project Manager: Celeste Clingan/Siva Raman Krishnamoorthy
Design Direction: Louis Forgione

Printed in United States of America
Last digit is the print number: 9 8 7 6 5 4 3 2 1

To my grandmother, Frances Jackson, who was crippled with rheumatoid arthritis and taught me so much about life and living.

—Donald Flemming

PREFACE

to the Third Edition

The third edition has finally arrived.
The same simple book is modestly revised.
The text has changes, but very slight.
But images have been added to make right.

MRI, CT and Ultrasound images are arranged
next to the plain film--to explain the change.
We still believe that the plain film is the start
of the workup of arthritis--the important part.

My thanks to Don Flemming and his partner in crime.
They did all of the work, despite lack of time.
I now continue to advise, consult and teach.
I pray you all success--for I'm also a priest.

Anne C. Brower

PREFACE

to the Second Edition

The second edition of "Black and White"
Is still quite simple and hopefully right
For all of its readers to use as a guide
To observe the joint where disease might hide.
The changes made are relatively few.
"Approach to the Foot" in Section I is new.
MR is revisited in greater detail
Yet compared to plain film, it still seems to pale.
An associate is added-Don Flemming his name
With enthusiasm and energy to this book he came.
He wrote, he edited, and better x-rays found.
His constant support was always around.
And now it's my hope that there will be space
In your office, your shelf, or some other place
For this book to be opened and frequently used
So problems in arthritis become easily defused.

Anne C. Brower

PREFACE

to the First Edition

This book is the result of requests from many residents who have heard my simplistic approach to the radiographic diagnosis of arthritic disease. All of the material in the book has been printed in some form in other books. The purpose of this work is to provide a small, practical book organized so as to allow relative ease in accurate diagnosis of arthritic disease through the radiograph. It is designed for practicing general radiologists, family practitioners, internists, and rheumatologists to use in day-to-day practice.

It is entitled *Arthritis in Black and White* to indicate that (1) it deals with arthritis as seen on the radiograph, and (2) it is a very basic, simple book illustrating the hallmarks of the more common arthropathies. It is not meant to be an extensive reference book; it does not illustrate all of the radiographic aspects of arthritic disease. It illustrates only the hallmarks of the arthropathies, not the deviations or "gray zones" of the various arthropathies.

The radiographic diagnosis of arthritic disease depends upon the excellence and appropriateness of the image obtained, as discussed in the first chapter of this book. The role of all imaging modalities is presented. Today, however, the plain film radiograph remains the imaging modality of choice. Therefore, the focus of this book centers on plain film interpretation.

The book is designed to be used easily and quickly in approaching any radiograph obtained on unknown arthritic disease. For the reader's convenience the book is divided into two sections. The first section illustrates an approach to analyzing the radiographic changes in a specific join and the common arthropathies that produce those changes in that particular joint. The second section illustrates the radiographic hallmarks of each of the common arthropathies. Thus the book might be used in the following way: When analyzing the radiograph of a knee on which the referring physician has questioned the possibility of rheumatoid arthritis, the user may turn to the chapter on rheumatoid arthritis in Part II and observe the hallmarks of the rheumatoid arthritis as it presents in the knee. If the problem radiograph does not fit the hallmarks of rheumatoid arthritis, the user may then turn to the chapter on the knee in Part I and through the approach described arrive at the appropriate diagnosis.

The radiographic diagnosis of arthritic disease is a difficult subject. I can only hope that this book will provide an easy starting place for the interested physician. However, I am reminded of a paragraph written by F. Spilsbury in 1774:

> The disorder termed the Gout is difficult to cure, and occasions exquisite pain and uneasiness to the patient, and trouble and perplexity to the physician to discover the nature, cause and a remedy for this excruciating malady; books upon books have been wrote in different ages by men of ingenuity and learning, and much practice without the desired amendation, as might reasonably be hoped for from their abilities and experience; that I am almost disheartened from throwing in my mite, did not the desire of relieving preponderate, therefore shall give my thoughts on the subject, crude and barren as they are.

Anne C. Brower

ACKNOWLEDGMENTS

This book, although a long-time dream, is now a reality because of the tremendous efforts of the many people I am deeply indebted to:

Karen Kellough—for her consistently accurate preparation of the manuscript.
Robert Irving—for his excellent photography of all the radiographs.
Ann Bignell—for her clear illustrations.
All my residents—for their inspiration.
Don Resnick—for his encouragement.
Larry Elliott—for his provision of time.
My Mother—for her understanding and support.

For changes in the Second Edition, I thank especially:

Saundra Cooper and DeLores Watson—for their roles in preparing the additions and corrections.
Robert Irving and Mike McKay—for their photographic images.
Syed Hassan—for the new illustrations.
Don Flemming—for his writing and constant support.
W. B. Saunders—Joan Sinclair for production of the final product.

–Brower

I have so much to be thankful for that this page could be longer than the book!

I am thankful for the support, encouragement and teaching that I have been blessed to receive from my current and past colleagues in the US Navy, Penn State Hershey Medical Center and the SSR.

I am deeply indebted to all of the students, residents and fellows that I have had the honor to teach and to all of the patients that have entrusted their care to me.

To all of my friends, but especially Kris Shekitka, Tom Smallman, Bill Corse and Carl Matyas, thanks for sharing the joys and disappointments of life with me.

This edition would not been possible without the dedication and creative spirit of Stephanie Bernard. It has been an honor to be your mentor, friend and colleague. A special thanks to Rebecca Gardner, David Mack and Rachel Miller of Elsevier for your professionalism and patience.

I have been blessed to be mentored by two remarkable radiologists, Anne Brower and Mark Murphey. To Anne, I would never have been an academic musculoskeletal radiologist without your guidance and support. Thank you for trusting me and for reminding me to not to forget my spiritual self. To Mark, thanks for putting up with me and for encouraging me to drive left despite my meager talent.

Thanks to my parents, Don and Barb, for providing a loving home and for all of the sacrifice and hard work that made my future possible. **I miss you, Dad.** To my brothers, Jeff and Kevin, thanks for being there for me. To my kids, Tim, Mike, and Erin, I am so very proud of you! To my wife and best friend, Sheri, always and all ways. I am looking forward to the next 36 years!!

–Flemming

1 Imaging Techniques and Modalities

Evaluation of any articular disorder involves imaging the affected joints with the most appropriate modality. Imaging documents not only the extent and severity of joint involvement but also the progression or regression of disease. More importantly, in the patient who presents with vague, complex, or confusing clinical symptoms, imaging often allows a specific diagnosis to be made. The modalities available for imaging are radiography, magnetic resonance imaging, ultrasonography, computed tomography, and bone scintigraphy. The role that each of these modalities may play in the evaluation of the patient with articular disease is discussed.

RADIOGRAPHY

Evaluation of articular disease should begin with the radiograph, which is the best modality to evaluate accurately any subtle change occurring in the bone. If high quality radiographs are obtained in properly positioned patients, accurate evaluation can often be made without further studies. The vast majority of modern radiology departments use computed radiography (CR) or digital radiography (DR) imaging equipment rather than film screen systems. Digital images from either of these modalities have lower spatial resolution than film screen systems but have comparable sensitivity to film for the detection of erosions and offer superior evaluation of the soft tissues. Tight collimation and proper exposure are critical for the optimization of a digital radiograph, and the imaging of both hands simultaneously on a large cassette or detector should be avoided with these systems. Digital radiography should be optimized with vendor-specific reconstruction algorithms and exposure factors. Optimum digital image quality can be dependent on the picture archival and communication system (PACS system) accepting vendor-specific correction factors, so the compatibility of imaging equipment and the PACS system should be verified at the time of equipment purchase and after any equipment software upgrade.

Evaluation of a digital image at a workstation is optimized by using high quality, high resolution, lumens balanced monitors that are calibrated frequently. Digital images, particularly of the hands and feet, should be magnified, panned, windowed, and leveled to be completely assessed.

For those departments still using film, the high quality study demands that high resolution, fine detail imaging system be used, especially in the extremities, to detect subtle disease. There are numerous film–screen combinations available, and the system used depends upon the individual radiography department. Generally, the lower the system speed, the higher the resolution. Most departments employ a single screen–film combination with system speeds of 80 to 100 for this necessary resolution.

The symptomatic joint should be imaged in appropriate positions. It should be radiographed in at least two different projections. Although one view may appear entirely normal, a second view taken at 90-degree angle to the first view may show significant abnormality (Fig. 1-1). Special views are available and should be used when imaging specific joint articular diseases. The important positions for several of the joints commonly imaged are discussed hereafter.

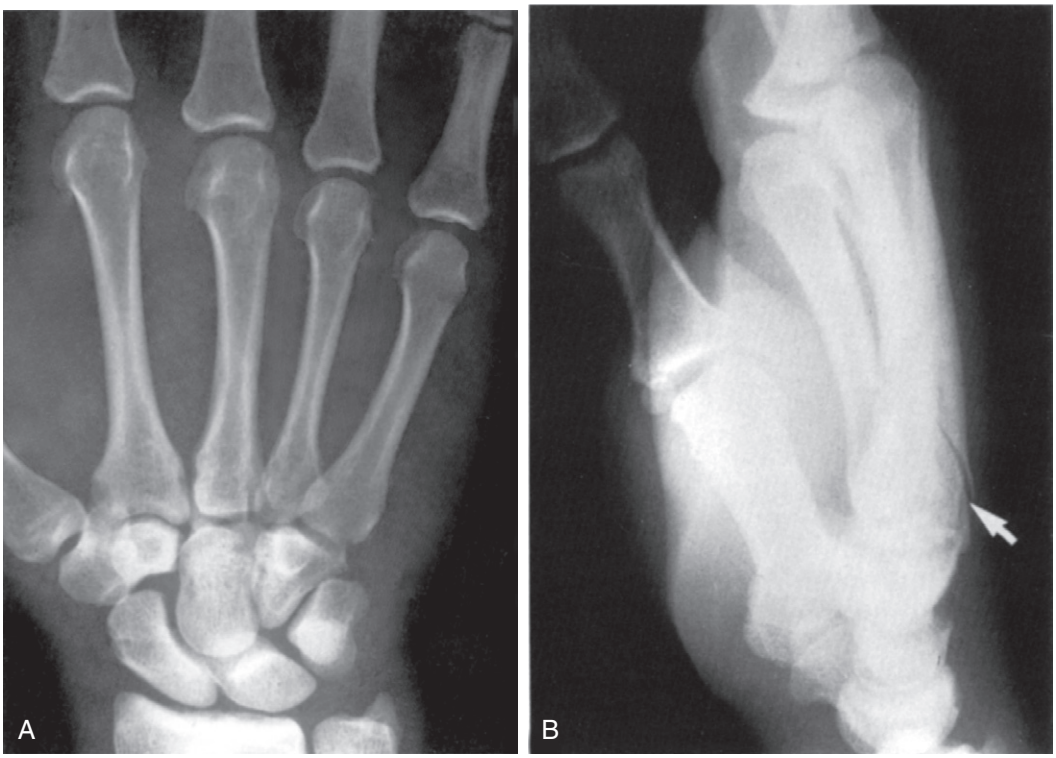

FIGURE 1-1. **A,** PA view of the metacarpals fails to reveal any significant bony abnormality. **B,** Lateral view of the same hand (taken at 90 degrees to the PA view) shows a fracture through the proximal end of the shaft of the third metacarpal (*arrow*).

Hand and Wrist

The posterior (PA) and Nørgaard views of the hands and wrists provide the most information if only two views are to be obtained. The PA view gives information on mineralization and soft tissue changes. The Nørgaard view is used to demonstrate early erosive disease. The Nørgaard view is an anterior-posterior oblique view, or the oblique view opposite that which is routinely obtained. It has been described as the "You're in good hands with Allstate" or "ball-catcher's" view. It profiles the radial aspect of the base of the proximal phalanges in the hand and the triquetrum and pisiform bones in the wrist (Fig. 1-2). The earliest erosive changes of any inflammatory arthropathy begin in these areas. Erosive changes occur between the triquetrum and pisiform before they occur around the ulnar styloid process (Fig. 1-3). The Nørgaard view will also reveal the reducible subluxations of inflammatory arthropathies and systemic lupus erythematosus, as the fingers are not rigidly positioned by the technician in this view (Fig. 1-4).

FIGURE 1-2. Nørgaard view of the hand. The blackened areas are those areas imaged specifically on this view to demonstrate the earliest erosive changes and inflammatory disease.

FIGURE 1-3. Nørgaard view of the hand demonstrating early erosive changes at the base of the second proximal phalanx, the base of the fourth and fifth metacarpal and the triquetrum as it articulates with the pisiform (*arrows*).

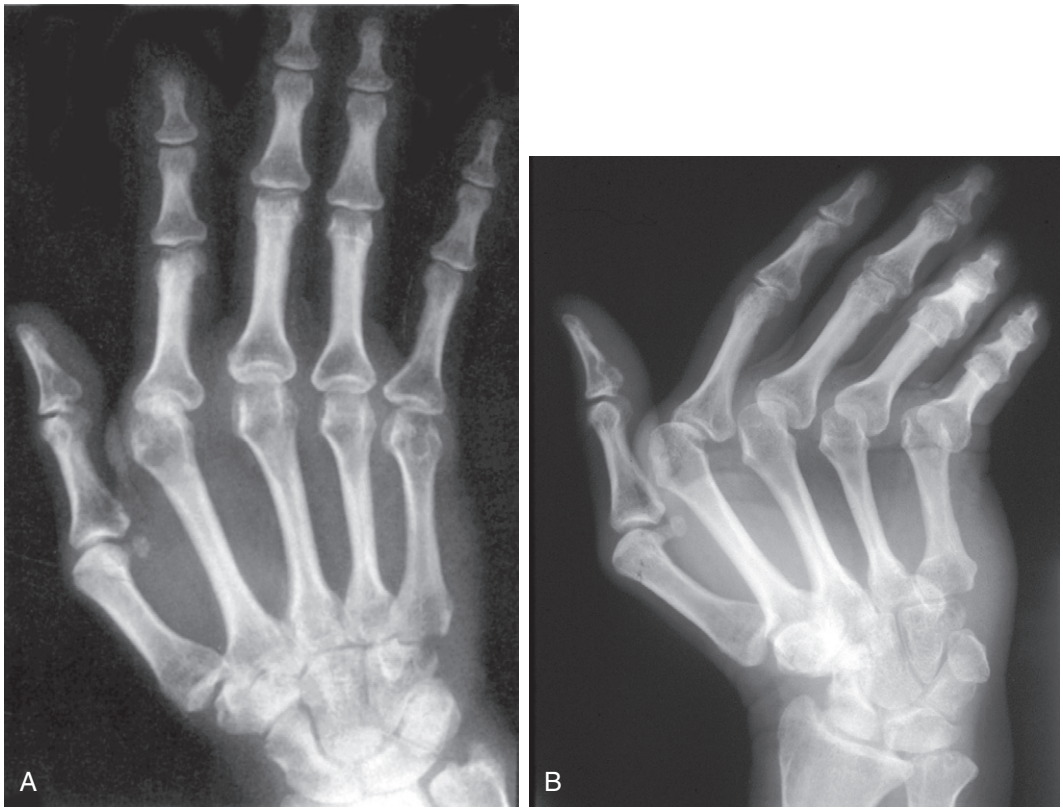

FIGURE 1-4. A, PA view of the hand in lupus, demonstrating minimal subluxation of the second proximal interphalangeal and metacarpal phalangeal joints. **B,** Nørgaard view of the same hand in which the fingers are not rigidly positioned. Extensive subluxations become apparent.

Foot

The anteroposterior (AP), oblique, and lateral views of the foot are usually obtained. One must be sure to obtain a high quality radiograph of the calcaneus in the lateral view. Observation of the attachments of the plantar aponeurosis and Achilles tendon is important in many of the arthropathies (Fig. 1-5).

FIGURE 1-5. Lateral view of the calcaneus showing erosive changes as well as bone productive changes on the inferior aspect of the calcaneus at the attachment of the plantar aponeurosis. *(From Brower AC: The radiographic features of psoriatic arthritis. In Gerber L, Espinoza L, editors:* Psoriatic arthritis,*Orlando, FL, 1985, Grune & Stratton, p. 125, reprinted with permission.)*

Shoulder

Anteroposterior views of the shoulder should be obtained in true external and internal rotation. Erosive changes can usually be identified in at least one of these views. External rotation is best for demonstrating the presence of osteophytes. Internal rotation demonstrates the traumatic lesion of the Hill-Sachs defect. Location of tendon calcification can be determined by observing change in the position of the calcification between the internal and external rotation. The straight AP view does not image the true glenohumeral joint. In order for this joint to be imaged accurately, the patient should be placed in a 40-degree posterior oblique position (Fig. 1-6).

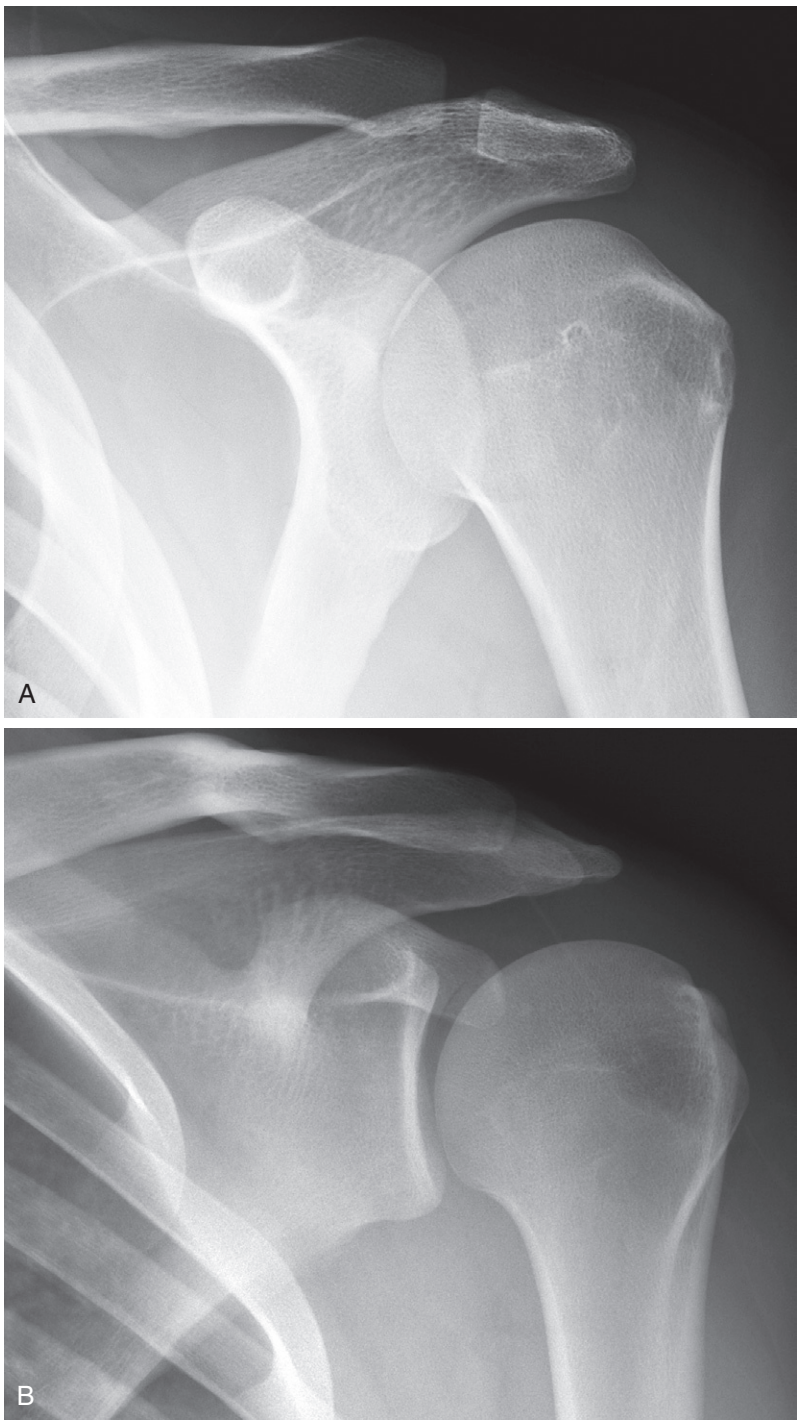

FIGURE 1-6. **A,** Normal AP view of the shoulder. **B,** AP view of the shoulder taken in 40-degree posterior oblique position. This allows accurate evaluation of the glenohumeral joint.

Knee

The AP radiograph of the knee should be obtained in the standing position. This allows for accurate evaluation of loss of cartilage. If the patient is not standing, then the medial and lateral compartments may appear perfectly normal (Fig. 1-7). In the standing position there may be asymmetry between the medial and lateral compartments, but unless the joint space measures less than 3 mm, cartilage loss is not the cause. The discrepancy between the compartments may be secondary to ligamentous instability. The standing AP view demonstrates displacement of the tibia on the femur and any pathologic degree of varus or valgus angulation. The knee should also be radiographed in a

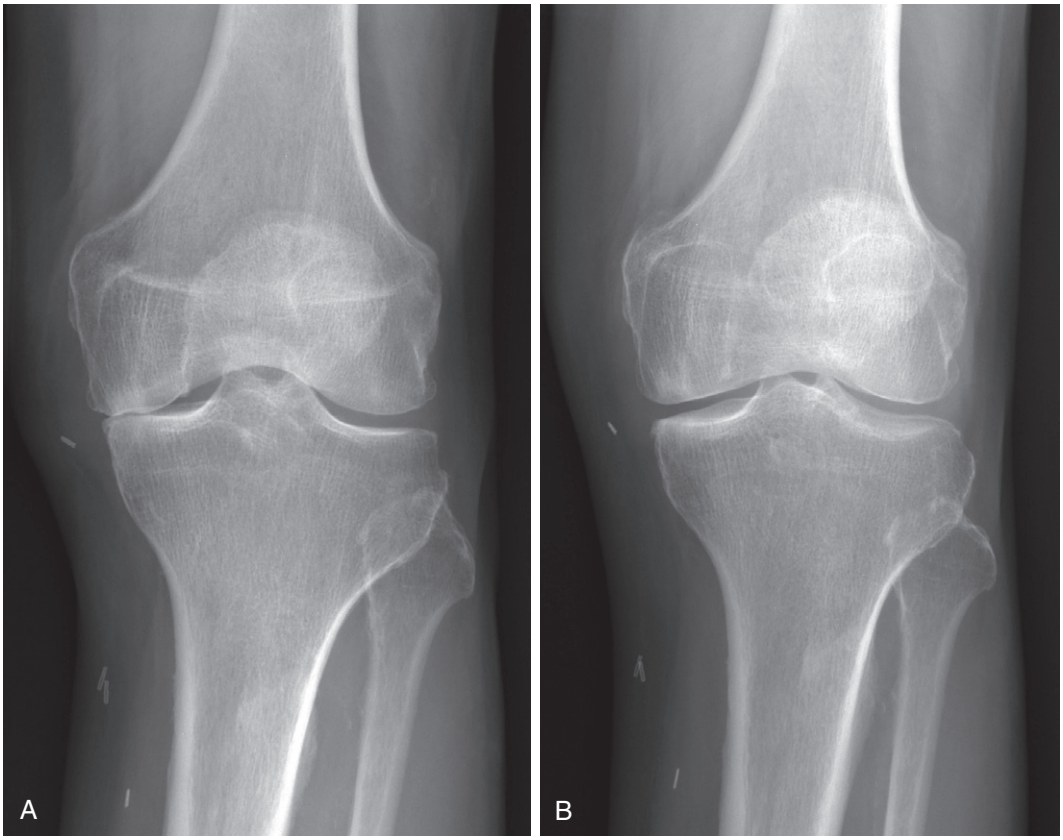

FIGURE 1-7. **A,** Standing AP view of the right knee. This view demonstrates near-total loss of the medial compartment joint space. **B,** Tabletop AP view of the same knee. Despite non-weight-bearing position, there is slight loss of the medial compartment with secondary osteoarthritic changes.

nonstanding lateral flexed position. This allows evaluation of the patellofemoral joint space as well as identification of an abnormal position of the patella. If the knee is flexed 45 degrees or more, then medial and lateral compartment narrowing can also be observed. On the lateral view, the medial plateau is the white line that curves downward; the lateral plateau is a white line that goes straight across or curves upward (Fig. 1-8).

FIGURE 1-8. Lateral view of the knee. The medial tibial plateau is the alignment curves downward (*arrow*) and the lateral plateau is a line that goes straight across (*arrowhead*).

Hip

The hip is usually radiographed in the AP and frog leg positions. In the AP view the hip is internally rotated to image the femoral neck to its fullest advantage. In the frog leg lateral view the hip is abducted. In this view, the anterior and posterior portions of the femoral head are imaged. This view is most important in evaluating underlying osteonecrosis. Although the entire head may appear to be involved on an AP view, the frog leg lateral view may demonstrate the abnormality to be limited to either the anterior or posterior section of the head. It is also the frog leg lateral view that demonstrates a subchondral lucency of osteonecrosis. In many patients, a vacuum phenomenon in the joint will be produced in the frog leg lateral view, helping to exclude the presence of synovial fluid. The vacuum phenomenon may also help in the evaluation of the cartilage present (Fig. 1-9).

FIGURE 1-9. Frog leg lateral view of the hip. A vacuum phenomenon has been introduced into the joint space (*arrows*) and allows evaluation of the thickness of the cartilage present. The cartilage is thinner in the posterolateral aspect of the hip joint in this patient with osteoarthritis.

Sacroiliac Joints

The modified Ferguson view is the only view necessary to evaluate the sacroiliac joints (Fig. 1-10). The patient is placed in a supine position and when possible, the knees and hips are flexed. The x-ray tube is centered on L5 to S1 and then angled 25 to 30 degrees toward the head. If it is angled too steep, the pubic symphysis will overlie the sacroiliac joints and obscure them, preventing accurate evaluation. The modified Ferguson view brings into profile the anterior/inferiormost aspect of the sacroiliac joints. It is this part of the joint that is most frequently affected in any disorder of the sacroiliac joints. Ninety percent of the time this view

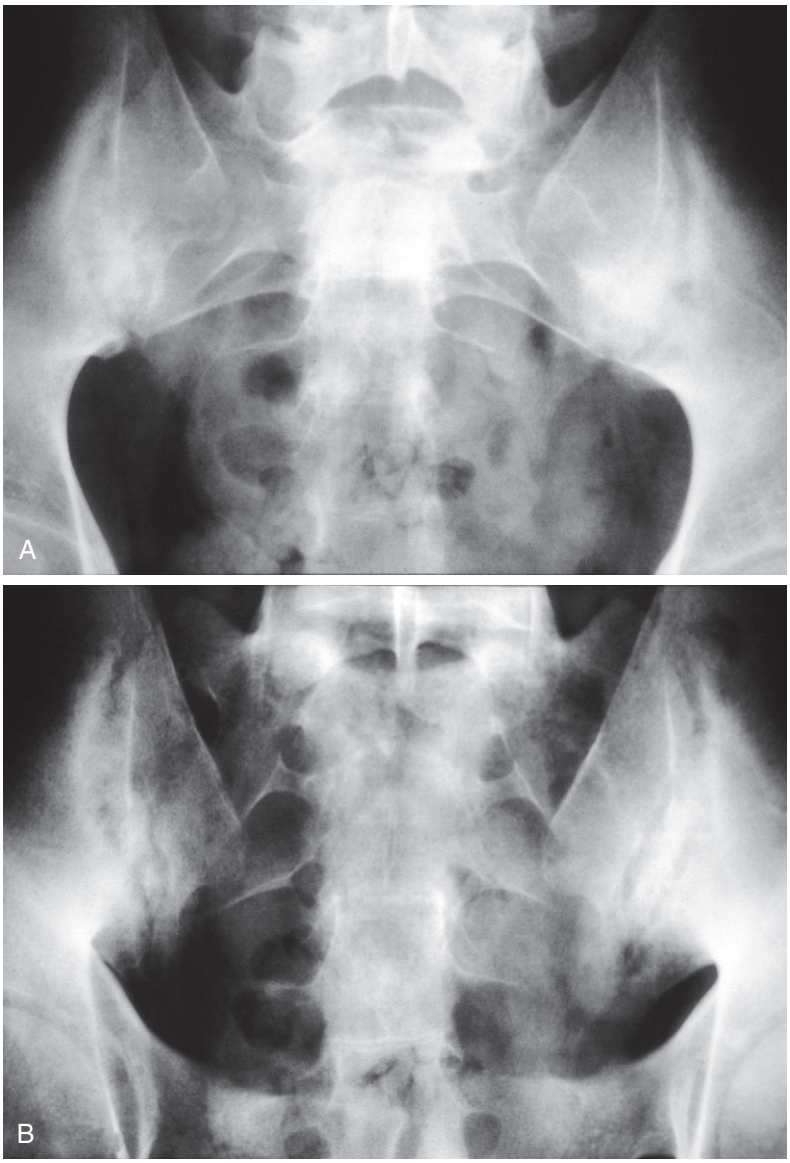

FIGURE 1-10. A, Normal AP view of the sacroiliac joints. Osteoarthritic changes are present in the right sacroiliac joint. The left sacroiliac joint appears ankylosed. **B,** AP Ferguson view of the same sacroiliac joints. The inferiormost aspect of the sacroiliac joint on the left side is normal; therefore, there is no ankylosis present. The apparent ankylosis is caused by a huge osteophyte that extends from the ilium across the sacroiliac joint the sacrum. *(From Brower AC: Disorders of the sacroiliac joint,* Radiolog *1(20):3, 1978; reprinted by permission.)*

provides the clinician with an image that can be accurately evaluated. Computed tomography and magnetic resonance imaging (MRI) may also be used if the pelvic soft tissues cause a problem in the plain film radiograph.

Cervical Spine

The lateral flexed view of the cervical spine is the single most important radiograph in the evaluation of cervical spine disease. Flexion opens the apophyseal joints and allows accurate observation of erosive disease. It demonstrates significant subluxation of one vertebral body on another. It also demonstrates abnormal laxity of the transverse ligament, which holds the odontoid adjacent to the atlas (Fig. 1-11). This finding is common in all inflammatory arthropathies but especially in rheumatoid arthritis.

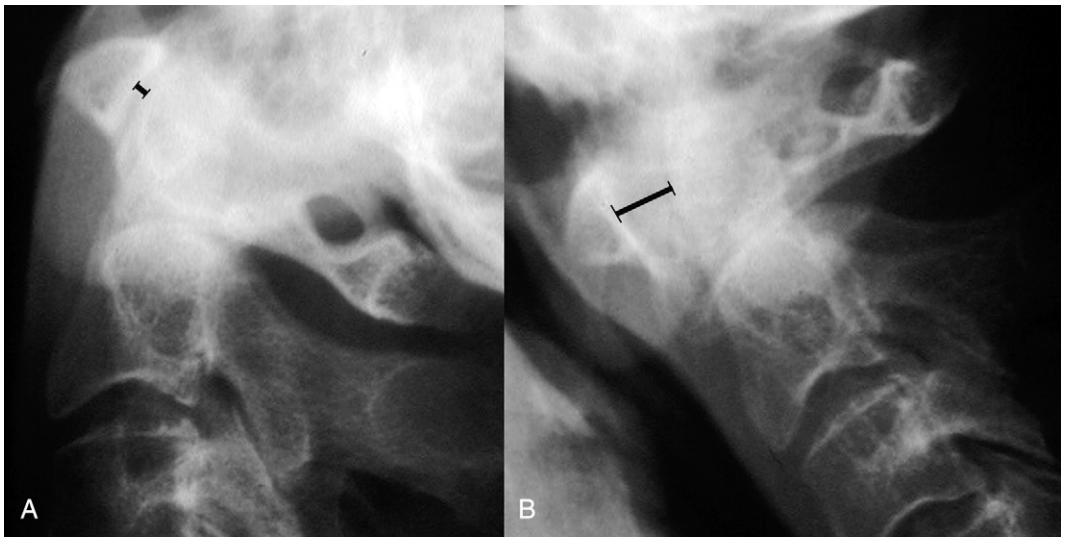

FIGURE 1-11. A, Lateral view of the upper cervical spine taken in extension. There is no evidence of subluxation. **B,** Lateral view of the same cervical spine taken in flexion. The distance between the odontoid and the atlas is increased to greater than 3 mm (*caliper line*). This indicates subluxation secondary to laxity of the transverse ligament.

Diagnostic Radiographic Survey

The distribution of the joint involvement is key to the diagnosis of the specific arthropathy. Therefore, it is also necessary to obtain radiographs of more than just the symptomatic joint. Simple radiographic surveys can be performed, tailored to the working clinical diagnosis. For example, if ankylosing spondylitis is the working diagnosis, then the survey should be tailored to the axial system; if rheumatoid arthritis is the working diagnosis, then the survey should be tailored to the appendicular system. For the patient with vague articular complaints that fit no specific pattern, the following "poor man's" survey would be appropriate:

1. Posteroanterior and Nørgaard views of both hands to include both wrists
2. Anteroposterior standing view of both knees
3. Anteroposterior view of the pelvis
4. Lateral flexed view of the cervical spine

This survey will provide sufficient diagnostic information while exposing the patient to a relatively low dose of radiation at a reasonable cost.

MAGNETIC RESONANCE IMAGING

Magnetic resonance (MR) imaging has made a major impact on the detection and evaluation of joint-based disease and is the most important imaging technique after radiography. This modality offers accurate, noninvasive assessment of pathology affecting joints, bone marrow, soft tissues, and the spine. It offers many advantages when compared to plain radiographs, including superior evaluation of soft tissues, marrow, and cartilage; lack of ionizing radiation; multiplanar evaluation of joints too difficult to image by plain radiography (e.g., temporomandibular joints and spine); and, if a contrast agent is necessary, an alternative agent (gadolinium) for individuals sensitive to iodine. The clinical and research use of MR imaging in the evaluation of arthropathies has expanded rapidly in an effort to exploit these advantages.

However, the advantages of MR imaging of the joint must be balanced against the cost of the examination, the length of the examination, and the discomfort for the patient. The use of MR in the evaluation of arthropathies can be separated into two categories: (1) assessment of complications of arthropathies, and (2) verification of an arthropathy and assessment of response to treatment. The use of MR in the primary evaluation of synovitis, detection of early erosions, and status of the articular surface is much more common now than it was 10 years ago. The problem with MR from a diagnostic perspective is that the examination is sensitive but not necessarily specific for the diagnosis of arthropathies. MR images should always be correlated with available radiographs whenever possible.

The inherent contrast resolution of MR offers the opportunity to evaluate the synovium, bone marrow, cartilage, soft tissues (ligaments, tendons, and muscle), and spine.

MR: Synovium

MR imaging can demonstrate disease of synovial-lined structures including synovitis, tenosynovitis, synovial cyst, and bursitis. The majority of these findings have been most extensively studied in rheumatoid arthritis but can be seen in any of the inflammatory arthropathies, infection, and even osteoarthritis. The MR demonstration of synovitis may be very important to the rheumatologist, if the physical examination is equivocal in establishing the diagnosis of an inflammatory arthritis or determining the effect of a particular treatment regimen on the synovium. Some investigators say that they can differentiate synovium from effusion on noncontrast spin echo images. Normal synovium is usually imperceptible on MR. Hypertrophied synovium may demonstrate intermediate signal on T1-weighted images relative to the low signal of joint effusion and show intermediate signal on T2-weighted images compared to the relatively high signal effusion (Fig. 1-12).

However, frequently synovitis cannot be differentiated from effusion without the use of intravenous gadolinium. Active synovitis enhances with the administration of gadolinium (Fig. 1-13), but the affected joint must be imaged immediately, as gadolinium will diffuse into the joint if imaging is delayed. This rapid diffusion of gadolinium precludes postcontrast imaging of joints outside the initial field of view.

FIGURE 1-12. Fat-suppressed fast spin echo (FSE) T2-weighted sagittal image of the knee in rheumatoid arthritis. The hypertrophied synovium (*arrows*) demonstrates lower signal than the surrounding high signal effusion.

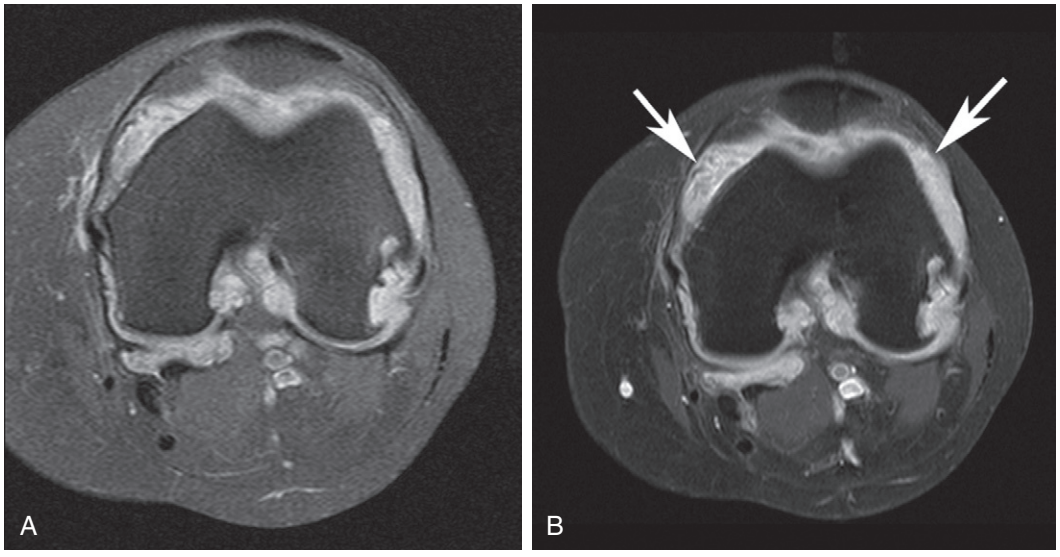

FIGURE 1-13. A, PD-weighted FSE fat-saturated axial image of the knee in rheumatoid arthritis shows high signal in the joint space. It is difficult to determine if this is effusion or synovitis. **B,** T1-weighted fat-saturated axial image following intravenous gadolinium administration shows enhancement of extensive synovitis (*arrows*).

Nonspecific synovitis is usually intermediate in signal on T1- and T2-weighted images. When the synovium is low in signal on T2-weighted images, the differential diagnosis becomes limited to the following: pigmented villonodular synovitis (PVNS), calcified synovial chondromatosis, hemophilia, amyloidosis, and chronic rheumatoid arthritis. The typical MR appearance of PVNS is foci of intermediate to low signal within the synovium, secondary to hemosiderin deposition, on T1- and T2-weighted images (Fig. 1-14). The diagnosis of synovial chondromatosis is suggested by the MR appearance of noncalcified loose bodies demonstrating intermediate signal on T1-weighted images and high signal on T2-weighted images (Fig. 1-15).

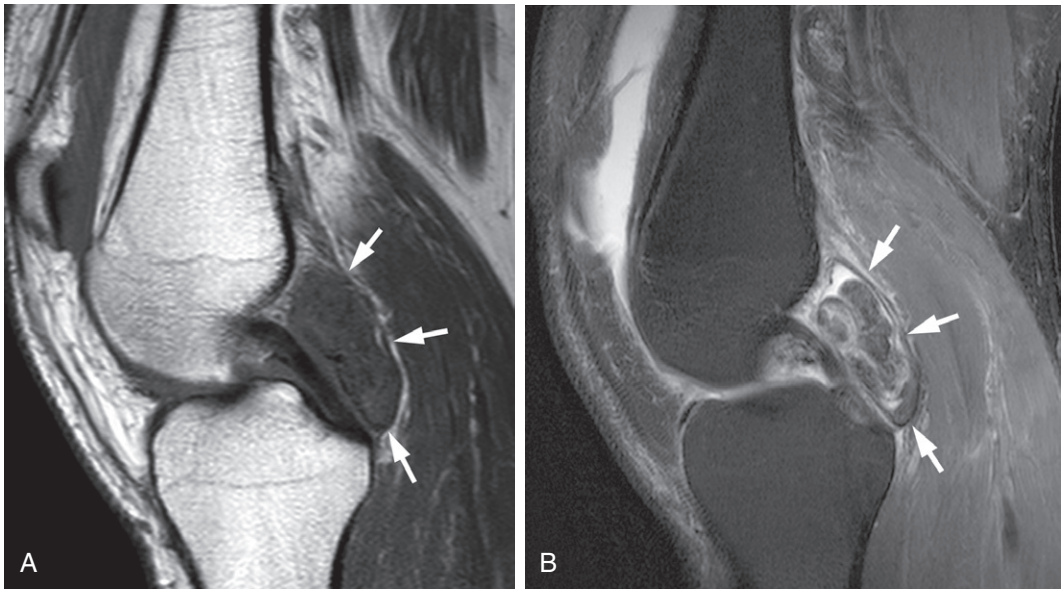

FIGURE 1-14. T1-weighted (**A**) and fat-saturated T2-weighted (**B**) sagittal images of the knee. Nodular mass (*arrows*) arising from the synovium demonstrates intermediate and low signal on T1-weighted images. The masses demonstrate predominantly low signal on T2-weighted images. The findings are classic for PVNS.

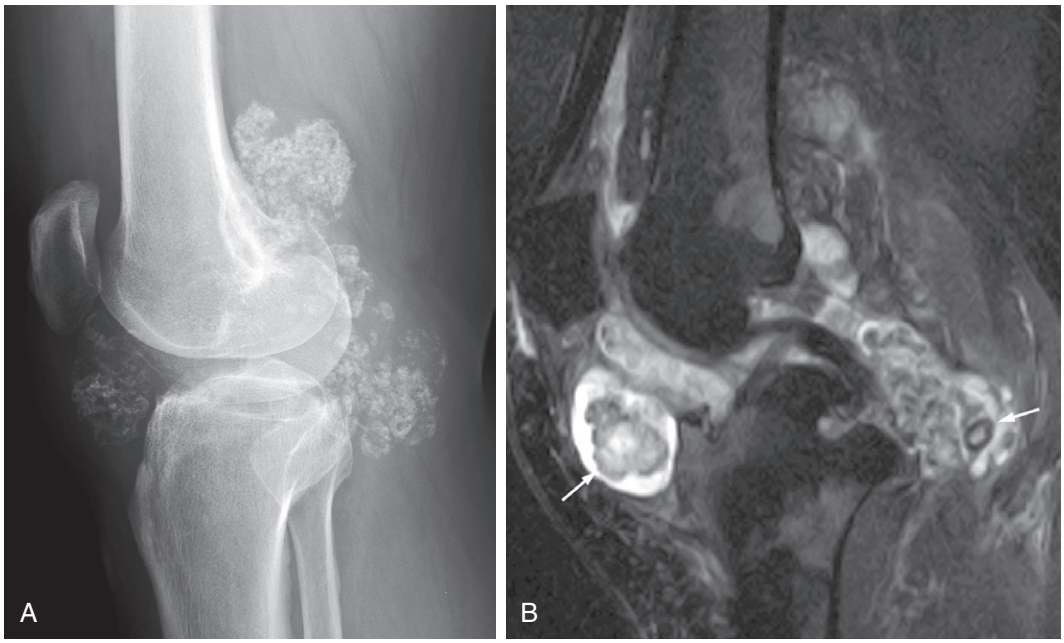

FIGURE 1-15. A, Lateral radiograph of the knee of synovial chondromatosis. Multiple ossific bodies are seen throughout the knee joint. **B,** T2-weighted fat saturated sagittal image demonstrates the multiple lobular, low signal bodies (*arrows*) outlined by high signal fluid.

MRI: Bone Marrow

MRI is exquisitely sensitive at detection of abnormalities of the bone marrow including erosions, osteonecrosis, fracture, and infection. Additionally, MRI detects these abnormalities earlier than plain radiography.

MR imaging has been shown to be superior to plain radiography for the detection and quantification of erosive disease particularly in the hands, wrists, and feet. Acute erosive disease is usually accompanied by synovitis. Erosions are best appreciated on T1-weighted images as interruption of subchondral bone and focal intermediate to low signal replacement of the adjacent bone marrow (Fig. 1-16). Fat-suppressed T2-weighted images should be evaluated for the presence of edema-like changes in the bone marrow adjacent to erosive disease. This finding heralds the progression of disease that can be later detected by radiography even with the administration of effective therapy (Fig. 1-17).

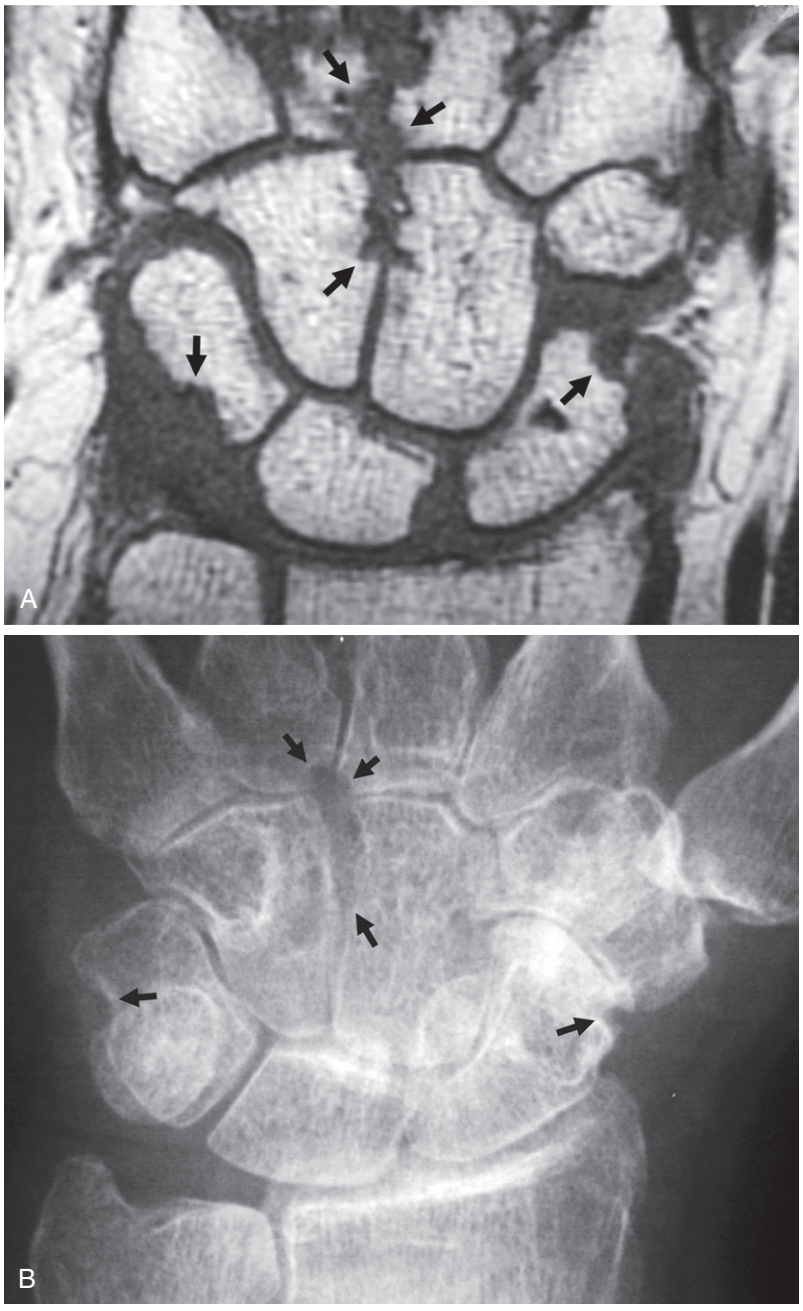

FIGURE 1-16. A, Coronal T1-weighted image of the wrist in a patient with rheumatoid arthritis. Focal interruptions in cortex are erosions (*arrows*). **B,** Some of the erosions seen on MR imaging are clearly visible on AP radiograph of the same wrist (*arrows*).

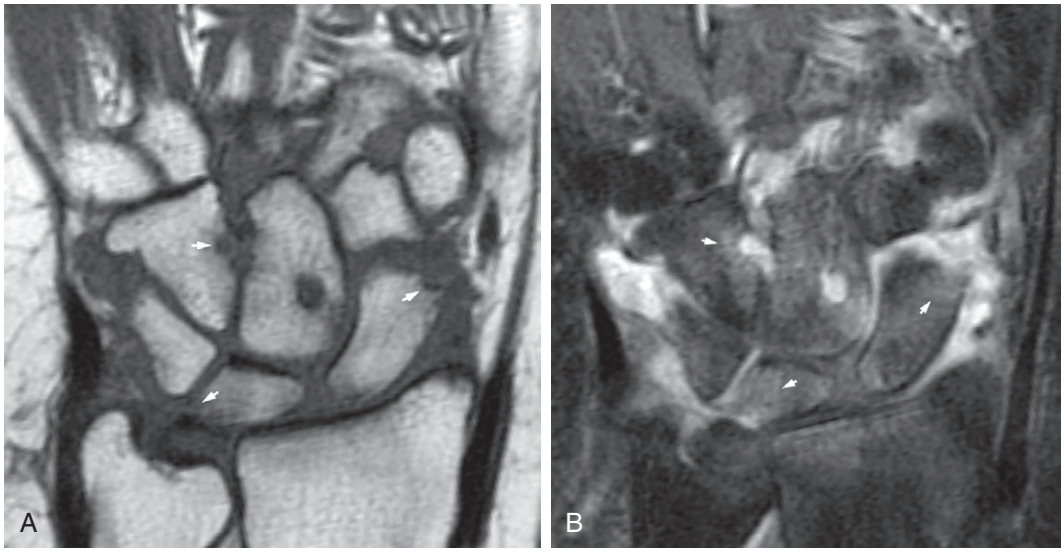

FIGURE 1-17. A, Erosions (*arrows*) are seen on coronal T1-weighted image of the wrist in a patient with rheumatoid arthritis. **B,** Fat-suppressed T2-weighted image demonstrates edema-like signal in the bone marrow adjacent to the erosive disease (*arrows*).

MR imaging offers the earliest and most sensitive detection of osteonecrosis. This is a common complication of systemic loose lupus erythematosus and steroid therapy. The MR signs of avascular necrosis (AVN) have been most extensively studied in the femoral head. The double line sign when seen in the femoral head is considered diagnostic of AVN. The double line sign consists of a linear band of low signal adjacent to a single linear band of high signal on T2-weighted spin echo sequences (Fig. 1-18). Fat signal is frequently preserved in the necrotic segment. Occasionally, the signal seen on T1- or T2-weighted images is nonspecific, depending on the stage of the osteonecrosis imaged, and in such cases the diagnosis of AVN should be made with caution.

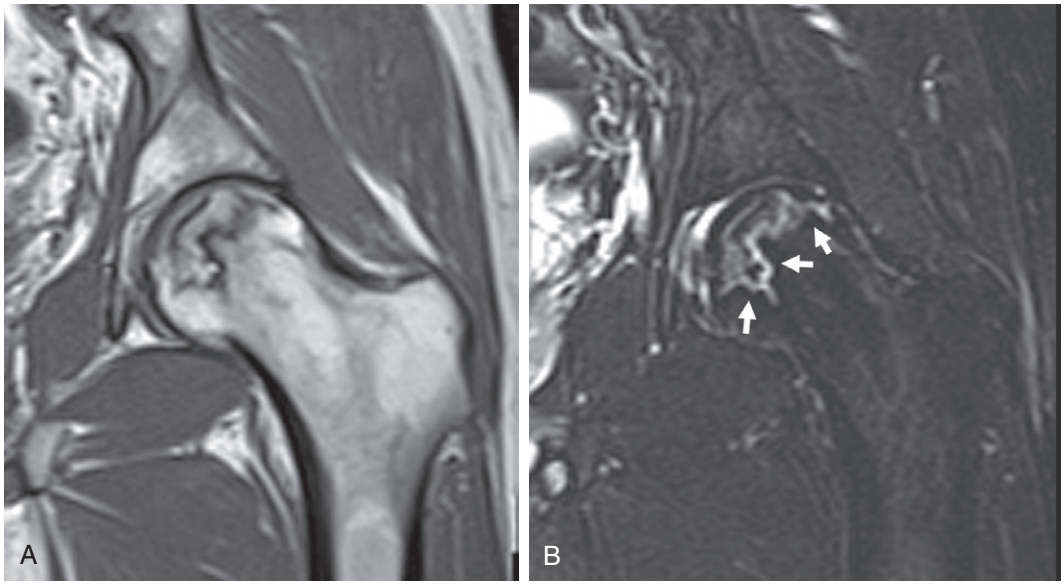

FIGURE 1-18. T1-weighted (**A**) and fat-saturated T2-weighted (**B**) coronal images of the left hip. Thin band of low signal is seen within the femoral head on both images. The wavy line of low signal is bordered by a thin line of high signal on the T2-weighted image, producing the "double line" sign. Fat signal is preserved in bone bounded by the double line sign (*arrow*). Findings are diagnostic of AVN of the femoral head.

Insufficiency fractures are easily and rapidly diagnosed with MRI. Insufficiency fractures present as a linear band of low signal on T1- and T2-weighted images surrounded by edema. Edema presents as intermediate signal on T1-weighted images and increased signal on T2-weighted images (Fig. 1-19). Insufficiency fractures can be quickly and accurately evaluated with T1-weighted images in the acute setting when osteoporosis hinders observation of such fractures on both plain film and scintigraphic images.

MR imaging has also been used to differentiate neuropathic osteoarthropathy from infection in the foot of a patient with diabetes. The value of MRI is in excluding infection. When no edema is demonstrated within the involved marrow, osteomyelitis can be confidently excluded. However both conditions can produce edema (low signal on T1-weighted images and high signal on T2-weighted images) in the affected marrow, soft tissues, and joint; therefore, they cannot be differentiated when this signal pattern is present. If the soft tissues are intact, then the diagnosis of osteomyelitis is less likely.

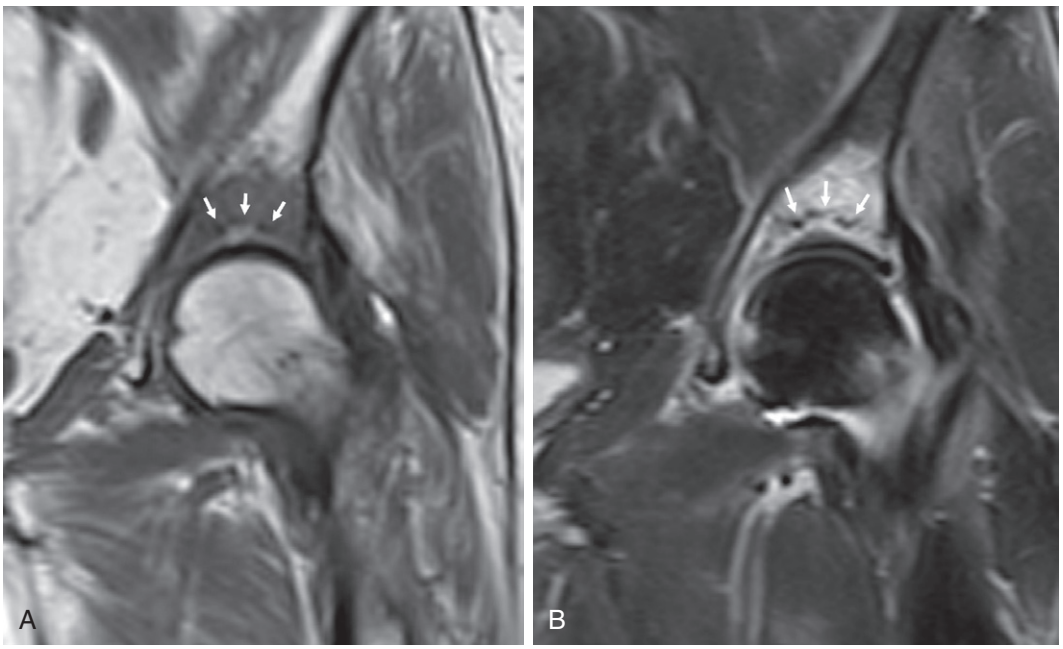

FIGURE 1-19. T1-weighted (**A**) and fat-saturated T2-weighted (**B**) coronal image of the hip. A linear band of low signal is seen paralleling the acetabular roof (*arrows*). This linear band is surrounded by intermediate signal on T1-weighted image and high signal on fat-saturated T2-weighted image. The findings are consistent with an insufficiency fracture.

MRI: Soft Tissues

MRI is an ideal modality to evaluate the soft tissues of an extremity and to evaluate both the primary manifestations and soft tissue complications of arthropathies. MRI can establish the diagnosis of ruptured tendons and ligaments. The rotator cuff is the most common tendinous structure evaluated by MRI, but other tendons, such as the Achilles and posterior tibial tendons, can be successfully evaluated. Rupture is diagnosed by visualization of discontinuity of the tendon or ligament. The ruptured tendon or ligament is frequently surrounded by fluid, as evidenced by high signal on T2-weighted images (Fig. 1-20).

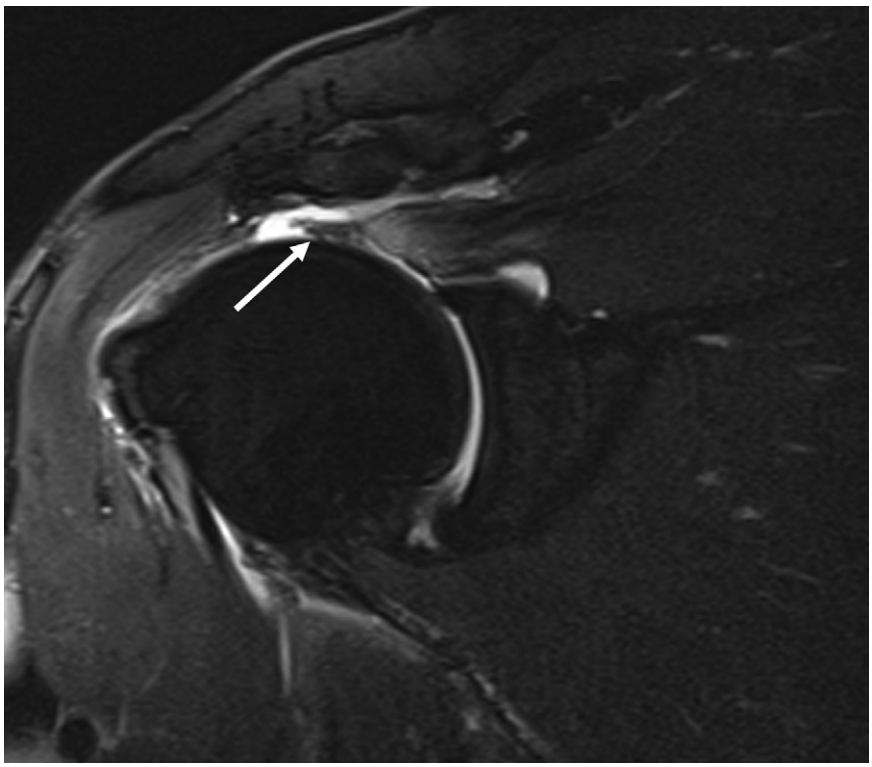

FIGURE 1-20. Fat-saturated T2-weighted coronal image of the shoulder demonstrates a full thickness tear of the supraspinatus tendon with the tendon retracted to the level of the glenoid (*arrow*). High signal fluid outlines the tendon margin.

MR: Cartilage

MR imaging offers direct imaging of both fibrocartilage and hyaline cartilage. Tears and degeneration of fibrocartilaginous structures, such as the meniscus of the knee, the labrum of the shoulder, and the triangular fibrocartilage complex of the wrist, can be demonstrated with spin echo and gradient recalled echo (GRE) sequences (Fig. 1-21). Direct imaging of the hyaline cartilage is possible particularly in larger joints like the knee. Standard sequences such as fat-suppressed proton-weighted (PD) images may demonstrate chondral disease in larger joints (Fig. 1-22), but imaging of hyaline cartilage can be very difficult due to poor spatial and contrast resolution in small joints such as the wrist. Subtle hyaline cartilage defects, however, may be visualized with

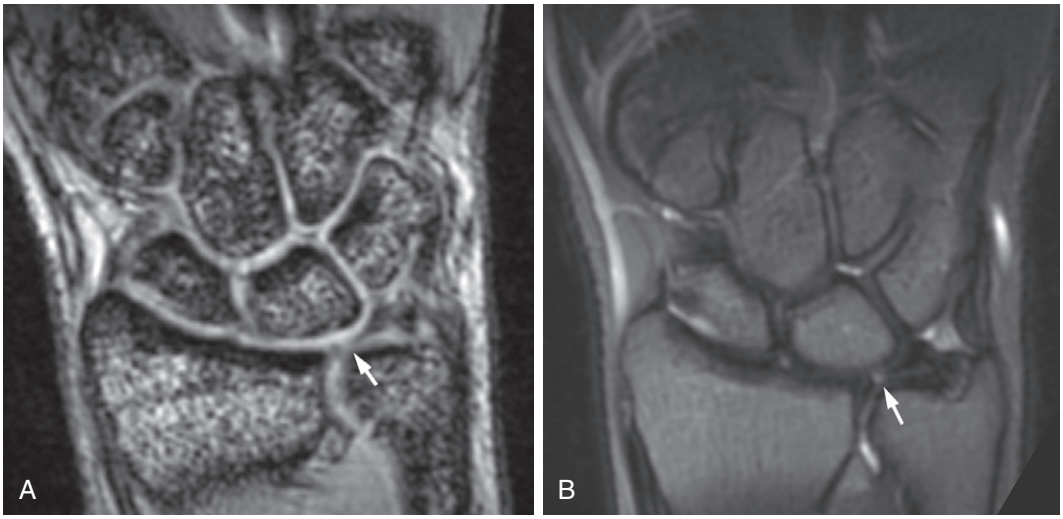

FIGURE 1-21. Gradient echo-weighted (**A**) and fat-saturated T2-weighted (**B**) coronal images of the wrist demonstrate a central tear in the triangular fibrocartilage disc with fluid in the tear (*arrows*).

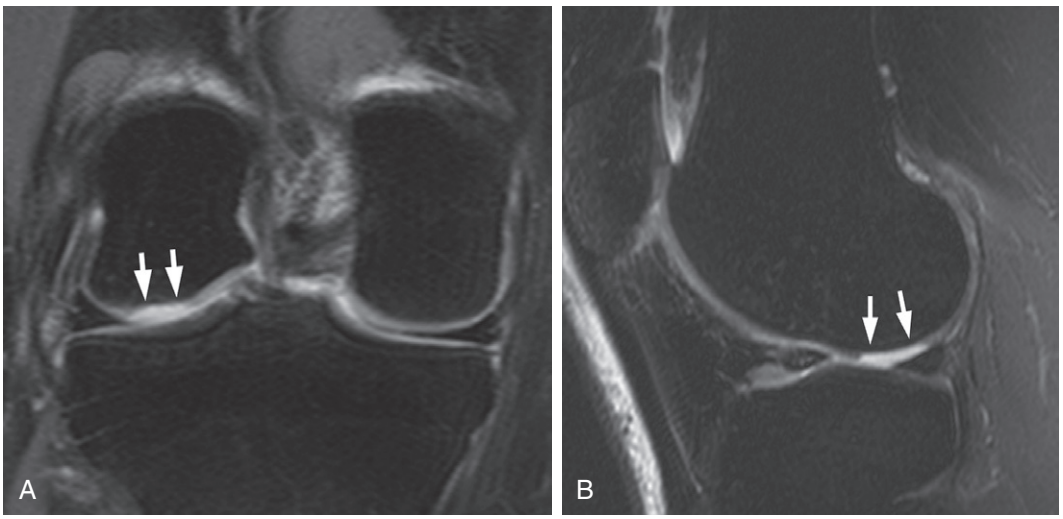

FIGURE 1-22. Coronal fat-suppressed proton density-weighted (**A**) and sagittal fat-saturated T2-weighted (**B**) images of the knee demonstrate a full thickness articular cartilage defect (*arrows*) of the lateral femoral condyle.

the use of intraarticular gadolinium or thin section GRE-type sequences. Cutting-edge MR imaging techniques for evaluation of cartilage include T2 mapping, dGEMRIC imaging, and T1rho sequences but these techniques are not widely used in clinical practice. MR imaging may be particularly useful in children when the epiphyses are largely cartilaginous. Erosion of this cartilage cannot be directly imaged by plain film radiography (Fig. 1-23).

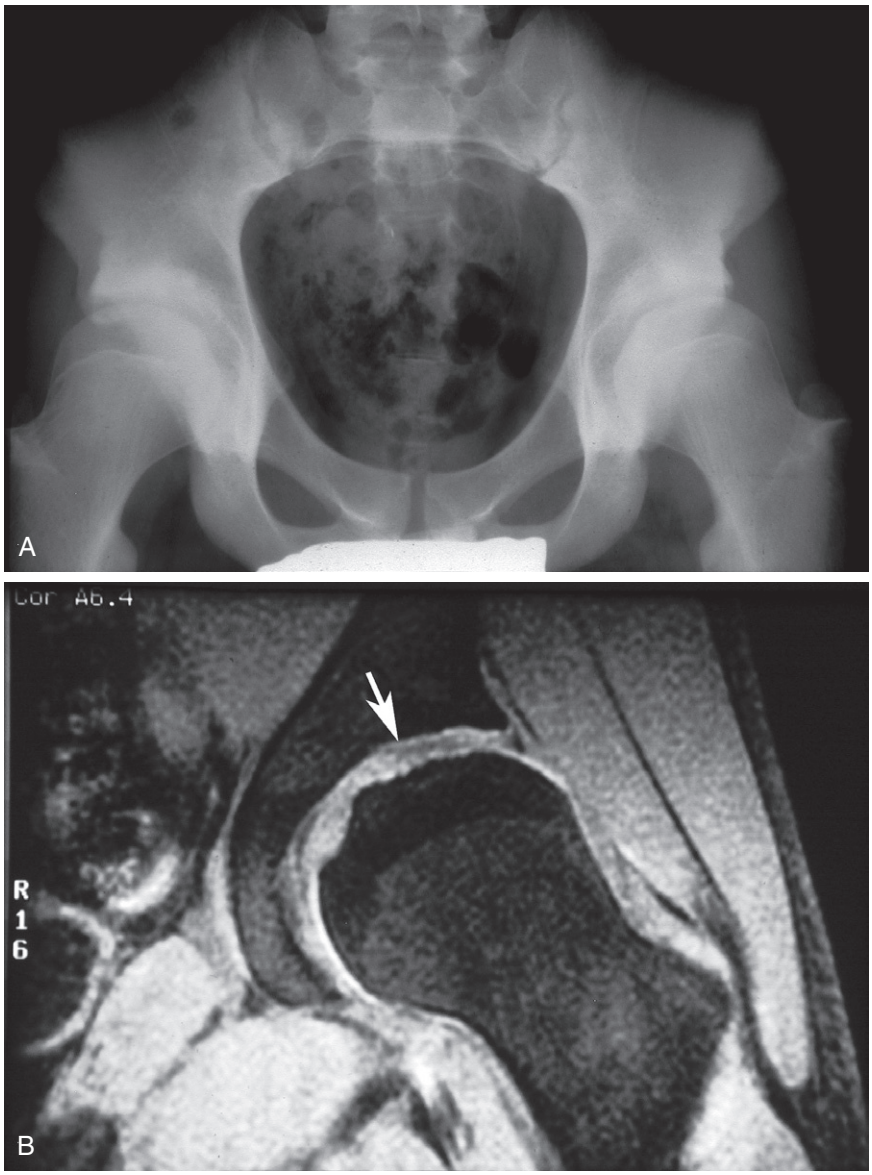

FIGURE 1-23. **A,** Radiograph of the hips in an adolescent male with juvenile idiopathic arthritis demonstrates enlargement of the femoral heads with lateral joint space narrowing. **B,** Fat-suppressed coronal spoiled gradient recalled echo image of the left hip demonstrates extensive irregularity and loss of normal high signal femoral and acetabular cartilage (*arrows*).

MR: Spine

MR imaging of the spine has proven to be clinically useful in the evaluation of complications of systemic arthropathies. Complications of rheumatoid arthritis at the craniocervical junction can be readily assessed, including cord impingement secondary to pannus at the C1-C2 joint, atlantoaxial subluxation, and cranial cervical settling (Fig. 1-24). In fact, any patient with rheumatoid arthritis who develops neurologic symptoms, progressive neurologic symptoms, or progressive radiographic changes in the cervical spine should have MR imaging of the cervical spine. MR imaging of the spine should also be performed in patients with ankylosing spondylitis and discovertebral destruction. In this scenario, as in neuropathic osteoarthropathy, the value of MR lies in excluding infection when no edema pattern is seen within the affected vertebral bodies.

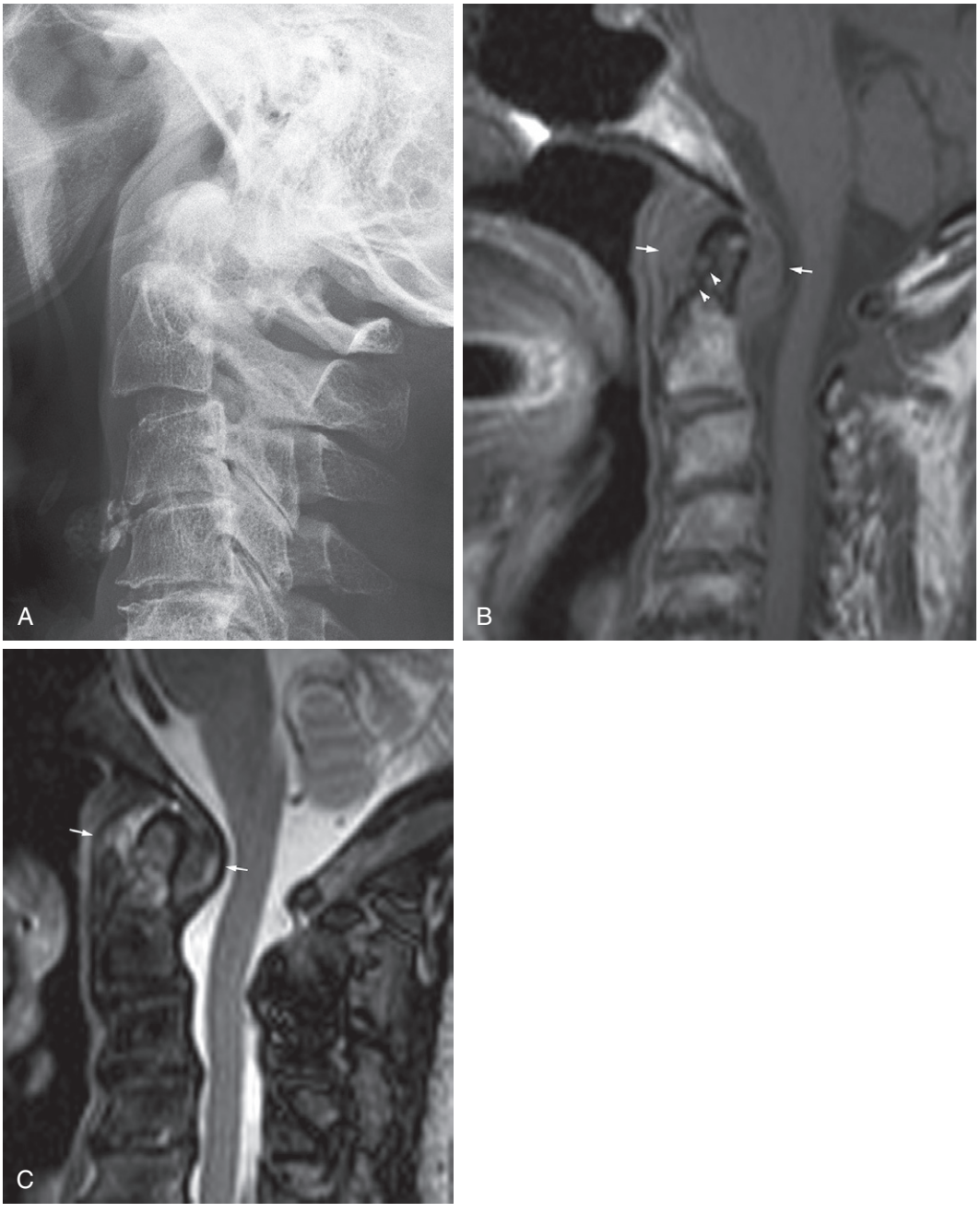

FIGURE 1-24. A, Lateral radiographs of the craniocervical junction demonstrate cortical irregularity to the odontoid process of C2 and soft tissue fullness anteriorly. Sagittal T1-weighted **(B)** and fat-saturated T2-weighted **(C)** images demonstrates an intermediate T1-weighted signal and heterogeneous intermediate to low signal T2-weighted mass surrounding and infiltrating the odontoid. This represents synovial hypertrophy (*arrows*) encroaching on the brainstem. Note the erosions of the dens best seen on T1-weighted image (*arrowheads*).

ULTRASONOGRAPHY

The role of ultrasound in the evaluation and treatment of articular pathology has expanded dramatically in the last 10 years. This modality is inexpensive, patient friendly, and relatively quick in comparison to MR imaging. Unlike MR imaging, multiple and bilateral joints may be rapidly assessed in the same sitting. Ultrasound also can assess some of the soft tissue complications of arthritis including tendon rupture, ligament rupture, cyst formation, and subcutaneous nodules. In addition to providing accurate diagnostic information, ultrasound offers the opportunity to guide aspiration of cysts and direct therapeutic injections without radiation exposure. However, this modality is best used by ultrasonographers who have a clear understanding of joint anatomy and experience in interpreting the findings of disease.

Ultrasound can detect important manifestations of inflammatory arthropathy including synovitis, tenosynovitis, and erosions. Ultrasound evaluation of synovitis is superior to physical examination. Synovitis is detected on gray scale imaging as hyper- or isoechoic material in a joint or tendon sheath (Fig. 1-25). Synovitis can be differentiated from hypoechoic fluid by gently compressing the area of concern. Synovitis is not compressible whereas uncomplicated

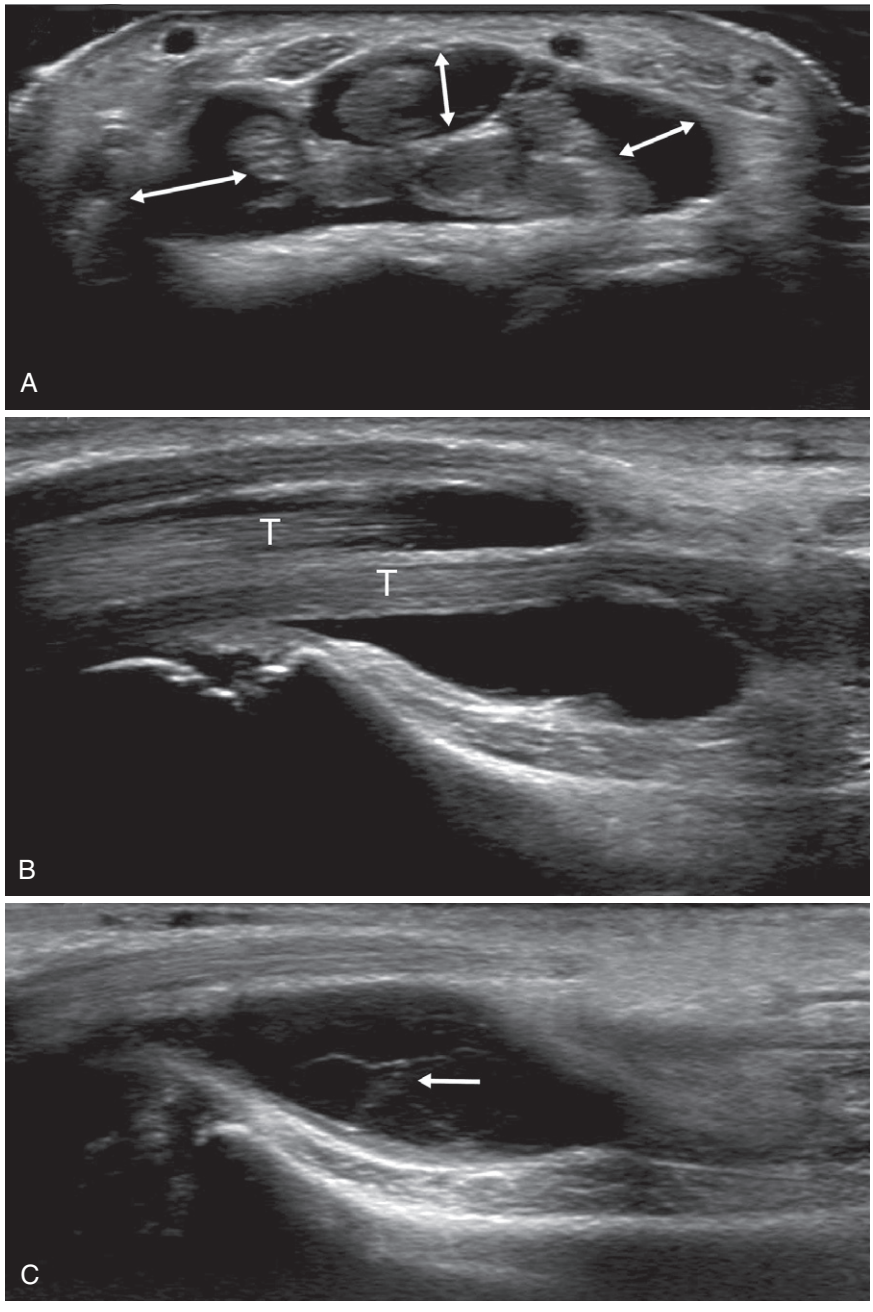

FIGURE 1-25. Axial (**A**) and sagittal (**B**) ultrasound of the flexor compartment of the wrist with tenosynovitis. Anechoic fluid (*arrows*) with mild peripheral synovial thickening surrounds the tendons (*T*). Sagittal image (**C**) (*arrow*) shows hyperechoic synovitis in tendon sheath fluid.

fluid can be readily displaced by applying pressure with the transducer. Synovitis is readily characterized by power Doppler interrogation with acute synovitis showing hypervascularity as long as the ultrasonographer does not compress the involved tissue with too much force. Power Doppler assessment of joints is so exquisitely sensitive that some authors describe being able to detect the enthesopathic changes of spondyloarthropathies. Erosions can be detected in the small joints of the hands, wrist, and feet, particularly at the dorsal aspect of the metacarpal heads and the distal ulna (Fig. 1-26). Ultrasound can show erosive disease at an earlier stage than can plain radiography, but it cannot assess the entirety of a joint, such as in the wrist, as well as MR imaging can. Ultrasound has become such a powerful adjunct to the evaluation of synovitis and erosive disease that these machines are now found in many rheumatologists' offices, and ultrasound training is integral to rheumatology fellowship education.

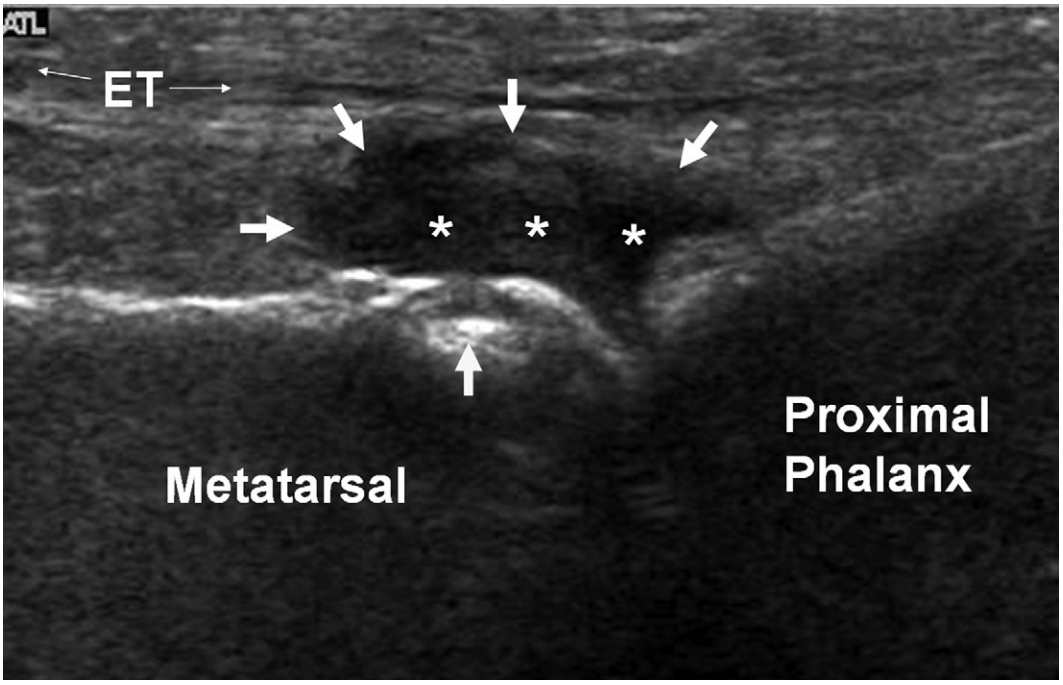

FIGURE 1-26. Sagittal ultrasound image of a metatarsal phalangeal joint. A focal interruption in the dorsal cortex of the metatarsal head (*arrow head*) indicates an erosion. Effusion (*white arrows*) and synovitis (*asterisks*) are appreciated at the dorsal aspect of the joint. *(Courtesy of Michael Bruno, Hershey, PA.)*

COMPUTED TOMOGRAPHY

The role of computed tomography (CT) in the evaluation of articular disorders has increased, particularly after the advent of volumetric helical CT scanning and the ability to reconstruct images in any plane. The exquisite detail of erosive changes imaged on a technically well done conventional radiograph is far superior to the bone detail observed on a CT image. However, CT is far superior to plain films for the evaluation of complex areas of anatomy such as the spine and sacroiliac joints (Fig. 1-27). CT and CT arthrography are frequently used to assess articular disorders in patients who cannot have MR imaging because of claustrophobia or implantable medical devices such as pacemakers. Creative uses of CT are being developed. Dual energy CT scanning has been shown to be a viable method of assessing disease activity in patients with gout. Despite the known utility of this modality, CT scanning can be associated with significant patient radiation, so this technique should be used thoughtfully and only when techniques such as MR or Ultrasound (US) imaging cannot be performed.

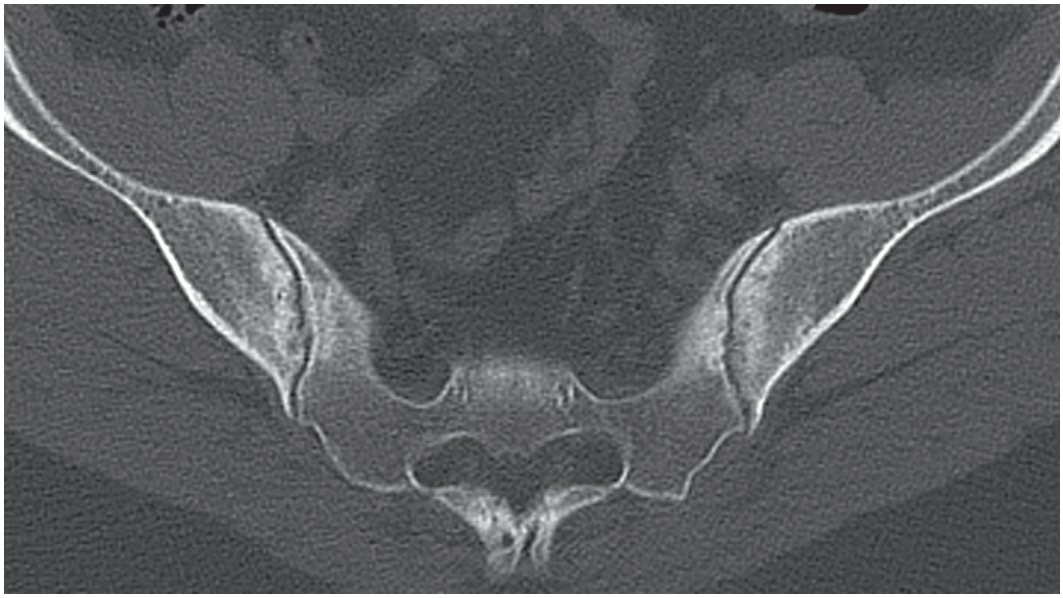

FIGURE 1-27. Axial CT image of the sacroiliac joints demonstrates the bilateral symmetric erosive changes of ankylosing spondylitis.

BONE SCINTIGRAPHY

Bone scintigraphy may be extremely helpful in evaluating the patient with articular disease. It is useful in three ways: (1) it may confirm the presence of disease, (2) it may demonstrate the distribution of disease, and (3) it may help to evaluate the activity of the disease. Bone scintigraphy is by far the most sensitive indicator of active disease. It will confirm the presence of hyperemia and inflammation that may not be apparent radiographically or on MR images. With careful observation of a high-resolution scintigraphic image of a joint, one may determine the exact location of the active disease. One may be able to distinguish tendinitis from synovitis, or synovitis from a primary bone lesion. While confirming abnormality in one joint, observation of increased activity in other areas of the body may help in making the correct diagnosis. An excellent example is the young adult who shows radiographic erosive changes in one sacroiliac joint. If bone scintigraphy shows increased uptake in that one sacroiliac joint only, infection becomes the working diagnosis. However, if bone scintigraphy shows increased uptake in both sacroiliac joints, reactive arthritis becomes the working diagnosis (Fig. 1-28).

Serial bone scintigraphy has also been helpful in evaluating activity of disease at a particular point in time. It may differentiate active disease from disease in remission. In osteonecrosis specifically, it may demonstrate the infarctive stage, the repair stage, and the inactive stage. Bone scintigraphy should be considered an integral part of the evaluation of the patient with articular disease.

Despite the inherent increased sensitivity of three-phase bone scintigraphy when compared to other modalities, the problem with this technique is the lack of specificity. Abnormal findings on scintigraphy have to be correlated with other imaging, which reduces the cost efficacy of the examination. Most rheumatologists and radiologists prefer evaluating arthropathies with radiographs, MR imaging, and ultrasound. However, in experienced hands bone scintigraphy can be a highly effective method of assessing articular disease activity. Future directions in scintigraphic imaging may lie in molecular imaging techniques that have not yet been fully developed.

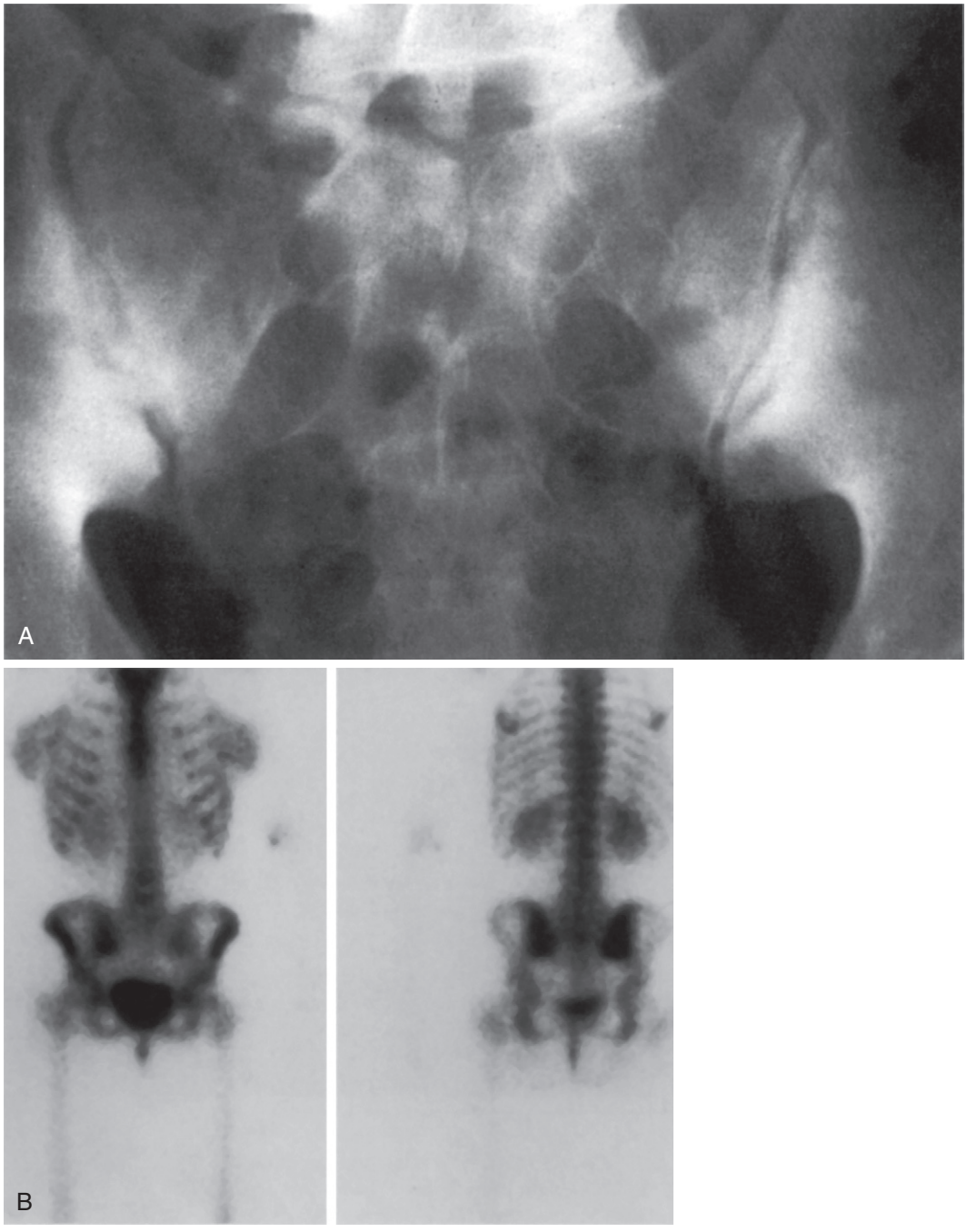

FIGURE 1-28. A, AP Ferguson view of the sacroiliac joints demonstrating erosive disease with repair involving the right sacroiliac joint. The left sacroiliac joint appears normal. Unilateral involvement of the right sacroiliac joint is most consistent with infection. **B,** bone scan of the same patient demonstrating increased activity in both sacroiliac joints. This would indicate involvement of the radiographically normal left sacroiliac joint and change the diagnosis from infection or early reactive arthritis.

SUGGESTED READINGS

Basu S, Zhuang H, Torigian DA, et al: Functional imaging of inflammatory diseases using nuclear medicine techniques, *Semin Nucl Med* 39:124–145, 2009.

Bjorkengren AG, Geborek P, Rydholm U, et al: MR imaging of the knee in acute rheumatoid arthritis: Synovial uptake of gadolinium-DOTA, *AJR Am J Roentgenol* 155:329–332, 1990.

Brower AC: Disorders of the sacroiliac joint, *Radiology* 1(20):3–26, 1978.

Campbell RS, Grainger AJ: Current concepts in imaging of tendinopathy, *Clin Radiol* 56:253–267, 2001.

De Leonardis F, Orzincolo C, Prandini N, et al: The role of conventional radiography and scintigraphy in the third millennium, *Best Pract Res Clin Rheumatol* 22:961–979, 2008.

Døhn UM, Ejbjerg B, Hasselquist M, et al: Detection of bone erosions in rheumatoid arthritis wrist joints with magnetic resonance imaging, computed tomography and radiography, *Arthritis Res Ther* 10:R25, 2008.

Gabriel H, Fitzgerald SW, Myers MT, et al: MR imaging of hip disorders, *Radiographics* 14:763–781, 1994.

Goldberg RP, Genant HK, Shimshak R, et al: Applications and limitations of quantitative sacroiliac joint scintigraphy, *Radiology* 128:683, 1978.

Jacobson JA, Girish G, Jiang Y, Resnick D: Radiographic evaluation of arthritis: inflammatory conditions, *Radiology* 248:378–389, 2008.

Jacobson JA, Girish G, Jiang Y, et al: Radiographic evaluation of arthritis: degenerative joint disease and variations, *Radiology* 248:737–747, 2008.

Johnson PT, Fayad LM, Fishman EK: CT of the foot: Selected inflammatory arthritides, *J Comput Assist Tomogr* 31(6):961–969, 2007.

Kainberger F, Mittermaier F, Seidl G, et al: Imaging of tendons—adaptation, degeneration, rupture, *Eur J Radiol* 25:209–222, 1997.

Karantanas AH: Acute bone marrow edema of the hip: role of MR imaging, *Eur Radiol* 17:2225–2236, 2007.

Keen HI, Brown AK, Wakefield RJ, et al: MRI and musculoskeletal ultrasonography as diagnostic tools in early arthritis, *Rheum Dis Clin North Am* 31:699–714, 2005.

König H, Sieper J, Wolf K: Rheumatoid arthritis: Evaluation of hypervascular and fibrous pannus with dynamic MR imaging enhanced with Gd-DTPA, *Radiology* 176:473, 1990.

Kursunoglu-Brahme S, Riccio T, Weisman MH, et al: Rheumatoid knee: Role of gadopentetate-enhanced MR imaging, *Radiology* 176:831, 1990.

Leach RE, Gregg T, Siber FJ: Weight-bearing radiography in osteoarthritis of the knee, *Radiology* 97:265–268, 1970.

Martel W, Poznanski AK: The effect of traction on the hip in osteonecrosis: A comment on the "radiolucent crescent line", *Radiology* 94:505–508, 1970.

Norgaard F: Earliest roentgenological changes in polyarthritis of the rheumatoid type: Rheumatoid arthritis, *Radiology* 85:325–329, 1965.

Østergaard M, Pedersen SJ, Døhn UM: Imaging in rheumatoid arthritis—status and recent advances for magnetic resonance imaging, ultrasonography, computed tomography and conventional radiography, *Best Pract Res Clin Rheumatol* 22:1019–1044, 2008.

Ragab Y, Emad Y, Abou-Zeid A: Bone marrow edema syndromes of the hip: MRI features in different hip disorders, *Clin Rheumatol* 27:475–482, 2008.

Robinson P: Sonography of common tendon injuries, *AJR Am J Roentgenol* 193:607–618, 2009.

Slivka J, Resnick D: An improved radiographic view of the glenohumeral joint, *J Can Assoc Radiol* 30:83–85, 1979.

Stiskal MA, Neuhold A, Szolar DH, et al: Rheumatoid arthritis of the craniocervical region by MR imaging: Detection and characterization, *AJR Am J Roentgenol* 165:585, 1995.

Swee RG, Gray JE, Beabout JW, et al: Screen-film versus computed radiography imaging of the hand: a direct comparison, *AJR Am J Roentgenol* 168:539–542, 1997.

Sy WM, Bay R, Camera A: Hand images: Normal and abnormal, *J Nucl Med* 18:419–424, 1977.

Tumeh SS: Scintigraphy in the evaluation of arthropathy, *Radiol Clin North Am* 34:215–231, 1996.

2 Evaluation of the Hand Film

Radiographs of the hands are probably the most informative part of any screening series for arthritis. It is suggested that two views be obtained for evaluation: a posteroanterior (PA) view and a Nørgaard view of both hands and wrists (see Chapter 1). The former is excellent for imaging mineralization and soft tissue swelling; the latter is necessary for imaging early erosive changes. Using these two views, a systematic approach to observation should be employed. One must observe (1) the radiographic changes occurring in a specific joint and (2) the distribution of these changes within the hand and wrist to make an accurate diagnosis.

RADIOGRAPHIC CHANGES

The radiographic changes occurring around a specific joint to be evaluated are soft tissue swelling, subluxation and dislocation, mineralization, calcification, joint space narrowing, erosion, and bone production. Each arthropathy has its own characteristic set of changes.

Soft Tissue Swelling

Symmetrical Swelling Around an Involved Joint (Fig. 2-1)

Symmetrical soft tissue swelling around a joint is a manifestation of synovitis. Soft tissue swelling is more readily appreciated with digital radiographic techniques than with film screen systems. Symmetrical swelling is most easily evaluated around the interphalangeal (IP) joints and wrist but can also be appreciated around the metacarpal phalangeal joint with careful evaluation. This type of swelling may be seen in any of the inflammatory arthropathies but is most common in rheumatoid arthritis.

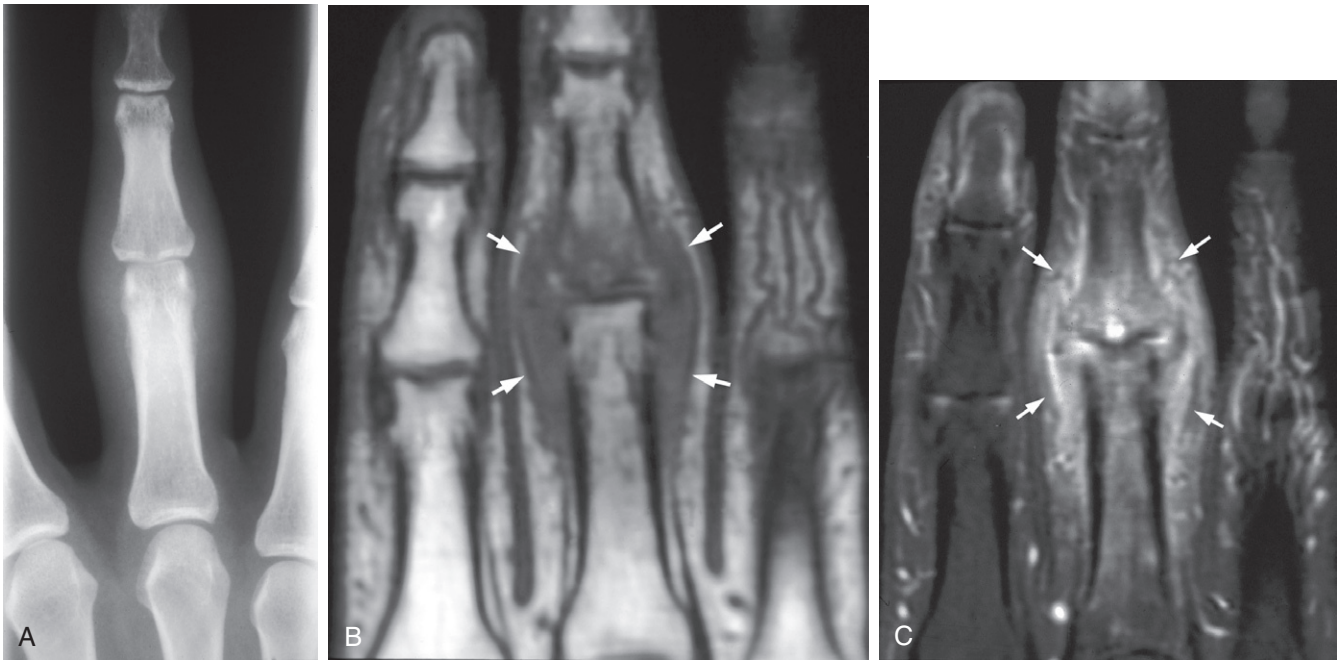

FIGURE 2-1. AP radiograph (**A**), T1-weighted coronal (**B**) and fat-suppressed T2-weighted coronal MR image (**C**) demonstrate symmetrical soft-tissue swelling (*arrows*) around the third PIP joint.

Asymmetrical Swelling Around an Involved Joint (Fig. 2-2)

Asymmetrical swelling may not be actual soft tissue swelling, but rather soft tissue asymmetry due to subluxation or an osteophyte. The osteophyte may have a nonopaque cartilage cap that distorts the soft tissue. This swelling is seen in osteoarthritis and erosive osteoarthritis. Such swellings around the distal interphalangeal (DIP) joints are called Heberden nodes and around the proximal interphalangeal (PIP) joints are called Bouchard nodes.

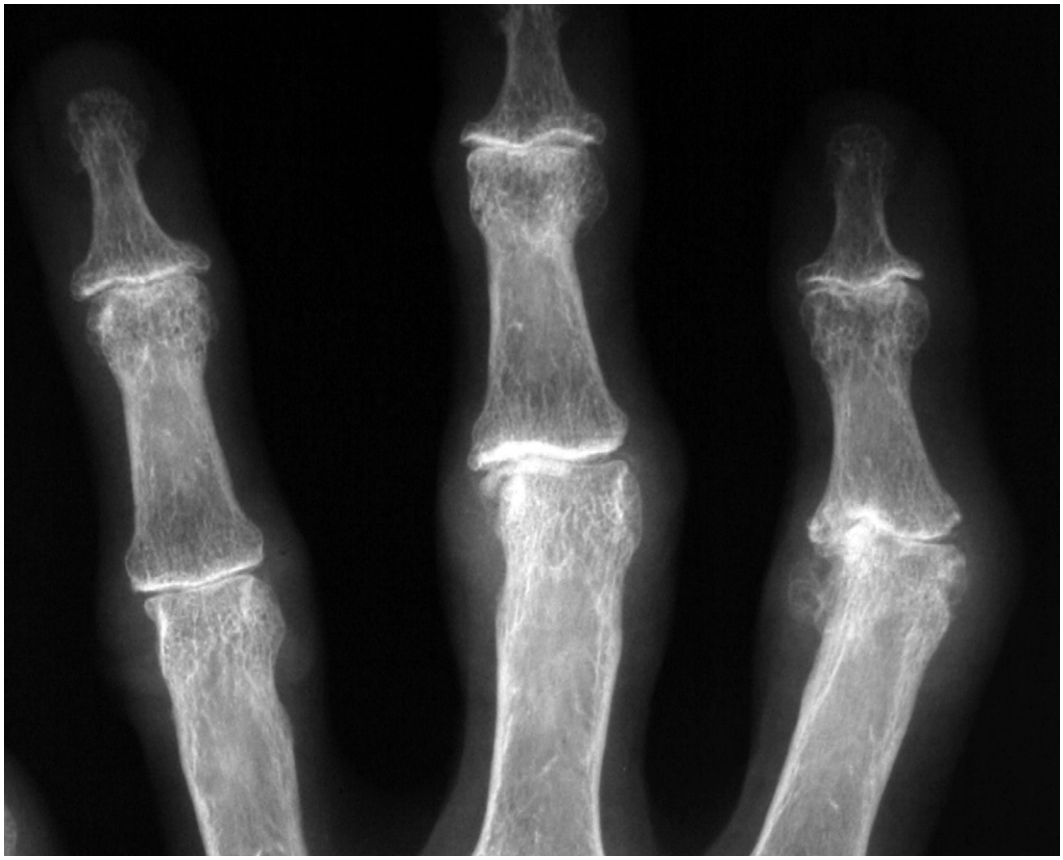

FIGURE 2-2. Distortion of the soft tissue secondary to subluxation and osteophytes in the second and third PIP joints of a patient with osteoarthritis.

Diffuse Fusiform Swelling of an Entire Digit (Fig. 2-3)

This swollen digit is reminiscent of a sausage or a cocktail hot dog. This type of swelling is seen commonly in psoriatic and reactive arthritis when it involves the hands or feet. The cause of this pattern of soft tissue swelling is not clear but may be related to either enthesopathy or flexor tenosynovitis.

FIGURE 2-3. Swollen digit resembling a sausage in psoriatic arthritis.

Lumpy, Bumpy Soft Tissue Swelling (Fig. 2-4)

Lumpy soft tissue swelling is produced by infiltration with a substance foreign to the normal tissues around the joint (i.e., urate crystals, xanthomatous tissue, or amyloid). An eccentric bump may be observed near or away from the joint. Such a swelling is most commonly seen in gout and rarely in xanthomatous or amyloid disease. Granulomatous involvement of the hand with sarcoid can also be associated with a soft tissue bump.

FIGURE 2-4. Soft tissue masses distributed asymmetrically around the proximal and distal interphalangeal joint of the second digit in patient with gout.

Subluxation

Subluxations may not be visualized on the PA view of the hands and wrists, because the technician will reduce any subluxation during positioning. Subluxations become apparent on the Nørgaard view, because the fingers are not supported in a fixed position. Subluxation is a prominent feature of rheumatoid arthritis and the arthritis of lupus. The proximal phalanges sublux in an ulnar and palmar direction in relationship to the adjacent metacarpals (Fig. 2-5). One can distinguish the arthritis of lupus from rheumatoid arthritis in that erosive disease is not present in the former. Subluxations do occur in osteoarthritis. These are usually in a lateral direction, deviating either radially or ulnarly (Fig. 2-6).

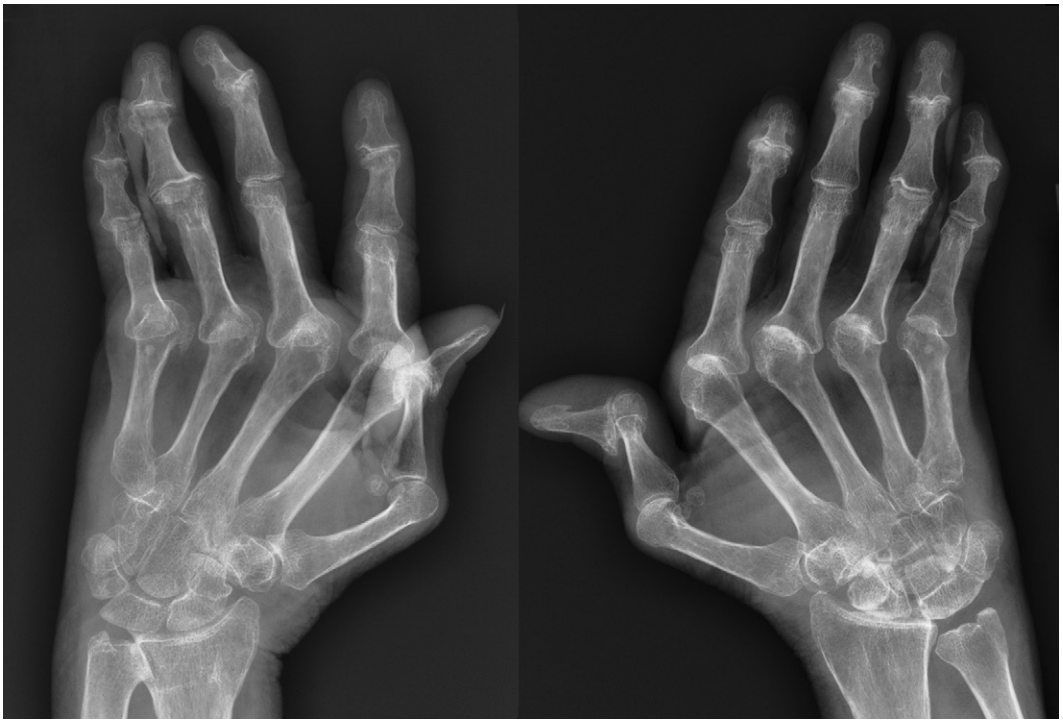

FIGURE 2-5. Subluxations of the proximal phalanges in an ulnar and palmar direction in relationship to the adjacent metacarpals in lupus arthritis. Ulnar subluxation of carpals.

FIGURE 2-6. Lateral subluxation of the middle phalanx in relationship to the proximal phalanx of the third digit in erosive osteoarthritis.

Mineralization

Overall mineralization is evaluated by observing the metacarpal shaft of the second or the third digit. The sum of the two cortices of the shaft should equal one half the width of the shaft in a normally mineralized digit (Fig. 2-7). The degree of generalized osteoporosis can be accurately judged by the sum of the two cortices in relationship to the width of the shaft (Fig. 2-8).

FIGURE 2-7. Shaft of the third metacarpal demonstrating normal mineralization. At the line drawn on the diaphysis, the sum of the two cortices equals half the width of the shaft.

FIGURE 2-8. Diffuse osteoporosis. At the line drawn on the diaphysis of the third metacarpal, the sum of the two cortices is clearly less than half of the width of the shaft.

Normal Mineralization (see Fig. 2-7)

Normal mineralization is typical of every arthropathy except rheumatoid arthritis. The maintenance of normal mineralization helps to distinguish the "rheumatoid variants"—psoriasis, reactive arthritis, and ankylosing spondylitis—from rheumatoid arthritis. The crystalline arthropathies and the osteoarthropathies maintain normal mineralization.

Diffuse Osteoporosis (see Fig. 2-8)

This change is associated only with rheumatoid arthritis. It is seen in the advanced stages of this disease. All other arthropathies tend to maintain normal mineralization. If one observes osteoporosis in a patient with another arthropathy, such as gout, then the generalized osteoporosis may be secondary to disuse, to medication or to the normal aging process. It should not be blamed primarily on the arthropathy.

Juxta-Articular Demineralization (Fig. 2-9)

This change has no objective criteria but is more readily appreciated in bilateral but asymmetric arthropathies. The metaphyseal-epiphyseal part of the digit is always less dense than the diaphysis, for the cortical bone is thinner in the metaphysis and epiphysis. Dramatic differences are easy to see. However, juxta-articular osteoporosis is a nonspecific finding; it is observed in many abnormal conditions, including posttraumatic change. It may be present in any of the arthropathies at any time. Observation of its presence only helps to establish that something is abnormal in the hand.

FIGURE 2-9. Juxta-articular osteoporosis of the Metacarpal Phalangeal joint (MCP) and IP joints of the fourth and fifth digits in patient with rheumatoid arthritis.

Calcification

Soft Tissue Mass Calcification (Fig. 2-10)

The urate crystals of gout are not radiopaque. However, when the urate crystals deposit in the soft tissues to form a tophus, calcium is precipitated with the urate crystals to varying degrees. Therefore the tophus may be just slightly denser than the surrounding soft tissue structure or it may be very densely calcified. In either case, such a tophus is part of the radiographic picture of gout.

FIGURE 2-10. Calcification in a soft tissue mass or tophus surrounding the second, third, and fifth PIP joints. Less dense tophi in the volar soft tissues of the thumb.

Cartilage Calcification (Chondrocalcinosis) (Fig. 2-11)

Calcium pyrophosphate dihydrate crystals deposit in hyaline and fibrous cartilage, producing a radiographic picture of calcified cartilage. When seen in two or more joints (meaning one knee and one wrist, not two knees), the radiographic diagnosis of calcium pyrophosphate dihydrate (CPPD) deposition disease can be made. In the older literature, "chondrocalcinosis" was associated with a long list of diseases. For example, it was listed as a manifestation of gout. However, it is now known that, although urate crystals deposited in soft tissues may precipitate calcium, urate crystals deposited in cartilage will not precipitate calcium. Therefore, a patient with known gout who demonstrates calcification of hyaline or fibrous cartilage must also have deposition of CPPD crystals in the cartilage; thus the patient has both gout and CPPD deposition. The only two diseases known to cause actual deposition of CPPD crystals in cartilage, other than idiopathic CPPD crystal deposition disease, are hyperparathyroidism and hemochromatosis.

FIGURE 2-11. Calcification in the triangular fibrocartilage of the wrist (*arrow*).

Tendinous and Soft Tissue Calcification (Fig. 2-12)

Hydroxyapatite crystals deposit in tendons and bursae, producing the classic tendinitis or bursitis of the shoulder. The second most common location for this deposition is over the greater trochanter. It can also cause a problem around the elbow or the wrist. Hydroxyapatite is also known to deposit in soft tissues in various systemic diseases, such as scleroderma, dermatomyositis, and renal osteodystrophy. However, patients have presented recently with hydroxyapatite deposition in numerous tendinous and soft tissue sites without an underlying systemic disease. Associated with this deposition, one can see erosive changes of the small joints of the hands adjacent to the concretion (Fig. 2-13). This disease entity has become known as hydroxyapatite deposition disease.

FIGURE 2-12. Hydroxyapatite deposition into a tendon.

FIGURE 2-13. Hydroxyapatite deposition into soft tissues surrounding PIP joints with erosive changes of the joints in a patient with hydroxyapatite deposition disease. *(Courtesy of Dr. M. K. Dalinka, Hospital of the University of Pennsylvania, Philadelphia.)*

Joint Space Narrowing

Maintenance of Joint Space

Although urate crystals may deposit within the cartilage of a joint and cause secondary loss of the joint space, gout is one of the few arthropathies that can cause significant changes around the joint while maintaining the joint space itself. A tophus deposited on the extensor aspect of a joint may cause significant erosive change of the dorsal aspect of the joint while preserving the flexor aspect (Fig. 2-14). Radiographically one may observe extensive erosion with a ghost of a joint space imaging through the erosion. In the rare instance of pigmented villonodular synovitis (PVNS) involving the wrist, the involved joint will usually be maintained.

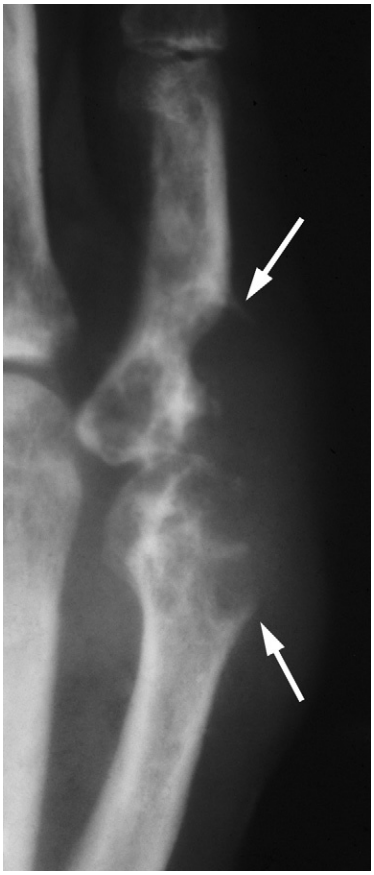

FIGURE 2-14. Extensive erosion of the dorsal aspect of the MCP joint, sparing the volar aspect of the joint. Erosive changes extend a considerable distance from the joint. Note sclerotic borders to erosions and the overhanging edge of cortex (*arrows*). The changes are typical of gout.

Uniform Narrowing (Fig. 2-15)

All of the arthropathies except for osteoarthritis produce uniform narrowing of the joint space. This includes the inflammatory arthropathies that erode the cartilage and all other arthropathies that deposit extra substance into the cartilage (i.e., the crystalline arthropathies, acromegaly, and Wilson disease).

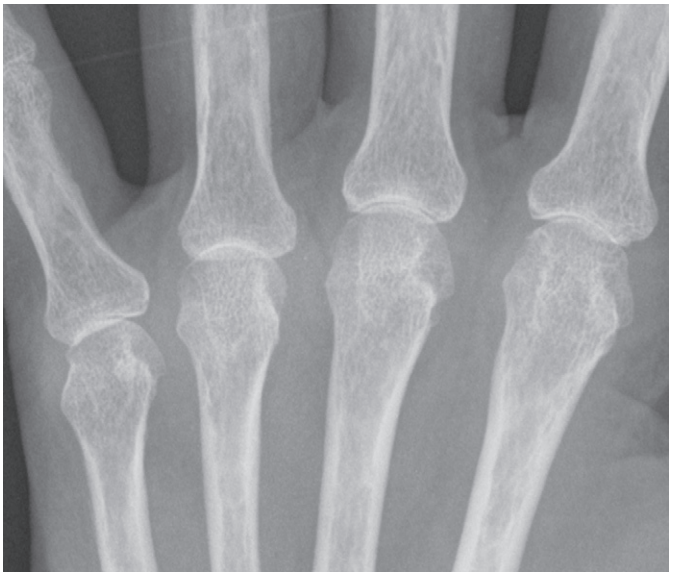

FIGURE 2-15. Uniform narrowing of the MCP joints in rheumatoid arthritis. Note also soft tissue swelling and erosion.

Nonuniform Narrowing (Fig. 2-16)

Nonuniform narrowing of the joint space is typical of osteoarthritis and erosive osteoarthritis.

FIGURE 2-16. Nonuniform narrowing of the PIP and DIP joints in patient with osteoarthritis.

Erosion

Aggressive Erosions

Aggressive erosions are actively changing while the radiograph is being taken. They have no sclerotic borders or evidence of reparative bone. In the inflammatory arthritides, early erosions are seen in the "bare" areas of bone. The bare area is located within the joint, between the edge of the articular cartilage and the attachment of the synovium. The very first radiographic change is a disruption of the white cortical line in the bare area, giving a "dot-dash" appearance (Fig. 2-17). These early erosions are best seen in the metacarpal heads or on the Nørgaard view at the base of the proximal phalanges on the radial side (Fig. 2-18). As these erosions progress, they involve more and more of the joint, ignoring the original barrier of cartilage (Fig. 2-19). Eventually the entire joint may be destroyed. The end of the proximal bone may be eroded in such a fashion as to appear whittled or pointed, while the end of the adjacent distal bone becomes splayed or cup-like (Fig. 2-20). This type of erosion has been called a "pencil-in-cup" deformity and is most commonly seen in patients with psoriatic arthritis.

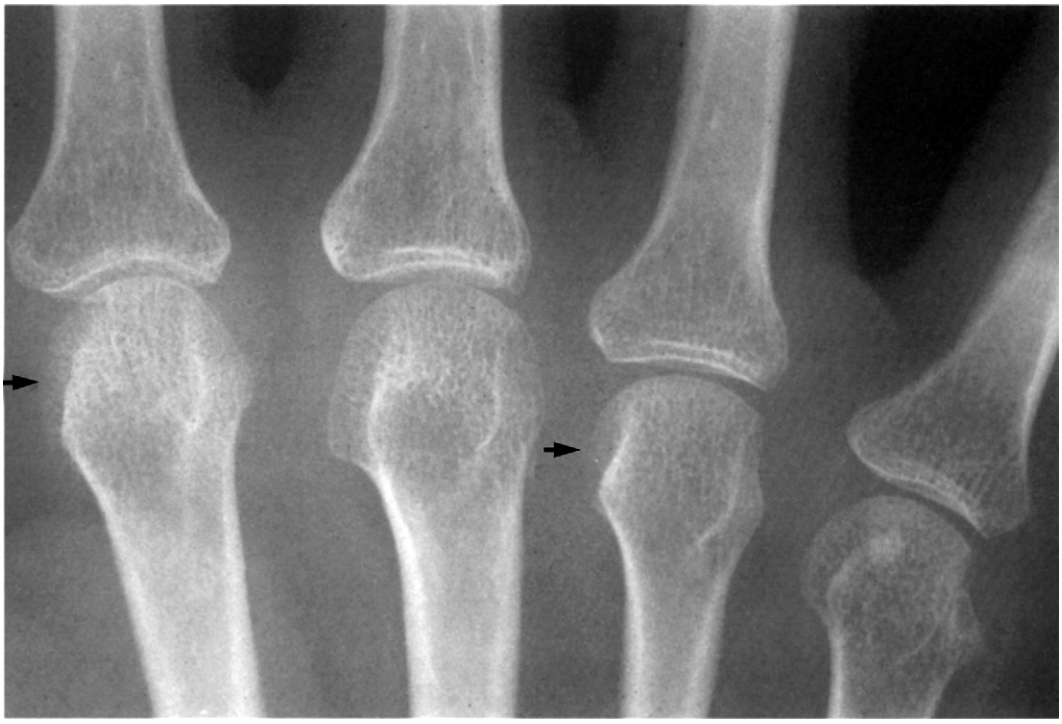

FIGURE 2-17. Disruption of the white cortical line on the radial aspect of the heads of the second and fourth metacarpals (*arrows*). These are early aggressive erosions in the bare areas of the metacarpal head in rheumatoid arthritis.

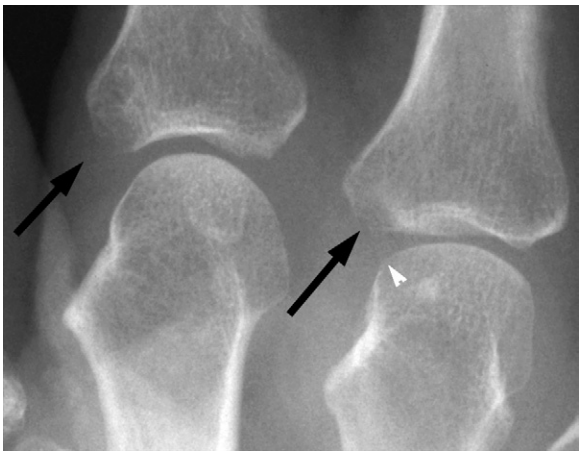

FIGURE 2-18. Erosion of the bases of the proximal phalanges on the radial aspect in a patient with rheumatoid arthritis (*arrows*). There is also adjacent erosion of the metacarpal head (*arrowhead*).

FIGURE 2-19. Extensive erosion of the MCP joints in a patient with rheumatoid arthritis.

FIGURE 2-20. "Pencil-in-cup" erosive change of the IP joint of the thumb in patient with psoriatic arthritis.

Nonaggressive Erosions

Nonaggressive erosions have a fine sclerotic border outlining the edge of the erosion. In the case of the inflammatory arthritides, this is a sign that repair has occurred or that the disease is in remission (Fig. 2-21). In other arthropathies it indicates the indolence of the erosion (Fig. 2-22). It is most commonly seen in gout. Such an erosion is caused by an adjacent tophus. The bone changes caused by the tophus occur extremely slowly and at such a rate that the bone has time to respond and repair.

FIGURE 2-21. Sclerotic border to an erosion at the base of the middle phalanx of the PIP joint in patient with rheumatoid arthritis in remission (*arrow*).

FIGURE 2-22. Large erosions with sclerotic borders involving the MCP joint of the fifth digit in gout. Overhanging edge of the cortex is evident (*arrow*). *(From Brower AC: The radiologic approach to arthritis,* Med Clin North Am *68:1593, 1984; reprinted by permission.)*

Location

The location of the erosion within a specific joint is important in distinguishing one arthropathy from another. The erosions of an inflammatory arthropathy occur at the margins of the joint. The erosions of erosive osteoarthritis tend to occur in the central portion of the joint. In diagnosing DIP joint disease, the erosive pattern is all-important. The marginal erosions of psoriasis have been compared to mouse ears (Fig. 2-23), and the central erosion of erosive osteoarthritis has been compared to a seagull (Fig. 2-24). The erosions of gout may occur away from the joint or on one side of the joint, leaving the rest of the joint intact (see Fig. 2-14).

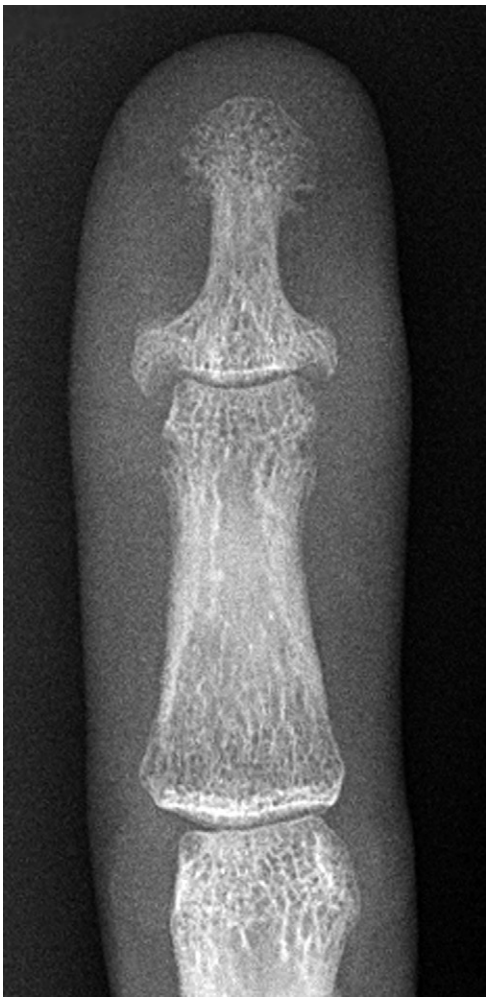

FIGURE 2-23. Marginal erosions resembling mouse ears in the DIP joint of a patient with psoriatic arthritis.

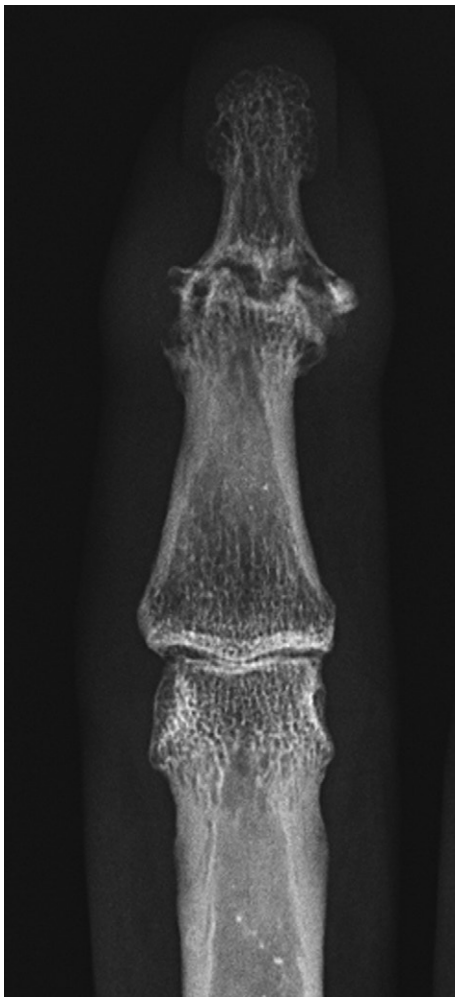

FIGURE 2-24. Central erosion combined with osteophytes to create a seagull appearance in the DIP joint of a patient with erosive osteoarthritis.

Bone Production

There are two different kinds of bone production. One is new bone added in the form of periostitis, enthesitis, or ankylosis. The second form of bone production is a reparative response.

New Bone Production of Enthesopathies

Periosteal New Bone Formation. This is new bone that is deposited along the shaft of the phalanx or in the metaphysis just behind an erosion (Fig. 2-25). Initially this response is exuberant and fluffy in appearance, but with time it becomes incorporated into the parent bone as solid bone formation (Fig. 2-26). This may lead to the appearance of a widened phalanx. This type of new bone formation is characteristic of psoriatic arthritis and of reactive arthritis when it involves the hand. It is a feature that distinguishes the spondyloarthropathies from rheumatoid arthritis.

FIGURE 2-25. Periosteal reaction along the shaft of the proximal phalanx (*arrows*) and new bone formation (*arrowhead*) behind erosive changes involving the PIP joint in a patient with psoriatic arthritis.

FIGURE 2-26. Solid periosteal new bone formation along the shafts of the second and third proximal phalanges in a patient with psoriatic arthritis.

Bone Formed at Tendinous Insertions. New bone can be formed at any tendinous or ligamentous insertion and is associated with the spondyloarthropathies. Again, this distinguishes the spondyloarthropathies from rheumatoid arthritis.

Bone Ankylosis. This is bony bridging of a joint and is seen only in arthropathies that aggressively destroy the cartilage of the joint. It is therefore seen primarily in the inflammatory arthropathies. In rheumatoid arthritis, bone ankylosis will occur in the carpal area but will not occur distal to the carpal area. In the spondyloarthropathies, bone ankylosis will occur not only in the carpals but also in the IP joints. This is another distinguishing feature in separating the spondyloarthropathies from rheumatoid arthritis. Bone ankylosis will occur in erosive osteoarthritis, because of its inflammatory component, but not in primary osteoarthritis (Fig. 2-27). Bone ankylosis is not a feature of the crystalline arthropathies.

FIGURE 2-27. Bone ankylosis of the fourth DIP joint in a patient with erosive osteoarthritis.

Reparative Response

Overhanging Edge of Cortex. This is a characteristic of a chronic, indolent type of erosion and therefore is seen most commonly in gout. As the underlying bone is remodeled by the adjacent tophus, it may elevate the adjacent periosteum. Bone formation induced by the periosteum will produce an appearance of an elevated or overhanging edge (see Figs. 2-14 and 2-22). This characteristic is seen in at least 40 percent of the erosions produced in gout.

Subchondral Bone (Fig. 2-28). This is reparative bone laid down just beneath the white cortical line. It occurs with degeneration or slow loss of cartilage and is a hallmark of osteoarthritis. However, it is also a feature of the crystalline arthropathies or any arthropathy in which a substance is deposited in the cartilage and secondary loss occurs. This type of bone production is not seen in the inflammatory arthropathies unless the disease is in a state of remission.

Osteophytes (see Figs. 2-2, 2-6, and 2-16). Osteophytes are bone extensions of a normal articular surface. They occur where the adjacent cartilage has undergone degeneration and subsequent loss. On the lateral radiograph, the osteophytes at the articular surfaces of the phalanges extend toward the body (Fig. 2-29). Osteophytes formed on metacarpal heads extend in a palmar direction and, on the PA view, resemble hooks (Fig. 2-30). Osteophytes are a hallmark of osteoarthritis; however, they are also a feature of any arthropathy that leads to slow degeneration or loss of cartilage (i.e., the crystalline arthropathies and acromegaly).

FIGURE 2-28. Subchondral sclerosis and joint space narrowing between the trapezium, trapezoid, and distal navicular bones in a patient with osteoarthritis.

FIGURE 2-29. Lateral view of a finger showing osteophytes extending proximally at the DIP and PIP joints in a patient with osteoarthritis.

FIGURE 2-30. "Hook," or osteophyte, on the metacarpal heads in a patient with CPPD crystal deposition disease.

DISTRIBUTION

Having evaluated the radiographic changes surrounding a specific joint, one must examine the distribution within the hand and wrist.

Digit Involvement

Outlined here is the characteristic distribution within the digits.

- **I.** DIP and PIP involvement
  - **A.** Osteoarthritis—osteophytes without erosions
  - **B.** Erosive osteoarthritis—osteophytes and erosion
  - **C.** Psoriatic arthritis—erosion without osteophytes
- **II.** MCP and PIP involvement
  - **A.** Rheumatoid arthritis—erosions without new bone formation; spares the DIPs
  - **B.** Psoriatic arthritis, reactive arthritis, ankylosing spondylitis—erosions and new bone formation; will involve DIPs
- **III.** MCP involvement
  - **A.** Inflammatory arthropathies—erosions
  - **B.** CPPD—osteophytes
- **IV.** Random involvement
  - **A.** Gout

Carpal Involvement

The distribution of radiographic changes in the wrist is also important in separating the arthropathies. The wrist is divided anatomically into specific compartments (Fig. 2-31), each of which is affected by different arthropathies. The inflammatory arthropathies involve all compartments, causing erosions and joint space loss uniformly throughout the wrist (Fig. 2-32). New bone formation distinguishes the spondyloarthropathies from rheumatoid arthritis.

Osteoarthritis and erosive osteoarthritis involve only the first carpometacarpal joint and the first metacarpal carpal (basal) joint (see Fig. 2-28). The presence of erosion differentiates one from the other. If osteoarthritic changes are present in the wrist in some other distribution, then one must consider an etiology other than primary osteoarthritis. Wrist osteoarthritis often may be posttraumatic (Fig. 2-33).

CPPD involves the radiocarpal compartment and often extends in a stairstep pattern to involve the capitate-lunate joint (Fig. 2-34). The changes in this distribution are those of osteoarthritis. Gout has a predilection for the carpometacarpal compartment, producing punched-out erosions with sclerotic borders (Fig. 2-35).

FIGURE 2-31. Normal wrist with outline of the different compartments: (**1**) the radiocarpal compartment, (**2**) the midcarpal compartment, (**3**) the common carpometacarpal compartment, and (**4**) the first carpometacarpal compartment. *(From Brower AC: The radiologic approach to arthritis,* Med Clin North Am *68:1593, 1984; reprinted by permission.)*

FIGURE 2-32. Pancarpal loss of joint spaces in a patient with rheumatoid arthritis.

FIGURE 2-33. Narrowing of the radiocarpal joints with subchondral sclerosis involving the radius and lunate in a posttraumatic osteoarthritis. There is an old fracture of the radial styloid.

FIGURE 2-34. Narrowing of the radionavicular joint and the capitate-lunate joint with subchondral sclerosis surrounding these articulations in a patient with CPPD crystal deposition disease.

FIGURE 2-35. Erosive changes with sclerotic borders involving the third and fourth carpometacarpal joint spaces in a patient with gout.

COMMON ARTHROPATHIES OF THE HAND—A RADIOGRAPHIC SUMMARY

Seven radiographs are presented here (Figs. 2-36 to 2-42) illustrating the common arthropathies involving the hand and summarizing all the individual features discussed in this chapter.

FIGURE 2-36. Early rheumatoid arthritis.

Soft tissue change:	Symmetrical swelling around MCP joints and wrist
Subluxations:	None
Mineralization:	Juxta-articular osteoporosis
Calcification:	None
Joint spaces:	Maintained
Erosions:	Early aggressive (arrows)
Bone production:	None
Distribution:	PIPs, MCPs, and pancarpal

FIGURE 2-37. Late rheumatoid arthritis.

Soft tissue change:	Atrophy
Subluxations:	MCP joints (proximal phalanges subluxed ulnarly and palmarly)
Mineralization:	Diffuse osteoporosis
Calcification:	None
Joint spaces:	Uniform loss—PIPs, MCPs, and pancarpal
Erosions:	Large aggressive
Bone production:	None
Distribution:	PIPs, MCPs, and pancarpal

FIGURE 2-38. Psoriasis.

Soft tissue change:	Fusiform digit swelling—first, second, and fourth digits
Subluxations:	None
Mineralization:	Normal
Calcification:	None
Joint spaces:	Destroyed fourth DIP, first MCP-IP, and second DIP
Erosions:	Large, aggressive; pencil-in-cup erosion of fourth DIP and IP joint of thumb
Bone production:	Solid periosteal new bone formation fourth and fifth proximal phalanges (*arrows*); fluffy new bone around thumb
Distribution:	MCPs, PIPs, and DIPs, but in a 1st, 2nd and 4th ray distribution. The 3rd and 5th ray are minimally involved.

FIGURE 2-39. Osteoarthritis.

Soft tissue change:	Distortion around DIPs
Subluxations:	Laterally at second DIPs
Mineralization:	Normal
Calcification:	None
Joint spaces:	Nonuniform loss—best seen at second DIPs
Erosions:	None
Bone production:	Osteophytes at DIPs and PIPs; subchondral sclerosis—greater multangular, distal navicular, and base of first metacarpal
Distribution:	DIPs, PIPs; first carpometacarpal joint and greater multangular-navicular joint

FIGURE 2-40. Erosive osteoarthritis.

Soft tissue change:	Swelling at the third and fourth PIPs
Subluxations:	Laterally at third and fourth PIPs
Mineralization:	Normal
Calcification:	None
Joint spaces:	Nonuniform loss—best seen at third PIP and first IP
Erosions:	Central erosions—combined with osteophytes to produce "seagull" appearance
Bone production:	Osteophytes at PIPs, DIPs, first carpometacarpal joint and greater multangular-navicular joint; subchondral sclerosis at second to fourth DIPs, PIPs and IP joint of thumb; ankylosis fifth DIP
Distribution:	PIPs and DIP; first carpometacarpal and greater multangular-navicular joint

FIGURE 2-41. CPPD crystal deposition disease.

Soft tissue change:	None
Subluxations:	None
Mineralization:	Normal
Calcification:	Triangular cartilage (fibrous cartilage); between lunate and triquetrum (hyaline cartilage) (*arrows*)
Joint spaces:	Uniform loss of second through fourth MCPs, radiocarpal, and capitate-lunate
Erosions:	None
Bone production:	Osteophytes at MCP joints; subchondral sclerosis in navicular, capitate, lunate
Distribution:	MCPs, 1st metacarpal-carpal joint, radionavicular joint, and capitate-lunate joints

FIGURE 2-42. Gout.

Soft tissue change:	Soft tissue mass around second and fifth DIP, ulnar styloid
Subluxations:	Laterally at thumb IP joint
Mineralization:	Normal
Calcification:	In soft tissue masses—best seen at ulnar styloid
Joint spaces:	Maintained; loss at second through fifth MCPs, PIPs; nonuniform loss at first IP; destruction of 2nd and 5th DIPs
Erosions:	Nonaggressive; second and fifth DIP, second PIP (*arrow*), third and fourth intercarpal joint, scapholunate joint, ulnar styloid
Bone production:	Overhanging edge of cortex—second and fifth DIP joint
Distribution:	Carpometacarpal and scapholunate joint; randomly throughout fingers—second and fifth DIPs

SUGGESTED READINGS

Bonavita JA, Dalinka MK, Schumacher HR: Hydroxyapatite deposition disease, *Radiology* 134:621–625, 1980.

Brower AC: The radiologic approach to arthritis, *Med Clin North Am* 68:1593–1607, 1984.

Kidd KL, Peter JB: Erosive osteoarthritis, *Radiology* 86:640–647, 1966.

Levine RB, Edeiken J: Arthritis: A radiologic approach, *Appl Radiol* (July/Aug) 55, 1985.

Martel W: The overhanging margin of bone: A roentgenologic manifestation of gout, *Radiology* 91:755–756, 1968.

Martel W: Diagnostic radiology in the rheumatic diseases. In Kelley WN, Harris Jr ED, Ruddy S, et al, editors: *Textbook of rheumatology*, ed 4, Philadelphia, 1993, W.B. Saunders.

Martel W, Stuck KJ, Dworin AM, Hylland RG: Erosive osteoarthritis and psoriatic arthritis: A radiologic comparison in the hand, wrist, and foot, *AJR Am J Roentgenol* 134:125–135, 1980.

Martel W, Hayes JT, Duff IF: The pattern of bone erosion in the hand and wrist in rheumatoid arthritis, *Radiology* 84:204–214, 1965.

Nørgaard F: Earliest roentgenological changes in polyarthritis of the rheumatoid type: Rheumatoid arthritis, *Radiology* 85:325–329, 1965.

Peter JB, Pearson CM, Marmar L: Erosive osteoarthritis of the hands, *Arthritis Rheum* 9:365–388, 1966.

Peterson CC, Silbiger ML: Reiter's syndrome and psoriatic arthritis: Their roentgen spectra and some interesting similarities, *Am J Roentgenol Radium Ther Nucl Med* 101:860–871, 1967.

Resnick CS, Resnick D: Calcium pyrophosphate dihydrate crystal deposition disease, *Curr Probl Diagn Radiol* 11(6):1–40, 1982.

Resnick D: Rheumatoid arthritis of the wrist: The compartmental approach, *Med Radiogr Photogr* 52:50–88, 1976.

Resnick D: The "target area" approach to articular disorders: A synopsis. In Resnick D, Niwayama G, editors: *Diagnosis of bone and joint disorders with emphasis on articular abnormalities*, Philadelphia, 1995, W.B. Saunders.

Sartoris DJ, Resnick D: Target area approach to arthritis of the small articulations, *Contemp Diag Radiol* 8:1, 1985.

3 *Approach to the Foot*

A systematic assessment of foot radiographs for the manifestations of arthropathies is important, because the foot may be an early site of involvement in a systemic arthropathy such as rheumatoid arthritis, or it may be the only site of involvement in arthropathies such as gout or reactive arthritis. The foot, however, can be difficult to evaluate radiographically. Arches are present in the long and short axes of the foot that make assessment of articulations in more than one plane difficult. The wedge shape of the foot does not permit uniform exposure of the foot on a single radiograph. The hindfoot articulations are complex and often require either computed tomography (CT) or magnetic resonance (MR) imaging for accurate evaluation.

A screening study of the foot should include anteroposterior (AP), lateral, and oblique radiographs. The AP radiograph of the foot permits evaluation of the interphalangeal (IP), metatarsophalangeal (MTP), and the first and second metatarsal-tarsal (MTT) joints. The oblique radiograph is necessary to observe abnormalities of the third through fifth MTT joints, the midfoot, and any early erosive changes on the lateral aspect of the fifth metatarsal. The oblique radiograph also permits evaluation of the lateral sesamoid at the first MTP joint. The lateral radiograph provides orthogonal assessment of the forefoot articulations, the mid- and hindfoot articulations, and the calcaneus. On rare occasions, a sesamoid view may be necessary to observe the sesamoidal articulation with the first metatarsal head.

Successful assessment of the foot depends on systematically observing changes in four separate anatomic compartments: (1) the forefoot articulations (MTP, sesamoid-MTP, and IP joints), (2) the MTT joints, (3) the mid- and hindfoot articulations (tarsal joints), and (4) the ligamentous insertions about the calcaneus. As in the hand, the following radiographic changes should be assessed: soft tissue swelling, soft tissue calcification, bony mineralization, joint space narrowing, erosion, subluxation and dislocation, and bone production.

FOREFOOT

Arthropathies involving the IP joints and the MTP joints of the forefoot follow the same principles outlined in the chapter on the assessment of the hand. The sesamoid bones of the first MTP joint have a synovium-lined articulation with the plantar aspect of the first metatarsal head and, if involved, will demonstrate the manifestations of any of the arthropathies of the foot. This articulation should not be forgotten when assessing foot radiographs.

Soft Tissue Swelling

Symmetrical Swelling Around a Joint (Fig. 3-1)

Symmetrical swelling about a joint is a manifestation of synovial proliferation, effusion, and periarticular soft tissue edema associated with inflammatory arthropathies. Soft tissue swelling is easier to appreciate with digital radiographic techniques than with a film screen system.

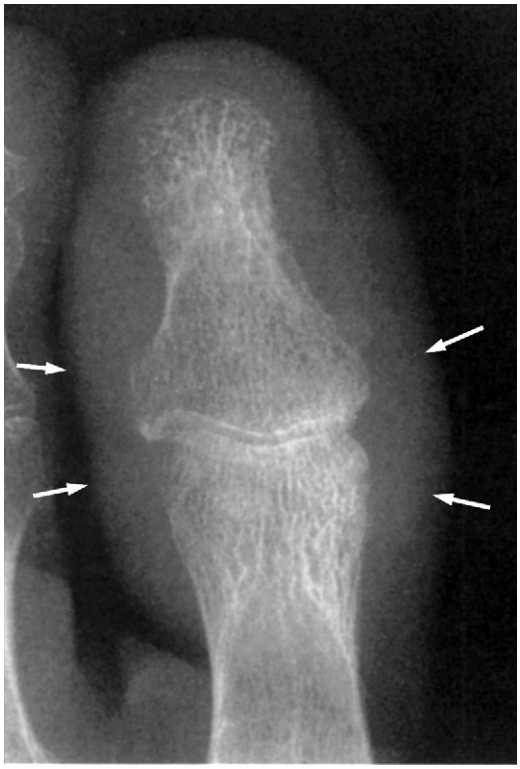

FIGURE 3-1. Symmetrical swelling (*arrows*) of soft tissues around the first IP joint in inflammatory arthritis.

Fusiform Swelling of an Entire Digit (Fig. 3-2)

The diffuse swelling of a digit resulting in a "sausage" or "cocktail hot dog" appearance is a manifestation of the spondyloarthropathies, trauma, and infection.

FIGURE 3-2. Diffuse soft tissue swelling of the second digit giving a "sausage" appearance in a patient with psoriatic arthritis.

Lumpy, Bumpy Soft Tissue Swelling (Fig. 3-3)

Soft tissue masses located eccentrically about a joint associated with cortical erosions are findings most commonly associated with gout, although these changes can be seen with amyloid, xanthomas, and sarcoid.

FIGURE 3-3. Corticated erosion (*arrowheads*) at the medial aspect of the first metatarsal head, lateral aspect of the second metatarsal head and destruction fifth IP joint with associated soft tissue masses (*arrows*) in patient with gout.

Soft Tissue Calcification

Mass (Fig. 3-4)

Gouty tophi may or may not contain varying amounts of calcium. Regardless of calcium content, gouty tophi are more radiopaque than the surrounding soft tissues.

FIGURE 3-4. Faintly calcified soft tissue mass overlying well-corticated erosions (*arrows*) on the medial aspect of the first MTP joint in patient with gout.

Tendinous or Ligamentous and Soft Tissue Calcification (Fig. 3-5)

Idiopathic hydroxyapatite deposition disease may present as calcification of the tendons of the medial flexor group (flexor hallucis longus, flexor digitorum longus, and posterior tibialis) or around the first MTP joint. Because soft tissue calcifications can be associated with renal osteodystrophy and scleroderma, these diseases must be excluded before diagnosing idiopathic disease.

FIGURE 3-5. Soft tissue calcification (*arrows*) medial to the first MTP joint in idiopathic hydroxyapatite deposition disease. There is no soft tissue mass outside the calcific deposit.

Mineralization

Normal

Generally bone mineralization is maintained in the spondyloarthropathies, thus distinguishing these erosive arthropathies from rheumatoid arthritis.

Juxta-Articular Osteoporosis (Fig. 3-6)

Juxta-articular osteoporosis is a nonspecific finding that can be seen in nonarthropathic conditions. In an arthropathy it is most commonly associated with inflammatory disease. Juxta-articular osteoporosis may be difficult to appreciate when the joints are diffusely involved. Resorption of subcortical bone in the medial aspect of the metatarsal head may be an indication of osteoporosis. Juxta-articular osteoporosis in acute reactive arthritis is the only feature that can radiographically distinguish this disease from psoriatic arthropathy.

DIFFUSE OSTEOPOROSIS

Generalized osteoporosis can be documented by assessing the cortical width in relation to the shaft width of the metatarsal bone. Generalized osteoporosis is usually seen in patients with rheumatoid arthritis.

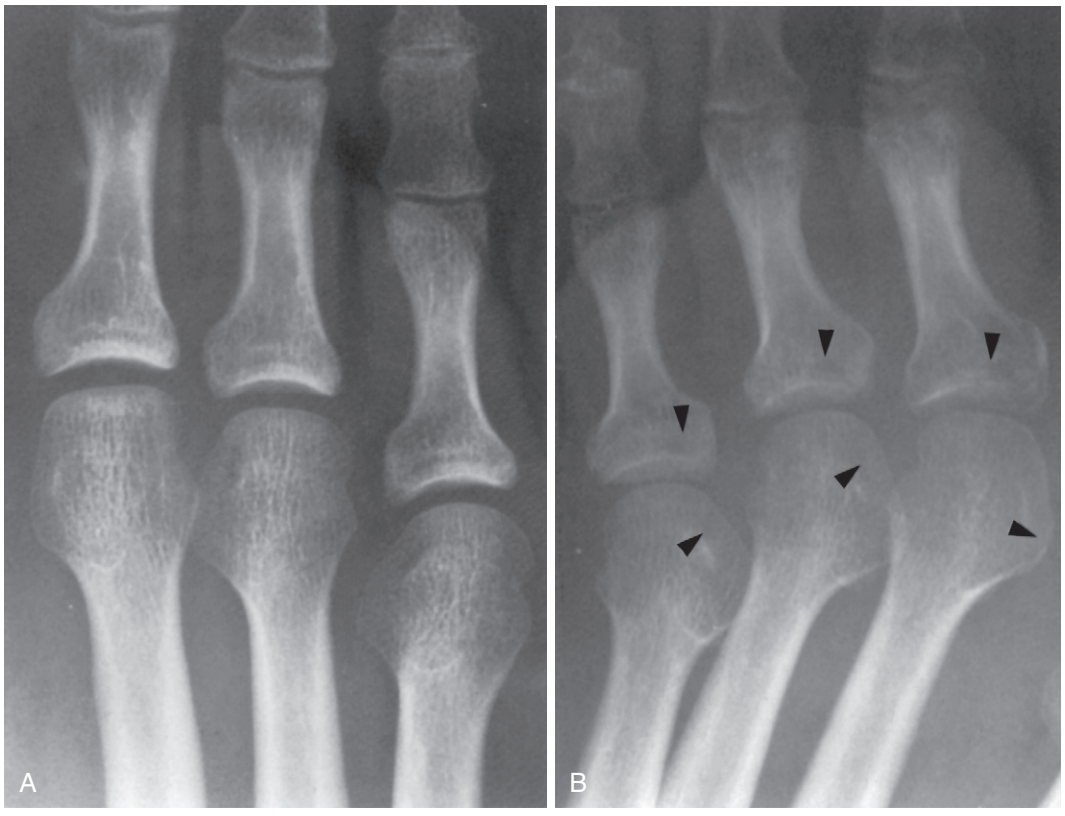

FIGURE 3-6. Juxta-articular osteoporosis in second through fourth MTP joints in right foot (**A**). This is better appreciated when nonaffected joints are available for comparison (**B**). There is loss of subchondral bone (*arrowheads*) when compared to normal in this patient with inflammatory arthritis.

Joint Space Change

Widening of Joint Space (Fig. 3-7)

Widening of a joint is often observed in acromegaly. Sometimes a joint involved by psoriatic arthropathy may appear widened secondary to fibrotic material replacing the joint.

FIGURE 3-7. Widened joints, flaring of phalangeal ends, and new bone formation in patient with acromegaly.

Normal (Fig. 3-8)

The joint space is typically maintained in gout in the face of periarticular well-corticated erosions with overhanging edges produced by tophaceous deposits.

Uniform Narrowing

Uniform joint space narrowing reflects uniform loss of the cartilage and is associated with both inflammatory arthropathies and deposition diseases.

Nonuniform Narrowing

Asymmetrical loss of cartilage is associated with mechanical osteoarthritis. Osteoarthritis is most commonly seen at the first MTP joint.

FIGURE 3-8. Sharply marginated erosions (*arrowheads*) associated with a soft tissue mass affecting the first MTP joint in patient with gout. Notice that the joint space is preserved.

Ankylosis (Fig. 3-9)

Distal IP and PIP joint ankylosis is associated with the spondyloarthropathies. Ankylosis of the MTP joints is rare.

FIGURE 3-9. Erosions and subluxations of MTP joints. Erosions at the first IP joint and ankylosis of the second and fourth DIPs and third and fourth PIPs joints in patient with psoriatic arthropathy.

Erosion

Aggressive Erosions

Aggressive erosions do not have corticated margins and are a manifestation of the inflammatory arthropathies. They tend to occur at the "bare area" of a bone, which is the area between where the synovial lining joins bone and the edge of the articular cartilage. Erosions are best seen on the AP view of the foot, which assesses the IP joints and the medial aspects of the second through fifth metatarsal heads (Fig. 3-10). The lateral aspect of the fifth metatarsal head is the earliest site of erosive disease in rheumatoid arthritis of the foot and is best seen on the oblique view (Fig. 3-11). The "pencil-in-cup" deformity is seen most frequently at the first IP joint and is most commonly associated with psoriatic arthritis, although it is also a manifestation of reactive arthritis (Fig. 3-12). Erosion of the distal tuft (acro-osteolysis) may be seen with reactive arthritis and psoriatic arthropathy (Fig. 3-13). Patients with acro-osteolysis in psoriasis may have nail changes that may be seen radiographically.

FIGURE 3-10. Erosive changes involving third through fifth MTP joints in rheumatoid arthritis. Erosive changes are manifested by loss of the white cortical line (*arrows*) along the medial aspect of the third through fifth metatarsal heads. There are also erosions of the lateral metatarsal heads of the third through fifth toes.

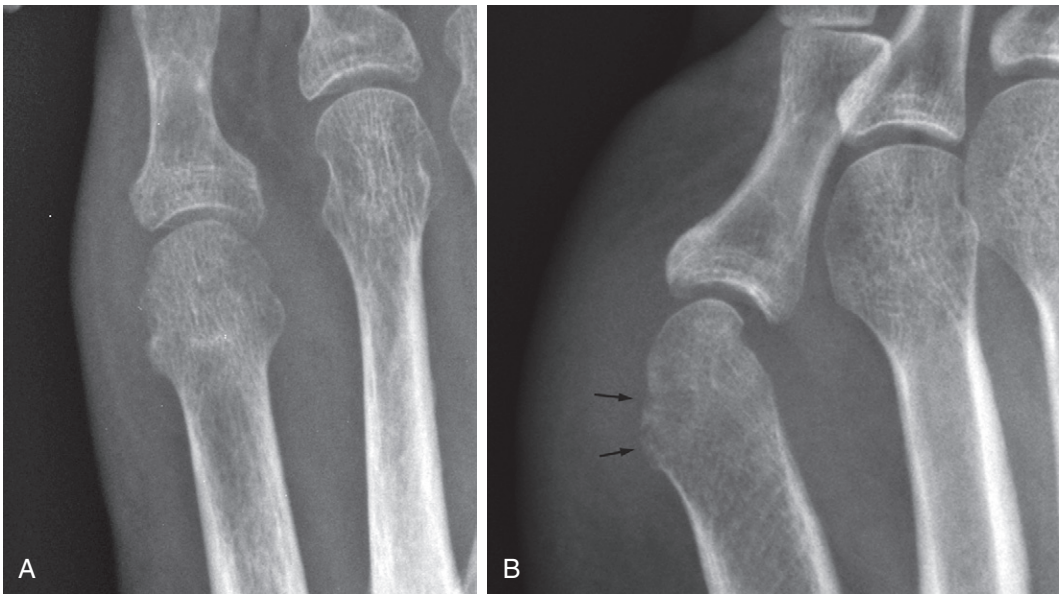

FIGURE 3-11. AP (**A**) and oblique (**B**) view of the foot. Erosion (*arrows*) along the lateral aspect of the fifth metatarsal head best seen in the oblique view of the foot.

FIGURE 3-12. "Pencil-in-cup" appearance of first IP joint in patient with psoriatic arthritis.

FIGURE 3-13. Acro-osteolysis and reparative new bone involving first and second distal phalanges producing increased density of phalanx in psoriatic arthritis.

Nonaggressive Erosions

An erosive process that is indolent will allow a reparative response to occur. This reparative response will be manifested by a sclerotic margin to the erosion. Such an erosion is classically associated with gout. The erosions of gout are most commonly seen at the dorsomedial aspect of first MTP or IP joint and may simulate subchondral cysts in the AP view. Careful evaluation of the oblique view or the lateral view will demonstrate the dorsally located well-corticated erosion with overhanging cortex associated with a soft tissue mass (tophus) (Fig. 3-14). Patients with inflammatory arthropathies whose disease is in remission may also exhibit erosions with sclerotic margins, but these erosions tend to be located along the plantar aspect of the foot (Fig. 3-15). Normally there is loss of joint space accompanying healed inflammatory erosions, whereas there is maintenance of the joint space with the erosions of gout.

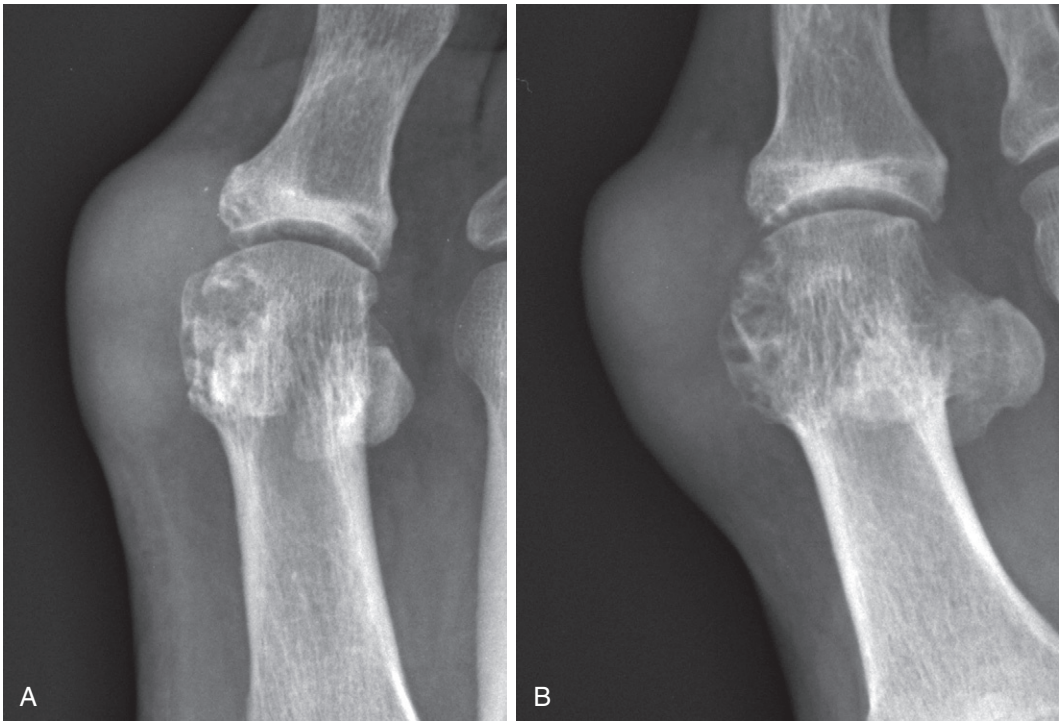

FIGURE 3-14. A, AP radiograph of big toe demonstrates cyst-like lucencies involving first metatarsal head and proximal phalanx. **B,** Oblique radiograph demonstrates that gouty tophus with associated erosion at medial aspect of first metatarsal head is responsible for the lucency seen in first metatarsal head on the AP radiograph.

FIGURE 3-15. Erosions (*arrows*) along plantar aspect of the fifth metatarsal head in patient with rheumatoid arthritis.

Bone Production

There are two different kinds of new bone production. One is in the form of added bone as a periostitis or enthesitis. The second is in the form of a reparative response.

New Bone of Enthesopathies

Periosteal new bone and bone formed at tendinous insertions are associated with the spondyloarthropathies. The periostitis of the spondyloarthropathies tends to be seen along the shafts of the phalanges and the metatarsal bones (Fig. 3-16). Periosteal new bone can also be seen at the base of the fifth metatarsal and along the medial aspect of the tarsal navicular (Fig. 3-17). New bone may be identified at any ligamentous attachment. New bone can also be seen within or just behind an erosion, giving the erosion a "paint brush" appearance (Fig. 3-18).

FIGURE 3-16. Periostitis along shafts of third metatarsal and the second and third proximal phalanges (*short arrows*). Marked juxta-articular osteoporosis, uniform joint space loss, and erosion (*long arrow*) are also seen at the third MTP joint in this patient with reactive arthritis.

FIGURE 3-17. Fluffy periostitis (*arrows*) along medial aspect of the navicular and first cuneiform in psoriatic arthritis. More solid-appearing new bone (*arrowhead*) has been added to the base of the fifth metarsal (MT) and lateral calcaneus.

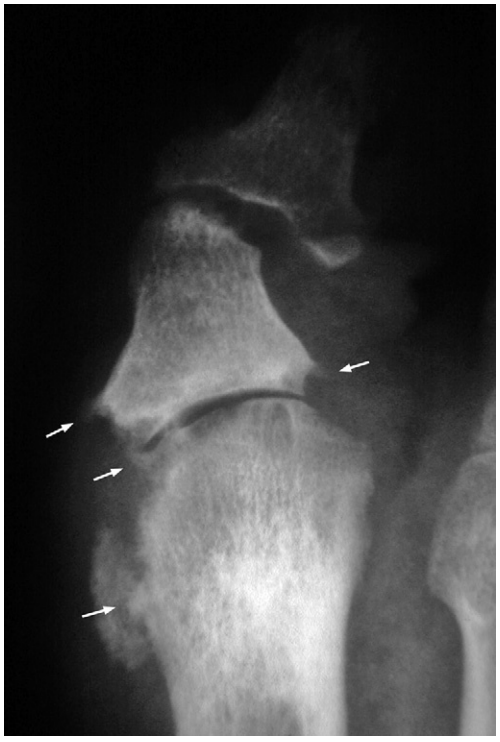

FIGURE 3-18. Erosions with "paint brush" appearance along medial aspect of first MTP joint. There is also new bone formation (*arrows*) at margins of erosions. Notice "pencil-in-cup" appearance of first IP joint in patient with psoriatic arthropathy.

Reparative Response

Overhanging Edge of Cortex. The slow erosive process of a gouty tophus will permit a reparative response and elevation of the cortex, which will manifest as an overhanging edge (Fig. 3-19).

Subchondral Bone. Subchondral sclerosis is reparative bone at the articular surface where the cartilage has been lost. It occurs in mechanical osteoarthritis and deposition arthropathies.

Osteophytes. Osteophytes are a hallmark of osteoarthritis. Primary osteoarthritis most commonly is seen at the first MTP joint. Osteoarthritis of the first MTP joint is usually associated with hallux valgus or hallux rigidus or limitus deformity. Osteophytes at the first MTP joint may

FIGURE 3-19. Well-corticated erosion involving medial aspect of first metatarsal head in patient with gout. Notice overhanging edges at the margins of the erosion (*arrow*).

impede dorsiflexion of the joint (Fig. 3-20). Osteoarthritis involving MTP joints other than the first is unusual, but it may be seen in any MTP joint that becomes the primary weight-bearing joint because of acquired or congenital shortening of the first metatarsal (Fig. 3-21). It can also be seen following avascular necrosis (AVN) of the metatarsal heads or in "burned-out" inflammatory arthritis. Osteoarthritis of IP joints other than the first is unusual and usually asymptomatic when present.

FIGURE 3-20. A, AP radiograph of first MTP in patient with hallux rigidus demonstrates marked joint space narrowing and osteophyte formation. **B,** On the lateral radiograph, a large dorsal osteophyte (*arrow*) mechanically impairs dorsiflexion of the great toe.

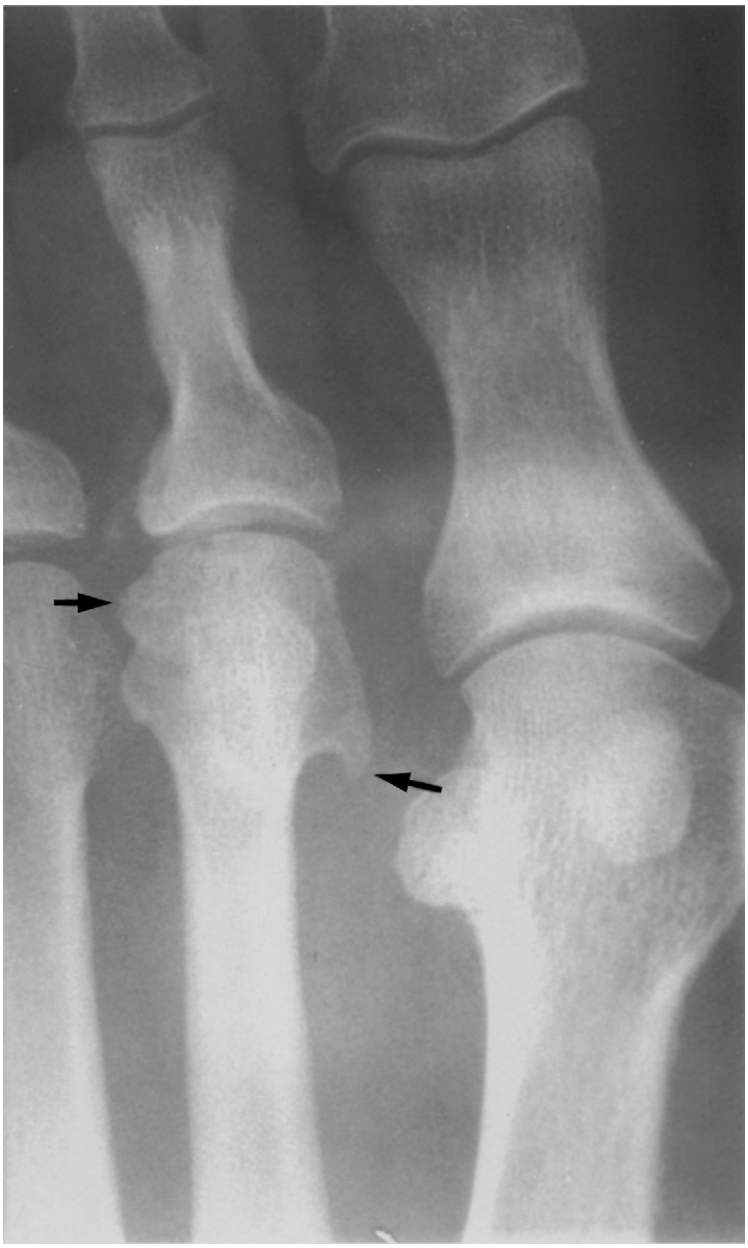

FIGURE 3-21. Osteoarthritis at second MTP joint manifested by subchondral sclerosis, osteophyte formation (*arrows*), and nonuniform joint space loss.

Subluxation

The most common subluxation of the foot occurs at the first MTP joint, where the proximal phalanx subluxes laterally (hallux valgus). Idiopathic hallux valgus usually leads to osteoarthritis of the first MTP joint. Hallux valgus and valgus deformity of the second through fourth MTP joints can be associated with any of the inflammatory arthropathies but is most commonly seen with rheumatoid arthritis (Fig. 3-22). The fifth MTP joint tends to sublux medially. The metatarsal heads tend to sublux in a plantar direction in rheumatoid arthritis. The altered mechanics of weight bearing may result in callus formation over the plantar aspect of the subluxed metatarsal heads. Reducible subluxations, as in the hands, can be seen in systemic lupus erythematosus and after rheumatic fever.

FIGURE 3-22. Severe hallux valgus and second MTP joint subluxation in patient with rheumatoid arthritis.

Distribution of Findings in Toes

Each arthropathy has a particular distribution in the toes. Rheumatoid arthritis is seen in the MTP and PIP joints (Fig. 3-23); the DIP joints are spared. Reactive and psoriatic arthritis have three different patterns of distribution: (1) limited to the DIPs and PIPs (Fig. 3-24), (2) involving a single or several digits at all joints (Fig. 3-25), and (3) similar to that of rheumatoid arthritis (Fig. 3-26). Gout usually involves the MTP and IP of the big toe (Fig. 3-27); when other toes are involved, the involvement is sporadic. Osteoarthritis most commonly involves the first MTP.

FIGURE 3-23. Erosions involving MTPs and first IP joints (*arrows*) and juxta-articular osteoporosis in patient with rheumatoid arthritis.

FIGURE 3-24. Erosive arthropathy limited primarily to IP joints. Notice acro-osteolysis of first and second distal phalanges, reparative new bone at margins of erosions (*arrowheads*), and "pencil-in-cup" appearance of the fifth IP joint in patient with psoriatic arthropathy.

FIGURE 3-25. Marginal erosions associated with reparative new bone limited primarily to the IP and MTP joint of the great toe in patient with psoriatic arthritis.

FIGURE 3-26. Psoriatic arthropathy involving IP and MTP joints. Distal interphalangeal joint involvement, ankylosis, reparative new bone, and normal mineralization differentiate this arthropathy from rheumatoid arthritis.

FIGURE 3-27. Erosions of tophaceous gout in typical distribution of the first MTP and IP joints. Intramedullary calcified tophaceous deposit is responsible for density seen at the IP joint.

METATARSAL-TARSAL JOINT

The arthropathies that involve the MTT joint are (1) rheumatoid arthritis, (2) gout, (3) osteoarthritis, and (4) neuropathic osteoarthropathy.

Rheumatoid arthritis of the MTT joints is common and manifests as symmetrical joint space narrowing and juxta-articular osteoporosis (Fig. 3-28). Erosions tend to be shallow and therefore difficult to appreciate. Soft tissue swelling may be difficult to appreciate, and subluxations that occur in the forefoot are not seen.

Gout usually involves the MTT joints and presents as it does in the first MTP joint. Corticated erosions frequently associated with soft tissue masses will be seen on the dorsal aspect of the MTT joints (Fig. 3-29). Osteoarthritis of the MTT joints most commonly occurs at the first metatarsal-cuneiform joint and presents with joint space narrowing, osteophyte formation, and subchondral sclerosis, typical of osteoarthritis involving other joints (Fig. 3-30). Osteoarthritis can involve the other MTT joints but is less common there and is usually associated with altered mechanics following trauma.

FIGURE 3-28. Marked MTT joint space narrowing, osteoporosis, and ankylosis in patient with rheumatoid arthritis.

FIGURE 3-29. Erosions (*arrowheads*) with sclerotic margins at the MTT joints in gout. The erosions involving the base of the fifth metatarsal are remote from the joint. Mineralized tophus is seen medially (*arrow*).

FIGURE 3-30. Oblique (**A**) and lateral (**B**) views of first MTT joint show large dorsal osteophyte (*arrow*), joint space loss, and subchondral sclerosis of osteoarthritis.

The neuropathic osteoarthropathy of the patient with diabetes most commonly involves the MTT joint. There is often an unsensed Lisfranc fracture-dislocation (Fig. 3-31). The radiographic findings tend to be dramatic and rapid in onset. If the foot is imaged in the acute phase, demonstrating the atrophic type of neuropathic joint with extensive resorption, it may be difficult to exclude infection (Fig. 3-32). Often, however, there is bone marrow edema

FIGURE 3-31. Severe Lisfranc fracture-dislocation in patient with neuropathic osteoarthropathy.

FIGURE 3-32. Extensive resorption of bone in the ankle, hindfoot, and midfoot in this patient with the atrophic form of neuropathic osteoarthropathy. *(Courtesy of Dr. C.S. Resnik, University of Maryland, Baltimore.)*

like changes that are intermediate in signal on T1-weighted images and high in signal on T2-weighted images. If an ulcer is appreciated in the soft tissues adjacent to abnormal bone marrow signal, then osteomyelitis is likely. If the soft tissues are completely intact, the likelihood of osteomyelitis is markedly reduced even in the face of dramatic signal abnormality in juxta-articular bone. Biopsy may be required to resolve the issue. The hypertrophic form of neuropathic osteoarthropathy tends to predominate. In this case, the radiographic findings are (1) dissolution of the joint, (2) sclerosis with osteophyte formation, (3) continued dislocation and subluxation, (4) extensive fractures with debris, and (5) joint distention (Fig. 3-33).

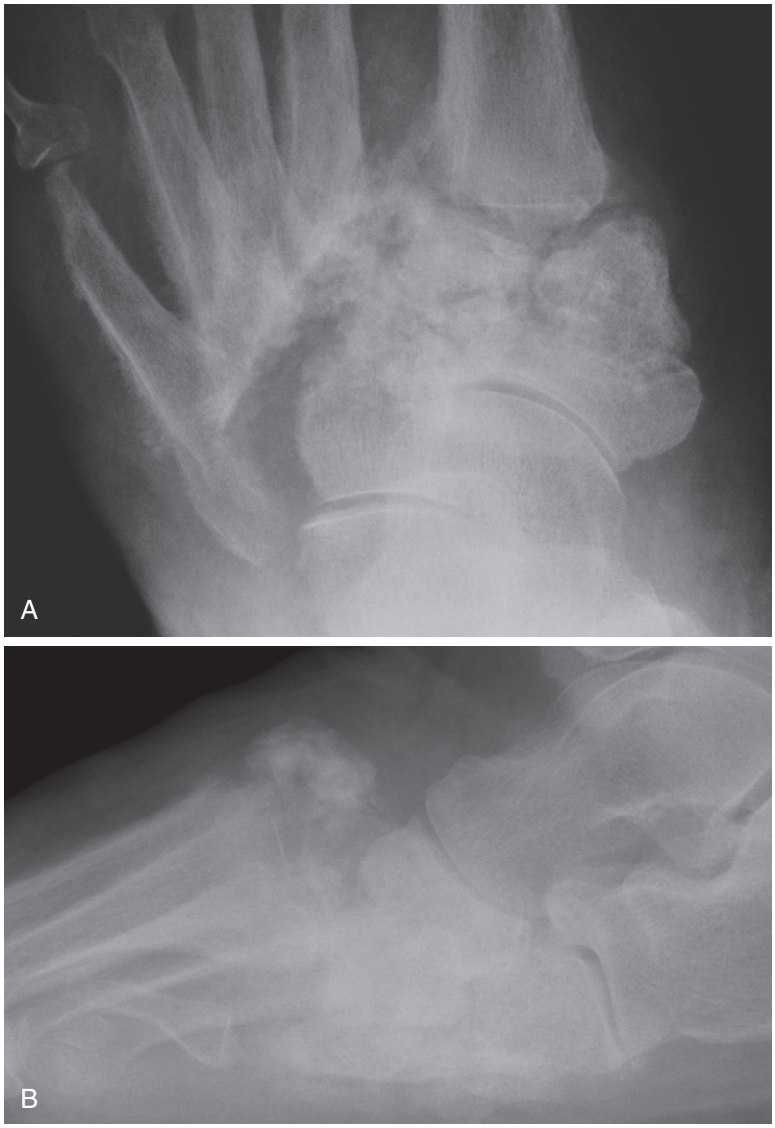

FIGURE 3-33. AP (**A**) and lateral (**B**) radiographs of MTT joints in a hypertrophic neuropathic foot. Notice the disorganization of the MTT and navicular cuneiform joints, with sclerosis, fractures, and debris.

TARSAL JOINTS

The tarsal joints can be the target of many arthritides but tend to have less dramatic radiographic manifestations when compared to the other joints of the foot. The exception is neuropathic osteoarthropathy, which tends to have dramatic findings wherever it presents. The most common arthropathies that involve the tarsal joints are rheumatoid arthritis and osteoarthritis.

Rheumatoid arthritis, as in the MTT joints, presents as bilateral symmetrical joint space narrowing with shallow erosions that are not usually visible. Osteophytes are lacking. Ankylosis of the tarsal joints can be seen (Fig. 3-34) as an unusual manifestation of rheumatoid arthritis. As a correlate to the hand, ankylosis of other joints in the foot is postsurgical.

FIGURE 3-34. Marked MTT joint space narrowing, osteoporosis, and ankylosis of several tarsal bones in rheumatoid arthritis.

Osteoarthritis involving any joint in the mid- and hindfoot is secondary to altered mechanics, most frequently following trauma (Fig. 3-35). The talonavicular joint is the most common hindfoot articulation to be affected by osteoarthritis. Joint space narrowing, subchondral sclerosis, and osteophytes are again seen.

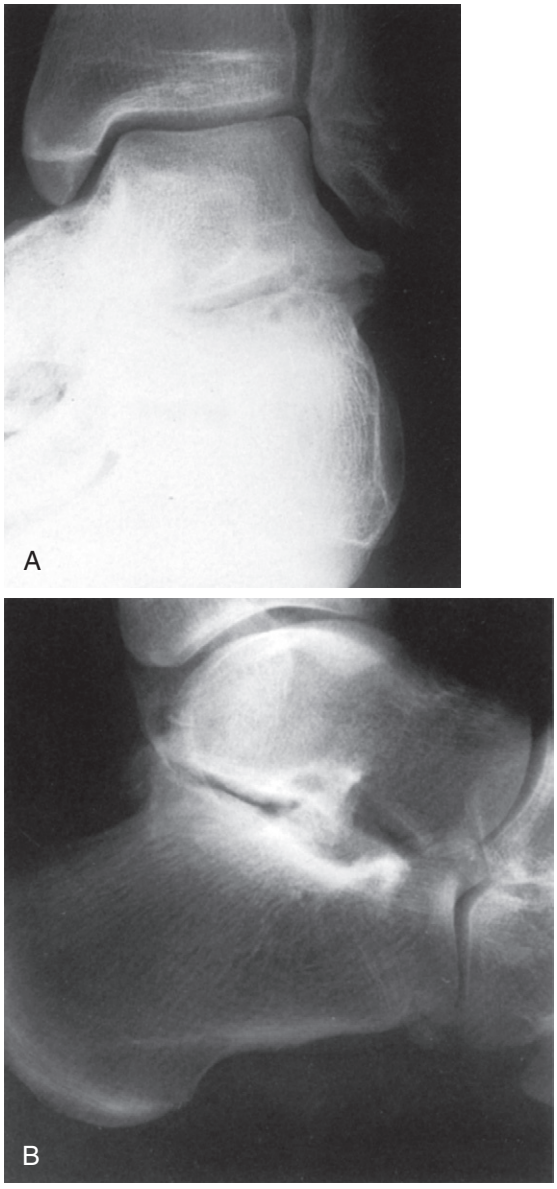

FIGURE 3-35. Internal oblique radiograph of ankle (**A**) and lateral radiograph of hindfoot (**B**) demonstrate joint space narrowing, subchondral sclerosis, and osteophyte of osteoarthritis involving the posterior talocalcaneal facet. This patient had a history of subtalar dislocation.

Osteoarthritic changes may be associated with tarsal coalition. Talocalcaneal coalition can produce a projection from the dorsal talus at the level of the joint known as the dorsal talar beak (Fig. 3-36). Joint space maintenance permits differentiation of the dorsal talar beak from the osteophytes associated with osteoarthritis. The dorsal talar beak also must be differentiated from the dorsal talar spur associated with the ankle capsular insertion that is posterior to the joint (Fig. 3-37).

FIGURE 3-36. Dorsal talar beak (*arrow*) at the level of the talonavicular joint in patient with surgically proven talocalcaneal coalition.

FIGURE 3-37. Dorsal talar spur (*arrow*) posterior to the talonavicular joint associated with ankle capsular insertion.

CALCANEUS

The calcaneus is frequently involved in inflammatory arthropathies. Erosions involving the calcaneus present at sites of ligamentous insertions. The posterosuperior and the plantar aspect of the calcaneus at the level of the plantar aponeurosis should be carefully evaluated for the presence of erosive changes.

The Achilles tendon inserts 1 to 2 cm inferior to the superior aspect of the calcaneus. A triangular lucent space containing the collapsed retrocalcaneal bursa is visualized between the calcaneus and the Achilles tendon in the normal state. Synovial inflammation will distend this bursa and obliterate the normal lucent triangle (Fig. 3-38). The synovial inflammation can eventually lead to erosions. As with erosions in other sites of the body, rheumatoid erosions will not be associated with bone production or "whiskering," which is seen in the spondyloarthropathies.

FIGURE 3-38. Distended retrocalcaneal bursa (*arrow*) associated with erosion (*arrowhead*) of the posterosuperior calcaneus in rheumatoid arthritis.

Erosions of the inferior surface of the calcaneus are also associated with the inflammatory arthropathies. Ill-defined erosions combined with whiskering and periosteal new bone at or anterior to the insertion of the plantar aponeurosis are hallmarks of the spondyloarthropathies (Fig. 3-39). The resulting bone production may produce a plantar spur, which can be differentiated from the calcaneal spur seen in normal patients by (1) the ill-defined margins of the spur and (2) the axis of the spur. The calcaneal spurs associated with the spondyloarthropathies tend to parallel the long axis of the calcaneus (Fig. 3-40), whereas "normal" calcaneal spurs tend to parallel the plantar aponeurosis. Bone production can be extensive and can produce an "ivory" appearance of the calcaneus (see Fig. 3-39).

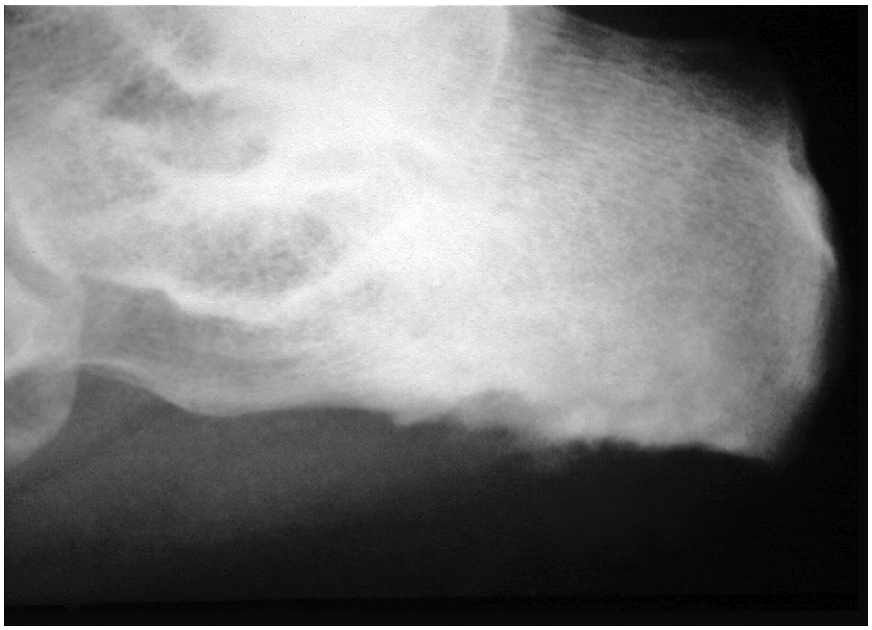

FIGURE 3-39. Extensive erosion of the inferior aspect of the calcaneus with sclerosis and ill-defined periostitis in psoriatic arthritis. The ivory appearance of the calcaneus is secondary to an extensive reparative response.

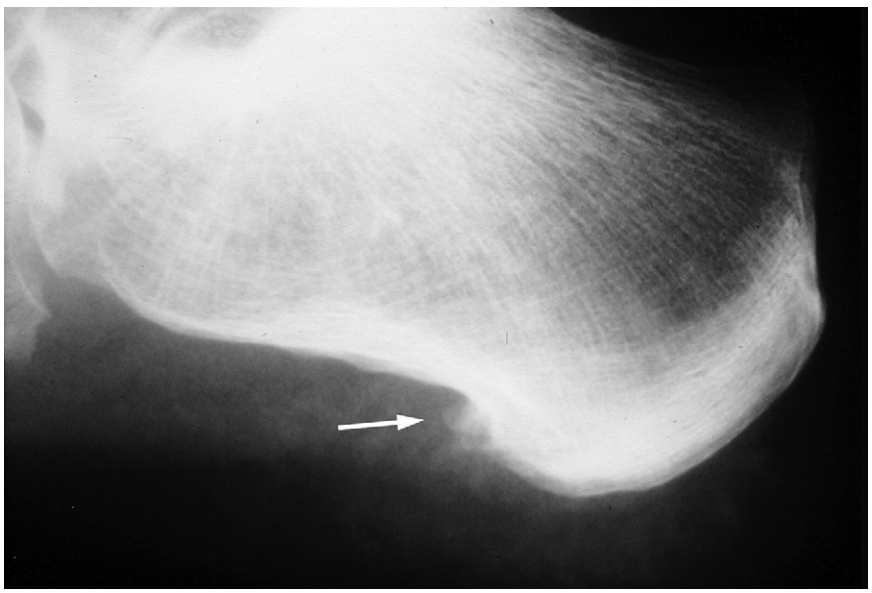

FIGURE 3-40. Ill-defined plantar calcaneal spur (*arrow*) that parallels the long axis of the calcaneus.

SUGGESTED READINGS

Chand Y, Johnson KA: Foot and ankle manifestations of Reiter's syndrome, *Foot Ankle* 1:167–172, 1980.
Egan R, Sartoris DJ, Resnick D: Radiographic features of gout in the foot, *J Foot Surg* 26:434–439, 1987.
Gold RH, Bassett LW: Radiologic evaluation of the arthritis foot, *Foot Ankle* 2:332–341, 1982.
Guerra J, Resnick D: Arthritides affecting the foot: Radiographic-pathological correlation, *Foot Ankle* 2:325–331, 1982.
Hammerschlag WA, Rice JR, Caldwell DS, et al: Psoriatic arthritis of the foot and ankle: Analysis of joint involvement and diagnostic errors, *Foot Ankle* 12:35–39, 1991.
Kumar R, Madewell JE: Rheumatoid and seronegative arthropathies of the foot, *Radiol Clin North Am* 25: 1263–1288, 1987.
Pavlov H: Imaging of the foot and ankle, *Radiol Clin North Am* 28:991–1018, 1990.
Resnick D, Feingold ML, Curd J, et al: Calcaneal abnormalities in articular disorders. Rheumatoid arthritis, ankylosing spondylitis, psoriatic arthritis, and Reiter syndrome, *Radiology* 125:355, 1977.
Zlatkin MB, Pathria M, Sartoris DJ, et al.: The diabetic foot, *Radiol Clin North Am* 25:1095–1105, 1987.

Approach to the Hip 4

The assessment of hip pain depends on a systematic review of a quality anteroposterior (AP) view of the pelvis. The femurs should be internally rotated approximately 15 degrees, the pelvis should not be oblique, and the sacrococcygeal junction should not project more than 4 cm superior to the superior pubic ramus. The following should be systematically assessed on the AP view of the pelvis: 1) hip joint space, 2) shape of the femoral head and femoral head neck junction, 3) geometry of the acetabulum, 4) evaluation of the sacroiliac joints and pubic symphysis, and 5) evaluation of the pubic rami, sacrum, and iliac wings for insufficiency fracture.

JOINT SPACE

The diagnosis of hip disease depends foremost on evaluation of the actual joint space. In some disorders the joint space is initially unaffected or even widened. Eventually, the femoral head migrates in one of three directions within the acetabulum, producing a specific pattern of joint space narrowing. The joint space narrows in a superolateral direction, a medial direction, or an axial (superomedial) direction (Fig. 4-1).

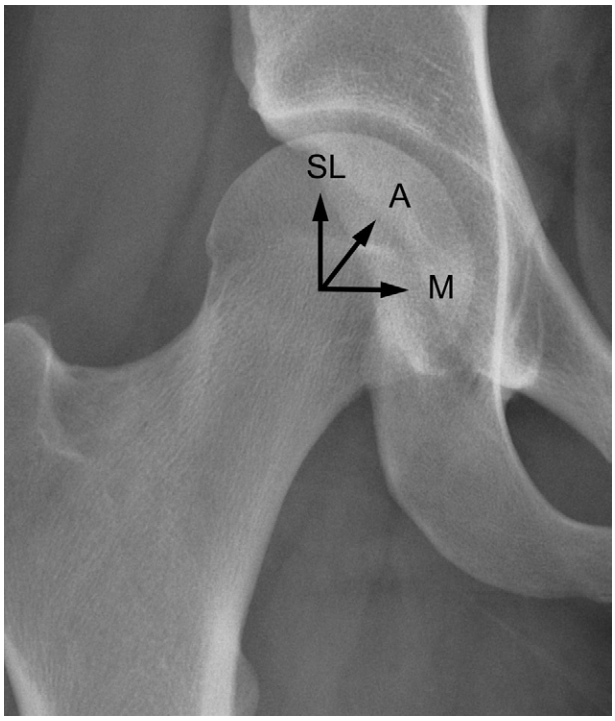

FIGURE 4-1. AP view of a normal hip. Arrows show direction of femoral head migration with cartilage loss: superolateral (SL), axial (A), or medial (M).

Superolateral Migration

Superolateral migration of the femoral head within the acetabulum indicates a nonuniform loss of cartilage. The cartilage loss is confined to the upper outer portion of the articulation. This is usually secondary to change in the normal mechanical stress across the hip joint and is characteristic of osteoarthritis (Fig. 4-2). With this cartilage loss, subchondral bone, or reparative bone, as well as small osteophytes, are formed on the lateral aspect of the femoral head and acetabulum. Weight bearing is then shifted from the center of the femoral neck to the medial cortex of the femoral neck. As a result, new bone is laid down in apposition to the medial cortex. As the disease progresses, a large medial osteophyte forms on the femoral head to fill the lack of congruity between the acetabulum and the femoral head. Cystic changes are also part of osteoarthritis.

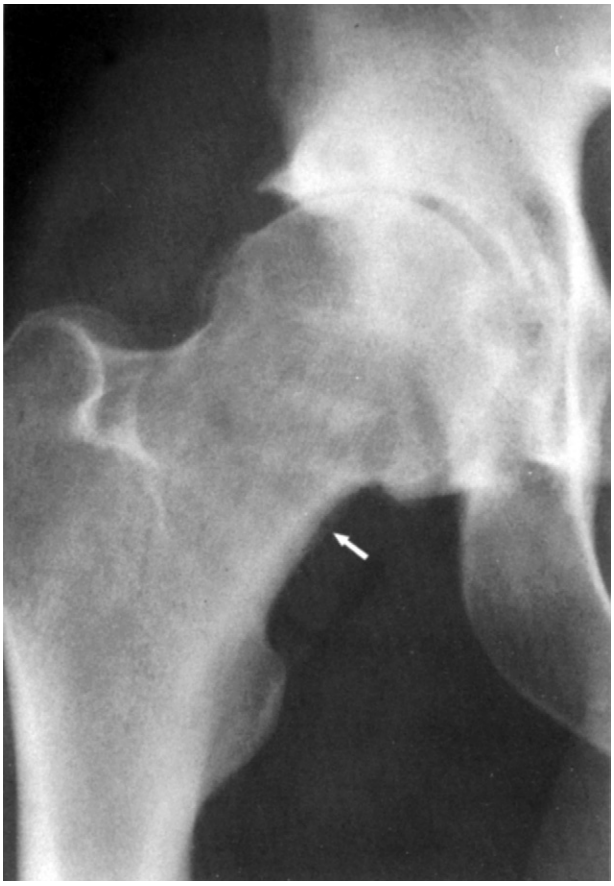

FIGURE 4-2. AP view of the hip demonstrating changes of osteoarthritis: nonuniform loss of cartilage with superolateral narrowing, osteophyte formation, subchondral sclerosis, and new bone apposition along the medial cortex of the femoral neck (*arrow*).

Medial Migration

Medial migration of the femoral head within the acetabulum can be seen in patients with primary osteoarthritis or in patients who have sustained an acetabular fracture (Fig. 4-3). Regardless, change in stress across the hip joint produces medial migration of the head in the acetabulum. The superolateral portion of the joint must widen, and the superior joint lines lose congruity when the head moves medial in the joint.

FIGURE 4-3. AP view of the hip showing fracture through the acetabulum. As a result, there is medial migration of the femoral head within the acetabulum, with osteoarthritic changes.

Axial Migration

Axial migration, also called superomedial migration, of the femoral head within the acetabulum indicates symmetrical uniform loss of cartilage. When the cartilage is affected uniformly, the earliest narrowing occurs along the axis of weight bearing on the axis of the femoral neck, as illustrated by a line drawn just superior to the fovea (Fig. 4-4). Axial migration is seen in any disease that destroys the cartilage in a uniform fashion. This includes the inflammatory arthropathies, the crystalline arthropathies, and other deposition arthropathies such as ochronosis and acromegaly. Upon observation of axial migration, one must evaluate the specific bone changes around the joint, such as mineralization, calcification, erosions, subchondral sclerosis, osteophyte formation, and cyst formation. The common arthropathies that produce axial migration are described here, with emphasis on their differential changes.

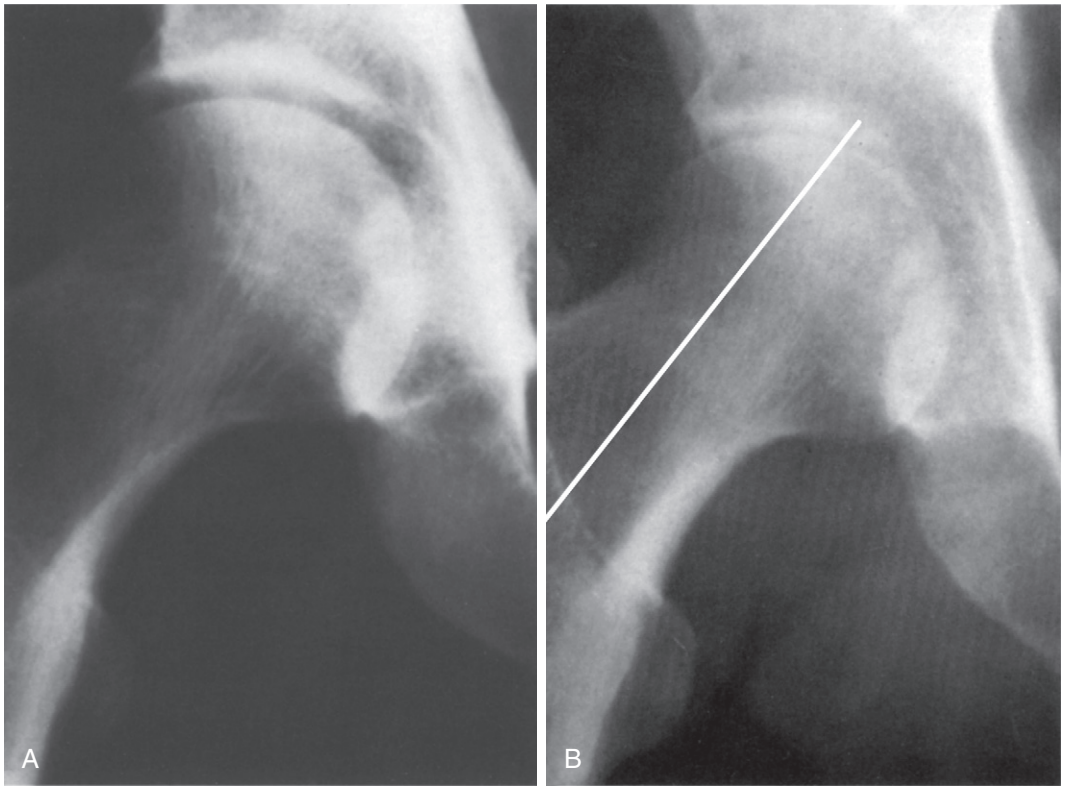

FIGURE 4-4. **A,** AP view of a normal hip. **B,** AP view of the same hip 1 year later demonstrating axial or superomedial migration. The narrowest portion of the hip joint is along a line just superior to the fovea.

Rheumatoid Arthritis (Figs. 4-5 and 4-6)

Rheumatoid arthritis is a bilateral symmetrical disease progressing from axial migration (Fig. 4-5) to acetabuli protrusio (Fig. 4-6). The bony structures are osteoporotic. There is little if any subchondral bone sclerosis. There is no osteophyte formation and no bone apposition along the inner aspect of the femoral neck. Erosions, when present, are relatively small. Synovial cysts may or may not be present. The hallmark is bilateral symmetrical axial migration with osteoporosis and lack of any evidence of bone repair.

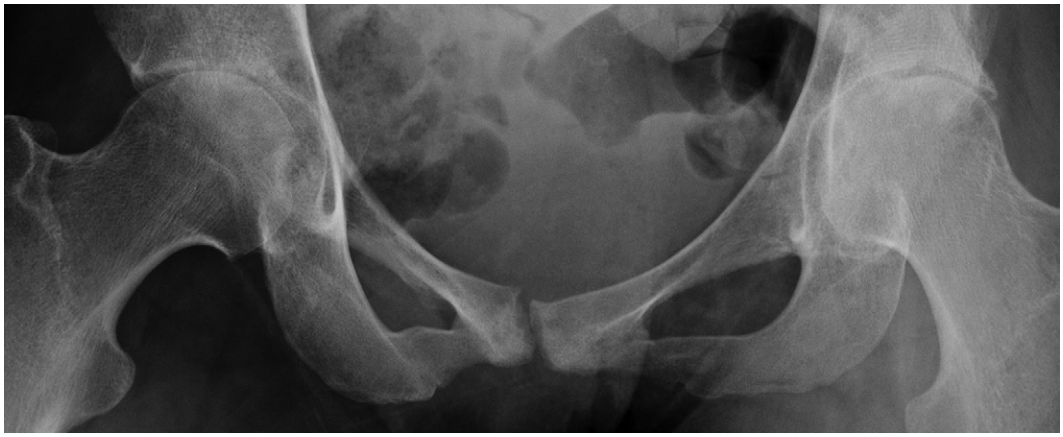

FIGURE 4-5. AP view of the pelvis showing bilateral symmetrical uniform narrowing of the hip joints. Both heads have moved in an axial direction. There is generalized osteoporosis. There is no evidence of osteophyte formation or bone apposition along the inner aspect of the femoral neck. There is little if any subchondral bone repair.

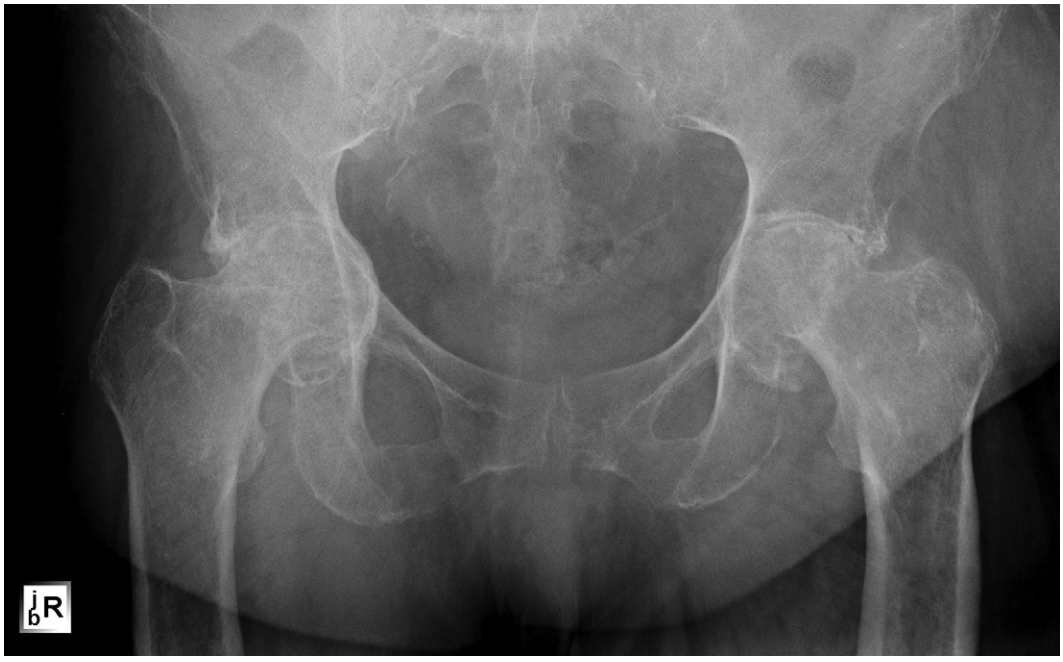

FIGURE 4-6. AP view of the pelvis showing severe changes of rheumatoid arthritis. There is left acetabular protrusio. Notice that the axial migration is actually superomedial. There is osteoporosis and lack of significant bone repair.

Ankylosing Spondylitis (Figs. 4-7 and 4-8)

Ankylosing spondylitis causes bilateral symmetrical axial migration of both hips, without producing the severe acetabuli protrusio seen in patients with rheumatoid arthritis. At first mineralization is maintained, and a cuff of osteophytes is seen at the junction of the femoral head and neck along with osteophytes at the superior and inferior borders of the acetabulum (Fig. 4-7). Unlike rheumatoid arthritis, ankylosing spondylitis is an ossifying disease. Erosive or cystic changes may not play a significant role in the changes in the hip. Instead the hip tends to progress to true bone ankylosis. The ankylosed femoral head tends to be almost normal in contour. Once ankylosis takes place, the surrounding bone structures become osteoporotic (Fig. 4-8).

FIGURE 4-7. AP view of the pelvis in a patient with ankylosing spondylitis. There is uniform loss of the cartilage with axial migration of both femoral heads. There is a cuff of osteophytes formed at the junction of the head and neck bilaterally. There are also osteophytes found on the superior and inferior aspects of the acetabulum. Notice the ankylosis of the sacroiliac joints and the "whiskering" of the ischial tuberosities.

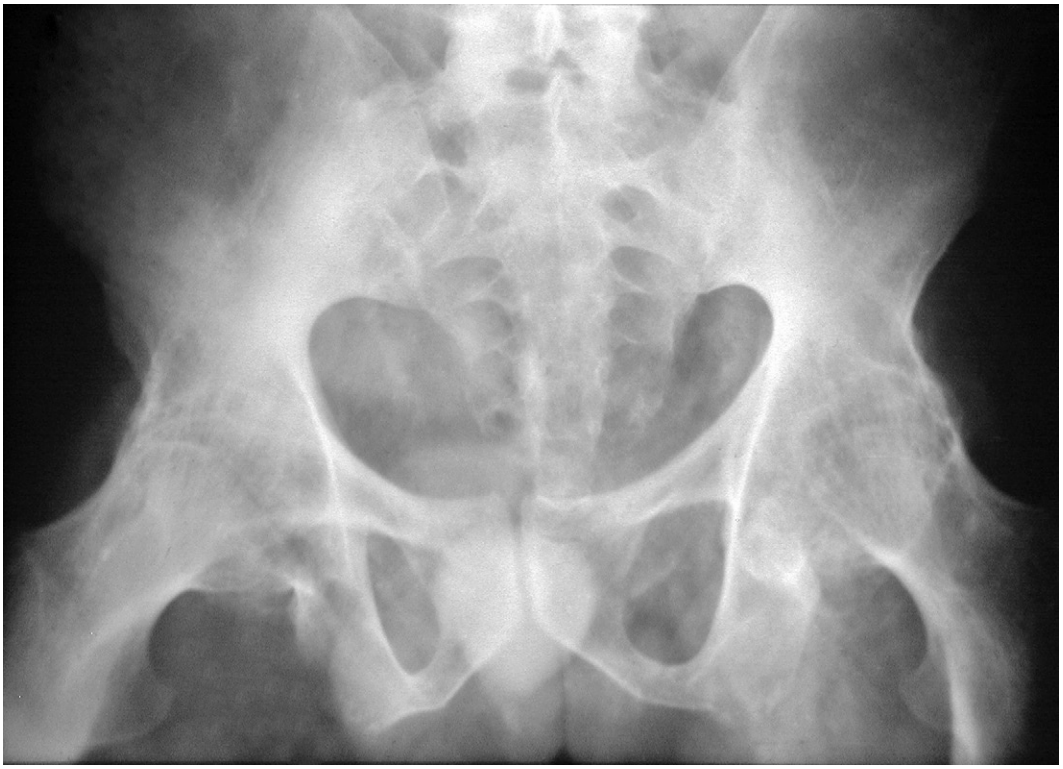

FIGURE 4-8. AP view of the pelvis in a patient with late-stage ankylosing spondylitis. There is total ankylosis of the sacroiliac joints and hip joints. Notice that through the ankylosis the contour of the femoral head is fairly well maintained. The bony structures are osteoporotic.

Calcium Pyrophosphate Dihydrate Crystal Deposition Disease (Figs. 4-9 and 4-10)

In calcium pyrophosphate dihydrate (CPPD) crystal deposition disease, both hips are involved either symmetrically or, more commonly, asymmetrically. Before axial migration occurs, one may observe calcification of the articular cartilage (Fig. 4-9). The axial migration rarely progresses to the extensive acetabuli protrusio seen in patients with rheumatoid arthritis. Unlike the inflammatory arthropathies, there is degeneration rather than active destruction of the cartilage. Therefore, the process is more indolent, and secondary osteoarthritic changes develop in the surrounding bones. Subchondral sclerosis, osteophyte formation, and cystic changes are seen (Fig. 4-10). The osteophytes formed tend to be smaller than those formed in osteoarthritis. Because there is no incongruity between the femoral head and the acetabulum, the large medial osteophyte seen in mechanical osteoarthritis is not seen in CPPD arthropathy. Cyst formation is more prevalent in CPPD arthropathy than in mechanical osteoarthritis. Severe CPPD arthropathy of the hip may resemble the changes of a neuropathic hip with no semblance of a joint space, massive bone repair, excessive osteophytosis, and bone debris.

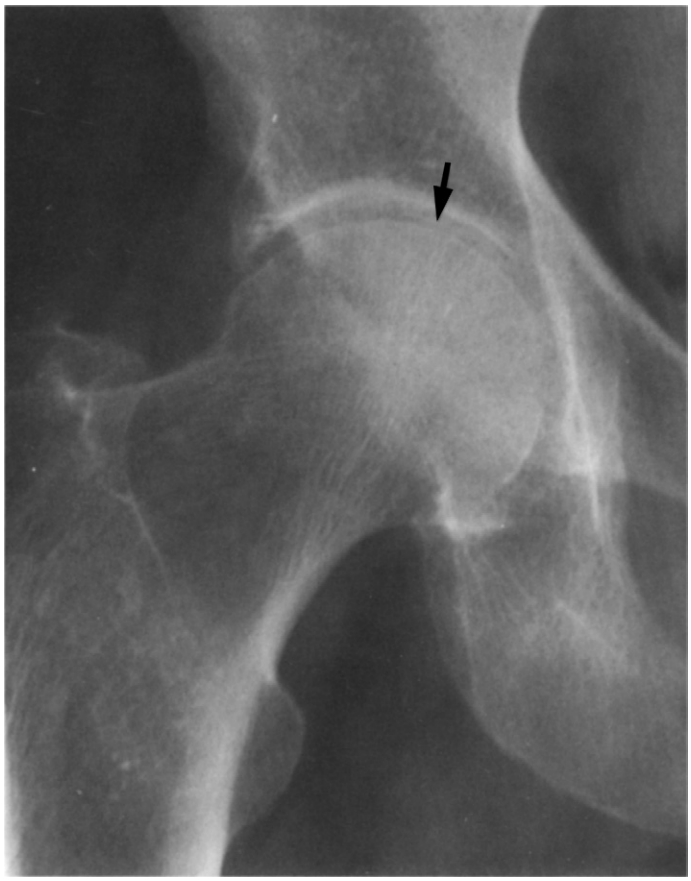

FIGURE 4-9. AP view of the hip demonstrating presence of chondrocalcinosis (*arrow*) and early axial migration of the head within the joint.

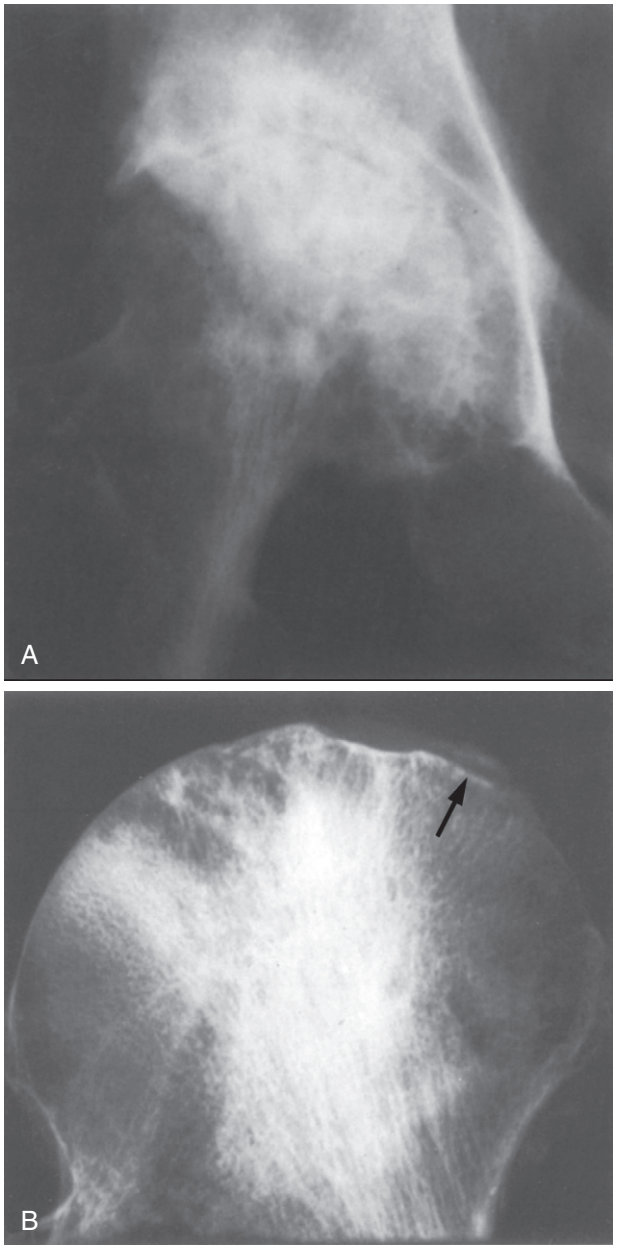

FIGURE 4-10. A, AP view of the hip in a patient with CPPD arthropathy. There is uniform loss of cartilage with axial migration present. There is significant subchondral bone repair and cyst formation. Osteophytes are also present. **B,** Specimen radiograph of the femoral head pictured in **A**. The cyst and reparative bone are well seen. Chondrocalcinosis is present in the remaining fragment of cartilage (*arrow*).

Septic Arthritis (Figs. 4-11 and 4-12)

Although the literature describes initial widening of a joint space with septic arthritis, usually we first see uniform narrowing of the joint space. The adjacent bony structures are osteoporotic. The diagnosis is clear when absence of the white cortical line along an extensive portion of the femoral head is observed (Fig. 4-11). Normally, as the entire white cortical line is lost and the underlying bone is destroyed, secondary reparative bone will be laid down behind the destruction. However, with an aggressive septic arthritis and resultant osteomyelitis, the entire femoral head and acetabulum can be destroyed without any evidence of repair (Fig. 4-12).

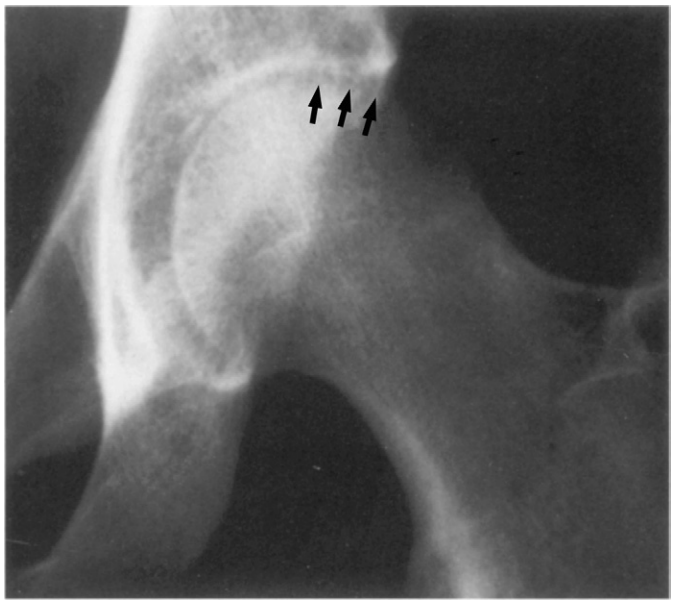

FIGURE 4-11. AP view of the hip with septic arthritis. There is axial migration of the femoral head within the acetabulum. There is significant loss of the white cortical line along the superolateral aspect of the femoral head (*arrows*).

FIGURE 4-12. AP view of the hip with septic arthritis going on to osteomyelitis. There has been total destruction of the femoral head and a large portion of the neck. There is considerable destruction of the acetabulum as well. Bone debris is seen within the joint space. This might be mistaken for a neuropathic hip except that the margin of destruction is extremely irregular and there is adjacent osteoporosis.

Secondary Axial Migration

Axial migration of the femoral head within the acetabulum may take place secondary to underlying bone disease rather than as primary disease of the cartilage (Fig. 4-13). The two most common bone diseases that cause this are Paget disease and renal osteodystrophy. In both instances, the underlying bone cannot absorb the normal stress applied to the acetabular area, and the acetabulum protrudes inward with weight bearing. The hip follows to maintain continuity within the acetabulum. Secondary degenerative changes commonly develop.

FIGURE 4-13. AP view of the pelvis of a patient with Paget's disease involving the right hemipelvis and left femur. The right hip has moved in an axial direction, with a resultant protrusion of the acetabulum secondary to the Paget's disease.

NORMAL JOINT SPACE

There are six common disorders involving the hip joint that will not cause loss of the actual joint until late in the disease. These are osteonecrosis of the femoral head, synovial osteochondromatosis, pigmented villonodular synovitis (PVNS), tuberculosis, developmental dysplasia of the hip, and femoroacetabular impingement.

Osteonecrosis (Figs. 4-14 to 4-16)

Osteonecrosis of the femoral head, no matter what the etiology, is a disorder of the femoral head. Only after the anatomical contour of the femoral head has been distorted and the overlying cartilage secondarily disrupted will the joint become involved with secondary osteoarthritis. In the earlier stages of osteonecrosis, the joint space is completely maintained and the acetabulum is completely normal. The first radiographic changes in the femoral head will be seen as smudginess of the normal trabecular pattern (Fig. 4-14). (The role of scintigraphy and magnetic resonance (MR) imaging is discussed in Chapter 1.) As repair occurs, lytic and sclerotic areas will be seen throughout the femoral head. The subchondral crescent-shaped lucency, seen best with the frogleg lateral view, is a rather late stage of necrosis and indicates impending collapse of the femoral head and the overlying cartilage (Fig. 4-15). Once this collapse has occurred, secondary osteoarthritic changes will develop (Fig. 4-16). However, one can distinguish late-stage osteonecrosis with secondary osteoarthritis from late-stage biomechanical osteoarthritis; in the late stages of osteonecrosis and secondary osteoarthritis, the radiographic changes in the femoral head are far more extensive than those in the acetabulum, whereas in late-stage mechanical osteoarthritis, the bone changes are equally distributed between the acetabulum and the femoral head.

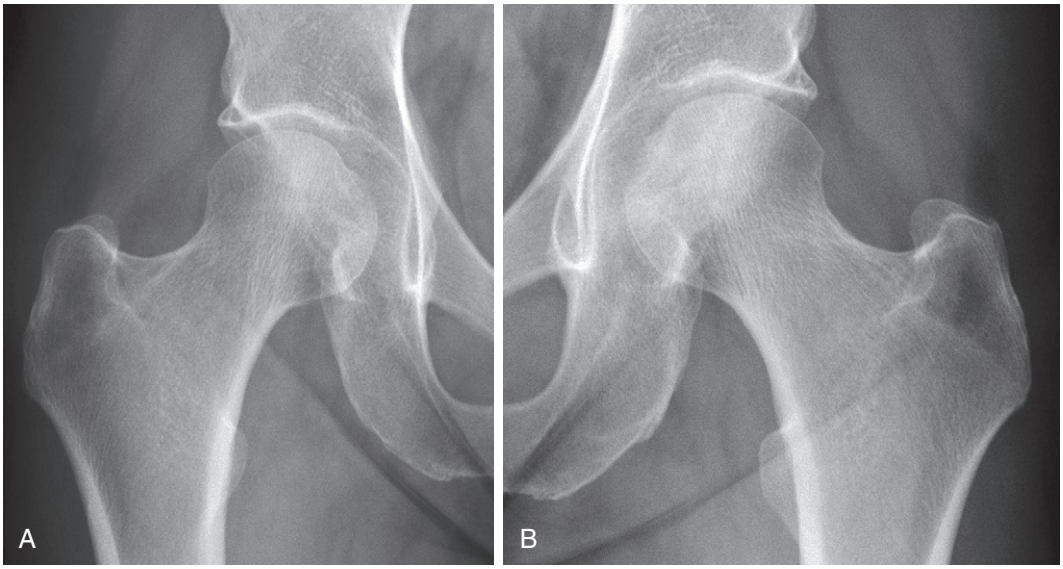

FIGURE 4-14. AP view of both hips demonstrating a normal right hip (**A**) and osteonecrosis of the left femoral head (**B**). Note that the joint space is maintained. The acetabulum is within normal limits. The trabecular pattern of the left femoral head has become smudgy as compared to the trabecular pattern of the left femoral head.

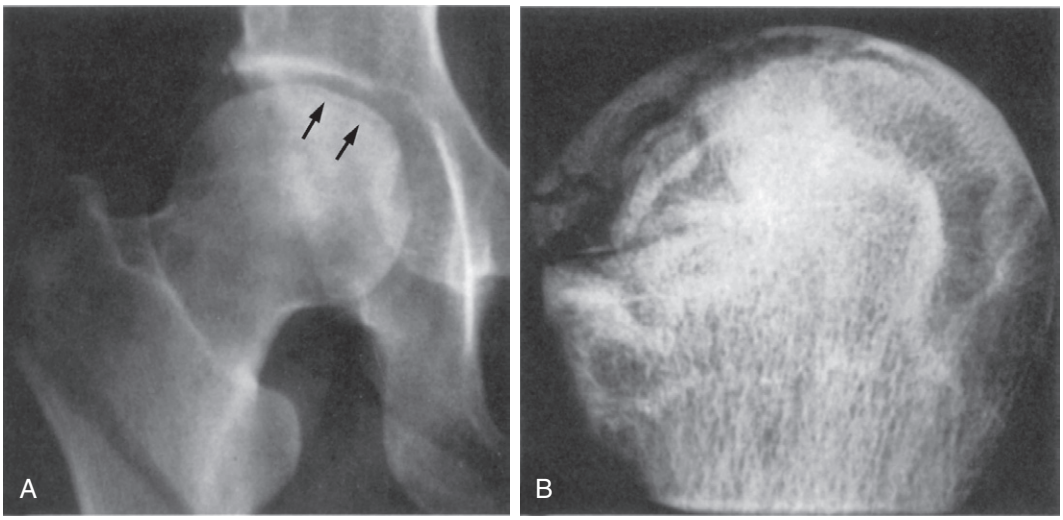

FIGURE 4-15. A, AP view of the hip showing osteonecrosis of the femoral head. The joint space is maintained. The acetabulum is within normal limits. There is smudginess of the trabecular pattern and a subchondral lucency (*arrows*), indicating impending collapse. **B,** Specimen radiograph of a femoral head with osteonecrosis. Subchondral lucency and collapse beneath are well demonstrated.

FIGURE 4-16. AP view of the hip with osteonecrosis and secondary superimposed osteoarthritic changes. Notice that most of the radiographic abnormalities are present in the femoral head rather than in the acetabulum. However, the joint space is now lost in the superolateral aspect.

Synovial Chondromatosis (Figs. 4-17 and 4-18)

There is no difficulty in making the diagnosis of synovial chondromatosis radiographically if the chondroid bodies are ossified sufficiently to be recognized (Fig. 4-17). If the bodies are not ossified, one must rely on other radiographic signs to make the diagnosis. The joint space is usually normal but may actually be widened or, late in the disease, narrowed. Osteoporosis of the bony structures may be present. The best radiographic sign is scalloping defects along the neck of the femur, usually most pronounced at the junction of the head and the neck (Fig. 4-18). If synovial chondromatosis is suspected and the chondroid bodies are not mineralized, the diagnosis may be confirmed through MR imaging.

FIGURE 4-17. AP view of the hip with synovial osteochondromatosis. The joint space is maintained. The joint capsule is filled with ossified chondroid bodies.

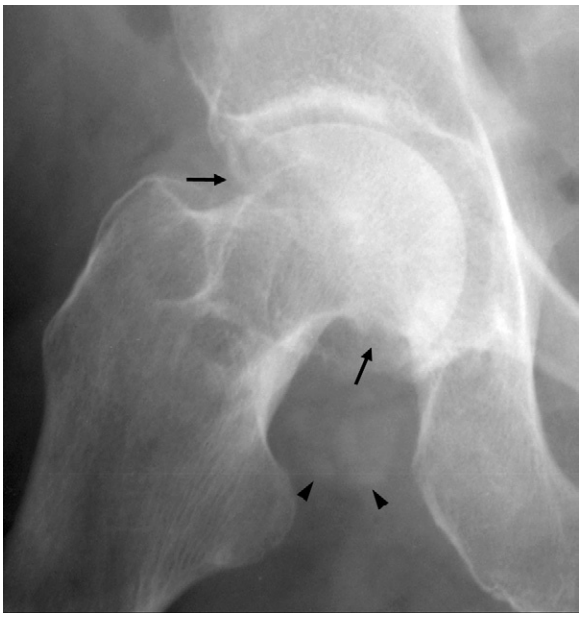

FIGURE 4-18. Synovial osteochondromatosis of the hip on frogleg view. There is surrounding osteoporosis. There are scalloped defects (*arrows*) on the femoral neck, one producing a sharp angle to the head as it joins the neck inferiorly. Faint ovoid densities are seen along the medial femoral neck (*arrowheads*).

Pigmented Villonodular Synovitis (Figs. 4-19 and 4-20)

The radiographic changes in PVNS are somewhat similar to those of synovial osteochondromatosis. The joint space may be normal, slightly widened, or, in the late stages, narrowed. Osteoporosis may or may not be present. Well-defined cysts are seen on both sides of the joint. Scalloping defects may be seen in the femoral neck, especially at the junction of the femoral head and neck. There is little evidence of bone

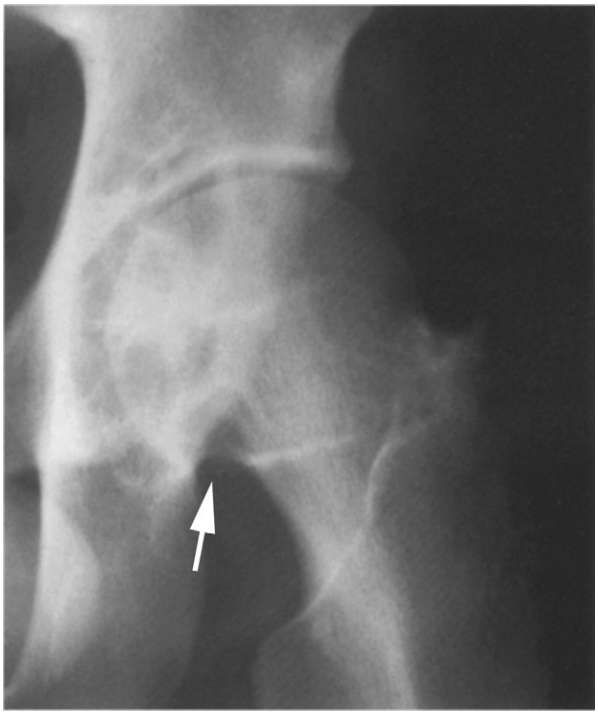

FIGURE 4-19. AP view of the hip in a patient with PVNS. The hip joint is maintained. There is normal mineralization present. There are cystic changes in the acetabulum as well as in the femoral head. The scalloping defect seen at the junction of the femoral head with the neck (*arrow*) demonstrates that the femoral head and neck are involved as well as the acetabulum.

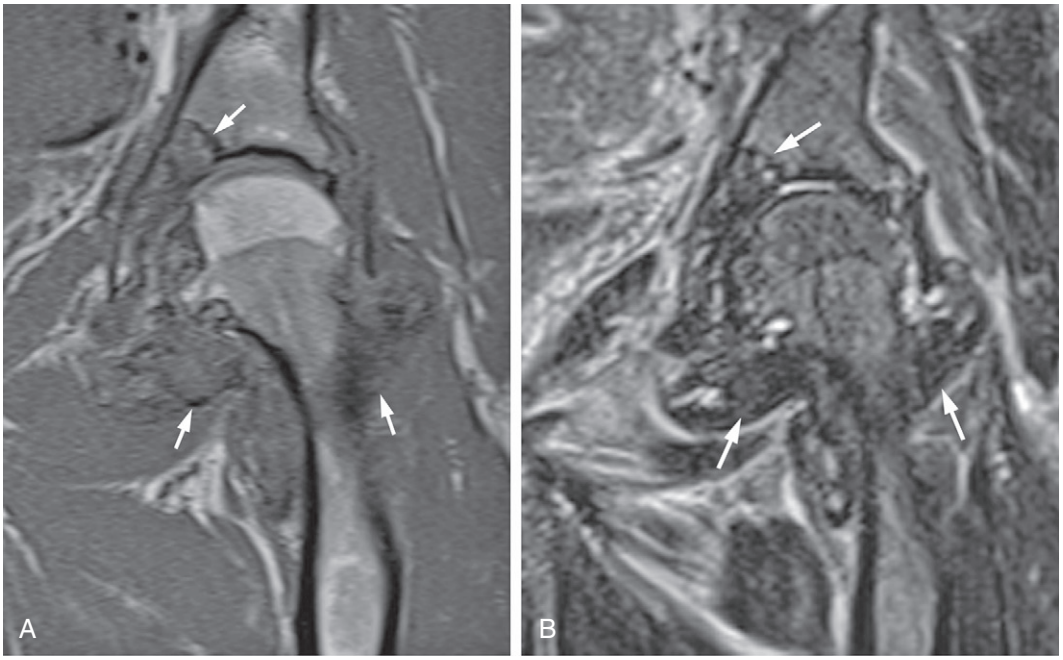

FIGURE 4-20. T1-weighted (**A**) and T2-weighted (**B**) coronal MR images of the left hip. Images show intermediate to low-signal T1 and low-signal T2 synovial proliferation. The areas of signal void (*arrows*) within the synovium are created by hemosiderin present in PVNS.

repair or osteophyte formation. The patient's age and the single joint involvement help to confirm the diagnosis, and the cystic changes help to distinguish it from synovial osteochondromatosis. Tuberculosis can present a similar appearance. The definitive diagnosis can be made through MR imaging.

Developmental Dysplasia of the Hip (Fig. 4-21)

Severe developmental dysplasia of the hip is recognized at an early age and does not usually present a diagnostic dilemma. However, subtle developmental dysplasia is easily overlooked. Subtle developmental dysplasia of the hip presents clinically as hip pain in a young person and radiographically is recognized by a shallow center edge angle, meaning under-coverage of the femoral head by the acetabulum. This entity is important to recognize as a source of early onset osteoarthritis because it is frequently associated with labral tear and cartilage damage of the anterior and superior acetabulum.

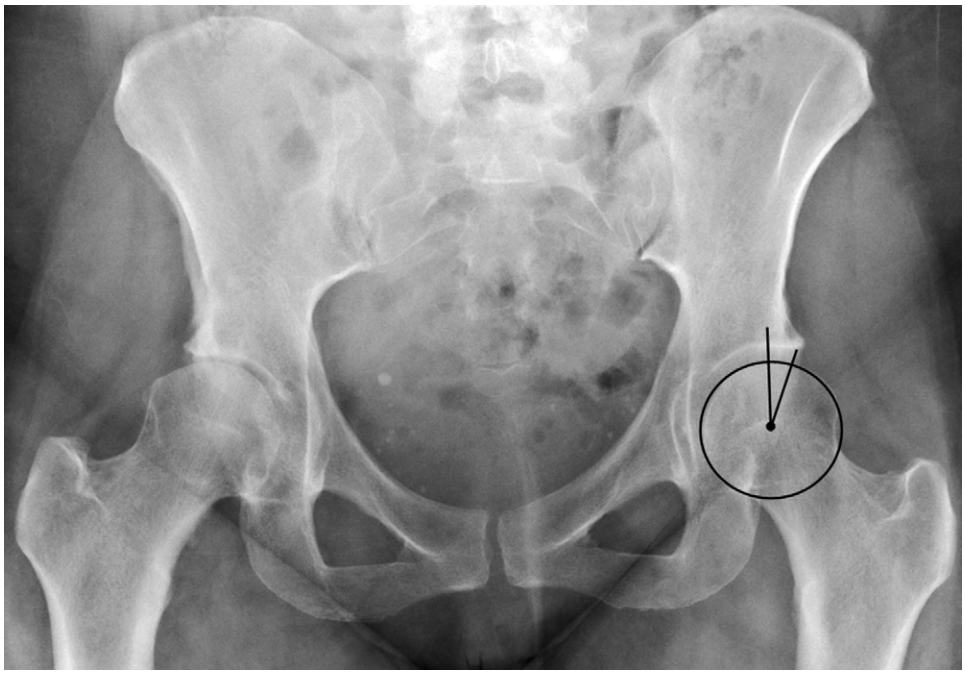

FIGURE 4-21. Developmental dysplasia of the hip in an adult. There is undercoverage of the femoral heads bilaterally with a measured center edge angle of less than 25 degrees (normal range is 25 degrees to 39 degrees). Superior joint space narrowing is present on the right.

Femoroacetabular Impingement (Fig. 4-22)

Femoroacetabular impingement (FAI) is a recently recognized disorder that is clinically associated with hip pain in young patients. Pain occurs at the limits of range of motion from impingement of the femoral neck against the acetabulum due to abnormal anatomy of either the femoral head neck junction (cam-type impingement) or the acetabulum (pincer-type impingement). An osseous bump at the superior lateral femoral head neck junction is the most common cause of cam impingement (Fig. 22A). Abnormal acetabular overcoverage, either focal or diffuse, may lead to pincer impingement (Fig. 22B). A subcortical lucency in the anterior femoral neck (synovial herniation pit) is frequently seen in the setting of pincer-type FAI.). Joint space is initially preserved but chronic impingement can lead to labral tear, cartilage destruction, and premature osteoarthritis.

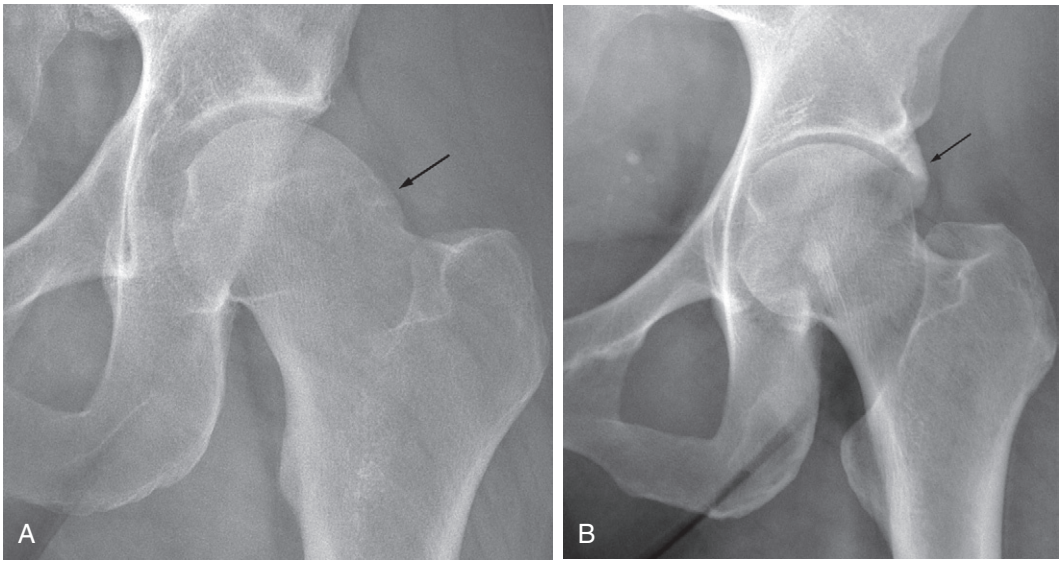

FIGURE 4-22. A, CAM-type femoroacetabular impingement with a dysplastic bony bump at the superolateral femoral head neck junction. **B,** Pincer-type femoroacetabular impingement with overcoverage of the femoral head by the acetabulum (*arrow*).

SUGGESTED READINGS

Bullough P, Goodfellow J, O'Conner J: Relationship between degenerative changes and load-bearing in human hip, *J Bone Joint Surg Br* 55:746–758, 1973.

Butt WP: Radiology of the infected joint, *Clin Orthop Relat Res* 96:136–149, 1973.

Dwosh IL, Resnick D, Becker MA: Hip involvement in ankylosing spondylitis, *Arthritis Rheum* 19:683–692, 1976.

Goldman AB, Bullough P, Kammerman S, et al: Osteitis deformans of the hip joint, *AJR Am J Roentgenol* 128:601–606, 1977.

Murray R: The aetiology of primary osteoarthritis of the hip, *Br J Radiol* 38:810–824, 1965.

Resnick D: Patterns of femoral head migration in osteoarthritis of the hip: Roentgenographic-pathologic correlation and comparison with rheumatoid arthritis, *Am J Roentgenol Radium Ther Nucl Med* 124:62–74, 1975.

Resnick D: Radiographic approach to hip disease, *Radiolog* 1(3):27, 1978.

Resnick D, Niwayama G, Goergen TG, et al: Clinical, radiographic and pathologic abnormalities in calcium pyrophosphate dihydrate deposition disease (CPPD): Pseudogout, *Radiology* 122:1–15, 1977.

Scott PM: Bone lesions in pigmented villonodular synovitis, *J Bone Joint Surg Br* 50:306–311, 1968.

Sweet DE, Madewell JE: Osteonecrosis: Pathogenesis. In Resnick D, editor: *Diagnosis of bone and joint disorders*, ed 4, Philadelphia, 2002, W.B. Saunders.

Tannast M, Siebenrock KA, Anderson SE: Femoroacetabular impingement: Radiographic diagnosis—what the radiologist should know, *AJR Am J Roentgenol* 188:1540–1552, 2007.

Zimmerman C, Sayegh V: Roentgen manifestations of synovial osteochondromatosis, *AJR Am J Roentgenol Radium Ther Nucl Med* 83:680–686, 1960.

Approach to the Knee 5

As in the hip, the diagnosis of a disorder of the knee depends foremost on the evaluation of true joint space involvement. This evaluation is made most accurately through an anteroposterior (AP) standing view of the knee and a flexed lateral view (see Chapter 1). The joint consists of three compartments: the medial tibiofemoral compartment, the lateral tibiofemoral compartment, and the patellofemoral compartment. The various arthropathies are characterized by the manner in which they affect these compartments. They separate into the following categories: those that affect all three compartments, those that preferentially involve a specific compartment, and those that initially do not involve any compartment.

TOTAL COMPARTMENT INVOLVEMENT

Total compartment narrowing indicates that all three compartments of the knee are involved in a uniform manner. This implies a primary abnormality of the underlying cartilage leading to loss of joint space. This loss may be caused either by aggressive destruction from inflammation or by slow degeneration secondary to deposition of foreign substance into the cartilage. The latter is seen in the late phases of the crystalline arthropathies, ochronosis, and acromegaly. The early phases of these arthropathies are discussed elsewhere in this chapter. However, once there is uniform loss of the cartilage, osteoarthritic changes are seen in the adjacent tibia, femur, and patella. Although it is difficult to distinguish one arthropathy from another in this osteoarthritic phase of disease, the uniform involvement of all compartments will separate these arthropathies from common mechanical osteoarthritis.

The arthropathies that produce total compartment involvement by aggressive destruction are the inflammatory arthropathies. Each has specific radiographic characteristics that distinguish it from the others.

Rheumatoid Arthritis (Figs. 5-1 and 5-2)

Rheumatoid arthritis is a bilateral symmetrical disease producing uniform loss of all compartments of the knee and generalized osteoporosis. Despite the fact that the knee is a weight-bearing joint, there is little evidence of bone repair or osteophyte formation in response to the cartilage loss (Fig. 5-1). Erosive changes may be present but are not a prominent part of the radiographic picture. Large synovial cysts may be present. A cyst may become so large that it resembles a bone neoplasm (Fig. 5-2). However, observation of uniform loss of joint space as well as smaller cysts in the adjacent bone should prevent an erroneous diagnosis. Occasionally there will be preferential narrowing of the lateral compartment. However, the relative lack of bone repair to this loss (osteophyte formation and subchondral sclerosis) should direct one away from the diagnosis of a mechanical osteoarthritis and toward the correct diagnosis of rheumatoid arthritis.

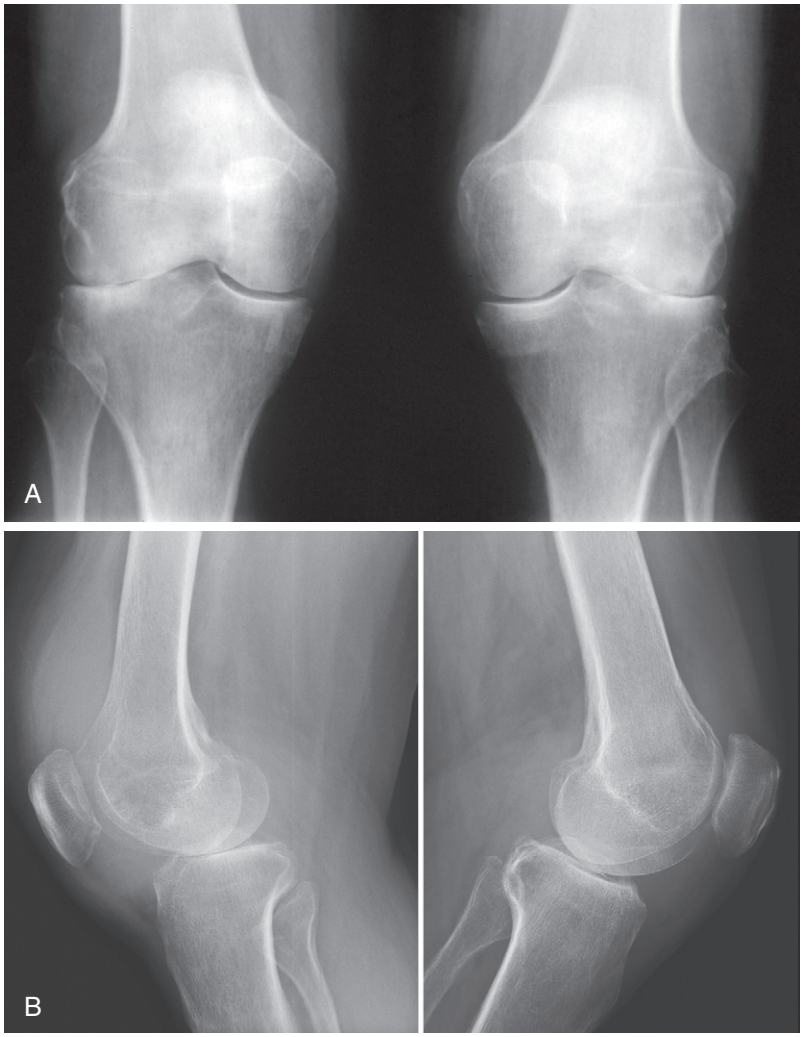

FIGURE 5-1. Anteroposterior standing view of both knees (**A**) and lateral view of both knees (**B**) in a patient with rheumatoid arthritis. There is loss of cartilage in all compartments. There is generalized osteoporosis with little to no evidence of bone repair. *(**A** from Kantor S, Brower AC: Radiographic assessment. In Rothermich N, Whisler R:* Rheumatoid arthritis, *Orlando, FL, Grune & Stratton, 1985, p 57; reprinted by permission.)*

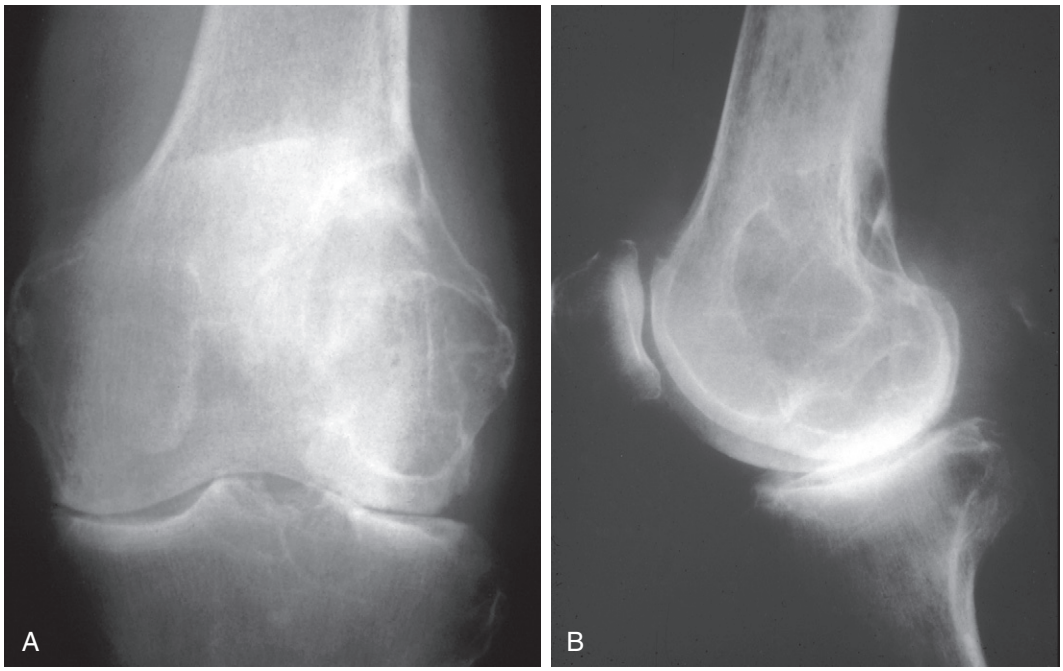

FIGURE 5-2. Anteroposterior (**A**) and lateral (**B**) views of the knee in a patient with rheumatoid arthritis. The large synovial cyst involves the lateral femoral condyle and resembles a giant cell tumor. However, there is narrowing of all compartments, generalized osteoporosis, and a synovial cyst involving the adjacent tibial plateau.

Psoriatic Arthritis or Reactive Arthritis (Fig. 5-3)

Psoriatic arthritis and reactive arthritis present similar radiographic changes. Both are bilateral but asymmetrical diseases involving one knee more than the other or involving one portion of the knee more than another. Unlike rheumatoid arthritis, bone mineralization is maintained. Also unlike rheumatoid arthritis, there is usually evidence of bone proliferation in the form of bone excrescences at ligamentous and tendinous attachments or a periosteal reaction.

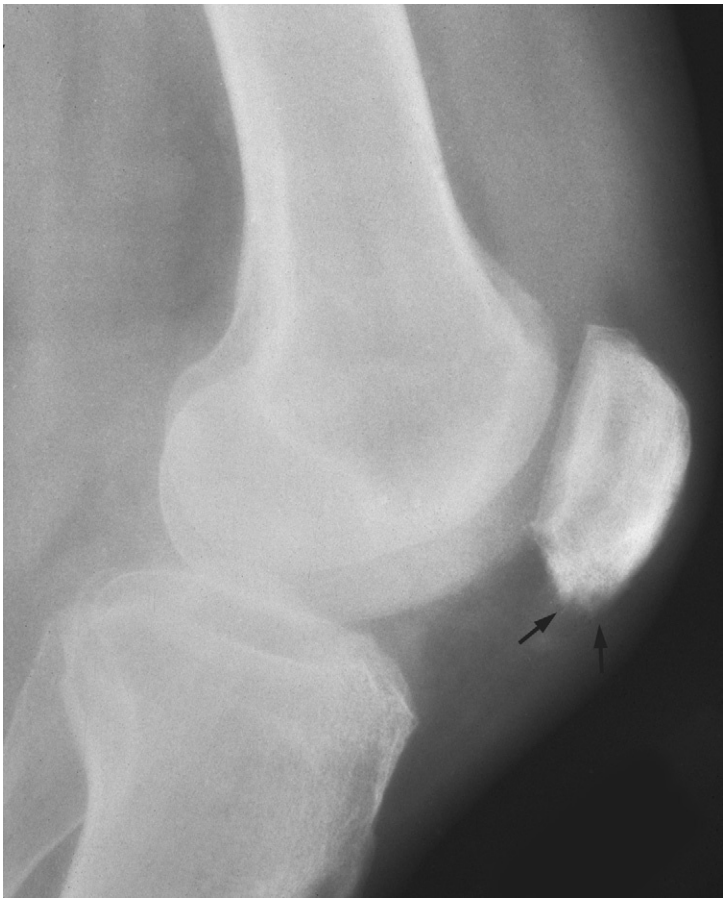

FIGURE 5-3. Lateral view of the knee in psoriatic arthritis. There is bone proliferation on the anteroinferior surface of the patella (*arrows*).

Ankylosing Spondylitis (Fig. 5-4)

Knee involvement in ankylosing spondylitis is uncommon. However, when knee involvement is present, ankylosis is the predominant part of the radiographic picture. Early in the disease process, small erosions with adjacent bone sclerosis will be present. However, in a relatively short period of time the joint may ankylose, leaving a normal contour to the ghost joint margins.

FIGURE 5-4. Lateral view of a knee in a patient with longstanding ankylosing spondylitis. The knee is ankylosed in a flexed position. The normal contours of the knee are seen through the ankylosis.

Juvenile Idiopathic Arthritis (Fig. 5-5)

Most frequently juvenile idiopathic arthritis presents as unilateral disease, but with total compartment involvement of the affected knee. The most prominent feature is overgrowth of the femoral and tibial epiphyses as well as overgrowth of the patella; with the overgrowth of the femoral condyles, the intracondylar notch appears widened. Joint space narrowing may not be prominent in the mono- or pauciarticular form of the disease. Because the cartilage is thicker in the child than in the adult, erosive disease and cyst formation, if present, are late manifestations. It may be difficult to distinguish these radiographic changes from those produced in hemophilia.

FIGURE 5-5. A, AP standing view of both knees in a patient with juvenile rheumatoid arthritis. The right leg is longer than the left leg. There is overgrowth of the femoral and tibial epiphyses in the right knee. There are uniform loss of cartilage and small erosive changes on the medial femoral condyle. **B,** Lateral view of the right knee. A large effusion is present. There is overgrowth of the femoral and tibial epiphyses. There is also overgrowth of the patella. The patella is elongated in configuration compared to the square configuration seen in the hemophilic knee (see Fig. 5-7).

Hemophilia (Figs. 5-6 and 5-7)

Hemophilia (Fig. 5-6) also produces overgrowth of the epiphyses and patella and widening of the intercondylar notch. There tends to be more cyst formation in the knee of the patient with hemophilia, secondary to intraosseous bleeding, than in the knee of a juvenile with rheumatoid arthritis. It has also been observed that the overgrown patella becomes square in hemophilia (Fig. 5-7) and elongated in the inflammatory arthropathy of childhood. The effusion of the hemophilic arthritis may be relatively dense secondary to chronic hemosiderin deposition in the synovium.

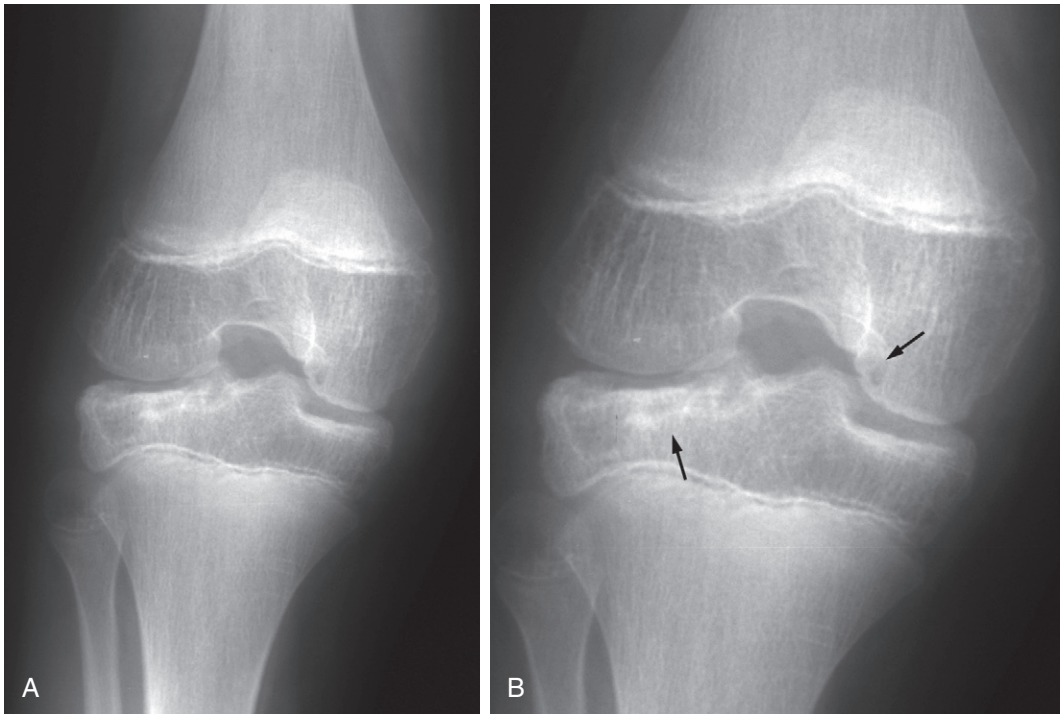

FIGURE 5-6. A, AP standing view of the knee in a patient with hemophilia. **B,** Close-up AP view of the right knee. There is overgrowth of the femoral and tibial epiphyses with widening of the intercondylar notch. There is mild uniform loss of the joint space visualized. A cyst is seen in the lateral tibial plateau and medial femoral condyle (*arrows*).

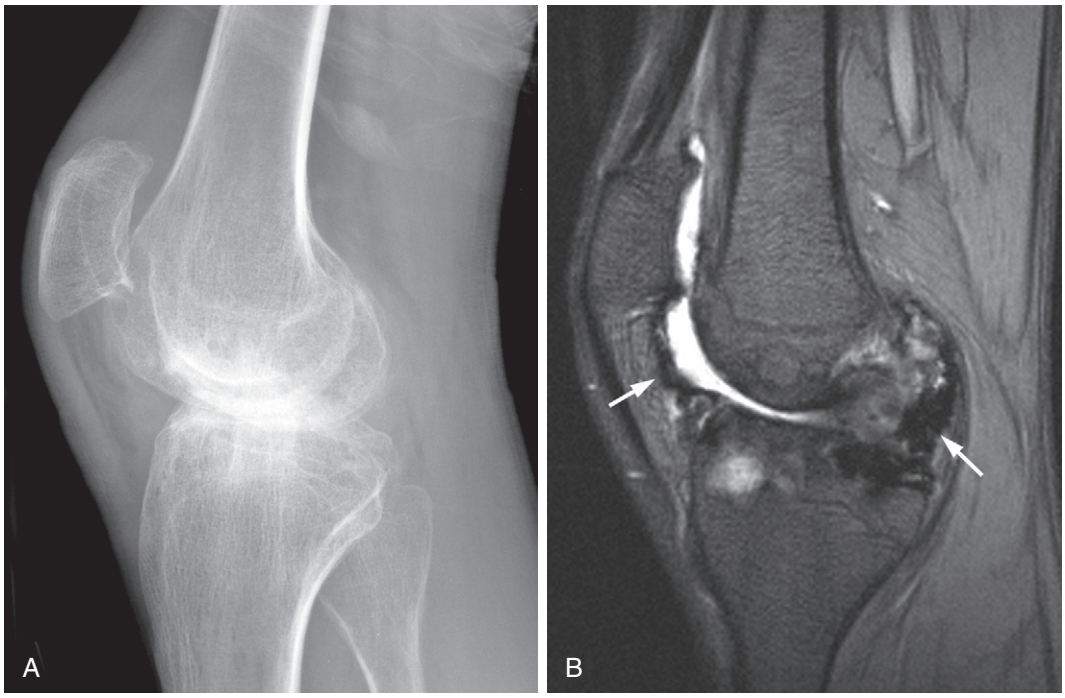

FIGURE 5-7. A, Lateral view of the knee in a patient with hemophilia. Synovial proliferation is seen. There is overgrowth of the femoral and tibial epiphyses as well as the patella, which is square in shape. Multiple cysts are seen in the epiphyses. **B,** Fast Spin Echo fat-suppressed T2-weighted sagittal MR image of the same knee demonstrating very low signal susceptibility artifact from hemosiderin staining of the synovium (*arrows*).

Septic Arthritis (Figs. 5-8 and 5-9)

Septic arthritis presents as unilateral involvement. In aggressive disease there will be evidence of effusion, uniform cartilage loss, juxta-articular osteoporosis, and diagnostic loss of the white cortical line (Fig. 5-8). As bone is destroyed, attempts at repair are usually made behind the destruction. In more indolent disease, such as tuberculous or fungal disease, there may be relative preservation of the joint space and erosions at the margins of the joint (Fig. 5-9). In childhood, an indolent infection may have a radiographic appearance similar to that of juvenile idiopathic arthritis.

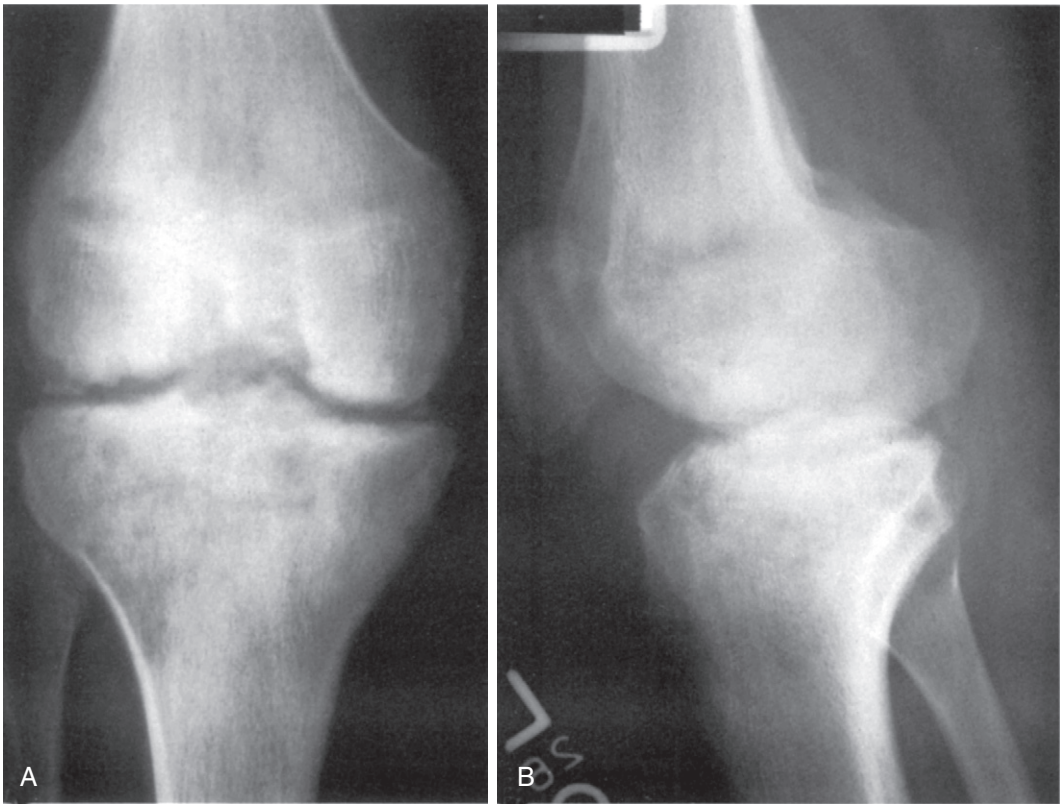

FIGURE 5-8. Anteroposterior (**A**) and lateral (**B**) views of a knee with septic arthritis. There is cartilage loss in all compartments of the knee. There is loss of the white cortical line best seen on the AP view. There is evidence of bone repair. *(From Resnick D, Niwayama G: Osteomyelitis, septic arthritis and soft tissue infection: The organisms. In Resnick D, Niwayama G, editors:* Diagnosis of bone and joint disorders, *vol 2, Philadelphia, W.B. Saunders, 1981; reprinted by permission.)*

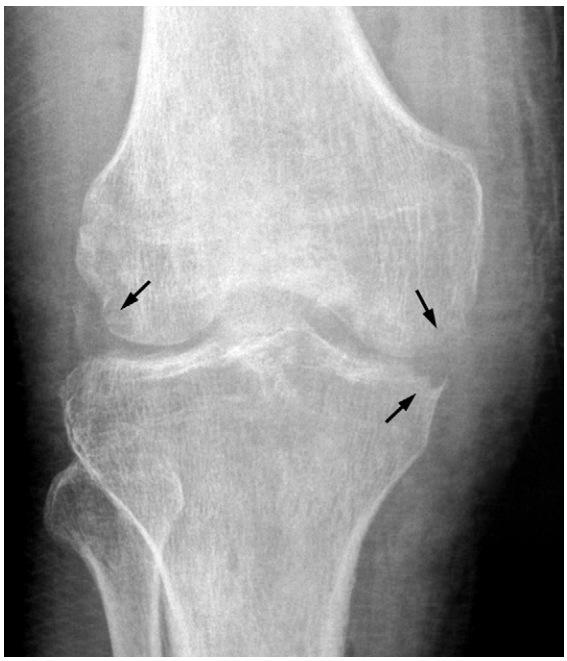

FIGURE 5-9. AP view of a knee of a patient with tuberculous arthritis. The joint space appears to be preserved. Erosions are present at the margins of the joint (*arrows*).

PREFERENTIAL COMPARTMENT LOSS

Two common arthropathies involve specific compartments in the knee joint, and knowledge of this specific compartment involvement helps the radiologist to make the correct diagnosis. These two arthropathies are (1) primary osteoarthritis and (2) calcium pyrophosphate dihydrate (CPPD) crystal deposition disease.

Osteoarthritis (Fig. 5-10)

Osteoarthritis of the knee is the most common arthropathy of the knee. It develops from change in the normal mechanisms of weight bearing across the knee joint. It is seen most commonly in patients with past significant trauma and in obese females. The normal standing knee shows slight valgus angulation. Most osteoarthritic knees stand in varus. There is preferential loss of the medial tibiofemoral compartment and associated loss of the patellofemoral compartment. As the cartilage is lost, there is evidence of bone repair with subchondral sclerosis and osteophyte formation. Cystic changes are part of the radiographic picture. Occasionally the lateral tibiofemoral compartment shows preferential loss, and an extreme valgus deformity is demonstrated on standing views. The patellofemoral compartment is not as commonly affected with lateral compartment involvement as with medial compartment involvement.

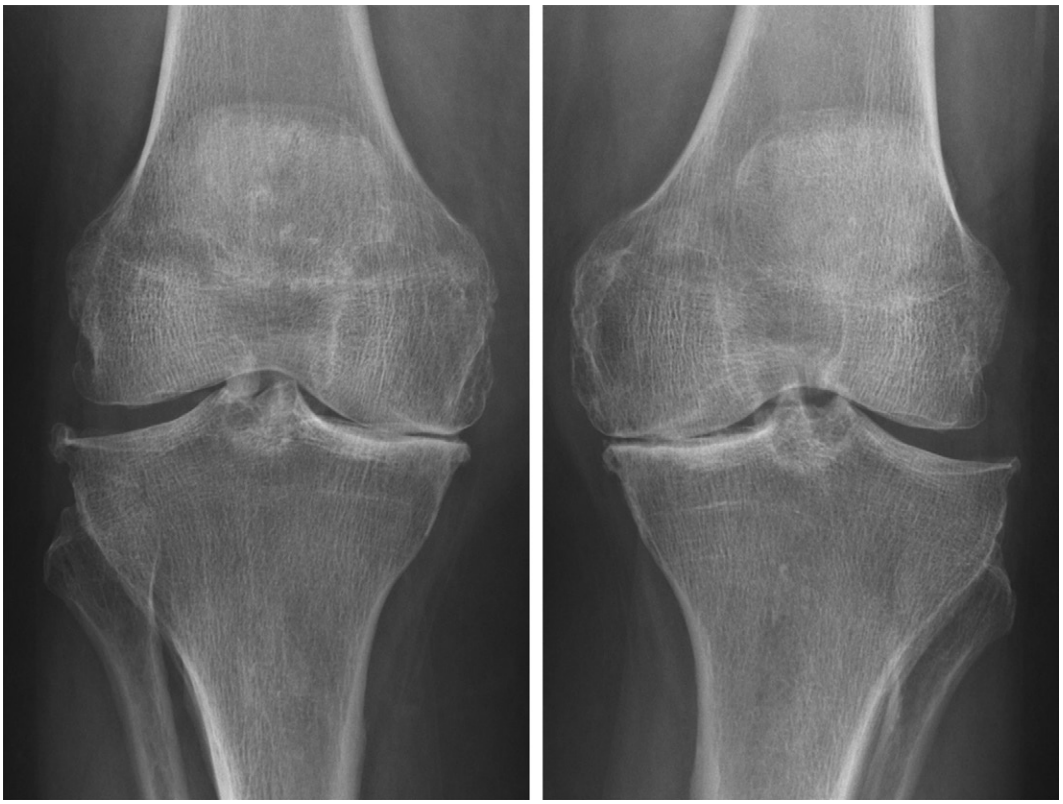

FIGURE 5-10. AP standing view of both knees in a patient with osteoarthritis. There is preferential loss of the medial tibiofemoral compartment. There is subchondral bone formation and osteophyte formation.

When osteoarthritic changes become exuberant, one must consider the possibility of a neuropathic joint (Fig. 5-11). The early radiographic changes in the neuropathic knee are massive recurrent effusions, subluxations, pathological fracture, and bone debris within the joint. As the process progresses, there is complete dissolution of the joint space, exuberant bone formation or eburnation, massive osteophytosis, and bone fragmentation.

FIGURE 5-11. AP view of a neuropathic knee. There are joint dissolution, subluxation, eburnation, fragmentation, and osseous debris.

CPPD Crystal Deposition Disease (Figs. 5-12 and 5-13)

CPPD crystal deposition disease is the second most common arthropathy of the knee, and it is seen predominantly in the elderly. There is preferential involvement of the patellofemoral joint space (Fig. 5-12). The narrowing of this joint space is accompanied by subchondral bone sclerosis and osteophyte formation on the posterior aspect of the patella and the anterior aspect of the femoral condyles. The narrowing may be so severe as to allow the motion of the patella to create a scalloped defect in the femur superior to the location of the patella in the flexed view. The defect is actually where the patella abuts the femur in extension. This radiographic change may be present even though the medial and lateral tibiofemoral compartments are unaffected. However, usually one can identify chondrocalcinosis in the maintained compartments. In some patients all compartments of the knee may be involved, with cartilage loss and osteoarthritic changes. In such patients, the presence of chondrocalcinosis may be impossible to identify. It is the one arthropathy in which the osteoarthritic changes may become so exuberant as to resemble those of a neuropathic knee (Fig. 5-13).

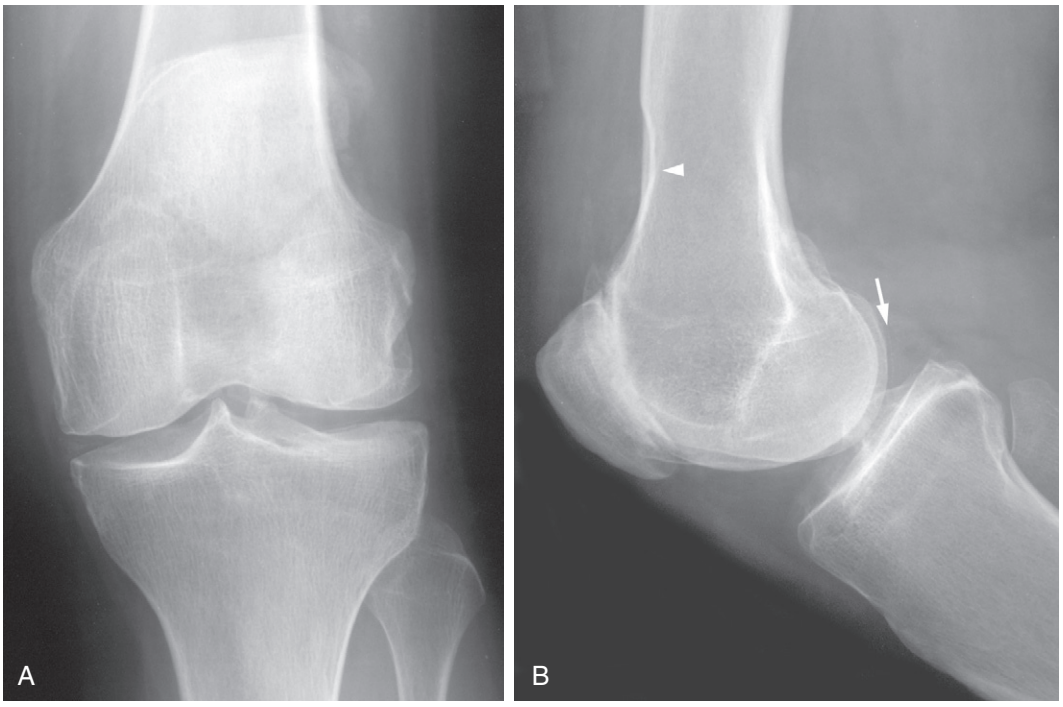

FIGURE 5-12. AP (**A**) and lateral (**B**) views of a knee in a patient with CPPD arthropathy. The medial and lateral tibiofemoral compartments are maintained, and chondrocalcinosis is identified (*arrow*). There is total loss of the patellofemoral joint space with adjacent subchondral new bone formation. A scalloped defect is seen in the femur (*arrowhead*) that is created by the patella as it abuts the femur when the knee is in extension.

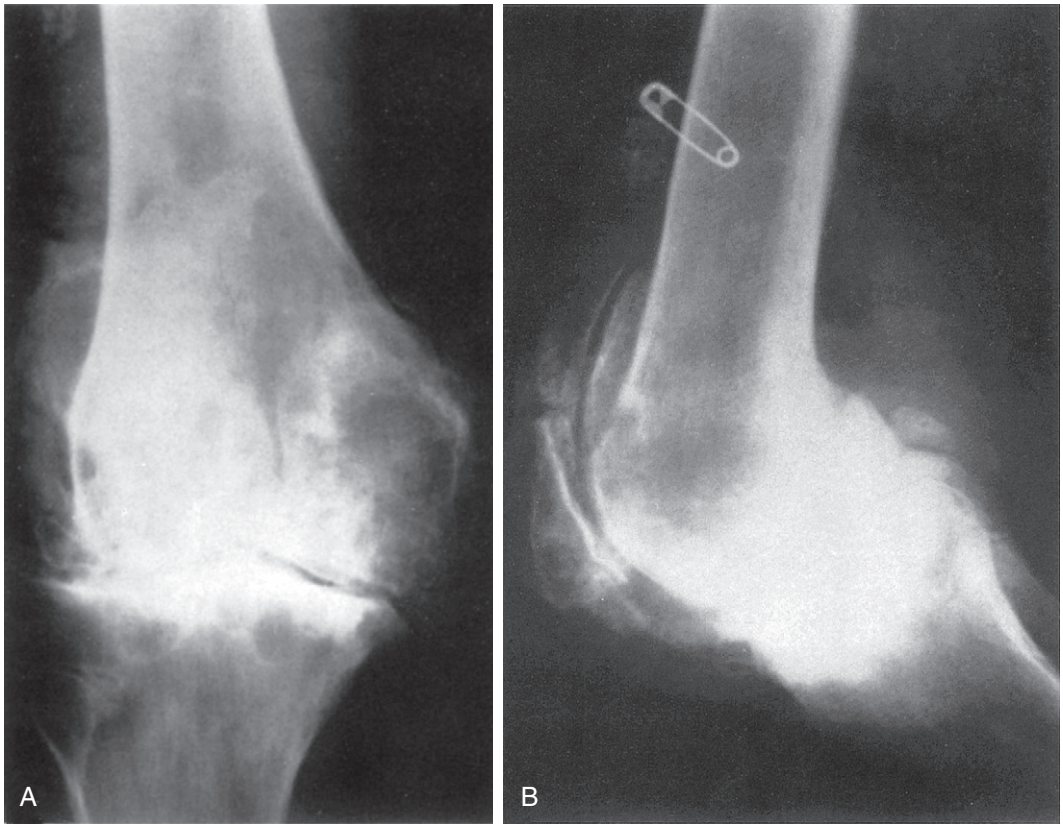

FIGURE 5-13. Anteroposterior (**A**) and lateral (**B**) views of a knee in a patient with CPPD arthropathy. There is extensive eburnation, massive osteophytosis, fragmentation, and osseous debris. The appearance suggests a neuropathic knee.

NORMAL JOINT SPACE

As in the hip, there are four common disorders of the knee joint that do not cause actual loss of the joint until late in the disease. These are osteonecrosis, osteochondritis dissecans, synovial osteochondromatosis, and pigmented villonodular synovitis (PVNS).

Osteonecrosis (Figs. 5-14 to 5-16)

Osteonecrosis of the femoral condyle has long been recognized as occurring in certain diseases, such as systemic lupus erythematosus, and as a complication of steroid therapy. Only recently has it been recognized as a relatively common idiopathic disorder in the elderly. Since it is a disease process of the femoral condyle, initially the joint itself is not affected. First detection of this disorder is usually made through bone scintigraphy or magnetic resonance (MR) imaging (see Chapter 1). Radiographically one initially sees ill-defined areas of lucency and bone repair in the involved condyle (Fig. 5-14). A subchondral lucency and displacement of the cortical fragment inward are pathognomonic of osteonecrosis (Fig. 5-15). As the disease progresses, there is marked deformity to the femoral condyle (Fig. 5-16); only in the late phases does secondary osteoarthritis develop. Although either condyle may be affected, it occurs more commonly in the medial condyle.

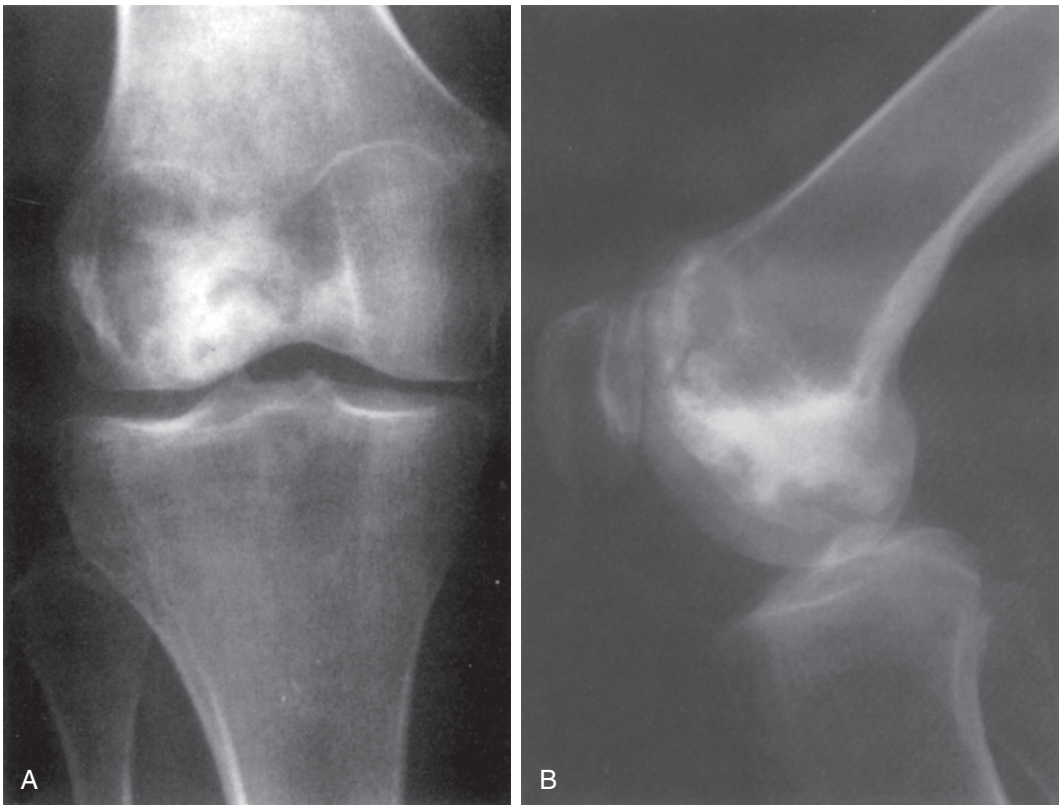

FIGURE 5-14. AP (**A**) and lateral (**B**) views of the knee with osteonecrosis of the lateral femoral condyle. The joint space is maintained. The radiographic abnormalities are identified as ill-defined areas of lucency and bone repair.

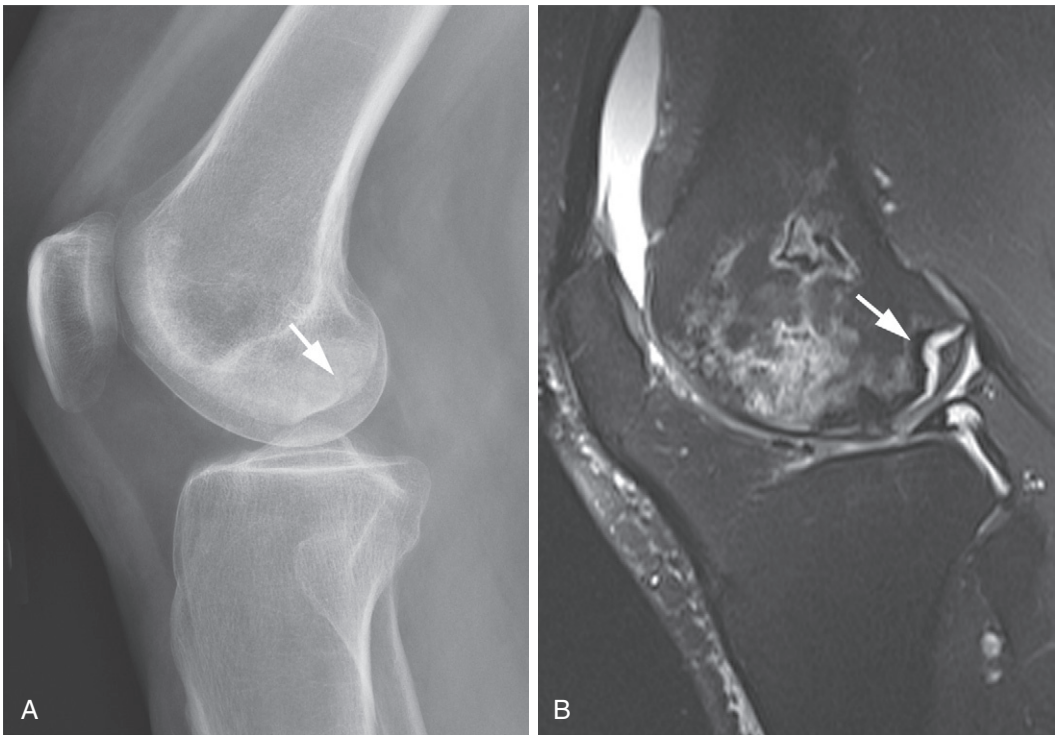

FIGURE 5-15. Lateral view of the knee (**A**) shows collapse of the articular surface of the lateral femoral condyle (*arrow*). Sagittal fat suppressed protien weighted MR image (**B**) shows fluid signal extending through subchondral fracture of the lateral femoral condyle. Note the curvilinear lines of high and low signal in the adjacent epiphysis. These are pathognomonic radiological signs of osteonecrosis.

FIGURE 5-16. AP standing view of the knee in a patient with systemic lupus erythematosus. Lateral condyle is markedly deformed secondary to osteonecrosis. The lateral tibiofemoral compartment are minimally narrowed.

Osteochondritis Dissecans (Fig. 5-17)

Osteochondritis dissecans is a disorder of people who are relatively young. It is an osteochondral fragment and defect seen in the lateral anterior aspect of the medial femoral condyle. It is a result of chronic repetitive trauma to an area of normal irregular ossification during growth. The bone part of the fragment may be identified within the defect or free within the joint; also, it may not be visualized at all owing to resorption. However, the cartilage part of the fragment is present and may be imaged by MR imaging. The defect in the femoral condyle has a relatively well-defined sclerotic border. This definition and location distinguish osteochondritis dissecans from osteonecrosis of the femoral condyle.

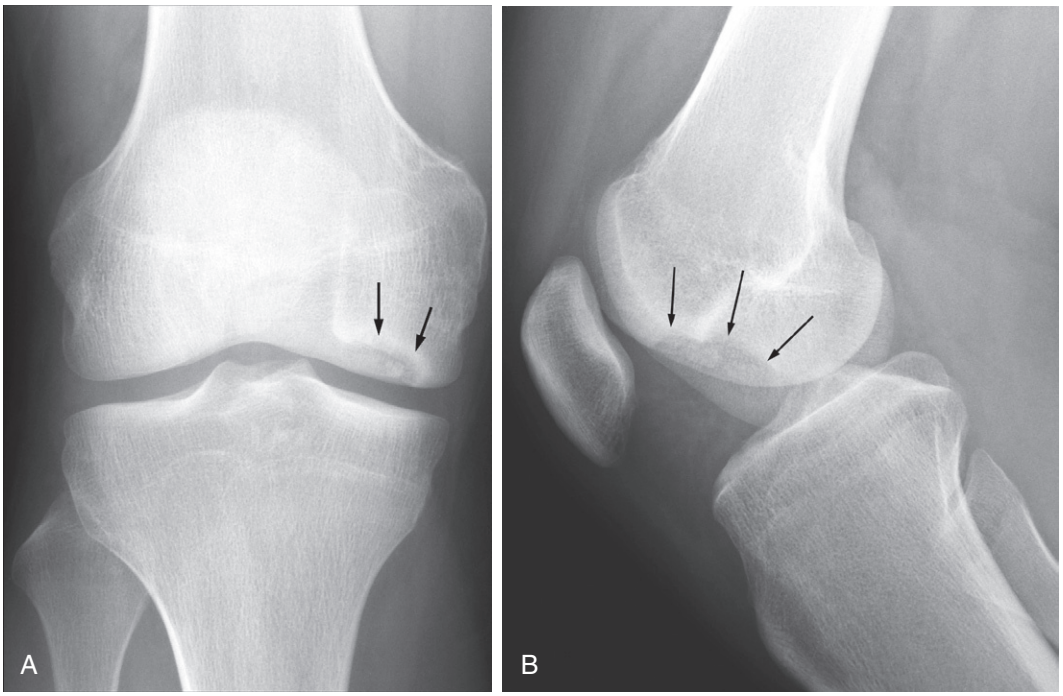

FIGURE 5-17. AP (**A**) and lateral (**B**) views of the knee of a patient with osteochondritis dissecans. A well-defined defect with a sclerotic border is seen in the lateral anterior aspect of the medial condyle (*arrows*). The osteochondral fragment is faintly delineated. An MR image may better characterize the status of the fragment.

Synovial Osteochondromatosis (Fig. 5-18)

As with the hip, there is no difficulty in making the diagnosis of synovial osteochondromatosis radiographically if the chondroid bodies are ossified sufficiently to be recognized. However, if the bodies are not ossified, then the clinical history must be used to suggest the diagnosis. The knee joint with its surrounding bursae and recesses is far more expansile than the hip joint. Therefore, the bones within the joint will not be affected except to develop secondary mechanical osteoarthritis. If the clinical history suggests the diagnosis and the chondroid bodies cannot be identified on the radiograph, MR imaging should be performed (see Chapter 1).

FIGURE 5-18. Lateral view of a knee with synovial osteochondromatosis. Multiple ossific bodies are seen throughout the knee joint.

Pigmented Villonodular Synovitis

The knee is the most common joint involved in PVNS. The joint space tends to be maintained until late in the disease. PVNS tends to cause joint space narrowing in one compartment of the knee rather than the entire knee. Cystic changes develop in both the tibia and the adjacent femur. There is little evidence of bone repair or osteophyte formation. The patient's age and single joint involvement will suggest the diagnosis; MR imaging will confirm it (see Chapter 1).

SUGGESTED READINGS

Butt WP: Radiology of the infected joint, *Clin Orthop Relat Res* 96:136–139, 1973.

Gilbert M, Cockin J: An evaluation of the radiological changes in haemophilic arthropathy of the knee. In Ala F, Dense WE, editors: *Proceedings of the 7th Congress of the World Federation of Haemophilia*, Amsterdam, 1973, Excerpta Medica, p 191.

Goldman AB: Some miscellaneous joint diseases, *Semin Roentgenol* 17:60–80, 1982.

Lagier R: Femoral cortical erosions and osteoarthrosis of the knee in chondrocalcinosis: An anatomo-radiological study of two cases, *Fortschr Geb Rontgenstr Nuklearmed* 120:460–467, 1974.

Martel W, Holt JF, Cassidy JT: Roentgenologic manifestations of juvenile rheumatoid arthritis, *AJR Am J Roentgenol Radium Ther Nucl Med* 88:400–423, 1962.

Milgram JW: Radiological and pathological manifestations of osteochondritis dissecans of the distal femur: A study of 50 cases, *Radiology* 126:305–311, 1978.

Resnick D, Niwayama G: The "target area" approach to articular disorders: A synopsis. In Resnick D, Niwayama G, editors: *Diagnosis of bone and joint disorders*, ed 3, Philadelphia, 1995, W.B. Saunders.

Resnick D, Niwayama G, Goergen TG, et al: Clinical, radiographic and pathologic abnormalities in calcium pyrophosphate dihydrate deposition disease (CPPD): Pseudogout, *Radiology* 122:1–15, 1977.

Scott PM: Bone lesions in pigmented villonodular synovitis, *J Bone Joint Surg Br* 50:306–311, 1968.

Thomas R, Resnick D, Alazraki NP, et al: Compartmental evaluation in osteoarthritis of the knee, A comparative study of available diagnostic modalities, *Radiology* 116:585–594, 1975.

Williams JL, Cliff MM, Bonakdarpour A: Spontaneous osteonecrosis of the knee, *Radiology* 107:15–19, 1973.

Zimmerman C, Sayegh V: Roentgen manifestations of synovial osteochondromatosis, *AJR Am J Roentgenol Radium Ther Nucl Med* 83:680–686, 1960.

Approach to the Shoulder 6

Pain in the shoulder is a common problem affecting all ages of the general population. It is the second most common cause of musculoskeletal pain. Radiographic diagnosis of the disease entity causing nonspecific pain begins with evaluation of how the shoulder joint has been affected. There are three areas in the shoulder joint to be observed: (1) the glenohumeral joint, (2) the subacromial space, and (3) the acromioclavicular joint.

GLENOHUMERAL JOINT INVOLVEMENT

Narrowing of the glenohumeral joint space with lack of involvement of the acromioclavicular (AC) joint or the subacromial space is usually accompanied by radiographic changes of osteoarthritis. It must be remembered that although the shoulder is not a weight-bearing joint, mechanical contact forces across the joint can actually be quite high with lifting of any weight. Primary osteoarthritis of the shoulder can be seen particularly in elderly women. However, because osteoarthritic changes of the glenohumeral joint are relatively rare, the primary underlying abnormality in the cartilage must be considered. This abnormality may be disruption, deformity, or deposition.

Disruption of the cartilage can occur either in chronic repetitive trauma, such as recurrent dislocations, or in late-stage osteonecrosis. In the posttraumatic shoulder, a Hill-Sachs deformity, a "trough sign," or a Bankart lesion may be identified in addition to the glenohumeral joint space narrowing and osteoarthritic changes. In late-stage osteonecrosis, the humeral head will be flattened and often fragmented.

Distortion of the underlying cartilage occurs in epiphyseal dysplasia or dysplasia of the scapular neck. In both instances the glenohumeral joint space narrowing and osteoarthritic changes will be superimposed on a recognizably dysplastic humeral head or flattened glenoid (Fig. 6-1).

FIGURE 6-1. Axillary view of the shoulder. There is osteophyte and subchondral cyst formation involving the posterior glenoid, which is dysplastic and retroverted.

Deposition of a foreign substance into the cartilage is the most common cause of cartilage degeneration. This is observed in calcium pyrophosphate dihydrate (CPPD) crystal deposition disease, acromegaly, and ochronosis. The most common of these is CPPD crystal deposition disease.

CPPD Crystal Deposition Disease (Fig. 6-2)

Observation of osteoarthritis involving both glenohumeral joints in a patient strongly suggests CPPD arthropathy. Early, before the joint is narrowed, chondrocalcinosis may be identified. With glenohumeral joint space narrowing, one will see subchondral sclerosis, osteophytosis, and occasionally cyst formation. The osteophyte will be seen best on the external rotation anteroposterior (AP) view. One may be able to identify calcification in the cartilage of the AC joint or glenohumeral joint, making the diagnosis more definitive.

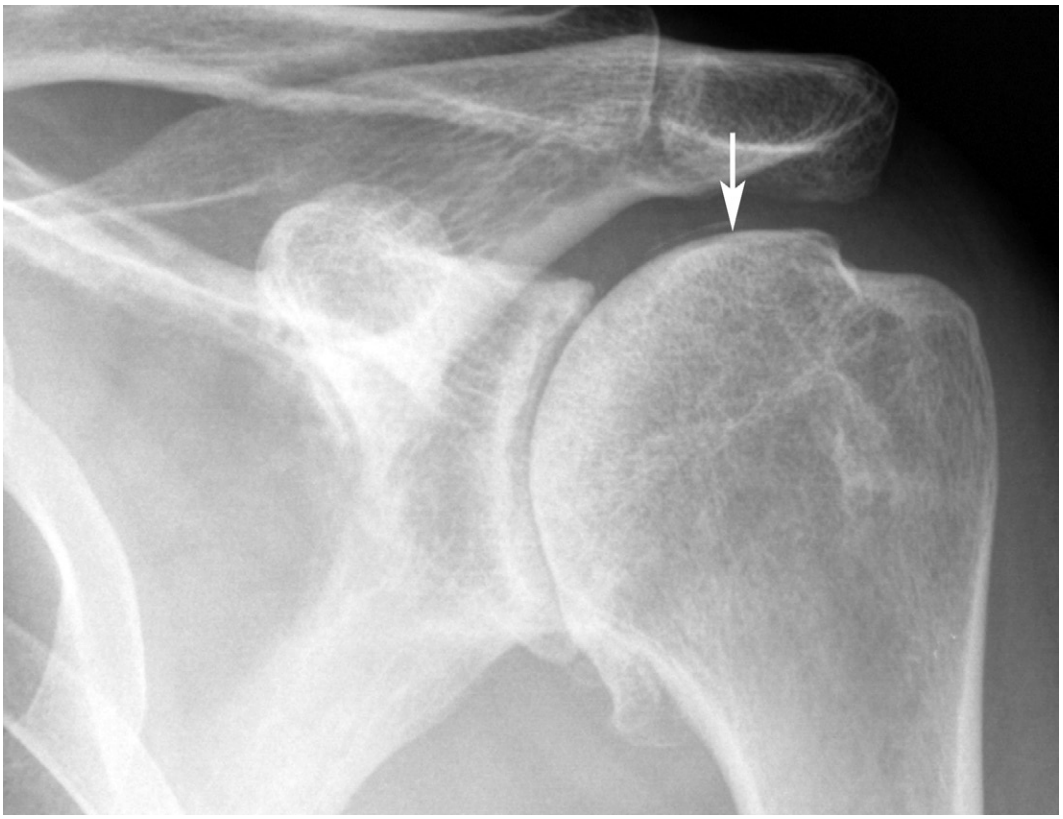

FIGURE 6-2. AP view of the shoulder of patient with CPPD arthropathy. There is narrowing of the glenohumeral joint space with preservation of the subacromial and AC joint spaces. A huge medial osteophyte is identified on the humeral head. There is subchondral sclerosis of both the humeral head and the glenoid. Chondrocalcinosis is seen in the superior humerus (see arrow).

SUBACROMIAL SPACE INVOLVEMENT

Isolated loss of the subacromial space occurs in a chronic rotator cuff tear and in certain positions in the shoulder impingement syndrome. If there is less than 7 mm between the undersurface of the acromion and the top of the humeral head, this space is considered narrowed.

Chronic Rotator Cuff Tear (Figs. 6-3 and 6-4)

The glenohumeral joint space is initially preserved. The humeral head appears superior to its normal articulation with the glenoid, and the space between the acromion and humeral head measures less than 7 mm (Fig. 6-3). There is osseous erosion of the undersurface of the acromion, with adjacent bone sclerosis. There may be sclerosis of the articulating humeral head as well. These radiographic changes are seen only in a chronic tear. There are no plain film findings in an acute rotator cuff tear; the radiographic diagnosis must be made through another modality, such as computed tomography (CT) arthrography, ultrasonography, or magnetic resonance (MR) imaging.

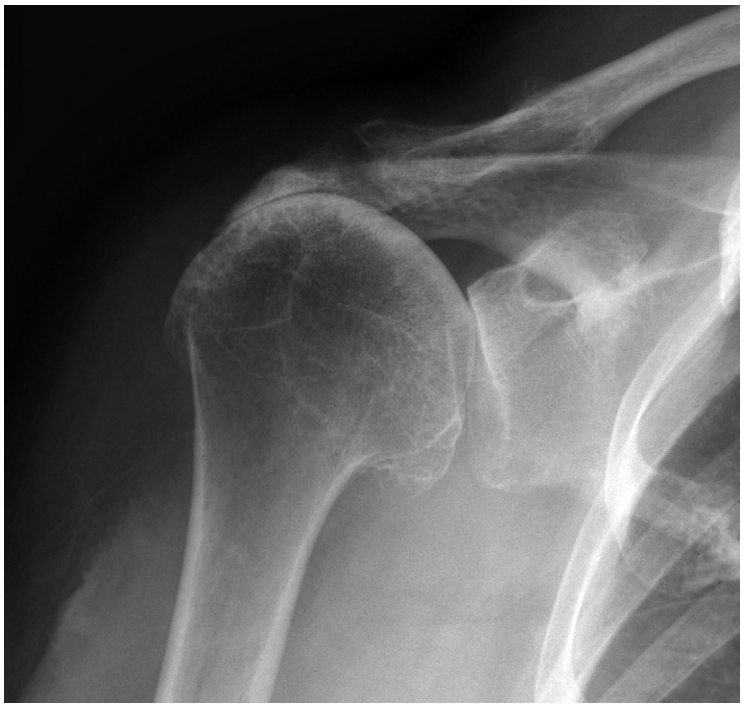

FIGURE 6-3. AP view of the shoulder demonstrating changes of a chronic rotator cuff tear. The humeral head abuts and remodels the undersurface of the acromion and clavicle. There is glenohumeral joint space osteoarthritis.

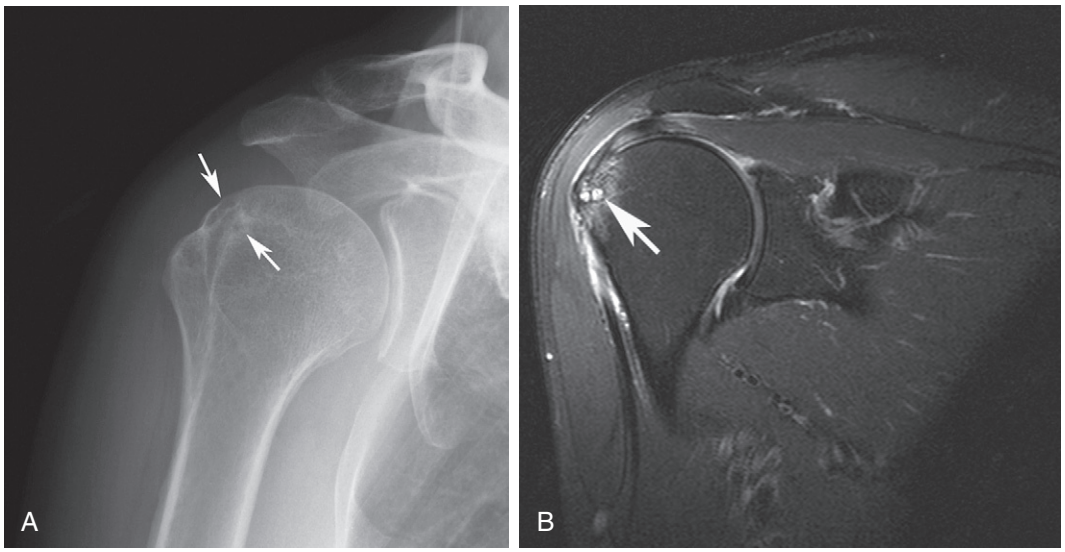

FIGURE 6-4. A, Posterior oblique view of the shoulder shows subcortical cysts in the anterior greater tuberosity (*arrows*). **B,** Coronal fat-suppressed T2-weighted image shows subcortical cysts (*arrow*) and tendinopathy in the adjacent anterior supraspinatus tendon.

Indicators of rotator cuff tendon disease are subcortical cyst formation and cortical irregularity of the greater tuberosity (Fig. 6-4). These findings are only manifestations of rotator cuff degeneration and are not specifically associated with rotator cuff tear as is narrowing of the humeral acromial space.

Shoulder Impingement Syndrome (Figs. 6-5 and 6-6)

In the shoulder impingement syndrome, pain is caused when the periarticular soft tissues, such as the rotator cuff, biceps tendon, or subacromial bursa, are trapped between the greater tuberosity of the humeral head and the coracoacromial ligamentous arch. Pain is produced on abduction or elevation of the externally rotated arm. On the normal AP view of the shoulder, bone excrescences are seen on the undersurface of the acromion (Fig. 6-5). These excrescences may be better visualized on an AP view in which the tube is angled 30 degrees caudally. Often there is some flattening, bone sclerosis, and bone proliferation at the greater tuberosity. If the shoulder is radiographed in external rotation and abduction, the greater tuberosity appears to abut the acromion (Fig. 6-6). Frequently, a coexistent chronic rotator cuff tear is present.

FIGURE 6-5. AP view of the shoulder in external rotation showing shoulder impingement syndrome. The glenohumeral joint space is preserved. The subacromial joint space appears preserved. There is a bone excrescence seen on the undersurface of the acromion (*arrows*). There is adjacent sclerosis of the acromion. There is some flattening of the greater tuberosity where the rotator cuff attaches (*arrowhead*).

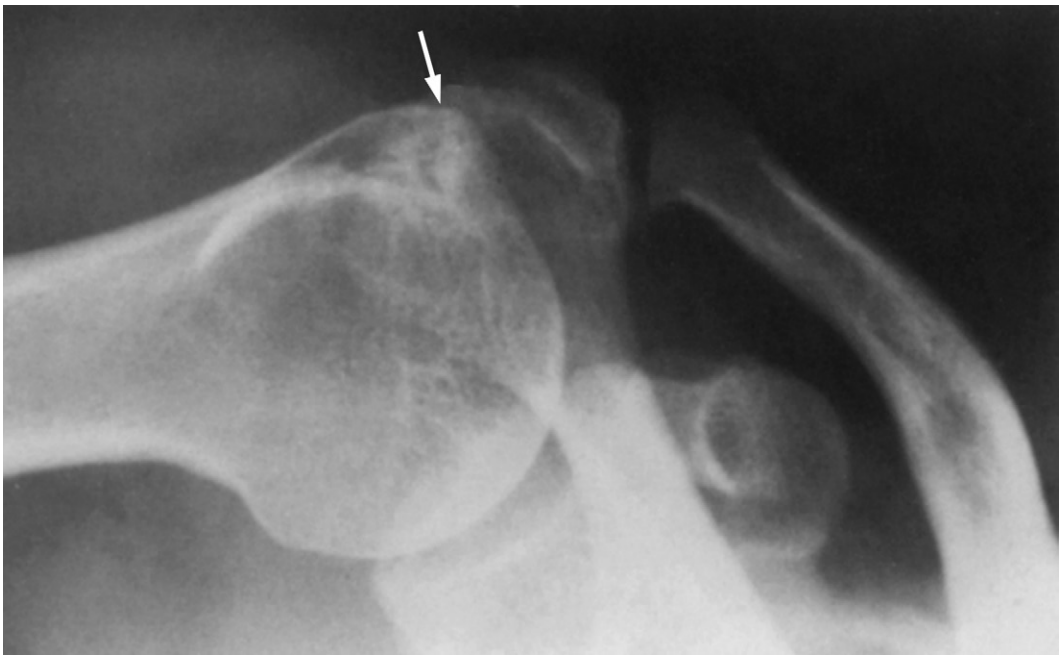

FIGURE 6-6. AP view of the shoulder positioned in external rotation and abduction. The glenohumeral joint space is preserved. The greater tuberosity abuts the acromion. There is flattening and bone sclerosis of the greater tuberosity (*arrow*). The findings are consistent with shoulder impingement syndrome.

ACROMIOCLAVICULAR (AC) JOINT INVOLVEMENT

Trauma is the most frequent cause of radiographic changes in the AC joint. Acute trauma may cause not only separation but also lysis of the distal end of the clavicle (Fig. 6-7). Osteoarthritis is the most common radiographic change seen at the AC joint and is believed to be secondary to past or chronic trauma. CPPD arthropathy may involve the AC joint, with calcification of the cartilage and later osteoarthritic changes. Various systemic diseases, such as hyperparathyroidism and scleroderma, will cause resorption of the distal end of the clavicle.

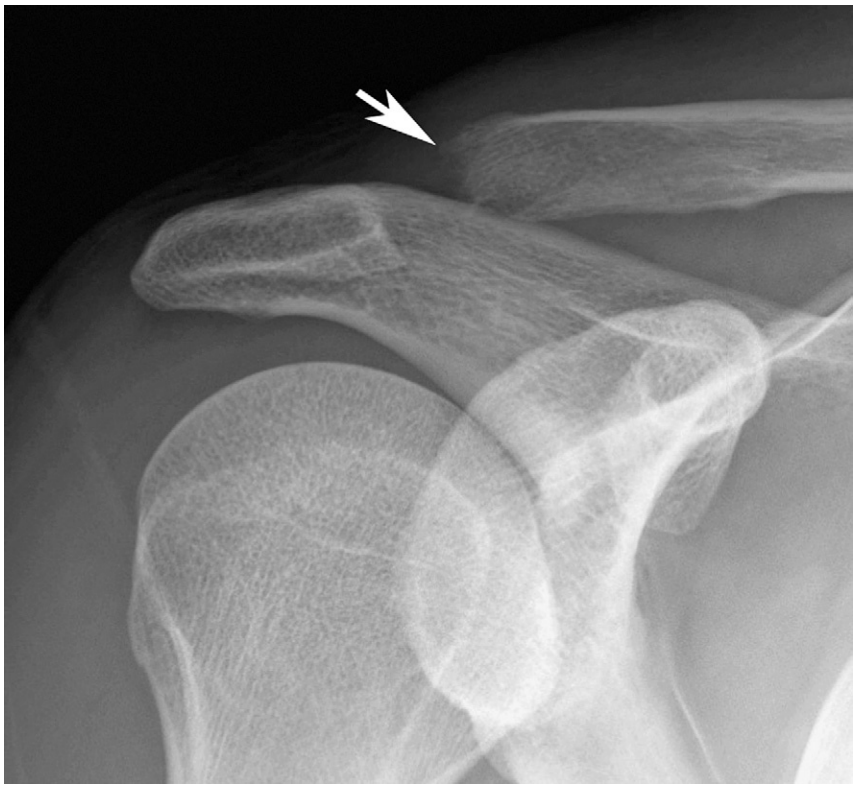

FIGURE 6-7. AP view of the shoulder obtained 3 months following injury to the AC joint. The glenohumeral joint is preserved. The subacromial space is preserved. There is resorption of the distal end of the clavicle (*arrow*).

TOTAL COMPARTMENT INVOLVEMENT

Involvement of the glenohumeral, subacromial, and AC joint spaces indicates an inflammatory arthropathy. However, the specific radiographic changes around these joint spaces distinguish one inflammatory arthropathy from another.

Rheumatoid Arthritis (Fig. 6-8)

When the shoulders are involved in rheumatoid arthritis, they are involved bilaterally and symmetrically. With loss of the glenohumeral joint space, the head moves inwardly; with involvement of the rotator cuff, the humeral head moves superiorly. Generalized osteoporosis is present. If erosions are present, they are usually juxta-articular on the humeral head. Lucencies in the humeral head representing intraosseous extension of synovitis may simulate neoplasm. The distal end of the clavicle may be resorbed. There is no evidence of bone sclerosis or osteophyte formation.

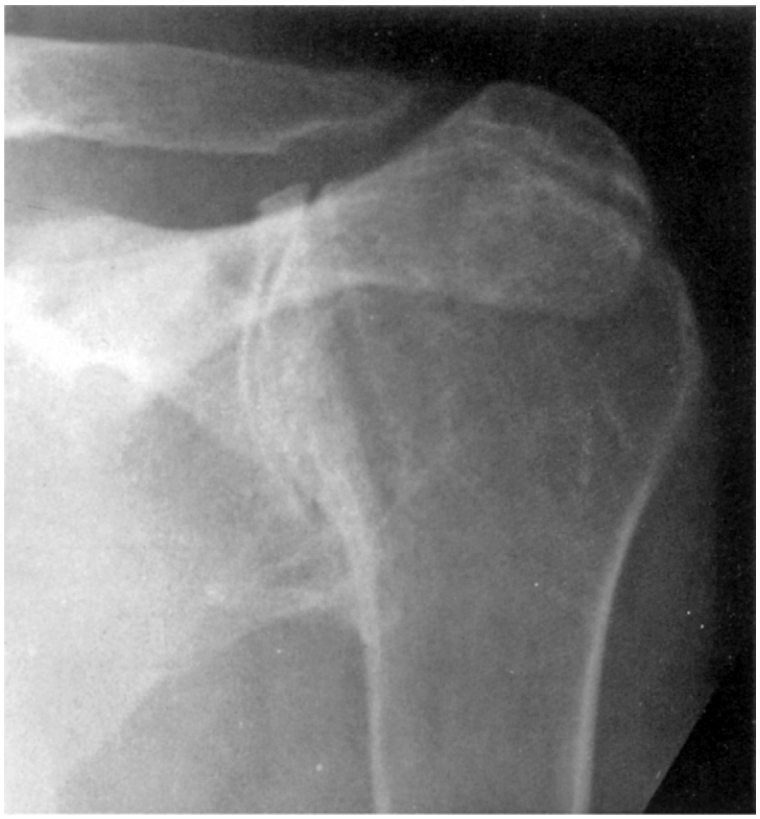

FIGURE 6-8. AP view of the shoulder of a patient with rheumatoid arthritis. There is generalized osteoporosis present. The humeral head has migrated inwardly and superiorly owing to loss of cartilage in the glenohumeral joint and the subacromial joint. There is erosion of the distal end of the clavicle.

Psoriatic Arthritis (Fig. 6-9)

In psoriatic arthritis, the shoulders are involved bilaterally but asymmetrically. The mineralization tends to be maintained. Although there is cartilage loss, erosive disease is usually less prominent than bone proliferation. Ossification occurs at the rotator cuff attachment and the coracoclavicular ligament.

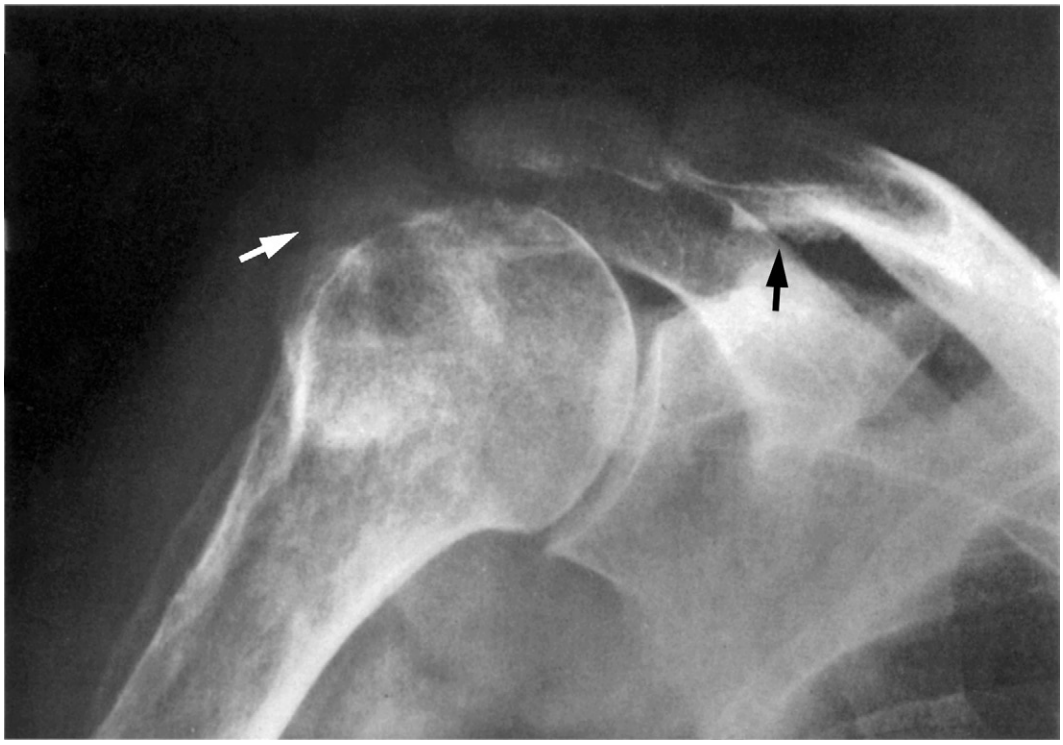

FIGURE 6-9. AP view of the shoulder of a patient with psoriatic arthritis. There is bone proliferation at the rotator cuff attachment and the coracoclavicular ligament (*arrows*). *(From Brower AC: The radiographic features of psoriatic arthritis. In Gerber L, Espinoza L, editors:* Psoriatic arthritis*, Orlando, FL, Grune & Stratton, 1985, p. 125; reprinted by permission.)*

Ankylosing Spondylitis (Fig. 6-10)

The shoulder may be affected in two ways in ankylosing spondylitis. The most common finding is relatively early ankylosis without evidence of erosive disease. However, in some individuals there may be a large erosion of the superolateral aspect of the humeral head, described as a "hatchet" deformity. Ankylosis may be superimposed on this hatchet-like erosion.

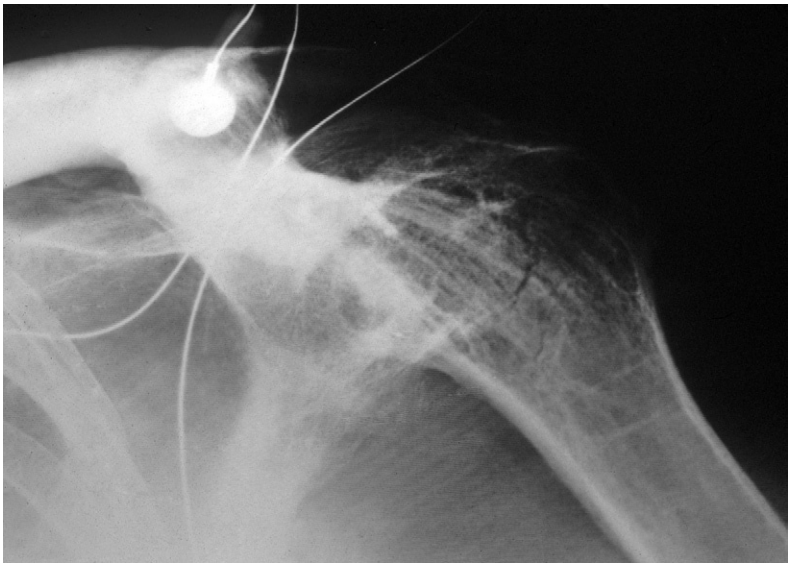

FIGURE 6-10. AP view of the shoulder in long-standing ankylosing spondylitis. The humeral head is ankylosed to the glenoid. There is extensive ossification of the coracoclavicular ligament.

Bleeding Abnormalities (Fig. 6-11)

Although the inflammatory processes cause a loss of all of the potential joint spaces in the shoulder, blood within the joint will initially create a widening of all of the joint spaces visualized. This can be seen after acute trauma, in patients with hemophilia, and in patients placed on anticoagulants. In these cases, the humeral head lies inferiorly and laterally in relation to the glenoid due to combination of acute effusion and deltoid muscle dysfunction. In hemophilia one may detect overgrowth of the humeral head and cystic changes on both sides of the joint secondary to intraosseous bleeding.

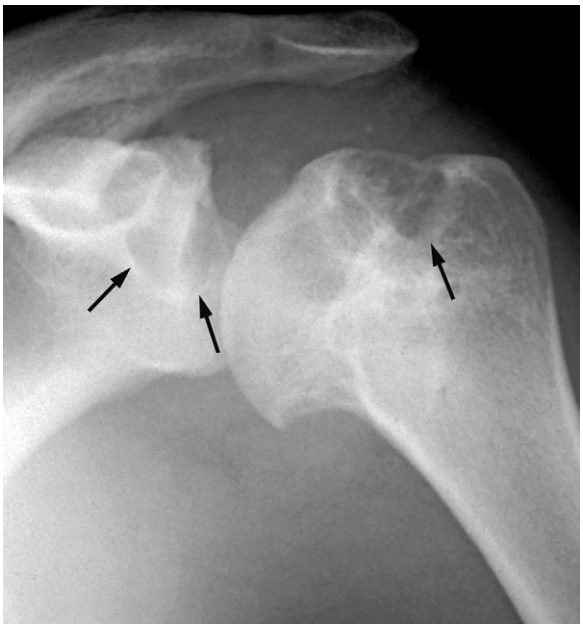

FIGURE 6-11. AP view of the shoulder of a patient with hemophilia. The humeral head has been displaced mildly inferiorly and laterally from its normal articulation with the glenoid. This is secondary to hemarthrosis. There are cystic changes in the glenoid and the humeral head consistent with intraosseous bleeding (*arrows*).

NORMAL JOINT SPACE

Two painful disorders of the shoulders do not cause change in any joint space early on. These are hydroxyapatite deposition disease and osteonecrosis.

Hydroxyapatite Deposition Disease (Figs. 6-12 and 6-13)

Hydroxyapatite deposition disease (HADD), commonly known as calcific tendinitis or bursitis, is the most common cause of shoulder pain. It is present in 40 percent of shoulder pain. It appears as amorphous calcification in one of the tendons surrounding the shoulder joint. One can usually identify which tendon is involved by observing the change in position of the calcification between internal and external rotation views. The calcification may break out of the tendon and deposit in the bursa. Should this happen, the bursa may become inflamed. This inflammation can then lead to erosive changes of the humeral head and acromion and joint destruction. This severe change is known as the "Milwaukee shoulder." Frank intraosseous extension of calcification into the humeral head or anterior proximal humerus (pectoralis major insertion) can mimic neoplasm. Some patients with chronic tendinitis and bursitis have degeneration of the rotator cuff. In such cases, one may see the changes of a chronic rotator cuff tear. Degeneration of the glenohumeral joint space has also been described with secondary osteoarthritis in the late phases of this disease.

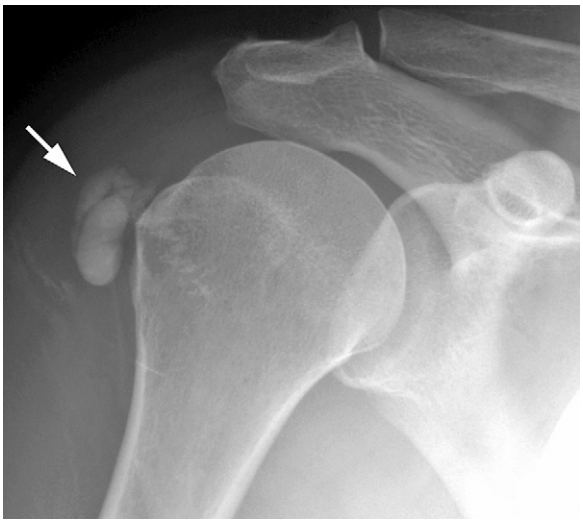

FIGURE 6-12. AP view of the shoulder showing normal glenohumeral, subacromial, and AC joint spaces. There are no significant bone abnormalities. There is a large amorphous calcific deposit seen in the area of the rotator cuff tendon attachments (*arrow*), which is indicative of HADD.

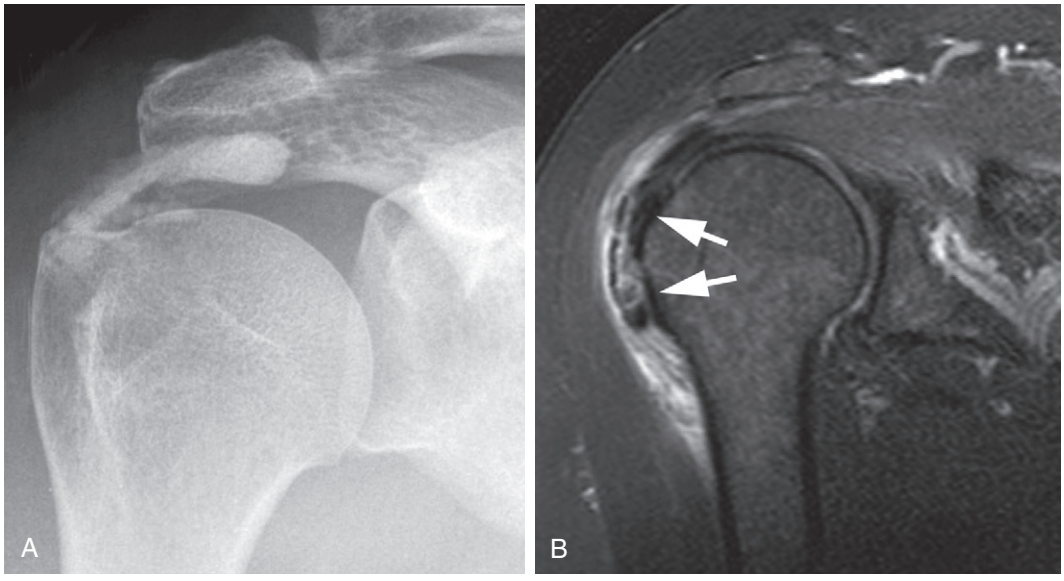

FIGURE 6-13. A, AP view of the shoulder demonstrating amorphous calcification in the rotator cuff attachment and subacromial bursa seen in HADD. **B,** Fat-suppressed T2-weighted coronal image demonstrates HADD as low signal in the tendon and bursa (*arrows*) with surrounding high signal inflammatory changes in the bursa and surrounding soft tissues.

Osteonecrosis (Fig. 6-14)

Osteonecrosis of the shoulder, as with any other joint, is a disorder of the bone and not of the cartilage. Therefore, in the early phases no change occurs in the joint space. The first radiographic manifestation of osteonecrosis is smudging of the trabecular pattern near the articular surface of the humeral head. This is usually followed by a subchondral lucency beneath the articular surface, indicating imminent collapse of the articular bone into the bone beneath. Once collapse has occurred, there is disruption of the cartilage over the humeral head and the appearance of secondary osteoarthritis changes.

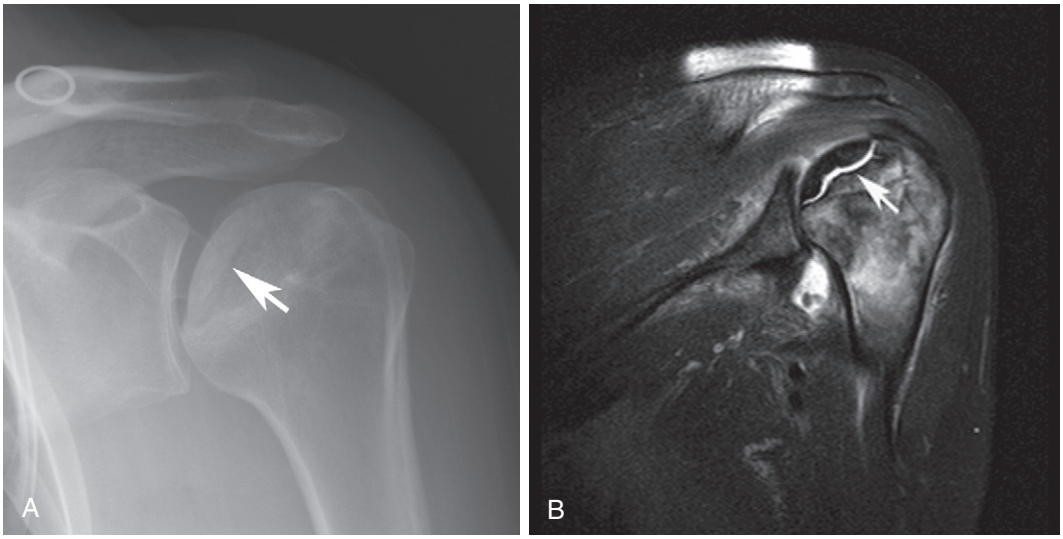

FIGURE 6-14. A, Posterior oblique view of the shoulder demonstrating osteonecrosis. The glenohumeral, subacromial, and AC joint spaces are maintained. There is subchondral bone sclerosis of the humeral head. There is collapse of the articular surface with a subchondral lucency present, indicating a subchondral fracture (*arrow*). **B,** Coronal fat-suppressed T2-weighted image shows fluid signal (*arrow*) in the subchondral fracture. Notice the preserved low signal of fat in the necrotic fragment.

SUGGESTED READINGS

Bonavita J, Dalinka MK, Schumacher HR Jr: Hydroxyapatite deposition disease, *Radiology* 134:621–625, 1980.

Cone RO, Resnick D: Degenerative disease of the shoulder, *Australas Radiol* 28:232–239, 1984.

Cone RO, Resnick D, Danzig L: Shoulder impingement syndrome: Radiographic-evaluation, *Radiology* 150:29–33, 1984.

Fritz LB, Ouellette HA, O'Hanley TA, et al: Cystic changes at supraspinatus and infraspinatus tendon insertion sites: association with age and rotator cuff disorders in 238 patients, *Radiology* 244:239–248, 2007.

Kerr R, Resnick D, Pineda C, Haghighi P: Osteoarthritis of the glenohumeral joint: A radiologic-pathologic study, *AJR Am J Roentgenol* 144:967–972, 1985.

Kotzen LM: Roentgen diagnosis of rotator cuff tear: Report of 48 surgically proven cases, *Am J Roentgenol Radium Ther Nucl Med* 112:507–511, 1971.

McCarty DJ, Halverson PB, Carrera GF, et al: "Milwaukee shoulder"—association of microspheroids containing hydroxyapatite crystals, active collagenase and neutral protease with rotator cuff defects. 1. Clinical aspects, *Arthritis Rheum* 24:464–473, 1981.

Peterson CC Jr, Silbiger ML: Reiter's syndrome and psoriatic arthritis: Their roentgen spectra and some interesting similarities, *Am J Roentgenol Radium Ther Nucl Med* 101:860–871, 1967.

Petersson CJ, Redlund-Johnell I: Joint space in normal gleno-humeral radiographs, *Acta Orthop Scand* 54(2):274–276, 1983.

Resnick D: Patterns of peripheral joint disease in ankylosing spondylitis, *Radiology* 110:523–532, 1974.

Sbarbaro JL: The rheumatoid shoulder, *Orthop Clin North Am* 6:593–596, 1975.

7 The Sacroiliac Joint

The sacroiliac (SI) joint is perhaps the most difficult joint in the skeleton to image adequately to make an accurate diagnosis of a disorder affecting it. This is partially due to obscuration of the joint by multiple overlying soft tissue structures and variations in the obliquity of the joint within an individual and among individuals. A modified anteroposterior (AP) Ferguson view (see Chapter 1) is the most useful view to eliminate the confusing soft tissue shadows and to profile that part of the joint that is affected by all disease processes.

The SI joint consists of two parts: (1) the true joint and (2) the ligamentous attachment between the two adjacent bones (Fig. 7-1). The anteroinferior one third of the SI joint is a true synovial joint. The posterosuperior one third is fibrous. The transition between the true synovial and fibrous components of the joint is a region of complex anatomic variation that includes developmental defects in the articular cartilage. The iliac side is covered by fibrous cartilage that is 1 mm thick; the sacral side is covered by hyaline cartilage that varies from 3 mm to 5 mm in thickness. Owing to the thinness of the cartilage on the iliac side compared to the sacral side, all disease processes involve the iliac side first and the sacral side second. The cartilage-covered area is surrounded by synovium. The posterosuperior portion of the SI joint is nothing more than a cleft between the sacrum and the ilium. There is no cartilage covering either bone in this area. Intraosseous ligaments extend between the sacrum and ilium, joining the two bones together. The AP modified Ferguson view images the anteroinferior-most aspect of the SI joint, which is the area where disease first begins.

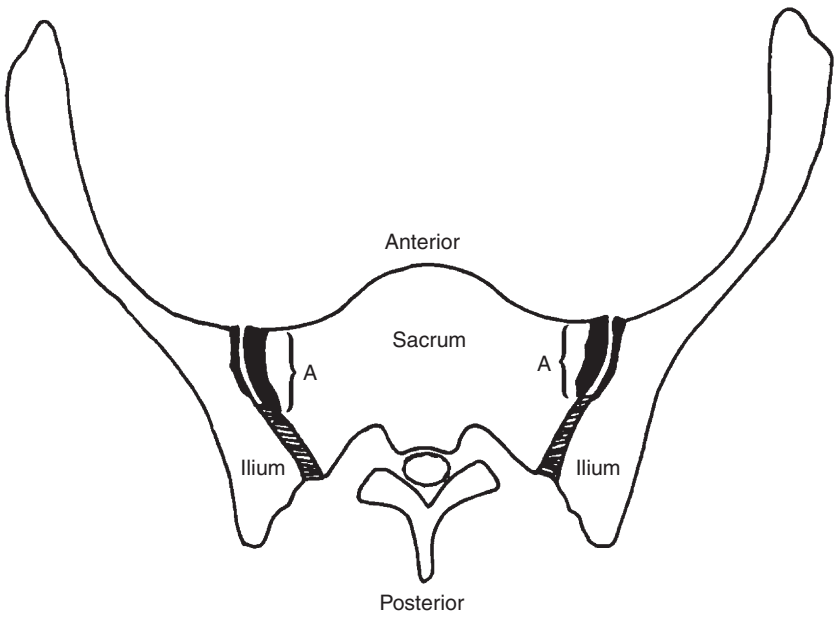

FIGURE 7-1. Anatomical drawing of the SI joints as viewed in an axial plane. The true synovial joint (**A**) is seen as the anterior one third of the cleft between the two bones. Note that the cartilage on the iliac side is thinner than the cartilage on the sacral side. The posterior portion of the cleft has no cartilage or synovium. Intraosseous ligaments join the sacrum to the ilium.

The obliquity of the SI joint varies from person to person. Therefore, no two individuals have identical-appearing SI joints. There are two criteria for determining normality of an SI joint. First, although the width of the SI joint varies from person to person according to the thickness of the cartilage on the sacral side, the SI joint should be of uniform width within the individual. Second, the white cortical line along the iliac and sacral side should be intact (Fig. 7-2). If these criteria are not met, then the SI joint must be considered abnormal. The diagnosis of disease involving the sacroiliac joint depends upon observing the following: (1) the width of the joint space, (2) the presence and type of erosions, (3) the presence and type of sclerosis, (4) the presence and type of bone bridging, and (5) the distribution of these changes.

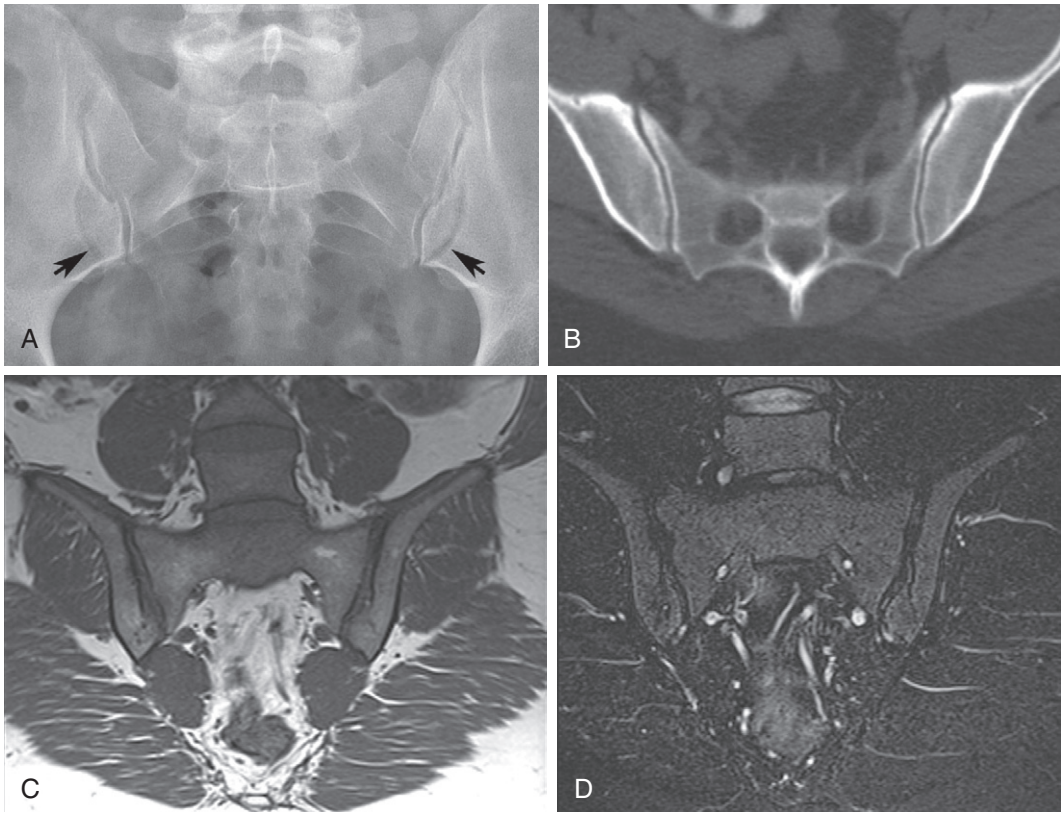

FIGURE 7-2. **A,** Normal AP view and **B,** computed tomography of the SI joints. Notice that the joint is of uniform width and the white cortical line (*arrows*) along the joint margins is intact. The anterior aspect of the joint (*arrow*) projects lateral to the posterior joint. Normal joint margins are thin bands of low signal on T1-weighted (**C**) and fat-suppressed T2-weighted (**D**) magnetic resonance images.

WIDTH OF THE JOINT SPACE

Apparent widening of the SI joint is observed with infection and the inflammatory spondyloarthropathies. Uniform narrowing of the SI joint is observed in rheumatoid arthritis. Irregularity of the width of the SI joint, where some parts are too narrow and other parts are too wide, is observed in the crystalline arthropathies and in osteoarthritis.

PRESENCE AND TYPES OF EROSIONS

Erosions are present in all of the inflammatory arthropathies. Small and succinct erosions tend to be present in ankylosing spondylitis and rheumatoid arthritis, whereas large and extensive erosions tend to be present in psoriatic, reactive, and septic arthritis. A large erosion may occur in gout, but it will have a sclerotic, well-defined border as opposed to the ill-defined border seen in the inflammatory arthropathies. Erosions are not seen in calcium pyrophosphate dihydrate (CPPD) crystal deposition disease or osteoarthritis.

PRESENCE AND TYPE OF SCLEROSIS

Reparative bone is seen behind or adjacent to erosive changes. This sclerosis tends to be minimal in ankylosing spondylitis and much more extensive in reactive, psoriatic, and septic arthritis. Reparative bone is seen in CPPD arthropathy, gout, and osteoarthritis. This sclerosis abuts the articular surface, usually at the inferior and superior aspects of the true joint. Sclerosis is seen in a wedge-shaped configuration on the iliac side of the SI joint in osteitis condensans ilii. The widest part of the wedge in osteitis condensans ilii is along the inferior aspect of the ilium.

PRESENCE AND TYPE OF BONE BRIDGING

There are two types of bone bridging: (1) a true bone ankylosis of the joint itself and (2) anterior osteophyte formation bridging across the ilium to the sacrum anterior to the joint. Bone ankylosis is seen in the inflammatory arthropathies and in septic arthritis. Anterior osteophyte formation is seen in the crystalline arthropathies and osteoarthritis.

DISTRIBUTION OF CHANGES

Disease entities are unilateral, bilateral and symmetrical, or bilateral and asymmetrical. Septic arthritis is almost always unilateral. Ankylosing spondylitis, spondylitis associated with bowel disease, CPPD arthropathy, and osteitis condensans ilii tend to be bilateral and symmetrical. Psoriatic arthritis, reactive arthritis, gout, and osteoarthritis tend to be bilateral and asymmetrical.

RADIOGRAPHIC CHANGES IN SACROILIAC JOINT DISORDERS

Generalized Inflammatory Disease

The most significant disorders of the SI joint are the inflammatory ones. Therefore, knowledge of radiographic changes occurring in these disorders is important. All of the inflammatory disease processes affect the SI joint in a specific sequence, varying only in degree of change within the sequence. Erosive changes begin on the iliac side of the SI joint. The earliest change observed is poor definition or loss of the white cortical line on the iliac side (Fig. 7-3). As the erosive disease progresses, the SI joint becomes apparently widened (Fig. 7-4). The body then responds by laying down reparative bone behind the erosive changes (Fig. 7-5). The reparative process then becomes the dominant part of the radiographic picture. Following this, bone ankylosis occurs across the SI joint (Fig. 7-6). Once the SI joint is ankylosed, the surrounding bone becomes osteoporotic secondary to loss of normal mechanical stress across the SI joint (Fig. 7-7). Although each inflammatory disease process goes through this sequence of events, disease entities can be distinguished through their extent and distribution of involvement. Specific disorders of the SI joints and their distinguishing radiographic characteristics are now illustrated and discussed.

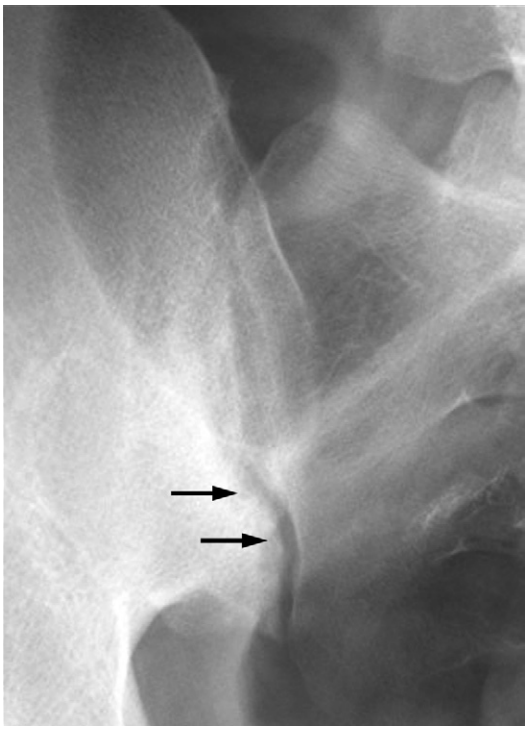

FIGURE 7-3. AP Ferguson view of the SI joint. The white cortical line is intact on the sacral side. It is ill-defined on the iliac side (*arrows*).

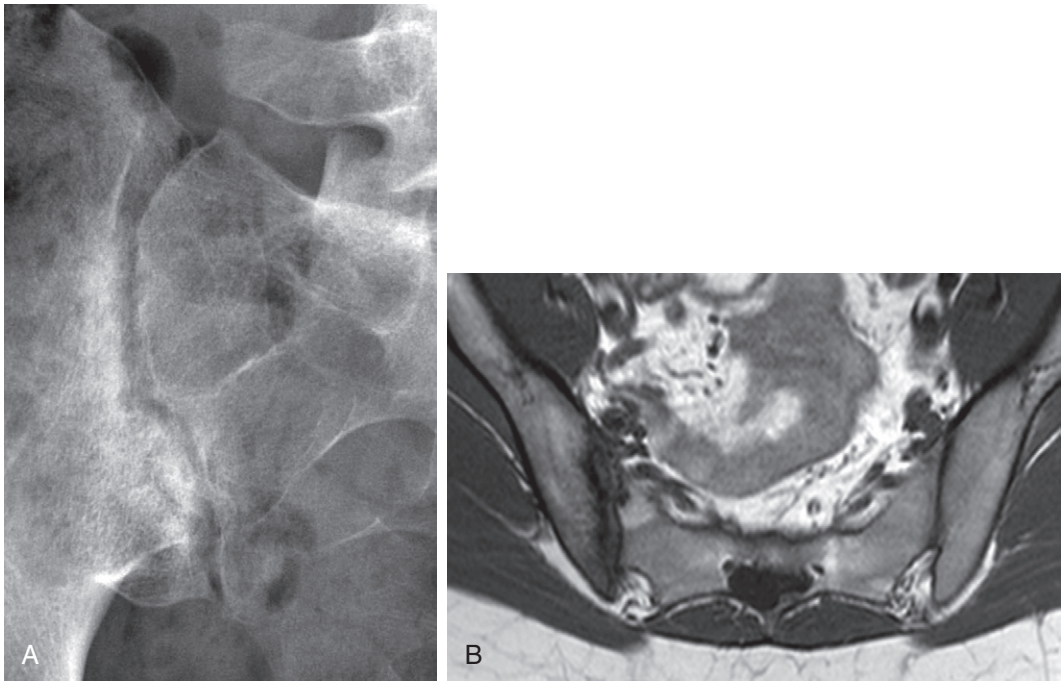

FIGURE 7-4. (**A**) AP view and (**B**) T1-weighted MR image of the SI joint showing erosion on the iliac side giving an appearance of widening of the joint. Notice that the cortical line on the sacral side is intact.

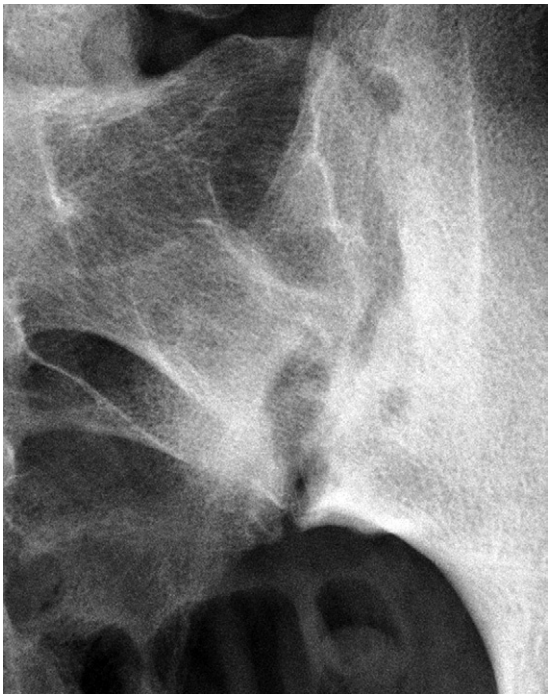

FIGURE 7-5. AP view of an SI joint showing extensive erosive changes on both the iliac and sacral sides. There is extensive bone repair behind the erosive changes on both sides.

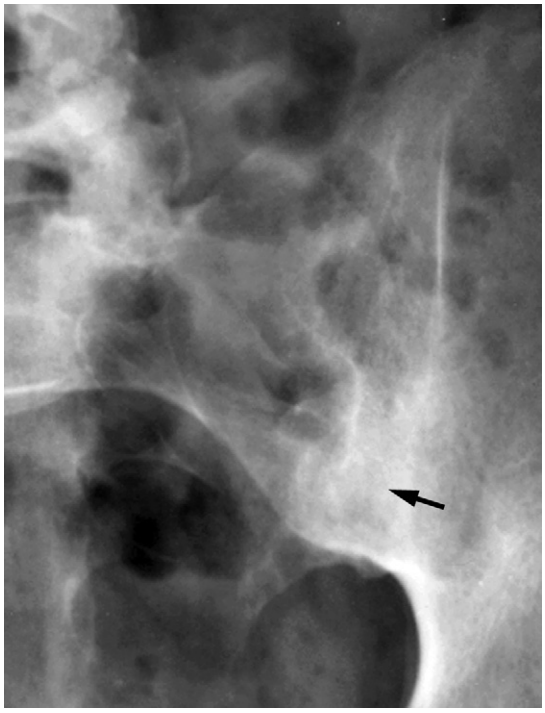

FIGURE 7-6. AP Ferguson view of the SI joint showing bone ankylosis (*arrow*) across the SI joint.

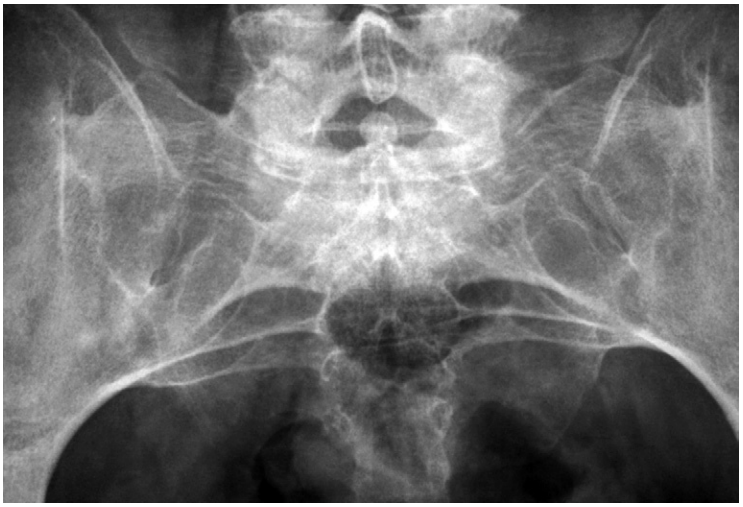

FIGURE 7-7. AP view of the SI joints showing total bone ankylosis across the joints and secondary osteoporosis.

Ankylosing Spondylitis (Figs. 7-8 and 7-9)

The first radiographic change observed in ankylosing spondylitis is found in the SI joints. It involves the joints bilaterally and symmetrically. The erosions appear to be small and succinct, presenting an edge that has been likened to the perforated edge of a postage stamp (Fig. 7-8). The amount of sclerosis, or bone repair, is also somewhat limited. Rather early in the disease, before the erosions or sclerosis become too extensive, bone ankylosis takes place. The ankylosis occurs not only in the true synovial aspect of the joint but also in the posterosuperior cleft of the joint (Fig. 7-9). Ankylosing spondylitis is an ossifying disease; it will ossify the ligaments that join the sacrum to the ilium in the posterosuperior aspect of the joint. Radiographically this is seen as a "star" with radiations from its center. A similar sequence of changes is observed in the arthropathy associated with bowel disease.

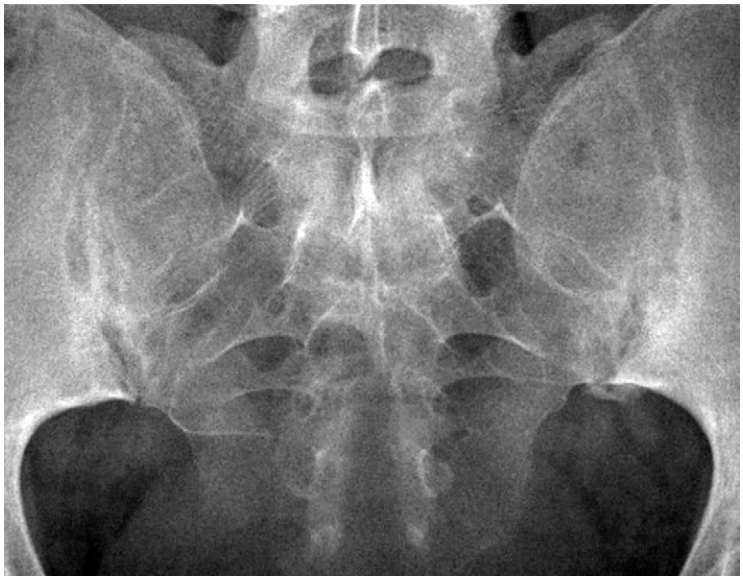

FIGURE 7-8. AP Ferguson view of the SI joints in a patient with ankylosing spondylitis. There is bilateral symmetrical involvement. There are small, succinct erosions involving both sides of the joint, with limited bone repair.

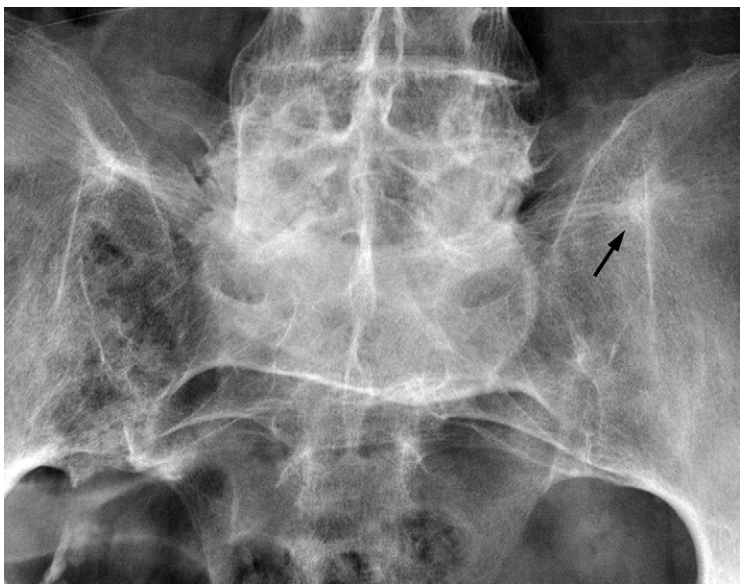

FIGURE 7-9. AP view of the SI joints in longstanding ankylosing spondylitis. Both SI joints are completely ankylosed. A "star" is seen at the superior aspect of the joint (*arrow*) representing ossification of the ligaments between the sacrum and the ilium.

Psoriatic Arthritis and Reactive Arthritis (Figs. 7-10 and 7-11)

One cannot distinguish psoriatic arthritis from reactive arthritis by observing the radiographic changes in the SI joint. Both present involvement of the SI joints in a bilateral and asymmetrical fashion (Fig. 7-10). The erosive component appears to be much more extensive than that seen in ankylosing spondylitis (Fig. 7-11). Likewise, the bone repair is more extensive. Ankylosis may or may not occur, but when it does, it occurs later in the disease process. Because the disease process is usually bilateral and asymmetrical, in the early stages it may present as unilateral involvement that may be subtle. Scintigraphy may be useful in distinguishing true unilateral disease from subtle bilateral, asymmetrical disease (see Chapter 1). However, once the changes become obvious on one side, there should be subtle changes involving the opposite side as well.

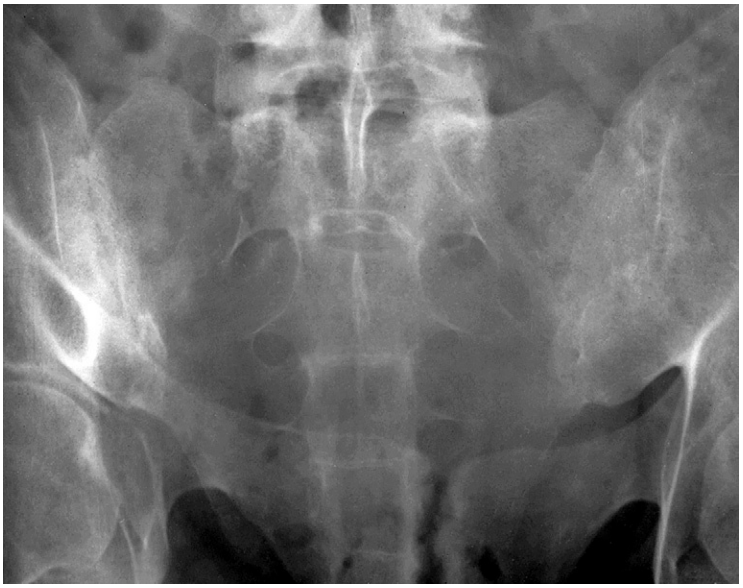

FIGURE 7-10. AP Ferguson view of the SI joints in a patient with psoriatic arthritis. There is bilateral asymmetrical involvement. There is ankylosis of the left SI joint. The right SI joint shows erosive changes with extensive bone repair. Ankylosis is beginning to occur.

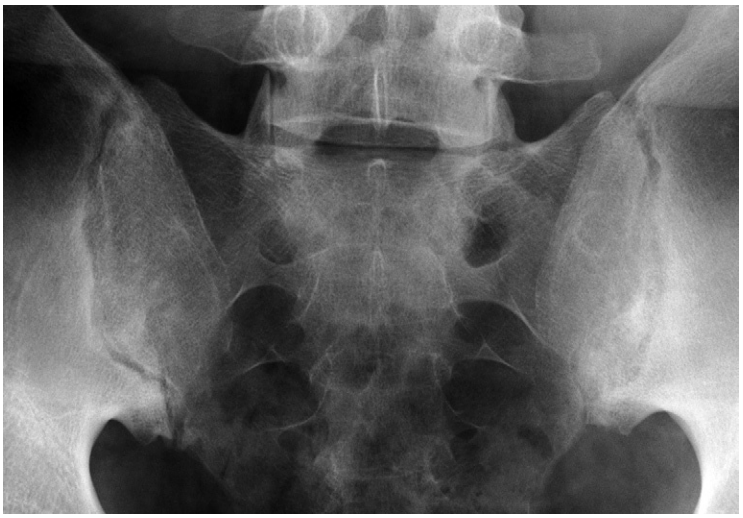

FIGURE 7-11. AP view of the SI joints in a patient with reactive arthritis. There is bilateral asymmetrical involvement. The right SI joint shows small erosive changes with some reparative bone formation. The left SI joint shows more erosive change with extensive bone repair.

Rheumatoid Arthritis (Figs. 7-12 through 7-14)

Rheumatoid arthritis causes symmetrical uniform narrowing of the SI joint with very little reparative bone and no evidence of osteophyte formation (Fig. 7-12). Occasionally erosive disease may be present, but never to the extent of presenting a widened joint space as seen in the spondyloarthropathies (Fig. 7-13). Bone ankylosis may occur, but this will be present in the synovial aspect of the joint only (Fig. 7-14). In contrast to the spondyloarthropathies, there is no ossification of the ligaments connecting the sacrum to the ilium. Involvement of the SI joints occurs late in rheumatoid arthritis and frequently goes unobserved because of the extensive involvement of the appendicular joints.

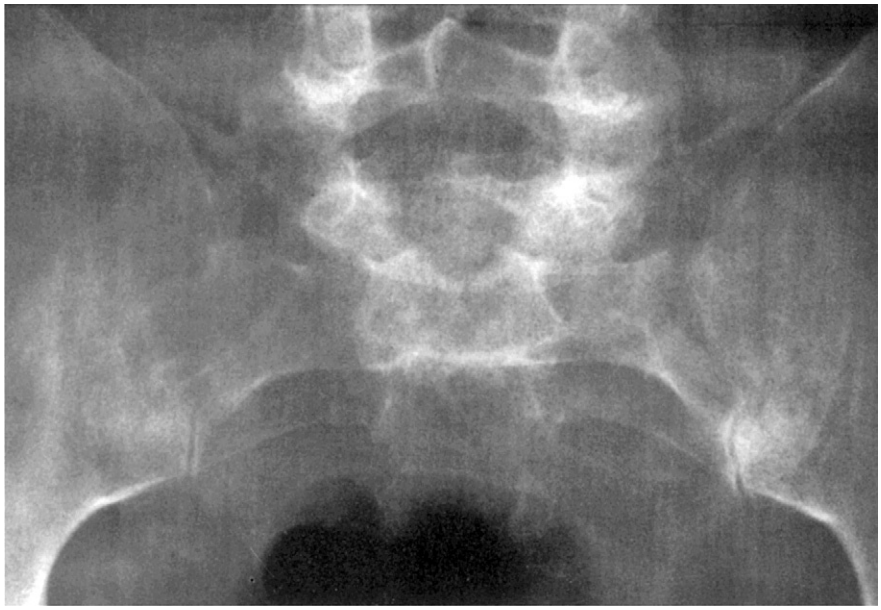

FIGURE 7-12. AP view of the SI joints in a patient with rheumatoid arthritis. There is bilateral symmetrical involvement with narrowing of both SI joints. No erosions are seen. There is minimal sclerosis around the left SI joint.

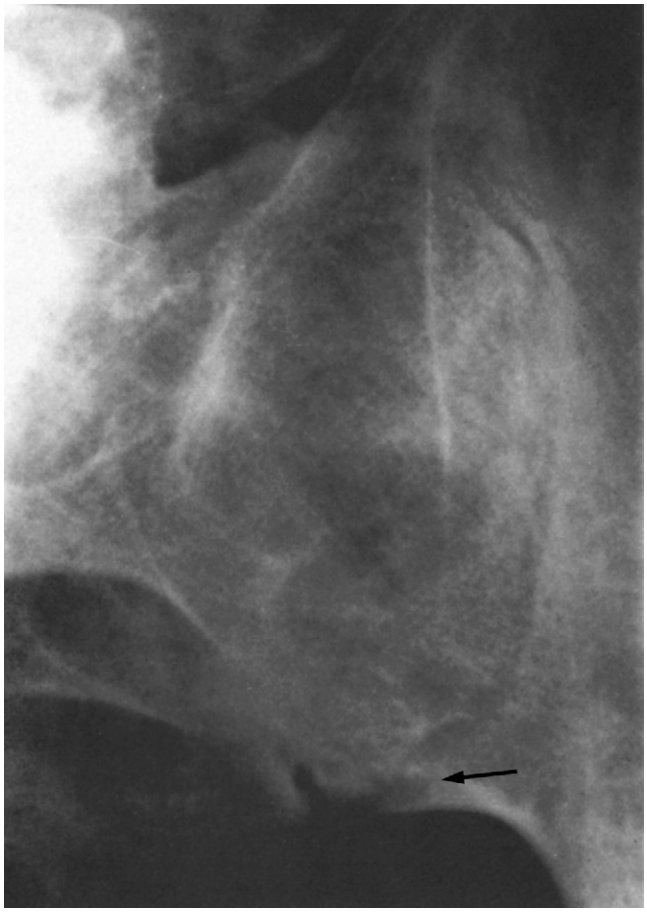

FIGURE 7-13. AP view of the SI joint in a patient with rheumatoid arthritis. Inferiorly there is a small erosion (*arrow*) without reparative response.

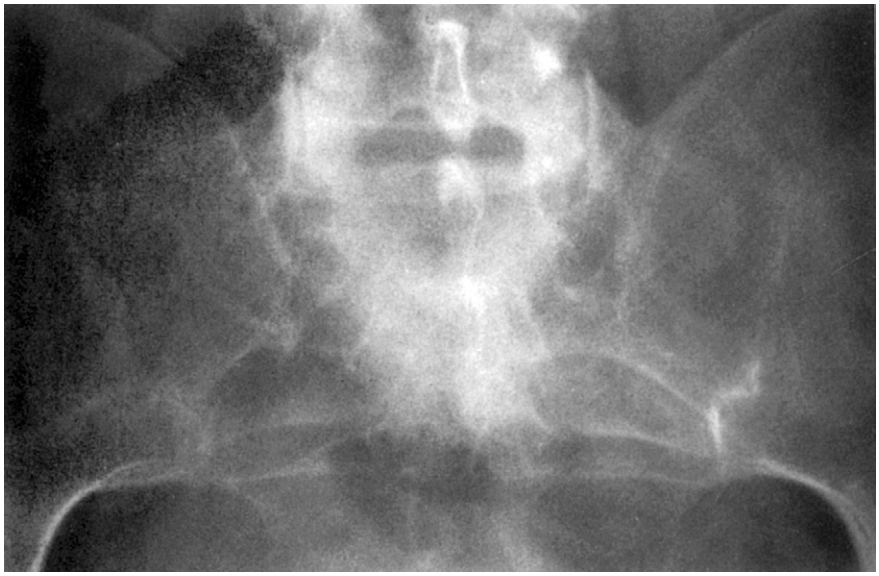

FIGURE 7-14. AP view of the SI joints in a patient with rheumatoid arthritis. There is bilateral bone ankylosis of the synovial part of the SI joint. There is no evidence of ligamentous ossification.

Infection (Figs. 7-15 through 7-17)

Septic arthritis is almost always unilateral in distribution. It leads to extensive erosion and extensive bone repair and may involve more than just the synovial aspect of the joint (Fig. 7-15). Tuberculous septic arthritis may cause the formation of a calcified abscess anterior to the SI joint (Fig. 7-16). Bone ankylosis may result from septic arthritis; septic arthritis is the most common cause of unilateral sacroiliac ankylosis (Fig. 7-17).

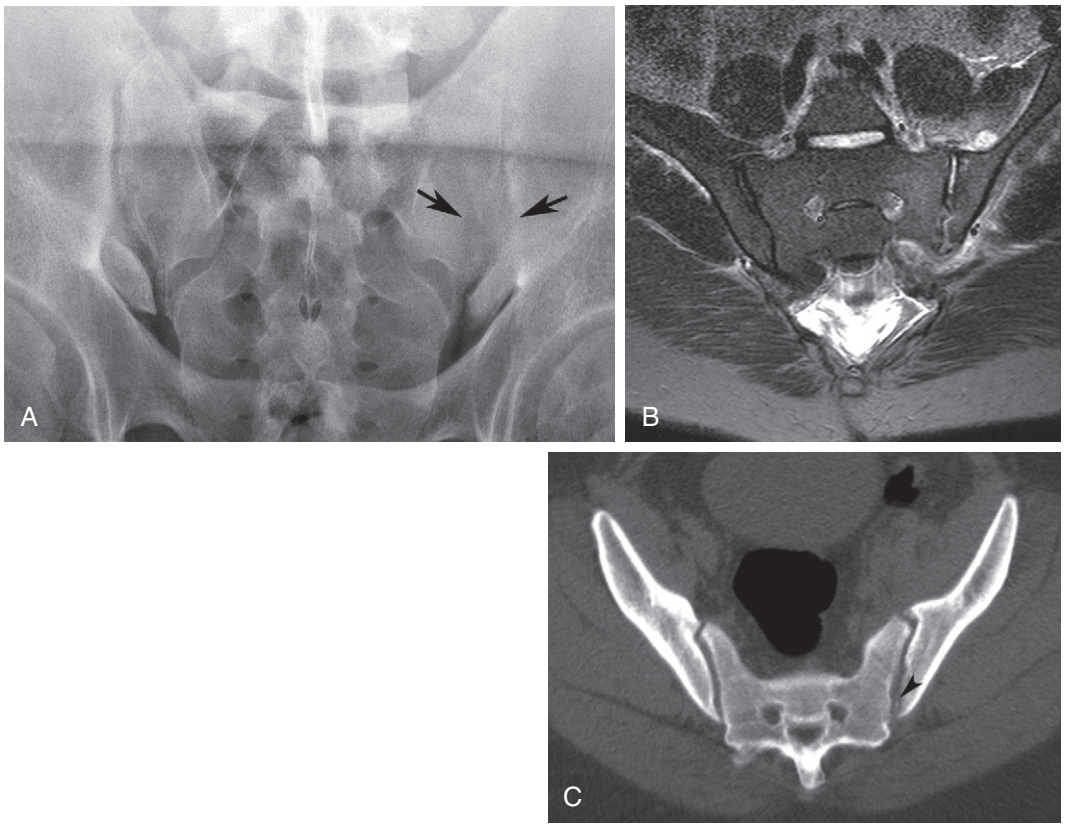

FIGURE 7-15. A, AP view of the SI joints in a patient with septic arthritis. The right SI joint is entirely normal. The left SI joint shows erosive changes (*arrows*). **B,** Coronal oblique fat-suppressed T2-weighted MR image shows erosions and soft tissue edema anterior and posterior to the joint. A small abscess is lateral and anterior to the joint. **C,** CT image shows erosions in the left joint and a small sequestrum is in the posterior joint space (*arrowhead*). Notice the extensive fat-stranding in the anterior soft tissues and bulging posterior joint capsule.

FIGURE 7-16. AP view of the SI joints in a patient with tuberculous septic arthritis. The left SI joint is normal. The right SI joint is obscured by a calcified abscess anterior to the SI joint.

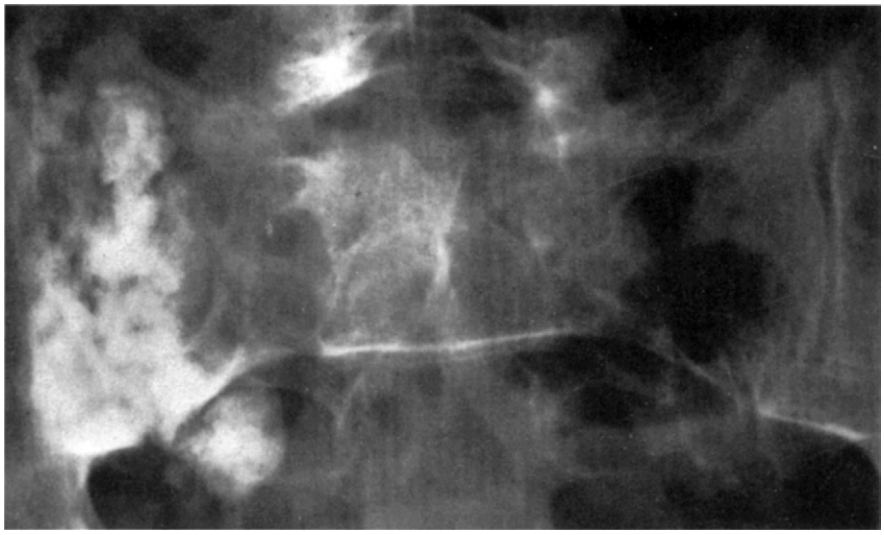

FIGURE 7-17. AP view of the SI joints in a patient with previously known septic arthritis. The right SI joint is normal. The left SI joint is completely ankylosed. *(From Brower AC: Disorders of the sacroiliac joint,* Radiolog *1(20):3, 1978; reprinted by permission.)*

Gout (Fig. 7-18)

Deposition of urate crystals into the cartilage leads to irregular loss of the joint space and superimposed osteoarthritis changes. In this instance it is impossible to distinguish gout from osteoarthritis. A tophus may form at the SI joint and create a large erosion of the anteroinferior aspect of the SI joint. However, this erosion, like those associated with tophi elsewhere, has a well-defined sclerotic border and occasionally an overhanging edge of cortex. Seven percent of the patients with radiographic gout demonstrate this classic lesion.

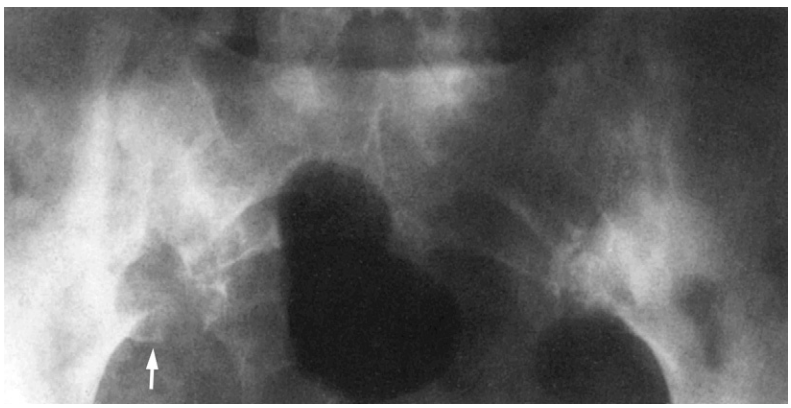

FIGURE 7-18. AP view of the SI joints in a patient with gout. The left SI joint shows changes of degenerative arthritis. There is patchy sclerosis on the iliac side. There is irregularity to the width of the joint space. The white cortical line on the sacral side is maintained. The right SI joint has a large erosion inferiorly. The erosion has a sclerotic rim and an overhanging edge of cortex (*arrow*). The erosion is classical of that produced by a tophus. *(From Brower AC: Disorders of the sacroiliac joint,* Radiolog *1(20):3, 1978; reprinted by permission.)*

CPPD Crystal Deposition Disease (Fig. 7-19)

The diagnosis of CPPD crystal deposition disease can be made when one sees calcification of the articular cartilage in both SI joints. This tends to be symmetrical when present. Should arthropathy develop secondary to this deposition, one may see air or a vacuum phenomenon within the SI joint. Eventually osteoarthritis changes may be seen.

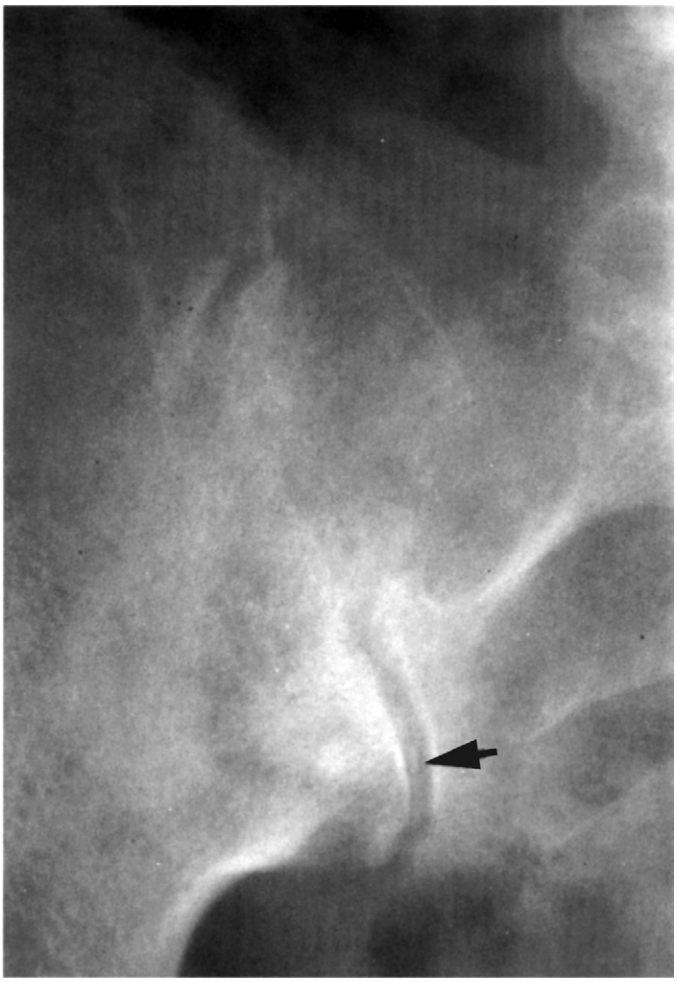

FIGURE 7-19. AP view of the SI joint in a patient with CPPD crystal deposition disease. Calcification (*arrow*) is seen within the inferior aspect of the joint.

Osteoarthritis (Figs. 7-20 to 7-22)

Osteoarthritis of the SI joints is a degeneration of the cartilage and associated bone changes secondary to abnormal mechanical stress across the joint. It is most commonly seen in males, especially those involved in heavy labor. It may be either bilateral and asymmetrical or unilateral. Irregular narrowing of the SI joint is observed to be most pronounced at the superior and inferior aspects of the true synovial joint (Fig. 7-20). Along with the narrowing, subchondral sclerosis develops in these areas. Erosive changes are not part of this arthropathy but subchondral cysts can be seen that may be confused with erosions on cross sectional imaging. The presence of nitrogen gas in the joint on computed tomography (CT) helps establish the diagnosis of osteoarthritis and excludes an inflammatory arthropathy (Fig. 7-21). Large osteophytes may develop superiorly and inferiorly and may bridge the ilium to the sacrum anterior to the actual joint. One may confuse this osteophyte formation with true bone ankylosis (Fig. 7-22); however, observation of part of the joint as normal should eliminate this confusing possibility. If necessary, a CT scan can be performed to demonstrate its anterior location.

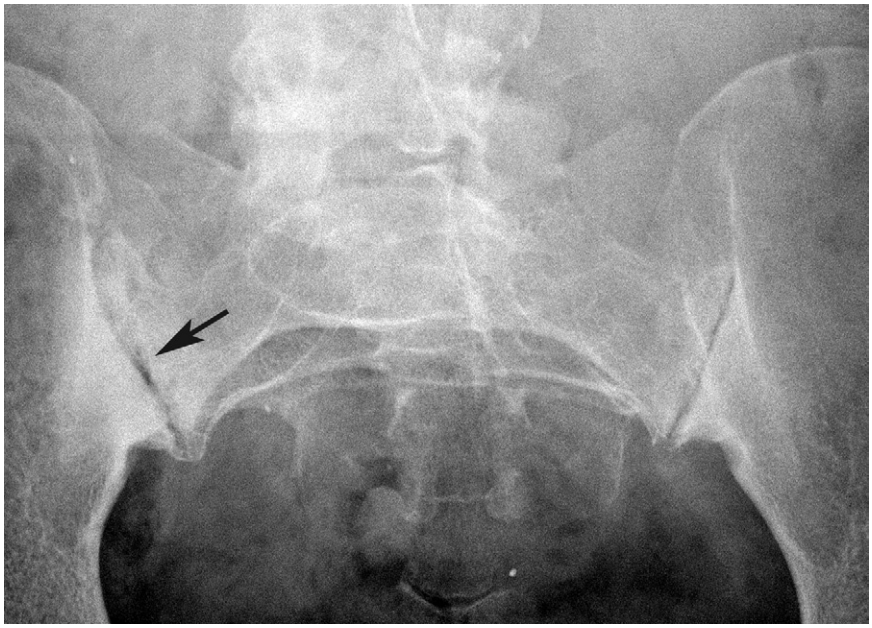

FIGURE 7-20. AP Ferguson view of the SI joints in a patient with osteoarthritis. There is bilateral asymmetrical involvement. The right SI joint shows sclerosis in the inferior aspect of the joint. The joint margin is still defined. Note the air vacuum phenomenon in joint (*arrow*). The left SI joint is irregularly narrowed. There is sclerosis present inferiorly in the joint.

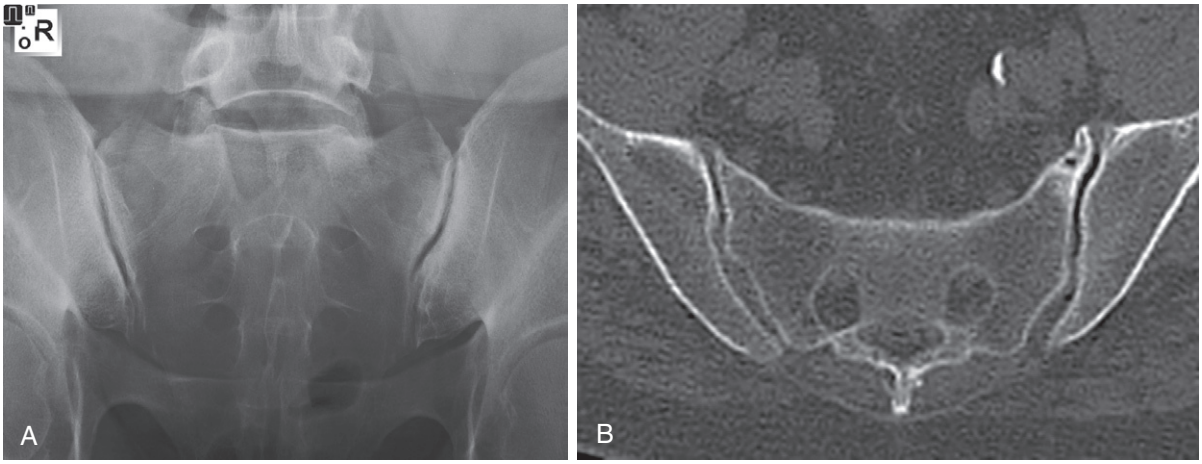

FIGURE 7-21. A, AP Ferguson view of the SI joints in a patient with osteoarthritis shows subchondral sclerosis in the superior left SI joint. Air is visible in the midportion of both SI joints. **B,** CT scan through the midportion of the SI joints shows mild subchondral sclerosis and a subchondral cyst in the anterior left SI joint. Air is seen in the left SI joint.

FIGURE 7-22. A, AP view of the SI joints in a patient with an osteophyte. The anterior inferior aspect of the left joint is obscured (*arrow*) but the posterior joint is maintained. There is sclerosis on the iliac side on the inferior aspect of the left SI joint. This might be confused with bone ankylosis. **B,** CT scan shows bridging by an anterior osteophyte extending from the left ilium to the sacrum.

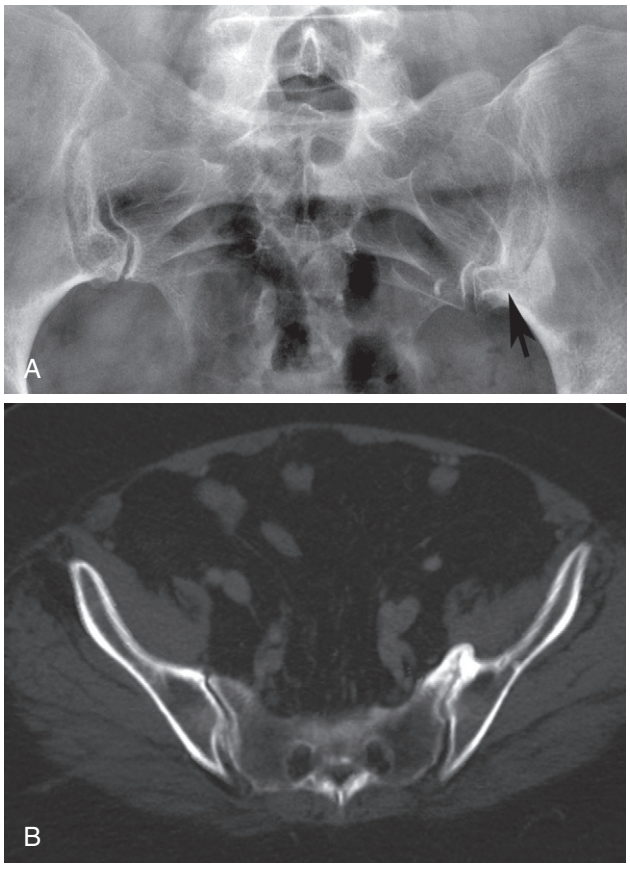

Osteitis Condensans Ilii (Figs. 7-23 and 7-24)

Osteitis condensans ilii is a disorder that surrounds the SI joint but does not affect the joint itself. It most commonly presents in multiparous females as a dome-shaped area of sclerosis on the iliac side of the SI joint. The widest portion of the sclerosis is found in the inferior aspect of the ilium (Fig. 7-23). There may be some sclerosis on the sacral side but always to a lesser extent than on the iliac side. Osteitis condensans ilii can be seen in males as well. It is believed to result from stress to this area secondary to instability at the pubic symphysis. Pain is usually present when the pubic symphysis is unstable. This instability can be demonstrated by "flamingo" views in which shifting weight from one leg to another shifts the apposition of the pubic rami (Fig. 7-24). Once the pubic symphysis is stabilized, either through surgery or through cessation of the activity that caused the instability, pain is no longer present. However, the radiographic changes may still be present. With time and continued pubic symphysis stability, the osteitis condensans ilii eventually resolves, with the iliac bone returning to normal.

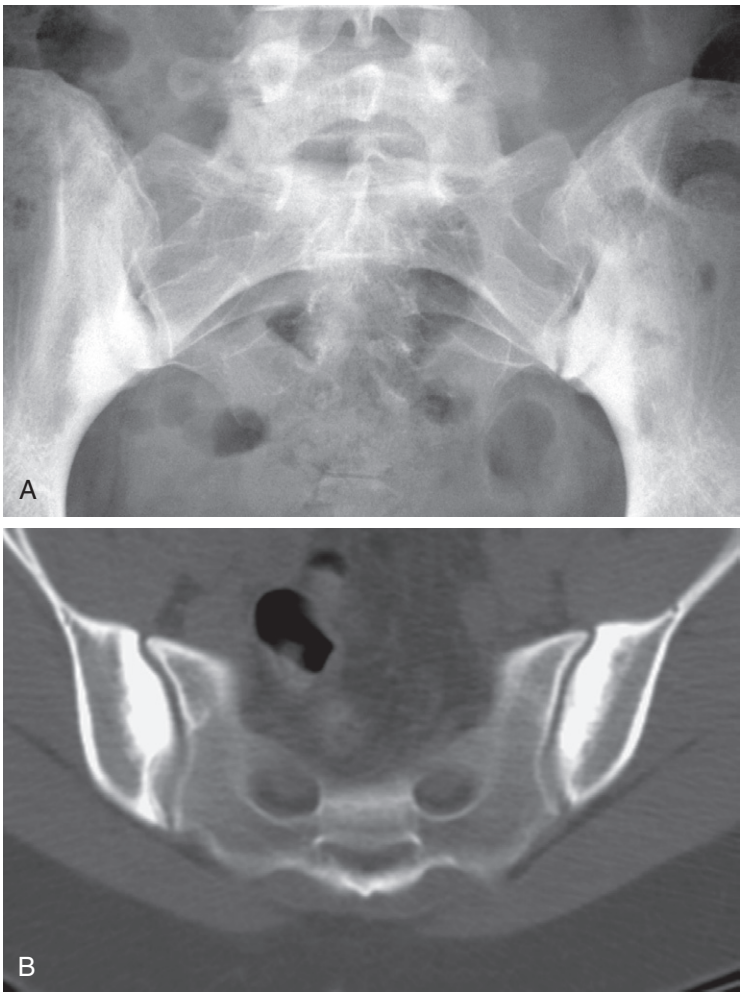

FIGURE 7-23. A, AP view of the SI joints in a patient with osteitis condensans ilii. There is bilateral symmetrical involvement. The actual joint spaces are normal. There is a triangular homogeneous sclerosis involving the inferior iliac side of the joint. **B,** Axial CT shows preserved joint space and sclerosis confined to the iliac side of the joint. There are no erosions.

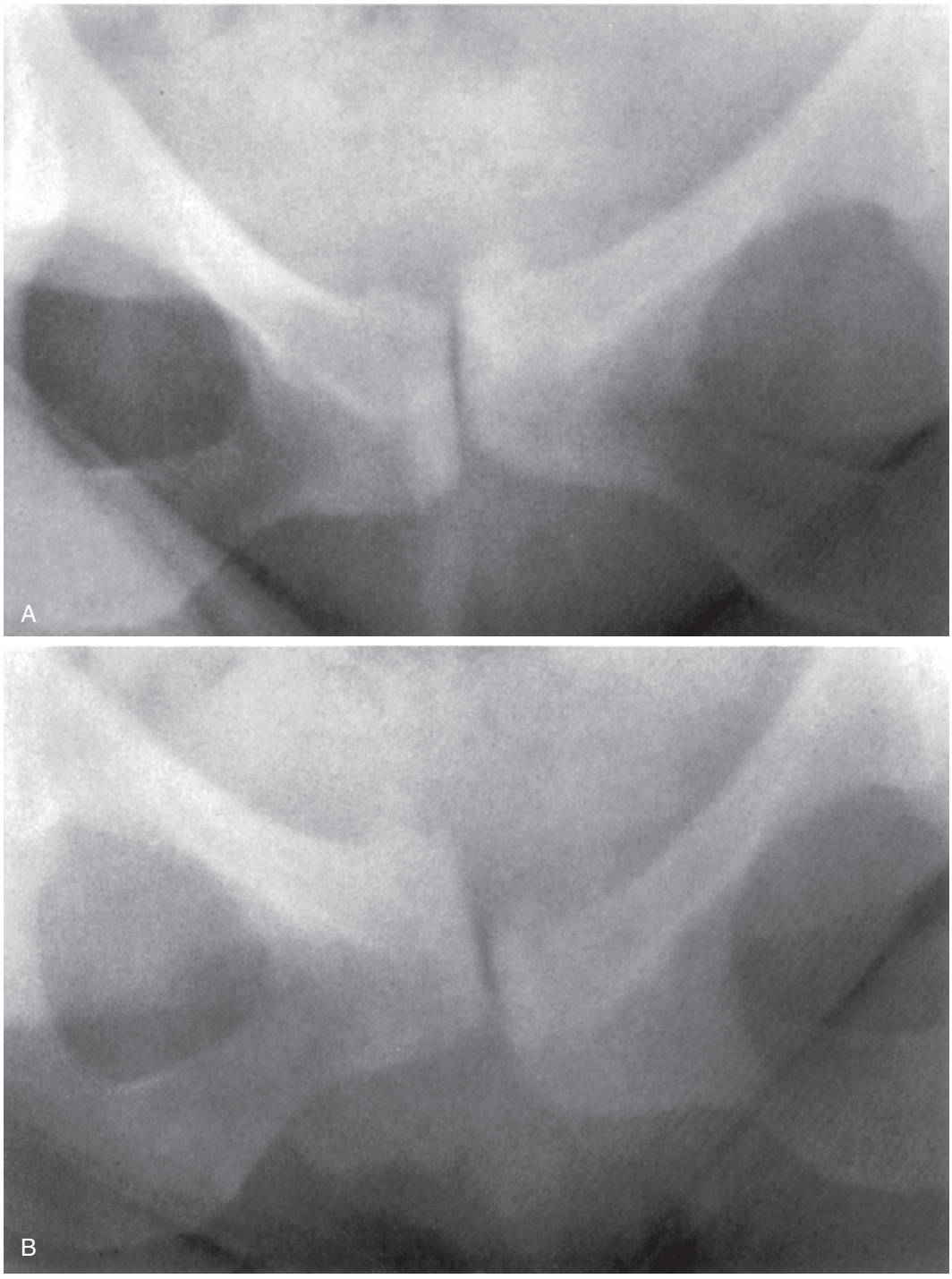

FIGURE 7-24. Instability of the pubic symphysis in a patient with osteitis condensans ilii. The instability is demonstrated by shifting weight from one leg (**A**) to the other (**B**), causing a shift in the position of the pubic rami.

SUGGESTED READINGS

Berens DL: Roentgen features of ankylosing spondylitis, *Clin Orthop Relat Res* 74:20, 1971.
Brower A: Disorders of the sacroiliac joint, *Radiolog* 1(20):3, 1978.
Dixon A, Lience E: Sacro-iliac joint in adult rheumatoid arthritis and psoriatic arthropathy, *Ann Rheum Dis* 20:247–257, 1961.
Gillespie HW: Osteitis condensans, *Br J Radiol* 26:16–21, 1953.
Harris NH, Murray RO: Lesions of the symphysis in athletes, *Br Med J* 4:211–214, 1974.
Jajic I: Radiological changes in the sacroiliac joints and spine of patients with psoriatic arthritis and psoriasis, *Ann Rheum Dis* 27:1–6, 1968.
Malawista SE, Seegmiller JE, Hathaway BE, et al: Sacroiliac gout, *JAMA* 194:954–956, 1965.
Numaguchi Y: Osteitis condensans ilii, including its resolution, *Radiolog* 98:1–8, 1971.
Resnick D: Disorders of the axial skeleton which are lesser known, poorly recognized or misunderstood, *Bull Rheum Dis* 28:932–939, 1977–1978.
Resnick D, Niwayama G, Goergen TG: Comparison of radiographic abnormalities of the sacroiliac joint in degenerative disease and ankylosing spondylitis, *AJR Am J Roentgenol* 128:189–196, 1977.
Resnick D, Niwayama G, Goergen TG: Degenerative disease of the sacroiliac joint, *Invest Radiol* 10:608–621, 1975.
Tuite MJ: Sacroiliac joint imaging, *Semin Musculoskelet Radiol* 12:72–82, 2008.

The "Phytes" of the Spine 8

In evaluating the spine, one observes the size, shape, and mineralization of the different vertebral bodies. These parameters become abnormal in various systemic diseases. For example, a large vertebral body is seen in Paget disease, a flattened vertebral body in eosinophilic granuloma, an H-shaped vertebral body in sickle cell disease, a sclerotic vertebral body in lymphoma, and an osteoporotic body in hyperparathyroidism. The arthropathies tend not to involve the vertebral body itself but primarily the apophyseal joints and the disc spaces. The most common arthropathy involving the apophyseal joints is osteoarthritis, which produces narrowing of the apophyseal joints, reparative bone, and osteophyte formation (Fig. 8-1). The inflammatory arthropathies cause erosive changes of the apophyseal joints, with or without eventual ankylosis. The inflammatory arthropathies may affect the disc space, but the most common disc space disorder is degeneration either idiopathically or secondary to abnormal deposition of material into the disc substance. Radiographic signs of disc degeneration are vacuum phenomenon, calcification, disc space narrowing, and reparative response in adjacent vertebral bodies.

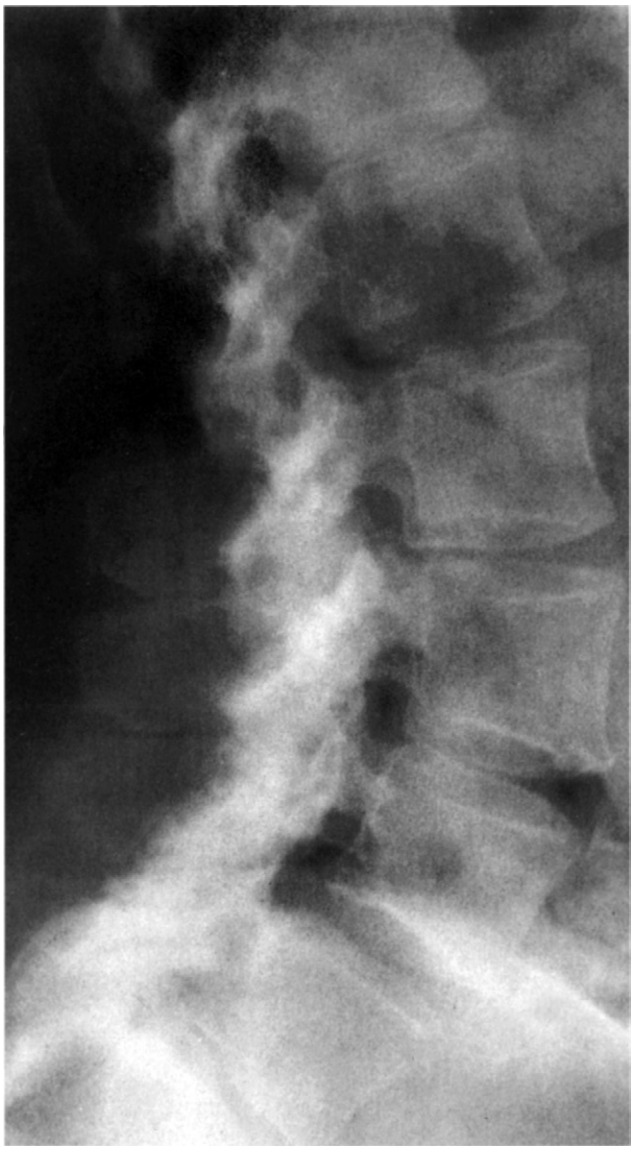

FIGURE 8-1. Lateral view of the lumbosacral spine in a patient with osteoarthritis of the apophyseal joints. Notice the absence of osteophyte formation and bone sclerosis of the vertebral bodies. There is loss of the apophyseal joint spaces with extensive surrounding bone repair. *(From Brower AC: The significance of various phytes of the spine,* Radiolog *1[15]:3, 1978; reprinted by permission.)*

However, many of the arthropathies lead to the development of various kinds of "phytes." The diagnosis of an arthropathy can be made through careful observation of the type of phyte that is produced. There are four different types of phytes: (1) the syndesmophyte, (2) the marginal osteophyte, (3) the nonmarginal osteophyte, and (4) the paraspinal phyte.

In order to understand the various kinds of phytes that distort the vertebral body and surround the disc, the anatomy of the disc interspace and surrounding soft tissues must be understood (Fig. 8-2). The central portion of the disc is known as the nucleus pulposus. This is surrounded by a fibrous ring called the annulus fibrosus. The nucleus pulposus and the inner portion of the annulus fibrosus are surrounded superiorly and inferiorly by the cartilaginous end-plate of the vertebral body. This cartilaginous vertebral end-plate does not extend to the borders of the bony vertebral body. Where the cartilaginous end-plate ends, the outermost fibers of the annulus fibrosus, called the Sharpey fibers, penetrate and connect the bone of one vertebral body to the bone of the adjacent vertebral body. The anterior longitudinal ligament adheres closely to the anterior border of the midportion of the vertebral body. At a level approximately 3 mm from the ends of the vertebral body, the anterior longitudinal ligament pulls away from the vertebral body and no longer closely adheres. It traverses the disc area in apposition to the Sharpey fibers and becomes closely adhered to the adjacent vertebral body 3 mm beyond the end-plate. The posterior longitudinal ligament adheres to the vertebral body in its entire length and is more intimately apposed to the Sharpey fibers posteriorly.

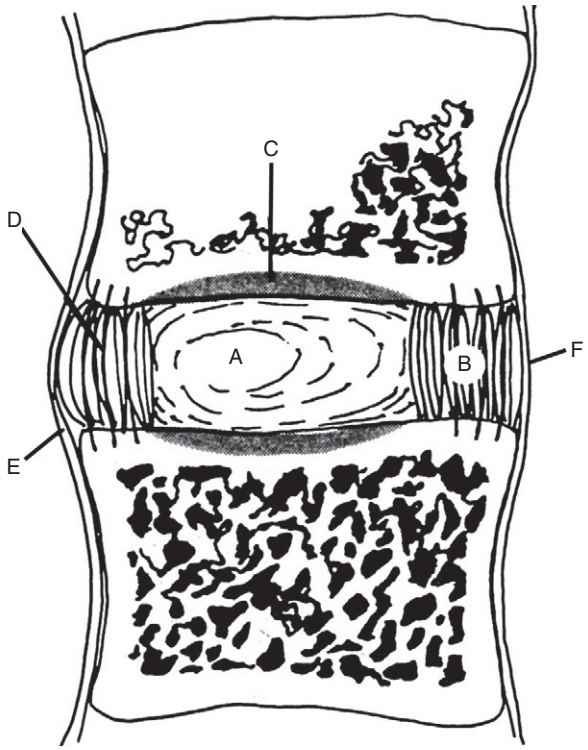

FIGURE 8-2. Anatomical drawing of the disc space and surrounding vertebral bodies. A = nucleus pulposus; B = annulus fibrosus; C = cartilaginous portion of the vertebral end-plate; D = Sharpey fibers; E = anterior longitudinal ligament; F = posterior longitudinal ligament.

SYNDESMOPHYTE

The syndesmophyte is a vertical ossification bridging two adjacent vertebral bodies (Fig. 8-3). It is the ossification of the Sharpey fibers of the annulus fibrosus. Because these fibers extend into the bone portion of the vertebral body, the syndesmophyte becomes a contiguous part of the vertebral bodies involved. The deep layers of the longitudinal ligaments may become ossified as well in forming this bridge. The syndesmophyte is the hallmark of ankylosing spondylitis. However, it may be seen in any of the spondyloarthropathies including reactive arthritis, psoriasis, and those associated with bowel disease.

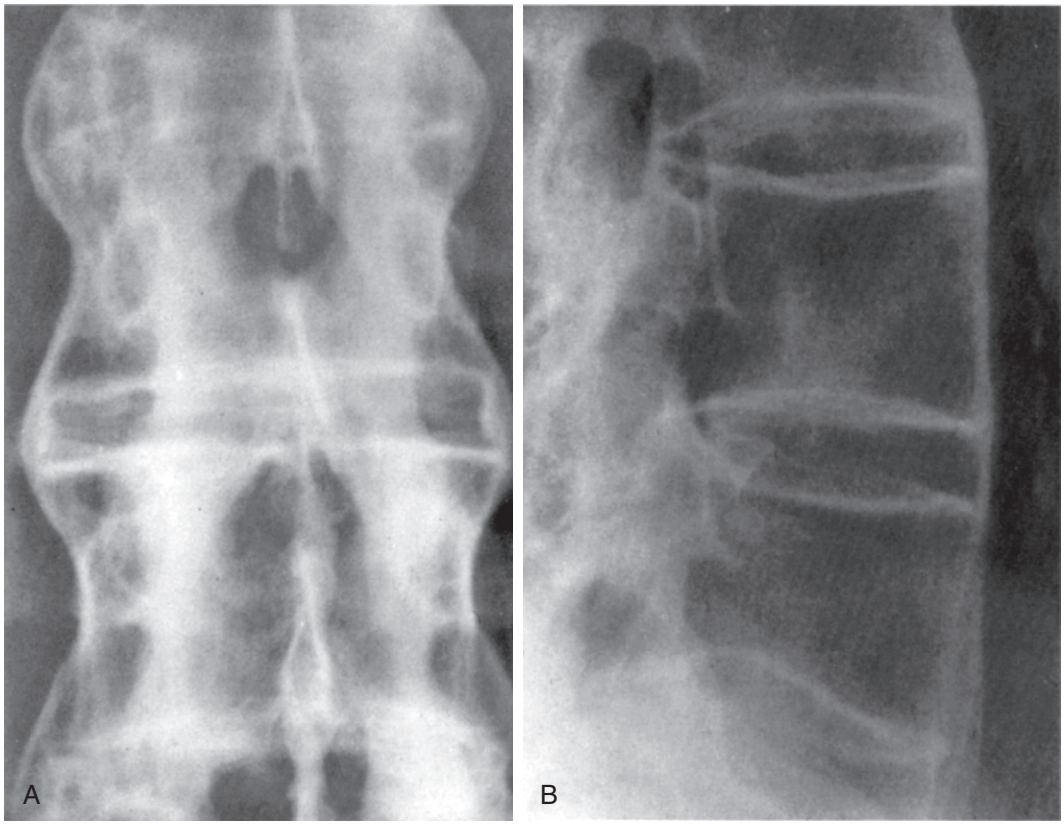

FIGURE 8-3. AP (**A**) and lateral (**B**) views of lumbar vertebral bodies jointed by syndesmophytes. At the disc level, the ossification is occurring in the annulus fibrosus and the deep layers of the anterior longitudinal ligament. *(**B,** from Brower AC: The significance of various phytes of the spine,* Radiolog *1[15]:3, 1978; reprinted by permission.)*

MARGINAL OSTEOPHYTE

The marginal osteophyte is a horizontal bony extension of the vertebral end-plate (Fig. 8-4). It is an integral part of the vertebral body in that it has a medullary canal contiguous with the medullary canal of the vertebral body and a cortex contiguous with the cortex of the vertebral body end-plate. Small marginal osteophytes are most commonly associated with degenerative disc disease and spondylosis deformans. Larger marginal osteophytes may turn from their horizontal course in a vertical direction and join with another marginal osteophyte from an adjacent vertebral body to form a bridge. These larger bridging marginal osteophytes are often posttraumatic but may be seen in combination with other types of phytes that are more diagnostic of the underlying disease entity.

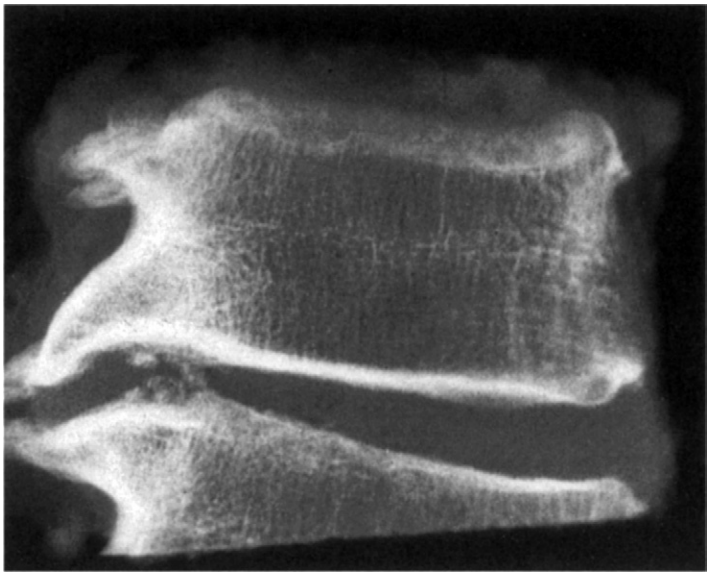

FIGURE 8-4. Specimen radiograph of disc space and surrounding vertebral bodies showing presence of marginal osteophytes. Notice that the medullary portion of the osteophyte is contiguous with the medullary portion of the vertebral body and that the cortex of the osteophyte is contiguous with the cortex of the vertebral body.

NONMARGINAL OSTEOPHYTE

A nonmarginal osteophyte is a horizontal extension or osteophyte of the vertebral body observed 2 mm to 3 mm away from the actual vertebral end-plate (Fig. 8-5). Again, a nonmarginal osteophyte appears to be an integral part of the vertebral body, with its medullary canal and cortex connecting with that of the vertebral body. Small ones are associated with degenerative disc disease and spondylosis deformans. These are called traction osteophytes and are believed to indicate an element of instability in the spine. Like the marginal osteophyte, the nonmarginal osteophyte may also turn vertically and join a similar nonmarginal or marginal osteophyte from an adjacent vertebral body (Fig. 8-6). These larger nonmarginal osteophytes (sometimes called nonmarginal syndesmophytes) are seen in psoriatic arthritis and reactive arthritis.

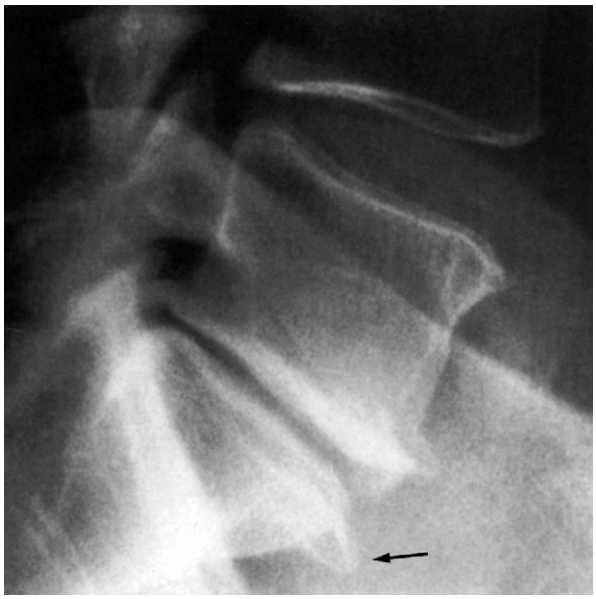

FIGURE 8-5. Lateral view of L5-S1 demonstrating a nonmarginal osteophyte (*arrow*) on S1.

FIGURE 8-6. Specimen radiograph of disc and adjacent vertebral bodies demonstrating a large nonmarginal osteophyte (*arrow*) joining a large marginal osteophyte.

PARASPINAL PHYTE

The paraspinal phyte is the ossification of the soft tissue structures that surround the vertebral body. This ossification is not an integral part of the vertebral body and can be separated from it (Fig. 8-7). Radiographically, the paraspinal phyte is observed most often as ossification of a longitudinal ligament. A lucent line can be seen to separate this ossification from the cortex of the vertebral body. The paraspinal phyte is most commonly associated with diffuse idiopathic skeletal hyperostosis (DISH).

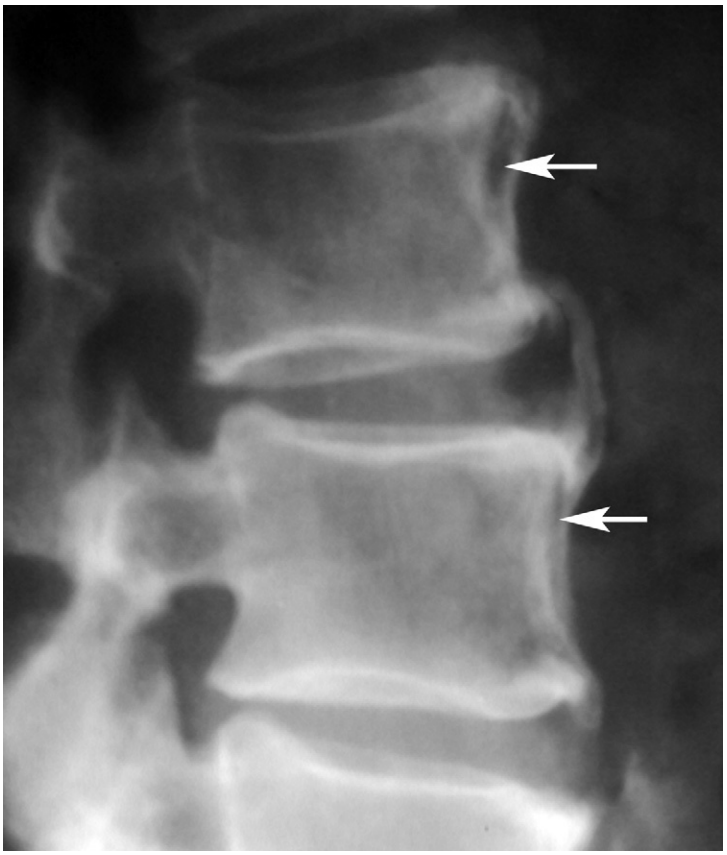

FIGURE 8-7. Lateral view of the lumbar spine demonstrating paraspinal phytes. This is ossification of the soft tissues and structures that surround the vertebral body. Notice that these phytes are not a contiguous part of the vertebral body. Lucent line separates the ossification from the vertebral body (*arrows*).

DISEASES PRODUCING PHYTES OF THE SPINE

Having described the various phytes that occur around the spine, we will now discuss common specific disease entities that produce phytes and the type and location of the phytes produced.

Degenerative Disc Disease—Primary and Secondary (Figs. 8-8 to 8-11)

Degenerative disc disease, or intervertebral osteochondrosis, is perhaps the most common positive radiographic finding in patients with back pain. If it occurs at one level, it is usually secondary to either the normal aging process or a premature aging process secondary to trauma. There is loss of normal resiliency of the nucleus pulposus and, with this, loss of normal disc height. As one observes the normal spine, the intervertebral disc spaces should increase as one descends the spine except at the level of C7-T1 and L5-S1, which are considered transitional areas. A disc space is considered narrow if the height is less than or equal to the one above it. Disc space narrowing is the most common radiographic sign of disc disease. Calcification or a vacuum phenomenon (air density) observed in a disc space is an absolute sign of disc degeneration. The vertebral bodies adjacent to the degenerated disc develop small marginal osteophytes or small nonmarginal osteophytes along with a degree of subchondral bone repair (Fig. 8-8). The nonmarginal osteophyte is called a traction osteophyte and indicates instability of the spine in this area.

When one observes degenerative disc disease at multiple levels without obvious structural abnormality, such as rotoscoliosis, one must consider an underlying arthropathy. The most common cause today would be calcium pyrophosphate dihydrate (CPPD) crystal deposition disease, in which one might find calcification in the soft tissue structures near the disc space. Acromegaly can be diagnosed when degenerative disc disease is observed in a patient with increase in the anteroposterior (AP) diameter of the vertebral bodies (Fig. 8-9).

FIGURE 8-8. Lateral view of L5-S1. This demonstrates narrowing of the disc space with a vacuum phenomenon. Small marginal osteophytes are present along with subchondral bone repair.

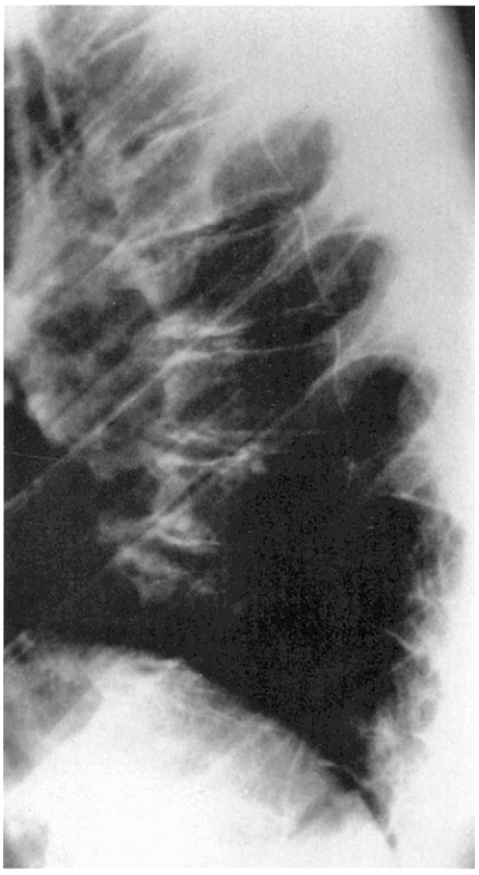

FIGURE 8-9. Lateral view of the thoracic spine in a patient with acromegaly. There is loss of disc height along with osteophyte formation. There is definite increase in the AP diameter of the vertebral body.

Ochronosis causes degenerative disc disease at all levels manifested by calcification or the vacuum phenomenon at all levels in the spine (Fig. 8-10). Although there is subchondral sclerosis in the vertebral bodies, there is remarkable absence of osteophyte formation. Sometimes the disc loss is so profound that the spine, while not truly ankylosed, is functionally ankylosed.

Observation of extreme or excessive degenerative disc disease should suggest a neuropathic spine. There may be dissolution of the disc space, tumbling of one vertebral body into another, reparative bone involving the entire vertebral body, massive osteophyte formation, and bone fragmentation (Fig. 8-11). Although once associated with tabes dorsalis, today this change is also observed in diabetic patients.

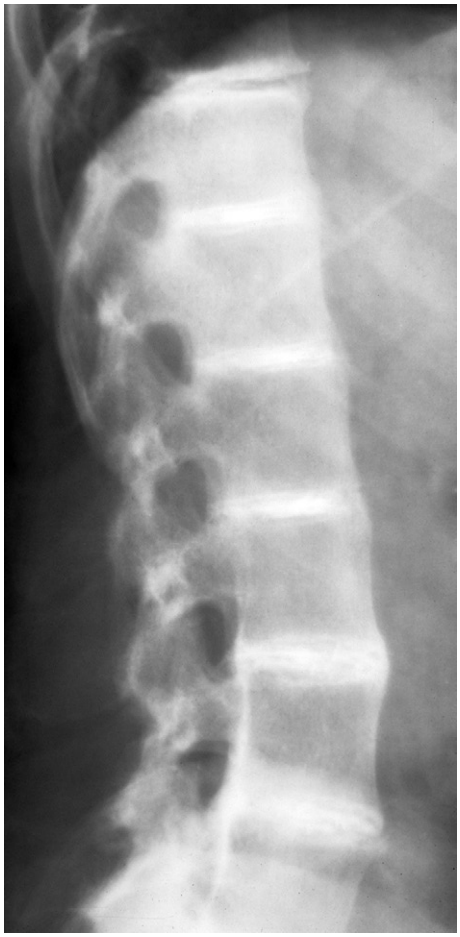

FIGURE 8-10. Lateral view of the lumbar spine in a patient with ochronosis. There is total loss of disc space at multiple levels. Calcification and the vacuum phenomenon are present at several levels. There is subchondral sclerosis but absence of osteophyte formation.

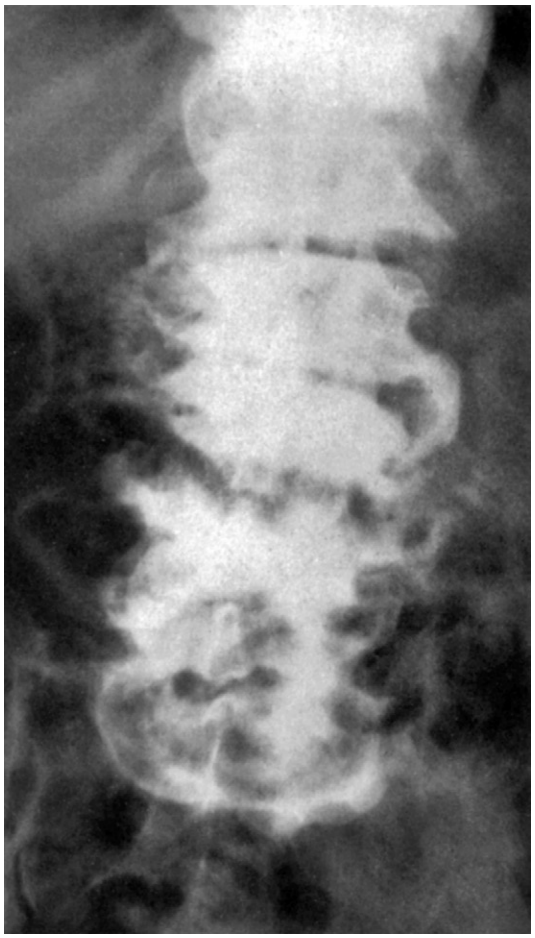

FIGURE 8-11. AP view of the lumbar spine in a patient with tabes dorsalis. There is severe loss of disc space, extensive reparative bone, massive osteophyte formation, and some bone fragmentation.

Spondylosis Deformans (Fig. 8-12)

The diagnosis of spondylosis deformans is made when one observes small marginal or nonmarginal osteophytes surrounding a disc *without* disc space loss or other signs of degenerative disc disease. Spondylosis deformans is thought to be a degeneration of Sharpey fibers, allowing anterior movement of the disc within the space. This anterior motion is believed to pull on the anterior longitudinal ligament, thus producing the small traction osteophyte. The small marginal osteophyte is produced secondary to the degeneration of Sharpey fibers.

FIGURE 8-12. Lateral view of the lumbar spine in a patient with spondylosis deformans. There is no loss of disc height. There are small marginal osteophytes and nonmarginal osteophytes. There is no vertebral body sclerosis.

Ankylosing Spondylitis (Fig. 8-13)

Ankylosing spondylitis produces syndesmophytes. It first ossifies the Sharpey fibers of the annulus fibrosus. It may then ossify the deep layers of the anterior longitudinal ligament. The vertebral bodies of the lumbar spine are normally concave anteriorly, and this curve will be lost because of bone formation in these structures. This ossification ascends the spine, from the lumbosacral spine to the cervical spine, in a symmetrical, succinct fashion. The final result is a "bamboo spine." It may or may not produce bony ankylosis of the apophyseal joints. The disc spaces are relatively well maintained throughout the spine. Once ankylosed, the disc spaces may become calcified.

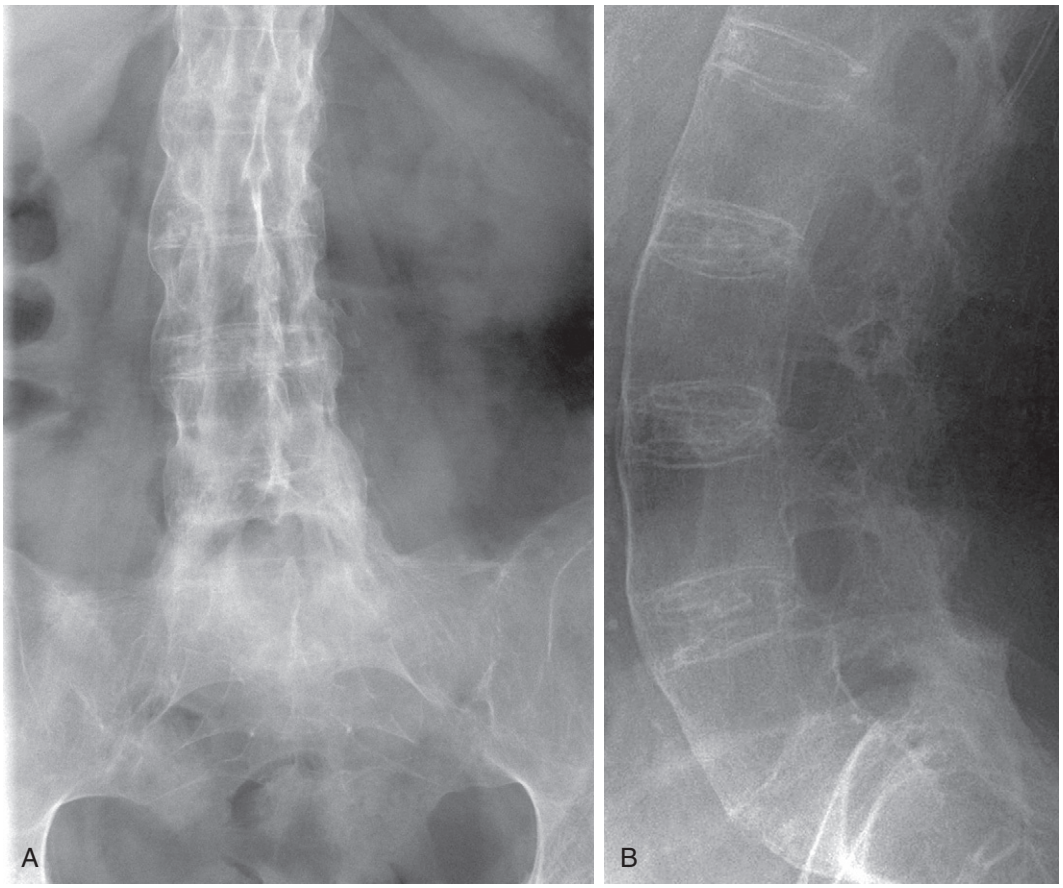

FIGURE 8-13. AP (**A**) and lateral (**B**) views of the lumbar spine in a patient with ankylosing spondylitis. Symmetrical syndesmophytes involve the entire spine. Notice the ankylosis of the apophyseal joints.

Psoriatic and Reactive Arthritis (Fig. 8-14)

Unlike ankylosing spondylitis, psoriatic and reactive arthritis's involvements of the spine are asymmetrical and exuberant. Although syndesmophytes may be present, more commonly there is production of bridging nonmarginal osteophytes. The syndesmophytes and nonmarginal osteophytes may be unilateral or bilateral, but in a skip distribution. Again, the apophyseal joints may or may not be ankylosed. The disc spaces tend to be maintained. One cannot distinguish the spine involvement in a patient with psoriasis from that in a patient with reactive arthritis. However, it is unusual for reactive arthritis but fairly common for psoriasis to involve the spine.

FIGURE 8-14. AP view of the lumbosacral spine in a patient with psoriatic arthritis. There are asymmetrical syndesmophytes and nonmarginal osteophytes.

Diffuse Idiopathic Skeletal Hyperostosis (Figs. 8-15 to 8-18)

The paraspinal phyte is the hallmark of DISH. DISH is not an arthropathy. It does not affect joint cartilage or articulating bone. Therefore, the apophyseal joints and the disc spaces are not affected. It is a bone-forming diathesis. It primarily ossifies ligaments and tendons, specifically at their attachments. In the spine, it ossifies the longitudinal ligaments. DISH is most commonly observed in the thoracic spine as excessive flowing ossification anterior to the vertebral bodies. Unlike ankylosing spondylitis, it does not ossify Sharpey fibers. Therefore, classically at the disc space levels, the ossification bulges anteriorly, producing a lucent Y- or T-shaped configuration between the ossification and the vertebral end-plates. The diagnosis of DISH is made when this flowing ossification involves four or more contiguous vertebral bodies with their intervening disc spaces (Fig. 8-15). In 10 percent of the patients with DISH, the ossification may be succinct enough to give an appearance similar to that of ankylosing spondylitis (Fig. 8-16). However, usually a lucency can be demonstrated between the ossification of the longitudinal ligament and the vertebral body, which cannot be identified in ankylosing spondylitis. In the cervical spine, this ossification may become so extensive as to cause dysphagia (Fig. 8-17).

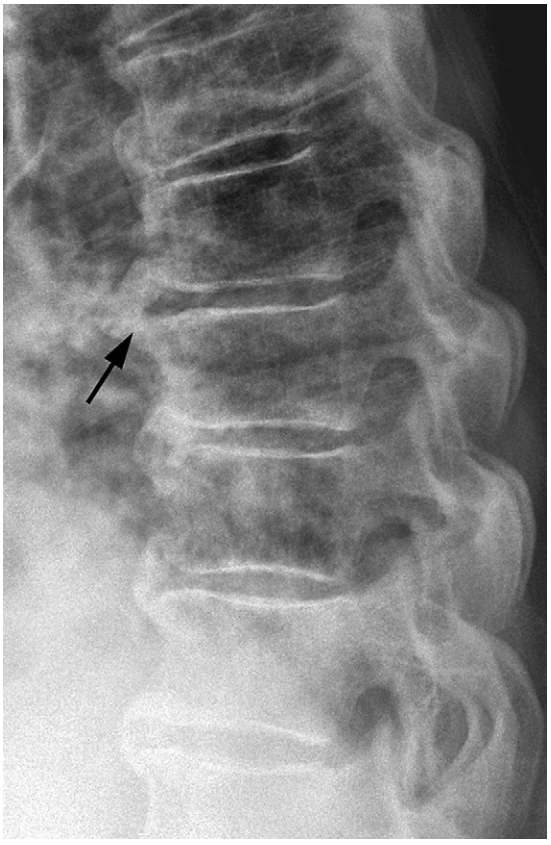

FIGURE 8-15. Lateral view of the thoracic spine in a patient with DISH. Flowing ossification or paraspinal phytes involve most of the thoracic spine. Notice the T- or Y-shaped lucency at the disc level demonstrating lack of ossification of the annulus fibrosus (*arrow*).

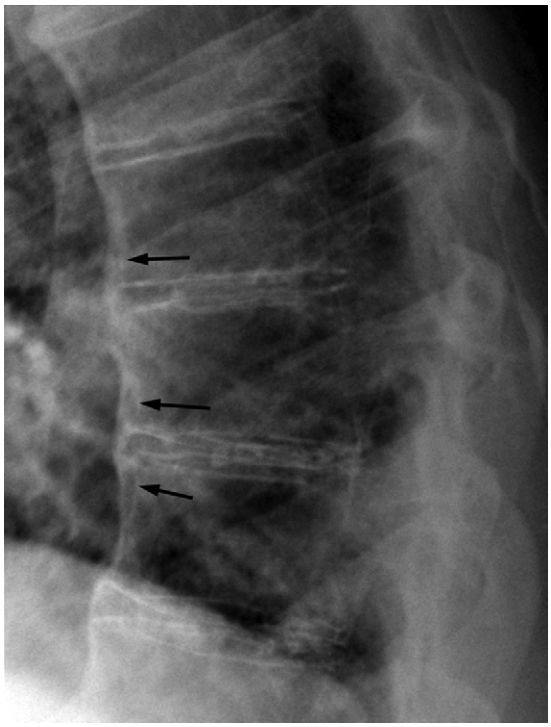

FIGURE 8-16. Lateral view of the thoracic spine in a patient with DISH. Although this appearance is similar to that of ankylosing spondylitis, a lucency (*arrow*) separates the following ossification from the vertebral body.

FIGURE 8-17. Lateral view of the cervical spine in a patient with DISH. Notice that the disc spaces are maintained and the apophyseal joints are free of disease. There is excessive bone formation anterior to the vertebral bodies.

When the lumbar spine is involved, paraspinal phytes are usually seen (Fig. 8-18). However, the lumbar spine may also manifest effusive nonmarginal and marginal bridging osteophytes. If the phytes in the lumbar spine suggest either DISH or a spondyloarthropathy, one need only observe the SI joints. These will be normal in DISH and abnormal in the spondyloarthropathies.

FIGURE 8-18. Lateral view of the lumbar spine in a patient with DISH. Notice the flowing paraspinal phytes.

SUGGESTED READINGS

Berens D: Roentgen features of ankylosing spondylitis, *Clin Orthop Relat Res* 74:20–33, 1971.
Brower A: The significance of the various phytes of the spine, *Radiolog* 1(15):3, 1978.
Feldman F, Johnson AM, Walter JF: Acute axial neuropathy, *Radiolog* 111:1–16, 1974.
Lang EK, Bessler WT: Roentgenologic features of acromegaly, *Am J Roentgenol Radium Ther Nucl Med* 86:321–328, 1961.
MacNab I: The traction spur. An indicator of segmental instability, *J Bone Joint Surg Am* 53:663–670, 1971.
McEwen C, DiTata D, Lingg C, et al: Ankylosing spondylitis and spondylitis accompanying ulcerative colitis, regional enteritis, psoriasis and Reiter's disease. A comparative study, *Arthritis Rheum* 14:291–318, 1971.
O'Brien WM, Bunfield WG, Sokoloff L: Studies on the pathogenesis of ochronotic arthropathy, *Arthritis Rheum* 4:137–152, 1961.
Peterson CC, Silbiger ML: Reiter's syndrome and psoriatic arthritis: Their roentgen spectra and some interesting similarities, *Am J Roentgenol Radium Ther Nucl Med* 101:860–871, 1967.
Resnick D: Disorders of the axial skeleton which are lesser known, poorly recognized or misunderstood, *Bull Rheum Dis* 28:932–939, 1977–1978.
Resnick D: Osteophytes, syndesmophytes and other "phytes", *Postgrad Radiol* 1:217, 1981.
Resnick D, Niwayama G: Radiographic and pathologic features of spinal involvement in diffuse idiopathic skeletal hyperostosis (DISH), *Radiology* 119:559–568, 1976.
Sokoloff L: Pathology and pathogenesis of osteoarthritis: Degenerative disease of the spinal column. In Hollander JL, editor: *Arthritis and allied conditions*, Philadelphia, 1966, Lea & Febiger, pp 855–857.

9 *Rheumatoid Arthritis*

In the practice of rheumatology, rheumatoid arthritis is considered the everyday disease. It is a symmetrical arthritis of the appendicular skeleton, sparing the axial skeleton except for the cervical spine. The common radiographic findings are as follows:

1. Periarticular soft tissue swelling
2. Juxta-articular osteoporosis progressing to generalized osteoporosis
3. Uniform loss of joint space
4. Lack of bone formation
5. Marginal erosions progressing to severe erosions of subchondral bone
6. Synovial cyst formation
7. Subluxations
8. Bilateral symmetrical distribution
9. Distribution in hands, feet, knees, hips, cervical spine, shoulders and elbows in decreasing order of frequency

Not all of these features are present at any one time, and no one abnormality is pathognomonic. However, combinations of many of these finding should lead to the correct diagnosis of rheumatoid arthritis. With the development of new drugs, many of these findings are becoming less frequent.

THE HANDS AND WRISTS

Radiographs of the hands are used by clinicians for two distinct purposes: (1) to help in early diagnosis and (2) to assess for disease progression. Therefore, the radiographic changes in the hands and wrists will be described in two separate categories: early changes, observed primarily for diagnosis, and late changes, observed primarily for disease state.

Early Changes

The plain film is still the first modality used for imaging for early changes. Though ultrasonography and magnetic resonance (MR) imaging are more sensitive for the detection of erosions, these modalities are more expensive, more time consuming, and not always available. The earliest changes seen radiographically are soft tissue swelling symmetrically around the joints involved and juxtaarticular osteoporosis. These changes are nonspecific but help to confirm the clinical impression of an inflammatory problem. Erosive disease is an indication of the aggressiveness of the arthropathy. Early erosions are subtle radiographically, and one must specifically look for them. The first erosive changes occur before there is loss of joint space. Erosions occur in the bare areas of the bone or in the bone within the joint space capsule that is not covered by articular cartilage. Radiographically, one loses the continuity of the white cortical line. On the posteroanterior (PA) view, this is best observed in the heads of the metacarpals (Fig. 9-1) and at the margins of the proximal interphalangeal (PIP) joints (Fig. 9-2). However, erosions are often first observed on the radial aspect of the base of the proximal phalanges. These changes are best imaged on the Nørgaard, or semisupinated oblique view of the hands (Fig. 9-3) (see Chapter 1).

FIGURE 9-1. Metacarpophalangeal joint: early changes. Loss of white cortical line (*arrowheads*) representing erosion of bare area.

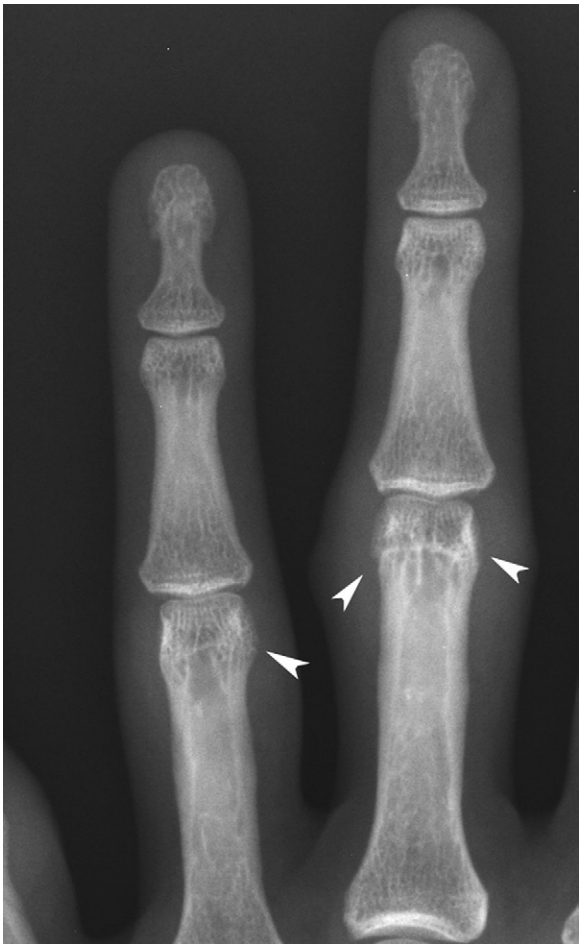

FIGURE 9-2. Proximal IP joint of a finger: early changes. Marginal erosion demonstrated (*arrowheads*).

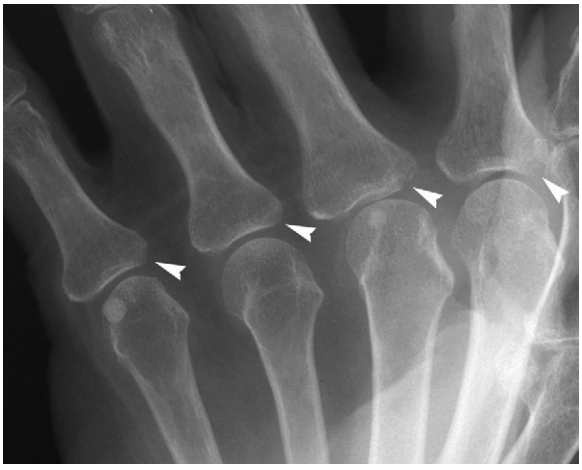

FIGURE 9-3. Metacarpophalangeal joint: early changes. Nørgaard projection demonstrating erosion of the radial aspect at the base of the proximal phalanx (*arrowheads*).

In the wrist, early erosions must be looked for in specific locations. They commonly occur at the waist of the navicular, the waist of the capitate, the articulation of the hamate with the base of the fifth metacarpal, the articulation of the first metacarpal with the trapezium, the radial styloid, and the ulnar styloid. These can all be imaged on the PA view (Fig. 9-4 A and B). The Nørgaard view profiles the pisiform and triquetrum and often demonstrates erosive changes between these two bones before erosions are seen on the ulnar styloid (Fig. 9-4 C).

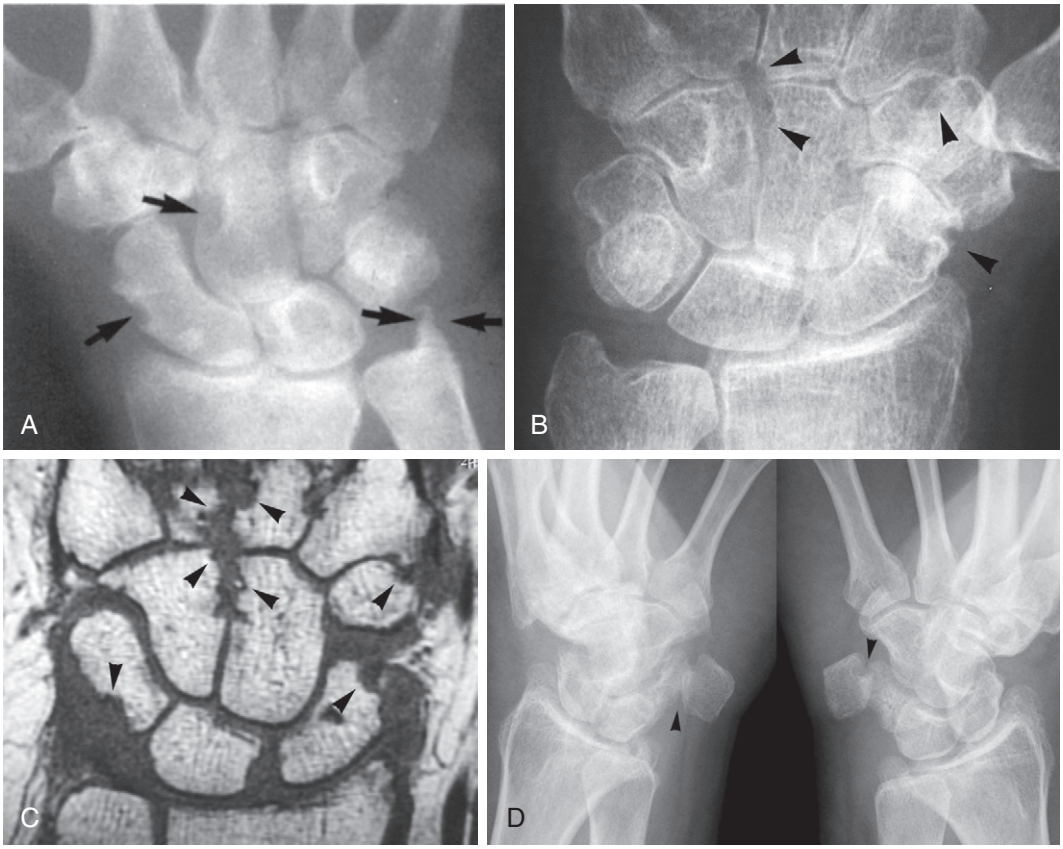

FIGURE 9-4. **A,** PA view of the wrist demonstrating early changes. Erosion of the waist of the navicular, the waist of the capitate, and the ulnar styloid (*arrows*). Notice that mineralization is normal and joint spaces are maintained. **B** and **C**, PA view of the wrist and coronal T1-weighted MR image showing juxta-articular osteoporosis and diffuse loss of joint spaces in a pancarpal distribution. Notice erosions (*arrowheads*). **D,** Nørgaard view of the wrist demonstrating erosive changes between the triquetrum and the pisiform bilaterally (*arrows*). Notice that the ulnar styloid is intact.

Late Changes

In the hand, the metacarpophalangeal (MCP) joints and/or the PIP joints are uniformly involved. In the wrist, all the carpals are affected as a unit. As the disease progresses, the cartilage and apparent joint space are lost uniformly (Fig. 9-5). As the cartilage is lost, the soft tissue swelling caused by the rheumatoid synovitis decreases. Juxta-articular osteoporosis progresses to diffuse osteoporosis. The subtle marginal erosions continue to progress, involving more and more of the articular surface to become large subchondral erosions (Fig. 9-6). Subluxations occur at the MCP joints, with the proximal phalanges subluxing ulnarly and palmarly in relationship to the metacarpal heads (Fig. 9-7). Swan neck and boutonnière deformities develop in the distal phalanges. Ulnar subluxation (translocation) of the carpus can also be seen (Fig. 9-8). Although the subluxations occur secondary to inflammation of the tendons and ligaments surrounding the joint, erosive disease is usually present when the subluxations occur.

FIGURE 9-5. PA view of the hand in advanced stages of rheumatoid arthritis. Diffuse osteoporosis is apparent. Notice the uniform involvement of PIP joints, MCP joints, and carpal bones as a unit.

FIGURE 9-6. PA view of the hand in late stages of rheumatoid arthritis. Notice the profound osteoporosis. There is PIP, MCP, and pancarpal involvement. Notice the large subchondral erosion of the second MCP and the fourth PIP joints (*arrows*). *(From Brower AC: The radiologic approach to arthritis,* Med Clin North Am *68:1593, 1984; reprinted by permission.)*

FIGURE 9-7. PA view of the hand demonstrating late changes of rheumatoid arthritis. Notice the diffuse osteoporosis. There is actual soft tissue atrophy. There is involvement of the PIPs, the MCPs, and the carpals as a unit. There is severe erosion, so that normal bone contour is not present. The proximal phalanges are subluxating ulnarly and palmarly in relationship to the metacarpal heads.

FIGURE 9-8. PA view of the wrist shows advanced rheumatoid arthritis of the wrist. There are pancarpal joint space loss and erosive changes. Less than 50 percent of the lunate articulates with the radius indicating ulnar translocation of the carpus.

In the late stages of the disease, there is actually soft tissue atrophy. Diffuse osteoporosis is present. Subcutaneous rheumatoid nodules may develop in 25 percent of patients (Fig. 9-9). The nodules do not cause bone destruction. There is lack of recognizable joint spaces (see Fig. 9-7). Bone ankylosis of the carpals may occur (Fig. 9-10). Although there may be fibrous ankylosis of the phalanges, there should be no radiographic evidence of bone ankylosis distal to the carpals unless there has been surgical fusion. Despite extensive involvement of the PIPs and MCPs, the distal interphalangeal joints (DIPs) are usually spared. If there are erosive changes involving the DIPs, a second arthropathy such as erosive osteoarthritis should be considered. The hand may eventually become an arthritis mutilans (Fig. 9-11).

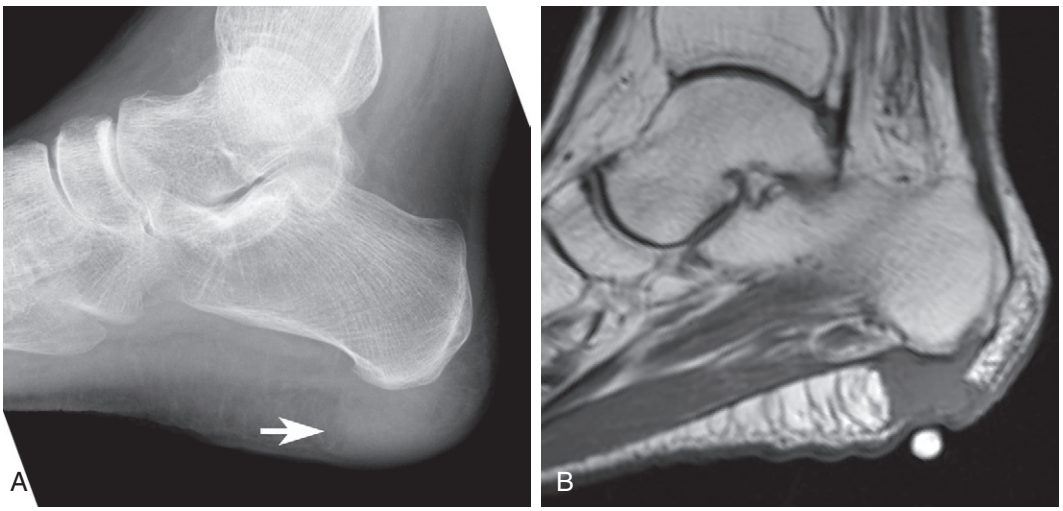

FIGURE 9-9. A, Lateral view of the calcaneus shows soft tissue density in the plantar soft tissues (*arrow*). **B,** Sagittal T1 image shows marker placed over intermediate signal rheumatoid nodule replacing the plantar fat pad.

FIGURE 9-10. PA view of the wrist demonstrating bone ankylosis of the carpal bones.

FIGURE 9-11. Arthritis mutilans.

THE FEET

The feet are involved in 80 to 90 percent of patients with rheumatoid arthritis. Some observers state that in 10 to 20 percent of patients, the feet are involved before the hands. However, generally the changes in the feet accompany or lag somewhat behind the changes in the hands. The radiographic changes in the feet are evaluated through an anteroposterior (AP) and a lateral view. Early involvement of the feet again shows juxta-articular osteoporosis and erosion of the bare areas on the heads of the metatarsals. The first erosive change is seen in the lateral aspect of the head of the fifth metatarsal (Fig. 9-12). There is loss of the white cortical line. The other metatarsal heads are eroded primarily medially and later laterally (Fig. 9-13). As the disease progresses, there are uniform loss of the cartilage in the MTP joints, progressive erosive changes, and subluxations of the proximal phalanges in a fibular direction in relationship to the metatarsals (Fig. 9-14). The metatarsal heads also subluxate in a plantar direction. There are dorsiflexion deformities of the PIP joints and a hallux valgus deformity of the big toe.

FIGURE 9-12. PA view of the MTP joints: early changes. Erosion of the lateral aspect of the head of the fifth metatarsal and the medial aspect of the head of the other metatarsals (*arrows*).

FIGURE 9-13. AP view of the forefoot with diffuse MTP joint space narrowing. Erosive changes of the medial aspects of metatarsal heads are larger than those on the lateral aspects.

FIGURE 9-14. AP view of the forefoot: late changes of rheumatoid arthritis. Note osteoporosis, severe erosive changes involving the heads of the metatarsals, hallux valgus deformity, and fibular subluxation of the proximal phalanges in relationship to the metatarsal heads.

Like the carpal bones in the wrist, tarsal bones of the foot are involved as a unit, with uniform joint space loss (Fig. 9-15). Bone ankylosis may occur in the tarsals but not distal to the tarsals (Fig. 9-16). Erosive changes may be present in the calcaneus at the attachment of the plantar aponeurosis or superior to the attachment of the Achilles tendon (Fig. 9-17).

FIGURE 9-15. AP view of the midfoot demonstrating uniform cartilage loss between all the tarsal bones.

FIGURE 9-16. Lateral view of the mid- and hindfoot showing severe osteoporosis and bone ankylosis.

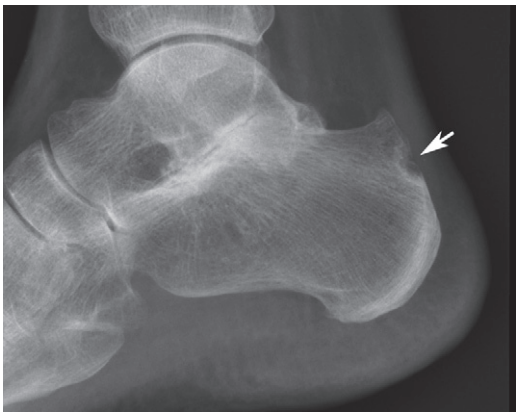

FIGURE 9-17. Lateral view of the calcaneus showing erosion superior to the attachment of the Achilles tendon (*arrow*). Notice the diffuse subtalar joint space narrowing.

THE HIPS

The hip joint is involved less frequently than the knee. It is affected in 50 percent of patients with rheumatoid arthritis. There is uniform loss of the cartilage and therefore axial migration of the femoral head within the acetabulum (Fig. 9-18). As the cartilage is lost, the head continues to move in an axial or a superior medial direction (Fig. 9-19). Bone is eroded away on the joint side of the acetabulum and laid down on the pelvic side producing a protrusion of the acetabulum. Both hips are affected in a symmetrical fashion.

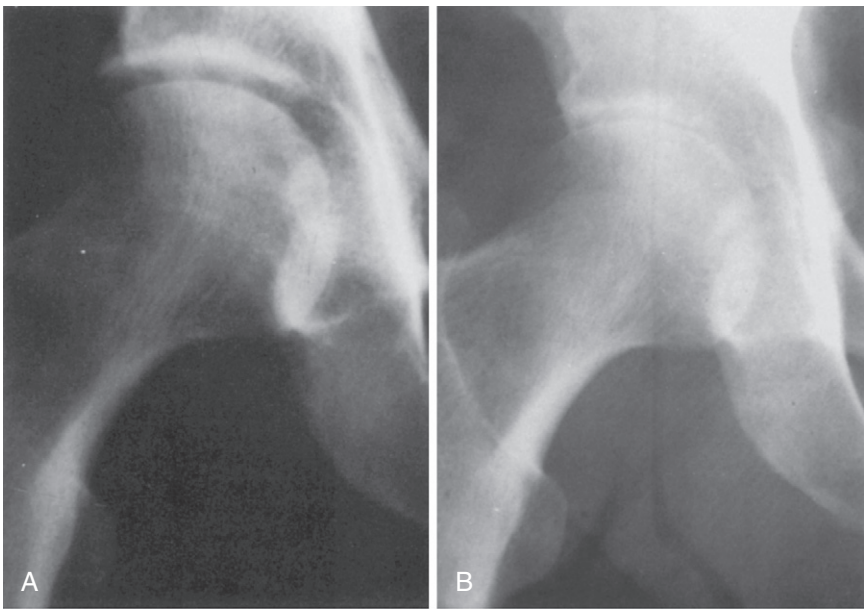

FIGURE 9-18. Rheumatoid hip: early changes. **A,** Normal hip. **B,** Same hip 1 year later showing uniform cartilage loss with axial migration.

FIGURE 9-19. AP view of both hips in a patient with rheumatoid arthritis. There is bilateral axial migration. There is minimal erosive disease. There is no evidence of osteophyte formation or reparative bone.

With cartilage loss, there are varying degrees of erosion and synovial cyst formation (Fig. 9-20). The changes in the femoral head also may be complicated by osteonecrosis secondary to steroid therapy. However, despite these changes and despite total loss of cartilage, the adjacent bone does not respond with repair phenomenon such as osteophytes or subchondral bone formation. Therefore, the typical rheumatoid pelvis shows bilateral symmetrical involvement of the hips with acetabula protrusio, osteoporosis, and noticeable absence of reparative bone and osteophyte formation (Fig. 9-21).

FIGURE 9-20. A, AP view of both hips in a patient with rheumatoid arthritis. Bilateral acetabuli protrusio is present. Small erosive changes involve both femoral heads and the acetabuli. There is no evidence of osteophyte formation or reparative bone present. **B,** Specimen radiograph of the femoral head in rheumatoid arthritis. Small erosions and cysts are demonstrated. There is no reparative bone. *(**A** from Brower AC: Disorders of the sacroiliac joint,* Radiolog *1[20]:3, 1978; reprinted by permission.)*

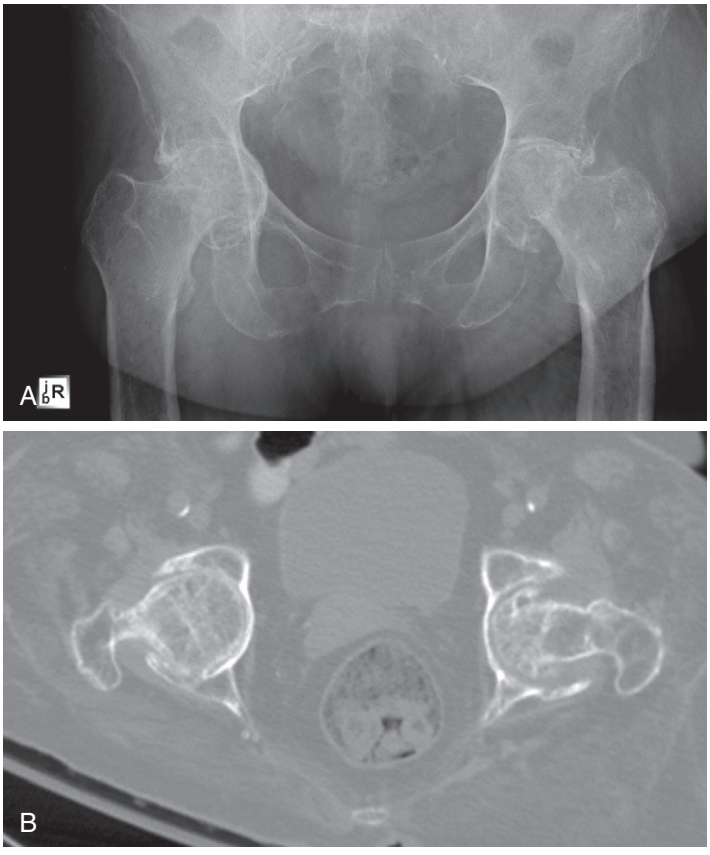

FIGURE 9-21. A, AP view of both hips in severe rheumatoid arthritis. There is severe bilateral acetabuli protrusio. Notice that the protrusion is in an axial direction. There is severe osteoporosis. There is no evidence of reparative bone. **B,** Axial computed tomography (CT) through the hips shows acetabuli protrusio and lack of reparative bone.

THE KNEES

The knees are involved in 80 percent of patients with rheumatoid arthritis. They are involved bilaterally and symmetrically. Radiographically, the knees must be evaluated with a standing AP view and a flexed lateral view to assess cartilage loss and alignment accurately. There is uniform loss of cartilage in all three compartments of the knee: the medial, lateral, and patellofemoral. Despite even severe loss of cartilage, there is little, if any, reparative response; there is a notable lack of subchondral bone and osteophyte formation (Fig. 9-22). Marginal erosions may occur but are not as prominent a part of the radiographic picture as they are in the hands. However, intraosseous synovial cysts may play a significant role. Such a cyst is produced by synovium breaking through the cartilage infiltrating into the bone. A ball-valve effect on the synovial fluid within the cyst causes enlargement of the cyst. Large cysts are called "geodes." Sometimes these geodes are mistaken for a bone neoplasm (Fig. 9-23). However, the presence of the uniform joint space narrowing and adjacent smaller cyst should indicate the correct diagnosis.

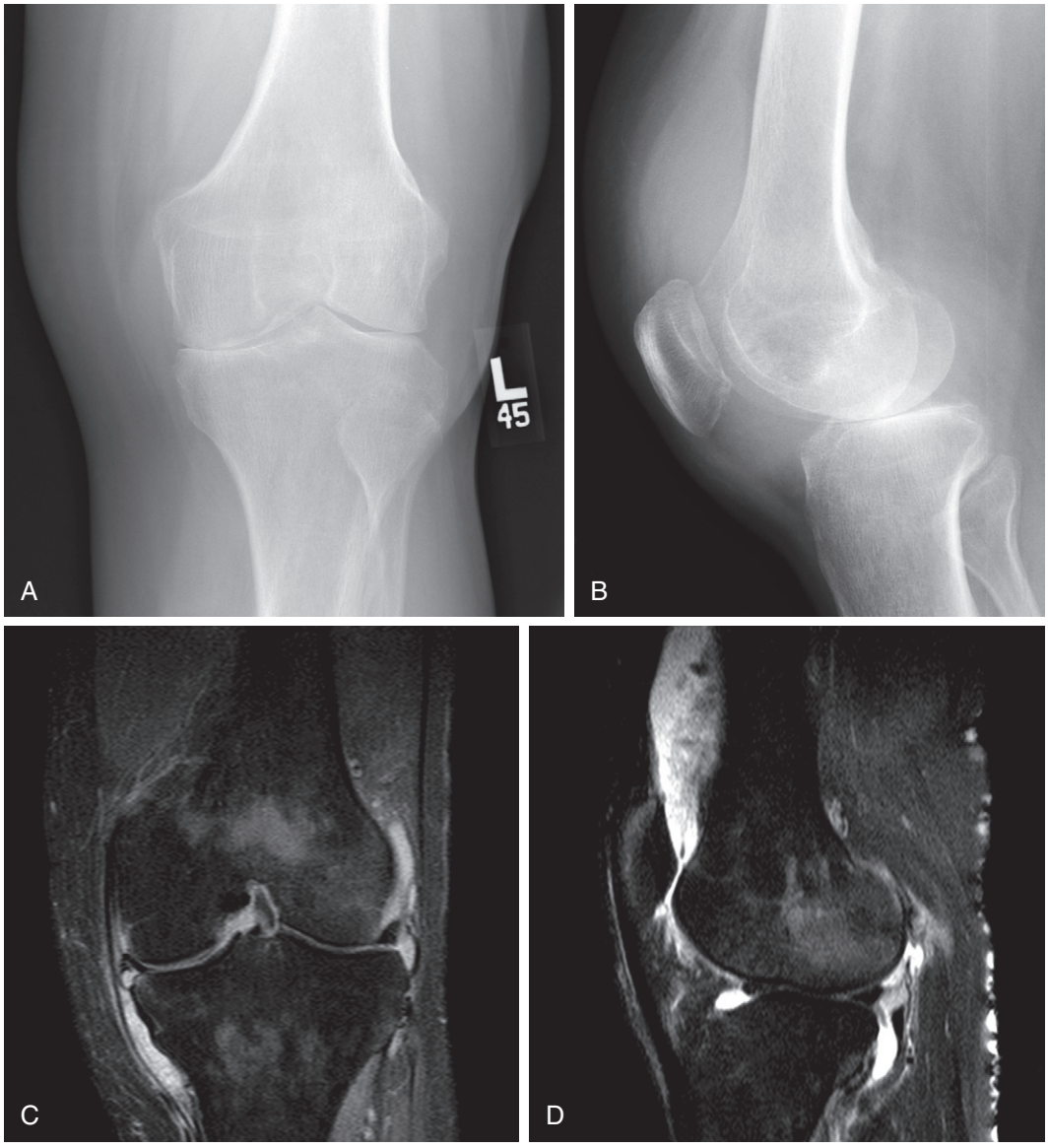

FIGURE 9-22. AP standing view (**A**) and lateral view (**B**) of both knees demonstrating cartilage loss of the medial and lateral compartments and large effusion. There is generalized osteoporosis present. Erosive disease is not a prominent feature. There is no evidence of bone repair. Coronal (**C**) and sagittal (**D**) fat-suppressed PD-weighted images show extensive synovitis with effusion and diffuse loss of articular cartilage.

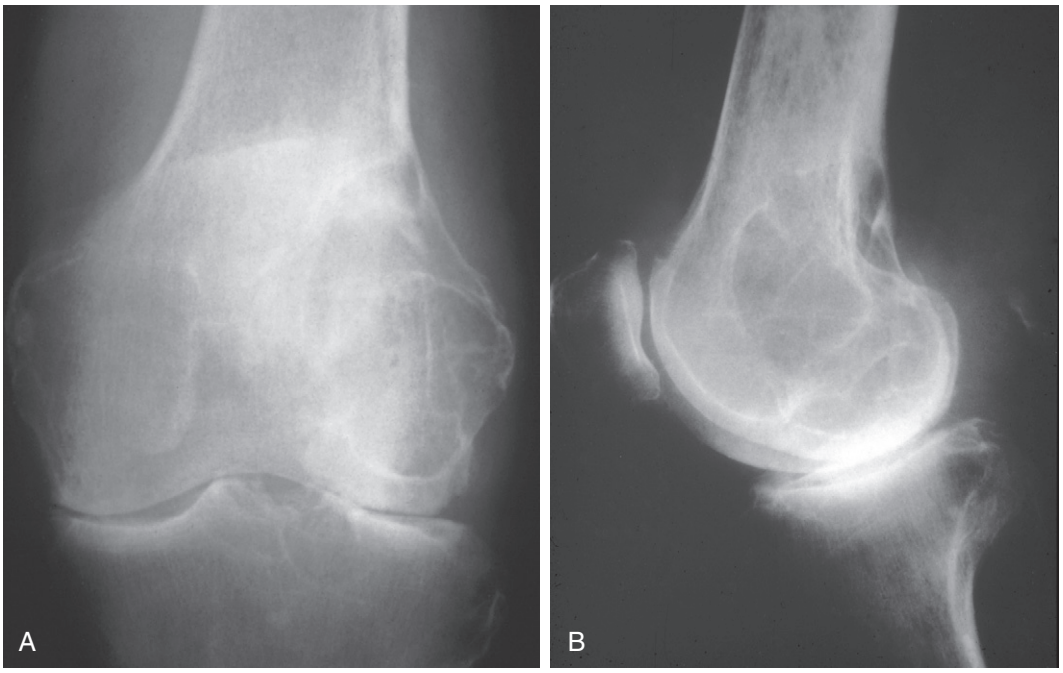

FIGURE 9-23. AP (**A**) and lateral (**B**) views of the knee in a patient with rheumatoid arthritis. A large synovial cyst involves the lateral femoral condyle and resembles a giant cell tumor. However, there is narrowing of the medial, lateral, and patellofemoral compartments. There is also a synovial cyst involving the adjacent tibial plateau. There is generalized osteoporosis. These related findings lead to the diagnosis of a rheumatoid "geode" rather than a giant cell tumor. *(From Kantor S, Brower AC: Radiographic assessment. In Rothermich N, Whisler R:* Rheumatoid arthritis, *Orlando, FL, Grune & Stratton, 1985, p. 57; reprinted by permission.)*

A Baker cyst, or synovial cyst extending into the soft tissues, is a frequent occurrence in rheumatoid arthritis. It extends posteriorly and may be directed inferiorly or superiorly in the soft tissues in the back of the knee. Ultrasound is often used to confirm the presence of a cyst. Rupture of a cyst with extravasation of cyst material into the surrounding muscle may cause symptoms similar to those of thrombophlebitis. However it must be remembered that a Baker cyst that has not ruptured can cause increased pressure on the deep venous system, producing a true thrombophlebitis.

THE ANKLES

The ankle is involved less frequently than the hand, foot, and knee. When involved, ankles show bilateral and symmetrical involvement. There is uniform loss of the cartilage in the ankle joint, with lack of reparative response (Fig. 9-24). Erosive changes do not play a prominent role. Synovial cysts may be present. The unique feature of ankle involvement is the periosteal reaction that may occur along the posterior shaft of the tibia. This may be just a manifestation of the patient's underlying disease; however, one must be careful to distinguish this periostitis from that occurring with a secondary stress fracture or osteomyelitis (Fig. 9-25).

FIGURE 9-24. AP view of the ankle in rheumatoid arthritis showing uniform narrowing of the joint space with severe osteoporosis of the surrounding bone structures.

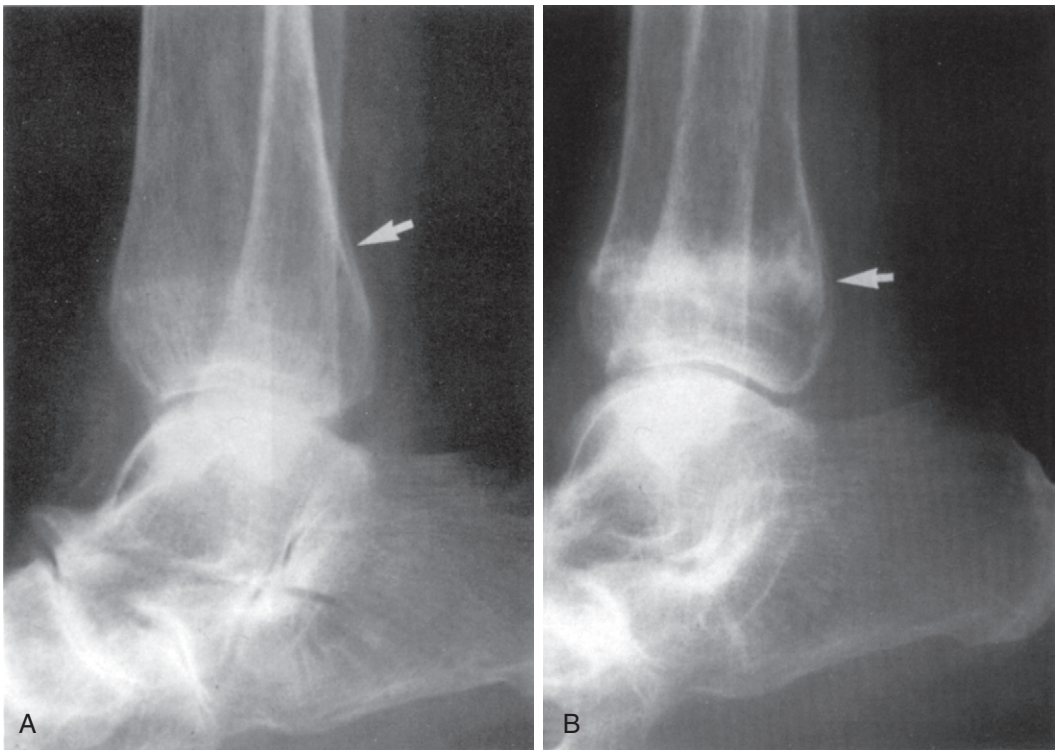

FIGURE 9-25. Lateral views of the ankle in rheumatoid arthritis. **A**, Generalized osteoporosis. Narrowing of the tarsal joints is visualized. There is a fine linear periosteal reaction posteriorly on the inferior aspect of the tibia (*arrow*). **B,** Ankle 10 days later demonstrating a stress fracture (*arrow*) of the distal tibia as the cause of the periosteal response.

THE SHOULDERS

Sixty percent of patients with rheumatoid arthritis ultimately have involvement of the shoulders. Radiographically there is uniform narrowing of all compartments of the shoulder joint: the glenohumeral, the acromial humeral, and the acromioclavicular (AC) joint. The humeral head therefore migrates proximally and superiorly in relationship to the glenoid (Fig. 9-26). There is usually an associated rotator cuff tear that allows the narrowing between the humerus and acromion. One may identify an actual erosion of the rotator cuff attachment (Fig. 9-27). Generalized osteoporosis is present. There is no evidence of bone repair or osteophyte formation. A synovial cyst may be present in the humeral head that may be mistaken for a chondroblastoma (Fig. 9-28); however, the joint space narrowing should preclude this diagnosis. There will be erosion of the distal end of the clavicle. Likewise, there may be erosion of the proximal end of the clavicle, as the sternoclavicular joint is also a synovial joint (Fig. 9-29).

FIGURE 9-26. AP view of the shoulder showing generalized osteoporosis. The humeral head has migrated proximally due to loss of cartilage in the glenohumeral joint. It has also migrated superiorly due to a rotator cuff tear. There is erosion of the distal end of the clavicle and remodelling of the medial humeral neck.

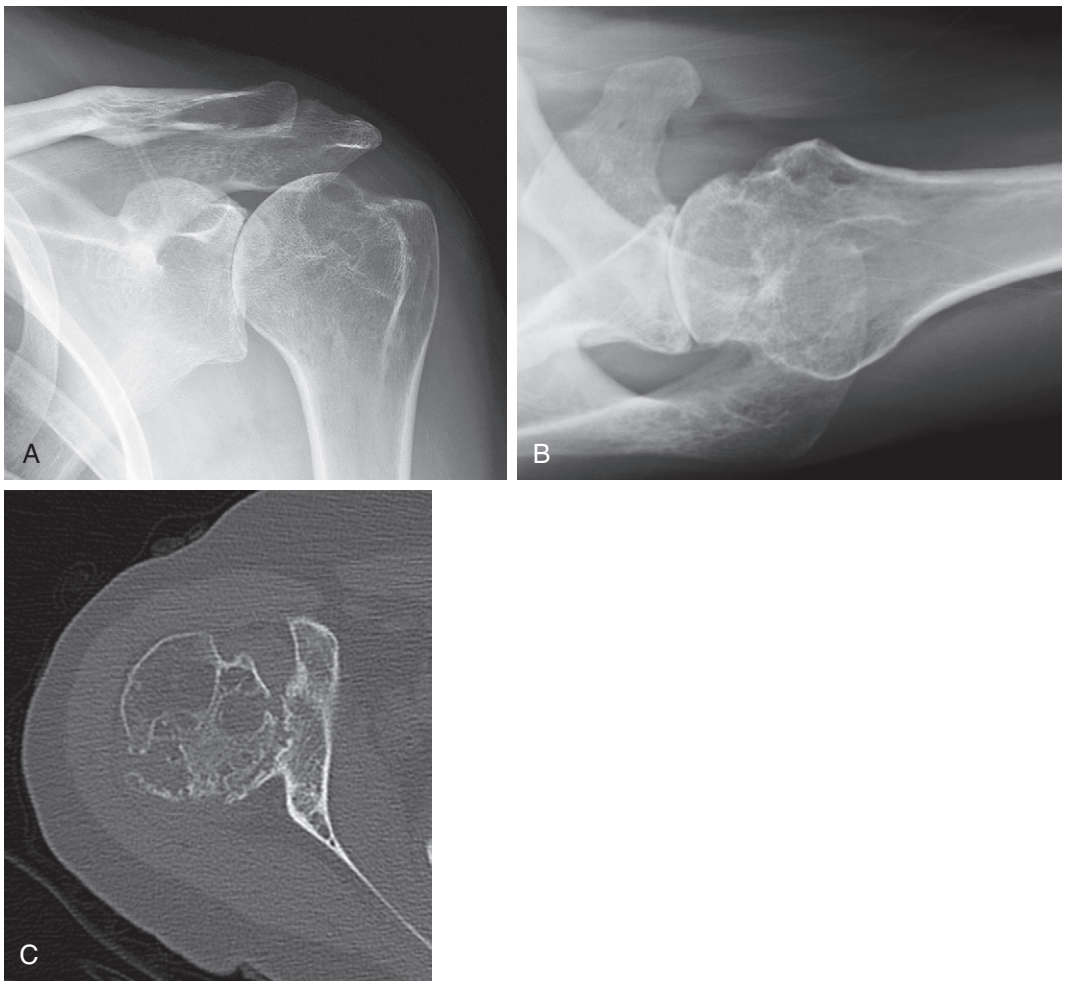

FIGURE 9-27. Posterior oblique (**A**) and axillary (**B**) view of shoulder of patient with rheumatoid arthritis. Humeral head has migrated inward and upward. Erosions are seen at attachment of the rotator cuff. **C,** Axial CT through the humeral head shows erosions and intraosseous cysts.

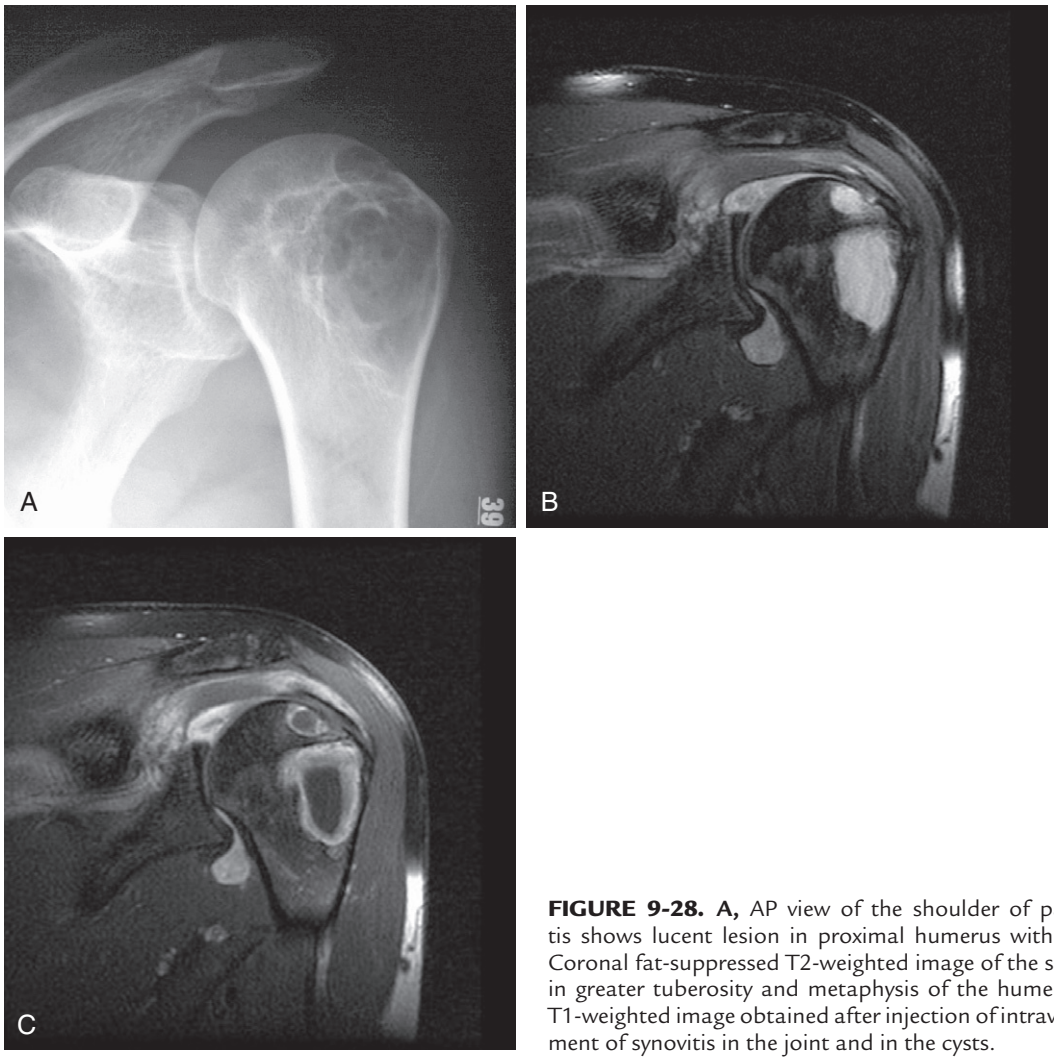

FIGURE 9-28. A, AP view of the shoulder of patient with rheumatoid arthritis shows lucent lesion in proximal humerus with thin sclerotic margination. **B,** Coronal fat-suppressed T2-weighted image of the shoulder shows high signal cysts in greater tuberosity and metaphysis of the humerus. **C,** Coronal fat-suppressed T1-weighted image obtained after injection of intravenous contrast shows enhancement of synovitis in the joint and in the cysts.

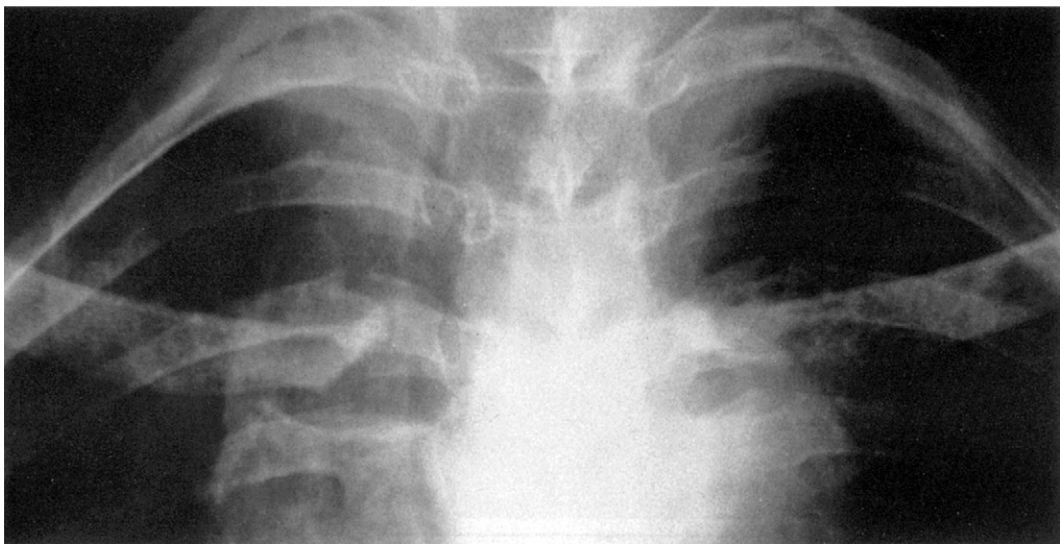

FIGURE 9-29. Erosive changes of the proximal end of the clavicle. *(From Kantor S, Brower AC: Radiographic assessment. In Rothermich N, Whisler R:* Rheumatoid arthritis, *Orlando, FL, Grune & Stratton, 1985, p. 57; reprinted by permission.)*

THE ELBOWS

The elbow is involved in 34 percent of patients with rheumatoid arthritis. When involved, the elbows show bilateral symmetrical involvement with uniform loss of the joint space. Generalized osteoporosis is present, and there is distinct lack of reparative bone and osteophyte formation (Fig. 9-30). The elbow joint may be so destroyed as to give the appearance of widening of the joint space (Fig. 9-31). Synovial cysts may occur around the elbow as well (Fig. 9-32).

FIGURE 9-30. AP view of the elbow showing uniform joint space loss between the radius and the humerus as well as between the ulna and the humerus. There is generalized osteoporosis. There is no evidence of reparative bone.

FIGURE 9-31. Lateral and AP views of the elbow showing such severe joint space loss as to give a widened appearance to the joint. Severe osteoporosis is present.

FIGURE 9-32. Lateral and AP views of the elbow. There are uniform joint space loss, osteoporosis, and synovial cysts (*arrows*).

THE SPINE

The thoracic and lumbar areas of the spine are usually not significantly involved in rheumatoid arthritis. However the cervical spine is involved in approximately 50 percent of individuals with rheumatoid arthritis. The most common abnormality seen in the cervical spine is atlantoaxial disease. The most frequent radiographic finding is laxity of the transverse ligament that holds the odontoid to the atlas. This laxity becomes apparent in the flexed lateral view of the cervical spine; unless the radiograph is taken in this position, this abnormality will be missed (Fig. 9-33). If every patient with rheumatoid arthritis had the cervical spine radiographed in a flexed position, 33 percent would demonstrate this abnormality. This laxity may become so severe as to require posterior fusion. It is believed that a gap of 8 mm or more between the odontoid and atlas requires surgical intervention (Fig. 9-34).

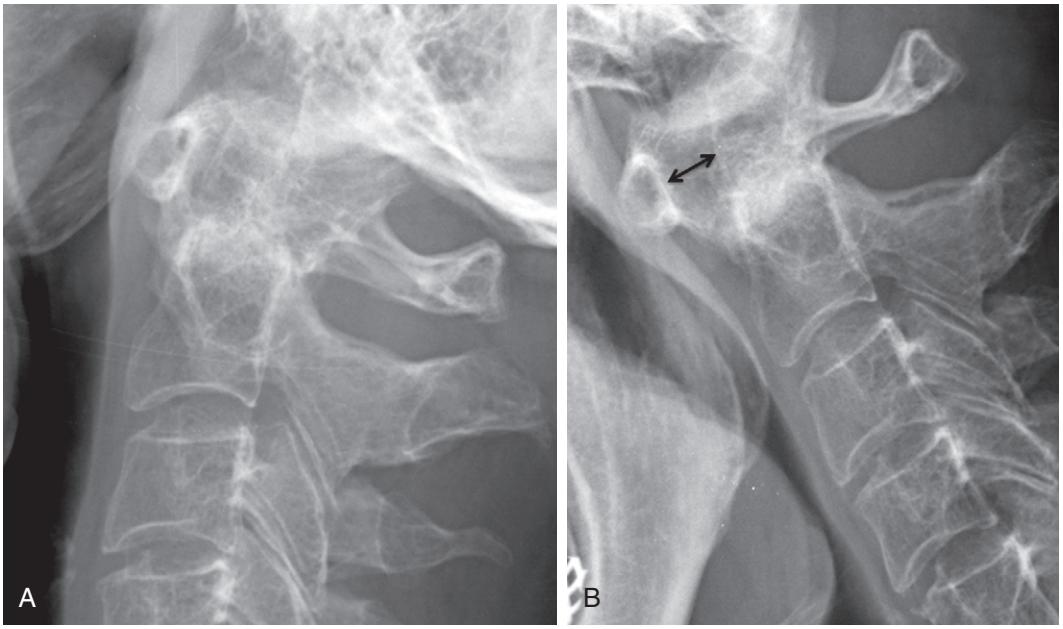

FIGURE 9-33. Lateral views of the C1-C2 area in patient with rheumatoid arthritis. **A,** Film was obtained in neutral position and shows no significant abnormality. **B,** Film taken with the neck in a flexed position demonstrates increased distance between the atlas and odontoid (*arrows*). This demonstrates nicely the laxity of the transverse ligament.

FIGURE 9-34. A, Lateral view of the upper cervical spine in patient with late rheumatoid arthritis. The distance between the atlas and the odontoid is greater than 8 mm, and there is marked narrowing of the spinal canal between the dens and posterior ring of C1 (*arrow*). Sagittal CT (**B**) and sagittal T2-weighted MR image (**C**) confirm marked compression of the spinal cord.

A more severe manifestation of atlantoaxial disease is vertical subluxation of the dens (Fig. 9-35) that is most accurately described as cranial cervical settling. Cranial cervical settling occurs because of extensive erosive changes between the atlantooccipital and atlantoaxial joint. The dens will project superior to the clivus and the anterior process of C1 will slide caudally on C2. One must assess the tip of the odontoid in relationship to the base of the skull. Erosion of the tip of the odontoid may serve as protection in patients with this malalignment; however erosion of the odontoid is not as common as subluxation of the atlantoaxial joint.

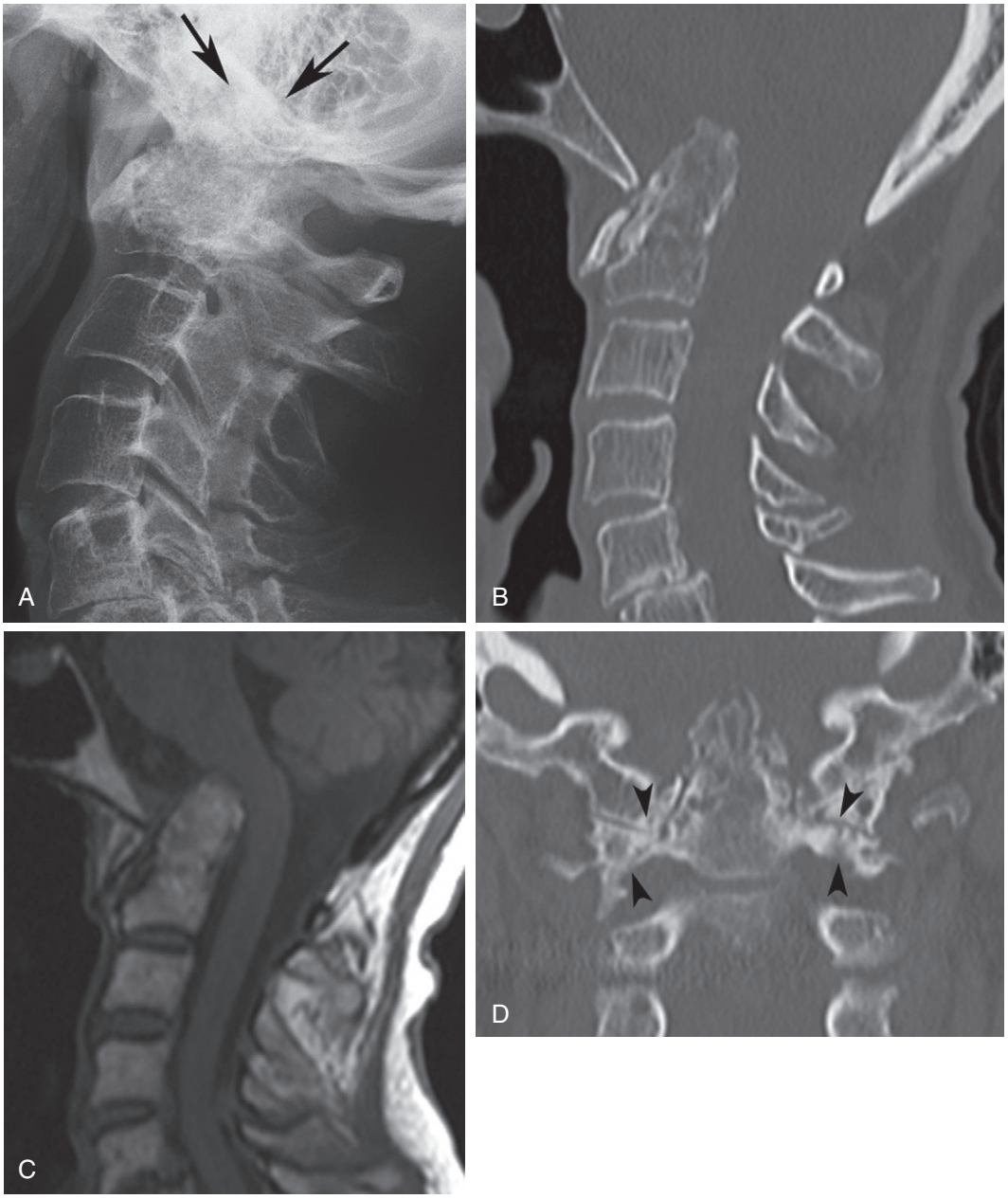

FIGURE 9-35. **A,** Lateral view of the upper cervical spine shows inferior displacement of the anterior arch of C1 on C2 and the tip of the dens projects superior to the clivus (*arrows*). **B,** Sagittal CT shows dens extending into foramen magnum. **C,** Sagittal T1-weighted MR image shows dens impinging on brain stem. **D,** Coronal CT shows erosive destruction of facets of C2 (*arrowheads*) that causes cranial cervical settling.

The apophyseal joints are commonly involved with erosive disease. Early erosive changes may be seen normally on the flexed lateral view of the spine (Fig. 9-36). Progressive involvement of the apophyseal joints leads to osteoporosis, disk space loss, and subluxations at multiple levels (Fig. 9-37). Very rarely, the apophyseal joints may ankylose.

FIGURE 9-36. Flexed lateral view of the cervical spine. Erosive changes (*arrow*) are seen at the apophyseal joint of C2-C3.

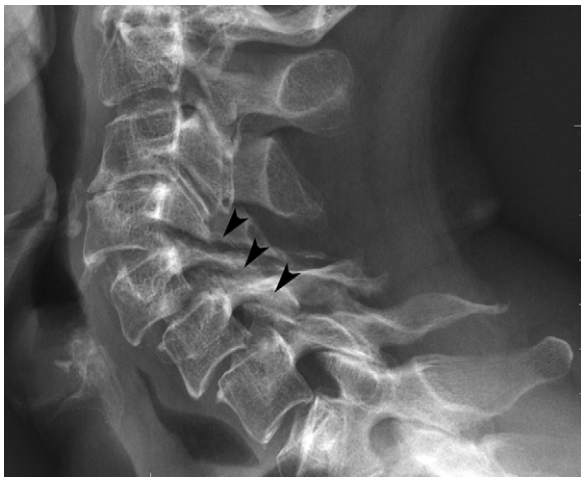

FIGURE 9-37. Lateral view of the cervical spine demonstrating late changes of rheumatoid arthritis. There is severe osteoporosis. There are anterior subluxations and severe erosions of facets (*arrows*) at C4-C5, C5-C6, and C6-C7.

Disc destruction and adjacent vertebral body destruction can occur from a synovitis extending from the joint of Luschka (Fig. 9-38). This must not be mistaken for infection. Despite the high percentage of patients with radiographically detectable cervical spine disease, only a small percentage eventually developed cervical myelopathy. MR imaging may be used to evaluate spinal cord involvement. It should be performed whenever the patient develops or changes neurologic symptoms or demonstrates progressive changes on serial radiographs of the cervical spine.

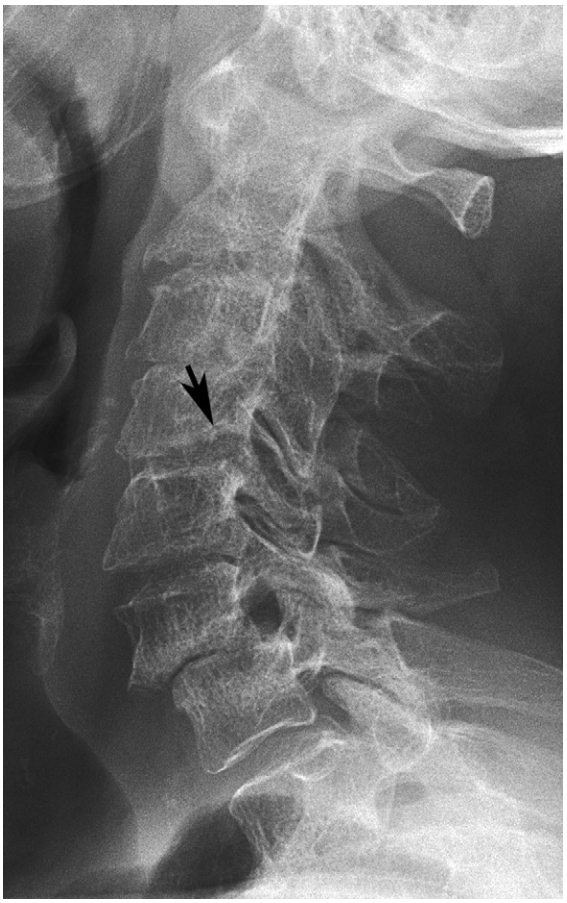

FIGURE 9-38. Lateral view of the cervical spine showing disc destruction at multiple levels and adjacent vertebral body destruction at C4-C5 (*arrow*). This is caused by a synovitis extending from the joint of Luschka.

THE SACROILIAC JOINTS

Involvement of the sacroiliac (SI) joints in rheumatoid arthritis is relatively insignificant. It occurs late in the patient's disease, if at all, and the patient and physician are more concerned about the involvement of the hands, feet, hips, or knees. Involvement of the SI joints is seen as a uniform narrowing of the joint space without evidence of bone repair or osteophyte formation (Fig. 9-39). Although erosive change can occur, it is never extensive enough to produce the apparent widening that one sees in the spondyloarthropathies. Bone ankylosis can occur, but only of the true synovial aspect of the SI joint (Fig. 9-40).

FIGURE 9-39. AP view of SI joints. There is bilateral symmetrical narrowing of the SI joints. There is generalized osteoporosis. There is no erosive disease and minimal bone repair.

FIGURE 9-40. AP view of the SI joints showing bone ankylosis of the synovial aspect of the joint.

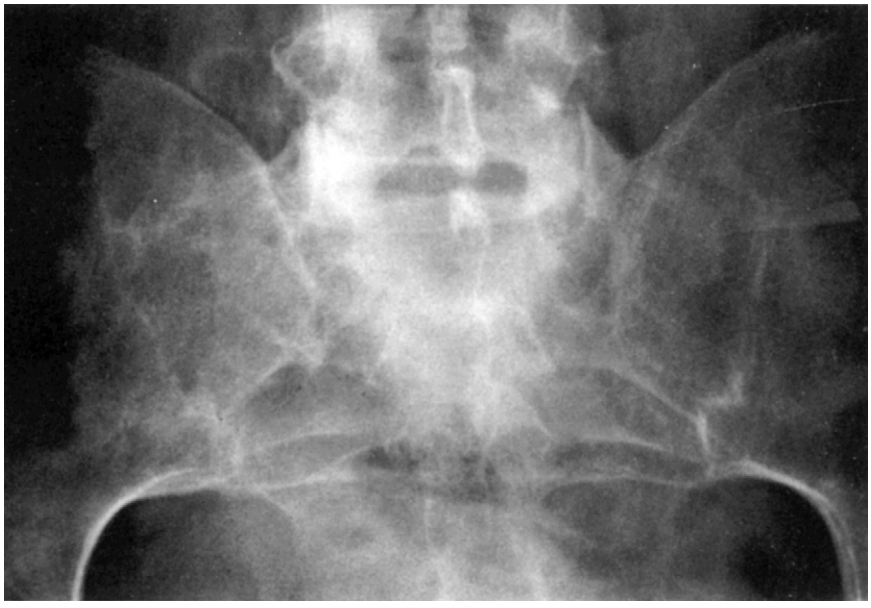

THE TEMPOROMANDIBULAR JOINT

The temporomandibular joint (TMJ) is often a forgotten joint in rheumatoid arthritis, but 80 percent of patients have symptoms in the TMJ. Osteoporosis, joint space narrowing, decreased range of motion, erosions of the condyles, and flattening of the temporomandibular fossa are the radiographic changes. These changes are best demonstrated through computed tomography (CT) and MR imaging (Fig. 9-41). Erosive disease may occur in the TMJ without significant erosive disease elsewhere in the body.

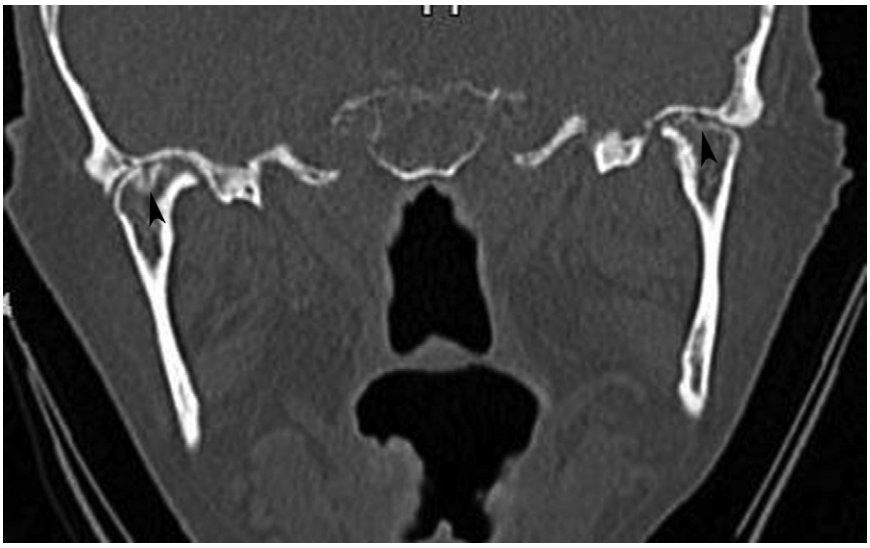

FIGURE 9-41. Coronal CT through the TMJs. There is osteoporosis, joint space loss, and erosion of the condyles (*arrow*).

SUMMARY

Rheumatoid arthritis is a common arthropathy with characteristic radiographic joint changes and distribution. Its hallmarks are symmetry, osteoporosis, uniform cartilage loss, erosions, and lack of bone response or proliferation.

SUGGESTED READINGS

Berens DL, Lockie LM, Lin RK, et al: Roentgen changes in early rheumatoid arthritis: Wrist-hands-feet, *Radiology* 82:645–654, 1964.

Brewerton DA: Hand deformities in rheumatoid disease, *Ann Rheum Dis* 16:183–197, 1957.

Brower AC: Radiographic assessment of disease progression in rheumatoid arthritis, *Rheum Dis Clin North Am* 17:471–485, 1991.

Calabro JJ: A critical evaluation of the diagnostic features of the feet in rheumatoid arthritis, *Arthritis Rheum* 5:19–29, 1962.

Chalmers IM, Blair GS: Rheumatoid arthritis of the temporomandibular joint: A clinical and radiologic study using circular tomography, *Q J Med* 42:369–386, 1973.

Good AE: Rheumatoid arthritis, Baker's cyst, and "thrombophlebitis, *Arthritis Rheum* 7:56–64, 1964.

Hastings DA, Parker SM: Protrusio acetabuli in rheumatoid arthritis, *Clin Orthop Relat Res* 108:76–83, 1975.

Kalliomäki JL, Viitanen S-M, Virtama P: Radiological findings of sternoclavicular joints in rheumatoid arthritis, *Acta Rheumatol Scand* 14:233–240, 1968.

Kirkup JR: Ankle and tarsal joints in rheumatoid arthritis, *Scand J Rheumatol* 3:50–52, 1974.

Komusi T, Munro T, Harth M: Radiologic review: The rheumatoid cervical spine, *Semin Arthritis Rheum* 14:187–195, 1985.

Magyar E, Talerman A, Fehér M, et al: The pathogenesis of the subchondral pseudocysts in rheumatoid arthritis, *Clin Orthop Relat Res* 100:341–344, 1974.

Martel W: Diagnostic radiology in the rheumatic diseases. In Kelley WN, et al, editors: *Textbook of rheumatology*, ed 3, Philadelphia, 1993, W.B. Saunders.

Martel W, Duff IF: Pelvo-spondylitis in rheumatoid arthritis, *Radiology* 77:744–756, 1961.

Martel W, Hayes JT, Duff IF: The pattern of bone erosion in the hand and wrist in rheumatoid arthritis, *Radiology* 84:204–214, 1965.

Nørgaard F: Earliest roentgenological changes in polyarthritis of the rheumatoid type: Rheumatoid arthritis, *Radiology* 85:325–329, 1965.

Park WM, O'Neill M, McCall IW: The radiology of rheumatoid involvement of the cervical spine, *Skeletal Radiol* 4:1–7, 1979.

Poleksic L, Zdravkovic D, Jablanovic D, et al: Magnetic resonance imaging of bone destruction in rheumatoid arthritis: Comparison with radiology, *Skeletal Radiol* 22:577–580, 1993.

Resnick D: Patterns of migration of the femoral head in osteoarthritis of the hip: Roentgenographic-pathologic correlation and comparison with rheumatoid arthritis, *Am J Roentgenol Radium Ther Nucl Med* 124:62–74, 1975.

Resnick D: Rheumatoid arthritis and related diseases. In Resnick D, editor: *Diagnosis of bone and joint disorders*, ed 3, Philadelphia, 1995, W.B. Saunders.

Resnick D: Rheumatoid arthritis of the wrist: The compartmental approach, *Med Radiogr Photogr* 52:50–88, 1976.

Sbarbaro JL: The rheumatoid shoulder, *Orthop Clin North Am* 6:593–596, 1975.

Weissman BN, et al: Prognostic features of atlantoaxial subluxation in rheumatoid arthritis patients, *Radiology* 144:745–751, 1982.

Weston WJ: The synovial changes at the elbow in rheumatoid arthritis, *Australas Radiol* 15:170–175, 1971.

10 *Psoriatic Arthritis*

For years psoriatic arthritis was considered part of the spectrum of rheumatoid arthritis. The classification of psoriatic arthritis as a "rheumatoid variant" persists today. However, the radiographic manifestations, along with clinical and laboratory data, establish psoriatic arthritis as a separate and distinct articular disorder. Psoriatic arthritis occurs in 5 to 8 percent of patients with severe and longstanding psoriatic skin disease. However, the arthropathy may coincide with or antedate the appearance of skin disease. In these patients, the radiographic examination becomes the determinate diagnostic study. The distinguishing radiographic features are as follows:

1. Fusiform soft tissue swelling
2. Maintenance of normal mineralization
3. Dramatic joint space loss
4. Bone proliferation
5. "Pencil-in-cup" erosions
6. Bilateral asymmetrical distribution
7. Distribution primarily in hands, feet, sacroiliac (SI) joints, and spine, in decreasing order of frequency

Although psoriatic arthritis differs from rheumatoid arthritis radiographically in many ways, the most significant difference is the presence of bone proliferation.

THE HANDS

The hands are most commonly involved in psoriatic arthritis. Although there may be nonspecific periarticular fusiform soft tissue swelling, there may be soft tissue edema beyond the joint, causing swelling of the entire digit in approximately 25 percent of patients. This dactylitis is described as sausage-like or resembling a cocktail hot dog (Fig. 10-1) on clinical examination and is highly specific for a spondyloarthropathy. Juxta-articular osteoporosis may occur in the early phases of the disease; however, it is transient. Normal mineralization is usually maintained even in the presence of severe erosive disease. Erosions occur initially at the margins of the joint but with time progress to involve the central area (Fig. 10-2). The erosion may become so extensive, destroying so much of the underlying bone, that the joint space may actually appear to be widened. The ends of the bones may become pointed, appearing as if destroyed by a pencil sharpener. The bone articulating with the pointed bone may become saucerized through erosion, producing the classic "pencil-in-cup" or "cup-and-saucer" appearance (Fig. 10-3). Erosions may also be appreciated involving the distal tufts of the fingers producing a pattern of acro-osteolysis.

FIGURE 10-1. Posteroanterior (PA) view of the hand showing classic radiographic changes of psoriatic arthritis: sausage-like swelling of the first, second, and third digits; normal mineralization; severe erosive changes creating the appearance of widened joint spaces of the second and third DIP joints; solid periosteal new bone added to the middle phalanx of third digit, widening the shaft; and fluffy new bone apposition adjacent to erosive changes (*arrows*).

FIGURE 10-2. A, Marginal erosions of the DIP joint. **B,** Marginal erosions have progressed to involve the central area of the PIP joint. Note ankylosis of DIP joint.

FIGURE 10-3. PA view of fourth digit in a patient with psoriasis demonstrating a classical "pencil-in-cup" deformity. Notice sausage-like swelling.

Bone proliferation is one of the most important features of psoriatic arthritis and is almost always present in some form. Bone proliferation takes place in four areas: adjacent to erosions, along shafts, across joints, and at tendinous and ligamentous insertions. The bone proliferation adjacent to erosive changes is observed as irregular excrescences with a spiculated, frayed, or fluffy appearance. With time these excrescences become well-defined bone (Fig. 10-4). Bone proliferation may be observed along shafts as a periostitis (Fig. 10-5). Initially it is exuberant and fluffy in appearance. Eventually it becomes solid new bone along the shaft of the phalanx, causing the widened appearance to the phalanx (see Fig. 10-1). Bone ankylosis across a joint is a common occurrence in distal interphalangeal (DIP) and proximal interphalangeal (PIP) joints (see Fig. 10-2 and 10-6). Bone proliferation occurring at tendinous and ligamentous insertions in the hand and wrist will be seen as a continuation of the periosteal response.

FIGURE 10-4. Bone proliferation (*arrows*) adjacent to erosive changes. Some excrescences are well defined, whereas others are more irregular in appearance.

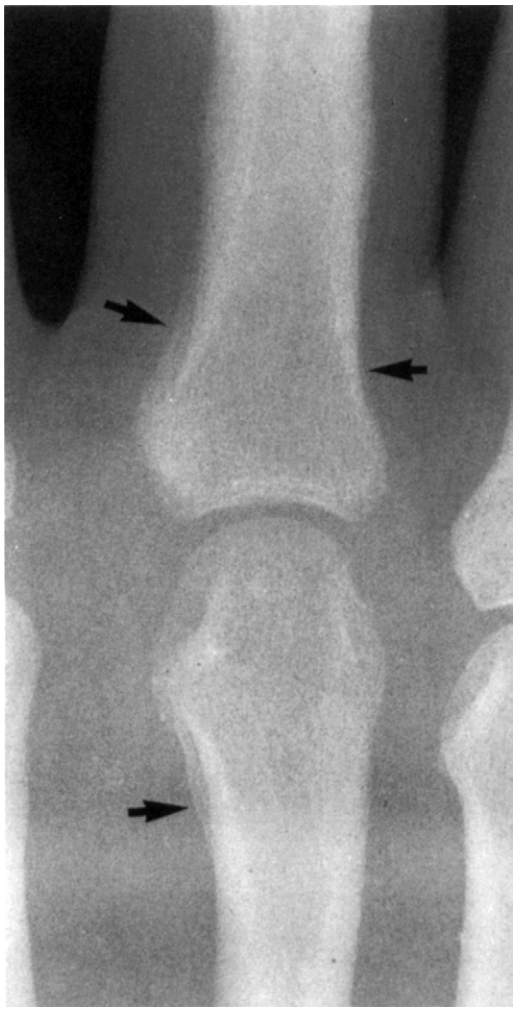

FIGURE 10-5. Periostitis (*arrows*) along the shafts of bones.

In the hand, psoriatic arthritis has three different patterns of distribution. The first pattern is primarily DIP and PIP involvement, with relative sparing of the metacarpophalangeal (MCP) and carpal joints (Fig. 10-7). The second pattern is ray involvement, wherein one to three fingers will be involved in all joints while the other fingers are spared. The carpal bones may or may not be involved (Fig. 10-8). The third pattern is similar to rheumatoid arthritis. In this distribution, other features will distinguish psoriatic arthritis from rheumatoid arthritis (Fig. 10-9). There is usually DIP involvement or evidence of bone proliferation (Fig. 10-10).

FIGURE 10-6. Bone ankylosis of the second and fifth DIP joints.

FIGURE 10-7. Involvement of IP joints with relative sparing of MCP joints. There are "pencil-in-cup" erosive changes involving the IP joint of the thumb and the DIP joint of the second and fifth digit.

FIGURE 10-8. PA view of the hand in patient with psoriasis. The fifth digit is involved in all joints, including the carpometacarpal joint, with erosion and bone production.

FIGURE 10-9. PA view of hand in a patient with psoriatic arthritis. There is pancarpal involvement with erosive change and partial ankylosis. There is uniform MCP involvement with erosive change; however, notice that the mineralization is normal. There is erosive change involving the PIP joint of the fifth digit and a "pencil-in-cup" erosion of the PIP joint of the fourth digit. There is bone ankylosis of the second and third PIP and second DIP joints.

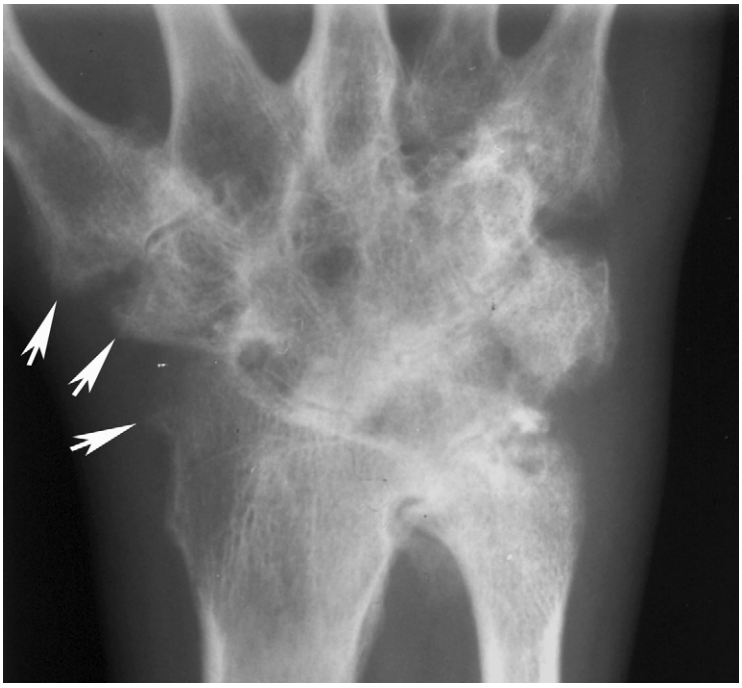

FIGURE 10-10. PA view of the wrist in a patient with psoriatic arthritis. There is pancarpal involvement with severe erosions of all the carpal bones. There is also evidence of bone ankylosis of the scaphoid to the trapezium and carpal to metacarpal bones. However, evidence of bone production, best seen at the radial aspect of the basal joint and radial styloid (*arrow*), distinguishes this psoriatic wrist from a wrist with rheumatoid arthritis.

THE FEET

The radiographic changes described in the hand are also found in the feet. An entire digit may be swollen and resemble a sausage (Fig. 10-11). Although there may be early juxta-articular osteoporosis, generally the mineralization is maintained. Severe erosive changes with pencil pointing are observed. Extensive destruction of the interphalangeal (IP) joint of the great toe is more common in psoriatic arthritis than in any other arthritis (Fig. 10-12). Bone proliferation is identified as periostitis, new bone formation around erosions, and bone ankylosis of IP joints (Fig. 10-13). Bone proliferation around the distal phalanx of a toe may produce an "ivory" phalanx (Fig. 10-14).

FIGURE 10-11. Soft tissue swelling of the entire second digit. Notice the fluffy periostitis (*arrow*) along the proximal phalanx. *(From Brower AC: The radiographic features of psoriatic arthritis. In Gerber L, Espinoza L, editors:* Psoriatic arthritis, *Orlando, FL, Grune & Stratton, 1985, p. 125; reprinted by permission.)*

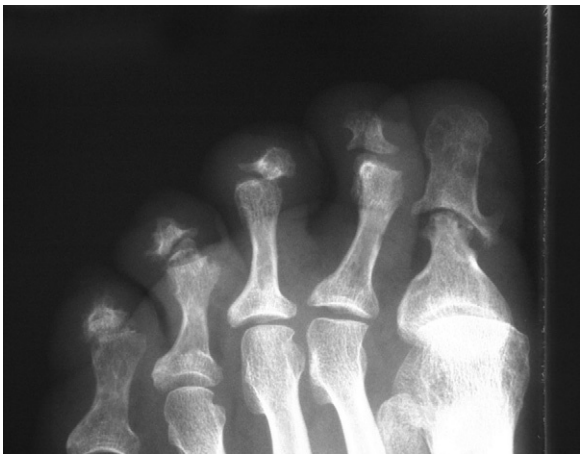

FIGURE 10-12. Anteroposterior (AP) view of the forefoot in a patient with psoriatic arthritis. Notice severe erosive changes of the DIP joints of the second, third, fourth, and fifth digits. There is total destruction of the IP joint of the big toe with complete distortion of the distal end of the proximal phalanx. Notice that mineralization is normal.

FIGURE 10-13. AP view of forefoot in a patient with psoriatic arthritis. Notice normal mineralization. There is pencil pointing of the distal metatarsals with subluxations and dislocations of the proximal phalanges. There is bone ankylosis of the PIP joint of the second and third digit.

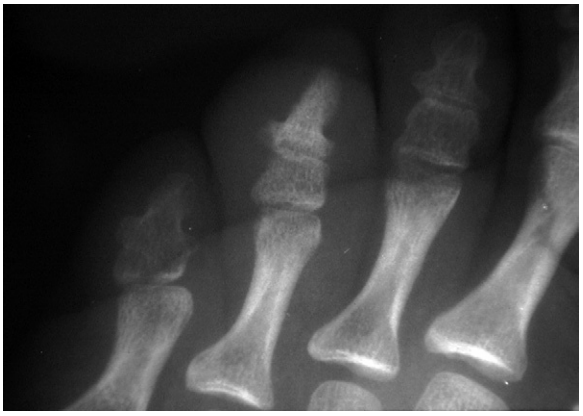

FIGURE 10-14. Erosion and bone proliferation of the distal phalanx of the fourth toe, producing an "ivory" appearance. Notice sausage-like appearance of soft tissue swelling.

As with the hand, three different patterns of distribution occur in the foot. Distal IP and PIP involvement is common (see Fig. 10-12); however, metatarsophalangeal (MTP) involvement is more common than MCP involvement (Fig. 10-15). Again, one to three rays may be affected, with the other rays being spared (Fig. 10-16).

FIGURE 10-15. AP view of forefoot in a patient with psoriatic arthritis. There is significant involvement of the MTP joints as well as ankylosis of the first IP joint.

FIGURE 10-16. AP view of the digits of the right foot in a patient with psoriasis. The fourth and fifth digits are involved with erosion and new bone production (*arrows*). The other digits are spared.

Radiographic changes are frequently seen on the posterior and inferior aspects of the calcaneus. Erosion and bone proliferation occur at the site of the Achilles tendon attachment posteriorly and superiorly (Fig. 10-17). Similar changes occur at the attachment of the plantar aponeurosis inferiorly, creating irregular and ill-defined spurs (Fig. 10-18). The spurs tend to point upward toward the calcaneus rather than downward along the course of the plantar aponeurosis as a normal heel spur points. Occasionally the entire inferior aspect of the calcaneus may be involved.

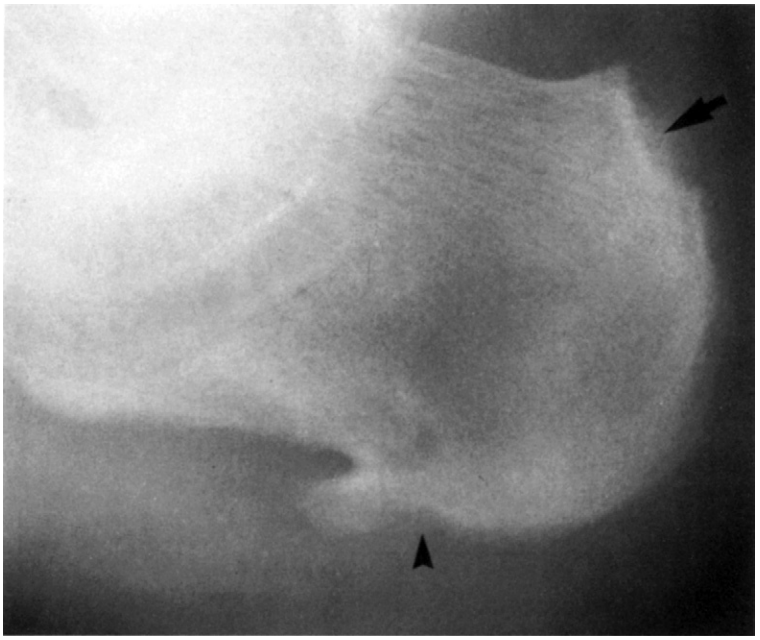

FIGURE 10-17. Erosion and bone production at the attachment of the Achilles tendon (*arrow*). There is also erosion of a calcaneal spur (*arrowhead*).

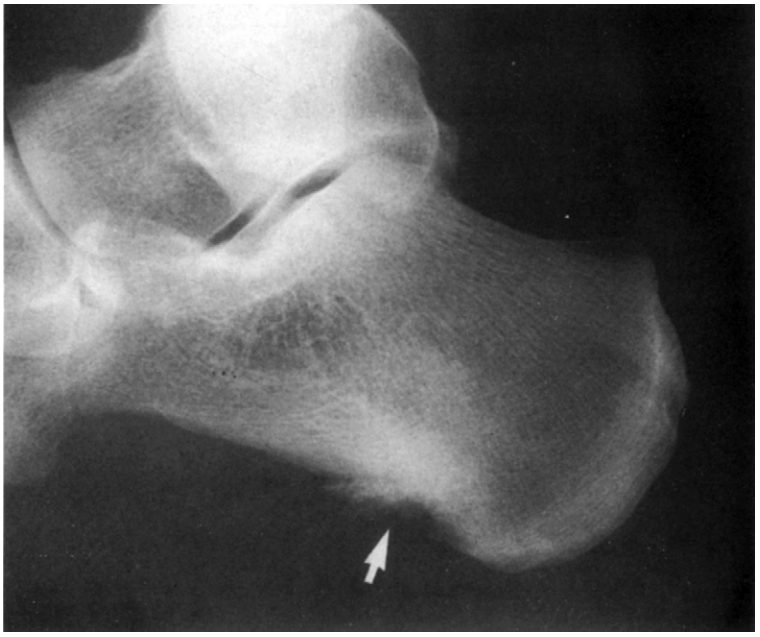

FIGURE 10-18. Erosion and bone proliferation at the attachment of the plantar aponeurosis (*arrow*). *(From Brower AC: The radiographic features of psoriatic arthritis. In Gerber L, Espinoza L, editors:* Psoriatic arthritis, *Orlando, FL, Grune & Stratton, 1985, p. 125; reprinted by permission.)*

OTHER APPENDICULAR SITES

The shoulder, elbow, knee, and ankle may be involved in psoriatic arthritis (Figs. 10-19 to 10-21). It is unusual for the hips to be affected. Bilateral but asymmetrical involvement is characteristic. Mineralization tends to be maintained. There is uniform loss of cartilage. Varying degrees of erosive changes and adjacent bone proliferation are characteristic. Bone proliferation at tendinous and ligamentous insertions is more frequently observed around the bigger joints. Common sites of proliferation are the femoral trochanters, the ischial tuberosities, the coracoclavicular ligament, the insertion of the rotator cuff, and the patellar tendons.

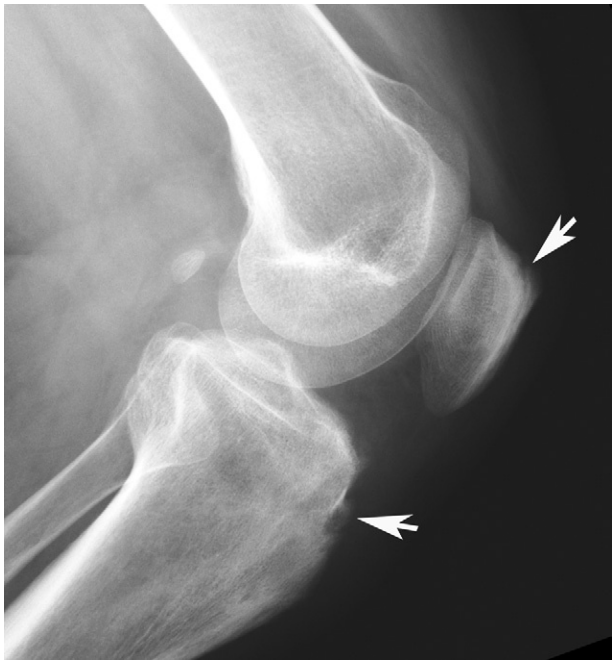

FIGURE 10-19. Lateral view of a knee of patient with psoriatic arthritis. There is narrowing of the joint spaces and bone proliferation on the superior surface of the patella and anterior proximal tibia (*arrows*).

FIGURE 10-20. AP view of the ankle. Notice soft tissue swelling. There is fluffy periosteal bone formation along the medial aspect of the distal tibia (*arrows*).

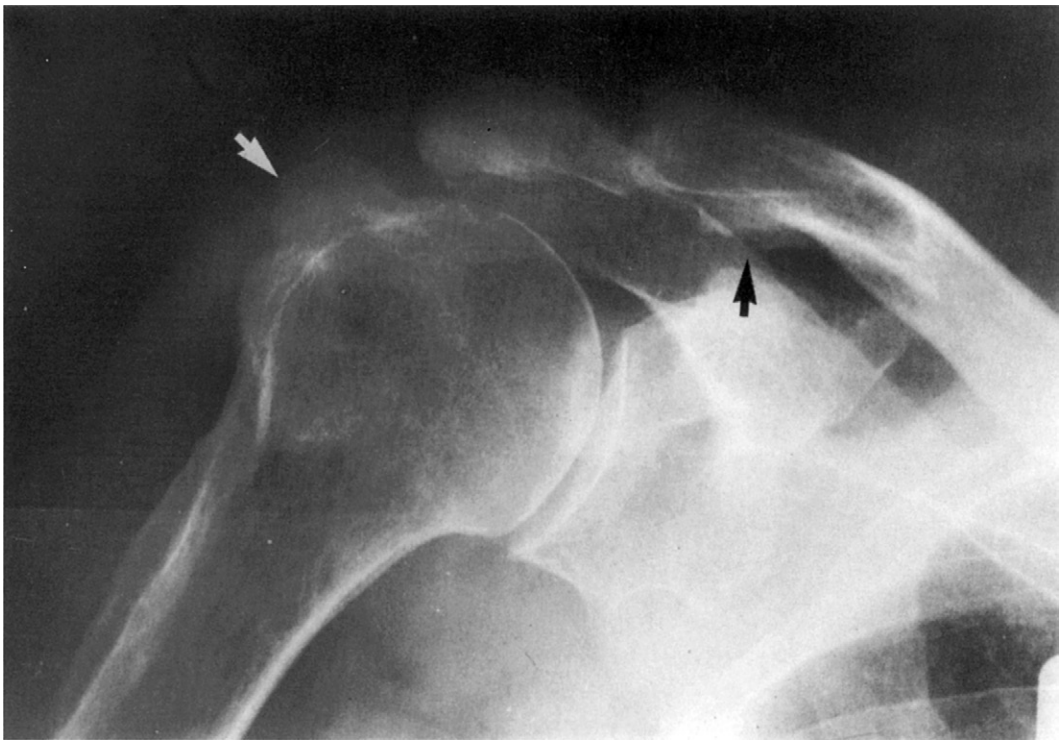

FIGURE 10-21. AP view of the shoulder in psoriatic arthritis. There is exuberant bone formation at tendon and ligamentous attachments (*arrows*). *(From Brower AC: The radiographic features of psoriatic arthritis. In Gerber L, Spinoza L, editors:* Psoriatic arthritis, *Orlando, FL, Grune & Stratton, 1985, p. 125; reprinted by permission.)*

THE SACROILIAC JOINTS

Thirty to 50 percent of patients with psoriatic arthritis have involvement of their SI joints. Although the involvement may be bilateral and symmetrical, it is usually bilateral and asymmetrical, with one side being more involved than the other (Fig. 10-22). Initially, erosive changes are seen on the iliac side of the true synovial joint. As the erosions enlarge and involve the sacral side, proliferative bone repair is observed. The erosions and bone repair are more extensive than that seen with ankylosing spondylitis (Fig. 10-23). Bony ankylosis may occur across the joint, but much less frequently than is observed in ankylosing spondylitis.

Outside the true synovial joint, ossification of the ligaments between the sacrum and ilium may occur even without ankylosis of the synovial joint. Ossification of other tendinous attachments, including the iliac crest, the ischial tuberosities, and the femoral trochanters, may be seen on the film of the pelvis.

FIGURE 10-22. AP Ferguson view of the SI joints in psoriatic arthritis. There is bilateral but asymmetrical involvement consisting of erosions and reparative bone, predominantly on the iliac side. *(From Brower AC: The radiographic features of psoriatic arthritis. In Gerber L, Espinoza L, editors:* Psoriatic arthritis, *Orlando, FL, Grune & Stratton, 1985, p. 125; reprinted by permission.)*

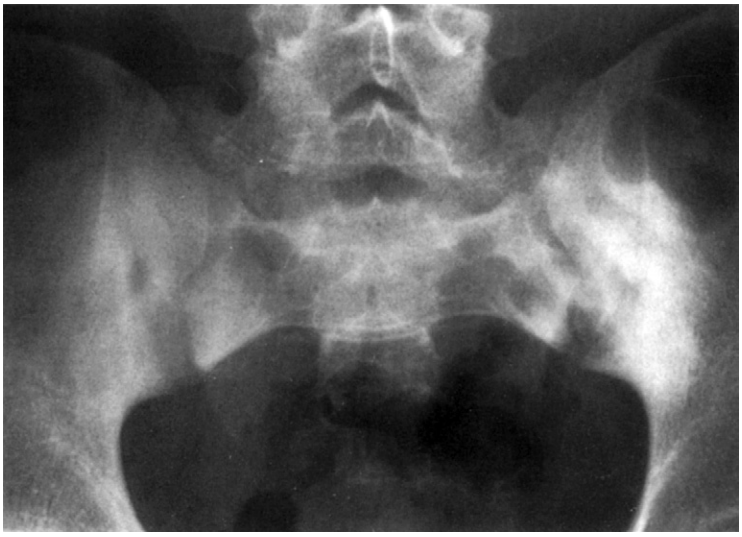

FIGURE 10-23. AP view of the SI joints in a patient with psoriatic arthritis. Large erosions and extensive bone repair are present.

THE SPINE

Spondylitis may occur usually with, but occasionally without, involvement of the SI joints. Involvement of the lumbar and thoracic spine is observed as paravertebral ossification. Large, bulky, bony outgrowths, unilateral or asymmetrical in their distribution, are characteristic and distinguish psoriasis from the succinct syndesmophyte of ankylosing spondylitis (Fig. 10-24). There is no squaring of the vertebral bodies and only occasional involvement of the apophyseal joints, which are two changes characteristic of ankylosing spondylitis.

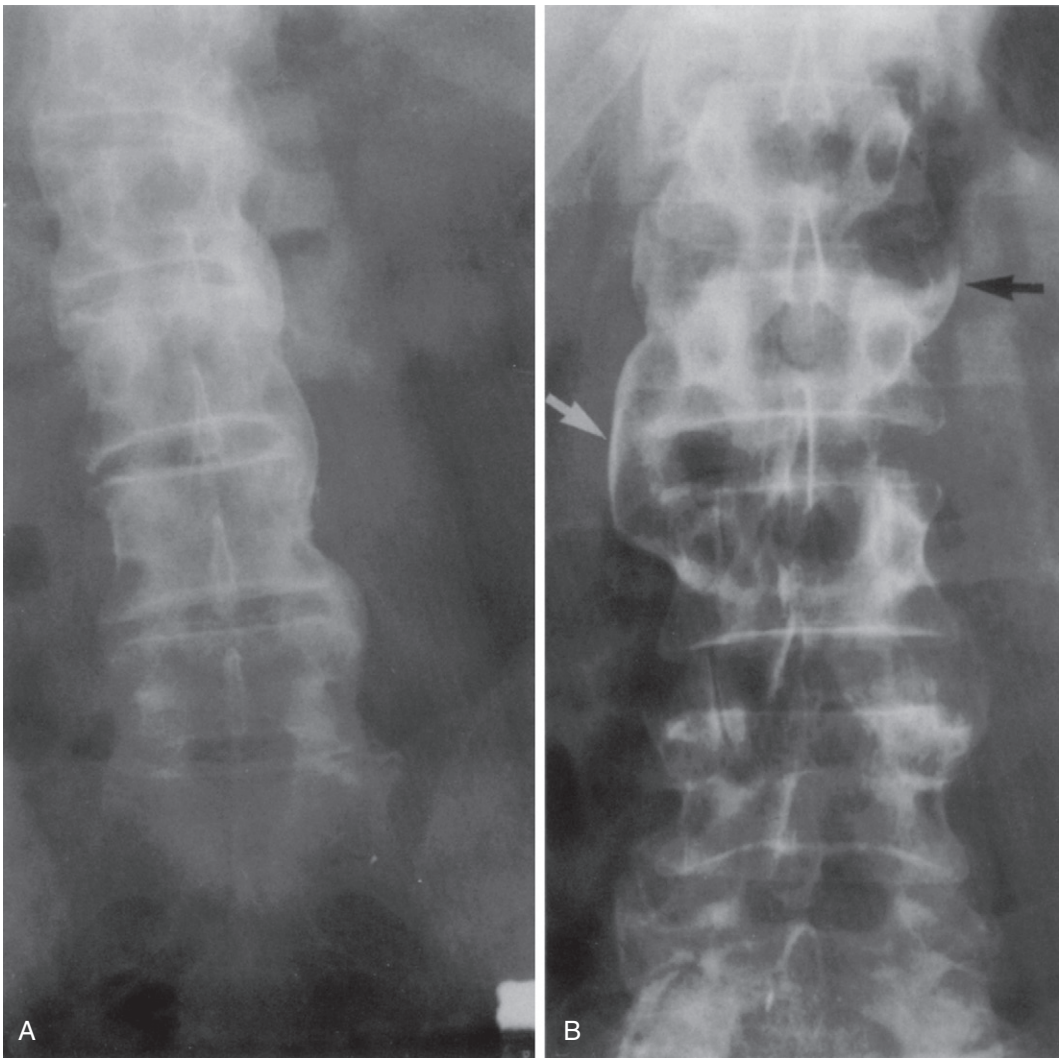

FIGURE 10-24. Psoriatic spondylitis. **A,** Asymmetrical, unilateral paravertebral ossifications. **B,** Large, bulky bone outgrowths joining underlying vertebral bodies. Notice the asymmetrical distribution (*arrows*). *(From Brower AC: The radiographic features of psoriatic arthritis. In Gerber L, Espinoza L, editors:* Psoriatic arthritis, *Orlando, FL, Grune & Stratton, 1985, p. 125; reprinted by permission.)*

The cervical spine may be involved, with or without involvement of the rest of the spine. In the cervical spine, the apophyseal joints are frequently affected, with narrowing, erosion, bone proliferation, and occasionally ankylosis (Fig. 10-25). There may be extensive bone proliferation along the anterior surface of the spine. Atlantoaxial subluxation, similar to that seen in rheumatoid arthritis, may also occur.

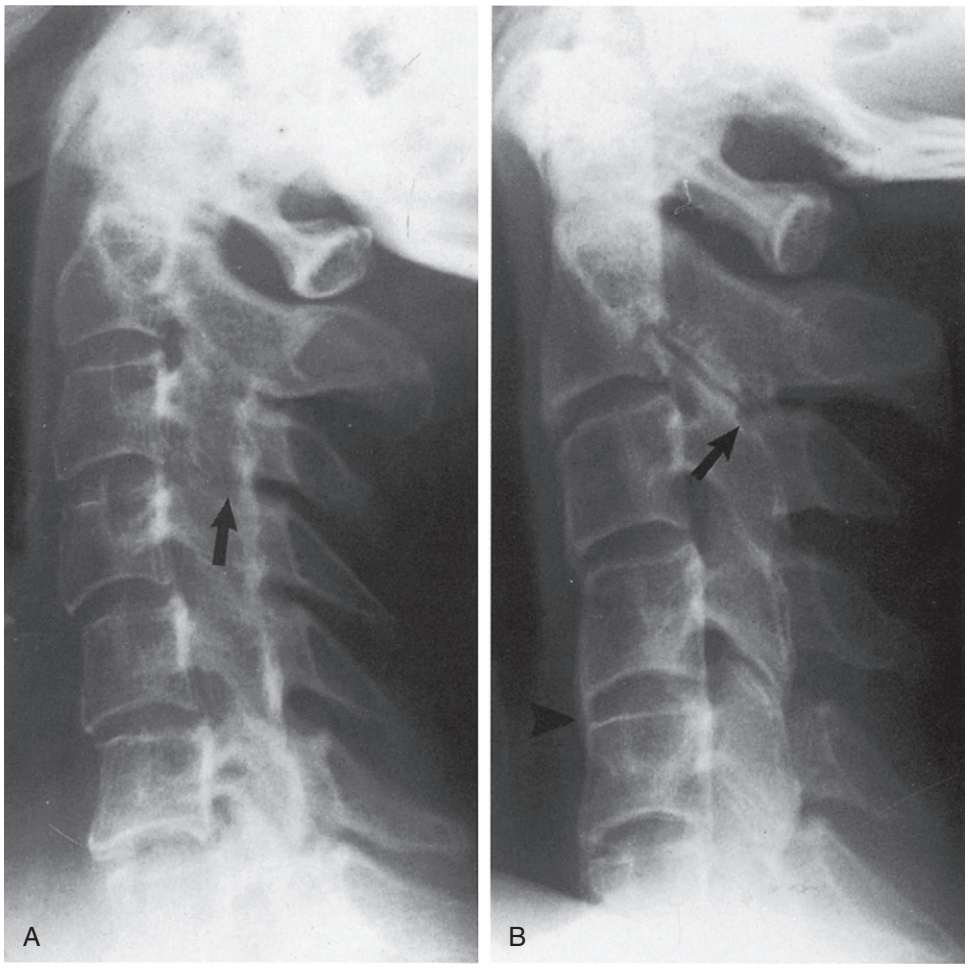

FIGURE 10-25. Cervical spine involvement in psoriatic arthritis. **A,** Apophyseal joint space narrowing, erosion (*arrow*), and ankylosis. **B,** Apophyseal joint space narrowing and erosion (*arrow*). There is also anterior paravertebral ossification present (*arrowhead*). *(From Brower AC: The radiographic features of psoriatic arthritis. In Gerber L, Espinoza L, editors:* Psoriatic arthritis*, Orlando, FL, Grune & Stratton, 1985, p. 125; reprinted by permission.)*

SUMMARY

Psoriatic arthritis presents specific radiographic changes in a specific distribution that allows the radiologist to make the diagnosis. It manifests a severe erosive element, as well as a bone productive element. The erosive changes help to distinguish it from ankylosing spondylitis, and the bone productive changes help to distinguish it from rheumatoid arthritis.

SUGGESTED READINGS

Avila R, Pugh DG, Slocumb CH, et al: Psoriatic arthritis: A roentgenologic study, *Radiology* 75:691–702, 1960.
Fawcitt J: Bone and joint changes associated with psoriasis, *Br J Radiol* 23:440–453, 1950.
Harvie JN, Lester RS, Little AH: Sacroiliitis in severe psoriasis, *AJR Am J Roentgenol* 127:579–584, 1976.
Jajic I: Radiological changes in the sacroiliac joints and spine of patients with psoriatic arthritis and psoriasis, *Ann Rheum Dis* 27:1–6, 1968.
Killebrew K, Gold RH, Sholkoff SD: Psoriatic spondylitis, *Radiology* 108:9–16, 1973.
Meaney TF, Hays RA: Roentgen manifestations of psoriatic arthritis, *Radiology* 68:403–407, 1957.
Peterson CC Jr, Silbiger ML: Reiter's syndrome and psoriatic arthritis: Their roentgen spectra and some interesting similarities, *AJR Am J Roentgenol Radium Ther Nucl Med* 101:860–871, 1967.
Resnick D, Broderick TW: Bony proliferation of terminal phalanges in: The "ivory" phalanx, *J Can Assoc Radiol* 28:187–189, 1977.
Resnick D, Niwayama G: On the nature and significance of bony proliferation in "rheumatoid variant" disorders, *AJR Am J Roentgenol* 129:275–278, 1977.
Resnick D, Niwayama G: Psoriatic arthritis. In Resnick D, editor: *Diagnosis of bone and joint disorders*, ed 3, Philadelphia, 1995, W.B. Saunders, p. 1075.
Sherman MS: Psoriatic arthritis: Observations on the clinical, roentgenographic, and pathological changes, *J Bone Joint Surg Am* 34:831–852, 1952.
Wright V: Psoriatic arthritis: A comparative radiographic study of rheumatoid arthritis and arthritis associated with psoriasis, *Ann Rheum Dis* 20:123–132, 1961.

11 Reactive Arthritis

Reactive arthritis (formerly known as Reiter disease) is usually associated with conjunctivitis and urethritis. It is a disease predominantly of males between 15 and 35 years of age and is transmitted through either epidemic dysentery or sexual intercourse. The arthritis may be present without documentation of the other clinical manifestations. In such cases, radiographic examination may provide the appropriate diagnosis. The classic radiographic features are as follows:

1. Fusiform soft tissue swelling
2. Early juxta-articular osteoporosis; reestablishment of normal mineralization
3. Uniform joint space loss
4. Bone proliferation
5. Ill-defined erosions
6. Bilateral asymmetrical distribution
7. Distribution primarily in feet, ankles, knees, and sacroiliac (SI) joints; hands, hips, and spine less frequently involved

Although the specific radiographic changes are identical to those of psoriatic arthritis, reactive arthritis has a characteristic but different distribution, thus allowing for accurate differential diagnosis.

THE FEET

The small articulations of the foot and the calcaneus are the most frequently involved joints in reactive arthritis. The arthritis is initially seen involving one joint only (Fig. 11-1). This monoarticular involvement could lead to a misdiagnosis of septic arthritis; therefore, the observation of the aggressiveness of the changes plays an important role in correct interpretation. There may be swelling of the entire digit (dactylitis), giving it an appearance of a sausage or cocktail hot dog. Early in the disease, juxta-articular osteoporosis is present and persists for a longer period of time than it does in psoriasis. Eventually normal mineralization returns. Early, a periostitis may be observed along the shafts of the phalanges (Fig. 11-2). Later, uniform joint space loss and marginal erosions with adjacent bone proliferation occur (Fig. 11-3). These changes are indistinguishable from the changes of psoriatic arthritis in the toes. Ankylosis of the joints does not occur as frequently as it does in psoriatic arthritis. Reactive arthritis also seems to prefer the metatarsophalangeal (MTP) joints (Fig. 11-4) and first interphalangeal (IP) joint over the distal interphalangeal (DIP) and proximal interphalangeal (PIP) joints seen classically in psoriatic arthritis.

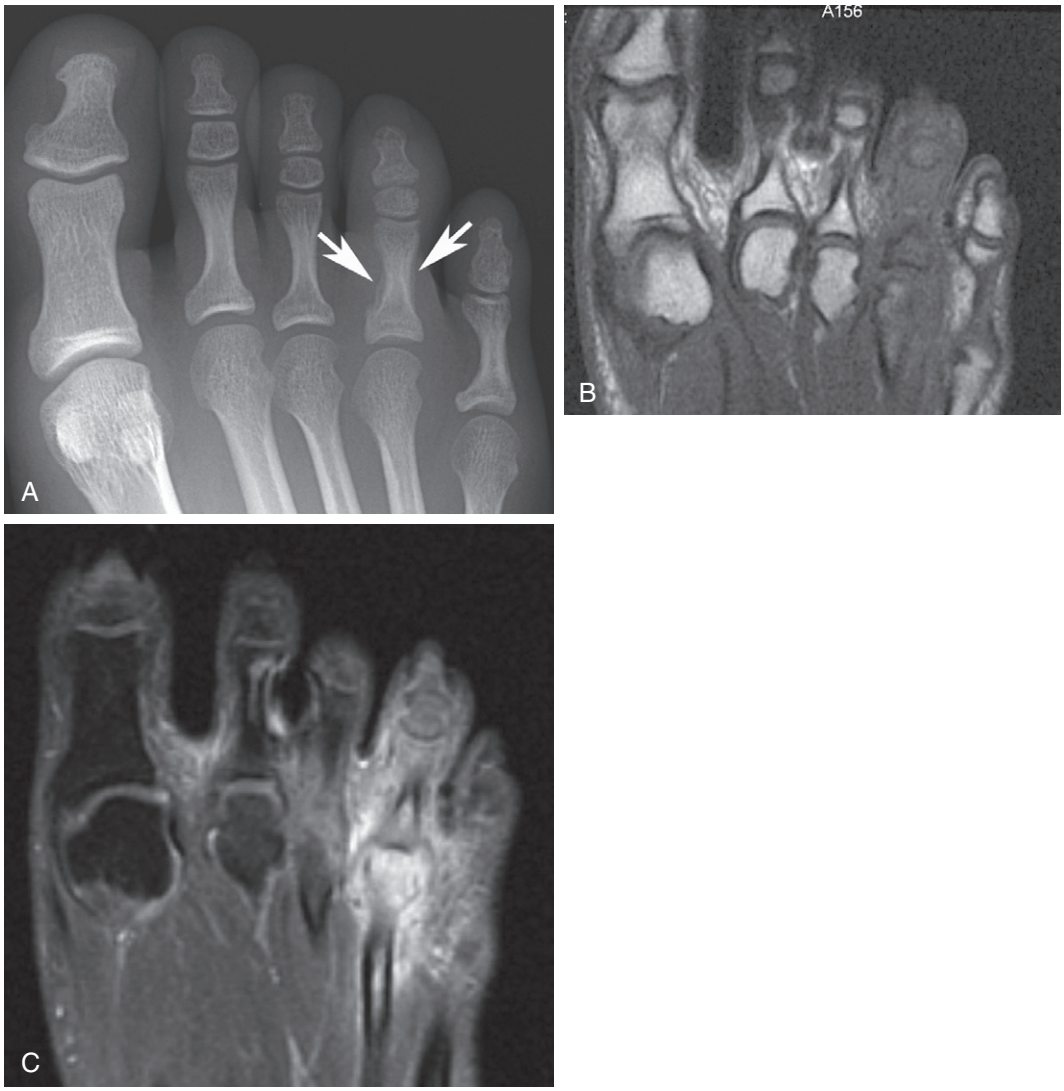

FIGURE 11-1. Anteroposterior (AP) view of the forefoot (**A**) in reactive arthritis. There is involvement of the fourth toe with sausage-like soft tissue swelling. There is new bone formation around the proximal phalanx (*arrows*). There is erosive change involving the juxta-articular areas of PIP joint. Axial T1-weighted image of the forefoot (**B**) shows intermediate signal replacing fat in the subcutaneous fat and marrow of the fourth toe indicating edema. Axial fat-suppressed T1-image through the forefoot following intravenous contrast administration (**C**) shows intense enhancement of synovitis in the fourth MTP joint.

FIGURE 11-2. MTP joints of patient with reactive arthritis. There is juxta-articular osteoporosis present in the third MTP joint. Periostitis is present along the shafts of the second, third, and fourth proximal phalanges and the neck of the third metatarsal.

FIGURE 11-3. AP view of the first through fourth toes in a patient with reactive arthritis. The second and third MTP joints are involved with erosive disease and adjacent bone proliferation (*arrows*).

FIGURE 11-4. AP view of the foot in reactive arthritis. There is dramatic involvement of all of the MTP joints, with juxta-articular osteoporosis, subluxations, erosive disease, and adjacent bone proliferation. The IP joints are relatively spared.

The calcaneus is involved in more than 50 percent of patients with reactive arthritis. Often it may be the only bone ever involved; hence the name "lover's heel." As in psoriatic arthritis, there is erosion and bone production at the attachment of the Achilles tendon and the plantar aponeurosis. Ill-defined spurs may develop at the aponeurotic attachment more frequently than at the Achilles tendon attachment (Fig. 11-5). They will tend to point upward and parallel the undersurface of the calcaneus (Fig. 11-6). Bone formation on the surface of the tarsal bones indicates midfoot involvement (Fig. 11-7).

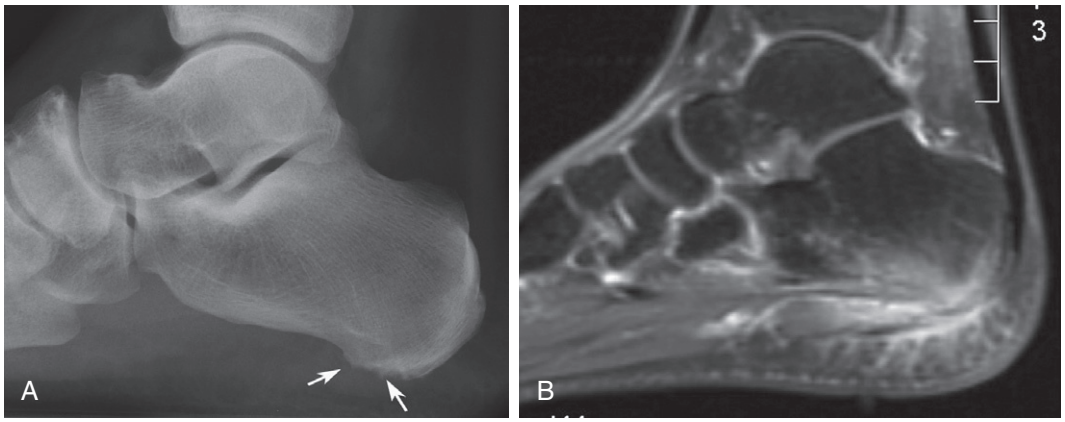

FIGURE 11-5. Lateral view of the calcaneus (**A**) in reactive arthritis. There is erosive change at the attachment of the plantar aponeurosis. There is adjacent proliferative bone production (*arrow*). Sagittal fat-suppressed T1-weighted image following intravenous contrast administration (**B**) shows enhancement of plantar aponeurosis and adjacent bone marrow.

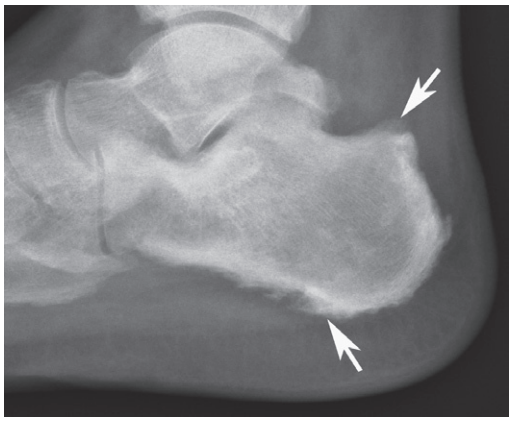

FIGURE 11-6. Lateral view of the calcaneus in a patient with longstanding reactive arthritis. There are erosive changes at both the posterior and plantar calcaneus. There is associated bone production (*arrows*). The calcaneal spur is pointing slightly toward the calcaneus.

FIGURE 11-7. AP view of the left midfoot involved with reactive arthritis. There is proliferative periostitis involving the medial aspect of the medial cuneiform and navicular (*arrows*). Notice the smooth surface of the unaffected right midfoot bones.

THE ANKLES

One or both ankles may be involved in 30 to 50 percent of patients with reactive arthritis (Fig. 11-8). There is usually soft tissue swelling and a fluffy periostitis involving the distal ends of the fibula and tibia. Uniform joint space loss may occur. Erosive disease is a less frequent manifestation.

FIGURE 11-8. AP view of the ankle involved with reactive arthritis. There is soft tissue swelling around the ankle. There is proliferative periostitis over the medial malleolus.

THE KNEES

Forty percent of the patients with reactive arthritis have involvement of one or both knees. The most common finding is the presence of a joint effusion. Juxta-articular osteoporosis may be observed, although eventually this is replaced with normal mineralization. Bone production observed as a periostitis or ossification of ligamentous and tendinous attachments is more common than erosive disease.

OTHER APPENDICULAR SITES

Whereas involvement of the joints of the lower extremities is common, involvement of the hip is relatively rare. Involvement of one or more joints in the upper extremity usually occurs before involvement of the hip. The most common area of involvement in the upper extremity is the hand. This is often limited to one digit (Fig. 11-9), although certainly several digits and the wrist may be involved (Fig. 11-10). Again the specific radiographic changes are identical to those seen in psoriatic arthritis, with erosive disease and evidence of new bone formation. There is a tendency toward persistent juxta-articular osteoporosis. Ankylosis of the IP joints is less frequent. The PIP joints are more frequently involved than the DIP joints or MCP joints.

FIGURE 11-9. Posteroanterior (PA) view of the hand in a patient with reactive arthritis. The only abnormality is the involvement of the IP joint and MCP joint of the thumb. There is soft tissue swelling around the IP joint with uniform loss of the joint space, erosive changes, and associated bone productive changes (*arrows*). There is joint space loss in the first MCP joint. There are bone productive changes seen around the sesamoid bone.

FIGURE 11-10. PA view of the hands in a patient with reactive arthritis. There is pancarpal involvement bilaterally. The PIP joints are involved, with extensive changes at the second PIP joint on the right and the fifth PIP joint on the left. The MCP joints are involved to a lesser extent, with the most dramatic changes being in the left fifth MCP joint.

THE SACROILIAC JOINTS

Early in the course of the disease, the SI joint is affected in 5 to 10 percent of patients; however, several years into the course of the disease, 40 to 60 percent have SI involvement. Although the involvement may be bilateral and symmetrical, it is usually bilateral and asymmetrical, with one side more extensively involved than the other (Fig. 11-11). Because of this asymmetrical involvement, radiographically it may appear as a unilateral involvement (Fig. 11-12). It then becomes important to distinguish reactive disease from septic arthritis of the SI joint. Magnetic resonance (MR) imaging or computed tomography (CT) aids immensely in establishing the correct diagnosis; in reactive arthritis, even though the radiographic changes may be unilateral, both SI joints show involvement with these modalities. As with psoriatic arthritis, erosive changes are first seen on the iliac side of the true synovial joint. As the erosions enlarge and involve the sacral side, proliferative bone repair is observed. Both may become quite extensive (Fig. 11-11). Ankylosis of the SI joint occurs less frequently than in psoriatic arthritis.

In addition to the changes in the SI joints, similar changes may occur at the pubic symphysis. Ossification of tendinous attachments may also be observed.

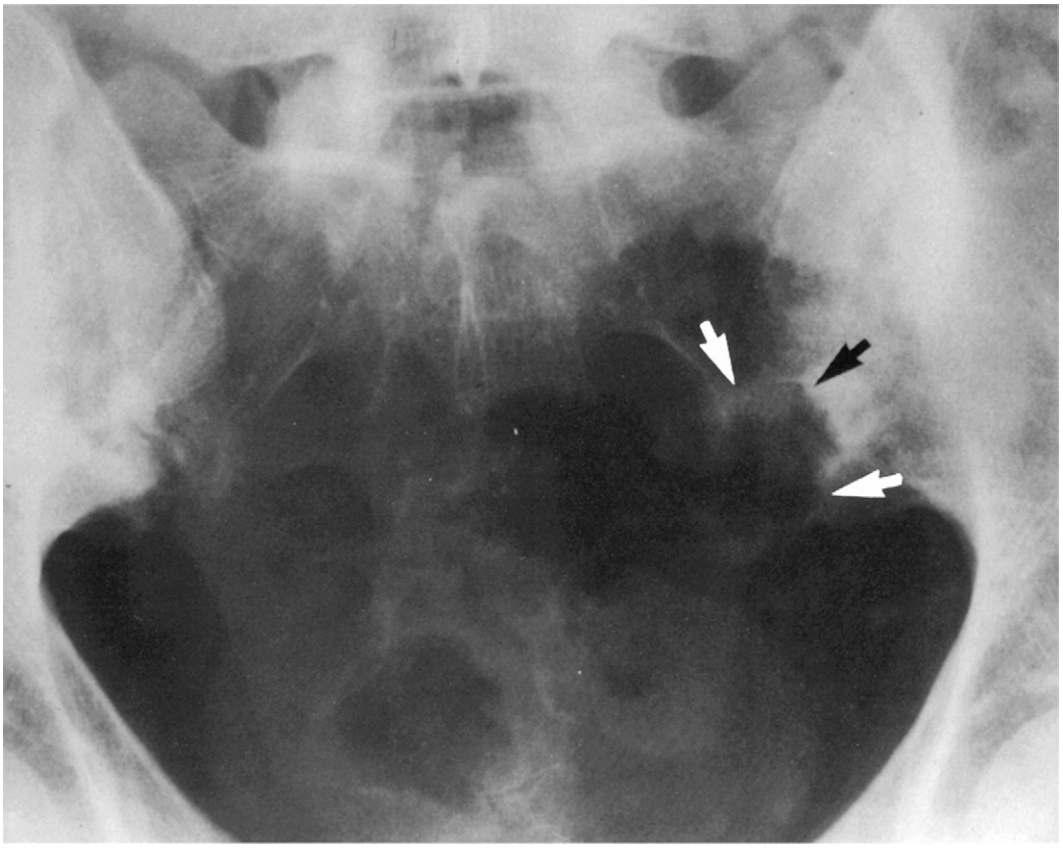

FIGURE 11-11. AP Ferguson view of the SI joints in a patient with reactive arthritis. There is bilateral asymmetrical involvement. Bone sclerosis is the prominent feature on the right side. A large erosion is seen in the inferior aspect of the left SI joint (*arrows*). *(From Brower AC: Disorders of the sacroiliac joint,* Radiolog *1(20):3, 1978; reprinted by permission.)*

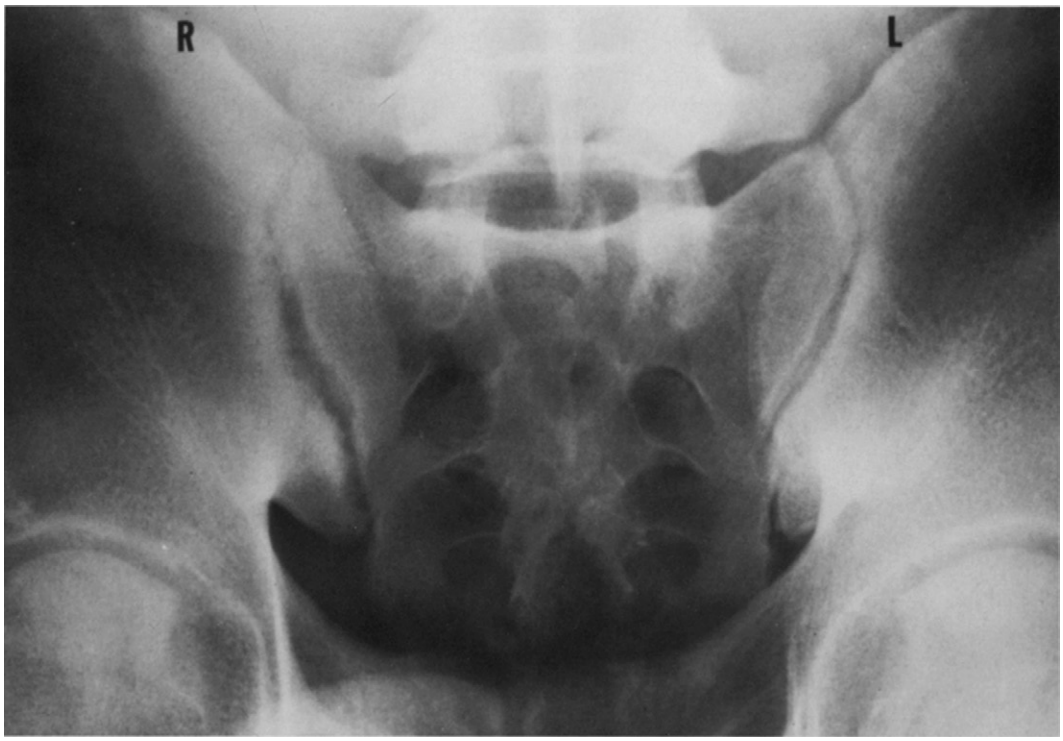

FIGURE 11-12. AP Ferguson view of the SI joints in a patient with reactive arthritis. The left SI joint is within normal limits. The right SI joint shows early changes of small erosions and adjacent sclerosis on the iliac side.

THE SPINE

Involvement of the spine in reactive arthritis is relatively rare and certainly less frequent than in psoriatic arthritis. Early spinal involvement occurs as paravertebral ossification somewhere around the lower three thoracic or upper three lumbar vertebral bodies (Fig. 11-13). In this location, if such ossification progresses, one observes large bulky bone bridges between adjacent vertebral bodies. As in psoriasis, their distribution will be unilateral or asymmetrical. As in psoriasis, there will be no squaring of the vertebral bodies and only occasional involvement of the apophyseal joints. In contrast to psoriasis, involvement of the cervical spine is extremely rare.

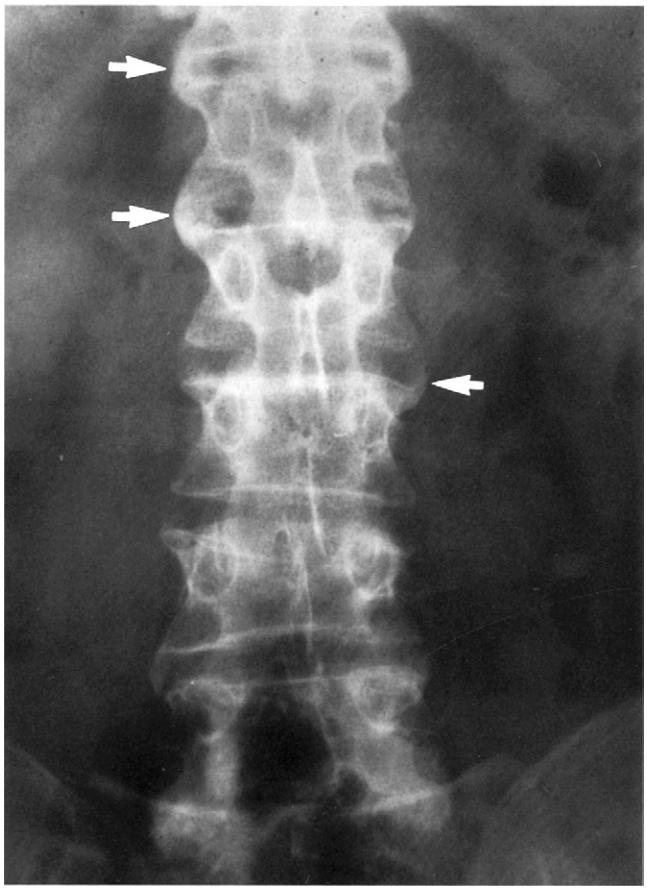

FIGURE 11-13. AP view of the lumbar spine in a patient with reactive arthritis. There is paravertebral ossification at the T12-L1, L1-L2, and L2-L3 disc spaces (*arrows*).

SUMMARY

The specific radiographic changes of reactive arthritis are indistinguishable from those of psoriatic arthritis. There is a tendency toward more juxta-articular osteoporosis and less ankylosis than in psoriatic arthritis; however, its characteristic lower extremity distribution is the most useful manifestation in distinguishing it from psoriatic arthritis.

SUGGESTED READINGS

Mason RM, Murray RS, Oates JK, Young AC: A comparative radiological study of Reiter's disease, rheumatoid arthritis, and ankylosing spondylitis, *J Bone Joint Surg Br* 41:137–148, 1959.

Murray RS, Oates JK, Young AC: Radiological changes in Reiter's syndrome and arthritis associated with urethritis, *J Fac Radiologists* 9:37–43, 1958.

Peterson CC Jr, Silbiger ML: Reiter's syndrome and psoriatic arthritis. Their roentgen spectra and some interesting similarities, *Am J Roentgenol Radium Ther Nucl Med* 101:860–871, 1967.

Resnick D: Reiter's syndrome. In Resnick D, editor: *Diagnosis of bone and joint disorders*, ed 3, Philadelphia, 1995, W.B. Saunders, p. 1103.

Reynolds DF, Csonka GW: Radiological aspects of Reiter's syndrome ("venereal" arthritis), *J Fac Radiologists* 9:44–49, 1958.

Sholkoff SD, Glickman MG, Steinback HL: Roentgenology of Reiter's syndrome, *Radiology* 97:497–503, 1970.

Sundaram M, Patton JT: Paravertebral ossification in psoriasis and Reiter's disease, *Br J Radiol* 48:628–633, 1975.

Weldon WV, Scalettar R: Roentgen changes in Reiter's syndrome, *Am J Roentgenol Radium Ther Nucl Med* 86:344–350, 1961.

12 *Ankylosing Spondylitis*

Ankylosing spondylitis is the chronic inflammatory disease that affects primarily the axial skeleton and only secondarily the appendicular skeleton. It is seen predominantly in males between the ages of 15 and 35 years. Of all the inflammatory arthropathies, it is the least erosive and the most ossifying. Ankylosis of a joint is the predominant characteristic. The common radiographic findings are as follows:

1. Normal mineralization before ankylosis; generalized osteoporosis after ankylosis
2. Subchondral bone formation present before ankylosis
3. Erosions—small, localized, and not a prominent part of the picture
4. Absence of subluxations
5. Absence of cysts
6. Ankylosis
7. Bilateral symmetrical distribution
8. Distribution in sacroiliac (SI) joints and the spine, ascending from the lumbar to the cervical; then hips, shoulders, knees, hands, and feet, in decreasing order of frequency

The axial distribution and the predominant ankylosing features make the radiographic diagnosis relatively easy.

THE SACROILIAC JOINTS

Although clinically ankylosing spondylitis is first suspected because of involvement of the costovertebral junction, radiographically the first involvement is seen in the SI joints. They are involved in a bilateral and symmetrical fashion (Fig. 12-1). Small, succinct erosions are seen first on the iliac side and then on the sacral side, giving the joint margin the appearance of the perforated edge of a postage stamp (Fig. 12-2). The erosions are surrounded by a small amount of bone repair. The erosions and sclerosis never become as extensive as those seen in the other spondyloarthropathies. The synovial aspect of the joint will ankylose relatively early. It is common for the entire SI joint, not only the true synovial aspect but also the ligamentous aspect, to ankylose. The ossification of the ligaments in the posterosuperior portion of the SI joint is seen radiographically as a "star" (Fig. 12-3).

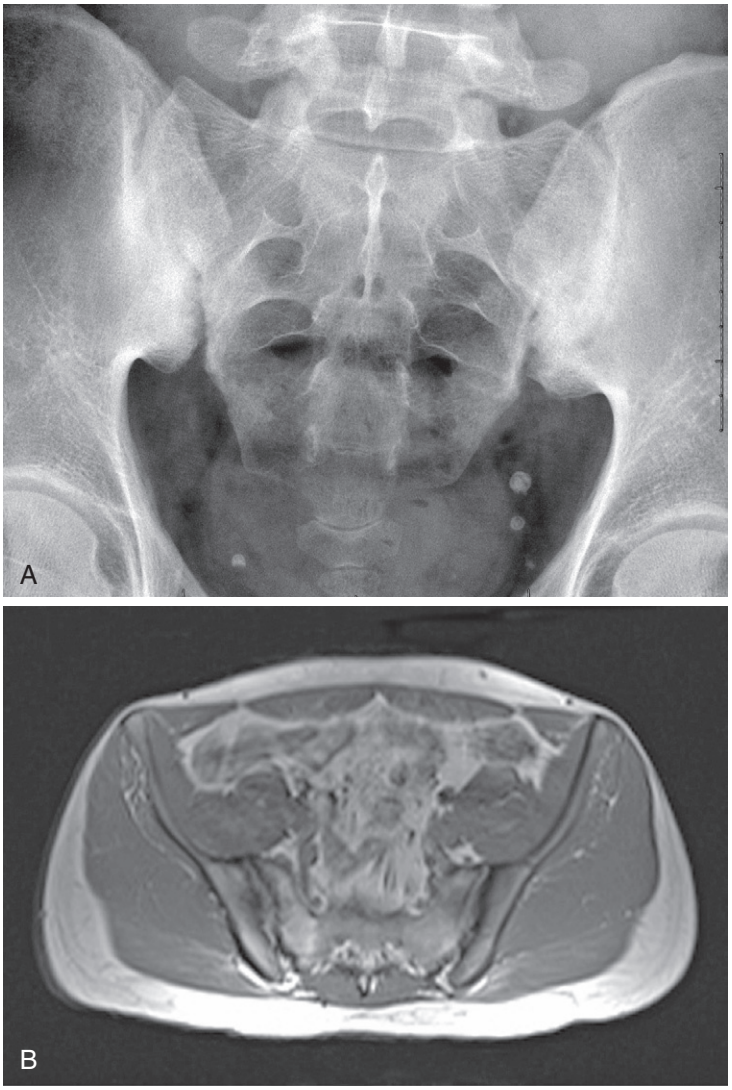

FIGURE 12-1. **A,** Anteroposterior (AP) view of the SI joints in a patient with early changes of ankylosing spondylitis. There is bilateral and symmetrical involvement. The erosions are succinct. There is minimal sclerosis. **B,** Coronal T1-weighted image shows erosion of the SI joints more prominently involving the ilium.

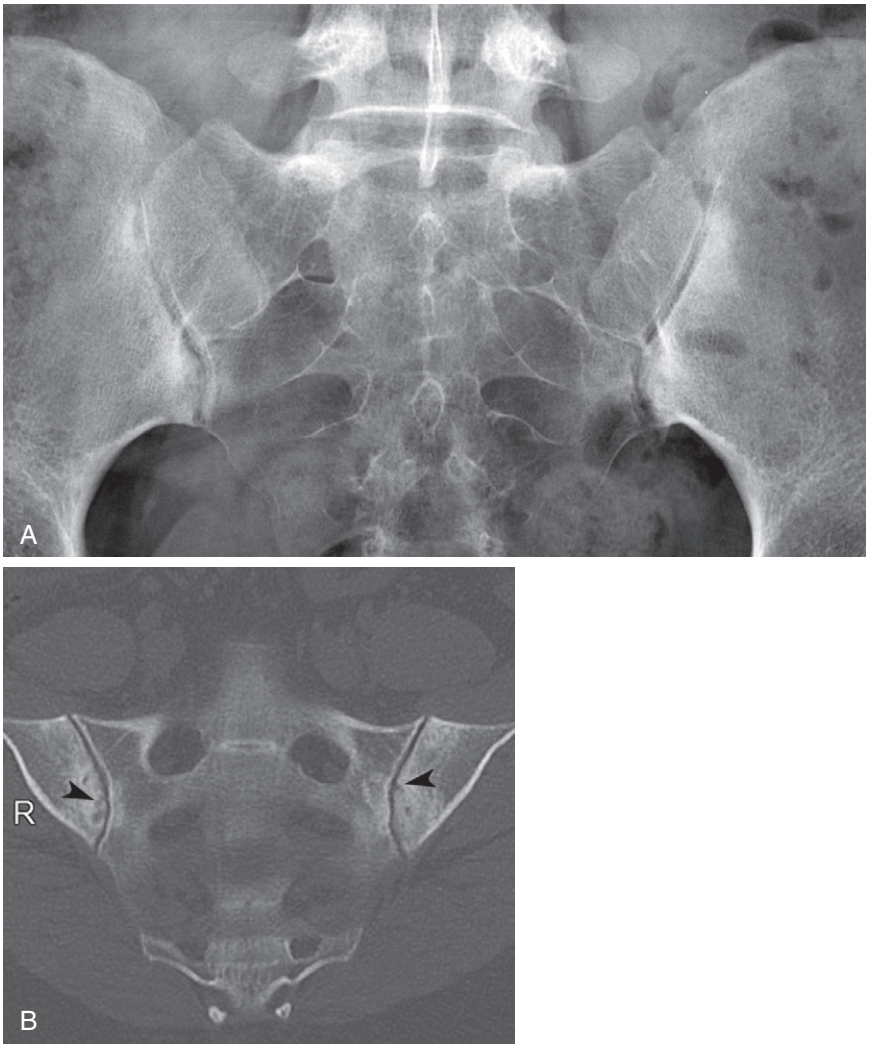

FIGURE 12-2. A, AP view of the SI joint in early ankylosing spondylitis. The erosions are small, giving the joint edge the appearance of the perforated edge of a postage stamp. A small amount of bone repair is present. **B,** Coronal CT image shows erosion (*arrows*) of the iliac portion of the SI joints and subchondral bone repair.

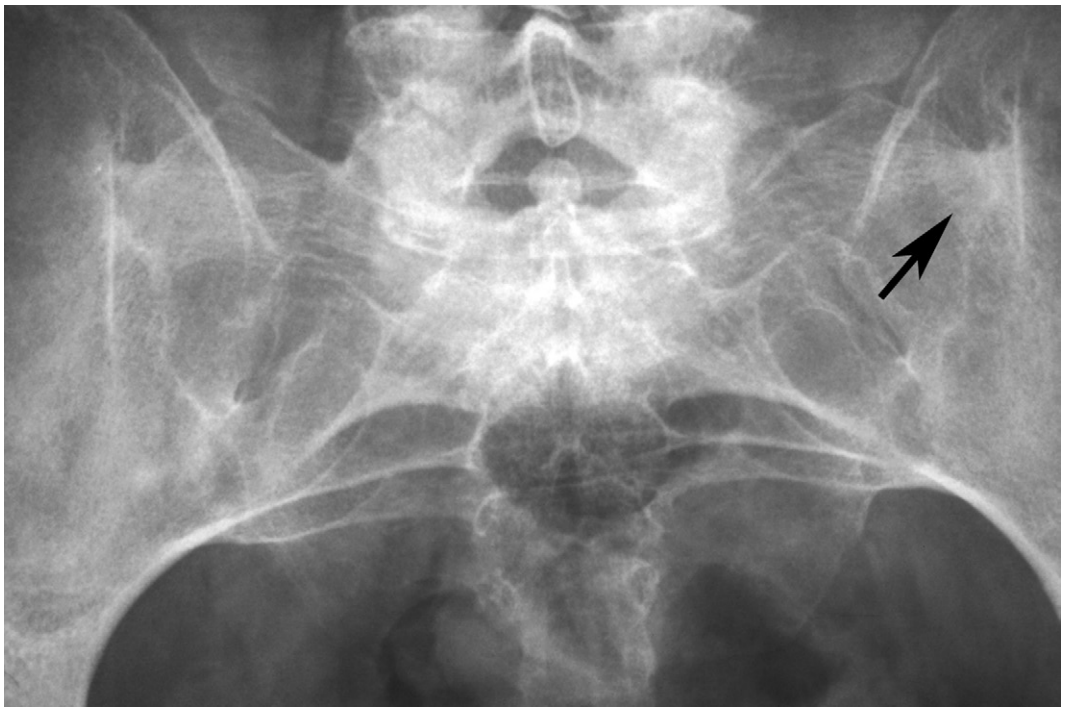

FIGURE 12-3. AP view of the SI joints in a patient with longstanding ankylosing spondylitis. Both SI joints are completely ankylosed. A "star" (*arrow*) represents the ossification of the ligaments in the posterosuperior portion of the joint.

Other changes in the pelvis may be seen concurrent with the changes in the SI joints. There may be ossification of the ligamentous attachments (enthesopathy) to the iliac crest and ischial tuberosities, giving a "whiskered" appearance (see Fig. 12-4). The pubic symphysis may be involved, with small succinct erosions and reparative response adjacent to the erosions, followed by total ankylosis (Fig. 12-5). The pubic symphysis is involved in 23 percent of patients.

FIGURE 12-4. AP view of the pelvis shows bone production at tendon insertions of the pelvis and proximal femurs. These changes are most prominent at the bilateral greater trochanter and ischial tuberosity. Both SI joints are ankylosed.

FIGURE 12-5. Pubic symphysis involved in ankylosing spondylitis. Erosive changes producing apparent widening and adjacent reparative response.

THE SPINE

Initial involvement of the spine may be seen in the T12-L1 area. However, usually spine involvement is identified by the radiologist in the lumbar area. It is then seen to progress upward through the thoracic spine to the cervical spine. Initially there is erosion of the corner of the vertebral body with secondary reactive sclerosis. This gives a squared appearance to the vertebral body, and the reactive sclerosis is identified as the "ivory" corner (Fig. 12-6). As the spine becomes immobilized, this reactive sclerosis disappears and one may identify nothing more than a squared vertebral body (Fig. 12-7).

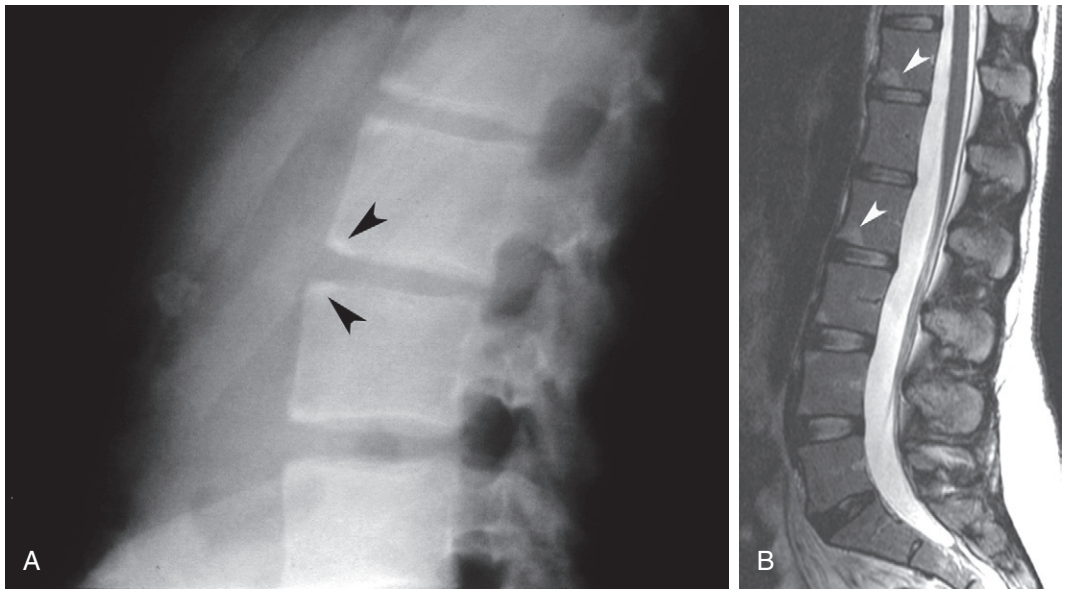

FIGURE 12-6. A, Erosion of the corner of the vertebral bodies and resultant reactive sclerosis give a squared appearance to the vertebral bodies and "ivory" corners (*arrowheads*) at multiple levels. **B,** Sagittal fat-suppressed T2-weighted image in a different patient shows edema-like changes (*arrowheads*) at the anterior part of the superior and inferior end-plate of multiple levels that are early changes of ankylosing spondylitis.

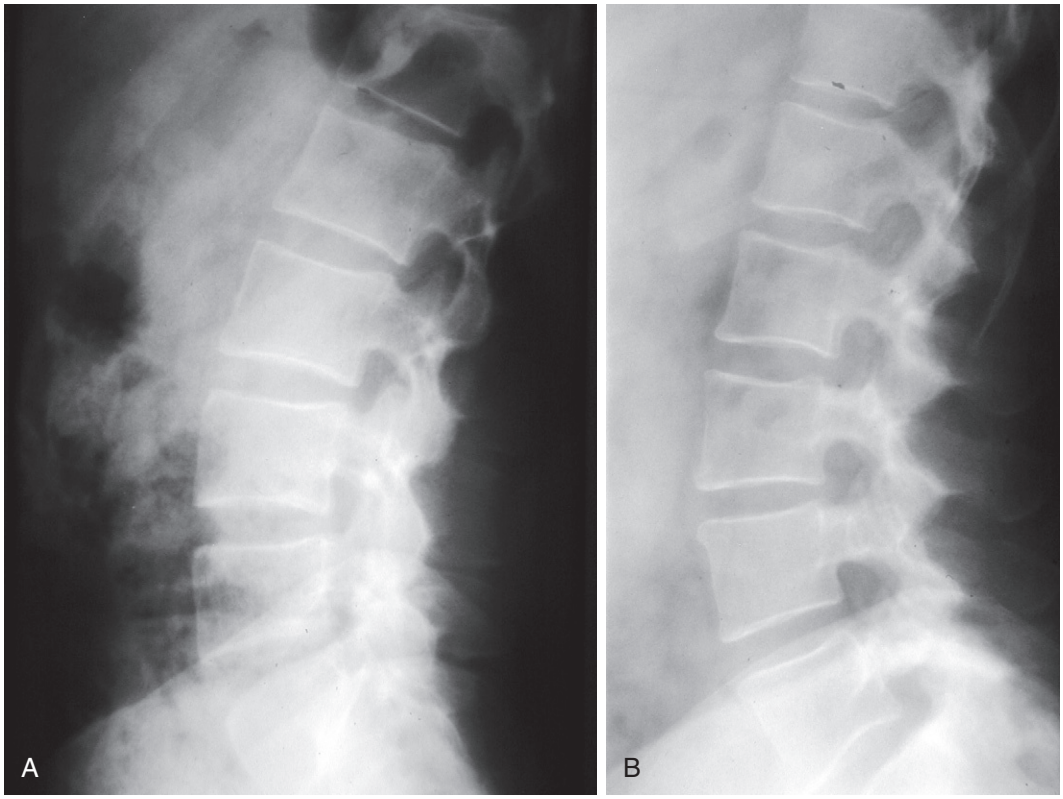

FIGURE 12-7. A, Lateral view of the lumbar spine in ankylosing spondylitis. There is loss of the normal anterior concavity and squaring of the vertebral bodies of the lumbar spine when compared to **B,** which is normal.

Ossification first takes place in the outer portion of the annulus fibrosus or in the Sharpey fibers. At first this ossification may not be visible radiographically, but lack of motion on physical examination and on flexion and extension films will indicate its presence (Fig. 12-8). This ossification will extend from the Sharpey fibers into the deep layers of the longitudinal ligaments. This ossification is called a syndesmophyte and ossifies one vertebral body to the adjacent vertebral body in a succinct fashion (Fig. 12-9). The syndesmophytes ascend the lumbar spine in a symmetrical fashion to eventually involve the thoracic spine and the cervical spine (Fig. 12-10). Bone formation anterior to the vertebral body will result in loss of normal anterior concavity of the lumbar spine vertebral bodies (Fig. 12-7). The disc spaces are generally preserved. Once ankylosis has taken place, disc calcification may develop (Fig. 12-11).

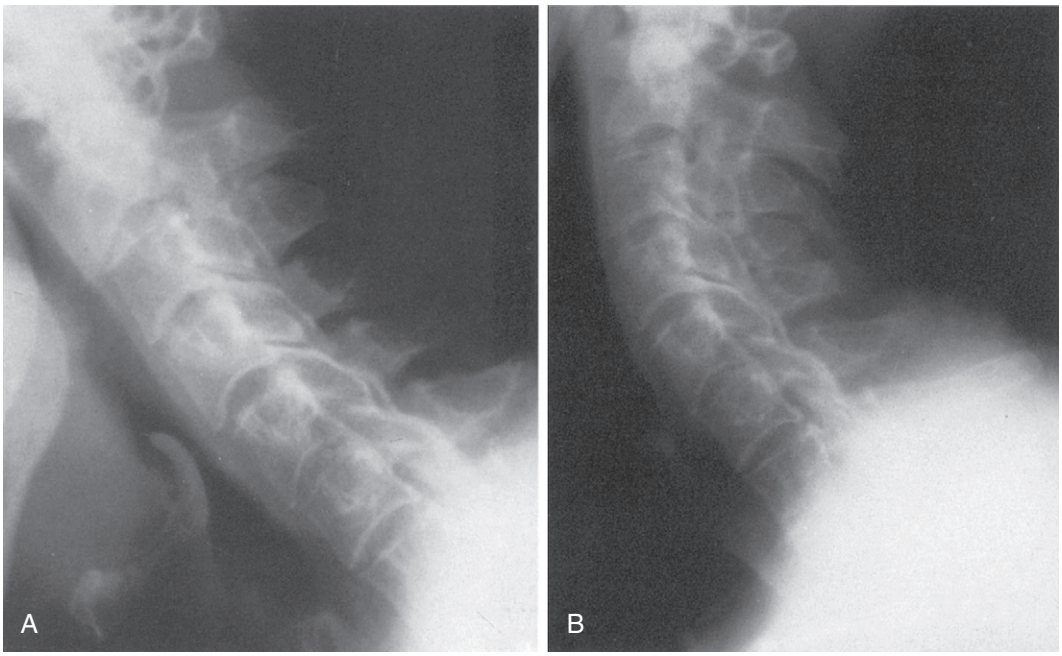

FIGURE 12-8. Lateral flexion (**A**) and extension (**B**) views of the cervical spine in ankylosing spondylitis. Despite the lack of visible ossification of the annulus fibrosus or anterior longitudinal ligament, there is no demonstrable motion between C5 and C6 or C6 and C7.

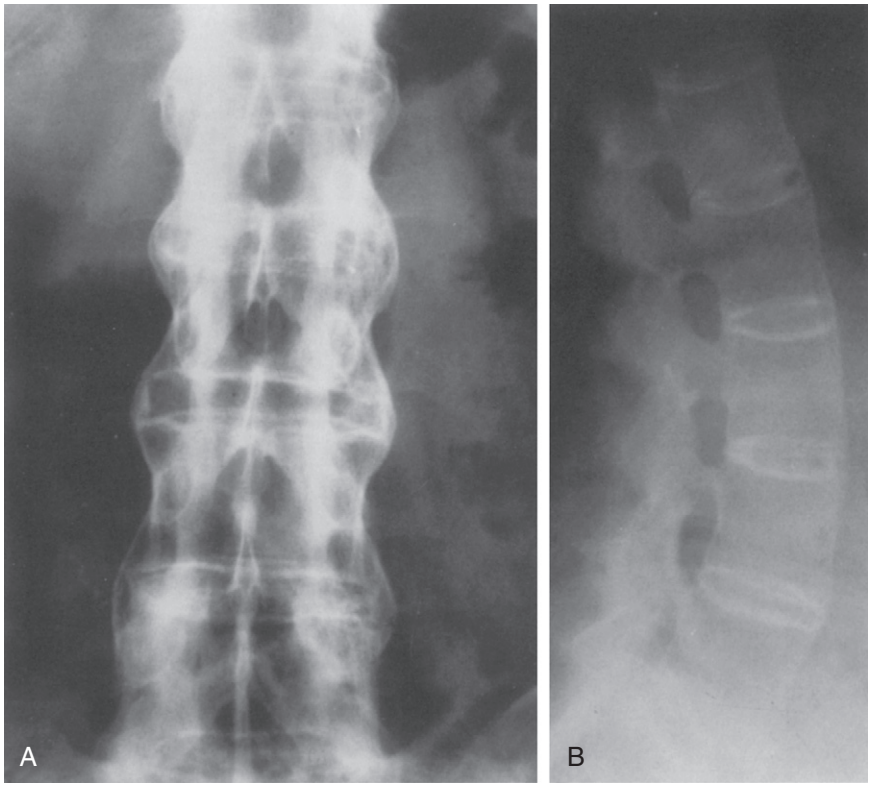

FIGURE 12-9. AP (**A**) and lateral (**B**) views of lumbar vertebral bodies showing succinct syndesmophytes of ankylosing spondylitis.

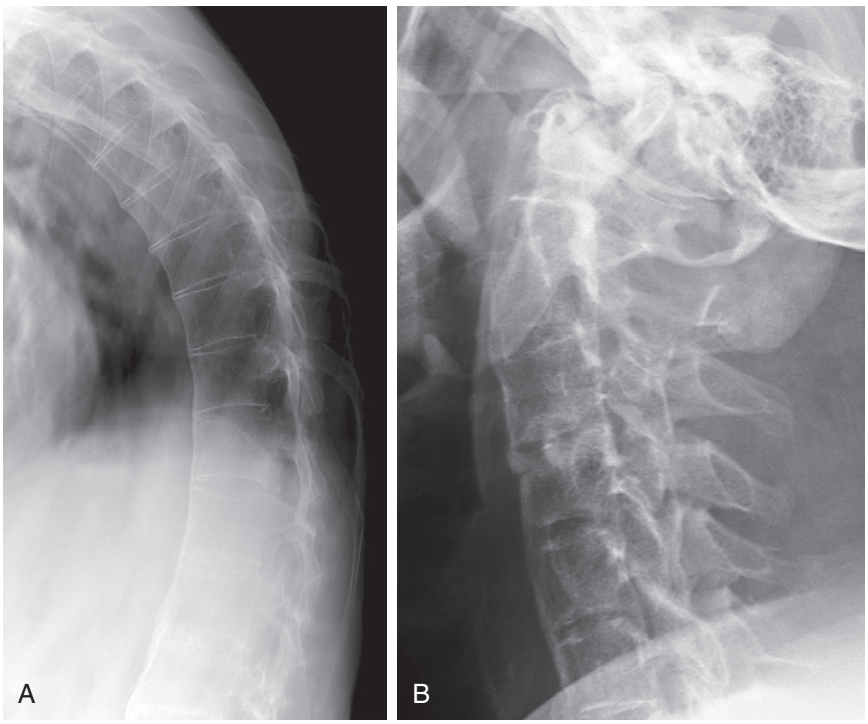

FIGURE 12-10. Lateral views of the thoracic spine (**A**) and the cervical spine (**B**) showing succinct ossification of the annulus fibrosus and deep layers of the anterior longitudinal ligament in ankylosing spondylitis.

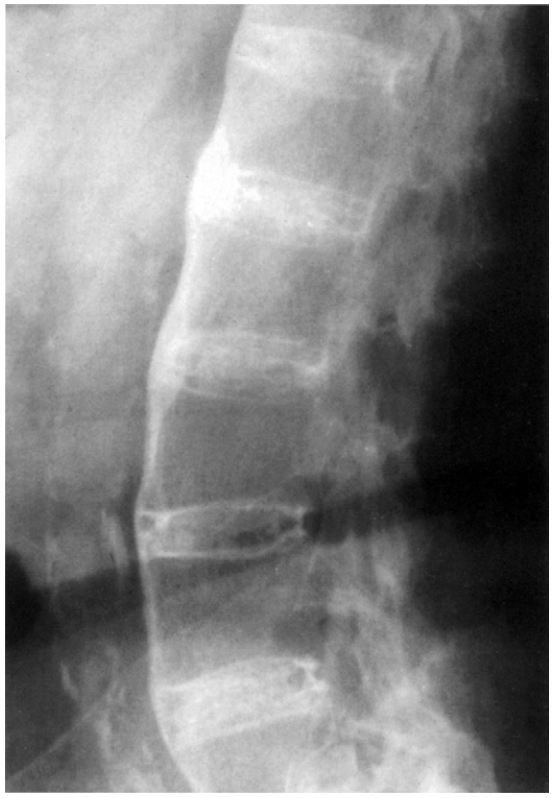

FIGURE 12-11. Lateral view of the lumbar spine in longstanding ankylosing spondylitis. Notice the succinct syndesmophyte formation. There is calcification of all discs.

The apophyseal joints may or may not be involved with erosive change and adjacent bone repair followed by ankylosis (Fig. 12-12). Ossification of all ligaments, including those between the spinous processes, may be present. The resulting appearance is that of a bamboo spine (Fig. 12-13).

FIGURE 12-12. Lateral view of the cervical spine showing syndesmophytes, osteoporosis, and ankylosis of the apophyseal joints.

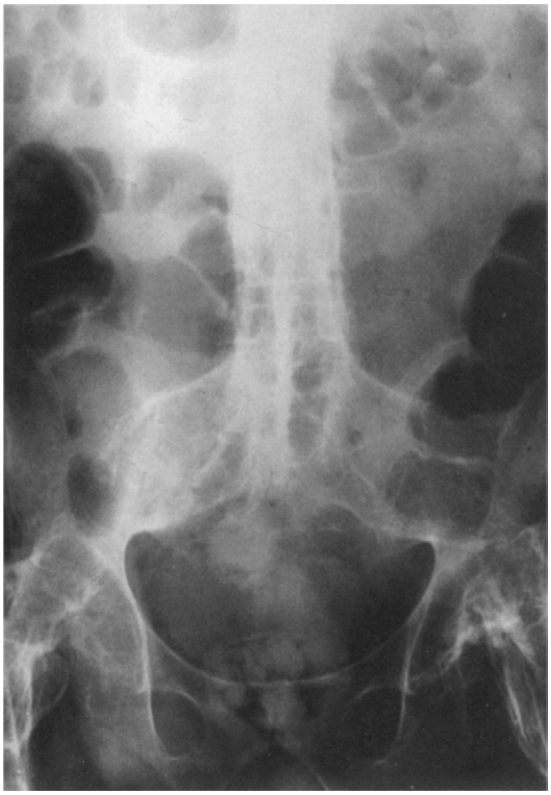

FIGURE 12-13. AP view of the lumbar spine and pelvis in a patient with longstanding ankylosing spondylitis. This is a classic bamboo spine. There is syndesmophyte formation and ossification of the ligaments between the spinous processes. There is ankylosis of the SI joints, the pubic symphysis, and both hips.

In the cervical spine, erosion of the odontoid process may occur. Atlantoaxial subluxation may also be demonstrated on flexed views taken in the lateral projection. Although these two findings are characteristic of rheumatoid arthritis, involvement of the rest of the spine with ankylosis should prevent erroneous diagnosis. Intubation of a patient with ankylosing spondylitis involving the cervical spine can result in a disastrous fracture if the intubator is unaware of the presence of the disease process (Fig. 12-14).

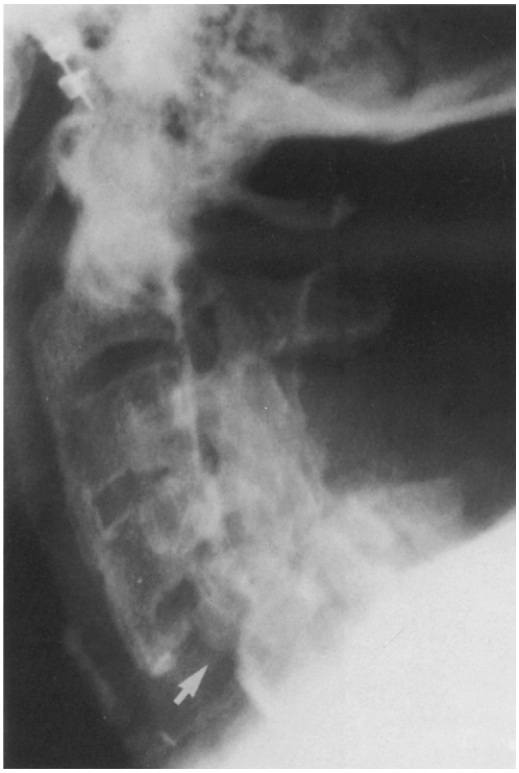

FIGURE 12-14. Lateral view of the cervical spine in a patient with ankylosing spondylitis. Notice the fracture at C4-C5 (*arrow*) incurred during intubation.

The ankylosed spine in this disease is more likely to fracture in the setting of trauma than a normal spine. Hyperextension injuries are more likely to induce fracture and the line of trauma tends to extend through the disc space. Any patient with ankylosing spondylitis that presents with posttraumatic back pain should be assumed to have a fracture and must be evaluated with computed tomography (CT) or magnetic resonance (MR) imaging (Fig. 12-15).

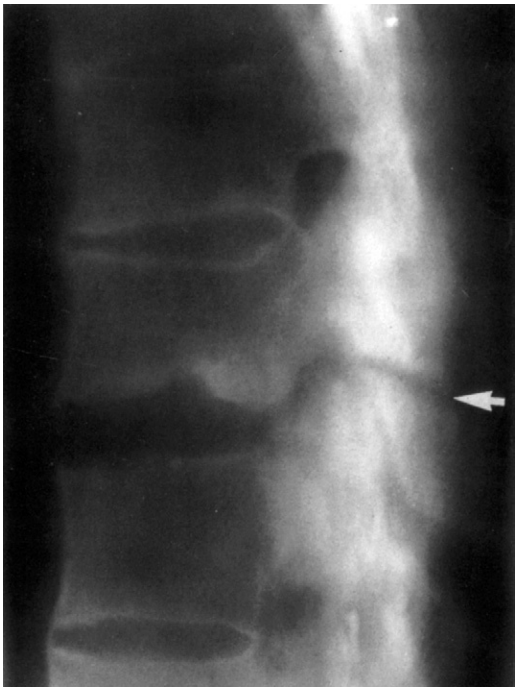

FIGURE 12-15. Tomographic cut taken in the lateral plane through the lower thoracic–upper lumbar spine area. There is ankylosis of the entire spine, except at T12-L1 (*arrow*). Here, there is distraction (widening) of the disc space and fracture through the posterior elements. *(Courtesy of Dr. C. S. Resnik, University of Maryland, Baltimore.)*

A common misdiagnosed complication of the bamboo spine is the pseudarthrosis that may develop in the lower thoracic–upper lumbar spine area. This develops around an area of true fracture or an area of skipped ossification (Fig. 12-15). It becomes the single point of motion in the entire spine and therefore undergoes disc degeneration and disintegration, erosion, and ebonation. The changes can resemble those of a severely degenerated disc, a septic discitis and osteomyelitis, or a neuropathic spine (Fig. 12-16). The etiology of these radiographic changes must be understood so that the correct diagnosis can be made.

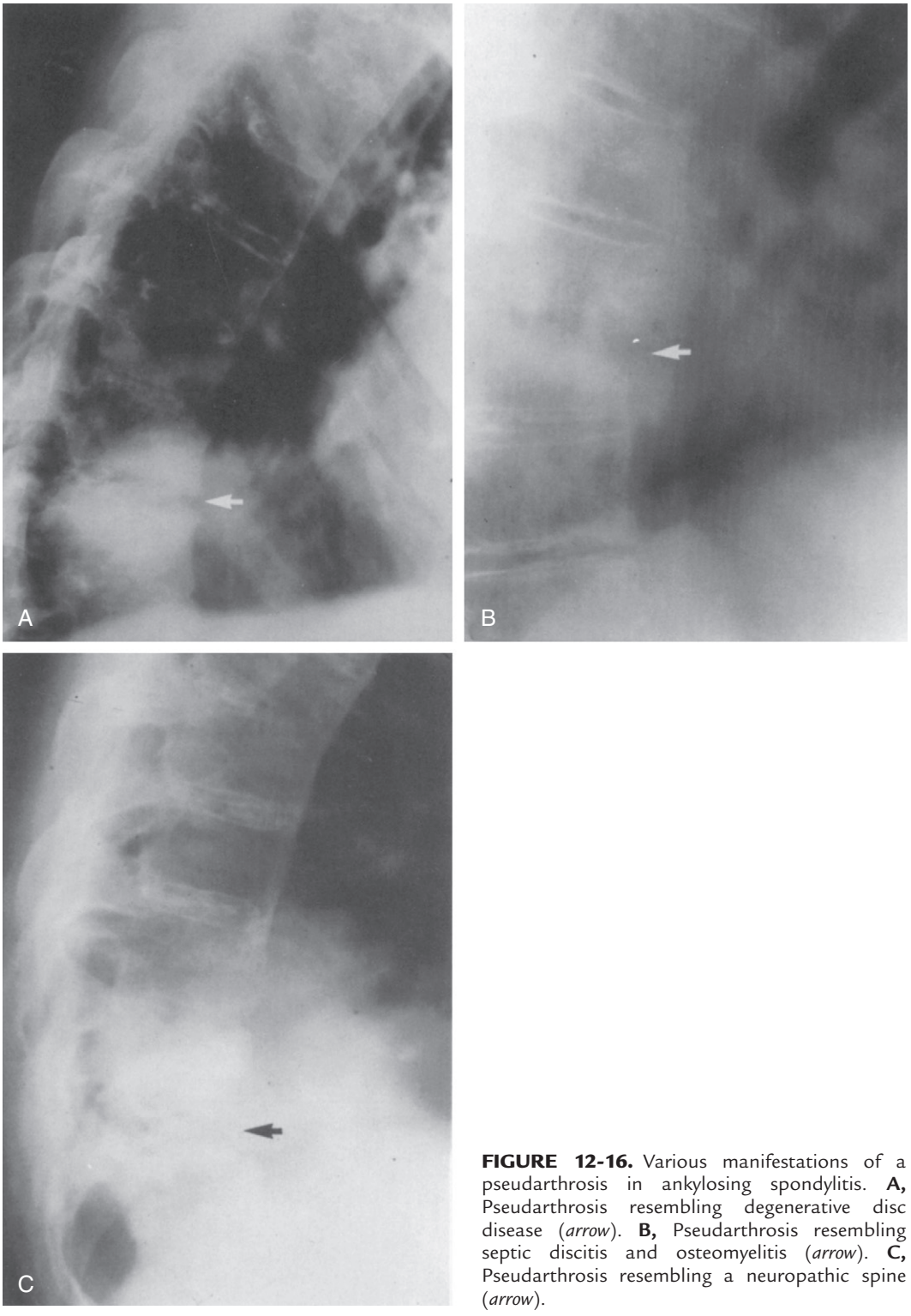

FIGURE 12-16. Various manifestations of a pseudarthrosis in ankylosing spondylitis. **A,** Pseudarthrosis resembling degenerative disc disease (*arrow*). **B,** Pseudarthrosis resembling septic discitis and osteomyelitis (*arrow*). **C,** Pseudarthrosis resembling a neuropathic spine (*arrow*).

THE HIP

After the axial skeleton, the most common joint to be involved is the hip. Two different types of involvement are described: the nondestructive and the destructive. The nondestructive is the more common type of involvement, and it is seen in the younger patient. There is a bilateral symmetrical involvement of both hips, with ankylosis a prominent part of the picture. There may be no loss of joint space, or there may be uniform loss of joint space with axial migration of the femoral head within the acetabulum. Very superficial erosions may be present, but basically the normal round contour of the femoral head is not distorted. Before true ankylosis takes place, normal mineralization will be present and a collar of osteophytes will be seen at the junction of the head and neck (Fig. 12-17). Once ankylosis has taken place, the surrounding bone becomes osteoporotic and this cuff of osteophytes disappears (Fig. 12-18).

The less common type of involvement of the hip tends to be a unilateral involvement. The progression of change is much slower. There is considerable destruction of the femoral head, with marked irregularity of the contour developing before progression to ankylosis.

FIGURE 12-17. AP view of the pelvis in a patient with ankylosing spondylitis. Normal mineralization is present. Both hips demonstrate uniform loss of cartilage with axial migration. A cuff of osteophytes is present at the junction of the head and neck as well as on the inferior and superior aspects of the acetabulum. There is ankylosis of the SI joints. There is ossification of the ligamentous attachments to the ischial tuberosities, giving a "whiskered" appearance.

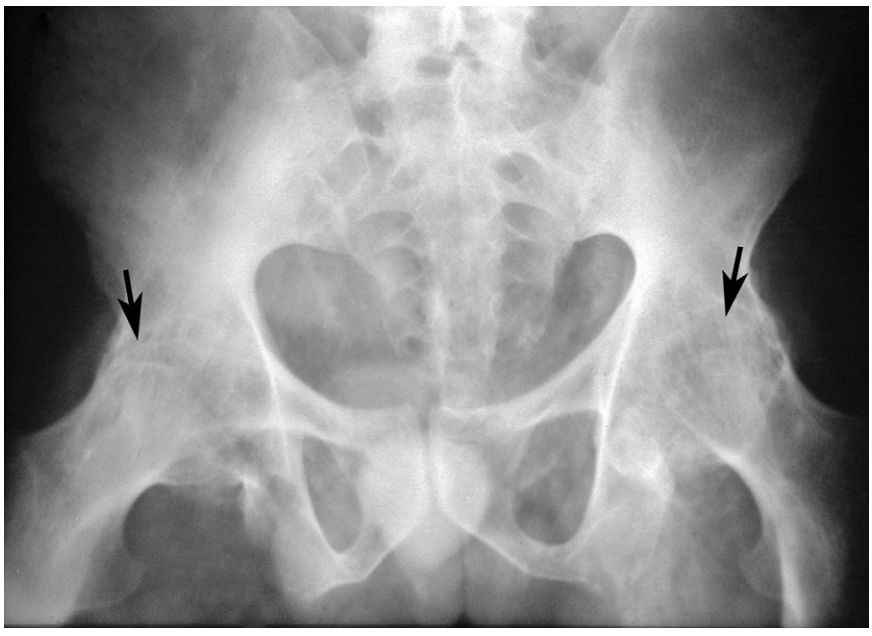

FIGURE 12-18. AP view of the pelvis in a patient with longstanding ankylosing spondylitis. There is generalized osteoporosis and ankylosis of the SI joints and both hips. Notice that the normal round contour of the femoral head is seen through the ankylosis (*arrows*).

THE SHOULDER

After the hip, the shoulder is the next most commonly involved joint. Again, there are two types of involvement, the nondestructive and the destructive. The nondestructive type shows a normally shaped humeral head ankylosed to the glenoid and extensive ossification of the coracoclavicular ligament (Fig. 12-19). The less common destructive type shows a large hatchet-shaped erosion of the humeral head (Fig. 12-20). Eventually ankylosis takes place, but not until the destruction has occurred.

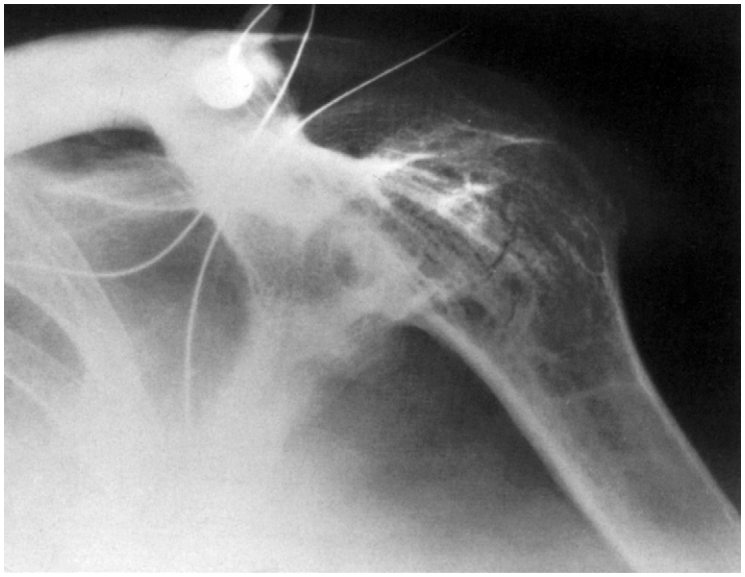

FIGURE 12-19. AP view of the shoulder in longstanding ankylosing spondylitis. The humeral head is ankylosed to the glenoid. There is extensive ossification of the coracoclavicular ligament.

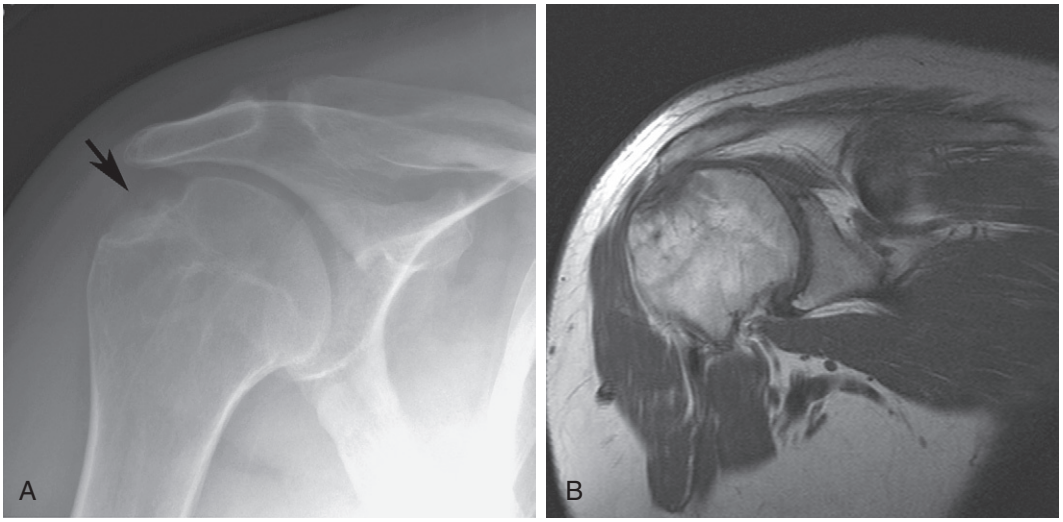

FIGURE 12-20. A, AP view of the shoulder shows a "hatchet" erosion in the lateral humeral head in ankylosing spondylitis. Bone formation is seen in the erosion (*arrow*). **B,** Coronal T1-weighted MR image through the erosion. The supraspinatus tendon (not shown) was intact.

OTHER JOINTS

The acromioclavicular (AC), sternoclavicular, and sternomanubrial joints are commonly affected joints. The knee is affected in 30 percent of patients with longstanding disease (Fig. 12-21). The elbows, hands, and feet are affected in approximately 10 percent of patients with longstanding disease (Fig. 12-22). In all of these areas, if erosive disease exists, then the erosions are relatively superficial, with minimal reparative bone response. The hallmark is always intraarticular ankylosis in a relatively short period of time.

FIGURE 12-21. Lateral view of the knee in a patient with longstanding ankylosing spondylitis. The knee is ankylosed in a flexed position. The normal contours of the articulating bones are seen through the ankylosis.

FIGURE 12-22. Lateral view of the hand in a patient with ankylosing spondylitis, showing ankylosis of all visible joints.

SUMMARY

The radiographic diagnosis of ankylosing spondylitis should not be a problem. Its predominance in the axial skeleton and its intraarticular ankylosis in a short period of time are classic and pathognomonic.

SUGGESTED READINGS

Berens DL: Roentgen features of ankylosing spondylitis, *Clin Orthop Relat Res* 74:20–33, 1971.
Cawley MI, Chalmers TM, Kellgren JH, et al: Destructive lesions of vertebral bodies in ankylosing spondylitis, *Ann Rheum Dis* 31:345–358, 1972.
Dihlmann W: Current radiodiagnostic concept of ankylosing spondylitis, *Skeletal Radiol* 4:179–188, 1979.
Dwosh IL, Resnick D, Becker MA: Hip involvement in ankylosing spondylitis, *Arthritis Rheum* 19:683–692, 1976.
Edeiken J, DePalma A, Hodes PJ: Ankylosing spondylitis, *Clin Orthop Relat Res* 34:62–72, 1964.
Forestier F: The importance of sacroiliac changes in early diagnosis of ankylosing spondyloarthritis, *Radiology* 33:389, 1939.
Levine DS, Forbat SM, Saifuddin A: MRI of the axial skeletal manifestations of ankylosing spondylitis, *Clin Radiol* 59:400–413, 2004.
Martel W: Diagnostic radiology in the rheumatic diseases. In Kelley WN, et al: *Textbook of rheumatology*, ed 4, Philadelphia, 1993, W.B. Saunders.
McEwen C, DiTata D, Lingg C, et al: Ankylosing spondylitis and the spondylitis accompanying ulcerative colitis, regional enteritis, psoriasis and Reiter's disease: A comparative study, *Arthritis Rheum* 14:291–318, 1971.
Pascual E, Castellano JA, Lopez E: Costovertebral joint changes in ankylosing spondylitis with thoracic pain, *Br J Rheumatol* 31:413–415, 1992.
Resnick D: Patterns of peripheral joint disease in ankylosing spondylitis, *Radiology* 110:523–532, 1974.
Resnick D, Niwayama G: Ankylosing spondylitis. In Resnick D, editor: *Diagnosis of bone and joint disorders*, ed 3, Philadelphia, 1995, W.B. Saunders, p. 1003.
Rivelis M, Freiberger RH: Vertebral destruction at unfused segments in late ankylosing spondylitis, *Radiology* 93:251–256, 1969.

13 Osteoarthritis

Osteoarthritis is the most common arthropathy. Although many arthropathies lead to secondary osteoarthritic changes, this chapter deals with primary osteoarthritis and osteoarthritis secondary to alteration of normal mechanics across a weight-bearing joint. The radiographic hallmarks of osteoarthritis are as follow:

1. Normal mineralization
2. Nonuniform loss of joint space
3. Absence of erosions
4. Subchondral new bone formation
5. Osteophyte formation
6. Cysts
7. Subluxations
8. Unilateral or bilateral asymmetrical distribution
9. Distribution in hands, feet, knees, and hips; sparing of shoulders and elbows

Except for the type of joint space loss, all of these features may also be seen in osteoarthritis developing secondary to an underlying cartilage problem. In secondary osteoarthritis the joint space loss is uniform; in primary or mechanical osteoarthritis the joint space loss is nonuniform.

THE HAND

Primary osteoarthritis in the hand involves the distal interphalangeal (DIP) joints and proximal interphalangeal (PIP) joints with relative sparing of the metacarpophalangeal (MCP) joints (Fig. 13-1). The soft tissue swelling around the DIP joint associated with osteophyte formation is called a Heberden node (Fig. 13-2); that around the PIP joint is called a Bouchard node. There is nonuniform loss of the joint space with subchondral sclerosis and osteophyte development in the area of greatest loss of cartilage. The osteophyte must not be confused with either the new bone formation of psoriasis or the saucerized flared edge of the bone caused by erosion of psoriasis. An osteophyte is an extension of a normal articular surface. In the interphalangeal (IP) joints the osteophyte extends laterally or medially and proximally toward the body (Fig. 13-3). Erosion and ankylosis, manifestations of inflammatory disease, are not present. Cyst formation is relatively rare in the digits.

FIGURE 13-1. Posteroanterior (PA) view of the hand in osteoarthritis. The interphalangeal (IP) joints are primarily involved, with cartilage loss, osteophyte formation, and subchondral sclerosis. The wrist shows involvement of the base of the first metacarpal as it articulates with the trapezium.

FIGURE 13-2. DIP joints in osteoarthritis. The soft tissue swelling associated with the osteophyte formation is called Heberden node.

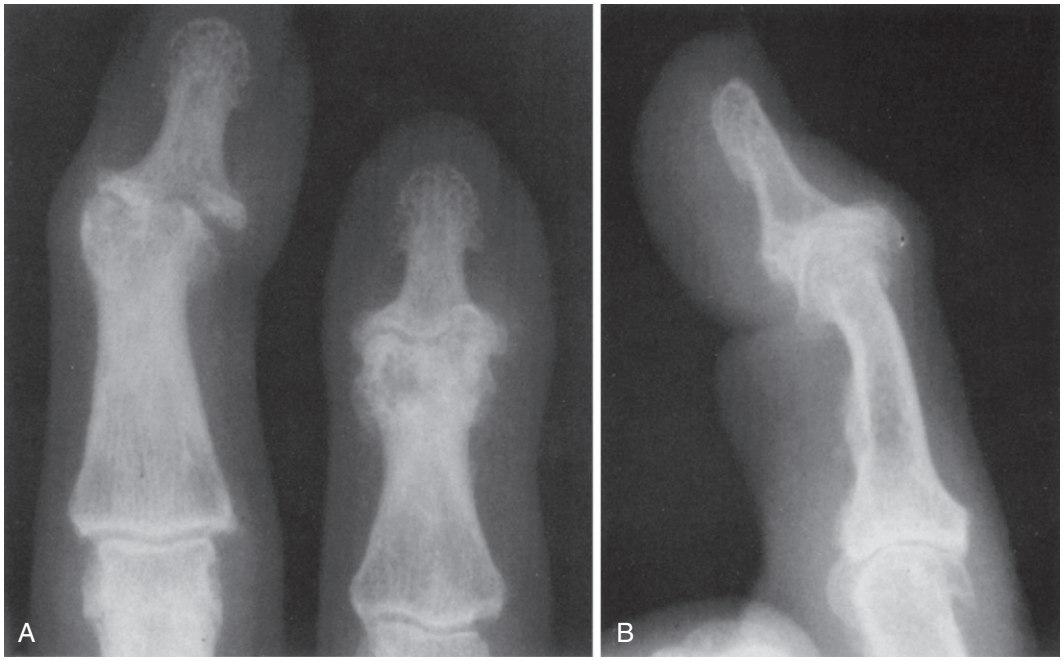

FIGURE 13-3. A, PA view of DIP joints showing nonuniform loss of joint space, subchondral sclerosis, and osteophyte formation extending laterally and medially. **B,** Lateral view of IP joints showing osteophytes extending proximally toward the body.

Primary osteoarthritis of the wrist involves only two joints: the joint between the base of the first metacarpal and the trapezium and the joint between the trapezium and the scaphoid (triscaphe joint) (Fig. 13-4). There may be radial subluxation of the base of the first metacarpal in relationship to the trapezium (Fig. 13-5). Large osteophyte formation is seen between the base of the first and second metacarpals. Eburnation and cyst formation are present. Osteoarthritic changes involving any other joint in the wrist must be considered secondary to another arthropathy, (e.g., calcium pyrophosphate dihydrate crystal deposition disease).

FIGURE 13-4. Osteoarthritis of the wrist. There is narrowing of the joint space between the base of the first metacarpal and the trapezium and between the trapezium and the scaphoid. There is subchondral sclerosis and osteophyte formation (*arrows*).

FIGURE 13-5. Osteoarthritis of the wrist. There is radial subluxation of the base of the first metacarpal in relationship to the trapezium. There is associated subchondral sclerosis and osteophyte formation. A cyst is present in the base of the first metacarpal (*arrow*).

Erosive osteoarthritis is a close relative of primary osteoarthritis and should be discussed at this time. Erosive osteoarthritis is seen primarily in postmenopausal females. It has the same distribution in the hand that primary osteoarthritis has, with involvement of the DIP and PIP joints in the fingers (Fig. 13-6) and the first carpometacarpal joint and the triscaphe joint in the wrist (Fig. 13-7). It is distinguished from osteoarthritis in that it has an inflammatory component superimposed on osteoarthritic changes. Therefore, in addition to osteophyte formation, erosive disease is present and ankylosis can occur (Fig. 13-8). Occasionally confusion exists between erosive osteoarthritis and psoriasis. Psoriasis has no osteophyte formation, and the erosions are marginal. Erosive osteoarthritis has osteophytes, and the erosions are more central in location.

FIGURE 13-6. PA view of a hand with erosive osteoarthritis. Normal mineralization is present. The DIP joints show osteophyte formation. The second PIP joint and third and fifth DIP joints show erosive changes and have the appearance of a seagull. There is ankylosis of the second DIP joint.

FIGURE 13-7. Wrist in patient with erosive osteoarthritis. There is loss of the joint space between the base of the first metacarpal and the trapezium and the trapezium and scaphoid. There is bone sclerosis and osteophyte formation. Erosive changes are seen in the base of the first metacarpal (*arrowhead*).

FIGURE 13-8. Erosive osteoarthritis involving the IP joints. Osteophyte formation is seen in nearly all the IP joints. There is bone ankylosis of the fifth PIP joint demonstrating the inflammatory component.

Martel has likened the appearance of the erosive osteoarthritic joint to that of a seagull and the appearance of the psoriatic arthritic joint to that of mouse ears (Fig. 13-9). The only other joints involved with erosive osteoarthritis are the IP joints of the feet. The presence of erosions and osteophytes in any other joint in the body indicates an underlying inflammatory arthropathy with secondary osteoarthritis, not erosive osteoarthritis.

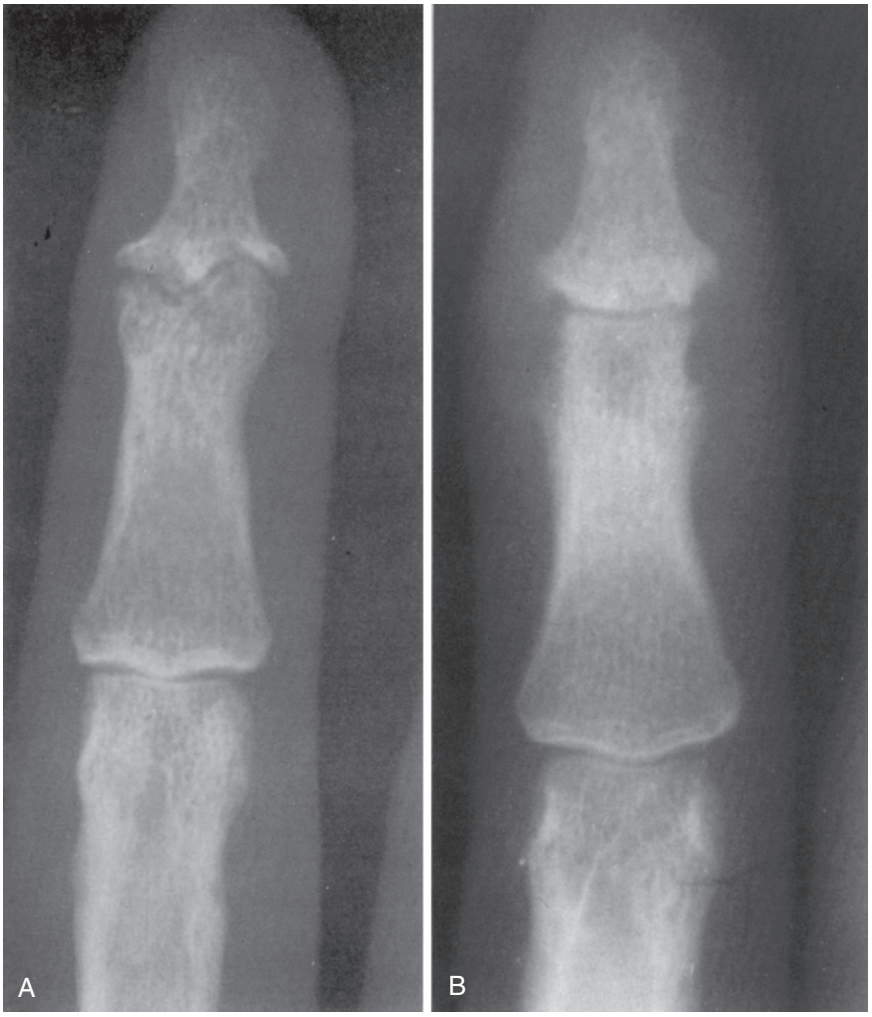

FIGURE 13-9. A, Erosive osteoarthritis involving the DIP joint demonstrating the appearance of a seagull. **B,** Psoriatic arthritis of the DIP joint demonstrating the appearance of mouse ears. *(**B** from Brower AC: The radiographic features of psoriatic arthritis. In Gerber L, Espinoza L, editors:* Psoriatic arthritis, *Orlando, FL, Grune & Stratton, 1985, p. 125; reprinted by permission.)*

THE FEET

The most common joint of the foot involved with osteoarthritis is the first metatarsophalangeal (MTP) joint. This is usually seen in association with a hallux valgus or a hallux rigidus deformity of the big toe. There is nonuniform loss of the joint space. Osteophyte formation, subchondral bone repair, and cyst formation are present (Fig. 13-10). In a hallux valgus deformity, the sesamoids appear lateral to their normal relationship with the metatarsal head. There may be thickening of the lateral cortex of the first metatarsal as weight is placed on this area (Fig. 13-11). Osteoarthritic changes may be seen elsewhere in the foot wherever the normal mechanics are changed (Fig. 13-12). For instance, a person with a tarsal coalition may develop osteoarthritis in the tarsal joints that are not congenitally fused.

FIGURE 13-10. Osteoarthritis of the first MTP joint with hallux rigidus. There is loss of the joint space, subchondral sclerosis, and osteophyte formation. A subchondral cyst is seen in the base of the proximal phalanx (*arrow*).

FIGURE 13-11. Osteoarthritis of the first MTP in a patient with a hallux valgus deformity. The sesamoids are lateral to the metatarsal head. There is narrowing of the joint space with subchondral bone and osteophyte formation. There is thickening of the lateral cortex of the metatarsal shaft (*arrow*).

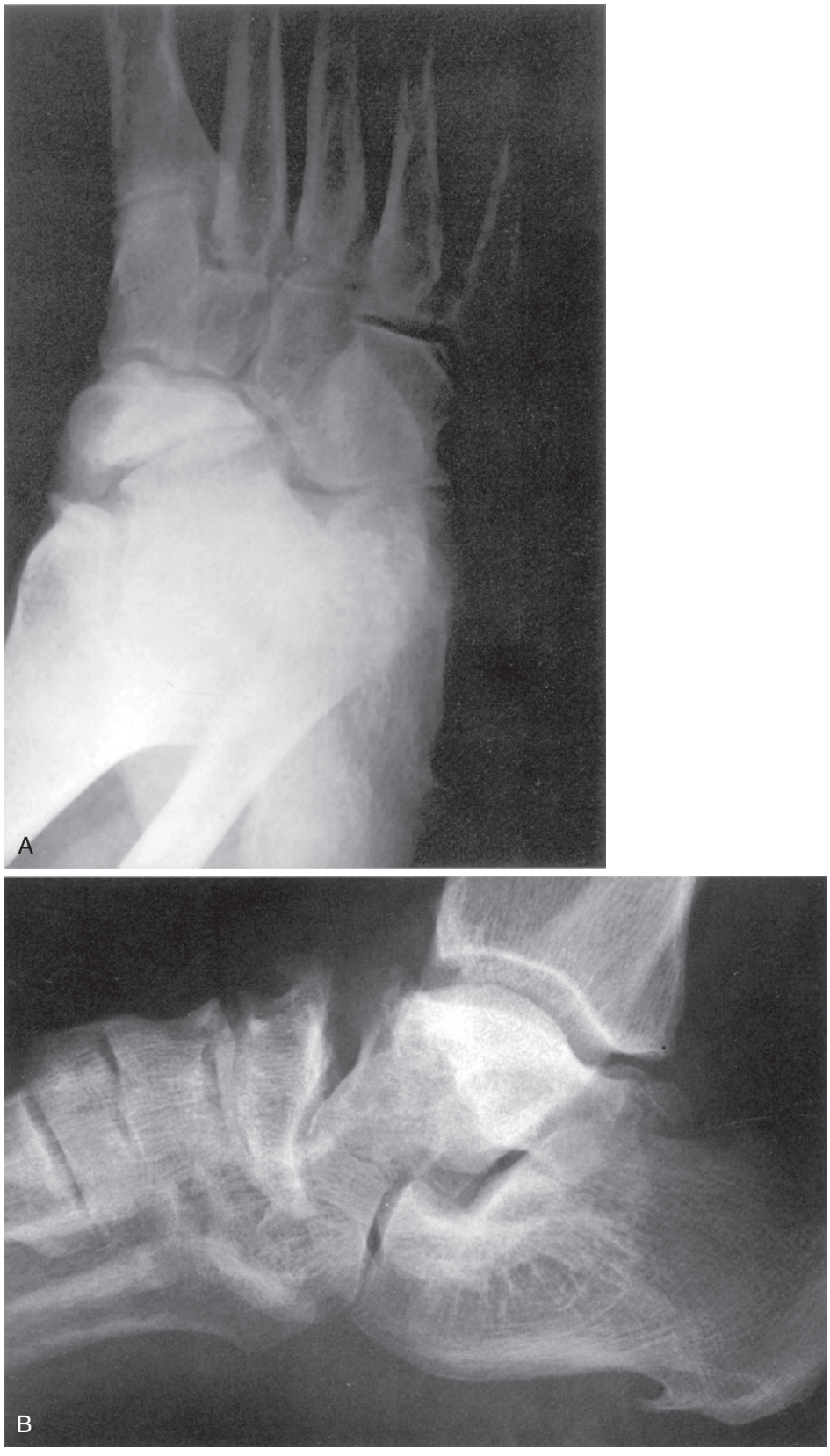

FIGURE 13-12. Anteroposterior (**A**) and lateral (**B**) views of the tarsal bones showing osteoarthritis secondary to a vertical talus.

THE HIPS

There is nonuniform loss of joint space in the hip joint that is radiographically identified as superolateral migration of the femoral head within the acetabulum (Fig. 13-13). If a vacuum phenomenon is produced within the joint, loss of cartilage is observed on the superolateral aspect of the hip joint, with maintenance of normal cartilage axially and medially (Fig. 13-14). As the cartilage is lost, subchondral bone formation and osteophyte formation are seen in this area of the joint (see Fig. 13-13). With this cartilage loss and migration of the head within the acetabulum, the head becomes noncongruent with the acetabulum. As a result, an osteophyte develops medially on the femoral head to fill the incongruity (Fig. 13-15). A ghost line of the original femoral head is often identified, with the osteophyte obviously being an addition to the head. The weight-bearing axis is shifted from its normal position to the medial neck of the femur, and new bone is added along the medial cortex (see Fig. 13-13). Although there is no actual erosion as seen in the inflammatory arthropathies, there may be wearing away or grinding down of the bone on both sides of the joint, giving a nubbin appearance to the femoral head and a more vertical orientation to the acetabulum (Fig. 13-16).

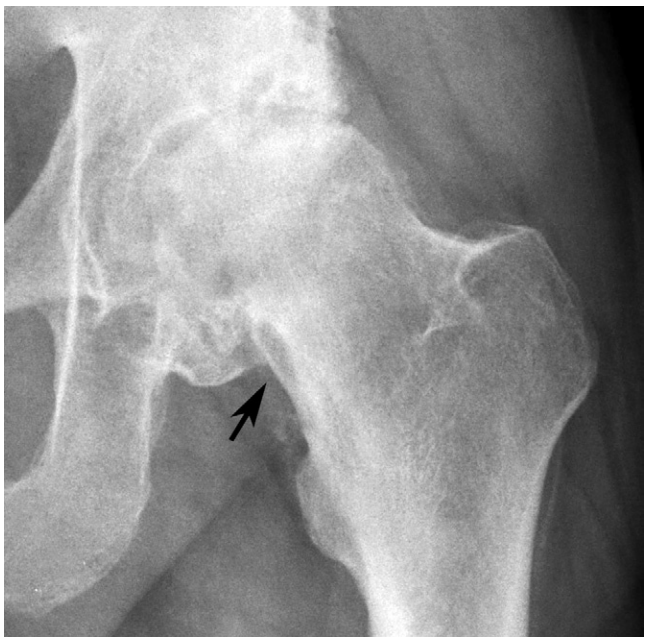

FIGURE 13-13. Osteoarthritis of the hip. There is nonuniform loss of the joint space with superolateral migration of the femoral head within the acetabulum. There is subchondral bone formation and an osteophyte seen on the lateral aspect of the acetabulum. There is new bone apposition along the medial cortex of the femoral neck (*arrow*).

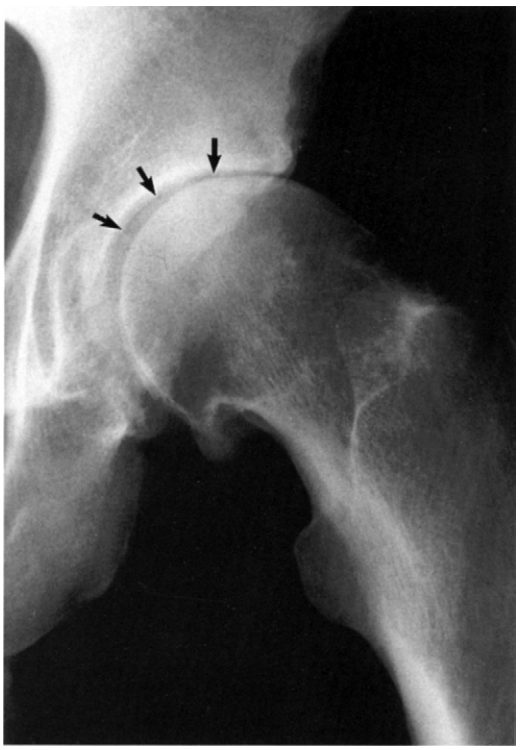

FIGURE 13-14. Frogleg lateral view of the hip in osteoarthritis. A vacuum phenomenon has been produced within the joint (*arrows*). This allows demonstration of the nonuniform loss of the cartilage, the greatest loss being superolaterally.

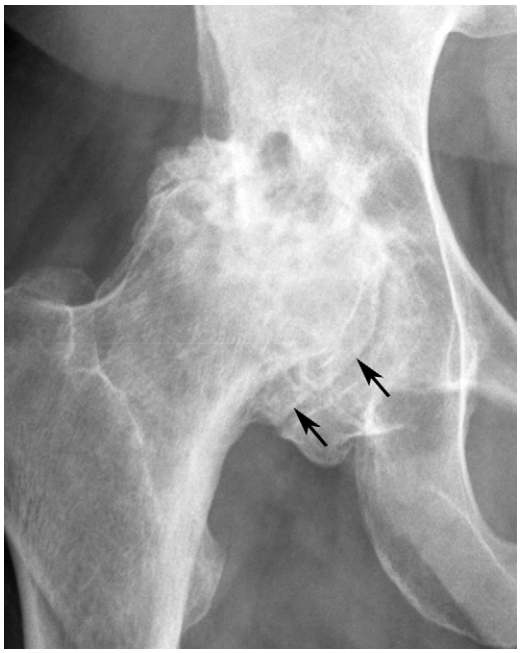

FIGURE 13-15. Anteroposterior (AP) view of the hip in osteoarthritis. The hip has moved in a superolateral direction within the acetabulum. There is subchondral sclerosis, osteophyte formation, and cyst formation. A large osteophyte has been added to the medial aspect of the femoral head (*arrows*); it fills the incongruity between the acetabulum and the displaced head.

FIGURE 13-16. Severe osteoarthritis of the hip. The femoral head has been mechanically eroded to half its normal size. The acetabulum has been eroded to a more vertical orientation. There are extensive subchondral bone formation, osteophyte formation, and marked thickening of the inner cortex of the femoral neck.

Cyst formation is part of osteoarthritis. The cysts of osteoarthritis have been classified as *intrusion cysts* and *contusion cysts* (Fig. 13-17). The intrusion cyst is seen immediately subchondrally and may have a wide, narrow, or radiographically absent communication with the joint space. The contusion cyst may be further from the joint than the intrusion cyst and is totally enclosed within the bone. Both have sclerotic borders and reparative bone surrounding them. A cyst may collapse, producing a bizarre configuration of the femoral head. Cysts can also be present before there is actual cartilage loss and later can cause secondary collapse of the joint.

Rarely, the disease in the hip may rapidly progress with destruction of the femoral head occurring in weeks or months simulating neuropathic disease or infection of the hip (Fig. 13-18). This form of osteoarthritis may be temporarily related to a steroid and anesthetic injection of the hip but has also been described without a preceding therapeutic injection. The etiology of rapid progressive osteoarthritis of the hip is unknown.

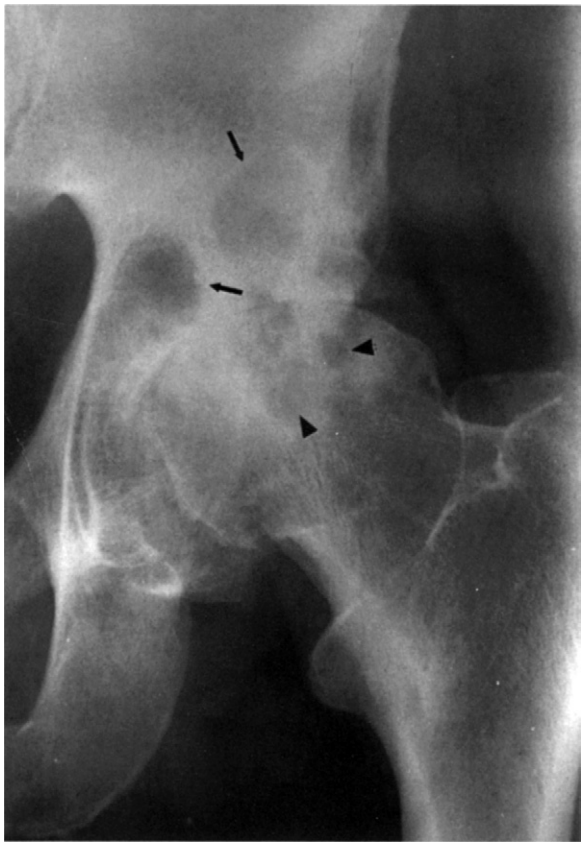

FIGURE 13-17. AP view of the hip with severe mechanical osteoarthritis. Intrusion (*arrows*) and contusion (*arrowheads*) cysts are present.

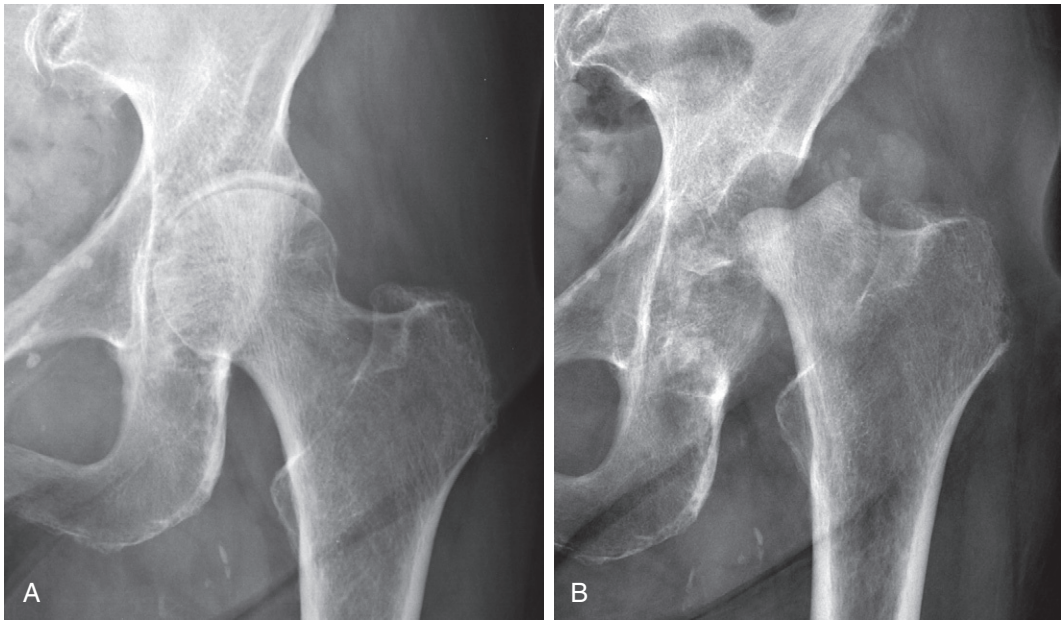

FIGURE 13-18. A, AP view of the hip with axial joint space narrowing and minimal osteoarthritis. **B,** AP view of the hip 3 months after an intraarticular steroid injection shows aseptic rapid destruction of the joint.

THE KNEES

Osteoarthritis of the knee is seen most commonly in the knee following trauma and in obese females. There is nonuniform loss of the joint space as manifested by preferential narrowing of one or two of three compartments. In some patients, the lateral tibiofemoral compartment is preferentially narrowed, with an exaggerated valgus deformity. More commonly, there is preferential narrowing of the medial tibiofemoral compartment accompanied by narrowing of the patellofemoral compartment (Fig. 13-19). In this scenario, there is a varus deformity in the standing knee, with lateral subluxation of the tibia in relationship to the femur. With this medial compartment loss and lateral subluxation, a large osteophyte forms on the medial aspect of the medial condyle (Fig. 13-20). Subchondral bone repair and cyst formation may be seen. There may be thickening of the medial cortex of the tibia as the axis of weight bearing is shifted to this area. Osteophyte formation and subchondral sclerosis develop in the posterior aspect of the tibia and the anterior aspect of the tibia and the femur (Fig. 13-21). Bone excrescences or exostoses may form and extend into the joint where cartilage has been lost (Fig. 13-22). Sometimes pieces of bone or cartilage break off and form loose bodies within the joint (Fig. 13-23). These changes should not be confused with primary synovial osteochondromatosis.

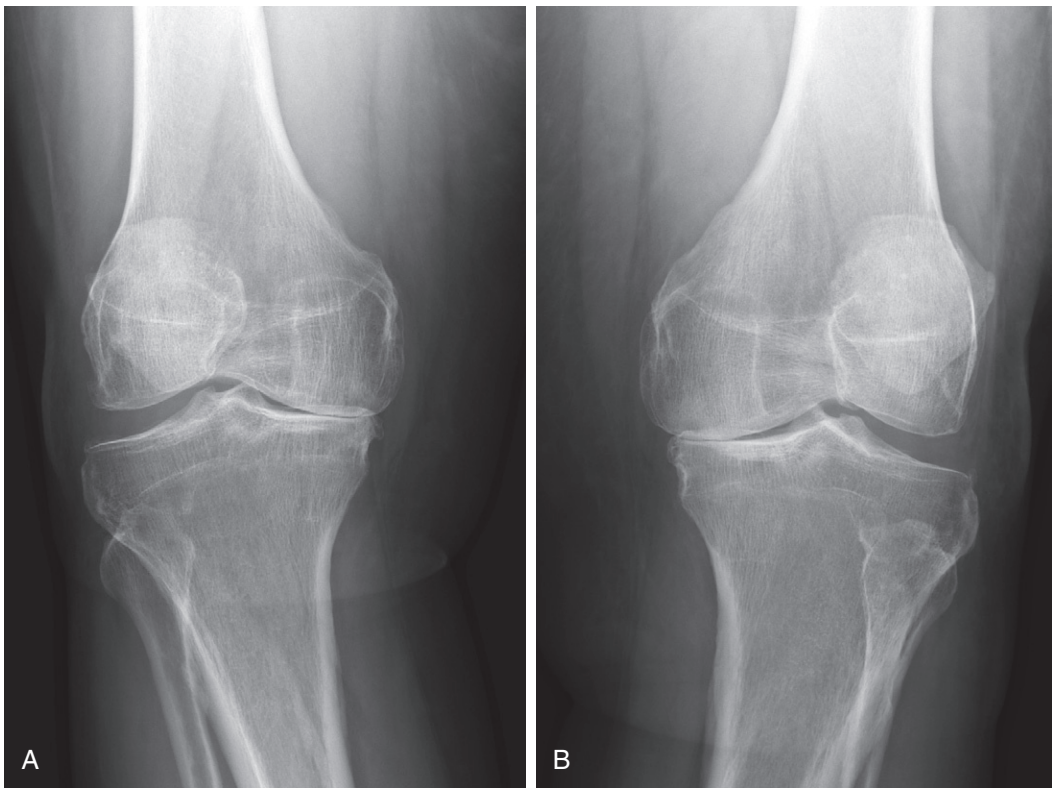

FIGURE 13-19. AP standing view of both knees in osteoarthritis. There is preferential narrowing of the medial tibiofemoral compartment with slight lateral subluxation of the tibia in relationship to the femur.

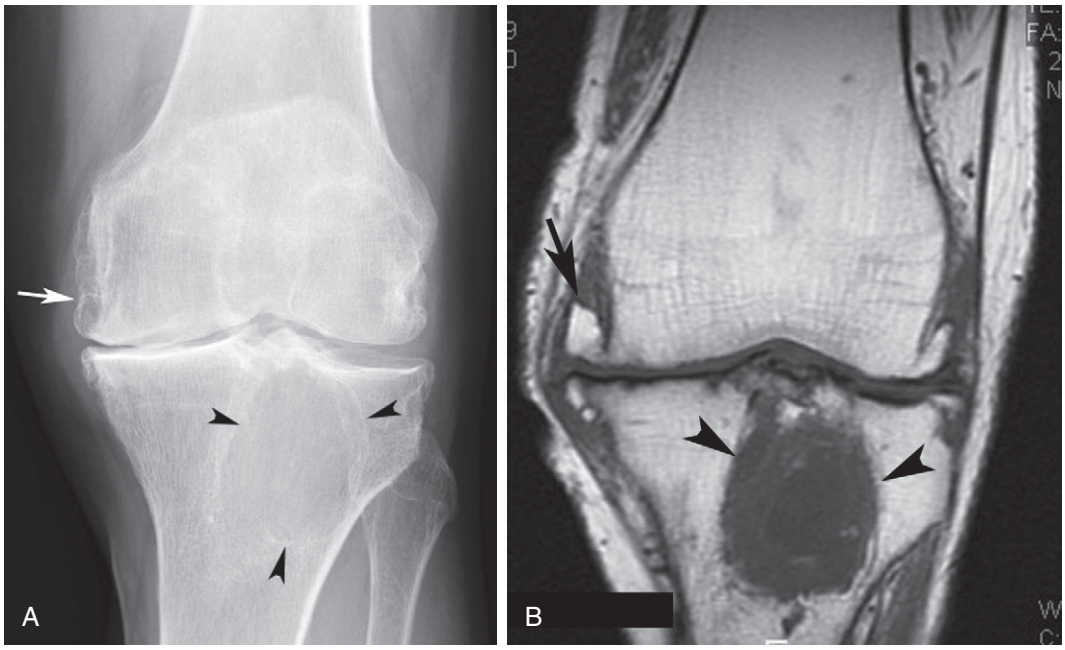

FIGURE 13-20. A, AP standing view of the knee. There is preferential medial compartment narrowing. A large osteophyte on the medial aspect of the medial condyle (*arrow*) might be mistaken for the original condyle. There is also a large subchondral cyst that might be mistaken for neoplasm (*arrowheads*). **B,** Coronal T1-weighted image of the knee confirms large medial osteophyte (*arrow*) and large subchondral cyst (*arrowheads*).

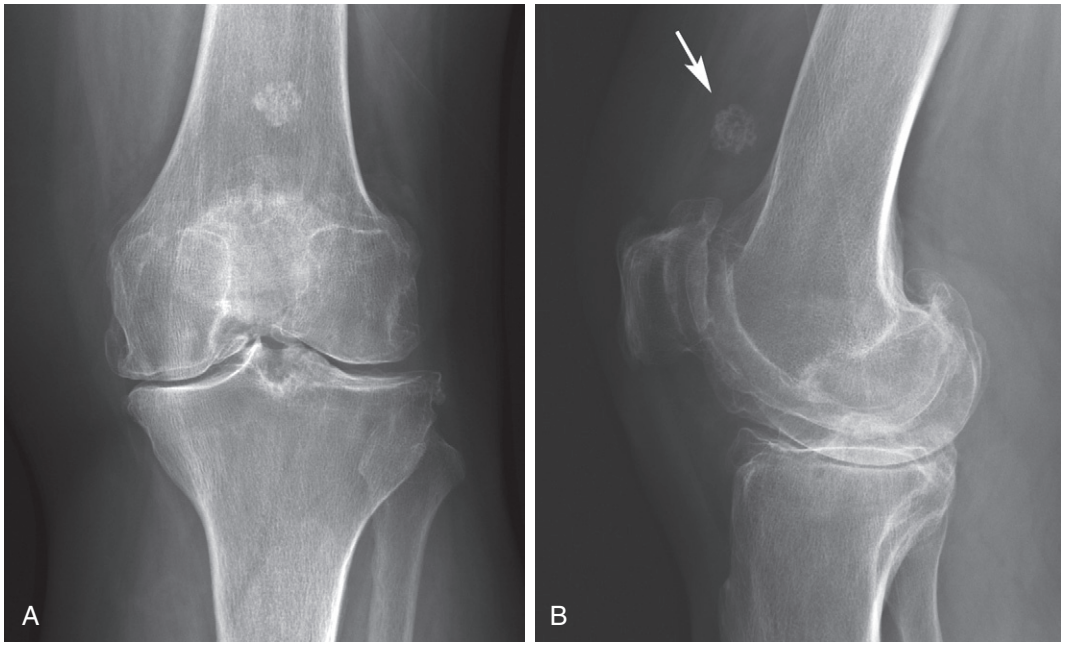

FIGURE 13-21. AP standing view (**A**) and lateral view (**B**) of the knee of a patient with osteoarthritis. There is preferential medial tibiofemoral and patellofemoral compartment narrowing. Varus deformity is noted on the AP view. There is extensive osteophyte formation medially on the AP view and anteriorly and posteriorly on the lateral view. Arrow points to loose body in the joint.

FIGURE 13-22. Tunnel view of a knee demonstrating bone excrescences extending into the joint from areas where cartilage has been lost (*arrows*).

FIGURE 13-23. Lateral view of a knee with osteoarthritis. There is loss of the joint spaces with osteophyte formation. Loose bodies are seen within the knee (*arrows*) that represent fragmentation of cartilage.

THE SACROILIAC JOINT (SI)

Osteoarthritis of the SI joint occurs most commonly in heavy laborers. The greatest loss of cartilage is seen in the superior and inferior aspects of the true synovial joint (Fig. 13-24). The loss is identified by the presence of subchondral bone repair. Osteophytes form superiorly and inferiorly and bridge across the ilium to the sacrum anteriorly. These osteophytes may be mistaken for bone ankylosis of the joint on an anteroposterior (AP) view. However, careful observation of a portion of the joint remaining unaffected should allow the correct diagnosis of osteoarthritis rather than inflammatory disease.

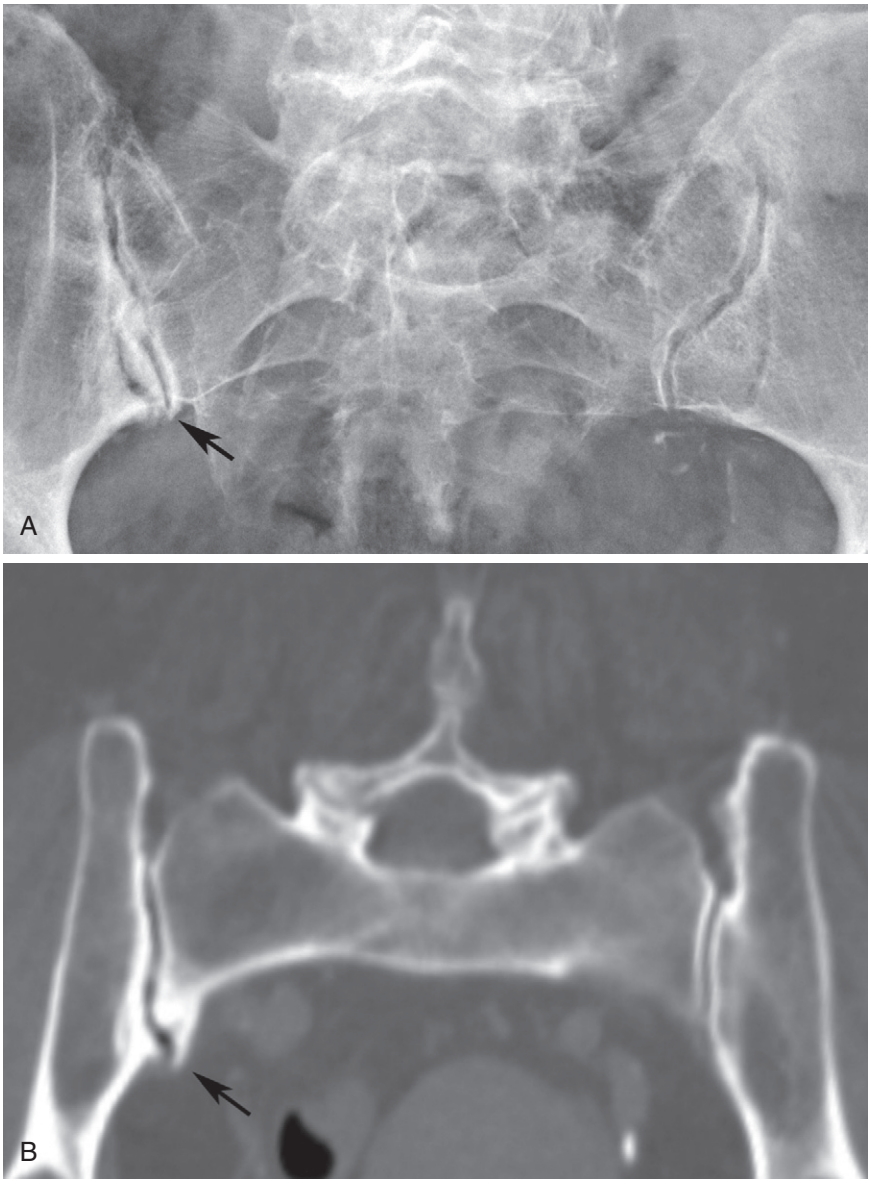

FIGURE 13-24. **A,** Sacroiliac joint in osteoarthritis. There is subchondral bone repair in the synovial aspect of the right sacroiliac joint. Osteophytes extend from the inferior sacroiliac joint (*arrow*). **B,** Coronal CT through the sacroiliac joints shows subchondral sclerosis and osteophyte formation (*arrow*) on the right.

THE SPINE

Osteoarthritis of the spine means osteoarthritis of the apophyseal joints (Fig. 13-25). This is commonly seen in the lower lumbar spine and in the lower cervical spine. It is seen as narrowing of the apophyseal joints and bone sclerosis. Severe osteoarthritis allows grade I spondylolisthesis (Fig. 13-26) in the lumbar spine and minimal subluxation in the cervical spine.

Narrowing or loss of disc height with osteophyte formation and subchondral bone sclerosis in the adjacent vertebral bodies should be called degenerative disc disease and not osteoarthritis. The disc is not a synovial joint, and disc degeneration should not be attributed to a disease that primarily involves the synovial joints. Degenerative disc disease is seen most commonly in the lumbar spine at L4-L5 and L5-S1 and in the cervical spine at C5-C6 and C6-C7 (Fig. 13-27).

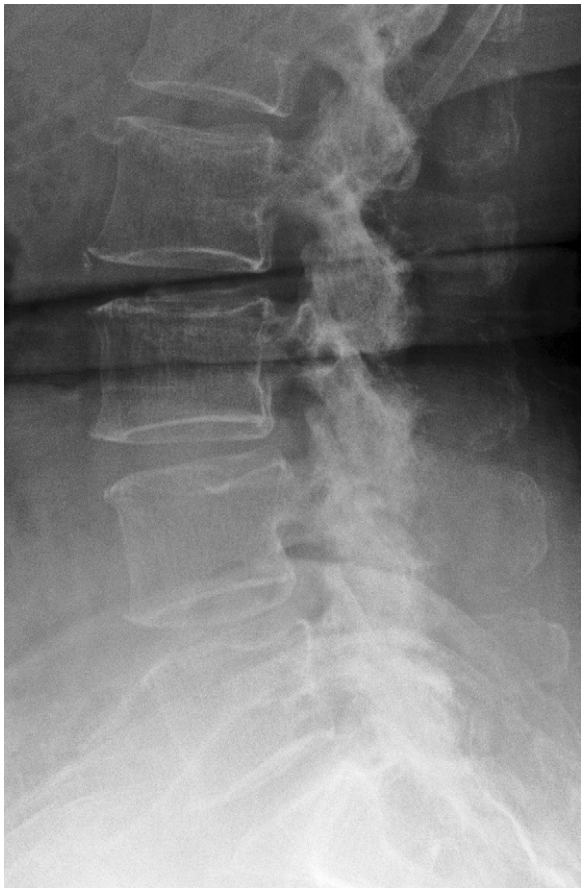

FIGURE 13-25. Lateral view of the lumbosacral spine showing osteoarthritis of the apophyseal joints. There is loss of the apophyseal joints with tremendous subchondral sclerosis present. The vertebral bodies and disc spaces are unaffected.

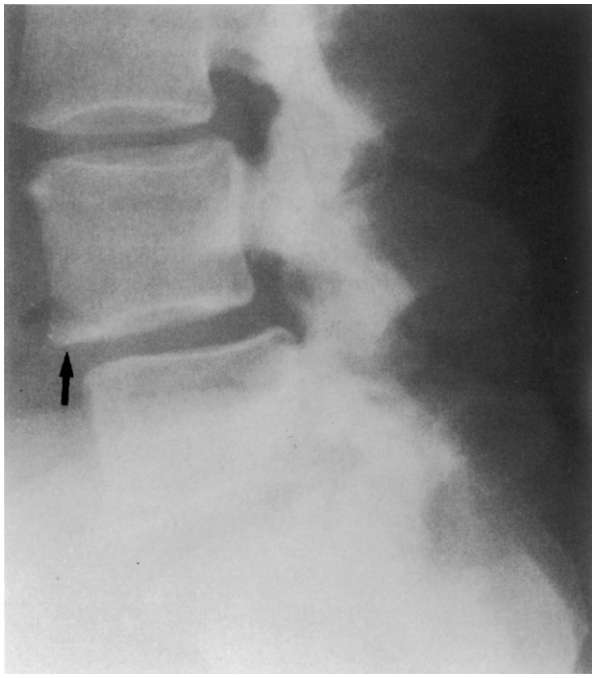

FIGURE 13-26. Lateral view of the lower lumbar spine with osteoarthritis. There is loss of the apophyseal joint spaces with adjacent subchondral sclerosis. There is a grade I spondylolisthesis of L4 in relationship to L5 (*arrow*).

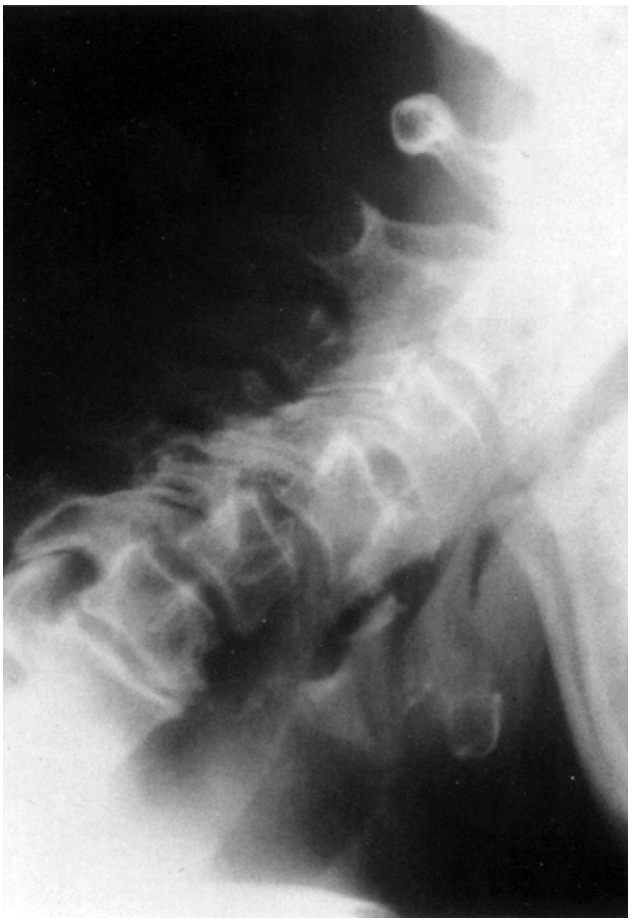

FIGURE 13-27. Lateral view of the cervical spine showing osteoarthritis of the apophyseal joints allowing subluxation of C4 on C5. Noted is associated degenerative disc disease at C5-C6 and C6-C7. C5 is subluxed on C6.

SUMMARY

The radiographic hallmarks of osteoarthritis are subchondral bone formation, osteophyte formation, and cysts. These changes may be seen secondary to a primary underlying arthropathy. In this instance the cartilage loss is uniform; however, if these radiographic findings occur with nonuniform loss of cartilage, the diagnosis must be primary osteoarthritis or osteoarthritis unrelated to a previous arthropathy.

SUGGESTED READINGS

Ahlback S: Osteoarthrosis of the knee: A radiographic investigation, *Acta Radiol Diagn (Stockh)* 277:7–72, 1968.

Cameron HU, Fornasier VL: Fine detail radiography of the femoral head in osteoarthritis, *J Rheumatol* 6:178–184, 1979.

Greenway G, Resnick D, Weisman M, et al: Carpal involvement in inflammatory (erosive) osteoarthritis, *J Can Assoc Radiol* 30:95–98, 1979.

Jeffery AK: Osteophytes and the osteoarthritic femoral head, *J Bone Joint Surg Br* 57:314–324, 1975.

Kellgren JH, Lawrence SJ, Bier F: Genetic factors in generalized osteoarthrosis, *Ann Rheum Dis* 22:237–255, 1963.

Kidd KL, Peter JB: Erosive osteoarthritis, *Radiology* 86:640–647, 1966.

Mann RA, Coughlin MJ, DuVries HL: Hallux rigidus: A review of the literature and a method of treatment, *Clin Orthop Relat Res* 142:57–63, 1979.

Martel W, Braunstein EM: The diagnostic value of buttressing of the femoral neck, *Arthritis Rheum* 21:161–164, 1978.

Martel W, Stuck KJ, Dworin AM, et al: Erosive osteoarthritis and psoriatic arthritis: A radiologic comparison in the hand, wrist, and foot, *AJR Am J Roentgenol* 134:125–135, 1980.

Mitchell NS, Cruess RL: Classification of degenerative arthritis, *Can Med Assoc J* 117:763–765, 1977.

Murray RO: The aetiology of primary osteoarthritis of the hip, *Br J Radiol* 38:810–824, 1965.
Ondrouch AS: Cyst formation in osteoarthritis, *J Bone Joint Surg Br* 45:755–760, 1963.
Resnick D: Patterns of migration of the femoral head in osteoarthritis of the hip: Roentgenographic-pathologic correlation and comparison with rheumatoid arthritis, *Am J Roentgenol Radium Ther Nucl Med* 124:62–74, 1975.
Resnick D, Niwayama G, Goergen TG: Degenerative disease of the sacroiliac joint, *Invest Radiol* 10:608–621, 1975.
Sims CD, Bentley G: Carpometacarpal osteoarthritis of the thumb, *Br J Surg* 57:442–448, 1970.
Smith D, Braunstein EM, Brandt KD, et al: A radiographic comparison of erosive osteoarthritis and idiopathic nodal osteoarthritis, *J Rheumatol* 19:896–904, 1992.
Thomas RH, Resnick D, Alazraki NP, et al: Compartmental evaluation of osteoarthritis of the knee: A comparative study of available diagnostic modalities, *Radiology* 116:585–594, 1975.
Trueta J: *Studies of the development and decay of the human frame*, Philadelphia, 1968, W.B. Saunders p. 335.

14 *Neuropathic Osteoarthropathy*

Neuropathic osteoarthropathy presents the most dramatic radiographic picture of all of the arthropathies. As a result, it may produce a diagnostic dilemma. Although it is known that various neurological disorders play a prominent role in the development of the osteoarthropathy, the exact pathogenesis has not been clearly established. Although chronic, repetitive, and undetected trauma creates many of the radiographic changes, it is not responsible for all of the changes seen. As long as trauma is believed to be the primary etiology, many neuropathic joints will continue to be misdiagnosed as infection or tumor.

The radiographic changes in neuropathic osteoarthropathy cover the complete spectrum of bone change from total resorption to excessive repair. At one end of the spectrum is the hypertrophic joint and at the other end is the atrophic joint. Each of these extremes is discussed separately.

THE HYPERTROPHIC JOINT

The hypertrophic joint, or bone productive joint, if put in a time sequence, should be called the "chronic joint." The radiographic changes present no diagnostic problem. The changes resemble osteoarthritis "with a vengeance." The hallmarks are the following:

1. Dissolution of normal joint articulation
2. Severe subluxation or dislocation
3. Excessive juxta-articular new bone formation
4. Mammoth osteophytes
5. Fragmentation and osseous debris
6. Pathological fractures
7. Unilateral or bilateral asymmetrical involvement
8. Distribution in weight-bearing joints (i.e., foot, ankle, knee, hip, spine)

The Foot and Ankle

Diabetes mellitus is the most common cause of neuropathic osteoarthropathy even though it occurs in only 5 to 10 percent of patients with diabetes. In patients who are diabetic, the forefoot and midfoot are the most commonly involved joints. However, in diabetes, infection is commonly present, and it becomes difficult to separate neuropathic changes from those of chronic osteomyelitis. The most common neuropathic change seen in the foot is radiographic evidence of a longstanding

Lisfranc fracture-dislocation with extensive eburnation and fragmentation around the tarsometatarsal joints (Fig. 14-1). Bizarre fractures of the calcaneus with dissolution of the talocalcaneal joint and tumbling of the talus into the calcaneus may be the neuropathic change (Fig. 14-2). In the ankle, the distal fibula may fracture pathologically and the talus may angulate within the ankle mortise. With time, massive bone sclerosis, osteophytosis, and osseous debris develop (Fig. 14-3).

FIGURE 14-1. Anteroposterior (AP) view of the forefoot in a diabetic patient. There is a Lisfranc fracture-dislocation of the tarsometatarsal joints. There is extensive subchondral sclerosis in the adjacent articulating bones.

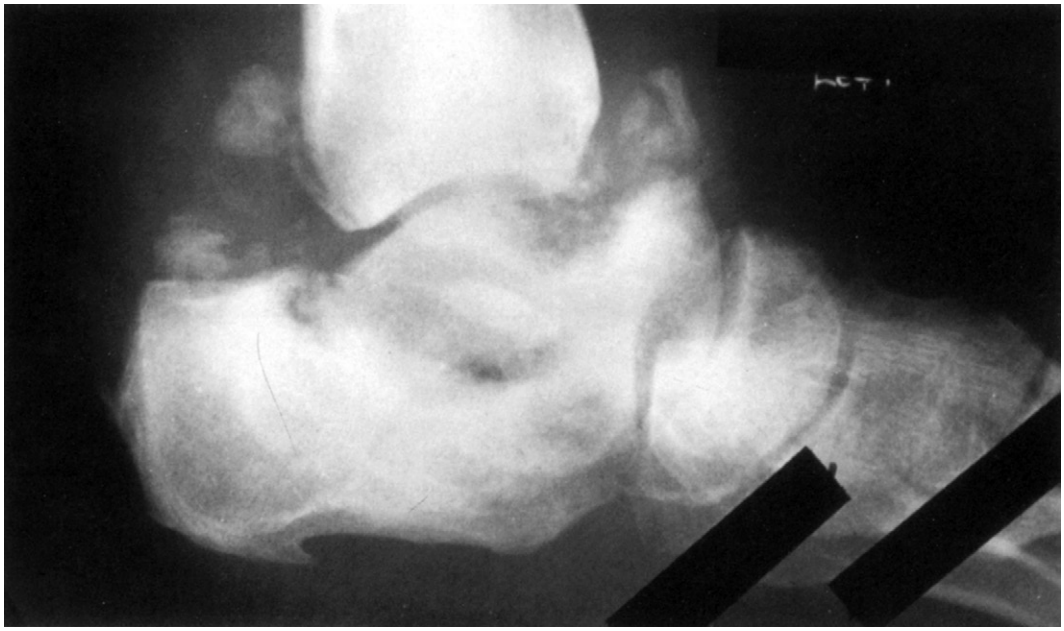

FIGURE 14-2. Lateral view of the hindfoot in a diabetic patient. This is dissolution of the talocalcaneal joint space, with the talus tumbling into the calcaneus. There is extensive subchondral bone formation. Fragments of bone are seen in the ankle joint. *(From Brower AC, Allman RM: Neuropathic osteoarthropathy in the adult. In Traveras JM, Ferruci JT, editors:* Radiology: Diagnosis/imaging/intervention, *vol 5, Philadelphia, J.B. Lippincott, 1986; reprinted by permission.)*

FIGURE 14-3. AP view of a neuropathic ankle. There is complete dissolution of the normal ankle joint. There is extensive subchondral sclerosis in both the tibia and adjacent talus. There is fragmentation within the joint space. An old healed fracture of the distal shaft of the fibula is evident.

Knee and Hip

These joints are most commonly involved in tabes dorsalis. Sixty to 70 percent of patients with this condition have lower extremity involvement. In the knee, the first radiographic change is recurrent massive effusion with some subluxation. Periarticular pathological fractures and bone debris within the joint may develop (Fig. 14-4). Eventually, with weight bearing, there is joint dissolution, subluxation, eburnation, and fragmentation (Fig. 14-5).

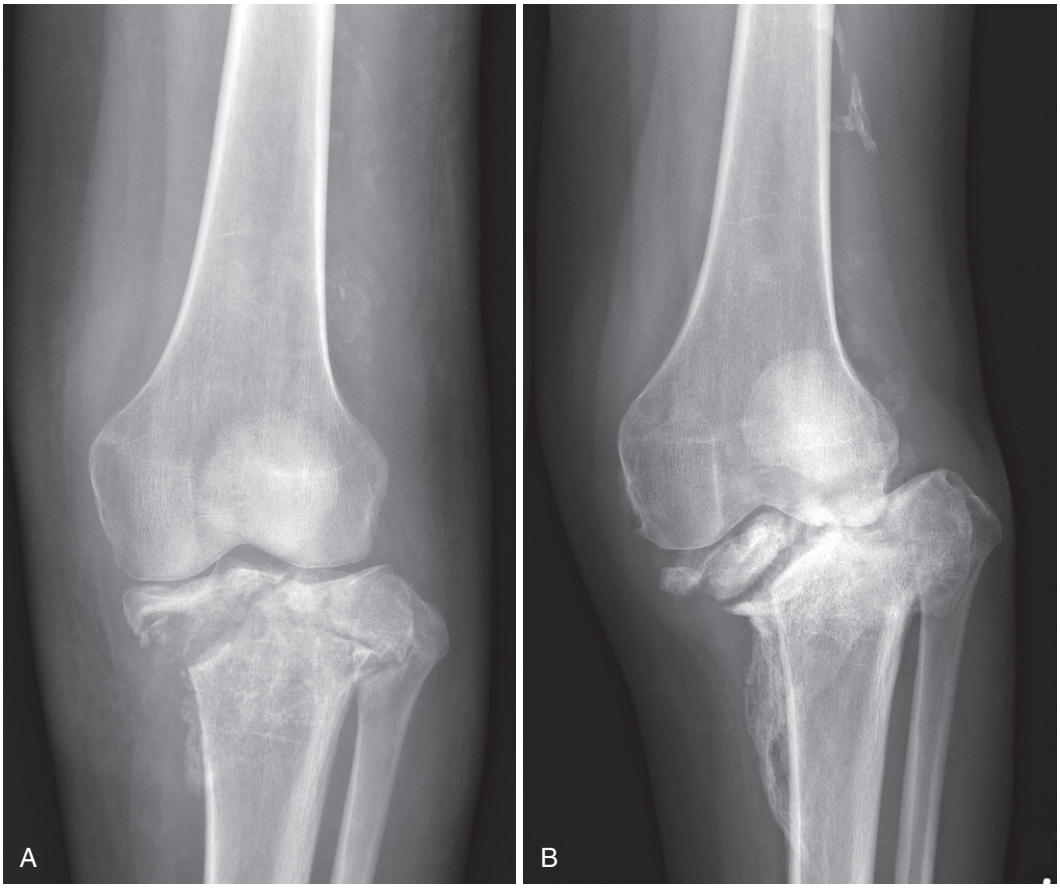

FIGURE 14-4. A, AP view of a neuropathic knee showing a pathological transverse fracture just beneath both the medial and lateral tibial plateau. Minimal ossification is seen medial to the tibial metaphysis and lateral to the femur. **B,** AP view of the knee 2 months later shows lateral subluxation of the knee and bone sclerosis in the proximal tibia.

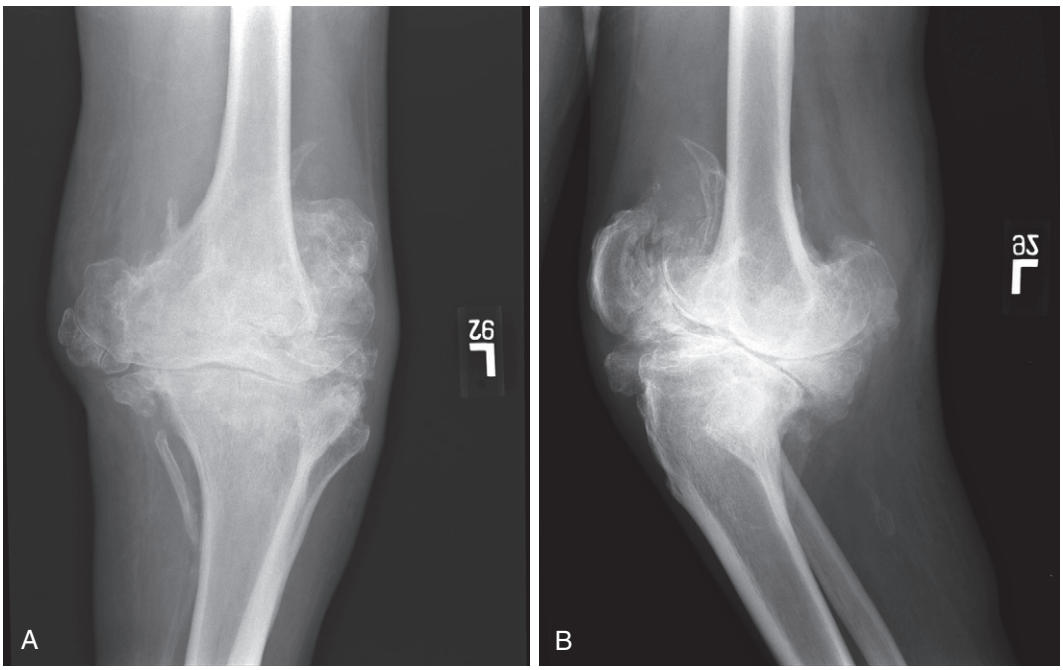

FIGURE 14-5. AP view (**A**) and lateral view (**B**) of a neuropathic knee showing marked loss of joint space, extensive anterior tibial subluxation, massive subchondral sclerosis, and fragmentation.

Early resorptive changes in the hip may or may not be seen prior to the hypertrophic changes. As long as the patient is weight bearing, productive bone changes develop around the femoral head, and a pseudoacetabulum is formed where the head has subluxed from the normal acetabulum (Fig. 14-6).

FIGURE 14-6. AP view of a hypertrophic neuropathic hip. The superior portion of the acetabulum has become eroded and remodeled, forming a large shallow pseudoacetabulum. There is massive bone formation in both the acetabulum and the femoral head. Osteophytosis and fragmentation are present as well.

The Spine

Although spine involvement is most commonly associated with tabes dorsalis, it may be observed in patients with diabetes. One or several disc levels and the adjacent vertebral bodies may be involved. The radiographic picture is one of bizarre and extreme degenerative disc disease (Fig. 14-7A). Eventually there is complete dissolution of the normal disc space, with massive sclerosis and excessive osteophytosis of the adjacent vertebral bodies (Fig. 14-7B). Bone fragmentation, although present, may be difficult to observe. One vertebral body appears to be tumbling into the adjacent vertebral body (Fig. 14-8).

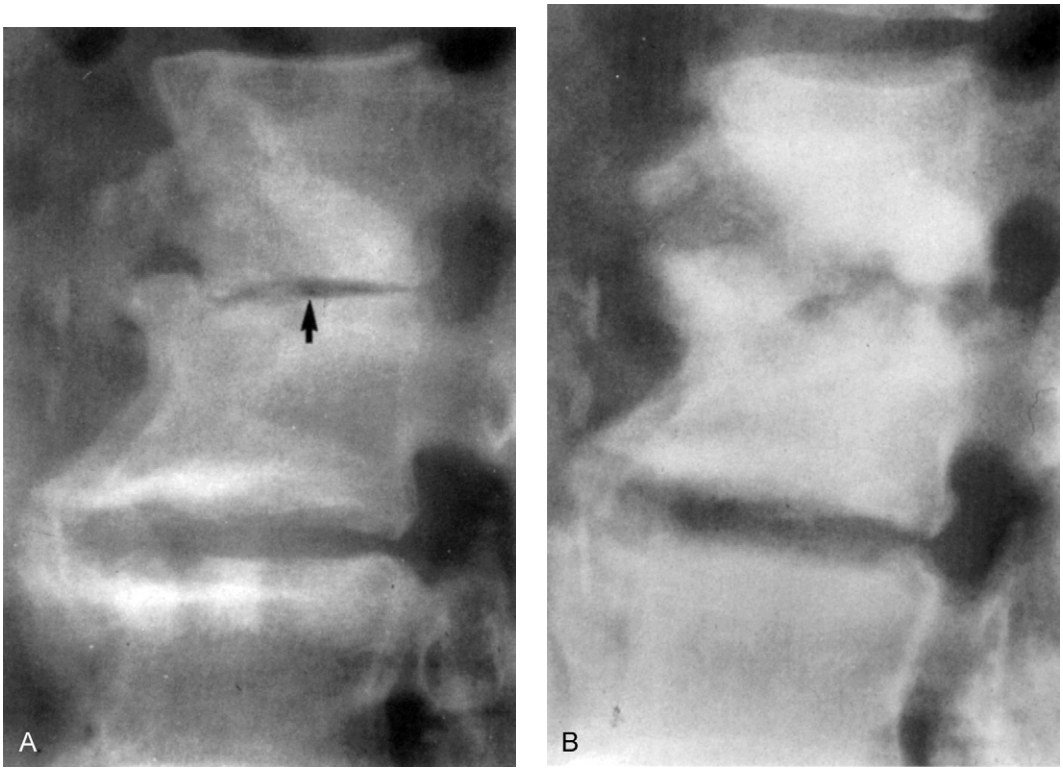

FIGURE 14-7. (A) A lateral view of three lumbar vertebral bodies. A vacuum phenomenon is present at the upper disc level (*arrow*). The superior vertebral body is tumbling into the inferior vertebral body. There is sclerosis involving half of the upper vertebral body and one third of the lower vertebral body. Although the changes resemble degenerative disc disease, the bone formation is more extensive, and the tumbling of one vertebral body into an adjacent vertebral body is unusual for uncomplicated degenerative disc disease. Lateral view of the lumbar spine shown in Figure 14-7**B** 1 year later. There is complete dissolution of the disc space, with massive eburnation in the adjacent vertebral bodies along with osteophyte formation.

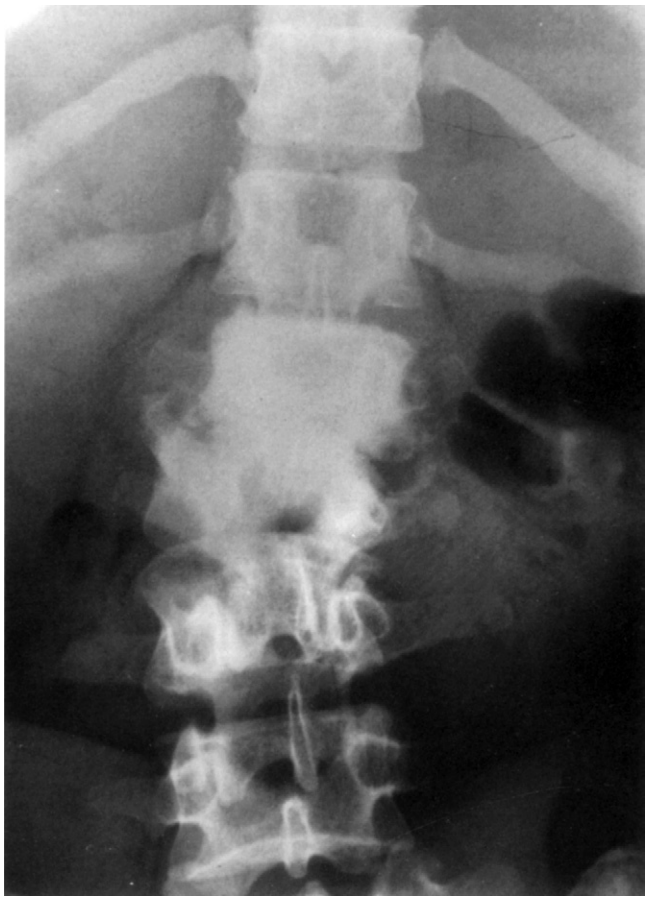

FIGURE 14-8. AP view of the upper lumbar spine in a patient with diabetes. L1 appears to be tumbling into L2. There is no evidence of a remaining disc space. Both vertebral bodies have become completely sclerotic. *(From Brower AC, Allman RM: Neuropathic osteoarthropathy in the adult. In Traveras JM, Ferruci JT, editors:* Radiology: Diagnosis/imaging/intervention, *vol 5, Philadelphia, J.B. Lippincott, 1986; reprinted by permission.)*

THE ATROPHIC JOINT

The atrophic or resorbed joint, if put in a time sequence, should be called the "acute joint." In this type of neuropathic joint, radiographs reveal change from normal to dramatic resorption within a period of 3 to 4 weeks. The radiographic appearance is often mistaken for a rampant infection or an aggressive bone tumor. The involvement of both sides of the joint excludes neoplasm; the sharp surgical edges of the resorbed bone and the maintenance of mineralization exclude infection. The radiographic hallmarks are the following:

1. Extensive bone resorption
2. Sharp edge that resembles surgical amputation between resorbed bone and remaining bone
3. Normal mineralization in remaining bone
4. Absence of bone repair
5. Soft tissue swelling
6. Bone debris in soft tissue
7. Unilateral or bilateral asymmetrical involvement
8. Distribution in non–weight-bearing joints, shoulder and elbow predominantly; also seen in a non–weight-bearing hip and knee; may be seen in early phase of any neuropathic joint.

The Shoulder and Elbow

The most common cause of neuropathic osteoarthropathy in the shoulder and elbow is syringomyelia. Twenty to 25 percent of patients with syringomyelia develop a neuropathic joint. In either the shoulder or elbow joint, soft tissue swelling is seen with osseous debris within it. Varying degrees of resorption of the articulating bones can be identified. The remaining ends of the bones appear to be surgically amputated (Figs. 14-9 to 14-11). In the shoulder, pathological fractures may be seen in the adjacent scapula or acromion (Fig. 14-12).

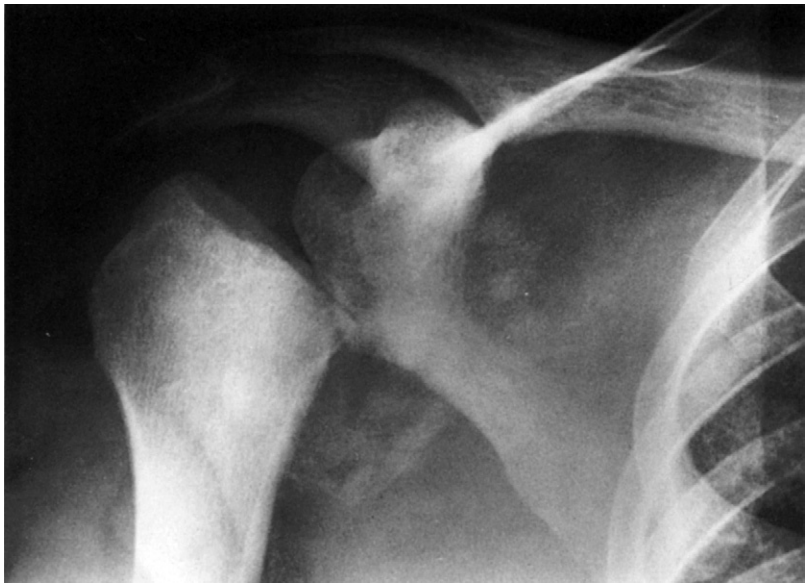

FIGURE 14-9. AP view of the shoulder in patient with syringomyelia. Part of the humeral head has been totally resorbed. There is a sharp edge to the remaining bone, giving the appearance of a surgical amputation. Debris is seen within the joint. *(From Brower AC, Allman RM: Neuropathic osteoarthropathy in the adult. In Traveras JM, Ferruci JT, editors:* Radiology: Diagnosis/imaging/intervention, *vol 5, Philadelphia, J.B. Lippincott, 1986; reprinted by permission.)*

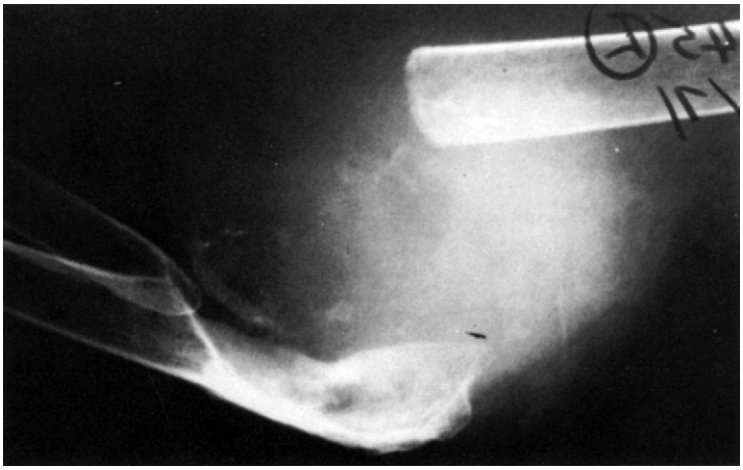

FIGURE 14-10. Lateral view of an elbow in patient with syringomyelia. There is tremendous soft tissue swelling in the area of the elbow joint. Ossific debris is seen within the soft tissue swelling. The proximal end of the radius appears whittled. The proximal end of the ulna is shallowed out, and the distal end of the humerus has a sharp surgical-appearing edge. Changes are classic for an atrophic neuropathic joint. *(From Brower AC, Allman RM: The neuropathic joint—a neurovascular bone disorder,* Radiol Clin North Am *19:571, 1981; reprinted by permission.)*

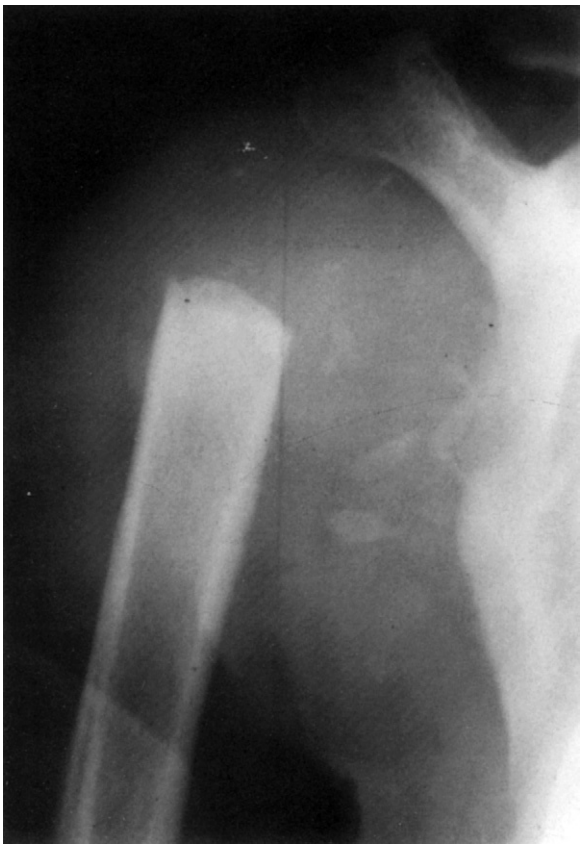

FIGURE 14-11. AP view of the shoulder in patient with syringomyelia. Soft tissue swelling is present in the area of the previous shoulder joint. Ossific debris is seen within the soft tissue. All of the humeral head and part of the proximal shaft have been resorbed. The remaining humerus is normally mineralized and has a sharp, surgical-appearing edge. *(From Brower AC, Allman RM: The pathogenesis of the neurotrophic joint: Neurotraumatic vs. neurovascular,* Radiology *139:349, 1981; reprinted by permission.)*

FIGURE 14-12. AP view of the shoulder in patient with syringomyelia. Half of the humeral head has been resorbed. The remaining humeral head is fractured from the remaining shaft. The acromion has been pathologically fractured from the scapula (*arrows*). Ossific debris is present within the joint. *(From Brower AC, Allman RM: The pathogenesis of the neurotrophic joint: Neurotraumatic vs. neurovascular,* Radiology *139:349, 1981; reprinted by permission.)*

The Hip

In the non–weight-bearing hip (e.g., in a patient with paraplegia), there are varying degrees of extensive resorption of the femoral head with a surgical sharp edge to the remaining bone (Fig. 14-13). Osseous debris is seen in the joint space. The hip may sublux laterally and superiorly to the acetabulum. After considerable time has passed, as long as the patient continues not to bear weight on the hip, a cortical border forms at the surgical edge of the resorbed bone. The acetabulum remodels to accommodate the subluxed hip (Fig. 14-14). The osseous debris becomes well-corticated bone fragments. However, the massive subchondral sclerosis and osteophytosis seen in a weight-bearing neuropathic hip do not occur.

FIGURE 14-13. AP view of an atrophic neuropathic hip. There has been complete resorption of the femoral head and most of the femoral neck. There has been some resorption and shallowing out of the acetabulum. There is a sharp edge to the remaining femur. The femur is subluxed laterally and superiorly to the acetabulum. *(From Brower AC, Allman RM: Neuropathic osteoarthropathy in the adult. In Traveras JM, Ferruci JT, editors:* Radiology: Diagnosis/imaging/intervention, *vol 5, Philadelphia, J.B. Lippincott, 1986; reprinted by permission.)*

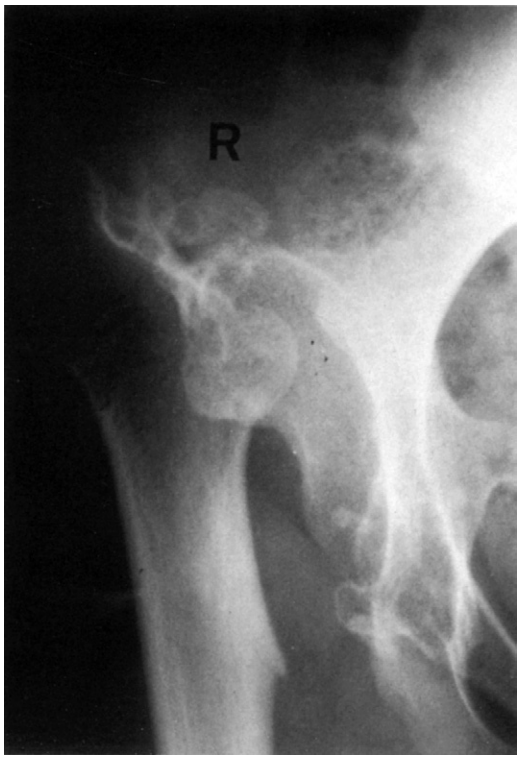

FIGURE 14-14. AP view of the same hip shown in Figure 14-14 3 years later. The femoral head and neck are absent. The remaining femoral shaft and adjacent acetabulum are well corticated. Bone fragments within the joint have become well corticated. There is absence of massive subchondral sclerosis and osteophytosis. *(From Bower AC, Allman RM: Neuropathic osteoarthropathy in the adult. In Traveras JM, Ferruci JT, editors:* Radiology: Diagnosis/imaging/intervention, *vol 5, Philadelphia, J.B. Lippincott, 1986; reprinted by permission.)*

COMBINED HYPERTROPHY AND ATROPHY

While the hypertrophic and atrophic joints represent the extremes of neuropathic osteoarthropathy, there are a large number of neuropathic joints that present with a combination of both bone resorption and bone production (Fig. 14-15). A segment of bone may be totally absent, while the remaining bone shows eburnation, fragmentation, and osteophytosis. Therefore in the ankle and foot of a patient with diabetes, one should be careful with interpreting this combination of resorption and production as infection. It must be recognized that the neuropathic joint goes through a spectrum of changes that are directly related to the amount of weight the joint bears. In the foot of a patient with diabetes, no imaging modality available can separate the acutely resorbing phase from infection.

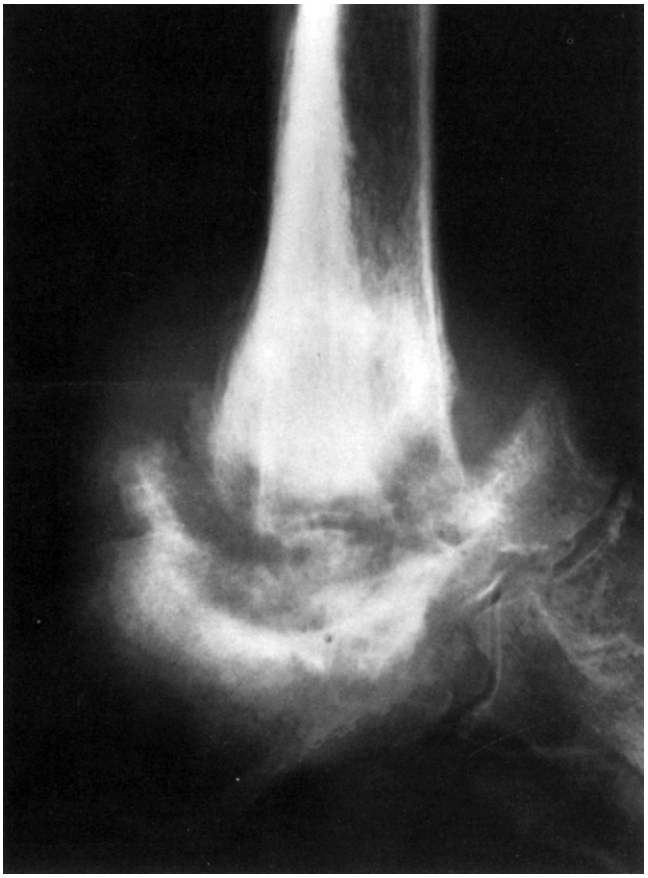

FIGURE 14-15. Lateral view of a neuropathic ankle. There is complete dissolution of the tibiotalar joint. Most of the talus has been resorbed, as has a portion of the calcaneus. The remaining calcaneus and the anterior portion of the talus show massive subchondral sclerosis and osteophytosis. There is also massive subchondral sclerosis present in the distal tibia, with some osteophytosis. This ankle represents the combination of bone resorption and production. *(From Brower AC, Allman RM: The pathogenesis of the neurotrophic joint: Neurotraumatic vs. neurovascular,* Radiology *139:349; 1981; reprinted by permission.)*

SUMMARY

Neuropathic osteoarthropathy is a dramatic arthropathy that is both easily diagnosed and easily misdiagnosed. It presents the spectrum of bone changes from extensive resorption to excessive production.

SUGGESTED READINGS

Brower AC, Allman RM: The neuropathic joint: A neurovascular bone disorder, *Radiol Clin North Am* 19:571–580, 1981.

Delano PJ: The pathogenesis of Charcots joint, *Am J Roentgenol Radium Ther Nucl Med* 56:189–200, 1946.

Feldman F: Neuropathic osteoarthropathy. In Margulis AR, Gooding CA, editors: *Diagnostic radiology*, San Francisco, 1977, University of California Press, p. 397.

Johnson JTH: Neuropathic fractures and joint injuries: Pathogenesis and rationale of prevention and treatment, *J Bone Joint Surg Am* 49:1–30, 1967.

Johnson LC: Circulation and bone (Charcot's disease and trophic change). In Frost HM, editor: *Bone biodynamics*, Boston, 1964, Little, Brown and Company, p. 603.

Katz I, Rabinowitz JG, Dziadiw R: Early changes in Charcot's joints, *Am J Roentgenol Radium Ther Nucl Med* 86:965–974, 1961.

Norman A, Robbins H, Milgram JE: The acute neuropathic arthropathy—a rapid, severely disorganizing form of arthritis, *Radiology* 90:1159–1164, 1968.

Yuh WT, Corson JD, Baraniewski HM, et al: Osteomyelitis of the foot in diabetic patients: Evaluation with plain film, Tc-99m MDP bone scintigraphy, and MR imaging, *Am J Roentgenol* 152:795–800, 1989.

Diffuse Idiopathic Skeletal Hyperostosis

15

Diffuse idiopathic skeletal hyperostosis (DISH), also known as ankylosing hyperostosis or Forestier disease, is not an arthropathy. The articular cartilage, adjacent bone margins, and synovium are not affected. DISH appears to be a bone-forming diathesis in which ossification occurs at skeletal sites subjected to stress, primarily at tendinous and ligamentous attachments. It is a common disorder, occurring in 12 percent of the elderly population. Its radiographic manifestations have been mistaken for ankylosing spondylitis, other spondyloarthropathies, and osteoarthritis. Although it may coexist with an arthropathy, it should not be mistaken for a manifestation of that arthropathy. Knowledge of the radiographic criteria allows the correct diagnosis to be made. The radiographic findings are the following:

1. Normal mineralization
2. Flowing ossification of at least four contiguous vertebral bodies
3. Preservation of disc spaces
4. Ossification of multiple tendinous and ligamentous sites in the appendicular skeleton
5. Absence of joint abnormality
6. Sporadic distribution
7. Distribution primarily in the spine

The radiographic manifestations of DISH divide into those associated with the spine and those that are extraspinal. Extraspinal changes without spinal involvement are possible but extremely unusual.

SPINAL MANIFESTATIONS

Ossification of the ligaments and soft tissues that surround the vertebral bodies occurs in DISH. This must be observed around four or more contiguous vertebral bodies in order to make the diagnosis of DISH. The thickness of the ossification can range from 1 to 20 mm. Bone excrescences of various shapes may be observed. The ossification may be so extensive as to render the spine as immobile as one with ankylosing spondylitis. Such a spine can fracture and develop a pseudoarthrosis similar to that which can occur in ankylosing spondylitis. Fracture may occur with relatively minor trauma, and these injuries can be easily overlooked (Fig. 15-1).

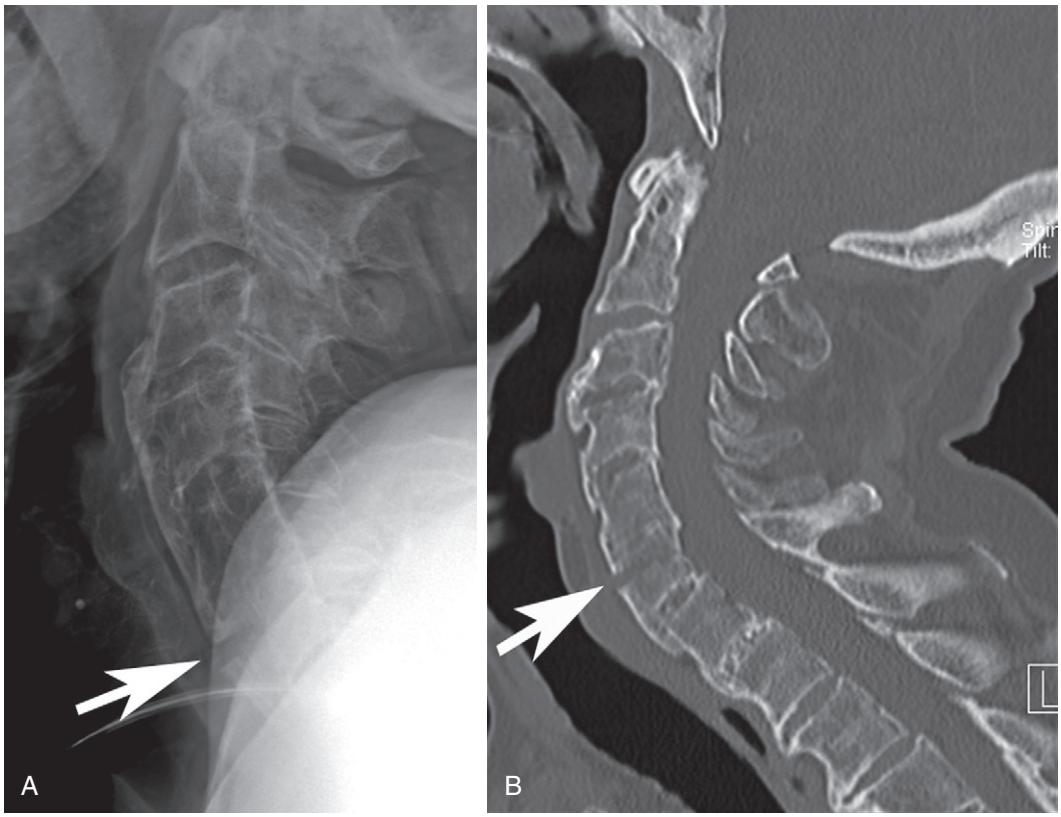

FIGURE 15-1. A, Lateral view of the cervical spine in trauma patient with DISH. Flowing anterior ossification is interrupted at the superior aspect of C6 (*arrow*). **B,** Sagittal computed tomography (CT) scan confirms a fracture extending through the superior end-plate of C6 (*arrow*).

The Thoracic Spine

The thoracic spine is the most common site of involvement. Flowing ossification is observed here in 97 to 100 percent of patients with DISH. It is usually seen anteriorly and on the right side in the lower thoracic spine, from T7 to T11 (Fig. 15-2). The thickness of the ossification can range from 1 to 20 mm. It may be smooth or bumpy in contour, depending upon the configuration of the bone excrescences at the disc levels. The radiolucent disc may appear to protrude into the flowing ossification, creating an L-, T-, or Y-shaped defect at the disc level (Fig. 15-3).

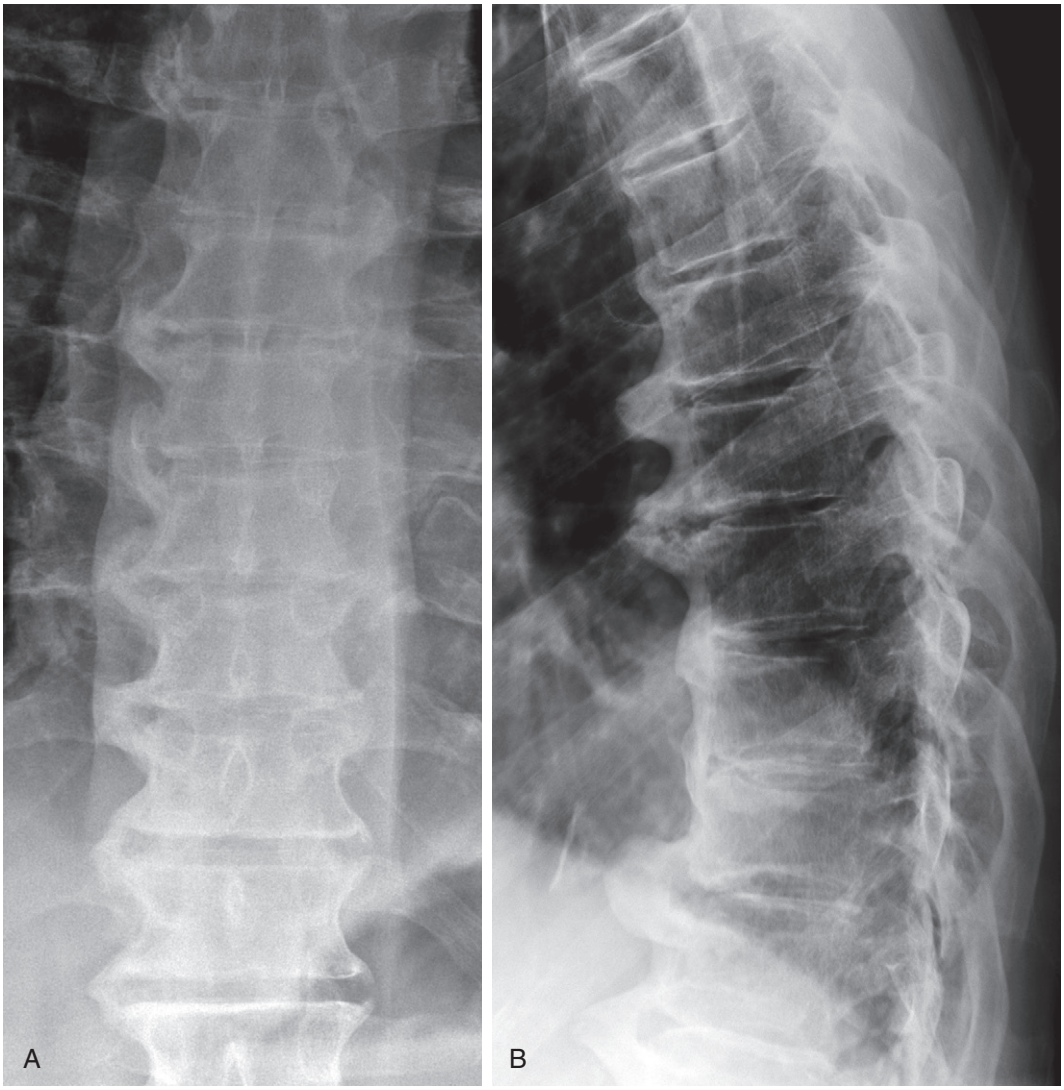

FIGURE 15-.2 Anteroposterior (**A**) and lateral (**B**) views of the thoracic spine in patient with DISH. Flowing ossification is noted anteriorly and on the right side of the spine. At least seven contiguous vertebral bodies are involved. The disc spaces are preserved. Radiolucency extends from the disc space into the ossification, creating a Y-shaped lucency and a bumpy bony excrescence at the disc level.

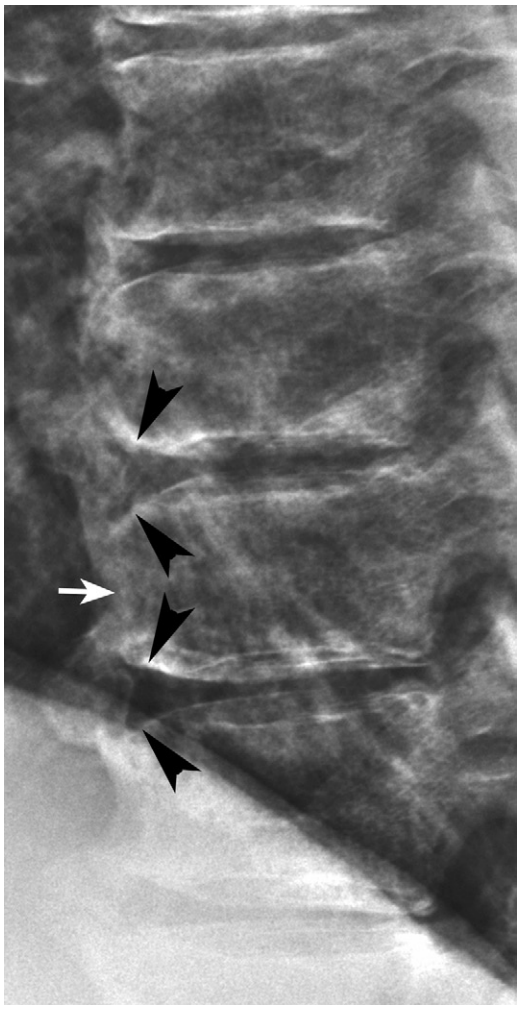

FIGURE 15-3. Lateral view of the lower thoracic spine in patient with DISH. Lucency separates the flowing ossification from the adjacent vertebral body (*arrow*). Lucent defects are seen in the bony excrescences at the disc level, creating a Y-shaped defect (*arrowheads*).

If the flowing ossification is thin and smooth, it may be mistaken for the ossification seen in ankylosing spondylitis (Fig. 15-4). Usually at some point a lucent line separates the flowing ossification from the adjacent vertebral body and thus distinguishes DISH from ankylosing spondylitis (Fig. 15-5).

FIGURE 15-4. Lateral view of the lower thoracic spine in patient with DISH. The flowing ossification is thin and smooth, resembling that of ankylosing spondylitis.

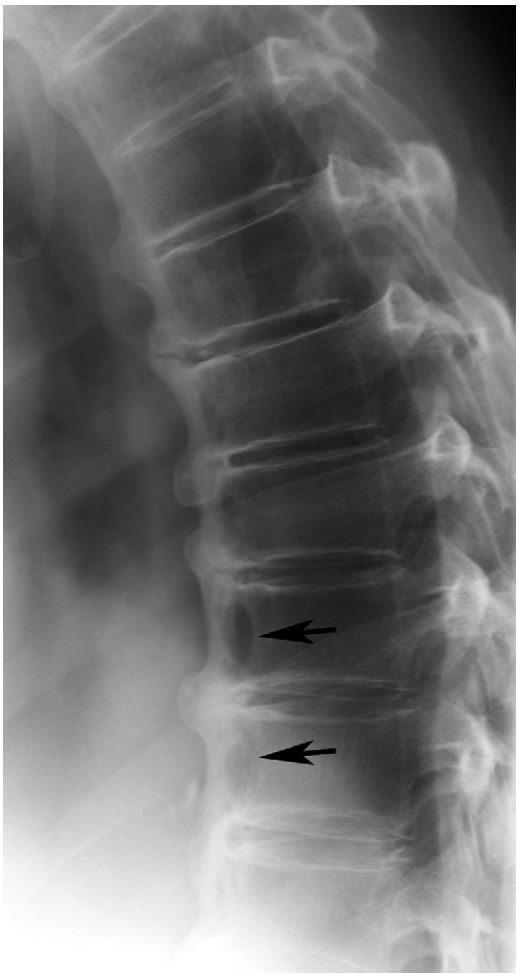

FIGURE 15-5. Lateral view of thoracic spine in patient with DISH. A lucent line separates the flowing ossification from the adjacent vertebral body (*arrow*), establishing the diagnosis of DISH rather than ankylosing spondylitis.

The Cervical Spine

The cervical spine is involved in 78 percent of patients with DISH. The abnormalities seen are most common in the lower cervical region. The flowing ossification anteriorly can vary from 1 to 12 mm in thickness. It may be very smooth in contour and appear to be an extension of the anterior border of the vertebral body (Fig. 15-6), or it may be very bumpy, with the bumps occurring at the disc levels (Fig. 15-7). The ossification may impinge upon the esophagus, causing dysphagia (Fig. 15-8). The disc heights are preserved, and the apophyseal joints are uninvolved. In some patients the posterior longitudinal ligament may be ossified, creating spinal stenosis.

FIGURE 15-6. Lateral view of the cervical spine in patient with DISH. There is thick but smooth ossification anterior to the vertebral bodies. The disc spaces are preserved, and the apophyseal joints are uninvolved.

FIGURE 15-7. Lateral view of the cervical spine in patient with DISH. There is thick, bumpy ossification anterior to the vertebral bodies. The disc spaces are maintained, and the apophyseal joints are uninvolved.

FIGURE 15-8. Lateral view of the cervical spine in patient with DISH. There is excessive flowing ossification anterior to the vertebral bodies. Barium introduced into the esophagus allows demonstration of impingement on the esophagus by the ossification (*arrow*). The disc spaces are maintained, and the apophyseal joints are uninvolved.

The Lumbar Spine

The lumbar spine is involved in 93 percent of patients with DISH. The ossification may be more profound than that seen in the thoracic or cervical spine (Fig. 15-9). Some patients show flowing ossification similar to that seen in the thoracic spine (Fig. 15-10). Others show huge bony protuberances or excrescences primarily at the disc levels, resembling excessive osteophytosis (Fig. 15-11). However, the disc space is usually maintained, and the apophyseal joints are uninvolved. Although DISH usually protects the patient from degenerative disc disease, it is possible for a patient to have both. Nevertheless, the two disorders should be recognized as separate entities so that the cause of clinical symptoms can be correctly addressed.

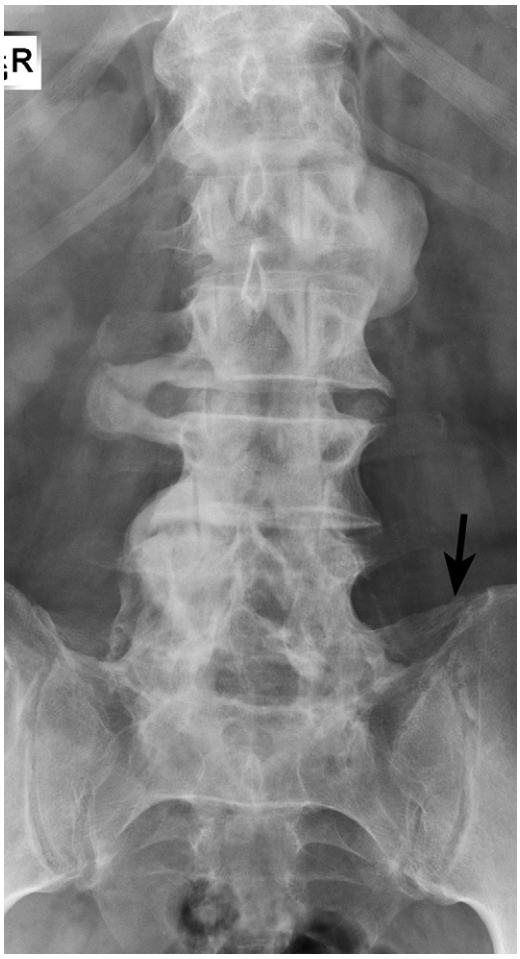

FIGURE 15-9. Anteroposterior (AP) view of the lumbosacral spine in patient with DISH. There is excessive flowing ossification bilaterally. The discs are preserved, and the sacroiliac (SI) joints are normal. There is ossification of the L5 iliolumbar ligament (*arrow*).

FIGURE 15-10. Lateral view of the lumbar spine in patient with DISH. There is flowing smooth ossification anterior to the vertebral bodies. The disc spaces are preserved, and the apophyseal joints are not involved.

FIGURE 15-11. Lateral view of the lumbar spine in patient with DISH. There is excessive bone formation anterior to the vertebral bodies, with huge bony excrescences at the disc levels. The discs are maintained.

EXTRASPINAL MANIFESTATIONS

The extraspinal radiographic manifestation of DISH is ossification of tendons and ligaments, predominantly at sites of attachment. Although such ossification occurs in the "normal" population, the number of sites is usually limited. In DISH, this ossification occurs at multiple sites. This ossification may be misinterpreted as osteophytosis in osteoarthritis. However, in DISH there is no radiographic change in the joint itself.

The Pelvis

One hundred percent of patients with extraspinal DISH have pelvic involvement. There is "whiskering" of the iliac crests, the ischial tuberosities, and the femoral trochanters (Fig. 15-12) similar to that seen in the spondyloarthropathies. Lack of involvement of the true synovial part of the sacroiliac (SI) joint distinguishes DISH from the spondyloarthropathies. Although DISH does not affect the synovial aspect of the SI joint, it may affect the rest of the joint (Fig. 15-13). The posterosuperior segment of the SI joint is not a joint, but a ligamentous bridge between the two bones. In DISH this area may ossify.

There may also be ossification across the superior aspect of the pubic symphysis (Fig. 15-14). Although the hip joint itself is preserved, bone excrescences may form at the acetabular margins (Fig. 15-15).

FIGURE 15-12. AP view of the pelvis in patient with DISH. There is ossification of the greater trochanters, ischial tuberosities, the lateral acetabular margin, and the iliac crests. The hip joint is preserved.

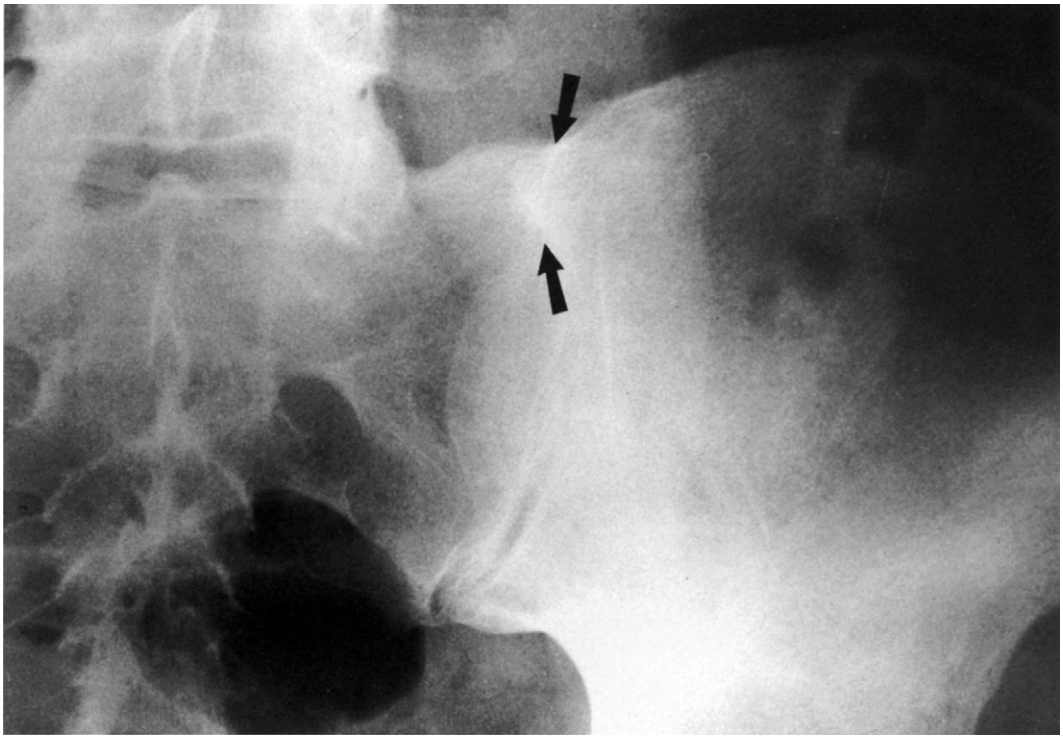

FIGURE 15-13. AP view of SI joint in patient with DISH. The true synovial joint is unaffected. The upper posterior ligamentous joint is ossified (*arrows*).

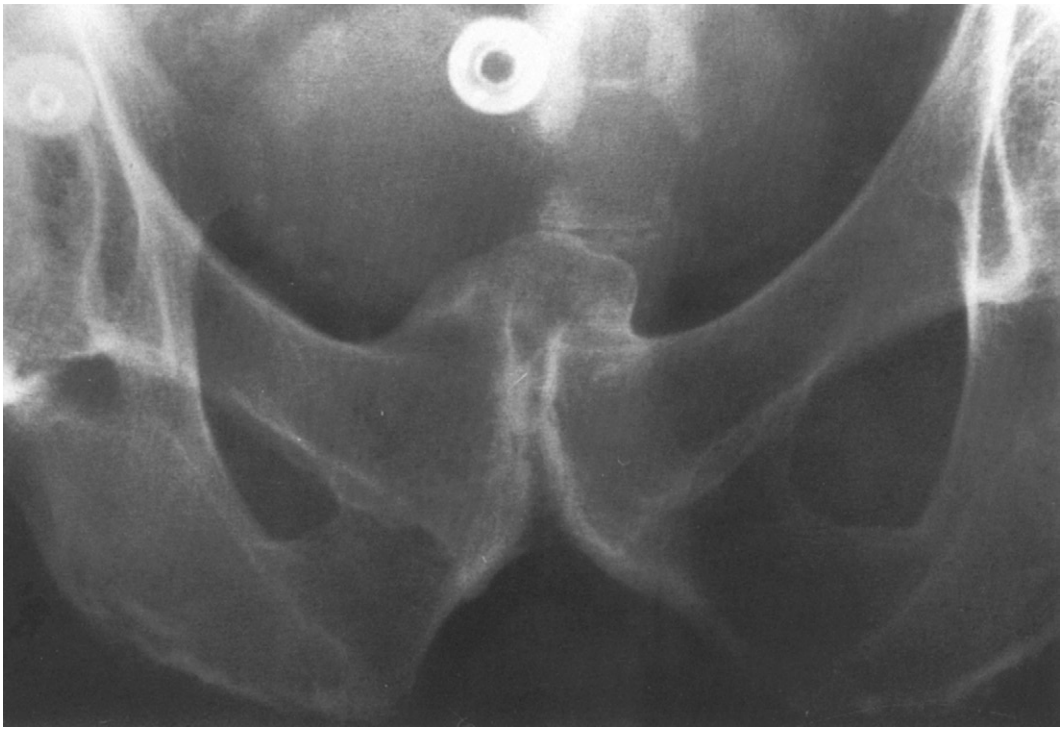

FIGURE 15-14. Pubic symphysis in patient with DISH. There is ossification bridging the pubic rami superiorly.

FIGURE 15-15. AP view of a hip in patient with DISH. Notice ossification around acetabulum, greater trochanter, and iliac tendon attachments. There are no changes that are indicative of an arthropathy of the hip.

The Foot

Ossification is seen on the calcaneus in 75 percent of patients with extraspinal DISH. This ossification occurs at the Achilles tendon and the plantar aponeurosis (Fig. 15-16). The ossification may become quite extensive; it may then fracture, resulting in disruption of the tendon. The common locations for ossification in the rest of the foot are the dorsal aspect of the talus, the dorsal and medial aspects of the tarsal navicular, the lateral and plantar aspects of the cuboid, and the lateral aspect of the base of the fifth metatarsal (Fig. 15-17).

FIGURE 15-16. Lateral view of the foot in patient with DISH. All joint spaces are preserved. Ossification is seen at the attachment of the plantar aponeurosis and the Achilles tendon. There is also ossification on the dorsal aspect of the navicular and the cuneiform, the base of the fifth metatarsal, and the distal tibia (*arrows*).

FIGURE 15-17. AP view of the foot shows ossification at the base of the fifth metatarsal and medial to the navicular and the cuneiform and lateral to the calcaneus (*arrows*).

The Knee

Ossification around the knee occurs in 29 percent of patients with extraspinal DISH. It is most commonly seen in the inferior and superior patellar tendon (Fig. 15-18). The anterior portion of the patella itself may have irregular new bone apposition. There may be ossification of the tibial tubercle in a fashion suggestive of Osgood-Schlatter disease. The medial collateral ligament ossifies, similar to Pellegrini-Stieda syndrome.

FIGURE 15-18. Lateral view of the knee in patient with DISH. Ossification of the superior and inferior patellar tendon as well as the tibial tubercle is seen.

The Elbow

Ossification around the elbow occurs in 49 percent of patients with extraspinal DISH. Spurring of the olecranon is the most common ossification. Around the elbow, ossification may become so extensive as to be misdiagnosed as osteoarthritis (Fig. 15-19). Absence of true joint changes should prevent the clinician from making a diagnosis of osteoarthritis. The correct diagnosis is important in the treatment of the patient, who may have limited range of motion in the elbow secondary to this ossification.

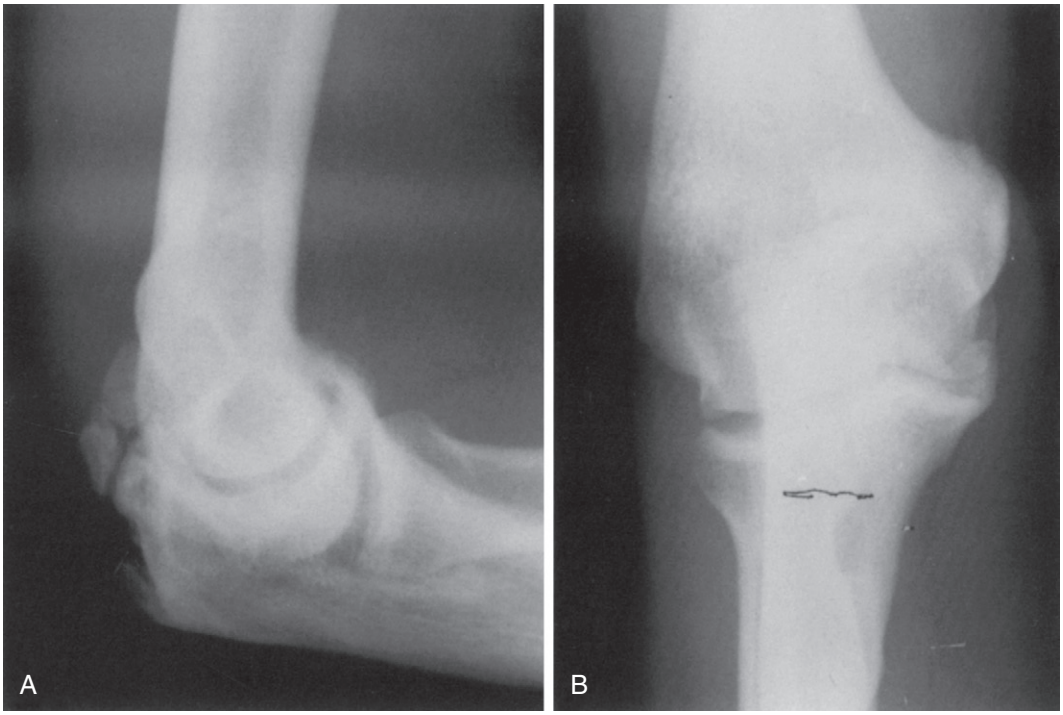

FIGURE 15-19. **A**, Lateral view of the elbow in patient with DISH. The bony excrescences seen around the elbow resemble the osteophytes of osteoarthritis. **B,** AP view of the same elbow shows that the joint is preserved. There is no subchondral sclerosis or cyst formation. The bony excrescences are ossified tendinous attachments. *(**A** from Brower AC: The significance of the various phytes of the spine,* Radiolog *1(15):3, 1978; reprinted by permission.)*

Other Sites

Ossification may occur in any ligamentous attachment. Other common sites are the deltoid protuberance on the humerus, the coracoclavicular ligament, the posterosuperior aspect of the femur, and the shafts of the phalanges (Fig. 15-20).

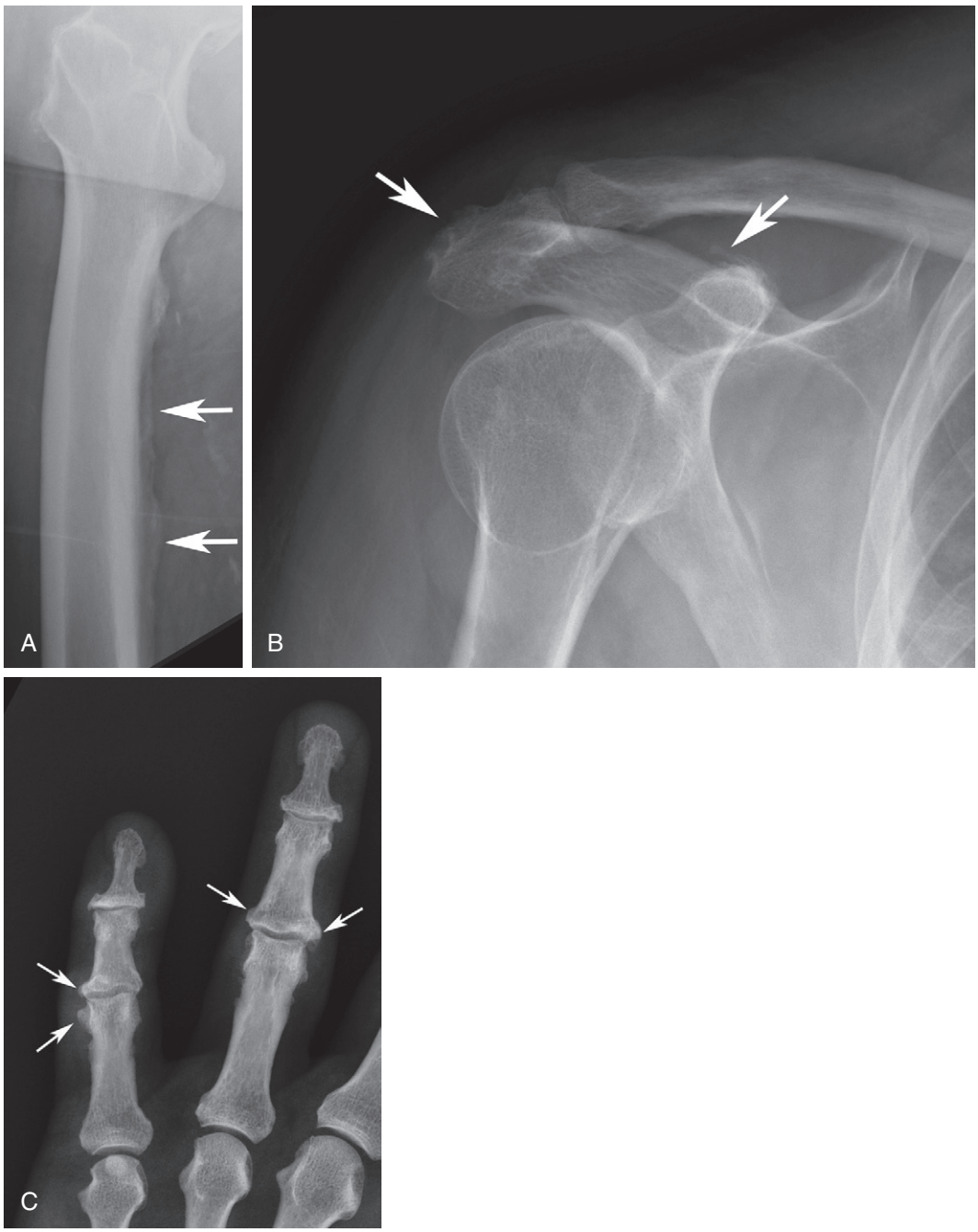

FIGURE 15-20. **A,** Lateral view of the femur in patient with DISH. There is ossification of ligamentous attachments posteriorly and superiorly along the femur (*arrows*). **B,** AP view of the shoulder in patient with DISH. There is ossification of the coracoclavicular ligament and the deltoid attachment (*arrows*). The joint itself is preserved. **C,** The fourth and fifth digit in a patient with DISH. There is ossification of ligamentous attachments (*arrows*).

SUMMARY

DISH is not an arthropathy but a bone-forming diathesis. It will not be misdiagnosed as an arthropathy if two observations are made: (1) the ossification present is in ligamentous and tendinous sites, and (2) the disc space or the joint space is preserved.

SUGGESTED READINGS

Burkus JK, Denis F: Hyperextension injuries of the thoracic spine in diffuse idiopathic skeletal hyperostosis: Report of four cases, *J Bone Joint Surg* 76A:237, 1994.

Forestier J, Lagier R: Ankylosing hyperostosis of the spine, *Clin Orthop Relat Res* 74:65, 1971.

Forestier J, Rotés-Querol J: Senile ankylosing hyperostosis of the spine, *Ann Rheum Dis* 9:321, 1950.

Mata S, Hill RO, Joseph L, et al: Chest radiographs as a screening test for diffuse idiopathic skeletal hyperostosis, *J Rheumatol* 20:1905, 1993.

Resnick D, Guerra J, Robinson C, et al: Association of diffuse idiopathic skeletal hyperostosis (DISH) and calcification and ossification of the posterior longitudinal ligament, *AJR Am J Roentgenol* 131:1049, 1978.

Resnick D, Niwayama G: Radiographic and pathologic features of spinal involvement in diffuse idiopathic skeletal hyperostosis (DISH), *Radiology* 119:559, 1976.

Resnick D, Shapiro R, Wiesner K, et al: Diffuse idiopathic skeletal hyperostosis (DISH) (ankylosing hyperostosis of Forestier and Rotés-Querol), *Semin Arthritis Rheum* 7:153, 1978.

Resnick D, Shaul SR, Robins JM: Diffuse idiopathic skeletal hyperostosis (DISH): Forestier's disease with extraspinal manifestations, *Radiology* 115:513, 1975.

Sutro CJ, Ehrlich DE, Witten M: Generalized juxta-articular ossification of ligaments of the vertebral column and of the ligamentous and tendinous tissues of the extremities (also known as Bechterew's disease, osteophytosis and spondylosis deformans), *Bull Hosp Joint Dis* 17:343, 1956.

Gout 16

Gout is the oldest recognized arthropathy. It was originally called podagra, from the Greek *pous*, meaning foot, and *agra*, meaning attack. In ancient history all arthritis was called gout. Today we know it to be a specific arthropathy secondary to deposition of monosodium urate crystals. It occurs in 0.3 percent of the population, and it accounts for 5 percent of all patients with arthritis. It is predominantly a disorder of males, occurring 20 times more frequently in males than in females. When it occurs in females, it is in the postmenopausal female.

There are two types of gout: (1) primary idiopathic gout due to an inborn error of metabolism, leading to the increase in uric acid in the blood; and (2) secondary gout associated with various diseases that cause increased production or decreased excretion of uric acid. Secondary gout does not usually produce radiographic changes.

Only 45 percent of patients with gout manifest radiographic bone changes, and then only 6 to 8 years after the initial attack. The radiographic changes indicate the chronicity of the disease process. Urate crystals deposit in tissues with poor blood supply, including cartilage, tendon sheaths, bursa, and so on. The radiographic presentation is dependent upon where the urate crystals are deposited. If they are deposited in cartilage, then the radiographic picture will be that of osteoarthritis; if they are deposited in soft tissue, then it will be that of chronic tophaceous gout. The hallmarks of osteoarthritis are discussed elsewhere. The radiographic features of chronic tophaceous gout are as follows:

1. Tophi
2. Normal mineralization
3. Joint space preservation
4. Punched-out erosions with sclerotic borders
5. Overhanging edge of cortex
6. Asymmetrical polyarticular distribution
7. Distribution in feet, ankles, knees, hands, and elbows, in decreasing order of frequency

Because the radiographic features of chronic tophaceous gout are pathognomonic of the disease no matter what joint is involved, the features are discussed in greater detail before describing the distribution. It must be remembered that osteoarthritis developing secondary to urate crystal deposition in cartilage cannot be distinguished from osteoarthritis secondary to any other etiology. One must rely on the radiographic findings of tophaceous deposit.

Tophi are soft tissue masses created by the deposition of urate crystals (Fig. 16-1). Urate crystals are not radiographically opaque. However, calcium may precipitate with the urate crystals to varying degrees, creating variation in the density of tophi (Fig. 16-2). Tophi are usually found in the periarticular area along the extensor surface of bone; however, they may be intraarticular or not associated with the joint at all.

FIGURE 16-1. Gout involving the fourth digit. The soft tissue mass surrounding the proximal interphalangeal (PIP) joint represents a tophus. Despite extensive involvement of the bone with erosion of the middle phalanx and bone spiculation (*arrows*) of the adjacent proximal phalanx, the PIP joint is only minimally narrowed. Mineralization is maintained.

FIGURE 16-2. Anteroposterior (AP) view of the hand in severe tophaceous gout. Calcium has precipitated with the urate crystals, giving density to the tophi. *(Courtesy of R.B. Harrison, University of Mississippi Medical Center, Jackson.)*

Tophi over an extended period of time erode the underlying bone. Because of the indolence of the process, the erosion produced usually has a sclerotic border. The erosion looks "punched out" and has frequently been described as a "mouse bite" (Fig. 16-3). Often as the erosion is developing, the proximal edge of cortex is remodeled in an outward direction, creating an overhanging edge (Fig. 16-4). This is seen in connection with 40 percent of the erosions identified. If the tophus is intraarticular and involves adjacent bones, then its extensor location and the indolence of the erosion allow preservation of the flexor portion of the joint space. Therefore on a radiograph, even when part of the joint is involved, the joint space appears to be preserved (Fig. 16-5).

FIGURE 16-3. Erosive changes of gout in the first metatarsophalangeal (MTP) joint. All erosions have sclerotic borders. One resembles a "mouse bite" (*arrow*).

FIGURE 16-4. Tophaceous gout involving the fifth metacarpophalangeal (MCP) joint. A soft tissue tophus is present laterally. Bone mineralization and joint space are maintained. The erosions have sclerotic borders. An overhanging edge of cortex is present (*arrow*).

FIGURE 16-5. AP view of the foot of patient with chronic tophaceous gout. Tophi involve the first, second, and third MTP joints and the first interphalangeal (IP) joint. Mineralization is maintained. Despite extensive erosion, the remaining joint space is preserved at each of the MTP joints. At the third MTP joint only a ghost outline of the joint space is observed (*arrows*), showing preservation of the plantar aspect of the joint, which has not been eroded by the dorsal tophus.

Urate crystals may deposit within the bone, producing an intraosseous tophus; the bone involved shows a lytic lesion, which may be expansile, with or without calcification (Fig. 16-6). The calcified tophus within the bone should not be mistaken for an infarct or enchondroma. Gout does not cause infarction; it replaces marrow.

FIGURE 16-6. **A,** AP view of toes of patient with tophaceous gout. The expansile lytic lesions involving the fifth proximal, middle, and distal phalanx represent intraosseous tophi. **B,** AP view of the great toe. The density within the first metatarsal head and phalanges is calcification within intraosseous tophaceous material. It should not be mistaken for an infarct.

Intraosseous deposit may also cause such destruction as to be misdiagnosed as infection. Usually preservation of the white cortical line of the involved joint surface will distinguish gout from infection (Fig. 16-7). Once the bone changes have occurred, they cannot be reversed; however, the urate crystals can disappear with treatment. Therefore, it is possible to see the bone changes of chronic tophaceous gout without the presence of the actual tophi (Fig. 16-8).

FIGURE 16-7. Posteroanterior (PA) view of the fourth finger with destruction of the distal interphalangeal (DIP) joint secondary to tophaceous gout. The preservation of the white cortical line of the articular surface of the distal proximal phalanx (*arrow*) goes against the diagnosis of infection.

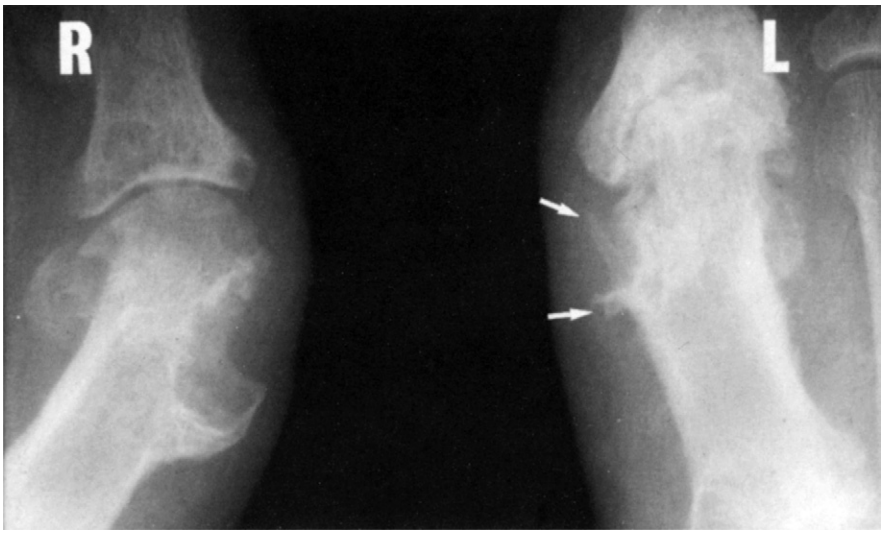

FIGURE 16-8. First MTP joints in treated gout. The large erosion with sclerotic border and overhanging edge of cortex involving the right metatarsal head was produced by a tophus that is no longer present. Urate crystals, no longer present, deposited in the soft tissues and the cartilage of the left MTP joint produced the joint space loss, the erosive changes, and the bone spiculation (*arrows*).

Normal mineralization is maintained. It is unusual to see even transient juxta-articular osteoporosis. Actually, bone production is a manifestation of the chronicity of the disease process. Bone production is seen as part of the osteoarthritic picture. It is also seen as the sclerotic border to the erosion and the overhanging edge of cortex. One may identify irregular bone spicules at sites of tendinous and ligamentous attachment (Fig. 16-9). Enlargement of ends of bones may also occur (Fig. 16-10).

FIGURE 16-9. AP view of both metatarsal joints in longstanding gout. Bone spicules are present (*arrow*). Despite the erosions, the metatarsal heads appear enlarged.

FIGURE 16-10. AP view of the great toe in patient with gout. Notice the enlargement of the bones around the MTP joint. Erosions with sclerotic borders are seen elsewhere (*arrows*).

The peripheral appendicular skeleton is the common site of involvement, with the foot being the classic location. It is extremely unusual to see the hip, shoulder, or spine involved with gout (Fig. 16-11).

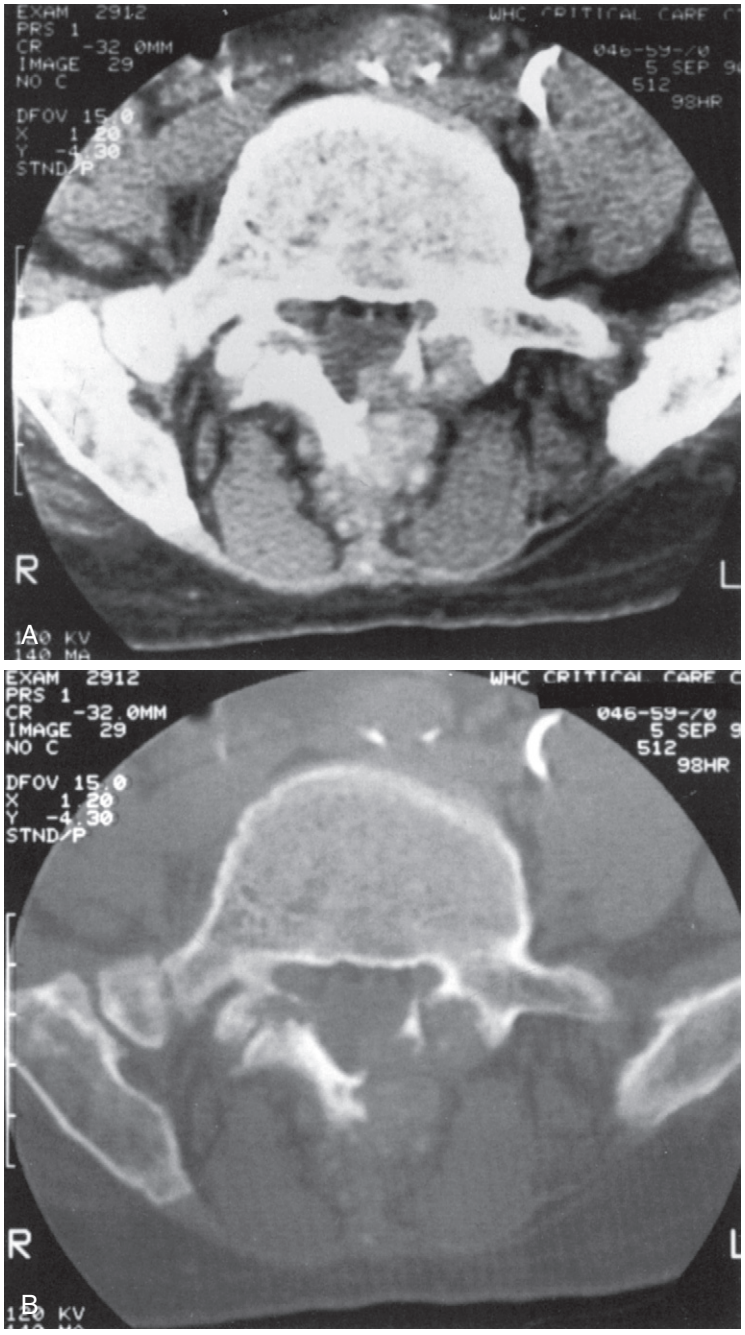

FIGURE 16-11. **A,** Axial CT image of the fifth lumbar vertebral body and posterior element. A large calcified tophus has eroded the lamina and posterior spinous process on the left. **B,** Same axial computed tomography (CT) image with bone windows. The eroded bone has sclerotic borders.

THE FOOT

Sixty-five percent of patients with gout experience their first attack in the first metatarsophalangeal (MTP) joint (Figs. 16-3, 16-8 to 16-10, and 16-12). Eventually, 90 percent of patients with gout have involvement of this particular joint. Sometimes it is difficult to distinguish gout from osteoarthritis in the MTP joint. Both may present with a hallux valgus deformity and productive bone changes. However, the tophus is usually present on the dorsal aspect of the joint and causes erosive changes on the dorsal surface of the first metatarsal head and to a lesser extent the adjacent proximal phalanx. In particular, the lateral view of the first MTP joint shows this tophus and erosion and distinguishes the process from the osteophytic and cystic changes of osteoarthritis (Fig. 16-13). The erosion may present medially on the first metatarsal head, and the tophus may be mistaken for a bunion (Fig. 16-14). Certainly presence of the overhanging edge of cortex distinguishes this from the cystic change of osteoarthritis. After the first MTP joint, the first interphalangeal (IP) joint and the fifth MTP joint are favored areas of involvement; however, any of the MTP joints may be involved (Fig. 16-5).

FIGURE 16-12. Oblique view of the first MTP joint in patient with gout. There is a large medial tophus. Erosions with sclerotic borders are present. There is bone formation with an overhanging edge (*arrow*). The joint space is minimally narrowed.

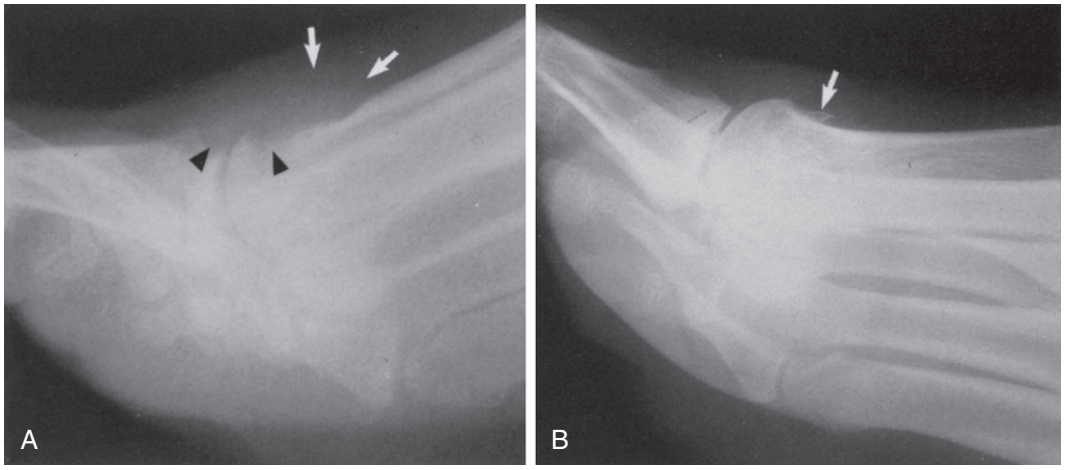

FIGURE 16-13. Gout versus osteoarthritis. **A,** Lateral view of the first MTP joint in patient with gout. A tophus is present dorsal to the first MTP joint (*arrows*). Bone erosion is present dorsally (*arrowheads*). **B,** Lateral view of the first MTP joint in patient with osteoarthritis. There is neither an identifiable tophus nor an erosion. An osteophyte is present (*arrow*).

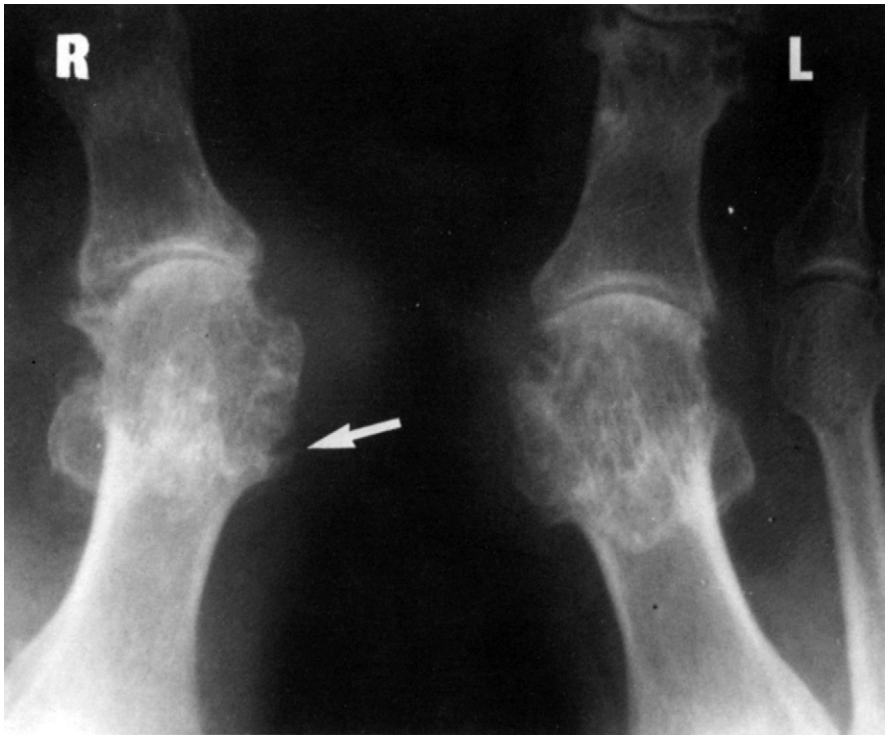

FIGURE 16-14. The first MTP joints in patient with gout. Although the osteophyte, subchondral sclerosis, and soft tissue mass at the right MTP joint might be interpreted as osteoarthritis with a bunion, the erosion with the overhanging edge of bone (*arrow*) indicates the correct diagnosis of gout. The changes in the left MTP joint are classic for gout.

The tarsal area is involved frequently, with swelling over the dorsum of the foot. Any of the tarsal joints may be involved (Fig. 16-15); however, there seems to be preference for the tarsometatarsal joints. Extensive destruction in this area by gout still produces punched-out erosions with sclerotic borders (Fig. 16-16).

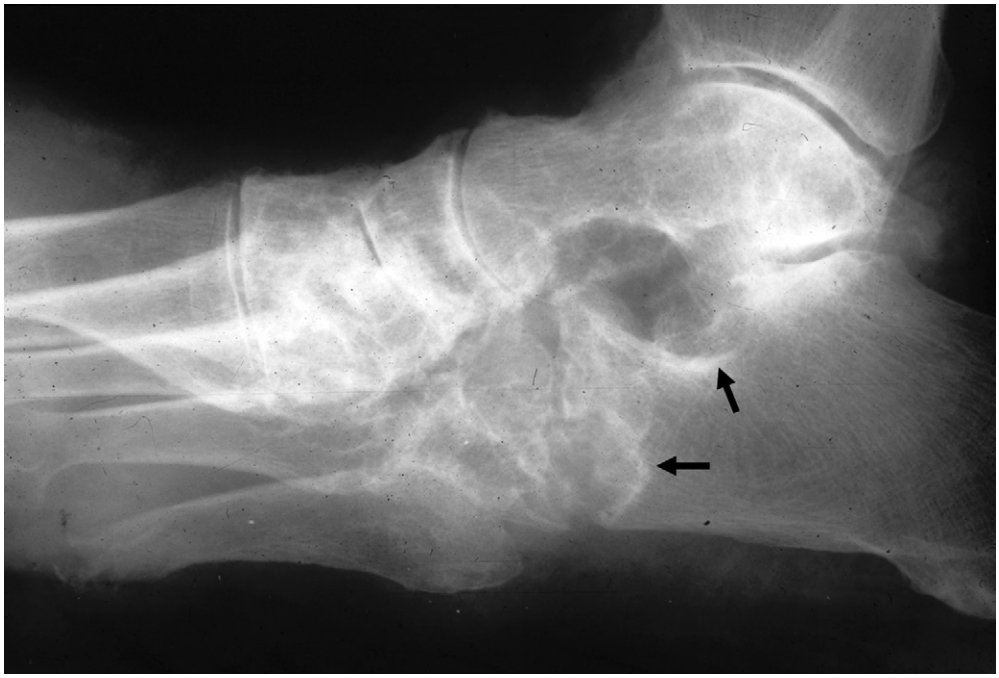

FIGURE 16-15. Lateral view of the foot in patient with gout. Large erosions with sclerotic borders are seen in the calcaneus as it articulates with the cuboid and the talus (*arrows*).

FIGURE 16-16. Midfoot in patient with gout. There are extensive erosive changes involving the tarsometatarsal joint spaces.

THE HAND

The hand, like the foot, is involved in a sporadic, asymmetrical fashion (Fig. 16-17). No one joint is preferred over another in the fingers. Mineralization is maintained. Tophi may or may not be identified. If erosive changes are present, then erosive areas have sclerotic borders and perhaps overhanging edges of cortex. The joint space may or may not be preserved. One may see a sporadic atypical distribution of osteoarthritic changes. There may be pancarpal involvement of the wrist (Fig. 16-18); however, frequently there is preferential involvement of the carpometacarpal joint space with erosive change (Fig. 16-19).

FIGURE 16-17. AP view of the hand of a patient with gout. Mineralization is normal. A tophus and associated erosion with a sclerotic border and overhanging edge of cortex are present at the fifth MCP joint. The second PIP joint shows enlargement of the bone ends with osteophytes and osteoarthritic bone spicules (*arrow*). The third DIP joint shows secondary osteoarthritic changes and an intraosseous tophus in the distal end of the middle phalanx. These changes represent the spectrum of gout.

FIGURE 16-18. AP view of the wrist shows a tophus adjacent to an eroded ulnar styloid. Erosions presenting as lucencies surrounded by sclerotic margins involve the carpal bones. Joint space is preserved despite extensive erosive changes.

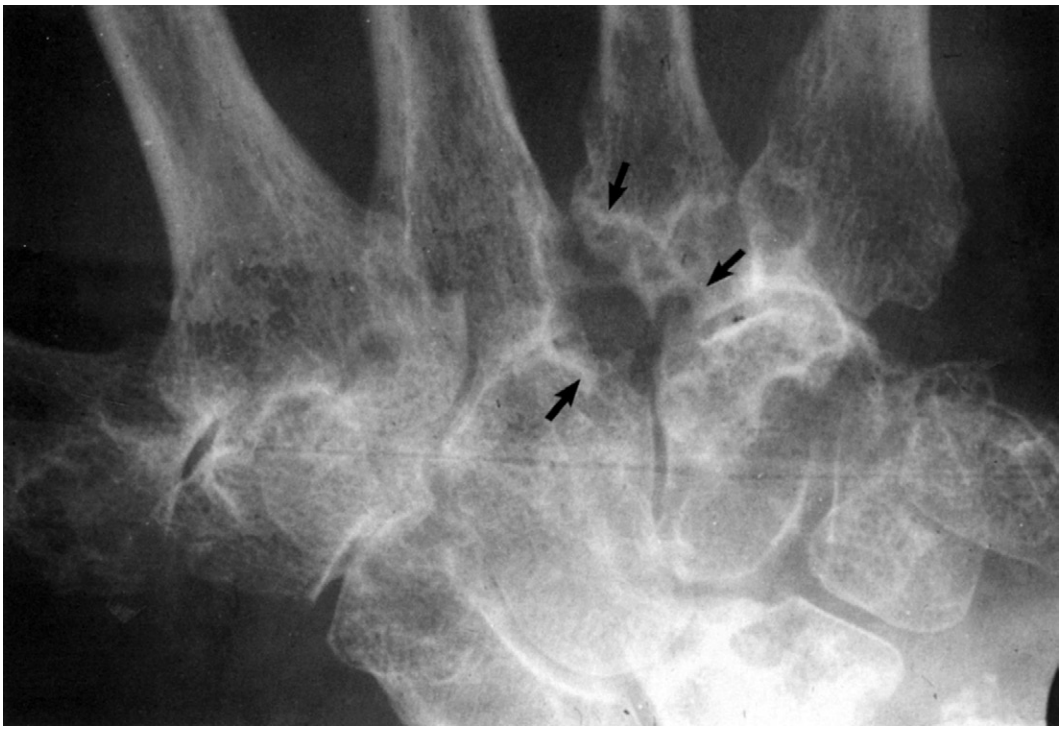

FIGURE 16-19. AP view of the wrist in patient with gout. There are punched-out erosions with sclerotic borders involving the bases of the third, fourth, and fifth metacarpals as they articulate with the capitate and hamate (*arrows*).

THE ELBOW

The elbow is involved in 30 percent of patients with gout. There is preferential olecranon bursal involvement with swelling over the extensor surface. Gout must always be considered in a patient with unilateral olecranon bursitis and is usually the diagnosis in a patient with bilateral olecranon bursitis (Fig. 16-20). The adjacent bone may or may not be involved. If it is involved, there may be either erosive (Fig. 16-21) or proliferative (Fig. 16-20) changes.

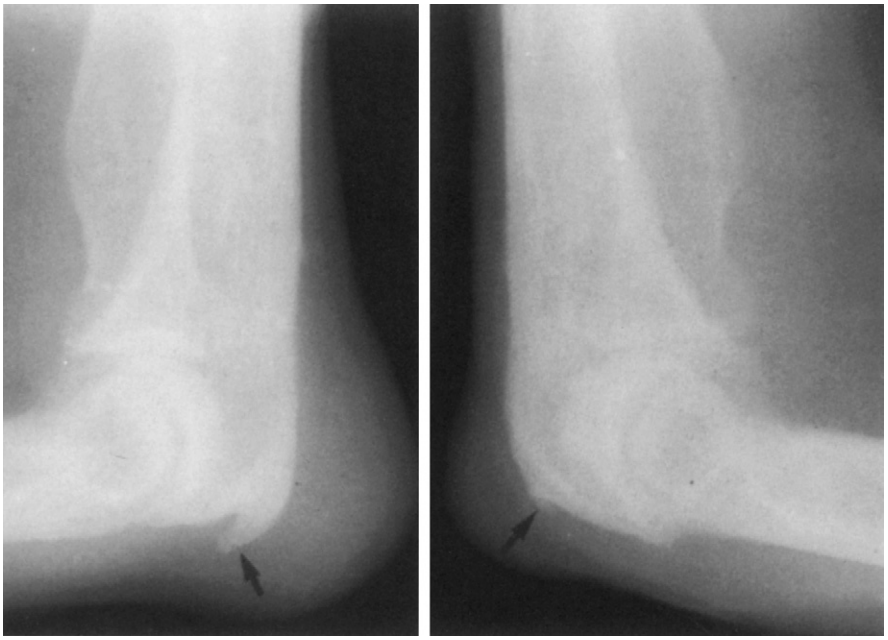

FIGURE 16-20. Lateral view of both elbows in a patient with gout. There is swelling of both olecranon bursae. There is also bone proliferation at both olecranons (*arrows*).

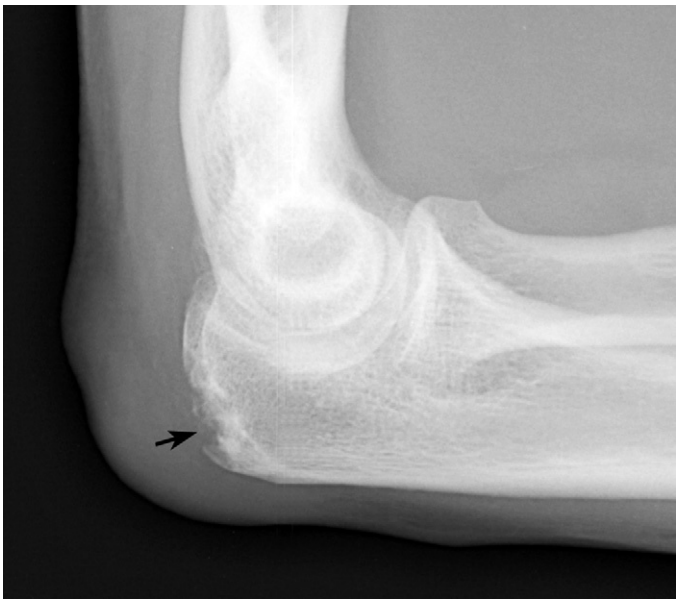

FIGURE 16-21. Lateral view of the elbow in gout. Bursitis is present. Erosion (*arrow*) is present in the olecranon.

OTHER APPENDICULAR SITES

The ankle and knee are frequently affected. The ankle tends to present the picture of tophaceous gout (Fig. 16-22), whereas the knee tends to present the picture of osteoarthritis (Fig 16-23). Tophus formation is frequently seen in the patella and patellar tendon (Fig. 16-24). The hip and shoulder are rarely involved.

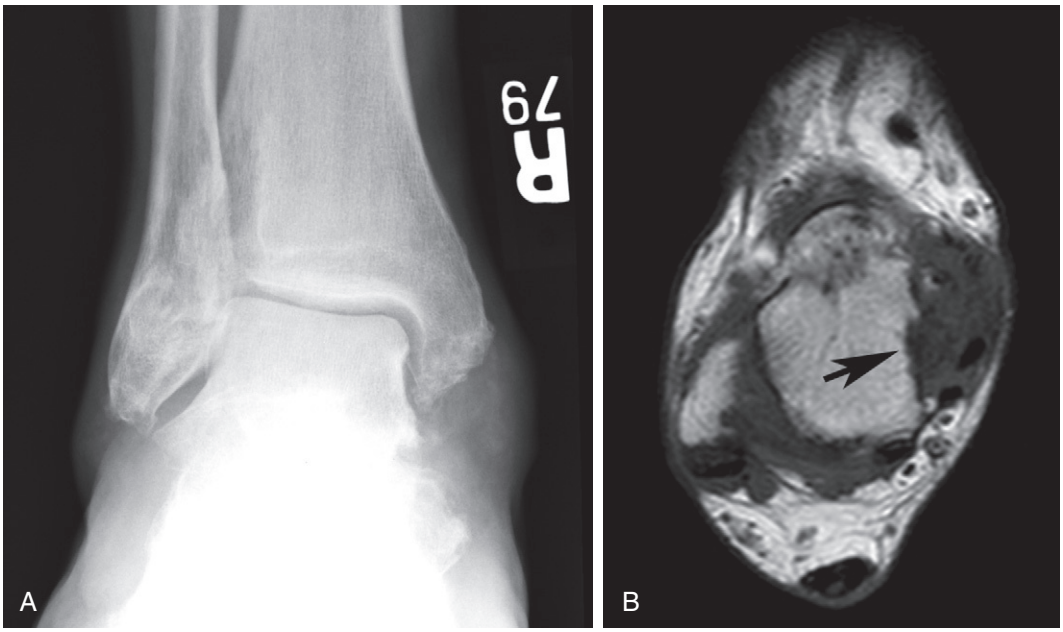

FIGURE 16-22. The ankle in patient with gout. **A,** AP view of the ankle shows a calcified tophus inferior to the medial malleolus. **B,** Axial T1-weighted image through the talus inferior to the medial malleolus. Tophus is intermediate and low signal soft tissue mass medial to the talus. There is an erosion of the medial talus (*arrow*).

FIGURE 16-23. AP view of the knee in patient with gout. The medial compartment is narrowed. There is an erosion of the medial tibial plateau. Small subchondral cysts are seen in the lateral tibial plateau.

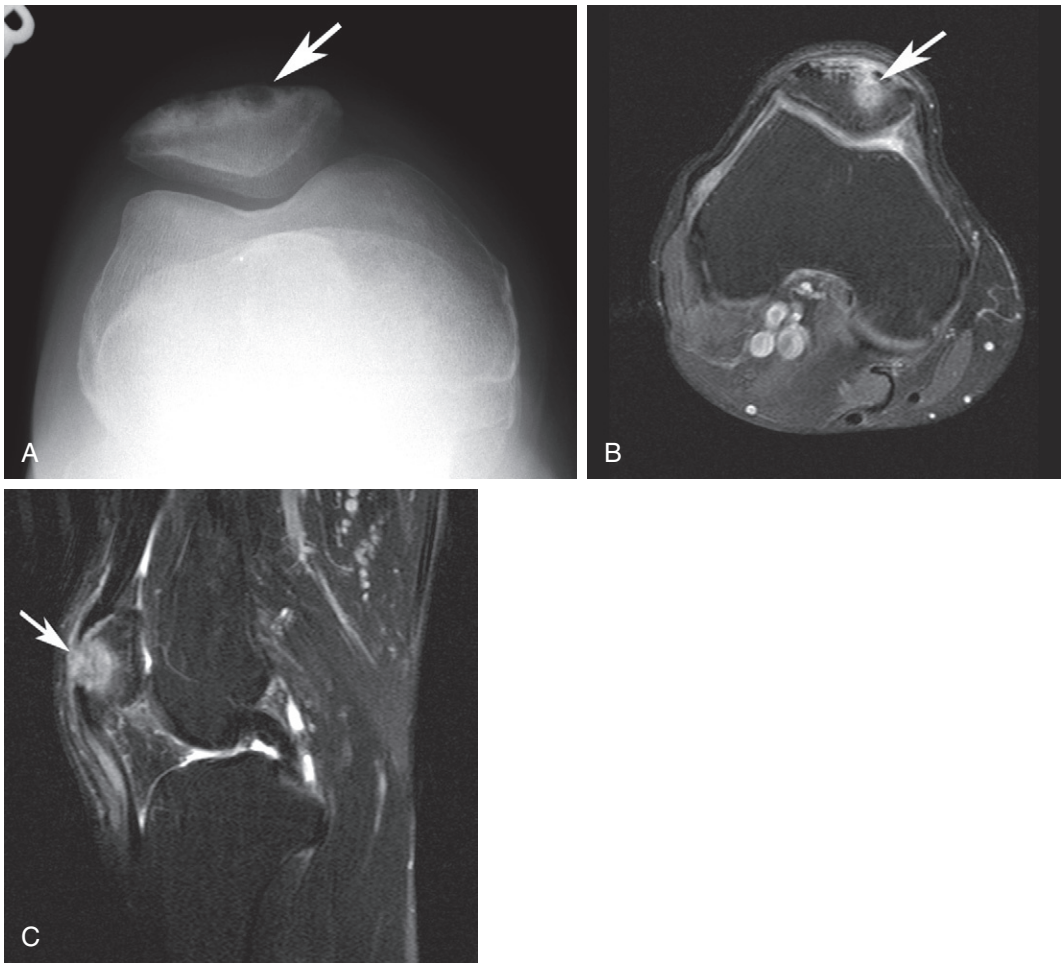

FIGURE 16-24. **A,** Sunrise view of the patella shows a focal lucency in the anterior patella (*arrow*). **B,** Axial fat-suppressed PD image of the patella shows intraosseous tophus (*arrow*) that accounts for patellar lucency. **C,** Sagittal fat-suppressed T2-weighted image shows tophus in patella (*arrow*) and tophaceous deposition in the patellar tendon.

THE SACROILIAC JOINT

Twelve percent of the patients with radiographic gout have involvement of the sacroiliac (SI) joint. Five percent present with an osteoarthritic picture indistinguishable from any secondary osteoarthritis. Seven percent show a classic change in the synovial aspect of the SI joint—there is a huge punched-out erosion with a sclerotic border (Fig. 16-25). A bone spicule representing an overhanging edge of cortex may be present. These changes are produced by a tophus, which may or may not be seen, depending upon the degree of calcification.

FIGURE 16-25. AP view of the pelvis in a patient with gout. Tophaceous deposits are present in the pubic symphysis and both SI joints. There are associated erosive changes with sclerotic borders and reparative bone.

SUMMARY

The radiographic changes of gout are identified relatively late in the disease process. The changes fit into two categories: (1) those of osteoarthritis indistinguishable from other causes of secondary osteoarthritis, and (2) changes that are pathognomonic of chronic tophaceous deposit.

SUGGESTED READINGS

Bloch C, Hermann G, Yu TF: A radiological reevaluation of gout: A study of 2000 patients, *AJR Am J Roentgenol* 134:781–787, 1980.
Martel W: Radiology of the rheumatic diseases. In Hollander JL, McCarty DJ Jr, editors: *Arthritis and allied conditions*, ed 8, Philadelphia, 1972, Lea & Febiger, p. 115.
Martel W: The overhanging margin of bone: A roentgenologic manifestation of gout, *Radiology* 91:755–756, 1968.
Resnick D: The radiographic manifestations of gouty arthritis, *Crit Rev Diagn Imaging* 9:265–335, 1977.
Vyhnanek L, Lavicka J, Blahos J: Roentgenological findings in gout, *Radiol Clin* 29:256–264, 1960.
Watt I, Middlemiss H: The radiology of gout, *Review Article, Clin Radiol* 26:27–36, 1975.
Wright JT: Unusual manifestations of gout, *Australas Radiol* 10:365–374, 1966.

Calcium Pyrophosphate Dihydrate Crystal Deposition Disease

17

Calcium pyrophosphate dihydrate (CPPD) crystal deposition disease is a common disorder and the most common crystal arthropathy. In a typical hospital population, one to three patients per week will be observed with some manifestation of this disorder. It typically affects the middle-aged and elderly population. Some estimate the frequency to be 5 percent of this population. The clinical picture varies from the pseudogout syndrome to asymptomatic joint disease. The radiographic picture also varies from chondrocalcinosis without arthropathy to severe arthropathy.

Chondrocalcinosis is the deposition of CPPD crystals into fibrous or hyaline cartilage. Chondrocalcinosis has been associated in the past with many diseases, such as diabetes, degenerative joint disease, and gout. However, the only two diseases that have definite significant association with CPPD crystal deposition are primary hyperparathyroidism and hemochromatosis. If a patient with gout demonstrates chondrocalcinosis on the radiograph, then the chondrocalcinosis is not secondary to deposition of urate crystals but secondary to deposition of CPPD crystals. The patient should be diagnosed as having two separate diseases, gout and CPPD crystal deposition disease (Fig. 17-1). In ochronosis, some patients have had CPPD crystals in the synovium but not in the cartilage.

Chondrocalcinosis is seen most frequently in the knee, pubic symphysis, and wrist (Fig. 17-2). At least one of these areas is involved in a patient with CPPD deposition disease. Therefore, when screening a patient for this disorder, one should obtain radiographs of these areas. Radiographic diagnosis can be made when two or more areas in the skeleton demonstrate chondrocalcinosis. CPPD crystals may also deposit in synovium capsules, tendons, and ligaments.

The arthropathy of CPPD radiographically resembles osteoarthritis. How its distribution within the skeleton as well as within the individual joint is distinctive, allowing separation from primary or mechanical osteoarthritis. The following are the radiographic features of CPPD crystal deposition disease:

1. Chondrocalcinosis
2. Normal mineralization
3. Uniform joint space loss
4. Subchondral new bone formation
5. Variable osteophyte formation
6. Cysts—more prominent than in osteoarthritis
7. Occasional neuropathic changes
8. Bilateral distribution
9. Distribution in knees, hands, and hips, in decreasing order of frequency; unlike osteoarthritis, the shoulder and elbow are involved

FIGURE 17-1. The wrist in a patient with gout and CPPD crystal deposition disease. The calcified mass lateral to the distal ulna is a calcified tophus of gout. Chondrocalcinosis (*arrows*) is also present, indicating CPPD crystal deposition disease.

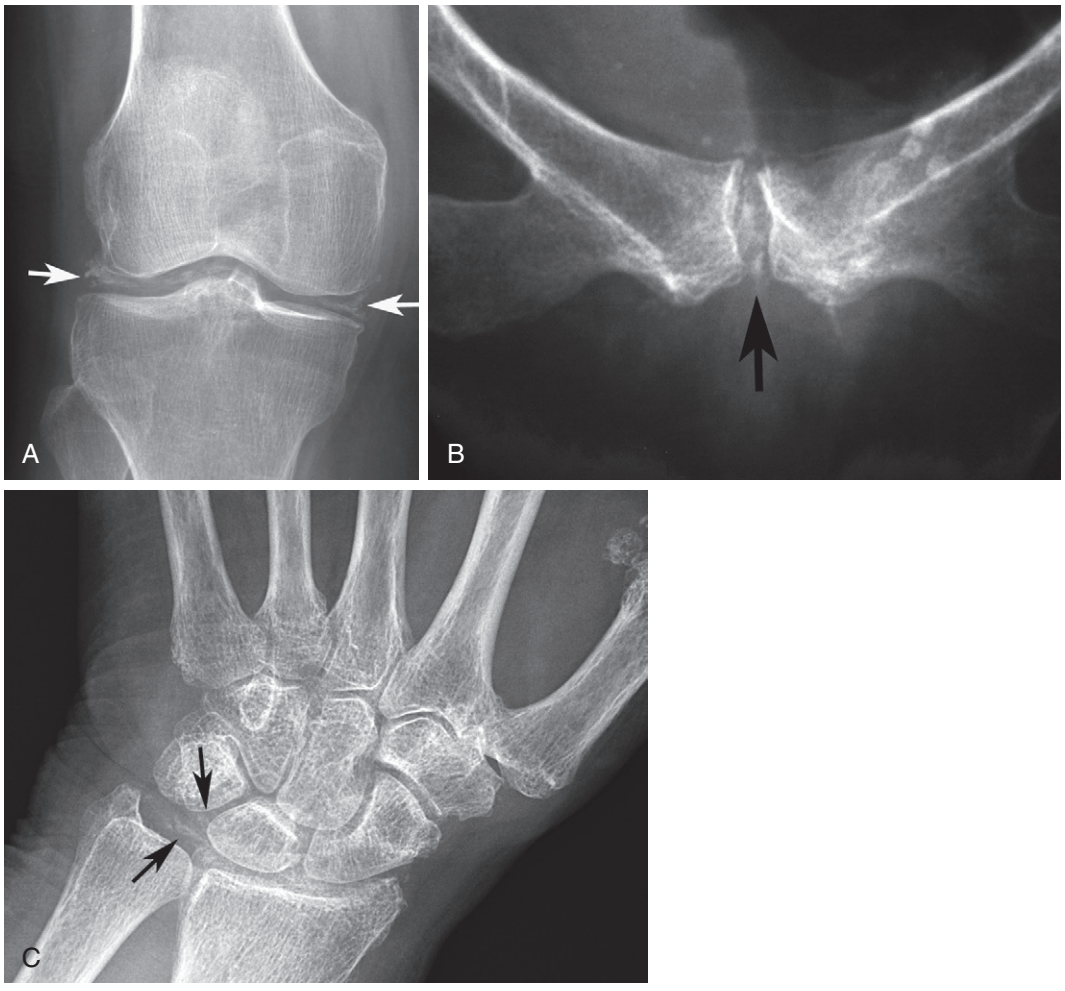

FIGURE 17-2. A, Chondrocalcinosis (*arrows*) in the knee. **B,** Chondrocalcinosis present in the fibrous cartilage of the pubic symphysis (*arrow*). **C,** Chondrocalcinosis in the wrist (*arrow*).

THE KNEE

The knee is the most commonly involved joint in CPPD crystal deposition disease. Eighty percent of patients show chondrocalcinosis, and 75 percent show changes of an arthropathy. The chondrocalcinosis is seen as (1) wedge-shaped calcification in the fibrocartilaginous menisci and (2) thin linear calcification in hyaline cartilage paralleling the femoral condyles or tibial platen (Fig. 17-3). Calcification may also be seen in the synovium, quadriceps tendon, or cruciate ligaments (Fig. 17-4).

In the arthropathy, there is often preferential narrowing of the patellofemoral joint space with sparing of the medial and lateral tibiofemoral compartments (Fig. 17-5). This patellofemoral narrowing is accompanied by subchondral bone sclerosis and osteophyte formation on the posterior aspect of the patella and the anterior aspect of the femoral condyles. There is often a scalloped defect seen in the femur proximal to the patella in the flexed knee. This scalloping is caused by abutment of the patella against the femur when the knee is in extension. Isolated patellofemoral involvement in the knee should always suggest CPPD crystal deposition disease.

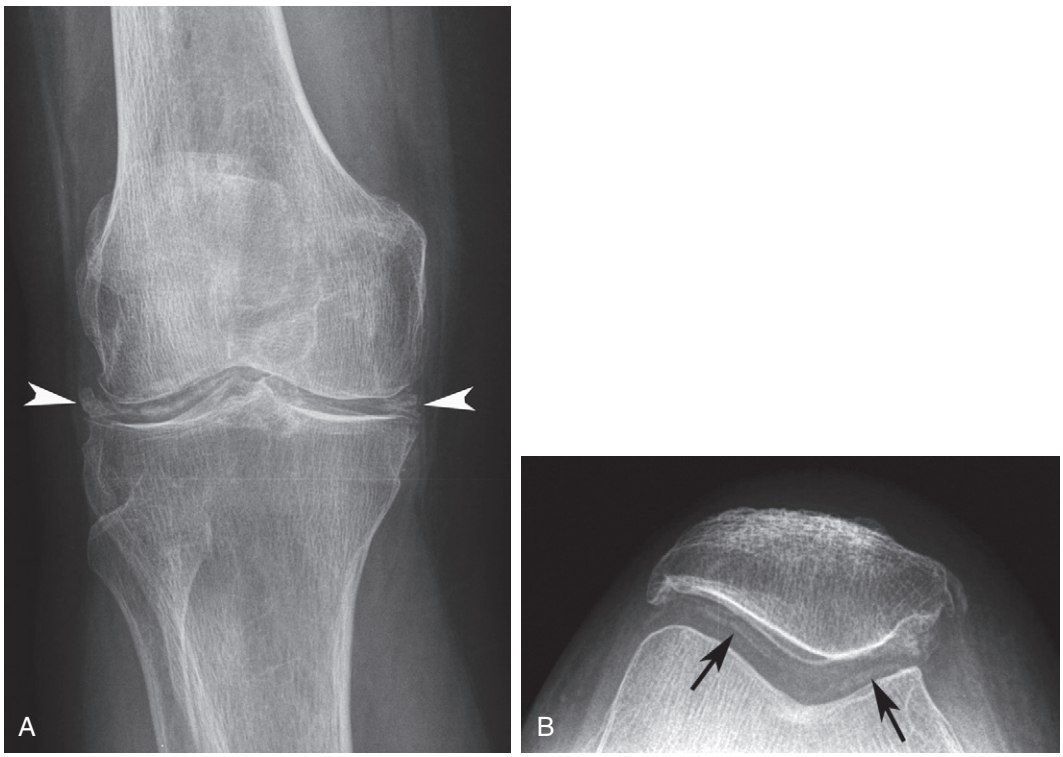

FIGURE 17-3. A, Anteroposterior (AP) view and (**B**) sunrise view of the knee demonstrating chondrocalcinosis. Wedge-shaped calcification is seen in the fibrocartilaginous meniscus (*arrowheads*), and curvilinear calcification is seen in the hyaline cartilage (*arrows*). The joint spaces are preserved.

FIGURE 17-4. Lateral view of the knee shows chondrocalcinosis in the quadriceps and gastrocnemius tendons (*arrows*). Typical calcification is also present in the joint.

FIGURE 17-5. Lateral view of the knee in the flexed position shows marked patellofemoral joint space narrowing with subchondral sclerosis and osteophyte formation. There is extensive remodelling of the anterior distal femur producing a notched appearance because of abnormal articulation of the patella with the femur in extension.

However, joint space narrowing may be seen in all three compartments, with the medial tibiofemoral compartment being involved more frequently than the lateral tibiofemoral compartment. In this case, the presence of chondrocalcinosis may be the only finding to distinguish this arthropathy from mechanical osteoarthritis. Occasionally the osteoarthritic changes become so severe that they resemble a neuropathic joint (Fig. 17-6). Such excessive changes should suggest CPPD arthropathy, rather than mechanical osteoarthritis.

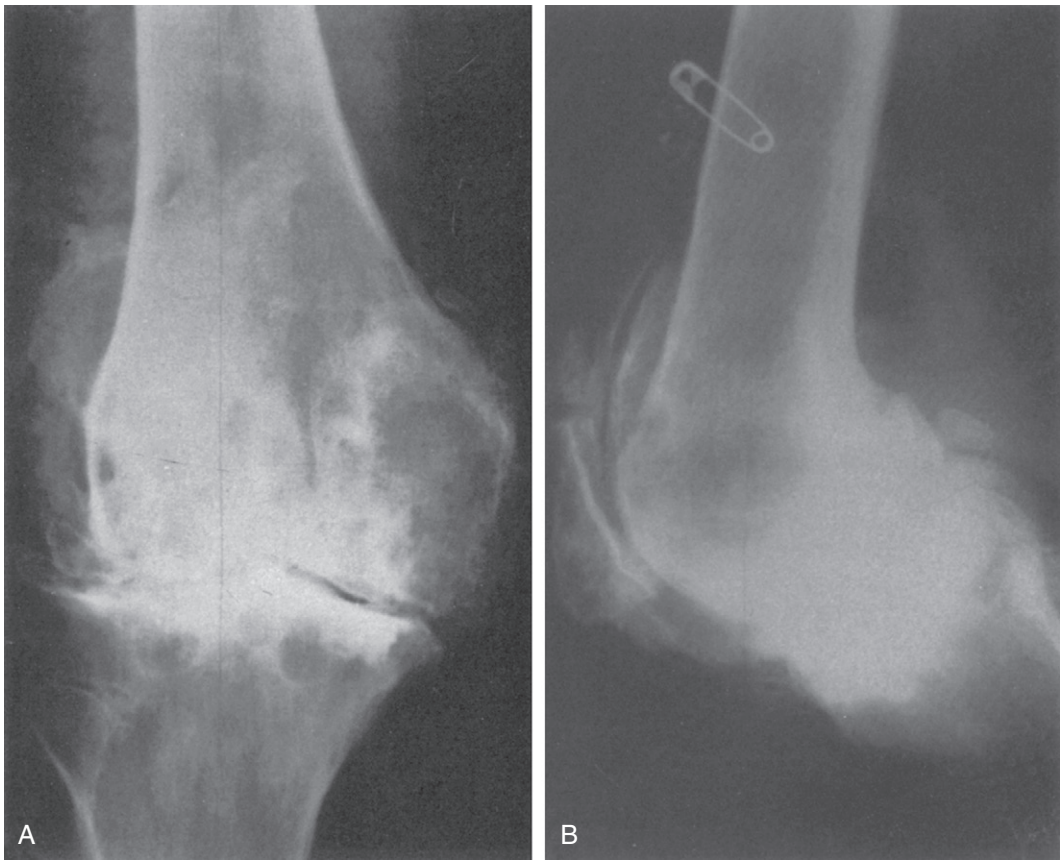

FIGURE 17-6. AP (**A**) and lateral (**B**) views of a knee in patient with CPPD arthropathy. There is loss of all compartments of the knee joint. There is extensive subchondral sclerosis and some cyst formation. There is fragmentation and bone debris in the joint. The findings resemble those of a neuropathic joint.

THE HAND

Chondrocalcinosis in the wrist is found in 65 percent of patients and the arthropathy in 70 percent of patients. Chondrocalcinosis is most frequently seen in the triangular fibrocartilage, hyaline cartilage, or ligament between the lunate and the triquetrum (Fig. 17-7). The hyaline cartilage may calcify around any of the carpal bones but most frequently between the scaphoid and lunate. This may lead to disruption of the scapholunate ligament and the resulting instability may produce osteoarthritis of the radioscaphoid joint. In the fingers, pyrophosphate deposition tends to occur in the synovium and capsule around the metacarpophalangeal (MCP) joints (Fig. 17-8).

FIGURE 17-7. The wrist in patient with CPPD arthropathy. There is chondrocalcinosis present in the triangular fibrocartilage (*arrowhead*) and in the hyaline cartilage between the lunate and triquetrum (*arrow*). There is also loss of the joint space between the navicular and the radius and between the lunate and capitate with subchondral bone formation.

FIGURE 17-8. MCP joints in patient with CPPD arthropathy. Calcification is present in the capsule.

The arthropathy in the hands is usually confined to the MCP joints. The interphalangeal (IP) joints are usually spared. The changes are those of osteoarthritis in the wrong distribution for primary osteoarthritis. There is joint space narrowing, subchondral bone formation, and variable osteophyte formation (Fig. 17-9). Occasionally there is cyst formation and resultant bone collapse. The arthropathy of the wrist most commonly affects the radiocarpal joint. Again, there are osteoarthritic changes in a distribution different from that of primary osteoarthritis. There is joint space narrowing, subchondral bone formation, and cyst formation (Fig. 17-10). The latter may dominate the radiographic picture. If there is dissociation between the scaphoid and lunate, there may be accompanying narrowing of the joint space between the lunate and capitate. The appearance has been described as a "stepladder" configuration (Fig. 17-11). This pattern of radioscaphoid and capitolunate joint space narrowing is known as scapholunate advanced collapse or SLAC wrist.

FIGURE 17-9. MCP joints in patient with CPPD arthropathy. There is sparing of the IP joints. There is loss of the MCP joints with chondrocalcinosis, osteophyte formation, and subchondral sclerosis.

FIGURE 17-10. A wrist in patient with CPPD arthropathy. Chondrocalcinosis is present (*arrow*). Osteoarthritic changes are present involving the radiocarpal joint and the lunate-capitate joint. Large cysts are present in the distal ulna and radius (*arrowheads*).

FIGURE 17-11. Posteroanterior (PA) view of the wrist in patient with CPPD arthropathy. There is scapholunate dissociation with secondary osteoarthritis at the radioscaphoid joint. Chondrocalcinosis is present in the triangular fibrocartilage (*arrow*).

THE HIP

Chondrocalcinosis is present in the hip in 45 percent of patients and the arthropathy in 30 percent of patients with CPPD. Chondrocalcinosis is seen as calcification of the fibrocartilage of the acetabular labrum and calcification of the hyaline cartilage paralleling the femoral head (Fig. 17-12). Most commonly the arthropathy causes uniform loss of cartilage and resultant axial migration of the femoral head within the acetabulum. This cartilage loss is accompanied by osteoarthritic changes (Fig. 17-13). However, the osteophytes may not be as large as those seen in mechanical osteoarthritis, for the hip is still in the normal axis of weight bearing. Subchondral cyst formation may dominate the picture (Fig. 17-14). If the axis of weight bearing remains in its normal position, then there is absence of the huge medial osteophyte and new bone apposition along the medial cortex of the femoral neck so commonly identified with mechanical osteoarthritis. Occasionally there may be bone collapse, destruction, and fragmentation leading to the appearance of a neuropathic joint.

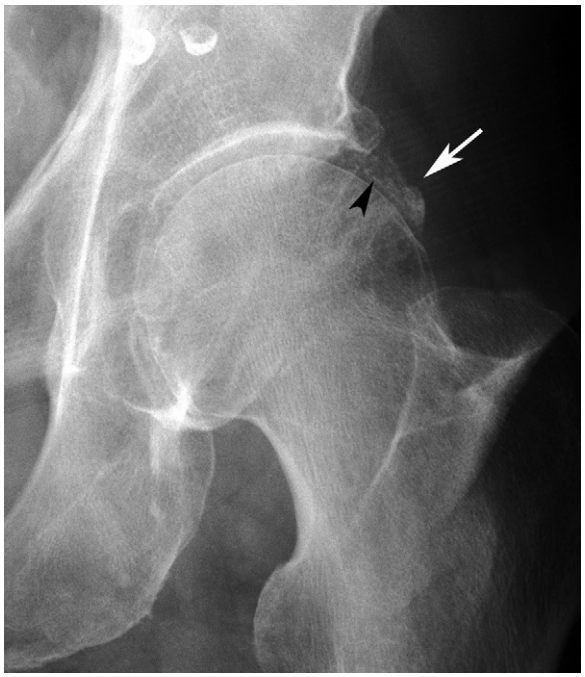

FIGURE 17-12. AP view of hip in patient with CPPD crystal deposition disease. Chondrocalcinosis is seen in hyaline cartilage (*arrowhead*) and in fibrous cartilage of the acetabular labrum (*arrow*).

FIGURE 17-13. AP view of the hip in patient with CPPD arthropathy. There is uniform loss of the cartilage with axial migration of the femoral head within the acetabulum. There are subchondral sclerosis and osteophyte formation.

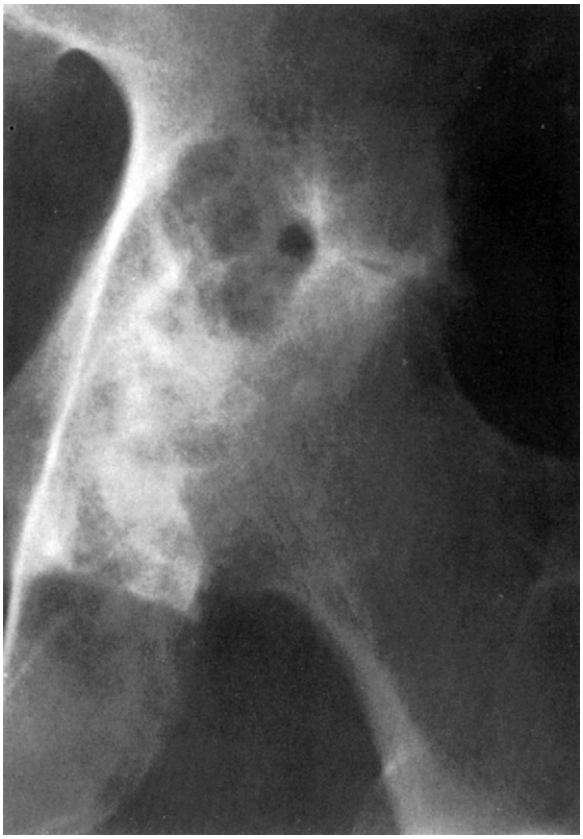

FIGURE 17-14. PA view of a hip in patient with CPPD arthropathy. There is uniform cartilage loss with axial migration of the femoral head within the acetabulum. There are subchondral sclerosis and extensive subchondral cyst formation. There is relative absence of osteophyte formation. There is no evidence of new bone apposition along the femoral neck. *(From Brower AC: The radiologic approach to arthritis,* Med Clin North Am *68:1593, 1984; reprinted by permission.)*

OTHER APPENDICULAR SITES

Unlike primary osteoarthritis, the non–weight-bearing joints, or the elbow and shoulder, are frequently involved. Again, chondrocalcinosis is seen more commonly than the actual arthropathy (Fig. 17-15). In both these areas, the arthropathy is one of osteoarthritis with subchondral bone formation, osteophyte formation, and subchondral cyst formation (Fig. 17-16). Similar changes may be seen in the acromioclavicular (AC) joint. The foot and ankle are less frequently involved. Chondrocalcinosis may be identified anywhere. Calcification may be seen in the synovium and capsule around the metatarsophalangeal (MTP) joints. In the foot, the arthropathy has a predilection for the talonavicular joint.

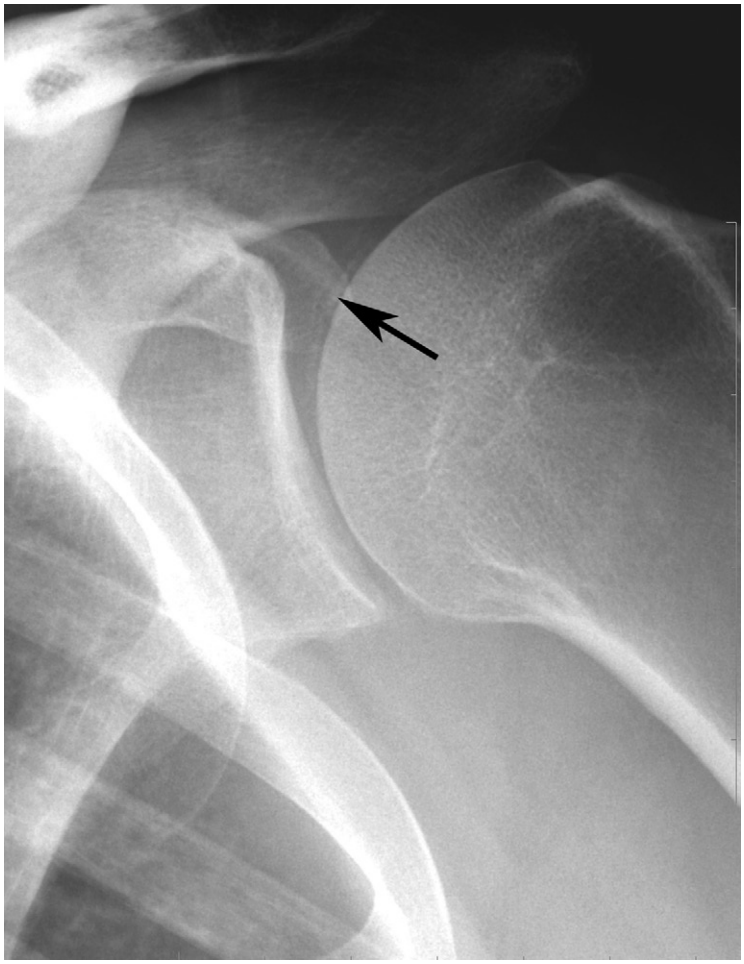

FIGURE 17-15. AP view of the shoulder demonstrating chondrocalcinosis of the hyaline cartilage (*arrow*).

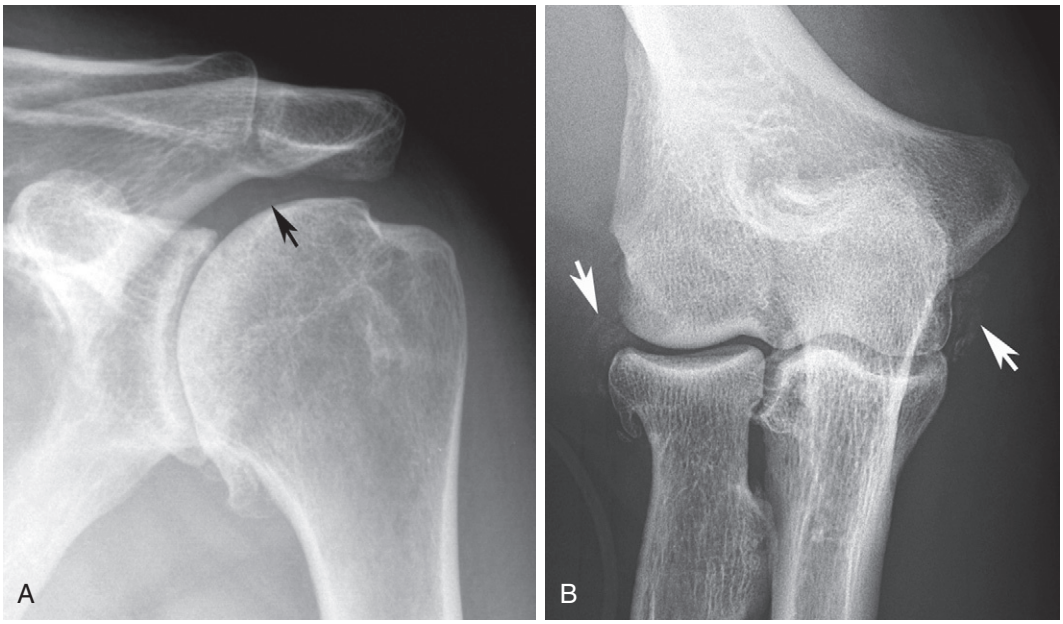

FIGURE 17-16. **A,** Shoulder in patient with CPPD arthropathy. There is loss of the glenohumeral joint space with subchondral sclerosis, osteophyte formation, and subchondral cyst formation. Chondrocalcinosis is seen in the superior humeral articular cartilage (*arrow*). **B,** Elbow in patient with CPPD arthropathy. There is calcification (*arrows*) and osteophyte formation.

THE SPINE

Spinal involvement is not uncommon and should be considered in any patient with evidence of degenerative disc disease at multiple levels. There is an increased incidence of the vacuum phenomenon at more than one level (Fig. 17-17). The diagnosis can be further defined by observing calcification in the soft tissue structures around the intervertebral disc space. The apophyseal joints may be involved as well, with osteoarthritic changes and resultant spondylolisthesis. These features can be observed in any part of the spine, cervical through lumbar.

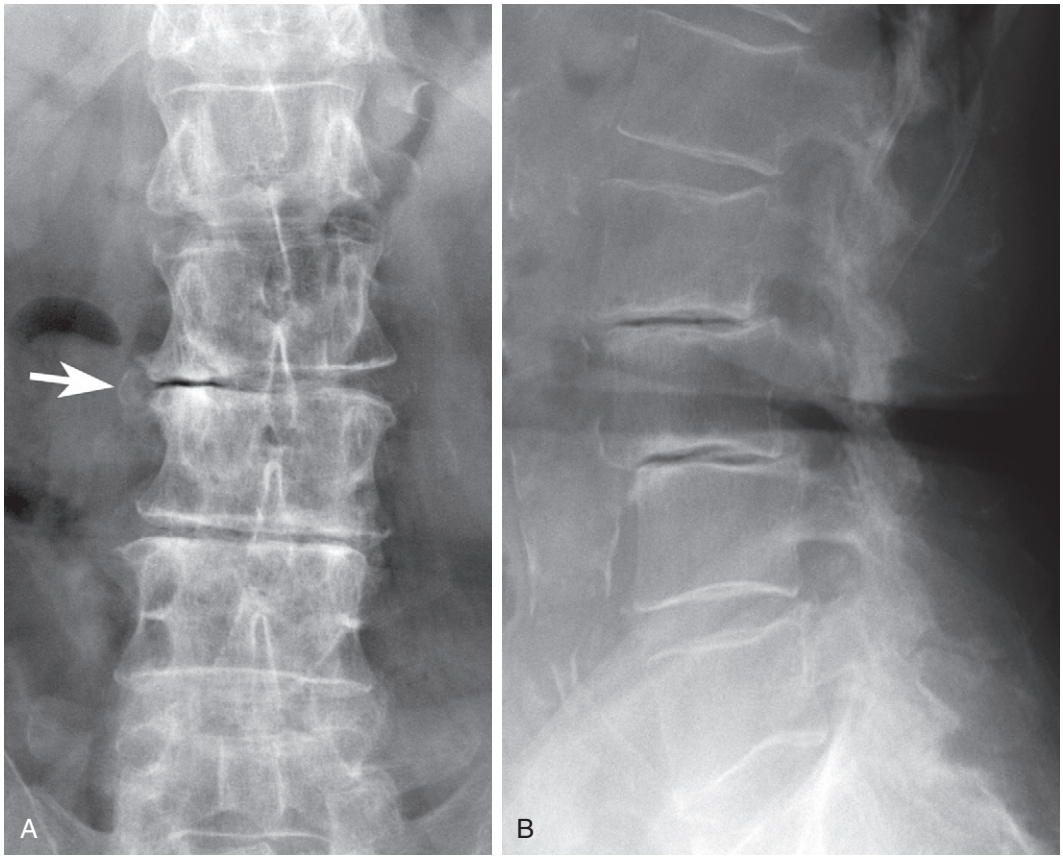

FIGURE 17-17. AP (**A**) and lateral (**B**) views of the upper lumbar spine showing the vacuum phenomenon at two disc levels. There is adjacent subchondral sclerosis and osteophyte formation. There is also calcification present in the soft tissue structures at the level of the disc (*arrow*).

One may also observe atlantoaxial subluxation in the cervical spine. This may be secondary to CPPD crystals depositing in the ligaments around the odontoid. Crystal deposition and synovitis at C1-C2 can be accompanied by cyst formation and dissolution of the dens. The bone resorption of the dens can lead to pathologic fracture (Fig. 17-18). Synovitis and destruction at C1-C2 can be confused with neoplasm on magnetic resonance (MR) imaging.

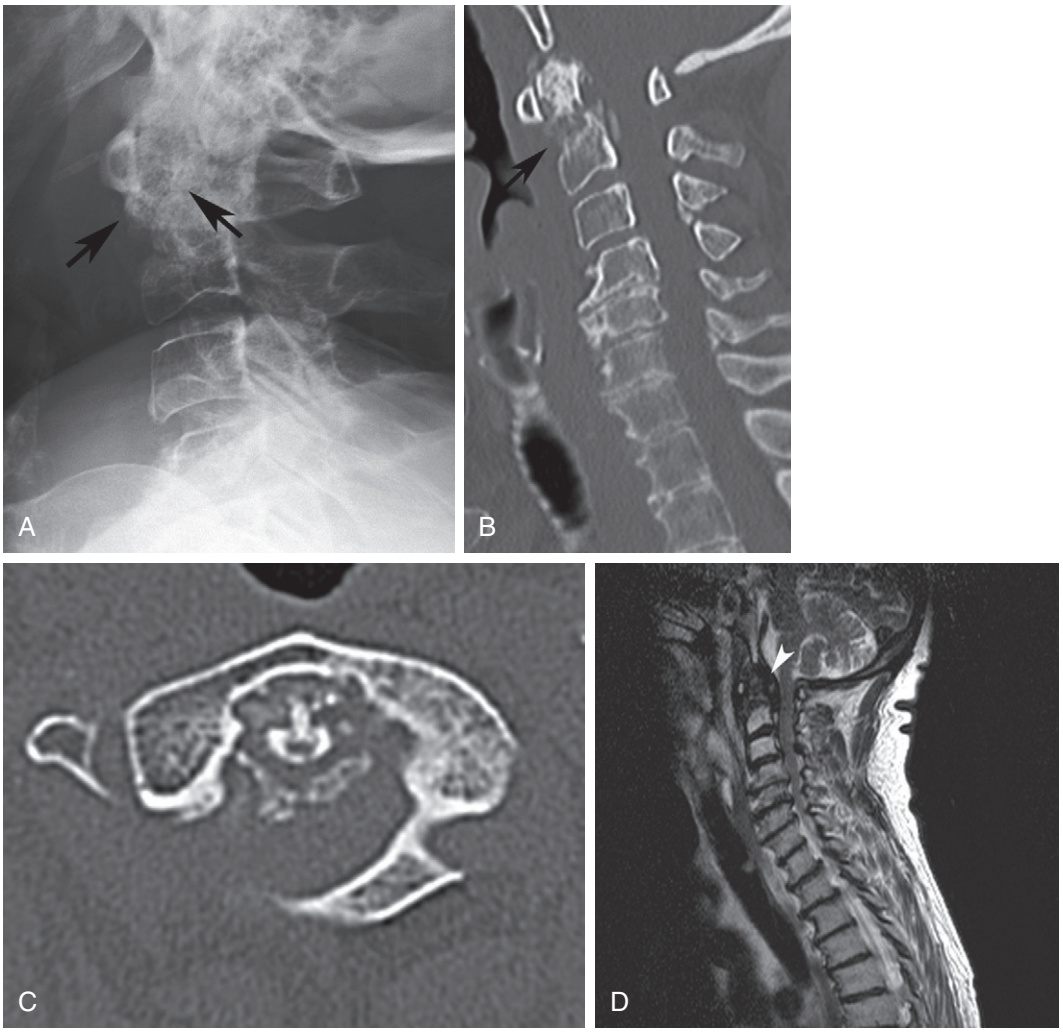

FIGURE 17-18. A, Lateral view of cervical spine showing a fracture at the base of the dens (*arrow*). **B,** Sagittal computed tomography (CT) image confirms fracture (*arrow*) and shows CPPD crystal in the soft tissues surrounding the dens. **C,** Axial CT images shows calcification surrounding the dens, which is eroded. **D,** Sagittal T2-weighted MR image of the cervical spine shows low signal of CPPD crystal posterior to the dens (*arrowhead*). There is marked narrowing of the cervical canal from disc-osteophyte formation.

UNUSUAL MANIFESTATIONS

Occasionally CPPD will deposit as a mass around a joint (tophaceous pseudogout), without any of the other typical manifestations of the disease in other joints. This happens most frequently around the temporomandibular joint, knee, and elbow (Fig. 17-19).

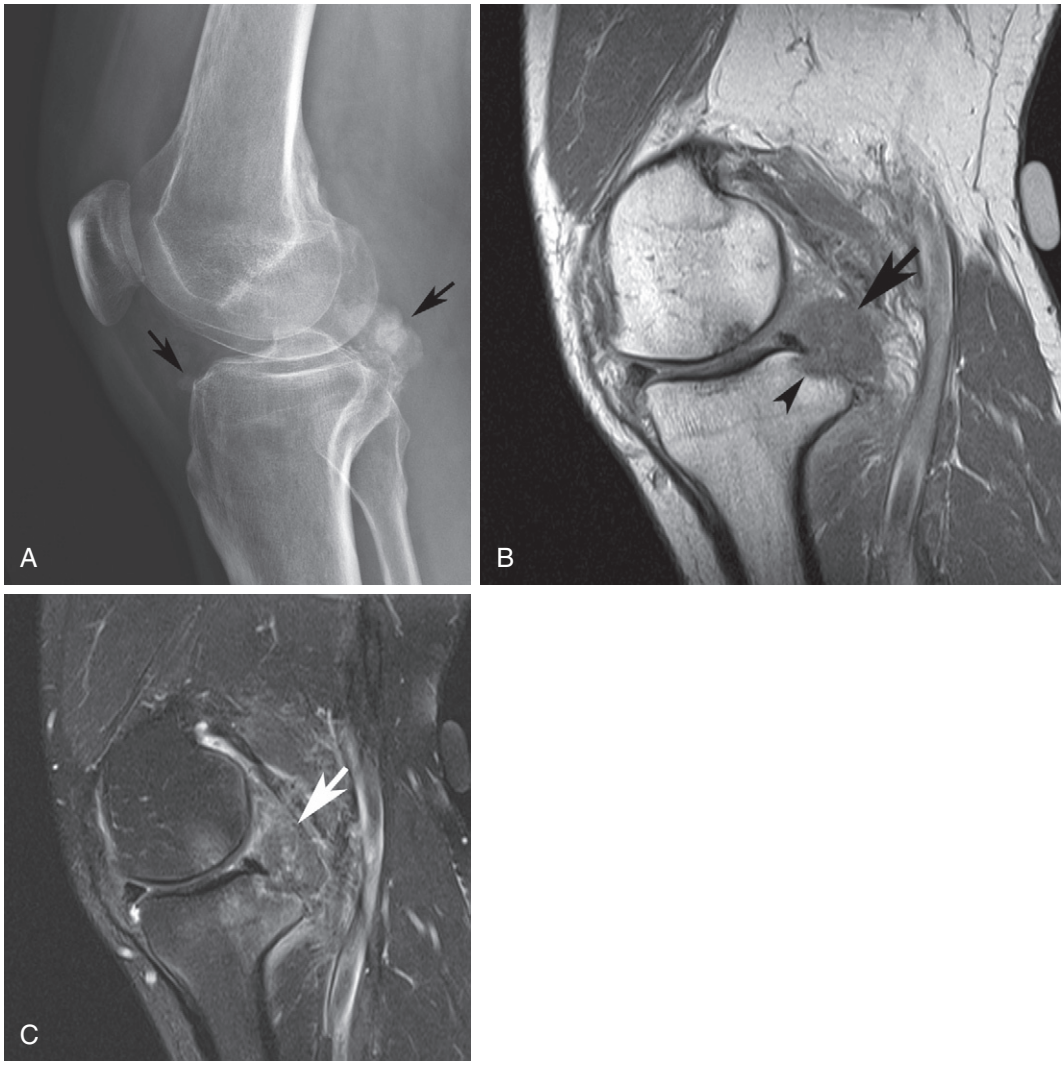

FIGURE 17-19. A, Lateral view of the knee shows tophaceous deposit of CPPD crystal in the posteromedial knee and anterior knee (*arrows*). Sagittal T1-weighted (**B**) and fat-suppressed T2-weighted (**C**) images show the tophus (*arrows*) and focal erosion of the posteromedial rim of the tibia (*arrowhead*).

SUMMARY

The radiographic hallmarks of CPPD crystal deposition disease are chondrocalcinosis and osteoarthritic changes in a specific distribution. Even in the absence of chondrocalcinosis, the specific distribution of osteoarthritic changes should suggest the correct diagnosis.

SUGGESTED READINGS

Adamson TC III, Resnik CS, Guerra J Jr, et al: Hand and wrist arthropathies of hemochromatosis and calcium pyrophosphate deposition disease: Distinct radiographic features, *Radiology* 147:377–381, 1983.

Chen C, Chandnani VP, Kang HS, et al: Scapholunate advanced collapse: A common wrist abnormality in calcium pyrophosphate dihydrate crystal deposition disease, *Radiology* 177:459–461, 1990.

Dirheimer Y, Wackenheim C, Dietemann JL: Calcification of the transverse ligament in calcium dihydrate deposition disease (CPPD), *Neuroradiology* 27:87, 1985.

Kakitsubata Y, Boutin RD, Theodorou DJ, et al: Calcium pyrophosphate dihydrate crystal deposition in and around the atlantoaxial joint: Association with type 2 odontoid fractures in nine patients, *Radiology* 216:213–219, 2000.

Lagier R: Femoral cortical erosions and osteoarthrosis of the knee with chondrocalcinosis: An anatomo-radiological study of two cases, *Fortschr Geb Rontgenstr Nuklearmed* 120:460–467, 1974.

Martel W, Champion CK, Thompson GR, Carter TL: A roentgenologically distinctive arthropathy in some patients with the pseudogout syndrome, *Am J Roentgenol Radium Ther Nucl Med* 109:587–605, 1970.

Martel W, McCarter DK, Solsky MA, et al: Further observations on the arthropathy of calcium pyrophosphate crystal deposition disease, *Radiology* 141:1–15, 1981.

McCarty DJ Jr.: Calcium pyrophosphate dihydrate crystal deposition disease—1975, *Arthritis Rheum* 19(Suppl 3):275–385, 1976.

Resnik CS, Miller BW, Gelberman RH, Resnick D: Hand and wrist involvement in calcium pyrophosphate dihydrate crystal deposition disease, *J Hand Surg Am* 8:856–863, 1983.

Resnik CS, Resnick D: Calcium pyrophosphate dihydrate crystal deposition disease, *Curr Probl Diagn Radiol* 11(6):1–40, 1982.

Resnick D, Niwayama G: Calcium pyrophosphate dihydrate (CPPD) crystal deposition disease. In Resnick D, editor: *Diagnosis of bone and joint disorders*, ed 3, Philadelphia, 1995, W.B. Saunders Company, p. 1556.

Resnick D, Niwayama G, Goergen TG, Utsinger PD: Clinical, radiographic and pathologic abnormalities in calcium pyrophosphate dihydrate deposition disease (CPPD): Pseudogout, *Radiology* 122:1–15, 1977.

Steinbach LS: Calcium pyrophosphate dihydrate and calcium hydroxyapatite crystal deposition diseases: Imaging perspectives, *Radiol Clin North Am* 42:185–205, 2004.

Zitnan D, Sitaj S: Natural course of articular chondrocalcinosis, *Arthritis Rheum* 19(Suppl):363–390, 1976.

18 Hydroxyapatite Deposition Disease

Hydroxyapatite deposition disease (HADD) is an extremely common disorder causing periarticular disease in the form of tendinitis or bursitis. Only rarely does it cause true articular disease. Calcium hydroxyapatite deposits in muscles, capsules, bursae, and tendon sheaths. Although this deposition is associated with many systemic diseases, such as collagen vascular diseases, renal osteodystrophy, hypervitaminosis D, and milk-alkali syndrome, in many patients it occurs idiopathically with no underlying systemic problem. The radiographic findings are as follows:

1. Periarticular calcification
   - **A.** Early deposition is linear and poorly defined, often blending with the soft tissues
   - **B.** With time this calcification becomes denser, homogeneous, well delineated, and circular
2. Soft tissue swelling
3. Normal adjacent joint and bone
4. Occasional joint effusion
5. Occasional osteoporosis, occasional reactive sclerosis, uncommon erosion or scalloping of adjacent bone
6. Single joint distribution; occasionally multiple joints may be involved either at the same time (33 percent of patients) or successively (67 percent of patients)
7. Distribution in shoulder, hip, wrist, elbow, and neck, in decreasing order of frequency

SHOULDER

The shoulder is the most common site of calcific tendinitis or bursitis. Calcium hydroxyapatite is said to be observed in 40 percent of the shoulders radiographed for shoulder pain. It usually locates first in a tendon. The actual tendon location can be identified by changes in rotation of the humerus on the radiograph (Fig. 18-1). Fifty-two percent of the calcific tendinitis occurs in the supraspinatus tendon, which can be seen in profile over the greater tuberosity on external rotation. Internal rotation of the humerus profiles the posterior aspect of the head on at the lateral aspect of the radiograph and the anterior head medially. Calcification in the infraspinatus tendon profiles

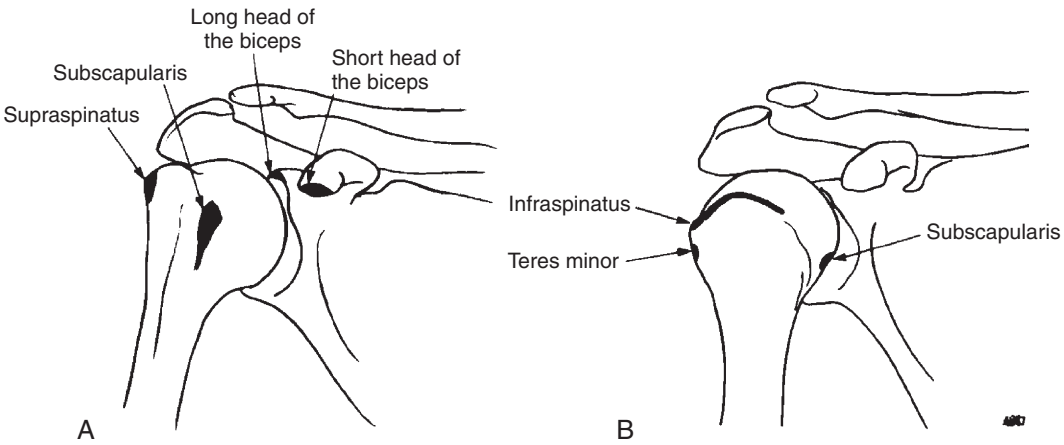

FIGURE 18-1 Locations of hydroxyapatite deposits in specific tendons as observed on anteroposterior (AP) view of the shoulder in (**A**) external rotation and (**B**) internal rotation.

posteriorly on internal rotation. Calcification of the teres minor also profiles posteriorly on internal rotation, but it is inferior to the infraspinatus calcification. Calcification in the subscapularis profiles anteriorly on internal rotation. Calcification of the long head of the biceps is seen on the superior aspect of the glenoid; that of the short head of the biceps is seen on the tip of the coracoid. Rotation does not change the location of calcification in the biceps.

Calcification in the rotator cuff area may eventually rupture into the bursa (Fig. 18-2). In some patients this has led to a secondary severe destructive arthropathy. The result of this particular sequence of events has been labeled the "Milwaukee shoulder" (Fig. 18-3).

FIGURE 18-2 AP view of the shoulder showing a large amorphous calcific deposit in the supraspinatus. The lateral aspect of the concretion is less distinct (*arrows*) indicating extension into the subacromial-subdeltoid bursa. The humeral head is inferiorly subluxed because of deltoid atony associated with acute bursal disease.

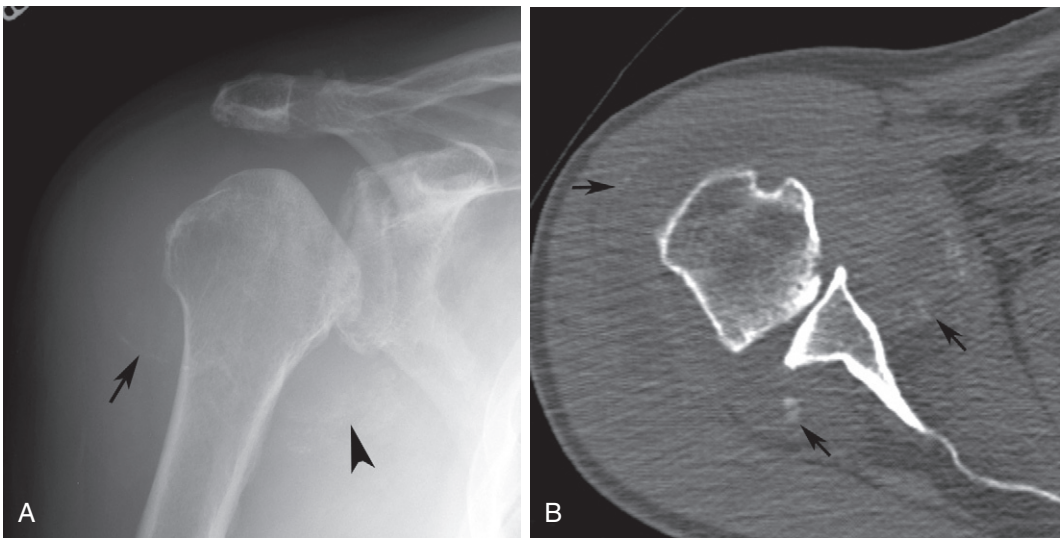

FIGURE 18-3 Patient with "Milwaukee shoulder." **A,** AP view of the shoulder shows destruction of the superomedial aspect of the humeral head and osteophyte formation in the glenohumeral joint. Faint calcification is visible in the periphery of the distended subacromial-subdeltoid bursa (*arrow*) and axillary recess (*arrowhead*). **B,** Axial computed tomography (CT) shows flattened appearance of the humeral articular surface and calcification at the periphery of the distended bursa and joint (*arrows*).

OTHER SITES

Around the hip, hydroxyapatite deposition may occur in the gluteal insertions into the greater trochanter and surrounding bursa. These calcifications may appear linear or cloud-like (Fig. 18-4). Calcification in the elbow occurs around the medial and lateral condyles of the humerus or in the triceps as it inserts into the olecranon (Fig. 18-5).

FIGURE 18-4 AP view of the hip demonstrating hydroxyapatite deposition into the gluteal insertions at the greater trochanter (*arrow*). The calcifications are both cloud-like and linear in their appearance.

FIGURE 18-5 Lateral view of the elbow demonstrating calcification in the common extensor tendon as it inserts into the lateral epicondyle.

In the wrist, the most frequent deposition occurs in the flexor carpi ulnaris. This is observed as calcification adjacent to the pisiform. Calcification may also be seen volar to the radiocarpal joint in the flexor carpi radialis or adjacent to the distal ulna and ulna styloid in the extensor carpi ulnaris (Fig. 18-6). Tendinitis may cause adjacent bone osteoporosis (Fig. 18-7).

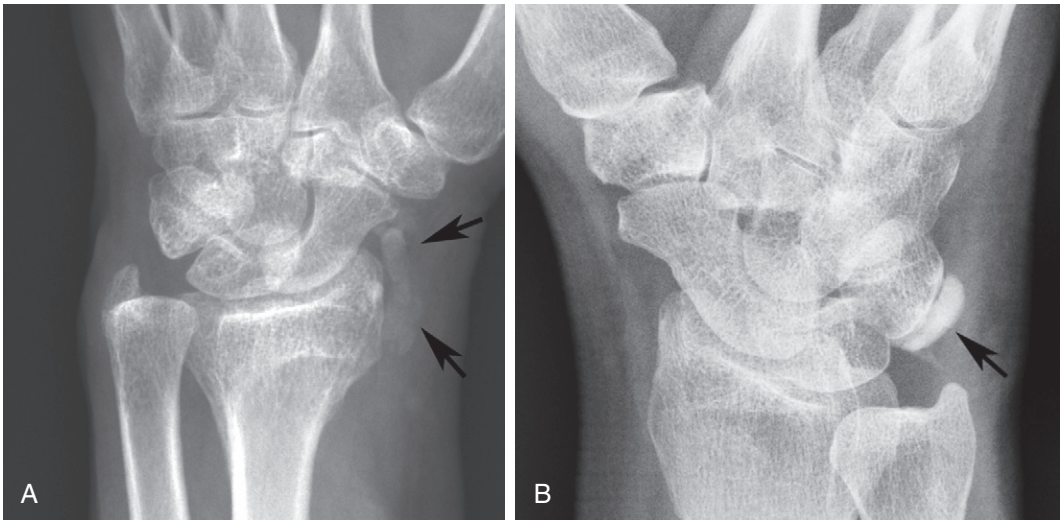

FIGURE 18-6 A, Oblique view of the wrist demonstrating calcification volar to the radius and scaphoid (*arrows*), most likely in the flexor carpi radialis. **B,** Oblique view of the wrist demonstrating calcification adjacent to the triquetrum and distal to the ulna (*arrow*). This most likely is in the extensor carpi ulnaris.

FIGURE 18-7 Posteroanterior (PA) view of the wrist showing calcification in the soft tissue radial to the radial styloid (*arrowhead*). The bone adjacent to this calcification is reacting with osteoporosis (*arrows*).

Perhaps the most painful hydroxyapatite deposition occurs in the neck in the longus colli muscle, which is the chief flexor of the cervical spine. The patient usually complains of tremendous pain on swallowing. Radiographically, one observes soft tissue swelling and amorphous calcification anterior to the C2 vertebral body just inferior to the body of the atlas (Fig. 18-8).

FIGURE 18-8 Lateral view of the upper cervical spine showing amorphous calcification inferior to the atlas and anterior to C2 lying in the longus colli muscle (*arrow*). There is adjacent soft tissue swelling.

It is now recognized that hydroxyapatite can deposit intraarticularly. Both periarticular and intraarticular deposition can lead to an arthropathy (Fig. 18-9). Most of the time an osteoarthritic radiographic picture has been described as part of the arthropathy. However, a severely destructive arthropathy has also been described involving the hand as well as the shoulder.

FIGURE 18-9 Two digits showing intra- and periarticular deposition of hydroxyapatite crystals. There is loss of the joint space, as well as erosive changes (*arrows*).

UNUSUAL MANIFESTATIONS

Deposition of HADD in the fingers may present clinically with redness and swelling that may mimic fracture or infection (Fig. 18-10). HADD may be associated with erosion of adjacent cortical bone and on rare occasion, deposition of crystal in the underlying bone marrow can be seen that leads to a diagnostic concern for osseous neoplasm. This phenomenon is most common at: (1) the posterior aspect of the proximal femur at the insertion of the gluteus maximus, (2) the insertion of the pectoralis major tendon on the anterior humerus, and (3) the greater or lesser tuberosity of the proximal humerus (Fig. 18-11).

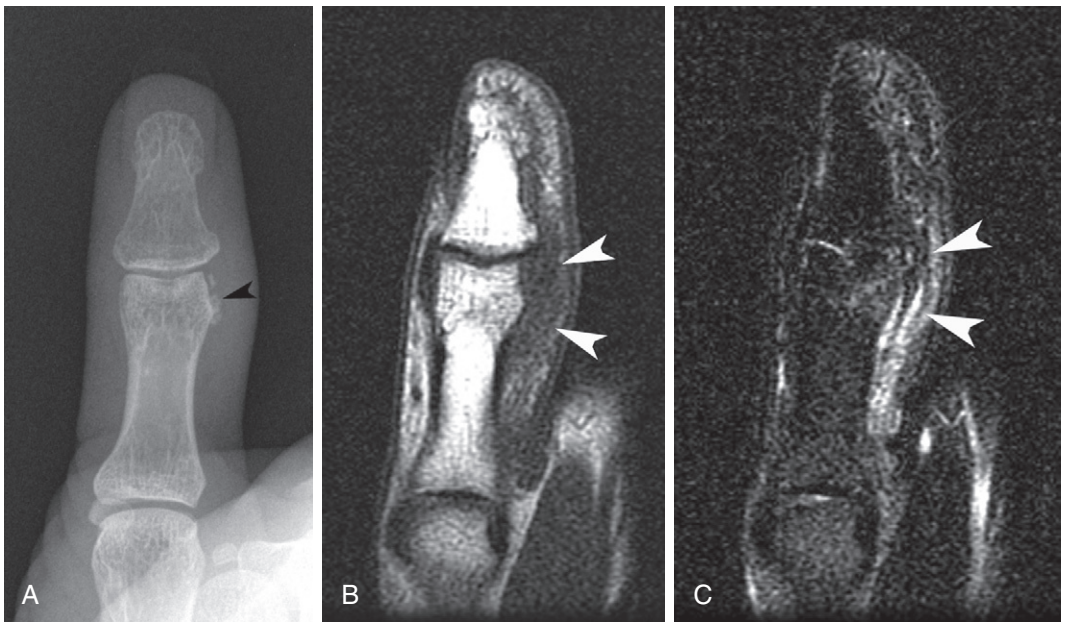

FIGURE 18-10 **A,** PA view of the thumb shows hydroxyapatite crystals in the ulnar capsule of the interphalangeal joint (*arrowhead*). Coronal T1-weighted (**B**) and fat-suppressed T2-weighted (**C**) images of the thumb show medial interphalangeal joint capsular thickening (*arrowhead*) and pericapsular edema from crystal deposition that may be confused with trauma. This underscores the importance of comparing magnetic resonance images to available plain radiographs.

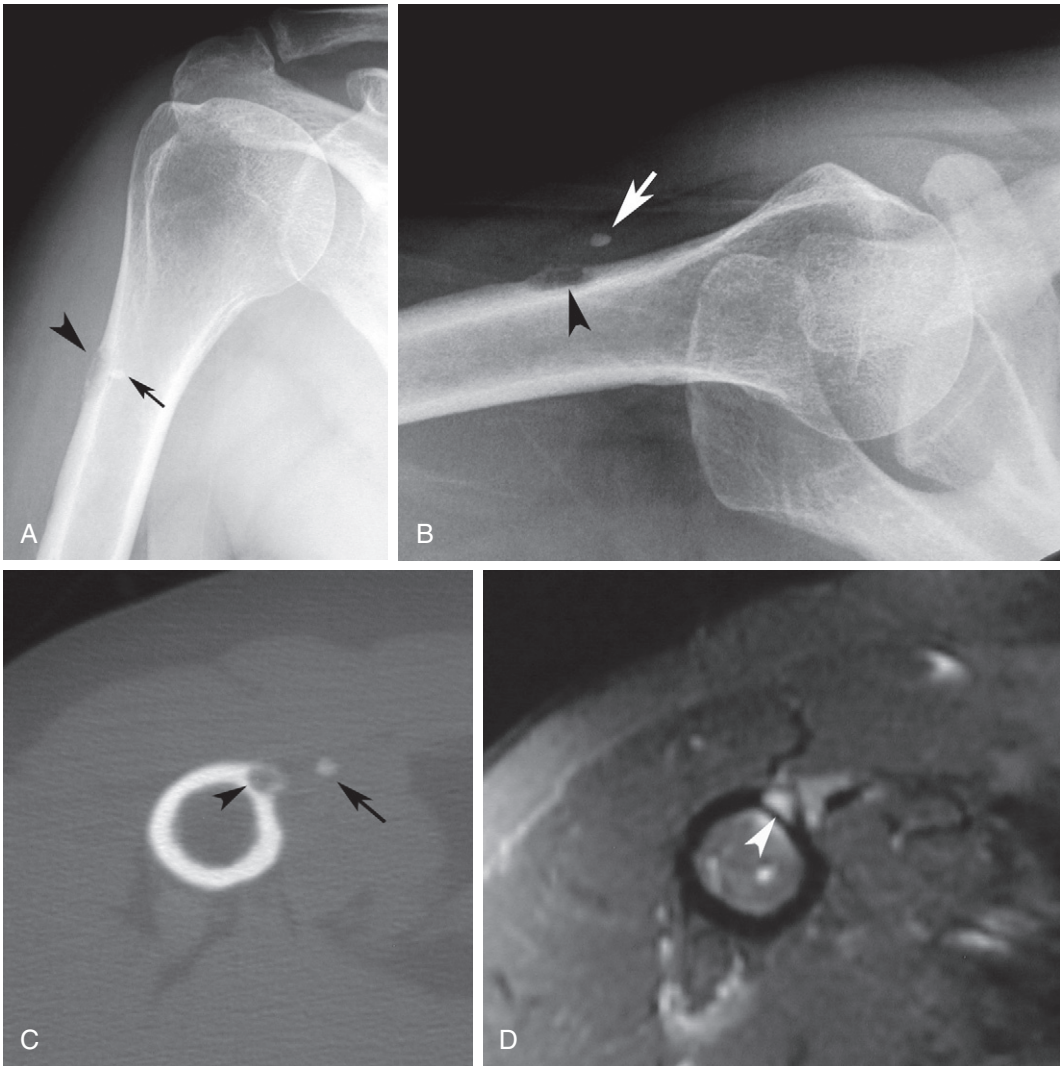

FIGURE 18-11 AP (**A**) and axial (**B**) view of the right shoulder show calcification in the soft tissues (*arrow*) adjacent to a focal erosion of the anterior cortex of the proximal humerus (*arrowhead*). **C,** Axial CT shows calcification is in pectoralis major tendon. **D,** Axial fat-suppressed T1-weighted image following intravenous contrast administration shows no mass lesion. There is enhancement of the humeral cortical erosion (*arrowhead*) and adjacent soft tissues.

SUMMARY

HADD is an extremely common disorder causing periarticular disease and only rarely causing intraarticular disease. The diagnosis is easily made by identifying calcification in the appropriate location. One must be careful to exclude an underlying systemic disease as the cause of this deposition.

SUGGESTED READINGS

Bonavita JA, Dalinka MK, Schumacher HR Jr: Hydroxyapatite deposition disease, *Radiology* 134:621–625, 1980.

Dalinka MK, et al: Periarticular calcifications in association with intra-articular corticosteroid injections (IACI), *Radiology* 153:615–618, 1984.

Dieppe PA, Doherty M, Macfarlane DG, et al: Apatite associated destructive arthritis, *Br J Rheumatol* 23:84–91, 1984.

Flemming DJ, Murphey MD, Shekitka KM, et al: Osseous involvement in calcific tendinitis: A retrospective review of 50 cases, *AJR Am J Roentgenol* 181:965–972, 2003.

Halverson PB, Carrera GF, McCarty DJ: Milwaukee shoulder syndrome: Fifteen additional cases and a description of contributing factors, *Arch Intern Med* 150:677–682, 1990.

Haun CL: Retropharyngeal tendinitis, *AJR Am J Roentgenol* 130:1137–1140, 1978.

Holt PD, Keats TE: Calcific tendinitis: A review of the usual and unusual, *Skeletal Radiol* 22:1–9, 1993.

McCarty DJ, Halverson PB, Carrera GF, et al: "Milwaukee shoulder"—association of microspheroids containing hydroxyapatite crystals, active collagenase, and neutral protease with rotator cuff defects. I. Clinical aspects, *Arthritis Rheum* 24:464–473, 1981.

Pinals RS, Short CL: Calcific periarthritis involving multiple sites, *Arthritis Rheum* 9:566–574, 1966.

Schumacher HR, Miller JL, Ludivico C, et al: Erosive arthritis associated with apatite crystal deposition, Arthritis Rheum 24:31–37, 1981.

19 Miscellaneous Deposition Diseases

Three deposition diseases are discussed in this chapter: hemochromatosis, Wilson disease, and ochronosis. Two of these diseases are extremely rare. Each has been associated with radiographic chondrocalcinosis, or calcification of hyaline or fibrous cartilage. However, if chondrocalcinosis is defined as the deposition of calcium pyrophosphate dihydrate (CPPD) crystals into hyaline or fibrous cartilage, then its association with all of these diseases becomes questionable. Whatever substance is deposited into the cartilage, degeneration and secondary osteoarthritis occur. Each of these diseases has specific changes that distinguish it from other arthropathies.

HEMOCHROMATOSIS

Primary hemochromatosis is an inherited disorder that leads to massive iron deposition throughout the body. The most common genetic defect is an autosomal recessive defect in the HFE gene on chromosome 6; 1 in 200 people of northern European descent are homozygous for this mutation. Despite the relatively common prevalence of this mutation the actual clinical presentation of hemochromatosis is relatively uncommon. The initial presenting complaint of patients with hemochromatosis is joint pain, so it is critical for radiologists to be alert for the radiographic presentation of hemochromatosis. Early recognition of this disorder can prevent hepatic fibrosis, cirrhosis, and myocardiopathy through appropriate therapeutic intervention. The arthropathy is seen in 24 to 50 percent of affected patients. The arthropathy may or may not have associated radiographic chondrocalcinosis. This raises some question about the cause of the arthropathy. Although chondrocalcinosis is frequently observed, it has not been determined whether the CPPD crystals actually cause degeneration of the cartilage or the crystals are deposited secondarily in already degenerated cartilage. It is known that iron inhibits pyrophosphatase activity in the cartilage, leading to the precipitation of CPPD crystals; however, it is not known whether the iron or the CPPD crystals cause the initial degeneration of the cartilage.

The arthropathy of hemochromatosis is almost identical to that of CPPD crystal deposition in that the radiographic picture is one of osteoarthritis in atypical sites for primary osteoarthritis. As in pyrophosphate arthropathy, subchondral cysts dominate the picture, and uniform, rather than nonuniform, loss of joint space is the rule. However, there are subtle differences that distinguish hemochromatosis from CPPD arthropathy. The radiographic findings in hemochromatosis arthropathy are:

1. Osteoporosis
2. Chondrocalcinosis—there appears to be more hyaline cartilage calcification than fibrous cartilage calcification when compared to CPPD arthropathy
3. Uniform joint space loss
4. Subchondral sclerosis
5. Subchondral cyst formation
6. Beak-like osteophytes
7. Slow progression of disease—no excessive neuropathic changes as seen in CPPD
8. Bilateral symmetrical distribution
9. Distribution in hand and wrist initially and most frequently, then knee and hip; late widespread involvement throughout the skeleton

The subtle changes that may distinguish hemochromatosis arthropathy from CPPD arthropathy are best seen in the hand and wrist.

Hand and Wrist

In the hand there is specific preference for the second and third metacarpophalangeal (MCP) joints with or without involvement of the other MCP joints and wrist (Fig. 19-1). There will be uniform loss of the joint space with subchondral sclerosis present. Small (1- to 3-mm) subchondral cysts may

be identified. There is a characteristic osteophytic beak on the medial aspect of the second and third metacarpals. There may be flattening or collapse of the heads of the metacarpals (Fig. 19-2). The fourth and fifth MCP joints may be involved, but the interphalangeal (IP) joints are usually spared. The MCP joints, particularly the fourth and fifth, are more frequently involved in hemochromatosis than they are in CPPD crystal deposition disease.

FIGURE 19-1. Posteroanterior (PA) view of the second through fifth MCP joints of a hand in patient with hemochromatosis. The fourth and fifth MCP joints are not affected. The second and third MCP joints show marked loss of the joint space. A characteristic osteophytic beak is present on the medial aspect of the head of the third metacarpal (*arrow*). There is flattening of both metacarpal heads.

FIGURE 19-2. PA view of the MCP joints in a patient with hemochromatosis. In this case all of the MCP joints are involved. There is flattening of the metacarpal heads, best illustrated in the fourth metacarpal head. There are numerous subchondral cysts present (*arrows*).

The wrist is less frequently involved in hemochromatosis than in CPPD crystal deposition disease; the distribution of the disease in the wrist also differs. Although the wrist may show involvement similar to that with CPPD arthropathy (Fig. 19-3), hemochromatosis usually involves primarily the common carpometacarpal, the midcarpal and the first carpometacarpal compartments, with sparing of the radiocarpal compartment. The changes seen are those of osteoarthritis in this distribution, with subchondral sclerosis and cyst formation.

Recognition of these findings should trigger a recommendation for screening for iron overload. This is best accomplished through assessment of serum iron transferrin saturation; a level of higher than 45 percent requires further evaluation for hemochromatosis including serum ferritin level and genetic testing.

FIGURE 19-3. PA view of the wrist. There is loss of the radiocarpal joint space with secondary osteoarthritic changes. There is no evidence of chondrocalcinosis.

Other Joints

In some patients, in the late phase of the disease there may be widespread involvement throughout the skeleton. It may be difficult to distinguish this involvement from that of CPPD arthropathy (Fig. 19-4). However, osteophytes, which have been described as "beak-like," may dominate the radiographic picture more frequently than in CPPD arthropathy. Generally the progression of the disease is very slow, whereas that in CPPD arthropathy can be extremely rapid. The kind of neuropathic changes seen in CPPD arthropathy are not seen in hemochromatosis.

FIGURE 19-4. Anteroposterior (AP) view of the hip in a patient with hemochromatosis. There is axial migration of the femoral head within the acetabulum. There is extensive subchondral cyst formation more prominent in the femoral head. There is some reparative bone present. There is no extensive osteophytosis present. This appearance resembles that of CPPD arthropathy of the hip.

WILSON DISEASE

Wilson disease is an extremely rare disease causing hepatolenticular degeneration. Copper is the substance deposited in the various tissues. The copper interferes with normal bone formation and causes osteogenic osteomalacia. An arthropathy occurs in 50 percent of affected patients; however, the arthropathy is usually a radiographic finding rather than a clinical problem.

Radiographic chondrocalcinosis has been reported very rarely in this already rare disease. However, there is some question about the etiology of the cartilage calcification. Pathologic proof of CPPD crystal deposition has not been made. In vitro studies have shown that copper ions inhibit pyrophosphatase activity in cartilage, allowing pyrophosphate dihydrate crystal deposition, but this phenomenon has yet to be proven in vivo. There is considerable bone fragmentation in the joint in Wilson disease, which could easily be mistaken for chondrocalcinosis.

The arthropathy of Wilson disease is quite distinctive, with marked irregularity to the cortical and subchondral areas of the articular surface giving a "paint brush" appearance. There is significant subchondral bone fragmentation, which in larger joints may resemble osteochondritis dissecans. Well-corticated ossicles may be seen in the joint. Other than these specific changes, the arthropathy resembles osteoarthritis in an unusual distribution for primary osteoarthritis. The arthropathy has been seen in the hand, wrist, foot, hip, shoulder, elbow, and knee.

OCHRONOSIS

Ochronosis is perhaps the oldest known metabolic disease. Patients exhibit an absence of the enzyme homogentisic acid oxidase. This absence allows the accumulation of homogentisic acid, which deposits in collagen as a dark pigment. This ochronotic pigment is believed to be a polymer of homogentisic acid. When deposited in cartilage, it causes discoloration and then eventual fragmentation of the cartilage. Ochronotic pigment is not radiodense. The calcification observed in this disease is calcium hydroxyapatite.

The arthropathy of ochronosis is not usually identified until the fourth decade. Although it is a rare arthropathy, it is radiographically distinctive. The radiographic findings are:

1. Osteoporosis—diffuse
2. Disc degeneration at multiple levels, with calcification or a vacuum phenomenon present
3. Uniform joint space loss
4. Extensive subchondral sclerosis
5. Relative absence of osteophytes
6. Intraarticular loose bodies
7. Bilateral symmetrical distribution
8. Distribution in spine, sacroiliac (SI) joints, knee, hip, and shoulder, in decreasing order of frequency

The radiographic changes divide into spinal and extraspinal manifestations. The radiographic changes in the spine have been confused with ankylosing spondylitis; those outside the spine have been confused with primary osteoarthritis or CPPD crystal deposition disease. Careful observation of the radiographic changes will prevent these errors from being made.

The Spine

The lumbar spine is the site most frequently involved and the cervical spine the least frequently involved. Ochronotic pigment deposits in the disc, causing degeneration of the disc. This disc degeneration is present at multiple levels and is manifested radiographically as loss of disc height and presence of disc calcification or the vacuum phenomenon (Fig. 19-5). The calcification seen in the disc space is not the ochronotic pigment, but calcium hydroxyapatite, as seen in any degenerative disc disease. With progressive degeneration of the disc, the actual disc space may become totally obscured. Ossification of the discs has been noted in some instances, with formation of very thick syndesmophytes between the vertebral bodies. Thus, the spine becomes ankylosed (Fig. 19-6).

The ankylosis of ochronosis may be mistaken for ankylosing spondylitis. However, in ankylosing spondylitis the syndesmophytes are thin and succinct and the disc spaces are usually maintained. Examination of the SI joints on the spine film also helps to distinguish ochronosis from ankylosing spondylitis. In ochronosis, the SI joints show changes of osteoarthritis, with narrowing, extensive sclerosis, and occasional vacuum phenomenon (Fig. 19-7). In ankylosing spondylitis, the SI joints show erosive changes followed by ankylosis.

Generalized osteoporosis of the vertebral bodies is present, except at the end-plates, where subchondral sclerosis occurs adjacent to the degenerated discs. There is a distinct lack of osteophytes present. Their absence helps to distinguish ochronosis from other diseases that cause degenerative disc disease at multiple levels.

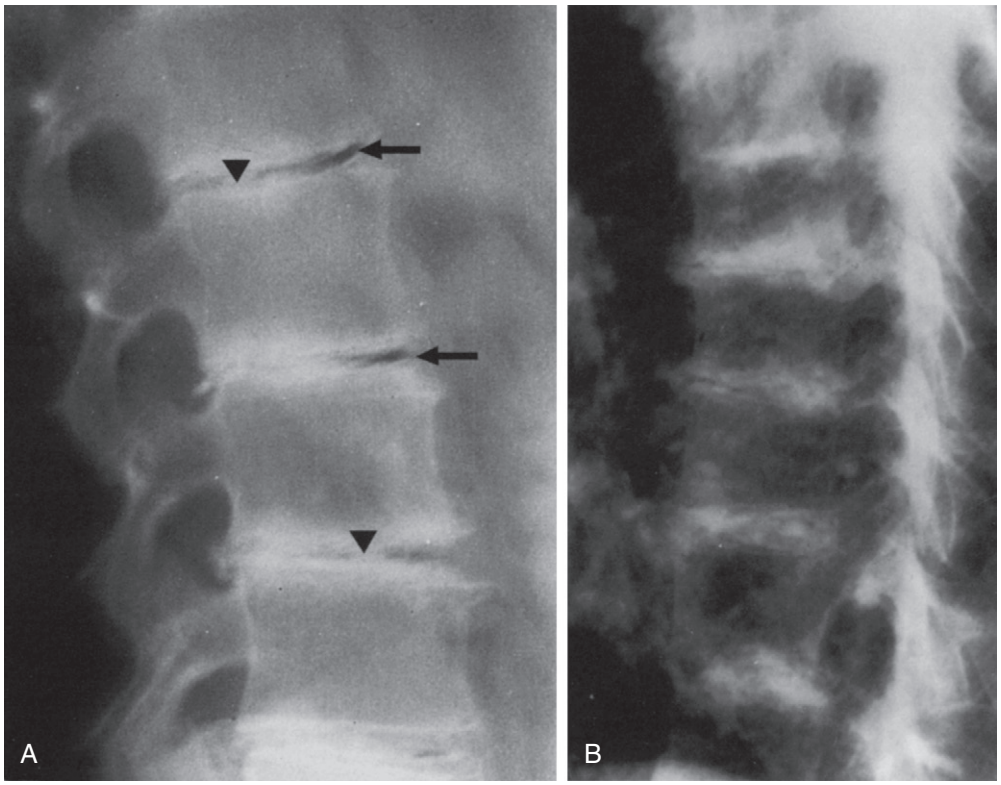

FIGURE 19-5. **A,** Lateral view of the lumbar spine showing evidence of loss of disc height at multiple levels. A vacuum phenomenon (*arrows*) and/or calcification (*arrowheads*) are seen at multiple levels. The bones are generally osteoporotic. The osteophytes are small and insignificant. **B,** Lateral view of the thoracic spine in ochronosis. The spine is generally osteoporotic. There is loss of disc height and disc calcification at all levels. There is a relative lack of osteophyte formation.

FIGURE 19-6. Lateral view of the lumbosacral spine in ochronosis. All disc spaces have been obliterated. A vacuum phenomenon is present at L2-L3 and L4-L5. At L3-L4 there has been ossification of the disc space causing ankylosis of the vertebral bodies. This appearance could be mistaken for ankylosing spondylitis except for the presence of the vacuum phenomenon at the other levels.

FIGURE 19-7. The SI joints in a patient with ochronosis. There is tremendous subchondral sclerosis on both sides of the SI joints bilaterally. There is a vacuum phenomenon present in both SI joints. There is no evidence of inflammatory erosion or bony ankylosis. These findings help to distinguish an ankylosed spine of ochronosis from that of ankylosing spondylitis.

The Knee

Outside of the spine, the knee is the most commonly involved joint in ochronosis. Chondrocalcinosis is not part of the radiographic picture. Although CPPD crystals have been identified in the synovium of the ochronotic knee, they have not been identified in the cartilage. The nonopaque ochronotic pigment deposits in the cartilage, causing degeneration. The radiographic changes are those of osteoarthritis superimposed on a uniform loss of joint space. Occasionally there is isolated lateral tibiofemoral compartment loss. The osteophytes are meager in comparison to the osteophytes seen in primary osteoarthritis (Fig. 19-8). There is a tendency toward fragmentation and the presence of multiple radiopaque intraarticular bodies. Sometimes tendinous calcification is observed.

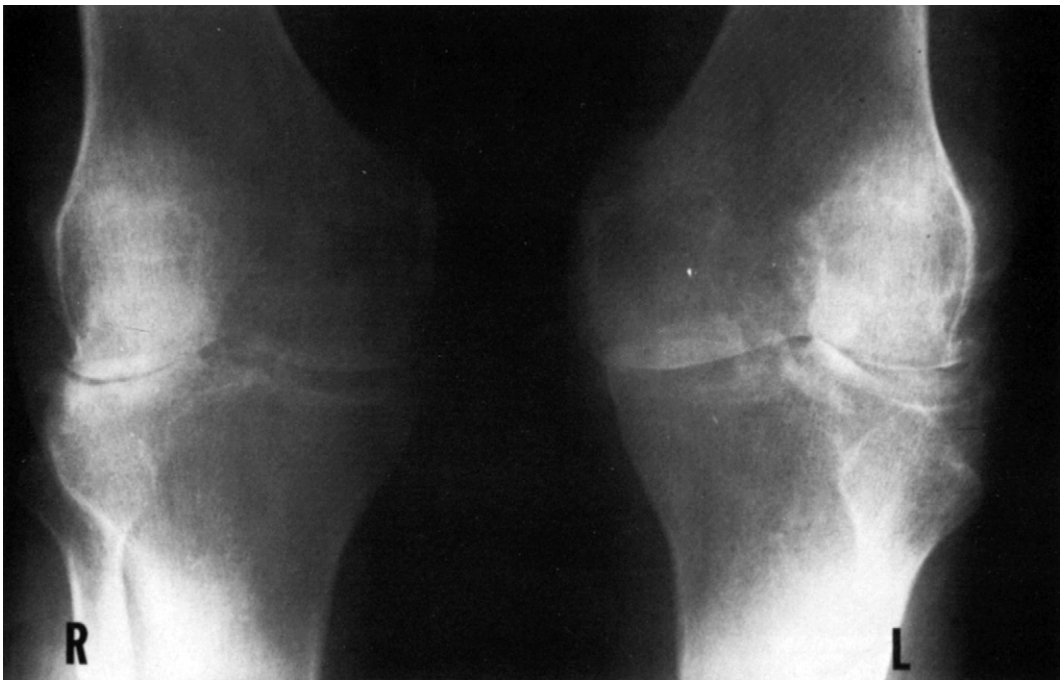

FIGURE 19-8. AP view of both knees in a patient with ochronosis. The right knee shows preferential lateral compartment narrowing. The left knee shows uniform narrowing. Subchondral bone sclerosis is superimposed upon the cartilage loss. There is minimal osteophyte formation considering the extensive loss of cartilage.

The Hip

The radiographic picture is that of osteoarthritis superimposed on uniform joint space narrowing. Again there is a lack of osteophytes, in contrast to the presence of osteophytes in primary osteoarthritis. In some patients severe destruction of the femoral head may be observed, with multiple intraarticular bodies (Fig. 19-9). The etiology of this destruction is unknown; it has been suggested that it is secondary to osteonecrosis superimposed on the ochronotic hip.

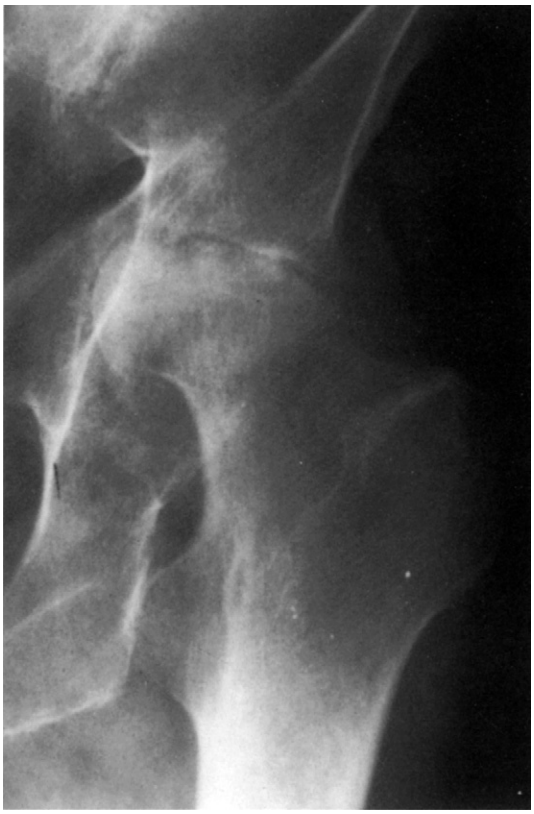

FIGURE 19-9. AP view of a hip in a patient with ochronosis. This hip demonstrates the severe destructive change that may occur in some patients with ochronosis.

The Shoulder

There is narrowing of the glenohumeral joint space with superimposed osteoarthritic changes. Fragmentation of the humeral head and tendinous calcification, if present, may help to distinguish ochronosis from osteoarthritis secondary to other deposition diseases.

SUMMARY

These three deposition diseases are relatively rare. They exhibit radiographic features of common arthropathies; however, each has distinctive features that separate it from other arthropathies. As long as the rare arthropathy is considered and the distinguishing features are observed, a correct diagnosis can be made.

SUGGESTED READINGS

Hemochromatosis

Atkins CJ, McIvor J, Smith PM, et al: Chondrocalcinosis and arthropathy: Studies in haemochromatosis and in idiopathic chondrocalcinosis, *Q J Med* 39:71–82, 1970.

Hirsch JH, Killien FC, Troupin RH: The arthropathy of hemochromatosis, *Radiology* 118:591, 1976.

Ross P, Wood G: Osteoarthropathy in idiopathic hemochromatosis, *AJR Am J Roentgenol Radium Ther Nucl Med* 109:575–580, 1970.

Schumacher HR Jr.: Hemochromatosis and arthritis, *Arthritis Rheum* 7:41–50, 1964.

Wilson Disease

Finby N, Bearn AG: Roentgenographic abnormalities of the skeletal system in Wilson's disease (hepatolenticular degeneration), *AJR Am J Roentgenol Radium Ther Nucl Med* 79:603–611, 1958.

Golding DN, Walshe JM: Arthropathy of Wilson's disease: Study of clinical and radiological features in 32 patients, *Ann Rheum Dis* 36:99–111, 1977.

Menerey KA, Eider W, Brewer GJ, et al: The arthropathy of Wilson's disease: Clinical and pathologic features, *J Rheumatol* 15:331–337, 1988.

Mindelzun R, Elkin M, Scheinberg IH, Sternlieb I: Skeletal changes in Wilson's disease: A radiological study, *Radiology* 94:127–132, 1970.

Ochronosis

Laskar RH, Sargison KD: Ochronotic arthropathy: A review with four case reports, *J Bone Joint Surg Br* 52:653–666, 1970.

O'Brien WM, LaDu BN, Bunim JJ: Biochemical, pathologic and clinical aspects of alcaptonuria, ochronosis and ochronotic arthropathy, *Am J Med* 34:813–838, 1963.

Pagan-Carlo J, Payzant AR: Roentgenographic manifestations in a severe case of alkaptonuric osteoarthritis, *Am J Roentgenol Radium Ther Nucl Med* 80:635–638, 1958.

Pomeranz MM, Friedman LJ, Tunick IS: Roentgen findings in alkaptonuric ochronosis, *Radiology* 37: 295–303, 1941.

Collagen Vascular Diseases (Connective Tissue Diseases)

20

The collagen vascular diseases (connective tissue diseases) are a group of diseases that have multiple, varied systemic manifestations. Articular symptoms play a minor role in the total clinical picture and usually produce little in the way of radiographic change in the joint. Although each disease has distinct features, there is a tendency toward overlap among the diseases. The diseases to be discussed are systemic lupus erythematosus, scleroderma, dermatomyositis, polyarteritis nodosa, and mixed connective tissue disease.

SYSTEMIC LUPUS ERYTHEMATOSUS

Systemic lupus erythematous (SLE) is the most common of the collagen vascular diseases. In this disease, articular symptoms are present in 75 to 90 percent of patients. The radiographic changes are:

1. Soft tissue swelling
2. Juxta-articular osteoporosis
3. Subluxations and dislocations
4. Absence of erosions
5. Absence of joint space loss
6. Calcification
7. Osteonecrosis
8. Bilateral and symmetrical distribution
9. Distribution in hand and wrist, hip, knee, and shoulder

The radiographic changes divide into three different categories: (1) deforming nonerosive arthritis, (2) osteonecrosis, and (3) calcification of soft tissue.

Deforming Nonerosive Arthritis

A deforming nonerosive arthritis is seen most commonly in the hands and wrists (Fig. 20-1). Early in the course of the disease, soft tissue swelling is seen, with eventual soft tissue atrophy. Juxta-articular osteoporosis is present that eventually becomes diffuse osteoporosis. When not distorted by subluxation or dislocation, the joint space appears preserved. Subluxation or dislocation without erosive disease is the hallmark of SLE. The subluxations are usually easily reducible.

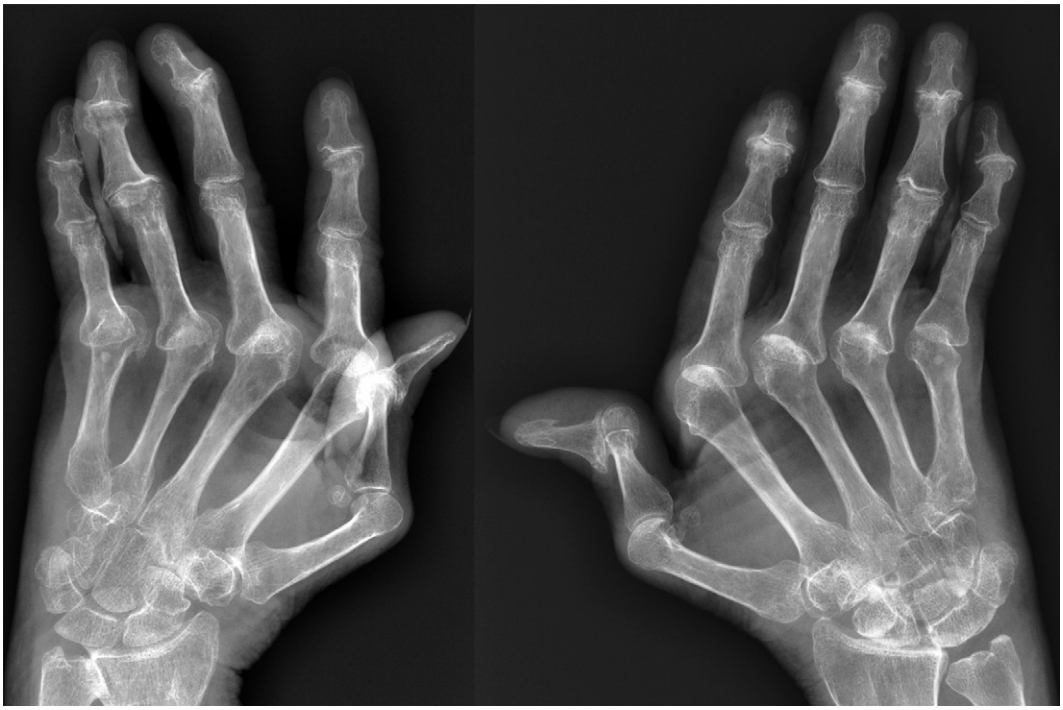

FIGURE 20-1. Posteroanterior (PA) view of both hands in a patient with SLE. Osteoporosis is present. Severe subluxations of all joints are present. There is no evidence of erosive disease. This is the classical deforming nonerosive arthritis of lupus.

Deformities may not be detected on the routine PA radiograph in which the technician has carefully positioned the digits for optimum imaging; however, on the Nørgaard view, in which the fingers are not positioned rigidly, the subluxations become apparent (Fig. 20-2). A similar deforming nonerosive arthritis may involve the knee or the shoulder, but it is more difficult to image radiographically.

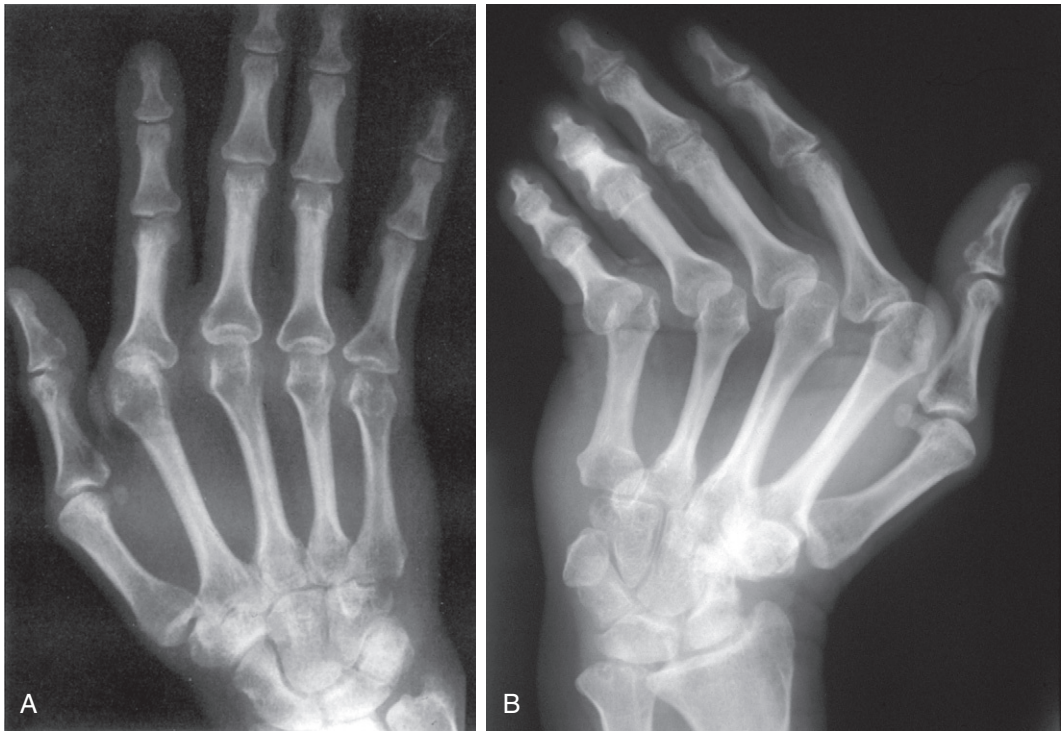

FIGURE 20-2. A, PA view of the hand in a patient with SLE. Juxta-articular osteoporosis is present. There is minimal subluxation of the MCP and PIP joints of the index finger. **B,** View of the same hand in the Nørgaard position. The fingers have not been rigidly positioned by the technician; therefore, severe subluxations of the MCP joints become apparent.

Osteonecrosis

Osteonecrosis is said to occur in 6 to 40 percent of patients with SLE. Although most of these patients are on steroids, it is known that SLE causes osteonecrosis even in the absence of steroid treatment. The patient with SLE with a significant vasculitic component who is being treated with steroids is extremely prone to osteonecrosis. The femoral heads, the humeral heads, the femoral condyles, the tibial plateaus, and the tali are the most common sites of osteonecrosis in SLE (Fig. 20-3); however, it has also been seen in the lunates, the scaphoids, and the metacarpal and metatarsal heads (Fig. 20-4). It usually occurs bilaterally and asymmetrically.

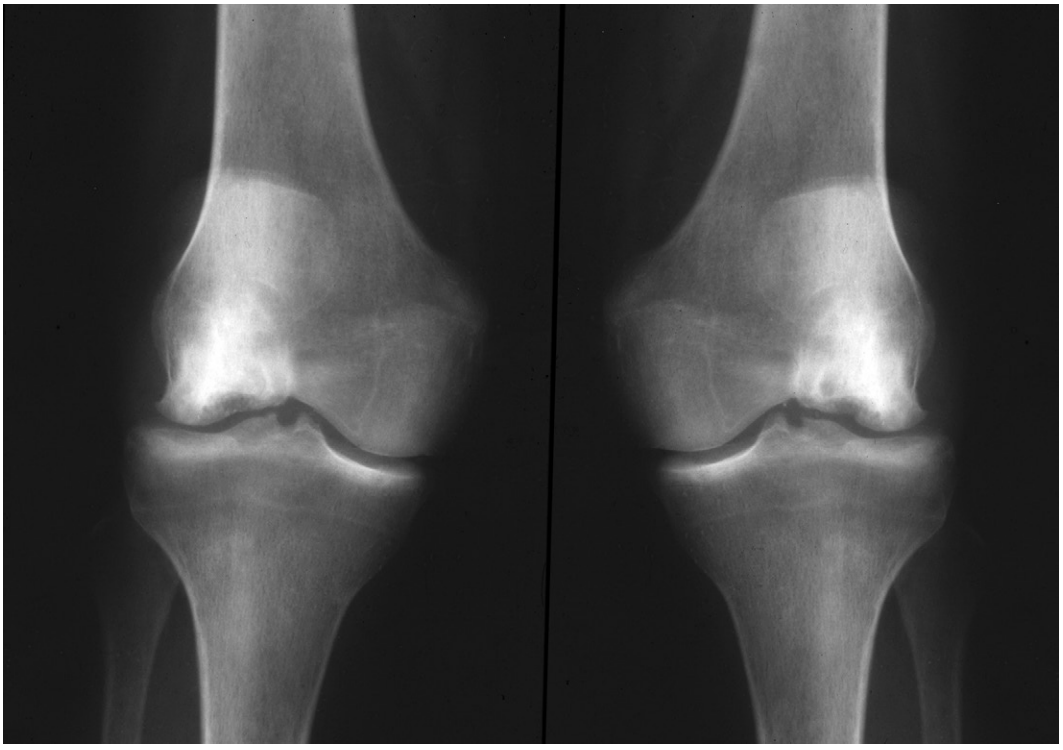

FIGURE 20-3. AP view of both knees in a patient with lupus. Osteonecrosis is observed in both lateral femoral condyles.

FIGURE 20-4. AP view of MTP joints in a patient with lupus. There is osteonecrosis present in the heads of the second and third metatarsals (*arrows*).

The radiographic findings are those observed in osteonecrosis of any etiology. Dead bone does not change radiographically. The radiographic changes observed are those of repair. The initial bone loss or osteoporosis in the repair process may not be appreciated radiographically. The first radiographic change may be increased smudgy density, which represents either dead bone that appears dense in comparison to the surrounding osteoporosis or reparative bone (Fig. 20-5). One may see a combination of osteoporosis and osteosclerosis. Advanced osteonecrosis is present when a subchondral lucency is seen (Fig. 20-6). The lucency is created by vacuum introduced between a distracted subchondral fragment and the remaining femoral head. It represents impending collapse of the articular segment into the underlying bone, if it has not already occurred. Once the articular surface has been deformed, the actual joint undergoes secondary osteoarthritic changes.

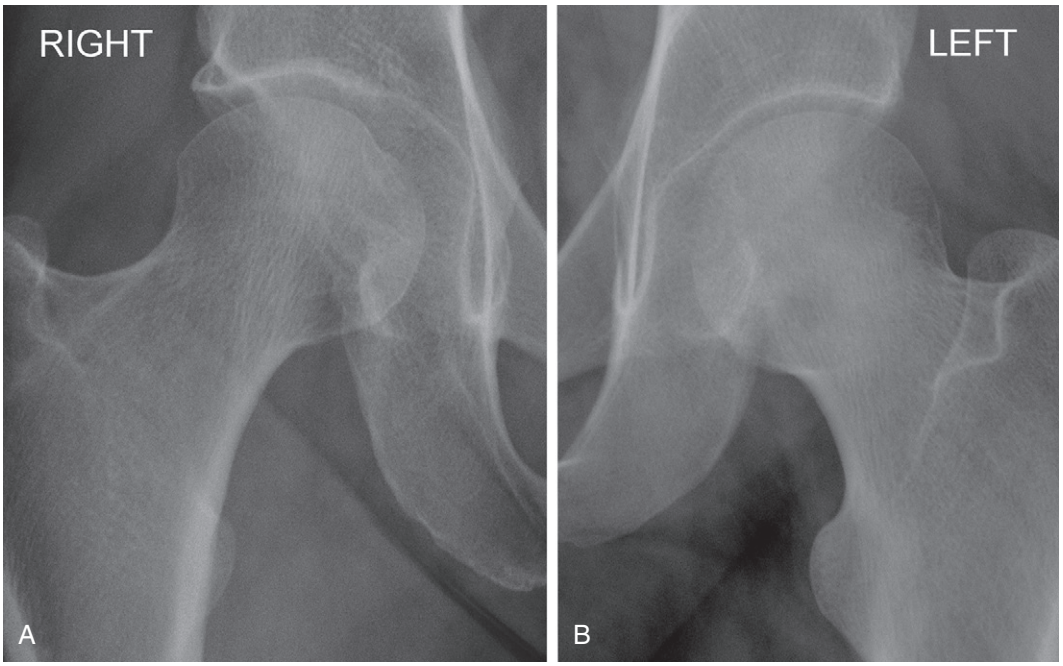

FIGURE 20-5. AP view of both hips in a patient with lupus. The right hip is normal. Increased smudgy density is observed in the left femoral head. This is an early radiographic change of osteonecrosis.

FIGURE 20-6. Specimen radiograph of a femoral head with advanced osteonecrosis. (The specimen was surgically removed from a patient with SLE.) There is a combination of osteoporosis and osteosclerosis present. A large subchondral lucency or vacuum separates the detached subchondral fragment from the underlying collapsed bone.

Calcification

Calcification may be present in the subcutaneous tissue in patients with SLE. It is usually linear and streaky in its appearance. There is no definite association of this calcification with the deforming nonerosive arthritis or with the osteonecrosis. If seen alone, this calcification is difficult to differentiate from that of other collagen vascular diseases.

SCLERODERMA

Forty-six percent of patients with scleroderma have articular symptoms. The radiographic changes appear to be limited to the hands and wrists. The radiographic changes are:

1. Resorption of soft tissue of the fingertip
2. Subcutaneous calcification
3. Erosion of the distal tuft
4. Acrosclerosis

The first visible radiographic change is the resorption of the soft tissue of the fingertip. In the normal finger, the soft tissues distal to the distal tuft usually measure 20 percent of the transverse dimension of the base of the distal phalanx (Fig. 20-7). This may or may not be accompanied by amorphous calcification (Fig. 20-8). Of the fingers involved, 40 to 80 percent have erosion of the distal tuft (acroosteolysis). It begins on the palmar aspect of the tuft and may progress to resorb the entire distal tuft (Fig. 20-9). Erosive disease can be seen in up to 25 percent of patients most commonly in the interphalangeal (IP) joints or the first carpometacarpal joint (Fig. 20-10).

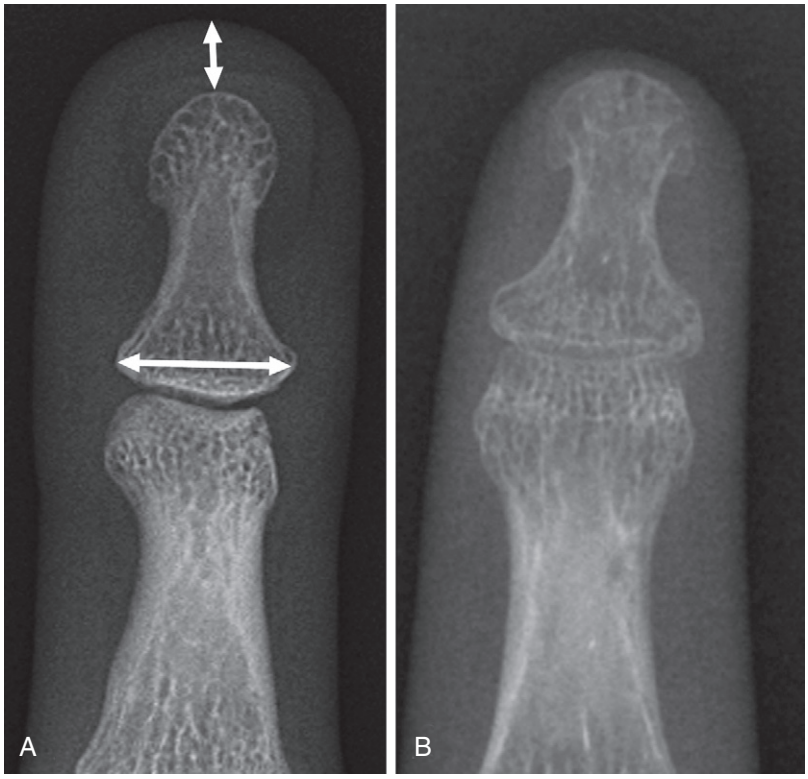

FIGURE 20-7. PA view of normal index finger (**A**) shows normal soft tissue (*short arrow*) distal to the distal tuft measuring more than 20 percent of the width of the distal phalanx (*long arrow*). PA view of index finger in patient with scleroderma (**B**) shows marked atrophy of distal soft tissues.

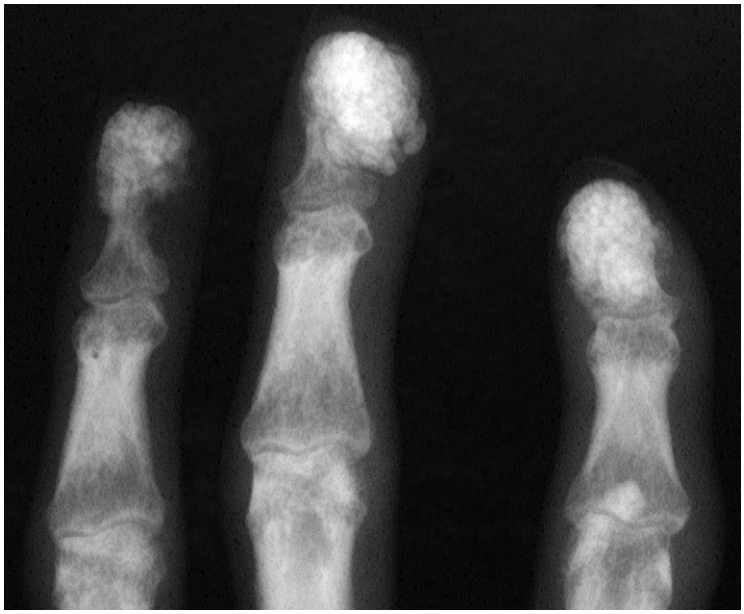

FIGURE 20-8. PA view of three digits in patient with scleroderma. There is amorphous calcification in the soft tissues of the distal phalanges. There are accompanying erosive changes of the distal tuft.

FIGURE 20-9. PA view of three digits in patient with scleroderma. There is amorphous calcification present in the soft tissues. Early resorption of the distal tuft is seen in the middle digit (*arrow*).

FIGURE 20-10. PA view of the hand in patient with scleroderma. Erosions and joint space loss are seen in the second MCP joint (arrows). There is pancarpal joint space loss with sclerosis and collapse of the lunate secondary to avascular necrosis. There is marked distal soft tissue atrophy of the second and third digits and acro-osteolysis of the thumb distal phalanx.

DERMATOMYOSITIS

In patients with dermatomyositis, the radiographic abnormality most commonly observed is soft tissue calcification (Fig. 20-11). This is present more often in children than in adults. It is usually identified along intermuscular fascial planes, but it may be present around joints or subcutaneously. If articular symptoms are present, then there are usually no radiographic findings around the joint. Sometimes transient osteoporosis may be seen, and there have been occasional reports of distal tuft resorption similar to that seen in scleroderma.

FIGURE 20-11. AP view of the thigh in dermatomyositis. Calcification is seen along intermuscular fascial planes as well as in subcutaneous tissue.

POLYARTERITIS NODOSA

The only radiographic change reported in polyarteritis nodosa is periosteal new bone formation. This has been limited primarily to the tibia and fibula and has appeared in a symmetrical fashion.

MIXED CONNECTIVE TISSUE DISEASE

Mixed connective tissue disease (MCTD) was originally defined in a patient having a combination of SLE and scleroderma. Today, a patient with MCTD may have features of SLE, scleroderma, and rheumatoid arthritis. The disease entity is defined serologically. Radiographically, the patient may have features of all three diseases involving primarily the hands, wrists, and feet. The radiographic features of scleroderma are soft tissue atrophy, calcification, and distal tuft resorption. Those of SLE are osteoporosis, subluxations, and/or osteonecrosis. Those of rheumatoid arthritis are erosive disease and joint space loss. In contrast to rheumatoid arthritis, the erosive disease may include the distal interphalangeal (DIP) joints as well as the proximal interphalangeal (PIP) joints, metacarpophalangeal (MCP) joints, and carpal joint spaces. One should identify at least one feature of scleroderma and one feature of lupus in order to make the diagnosis radiographically (Fig. 20-12). In some patients there is a unique feature of preferential ankylosis of the capitate to the trapezoid.

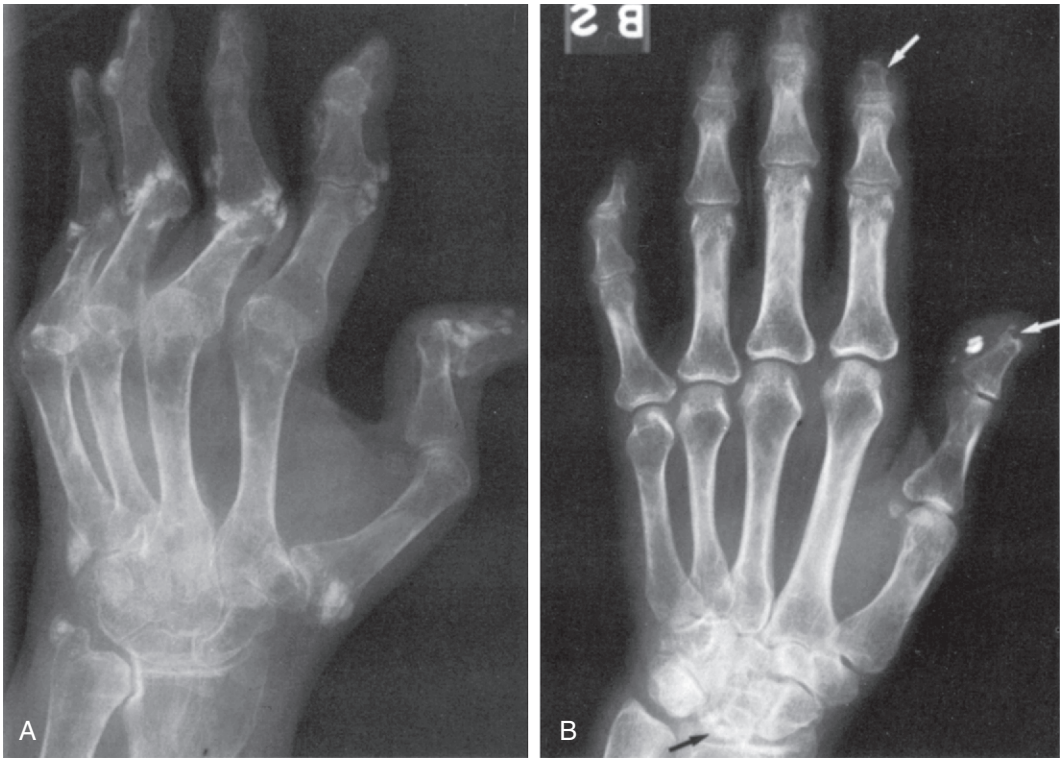

FIGURE 20-12. **A,** PA view of a hand in a patient with MCTD. There is diffuse osteoporosis present, with subluxations of the MCP and PIP joints. These are radiographic manifestations of SLE. There is also amorphous calcification in the soft tissues and loss of soft tissue in the distal phalanges. These are radiographic features of scleroderma. The combination is observed in MCTD. **B,** PA view of the hand in a patient with MCTD. There is osteonecrosis of the lunate (*black arrow*), a radiographic feature of lupus. There is amorphous calcification in the soft tissue of the thumb and resorption of the distal tufts of the thumb and index finger (*white arrows*). These are radiographic features of scleroderma. The combination is observed in MCTD.

SUMMARY

Although the collagen vascular diseases have individual specific manifestations, there is a tendency to overlap among the diseases. MCTD is a demonstration of this overlap; however, it is defined as a distinct entity serologically and should not be confused with the general overlap among these disease entities.

SUGGESTED READINGS

Aptekar RG, Klippel JH, Becker KE, et al: Avascular necrosis of the talus, scaphoid, and metatarsal head in systemic lupus erythematosus, *Clin Orthop Relat Res* 101:127–128, 1974.

Brower AC, Resnick D, Karlin C, et al: Unusual articular changes of the hand in scleroderma, *Skeletal Radiol* 4:119, 1979.

Budin JA, Feldman F: Soft tissue calcifications in systemic lupus erythematosus, *Am J Roentgenol Radium Ther Nucl Med* 124:358–364, 1975.

Fraser GM: The radiological manifestations of scleroderma (diffuse systemic sclerosis), *Br J Dermatol* 78:1–14, 1966.

Green N, Osmer JC: Small bone changes secondary to systemic lupus erythematosus, *Radiology* 90:118–120, 1968.

Klippel JH, Gerber LH, Pollak L, et al: Avascular necrosis in systemic lupus erythematosus: Silent symmetric osteonecrosis, *Am J Med* 67:83, 1979.

Labowitz R, Schumacher HR Jr: Articular manifestations of systemic lupus erythematosus, *Ann Intern Med* 74:911–921, 1971.

Saville PD: Polyarteritis nodosa with new bone formation, *J Bone Joint Surg Br* 38-B:327–333, 1956.

Silver TM, Farber SJ, Bole GG, et al: Radiological features of mixed connective tissue disease and scleroderma-systemic lupus erythematosus overlap, *Radiology* 120:269–275, 1976.

Steiner RM, Glassman L, Schwartz MW, et al: The radiological findings in dermatomyositis of childhood, *Radiology* 111:385–393, 1974.

Tuffanelli DL, Winkelmann RK: Systemic scleroderma: Clinical study of 727 cases, *Arch Dermatol* 84:359–371, 1961.

Udoff EJ, Genant HK, Kozin F, et al: Mixed connective tissue disease: The spectrum of radiographic manifestations, *Radiology* 124:613–618, 1977.

Weissman BN, Rappoport AS, Sosman JL, et al: Radiographic findings in the hands in patients with systemic lupus erythematosus, *Radiology* 126:313–317, 1978.

Yune HY, Vix VA, Klatte EC: Early fingertip changes in scleroderma, *JAMA* 215:1113–1116, 1971.

Juvenile Idiopathic Arthritis 21

There are a variety of disorders that affect the joints in children. In the past all of the disorders have been lumped together and labeled juvenile rheumatoid arthritis. Although each disorder has different clinical and radiographic manifestations and course, it may be impossible to distinguish one disorder from another at a specific time within the course of the disease. Therefore, the better term "juvenile idiopathic arthritis" has been applied to these disorders.

Juvenile idiopathic arthritis (JIA) includes juvenile-onset ankylosing spondylitis, psoriatic arthritis, inflammatory bowel disease, juvenile-onset adult-type (seropositive) rheumatoid arthritis, and Still's disease (seronegative chronic arthritis). All of these disorders, except for Still's disease, tend to occur in older children and therefore usually behave like their adult counterpart. Juvenile-onset adult-type (seropositive) rheumatoid arthritis differs from adult rheumatoid arthritis in two ways. First, a periostitis is frequently present in the metaphyses of the phalanges, metacarpals, and metatarsals. Second, there is significant erosive disease without joint space loss.

Still's disease (seronegative chronic arthritis) makes up 70 percent of the cases of JIA. There are three different clinical presentations of Still's disease, with some crossover within these three groups: (1) classic systemic disease with little to no radiographic articular changes, (2) polyarticular disease with less severe systemic manifestations, and (3) pauciarticular or monoarticular disease with infrequent systemic manifestations. Some of the children with pauciarticular or monoarticular disease progress to polyarticular disease. In all presentations the children are younger than those with other types of JIA. Because the articular changes are occurring in rapidly growing bones, the radiographic changes are quite different from those in the older child. The articular radiographic changes in Still's disease are as follows:

1. Periarticular soft tissue swelling
2. Osteoporosis—juxta-articular, metaphyseal lucent bands, or diffuse
3. Periostitis
4. Overgrown or ballooned epiphyses
5. Advanced skeletal maturation—premature fusion leading to decreased bone length
6. Late joint space loss
7. Late erosive disease
8. Ankylosis
9. Bilateral and symmetrical distribution in polyarticular disease; sporadic distribution in pauciarticular or monoarticular disease
10. Distribution in hand and wrist, foot, knee, ankle, hip, cervical spine, and mandible, in decreasing order in polyarticular disease; distribution in knee, ankle, elbow, and wrist in pauciarticular or monoarticular disease

The radiographic changes are those of chronic inflammation and hyperemia in a joint that is undergoing growth and change. The changes described may occur in any type of JIA if the disease begins at an early enough age.

THE HAND AND WRIST

The hand is less frequently involved than the wrist. The distribution of the disease within the hand differs from that of adult rheumatoid arthritis in that the distal interphalangeal (DIP) joints are involved as well as the proximal interphalangeal (PIP) joints and metacarpophalangeal (MCP) joints (Fig. 21-1). In early involvement there is periarticular soft tissue swelling and juxta-articular osteoporosis. In 23 percent of patients, a periostitis is present along the metaphyses and diaphyses of the phalanges and metacarpals (Fig. 21-2). As the disease persists, there is overgrowth and ballooning of the epiphyses (Fig. 21-3). Premature fusion of the growth plate follows, leading to brachydactyly (Fig. 21-4). However, despite these changes there is usually a noticeable absence of erosive disease, and the joint spaces tend to be preserved. With continuing osteoporosis, epiphyseal compression fractures develop, leading to flattening of the metacarpal heads and "cupping" of the proximal phalangeal ossification centers (Fig. 21-5). Even now growth deformity, rather than erosive disease, remains the prominent part of the radiographic picture.

FIGURE 21-1 Posteroanterior (PA) view of a hand in patient with JIA. There is generalized osteoporosis. There is some overgrowth of the articulating ends of the bones of the MCP joints and all IP joints.

FIGURE 21-2 PA view of the second finger in patient with JIA. There is soft tissue swelling centered on the MCP joint and osteoporosis of the second digit. There is periosteal reaction involving the distal second metacarpal.

FIGURE 21-3 PA view of the hand in patient with JIA. There is juxta-articular osteoporosis around all joints visualized. There is overgrowth of the articular ends of the bones of the MCP joints, PIP joints, and radius and ulna. There is pancarpal joint space narrowing of the wrist without erosions.

FIGURE 21-4 PA view of a hand in patient with JIA. There is diffuse osteoporosis. There is overgrowth of the metacarpal heads with premature fusion of the third metacarpal, leading to severe brachydactyly.

FIGURE 21-5 PA view of the hand in a patient with Still's disease. There is diffuse osteoporosis present. There is soft tissue swelling around the wrist, MCP joints, and all IP joints. There is deformity of the epiphyses secondary to compression fractures (*arrows*), and there is cupping of the proximal phalangeal ossification centers (*arrowheads*). The changes are primarily due to growth deformities rather than erosive changes.

The wrist is commonly involved. Early in the disease there is soft tissue swelling and juxta-articular osteoporosis. With persistence of the disease process, there is acceleration of growth maturation in the wrist, as seen by increase in the size of the carpal bones. The carpal bones become irregular in their contour secondary to erosions occurring at a young age and repairing with growth (Fig. 21-6). Nineteen percent of patients demonstrate ankyloses at the wrist. Usually one of the three compartments of the wrist is not ankylosed. Most frequently the common carpometacarpal and midcarpal compartments are ankylosed, with total sparing of the radiocarpal compartment (Fig. 21-7).

FIGURE 21-6 PA view of the wrist in a patient with Still's disease. The carpal bones are very irregular in their contour secondary to erosions occurring at a young age with subsequent repair.

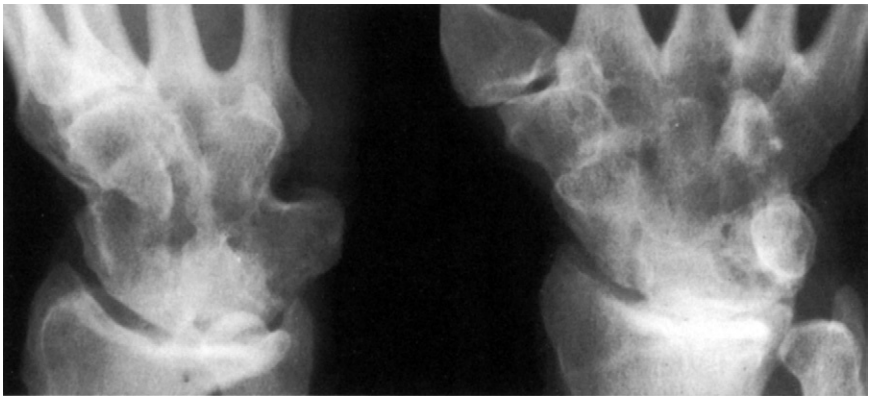

FIGURE 21-7 PA and oblique views of the wrist in a patient with Still's disease. There is ankylosis of the common carpometacarpal compartment and the midcarpal compartment. The radiocarpal compartment remains open.

THE FOOT AND ANKLE

The changes seen in the foot are similar to those seen in the hand. Initially there is soft tissue swelling and juxta-articular osteoporosis around the IP and metatarsophalangeal (MTP) joints. Periostitis may involve the metaphyses and diaphyses of the proximal phalanges and metatarsals. Eventually there is epiphyseal overgrowth with premature fusion of the growth plate and brachydactyly (Fig. 21-8). Involvement of the tarsal bones is similar to involvement of the carpal bones. The tarsals are irregular in their shape and contour. They may be enlarged. Bony ankylosis occurs here as it does in the carpal bones (Fig. 21-9). In the ankle, there may be a tibiotalar tilt secondary to overgrowth of the epiphysis and premature closure of the epiphyseal plate (Fig. 21-10).

FIGURE 21-8 Anteroposterior (AP) view of the foot in patient with JIA. There is diffuse osteoporosis. The metatarsal heads are overgrown with shortening of the third and fourth metatarsals. The fifth metatarsal head is flattened from subchondral fracture.

FIGURE 21-9 Lateral view of the ankle in a patient with JIA demonstrates ankylosis of the tarsal joints except at the tarsometatarsal compartment. There is also overgrowth of the articulating end of the tibia.

FIGURE 21-10 AP view of the ankle in a patient with JIA. There is overgrowth of the tibial and fibular epiphyses. The tibiotalar joint is slanted laterally.

THE KNEE

The knee is the joint most commonly affected in pauciarticular or monoarticular disease, and it is very frequently involved in polyarticular disease. Early in the course of the disease, soft tissue swelling and juxta-articular osteoporosis are present. In the knee, a metaphyseal lucent band, similar to that seen in leukemia, may be observed as a manifestation of juxta-articular osteoporosis. This is thought to be secondary to increased metaphyseal bone blood flow in the child, which accompanies increased blood flow to the inflamed synovium. Persistent hyperemia in and around the joint causes overgrowth of the femoral and tibial epiphyses (Fig. 21-11). There is widening of the intercondylar notch secondary to overgrowth of the femoral condyles. There is overgrowth of the patella with either elongation or squaring of its configuration. The radiographic changes in the knee are similar

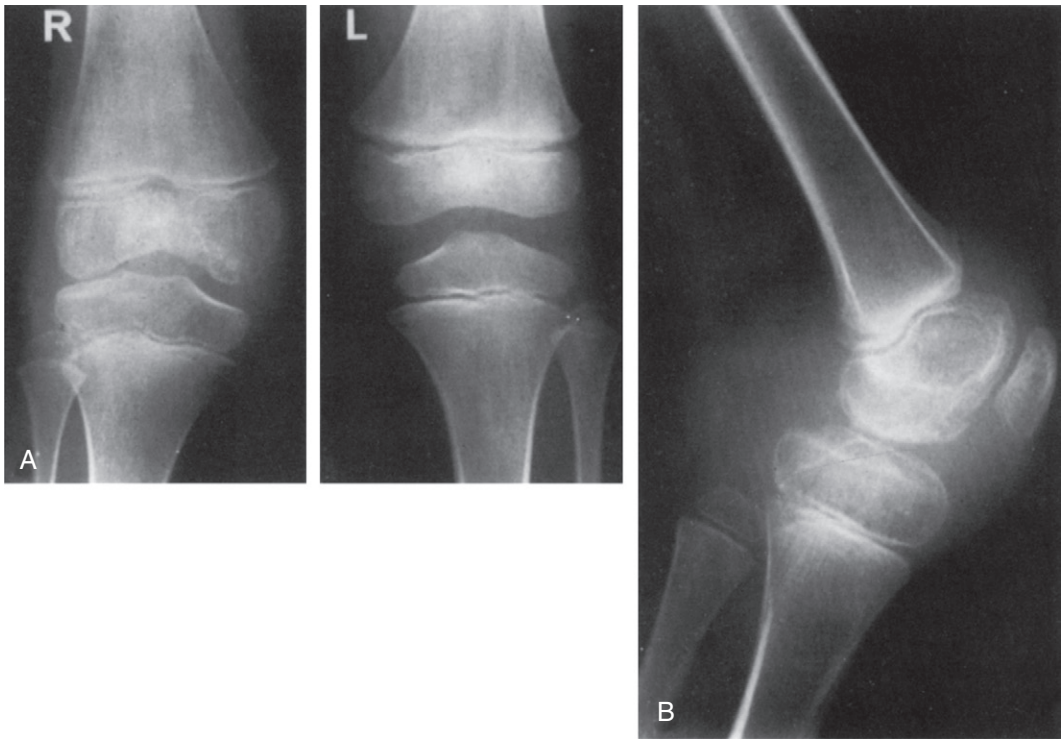

FIGURE 21-11 **A,** AP standing view of both knees in a patient with monoarticular disease. The left knee is normal. The right knee, although held in a somewhat flexed position, demonstrates overgrowth of the femoral and tibial epiphyses. The intracondylar notch appears widened. **B,** Lateral view of the involved knee showing a large synovial effusion. Again there is overgrowth of the epiphyses. In addition, there are overgrowth and elongation of the patella.

to those seen in hemophilia. Some authors have described the overgrown patella in hemophilia as more squared in appearance than in JIA. There also tend to be more cysts in the knee of a patient with hemophilia secondary to intraosseous bleeding. With persistent osteoporosis there are epiphyseal compression fractures, causing a flattened appearance of the femoral condyles. In severe involvement of the knee, there may be joint space narrowing and osseous erosions (Fig. 21-12).

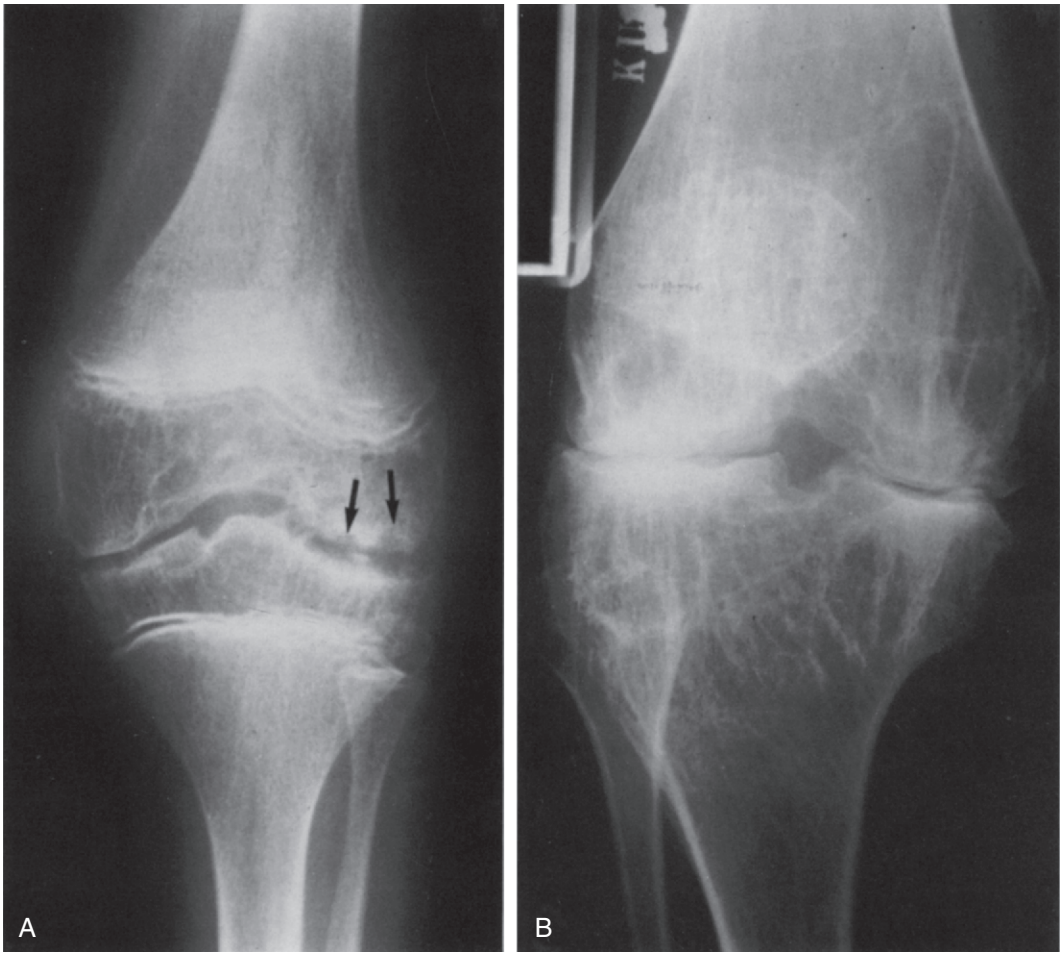

FIGURE 21-12 **A,** AP view of a knee in a patient with JIA. Soft tissue swelling is seen around the knee. There is overgrowth of the epiphyses and widening of the intracondylar notch. The joint space has become somewhat narrowed. The femoral condyles have become flattened. Osseous erosions are observed (*arrows*). **B,** AP view of the knee in an adult who had JIA. There is overgrowth of the articulating ends of the bones, indicating previous overgrowth of the epiphyses and premature fusion. There is total loss of the joint space. There is flattening of the condyles. Superimposed osteoarthritic changes are present.

THE HIP

The hip is less frequently involved in Still's disease; however, it is commonly involved in the other types of JIA. Again, the early change is juxta-articular osteoporosis. With time there is enlargement of the femoral epiphysis with premature fusion of the growth plate (Fig. 21-13). The femoral head may become irregular in its outline secondary to compression fractures and erosive changes (Fig. 21-14). In advanced disease, uniform joint space loss occurs with resultant protrusion of the acetabulum. Erosive changes become prominent (Fig. 21-15). In the very young patient, involvement of the hip may be accompanied by hypoplasia of the ilium and a coxa valga deformity of the proximal femur.

FIGURE 21-13 AP view of the hip in a patient with early monoarticular disease. There is severe osteoporosis of the bony structures. The femoral head is enlarged, with its lateral margin extending beyond the articulating acetabular surface. There is evidence of beginning fusion of the epiphyseal plate, which is premature for this patient.

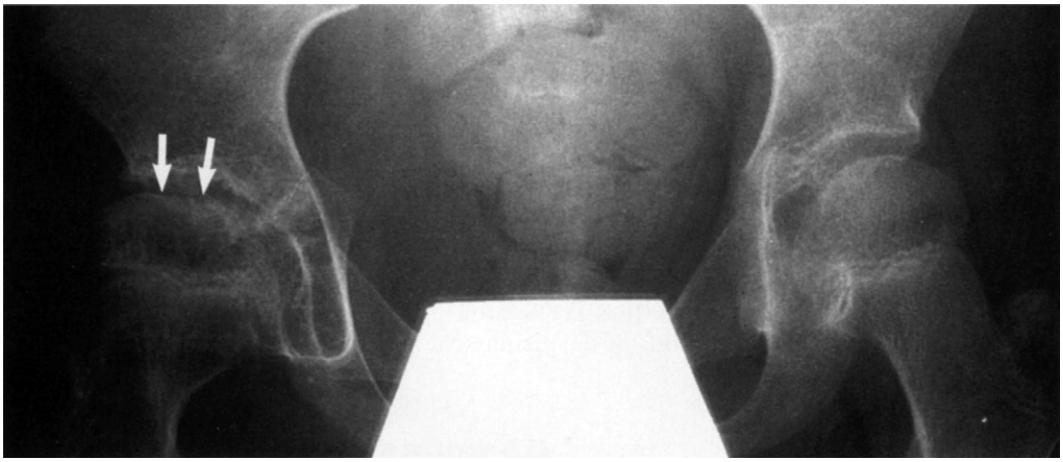

FIGURE 21-14 AP view of the pelvis in a patient with polyarticular JIA. Although both hips are involved, the right is more severely involved than the left. The right hip is more osteoporotic. The femoral head is irregular in its outline secondary to compression fractures (*arrows*).

FIGURE 21-15 AP view of the pelvis in patient with advanced disease of the hip joints. Erosive disease is present in both hips. Protrusion of the acetabulum has occurred on the right side. There is some atrophy of the left ilium.

THE CERVICAL SPINE

Atlantoaxial subluxation or odontoid erosion, as seen in adult rheumatoid arthritis, is common in juvenile-onset adult-type (seropositive) rheumatoid arthritis but is uncommon in Still's disease. In Still's disease the apophyseal joints are involved, with ankylosis beginning in the upper cervical spine. The apophyseal joint of C2-C3 is the most commonly ankylosed. The lower cervical spine is rarely involved and never without involvement of the upper cervical spine. With the ankylosis of the apophyseal joints there is decrease in the size of the adjoining vertebral bodies and decrease in the disc space (Fig. 21-16). This decrease in size of the vertebral bodies is believed to be secondary to the ankylosis of the apophyseal joints occurring at a very young age. It is not seen in juvenile-onset ankylosing spondylitis, in which the ankylosis of the apophyseal joints occurs at a much older age.

FIGURE 21-16 Lateral view of the neck in a child with JIA. There is total ankylosis of the apophyseal joints from C2 through C5. The apophyseal joints of C5-C6 and C6-C7 remain open.

THE MANDIBLE

Ten to 20 percent of the children with Still's disease have underdevelopment of the mandible. There is shortening of the body and the vertical rami of the mandible. A concavity develops on the undersurface of the mandibular body just anterior to the angular process, which is called antegonial notching (Fig. 21-17). The condyles of the mandible are flattened and poorly developed. This may or may not lead to temporomandibular joint (TMJ) changes.

FIGURE 21-17 Lateral view of the cervical spine in a patient with JIA. There is ankylosis of the C2-C3 apophyseal joints and the posterior edge of the vertebral bodies. There is also antegonial notching of the mandible (*arrows*).

SUMMARY

The radiographic changes in JIA depend upon the age of onset of the specific disease. If the disease begins in the older child, the radiographic findings mimic the similar adult arthropathy. If the disease onset is in the young child, growth disturbances, rather than joint space loss and erosion, become the predominant picture.

SUGGESTED READINGS

Ansell BM: Chronic arthritis in childhood, *Ann Rheum Dis* 37:107–120, 1978.

Ansell BM, Kent PA: Radiological changes in juvenile chronic polyarthritis, *Skeletal Radiol* 1:129–144, 1977.

Becker MH, Coccaro PJ, Converse JM: Antegonial notching of mandible: An often overlooked mandibular deformity in congenital and acquired disorders, *Radiology* 121:149–151, 1976.

Chaplin D, Pulkki T, Saarimaa A, Vainio K: Wrist and finger deformities in juvenile rheumatoid arthritis, *Acta Rheum Scand* 15:206–223, 1969.

Jacqueline F, Boujot A, Canet L: Involvement of hips in juvenile rheumatoid arthritis, *Arthritis Rheum* 4:500–513, 1961.

Martel W, Holt JF, Cassidy JT: Roentgenologic manifestations of juvenile rheumatoid arthritis, *Am J Roentgenol Radium Ther Nucl Med* 88:400–423, 1962.

Myall RWT, West RA, Horwitz H, Schaller JG: Jaw deformity caused by juvenile rheumatoid arthritis and its correction, *Arthritis Rheum* 31:1305–1310, 1988.

Reed MH, Wilmot DM: The radiology of juvenile rheumatoid arthritis: A review of the English language literature, *J Rheumatol Suppl* 31:2–22, 1991.

Sairanen E: On rheumatoid arthritis in children: a clinico-roentgenological study, *Acta Rheum Scand Suppl* 4:1–79, 1958.

22 *Hemophilia*

The joint changes in hemophilia are secondary to chronic repetitive hemarthrosis and intraosseous bleeding. Hemarthrosis occurs in 75 to 90 percent of patients with hemophilia. The first bleed usually occurs between the ages of 2 and 3. Repetitive bleeding episodes occur between the ages of 8 and 13, with 50 percent of patients developing permanent bone changes around the joint. The radiographic change in the joint depends upon the age of the patient at the time of the bleed, the site of the bleed, and the acuteness or chronicity of the bleed. The articular changes in hemophilia are as follows:

1. Radiodense soft tissue swelling
2. Osteoporosis—juxta-articular or diffuse
3. Overgrown or ballooned epiphyses
4. Subchondral cysts
5. Late uniform joint space loss
6. Late secondary osteoarthritic changes
7. Asymmetrical sporadic distribution
8. Distribution in knee, elbow, ankle, hip, and shoulder, in decreasing order; changes distal to the elbow or ankle are rare

Radiographic changes of hemophilia resemble those of juvenile idiopathic arthritis (JIA) except that there is usually no periostitis or bone ankylosis.

THE KNEE

The knee is the joint most commonly involved in hemophilia. In the acute hemarthrosis, joint effusion and juxta-articular osteoporosis are observed. If chronic bleeding occurs, the joint effusion becomes radiodense (Fig. 22-1). Chronic hyperemia to the joint leads to overgrowth or ballooning of the femoral and tibial epiphyses. The overgrowth of the femoral condyles causes widening of the intercondylar notch. This widening may be accentuated by the position of the knee, which is frequently held in fixed flexion. The condyles may appear flattened. The patella is ballooned and

squared inferiorly. Multiple subchondral cysts are usually visualized in the epiphyses (Fig. 22-2). If the chronic bleeding occurs in an older child, then the overgrowth of the epiphyses and widening of the intracondylar notch may not be as apparent as it is in the younger child (Fig. 22-3). In chronic phases of the disease, there may be uniform joint space loss with secondary osteoarthritic changes (Fig. 22-4).

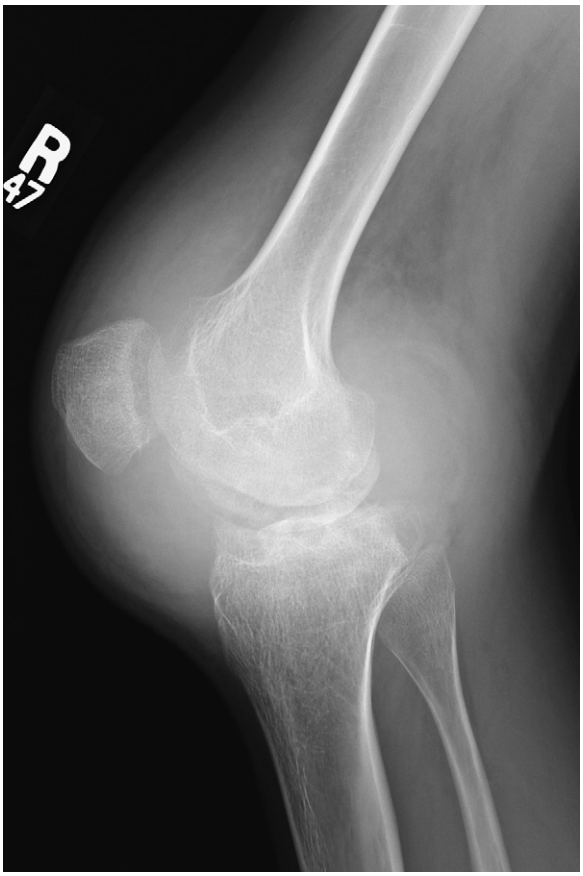

FIGURE 22-1. Lateral view of the knee in a patient with hemophilia. A radiodense effusion is present. There is overgrowth of the epiphyses, as well as ballooning and squaring of the patella.

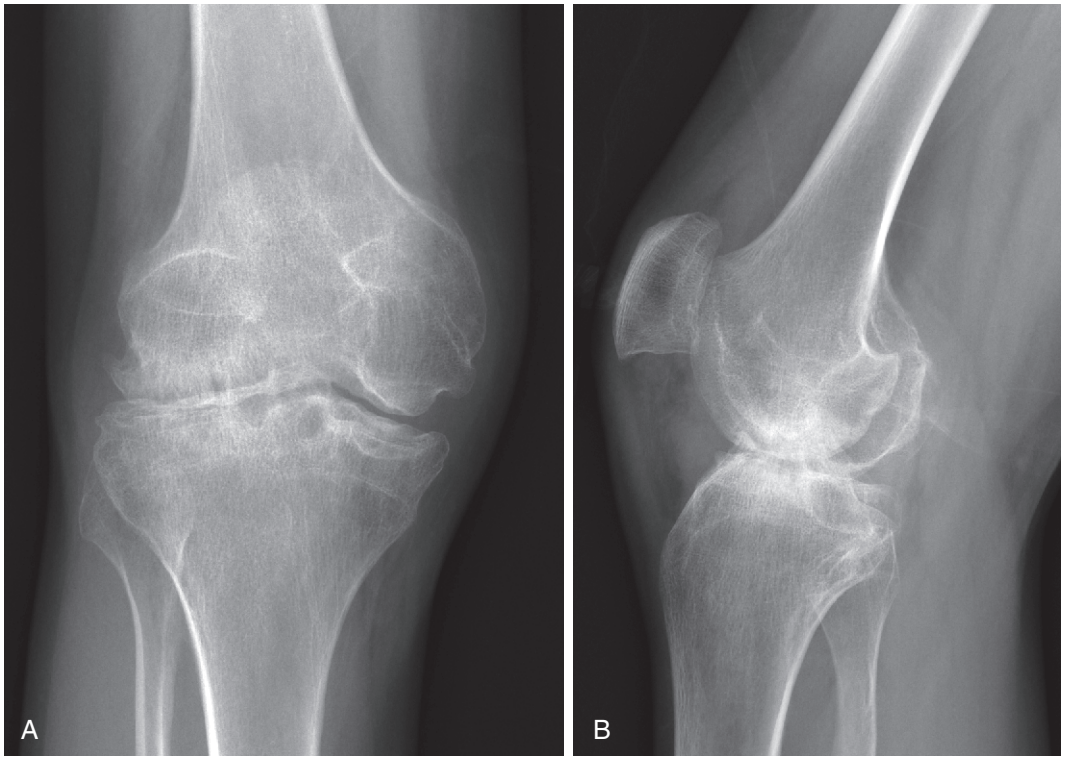

FIGURE 22-2. Anteroposterior (AP) (**A**) and lateral (**B**) views of knee in patient with hemophilia. There is overgrowth of the epiphyses, widening of the intracondylar notch, ballooning of the patella, and squaring of its inferior border. Subchondral cysts are present.

FIGURE 22-3. AP view of the knee in a 53-year-old patient with hemophilia. The overgrowth of the epiphyses and widening of the intracondylar notch are not as easily discernible as in Figure 22-2. There is uniform loss of the joint space and a subchondral cyst is present (*arrow*).

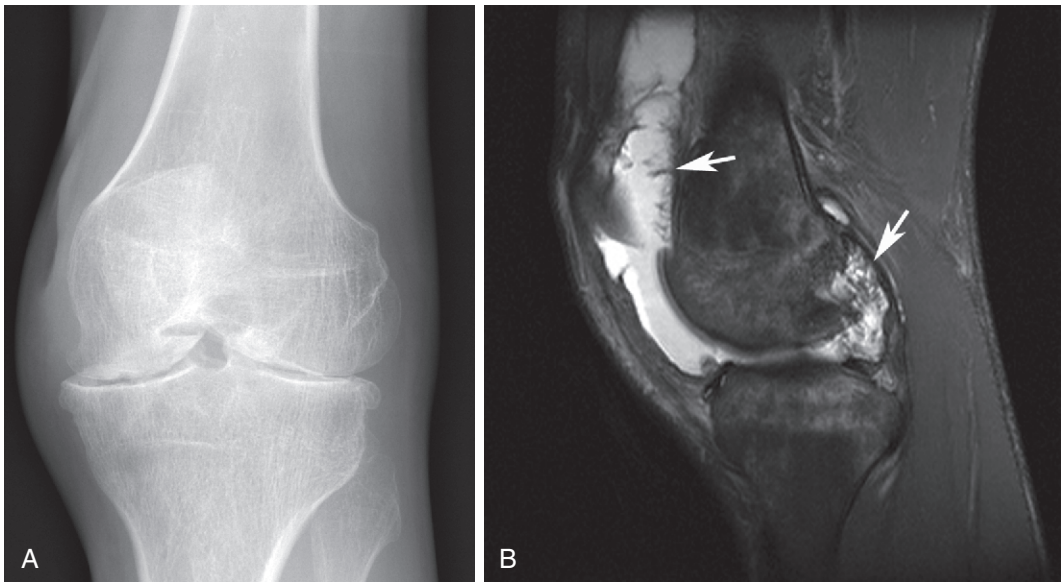

FIGURE 22-4. A, AP view of the left knee in a patient with longstanding hemophilia. The radiographic changes are those of chronic disease. There are ballooning of the epiphyses and widening as well as deepening of the intracondylar notche. There is flattening of the femoral condyles. There are superimposed secondary osteoarthritic changes. **B,** Sagittal fat-suppressed T2-weighted image in the same patient shows low signal synovitis (*arrows*) that might be confused with pigmented villonodular synovitis.

THE ANKLE

Again, in the acute bleed, soft tissue swelling and juxta-articular osteoporosis are observed. The soft tissue swelling becomes radiodense in the chronically affected joint (Fig. 22-5). There is overgrowth of the tibial epiphysis. This may be accompanied by premature fusion of the epiphyseal plate and abnormal growth or flattening of the talus. The combination leads to a tibiotalar slant (Fig. 22-6). In late involvement there may be uniform loss of the joint space with superimposed secondary osteoarthritic changes (Fig. 22-7).

FIGURE 22-5. Lateral view of the ankle in a patient with hemophilia. The tibiotalar joint is widened and the talus is positioned vertically by the fluid. The synovium is radiodense from hemosiderin deposition.

FIGURE 22-6. AP view of the ankle in a patient with longstanding hemophilia. There is ballooning of the epiphyses of the tibia and fibula. There is a tibiotalar slant indicating premature fusion of the epiphyseal plate.

FIGURE 22-7. AP view of the ankle in patient with hemophilia. There is joint space narrowing and collapse the talus with findings of secondary osteoarthritis.

THE ELBOW

Radiodense soft tissue swelling is seen around the elbow, accompanied by osteoporosis. If the patient is young, then there will be overgrowth of the epiphyses (Fig. 22-8). There may be widening of the olecranon fossa and the trochlear and radial notches in the ulna. The radial head may be enlarged and flattened. Subchondral cysts may be seen. Eventually there may be uniform loss of the joint space (Fig. 22-9).

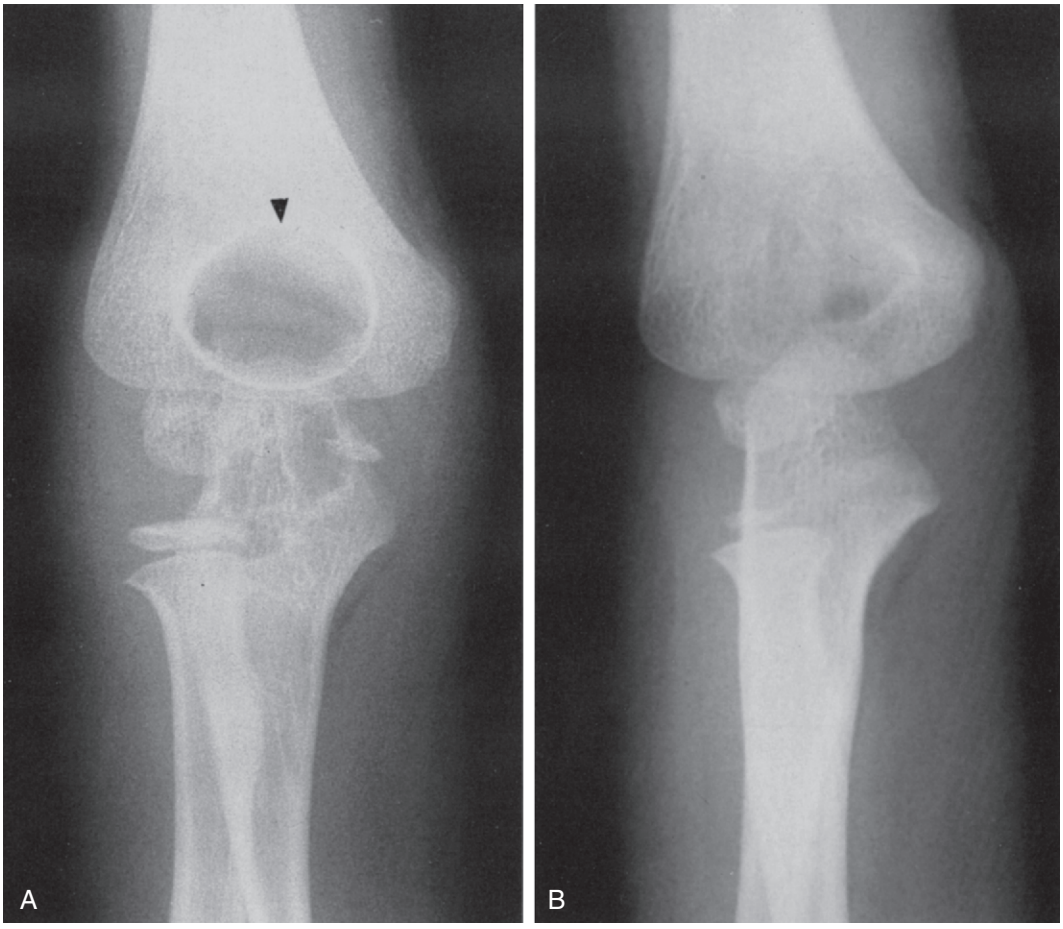

FIGURE 22-8. A, Right elbow shows changes of hemophilia. The olecranon fossa is enlarged (*arrowhead*). Cystic changes are seen in the ulna. All epiphyses are larger than in the comparison normal elbow (**B**).

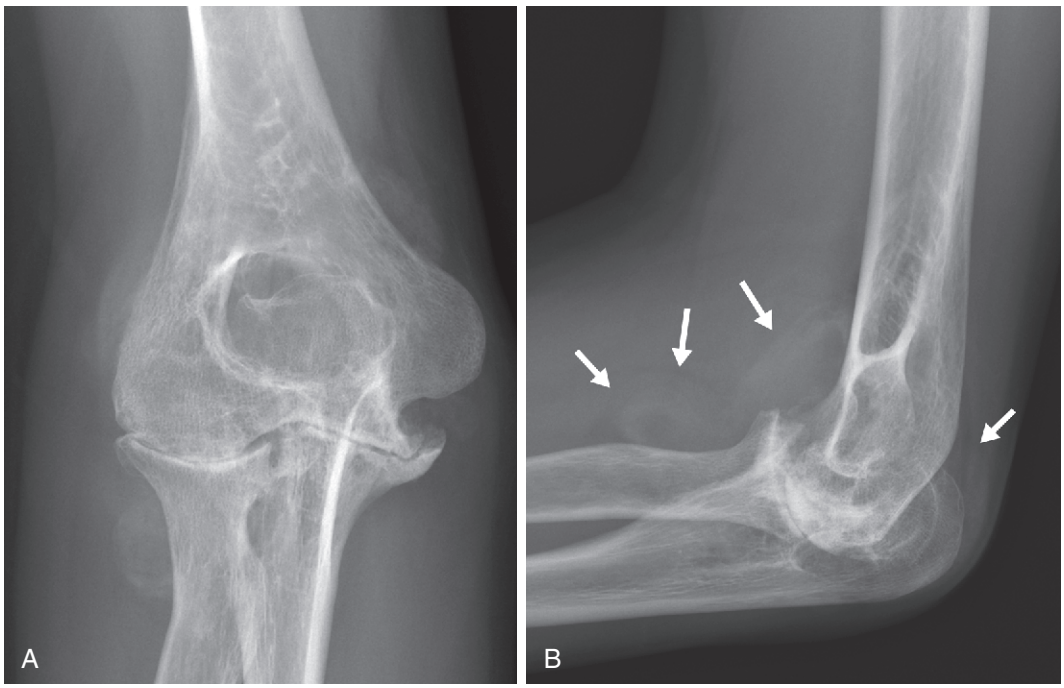

FIGURE 22-9. AP (**A**) and lateral (**B**) views of the elbow in a patient with longstanding hemophilia. Hypertrophy of the synovium is seen (*arrows*). There is loss or destruction of the joint space and enlargement and flattening of the radial head. The olecranon fossa is enlarged.

THE SHOULDER

Unlike the other joints described, the shoulder joint may show widening of the joint space with the hemarthrosis (Fig. 22-10). The humeral head is displaced inferiorly and laterally from its normal articulation with the glenoid. There may be radiodensity to the soft tissue around the shoulder. Overgrowth of the humeral epiphysis may be observed. Subchondral cyst formation is seen in the humeral head as well as in the glenoid (Fig. 22-11). Chronic involvement may lead to uniform joint space narrowing with secondary osteoarthritic changes.

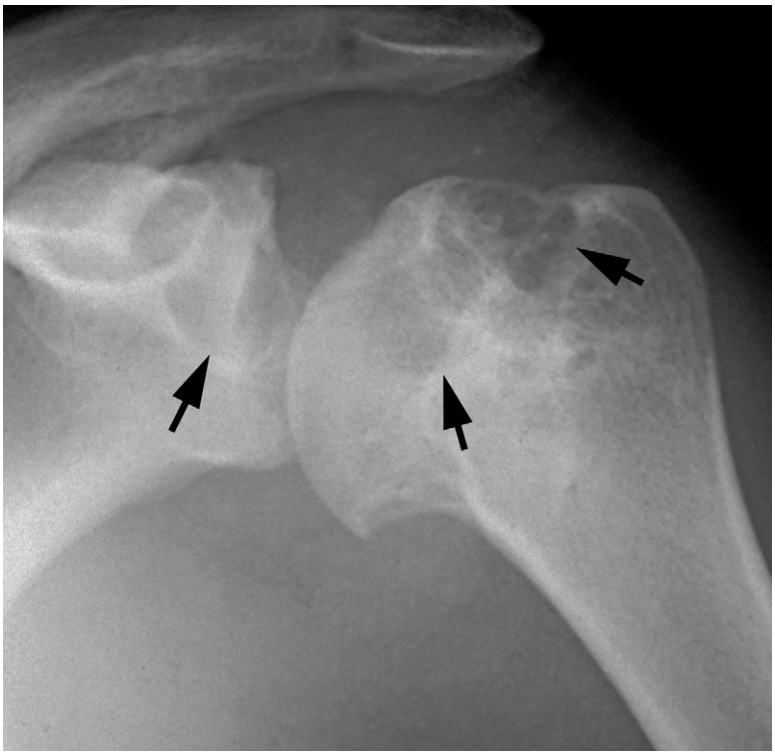

FIGURE 22-10. AP view of the shoulder in patient with hemophilia. The joint space is widened, with the humeral head displaced inferiorly and laterally from the articulating glenoid. Subchondral cysts are present (*arrows*).

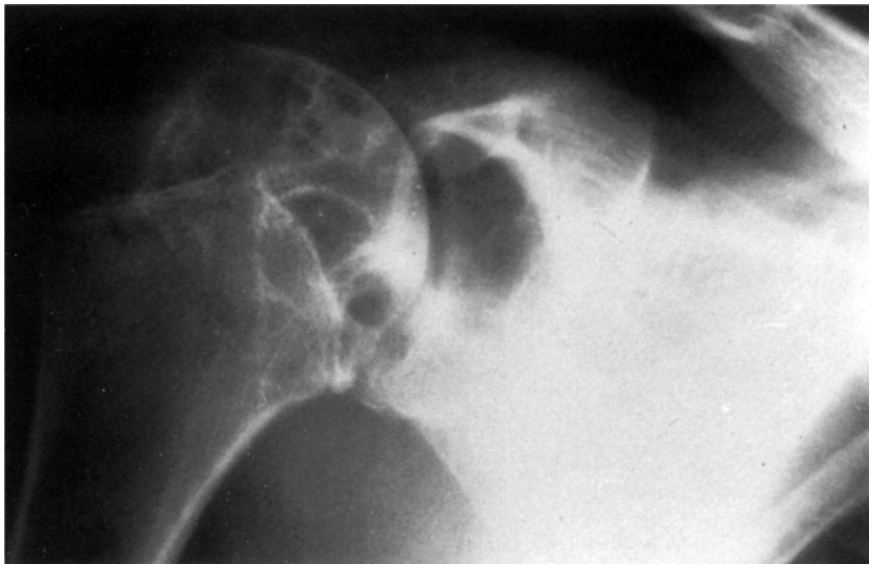

FIGURE 22-11. AP view of the shoulder in patient with hemophilia. The joint space appears to be maintained. There is juxta-articular osteoporosis. Huge subchondral cysts are present in the humeral head as well as the glenoid.

OTHER APPENDICULAR SITES

Changes in the hip are similar to those in the shoulder, with some overgrowth of the femoral head and subchondral cyst formation. With chronic bleeding the femoral head may undergo changes of osteonecrosis.

In the non–weight-bearing joints, actual widening of the joint space may be the initial radiographic sign of an acute hemarthrosis. If the chronic hemarthrosis occurs in a small joint or in a nongrowing joint, one should expect to see eventual uniform loss of joint space, with subchondral cyst formation dominating the picture (Fig. 22-12).

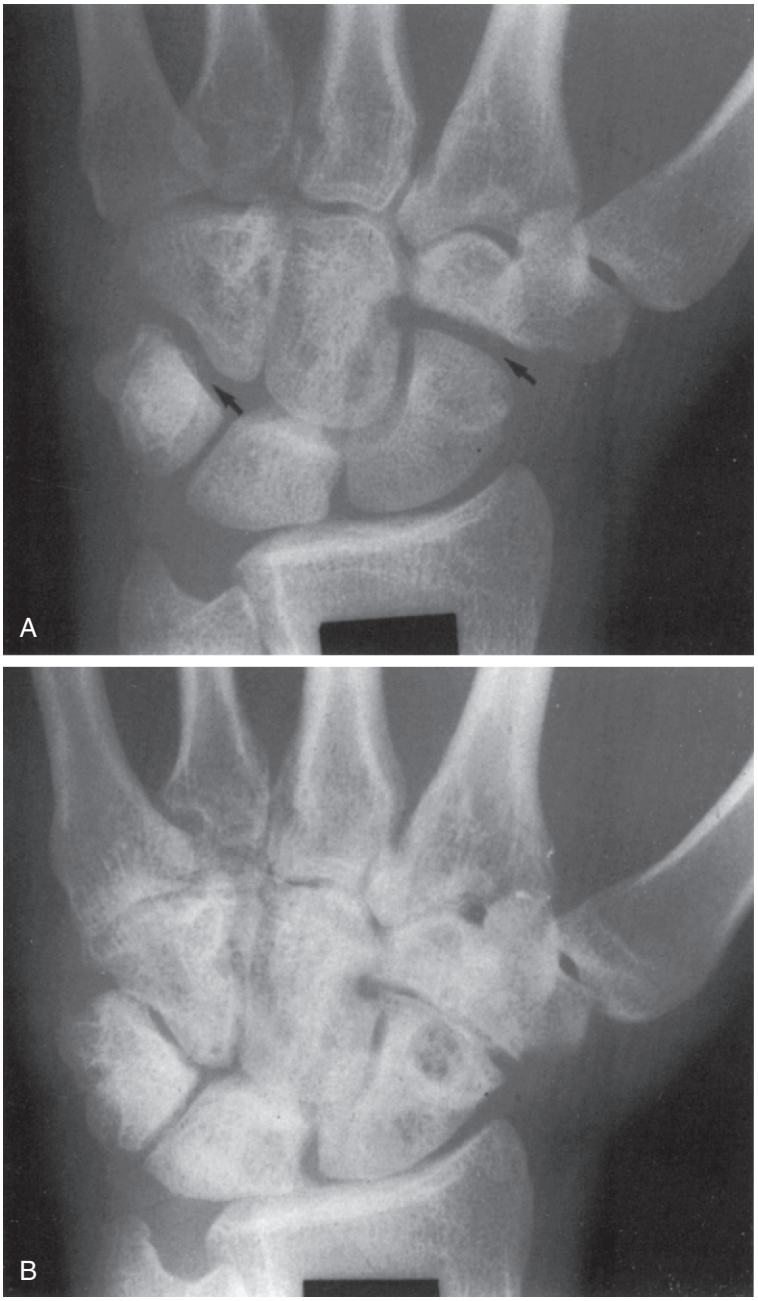

FIGURE 22-12. **A,** Posteroanterior (PA) view of the wrist in a patient with hemophilia with acute hemorrhage. There is widening of the carpal joint spaces best identified between the navicular and multangulars and between the triquetrum and hamate (*arrows*). **B,** The same wrist 3 years later. There is now narrowing of some of the carpal joint spaces, particularly that between the navicular and the multangulars. There is a large cyst in the articulating navicular and cystic changes in the other carpal bones as well.

PSEUDOTUMORS

Although the radiographic changes in hemophilia most frequently occur around the joint, changes may occur at a distance from the joint. Chronic repetitive bleeding into the bone, subperiosteally, or into the soft tissue presents as a mass called a "pseudotumor." The radiographic appearance depends upon the location and extent of the bleed. It will have the radiographic characteristics of an aneurysmal bone cyst. The intraosseous pseudotumor may be small or large and centrally or eccentrically located. It is usually a radiolucent lesion with a well-defined border that may or may not be sclerotic. It is often septated. There may be cortical destruction with varying degrees of periosteal bone formation. The most common sites are the femur, the pelvis, and the tibia, in decreasing order (Fig. 22-13). If the bleed is subperiosteal, then there may be scalloping of the underlying cortex as well as profound periosteal bone formation (Fig. 22-14). The periostitis may simulate that seen with malignancy. Knowledge of the patient's underlying disease should exclude this latter possibility. A soft tissue pseudotumor may cause pressure erosion on any adjacent bone.

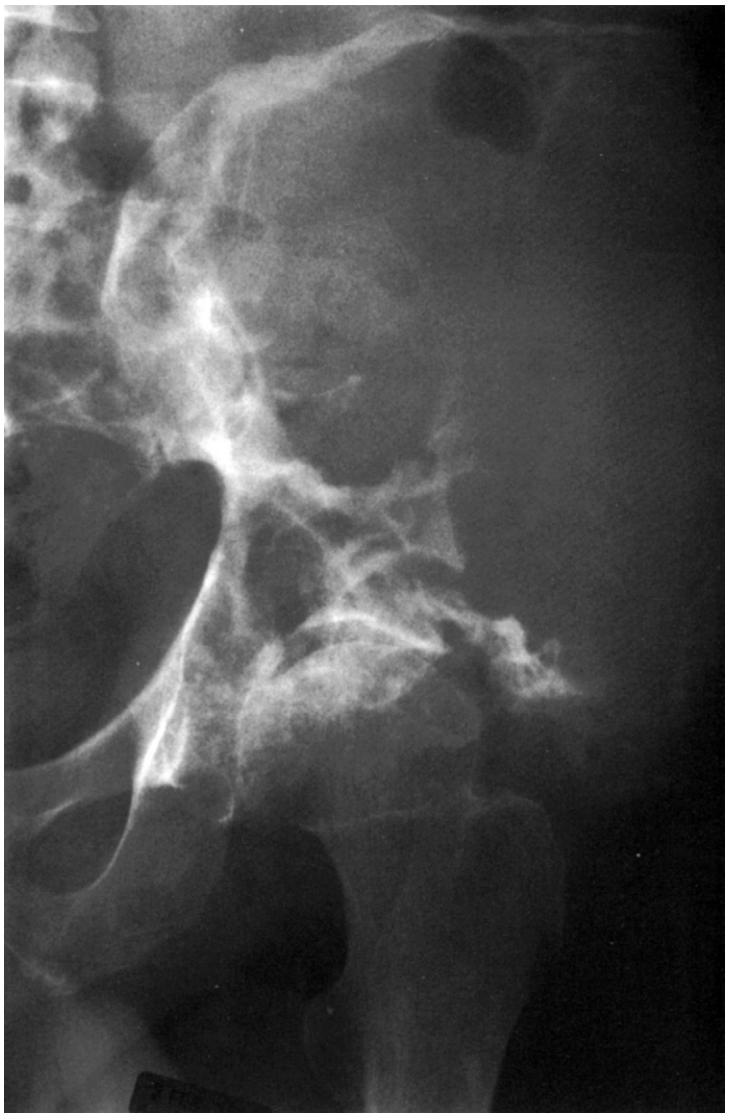

FIGURE 22-13. Huge pseudotumor involving the entire left ilium of a patient with hemophilia.

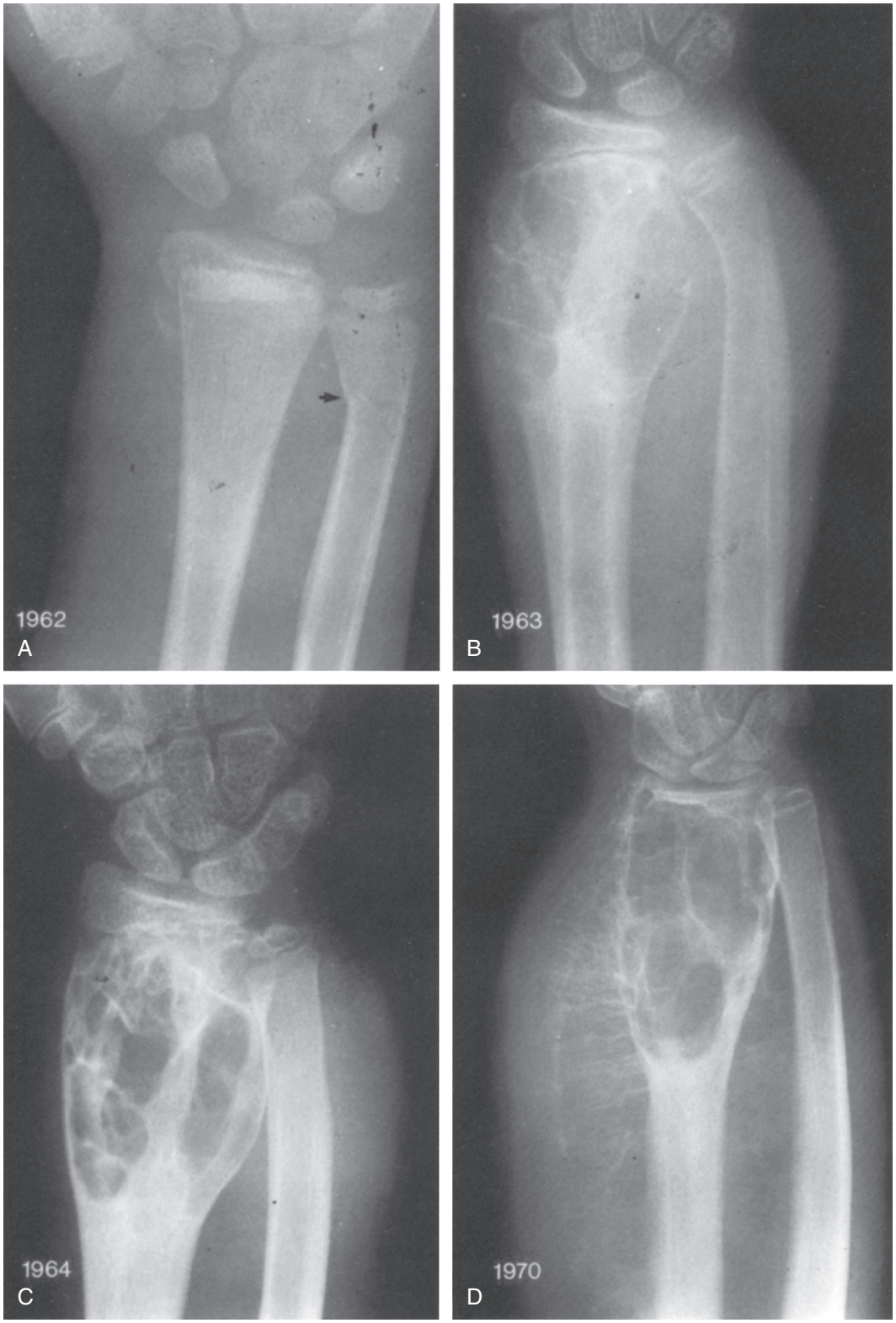

FIGURE 22-14. Evolution of a pseudotumor of hemophilia. **A,** PA view of the wrist in October 1962 showing a Salter II fracture of the distal radius and a torus fracture of the distal ulna (*arrow*). **B,** PA view of the same wrist in June 1963. Tremendous soft tissue swelling is present around the distal forearm. There is a bowing deformity of the distal end of the ulna. There is a large cystic septated lesion involving the distal diametaphyseal area of the radius. The cortex has been disrupted in places. There is solid periosteal response proximal to this lesion. **C,** PA view of the same wrist in August 1964. Patient received radiation therapy in the interval. There remains some soft tissue swelling around the distal ulna. The cystic septated lesion in the distal radius has become well corticated and well defined. **D,** PA view of the same wrist and distal radius and ulna in December 1970. The patient has continued to bleed into the forearm. In addition to the cystic septated lesion involving the distal end of the radius, there is now a large soft tissue mass with a spiculated periosteal reaction surrounding the distal end of the radius. This indicates not only intraosseous bleeding, but also subperiosteal bleeding, forming a huge pseudotumor.

SUMMARY

The bone changes in hemophilia divide into two categories: (1) those associated with bleeding into the joint and (2) those associated with bleeding into or adjacent to bone away from the joint. The arthropathy may mimic that of JIA; however, presence of radiodense soft tissue swelling and subchondral cysts should help to distinguish hemophilia from JIA. Radiographically, pseudotumors mimic aneurysmal bone cysts. However, knowledge of the patient's underlying disorder should lead to the correct diagnosis.

SUGGESTED READINGS

Brant EE, Jordan HH: Radiologic aspects of hemophilic pseudotumors in bone, *Am J Roentgenol Radium Ther Nucl Med* 115:525–539, 1972.

Gilbert M, Cockin J: An evaluation of the radiological changes in haemophilic arthropathy of the knee. In Ala F, Denson KWE, editors: *Proceedings of the 7th Congress of the World Federation of Haemophilia*, Amsterdam, 1973, Excerpta Medica, p. 191.

Handelsman JE: The knee joint in hemophilia, *Orthop Clin North Am* 10:139–173, 1979.

Jensen PS, Putman CE: Hemophilic pseudotumor: Diagnosis, treatment, and complications, *Am J Dis Child* 129:717–719, 1975.

Johnson JB, Davis TW, Bullock WH: Bone and joint changes in hemophilia; a long-term study in twelve Negro subjects, *Radiology* 63:64–71, 1954.

Jordan HH: *Hemophilic arthropathies*, Springfield, IL, 1958, Charles C Thomas.

Newcomer NB: The joint changes in hemophilia, *Radiology* 32:573–582, 1939.

Pettersson H, Ahlberg A, Nilsson IM: A radiologic classification of hemophilic arthropathy, *Clin Orthop Rel Res* 149:153–159, 1980.

Stoker DJ, Murray RO: Skeletal changes in hemophilia and other bleeding disorders, *Semin Roentgenol* 9(3):185–193, 1974.

Zimbler S, McVerry B, Levine P: Hemophilic arthropathy of the foot and ankle, *Orthop Clin North Am* 7:985–997, 1976.

Mass-Like Arthropathies 23

The articular disorders that will be discussed in this chapter, pigmented villonodular synovitis, synovial chondromatosis, and amyloidosis, share some common radiologic imaging characteristics. These entities are more common in large joints, the plain radiographic findings may be subtle, and the magnetic resonance (MR) findings are distinctive. Despite the fact that these conditions are relatively uncommon, most radiologists will see these diagnoses several times during a career and therefore must be well versed on their distinctive radiologic presentation.

PIGMENTED VILLODULAR SYNOVITIS

Pigmented villonodular synovitis (PVNS) is an uncommon neoplastic condition that arises in the synovium of joints, tendon sheaths, and bursae. It is a monoarticular disease with rare exception. The presentation in an affected joint or extremity may be focal or diffuse. The most common age at time of diagnosis ranges from 20 to 40 years, but this disease may be seen in children and older adults. The radiographic presentation of PVNS depends on whether the disease is extraarticular on intraarticular.

Extraarticular PVNS presents radiographically as a focal, noncalcified soft tissue mass in the hand and wrist (75%), followed by the foot or ankle. It is commonly known as giant cell tumor of the tendon sheath. The mass may cause scalloping or well-corticated erosion of adjacent bone (Fig. 23-1).

The intraarticular form of PVNS may be focal or diffuse. These patients usually present with complaints of pain or joint swelling. The focal intraarticular form of PVNS almost exclusively presents in the knee and will therefore have little radiographic changes (Fig. 23-2).

FIGURE 23-1. Oblique view of the foot in giant cell tumor of the tendon sheath. There are well corticated erosions in the third and fourth tarsometatarsal (TMT) joint (*arrowheads*). Lytic lesion with sclerotic margins in the proximal third metatarsal is caused by intraosseous extension of tumor.

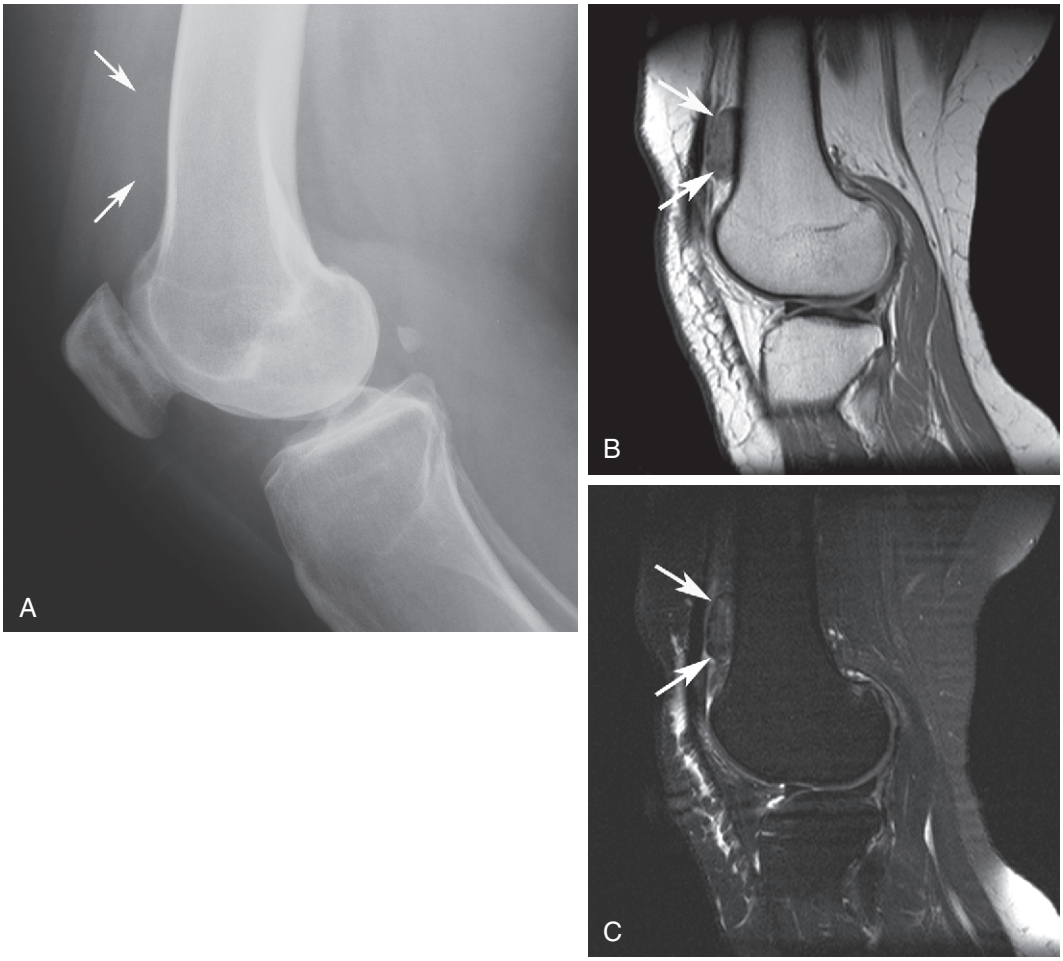

FIGURE 23-2. Focal PVNS of the knee. **A,** Lateral view of the knee shows subtle soft tissue mass anterior to the distal femur (*arrows*). Sagittal T1-weighted (**B**) and fat-suppressed T2-weighted (**C**) images of the knee show focal mass anterior to the distal femur with characteristic low T2 signal of PVNS.

The diffuse intraarticular form of the disease has been described in virtually every joint but is most commonly seen in the knee followed by the hip, ankle, shoulder, and elbow in decreasing order of frequency.

The radiographic findings in diffuse intraarticular PVNS are as follows:

1. Effusion
2. Soft tissue swelling
3. Preservation of joint space
4. Maintenance of bone mineralization
5. Well corticated extrinsic erosions in 50 percent of patients—usually seen where synovium is tightly applied to bone (i.e., neck of the femur in the hip, posterior femur, rim of medial and lateral tibial plateau in the knee)
6. No calcification

The MR appearance of PVNS is distinctive regardless of the form of the disease. The classic presentation is that of a mass with heterogeneous low to intermediate signal on T1- and T2-weighted images (Fig. 23-3). The extent of low signal is dependent on amount of hemosiderin in the lesion. The T2 low signal presentation of PVNS is distinctive; it is unfortunately not specific. Plain film radiography will help distinguish the low T2 signal from that occasionally seen in synovial chondromatosis, amyloid arthropathy, gout, or hemophilia.

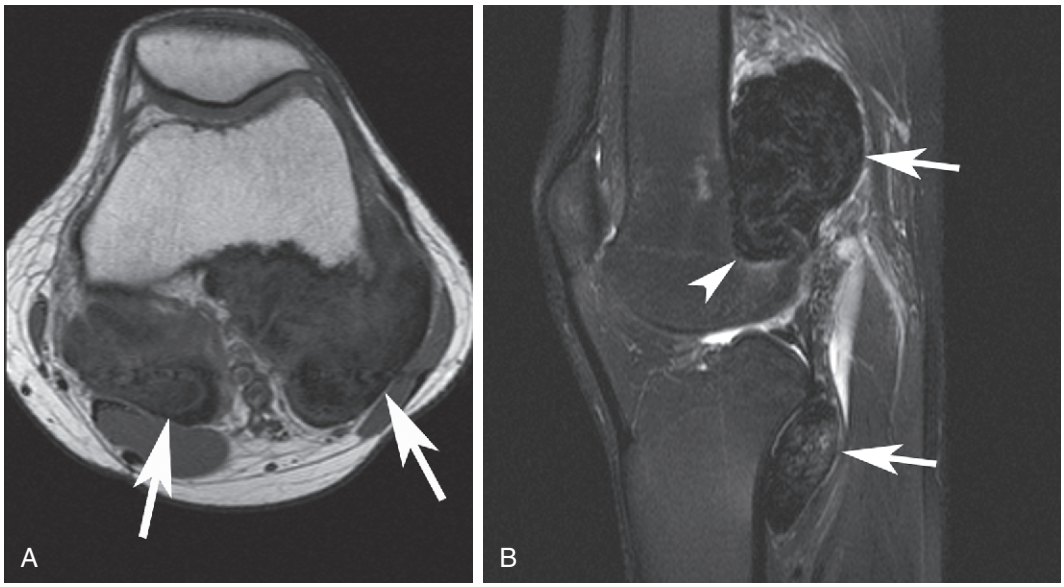

FIGURE 23-3. Axial T1-weighted (**A**) and sagittal fat-suppressed T2-weighted (**B**) MR images of the knee in patient with diffuse PVNS. Low signal masses (*arrows*) extend from the joint into the surrounding soft tissues. There is erosion of the posterior distal femur (*arrowhead*).

SYNOVIAL CHONDROMATOSIS

Synovial chondromatosis is a benign neoplastic disorder in which the synovium forms chondroid bodies. If and when these chondroids ossify, the diagnosis can be made from the plain radiograph (Fig. 23-4). When they do not calcify, then one must proceed to MR imaging to make the diagnosis. Though synovial chondromatosis has been described in every location, the knee is most commonly affected, followed by the hip, elbow, shoulder, and ankle in descending order of frequency. It is most commonly seen in 20- to 40-year-old men. The most common radiographic findings are:

1. Preserved joint space
2. Normal mineralization
3. Well-corticated erosions or scalloping of the adjacent bone in tight joints, which occurs in 30 percent of cases
4. If chondroid bodies ossify, they are numerous, small, and uniform in size

Synovial chondromatosis is not to be confused with the chondral and osseous fragments seen in a patient with severe osteoarthritis. In this latter situation, not only are there changes of osteoarthritis, but also the calcified fragments seen vary in size and shape.

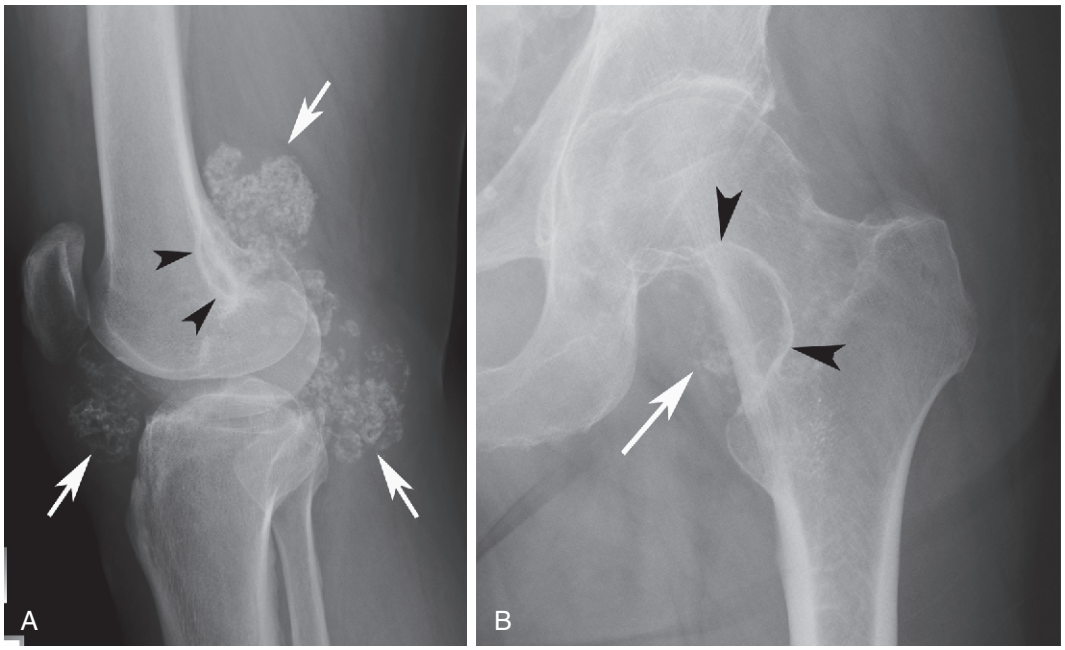

FIGURE 23-4. A, Lateral view of the knee shows extensive small intraarticular calcifications that are typical of primary synovial chondromatosis. There is erosion of the posterior distal femur (*arrowhead*). **B,** Anteroposterior (AP) view of the hip in a different patient with synovial chondromatosis. Calcification is less prominent (*arrow*). There is a large, well-corticated erosion of the femoral neck (*arrowheads*).

The MR image appearance of synovial chondromatosis is differentiated from PVNS on T2-weighted images. The unmineralized portions of synovial chondromatosis are intermediate to high in signal on fluid-sensitive sequences (Fig. 23-5). Low signal on T2-weighted images, which can cause confusion with PVNS, is an indication of mineralization. However, then plain film will make the diagnosis clear (Fig. 23-6).

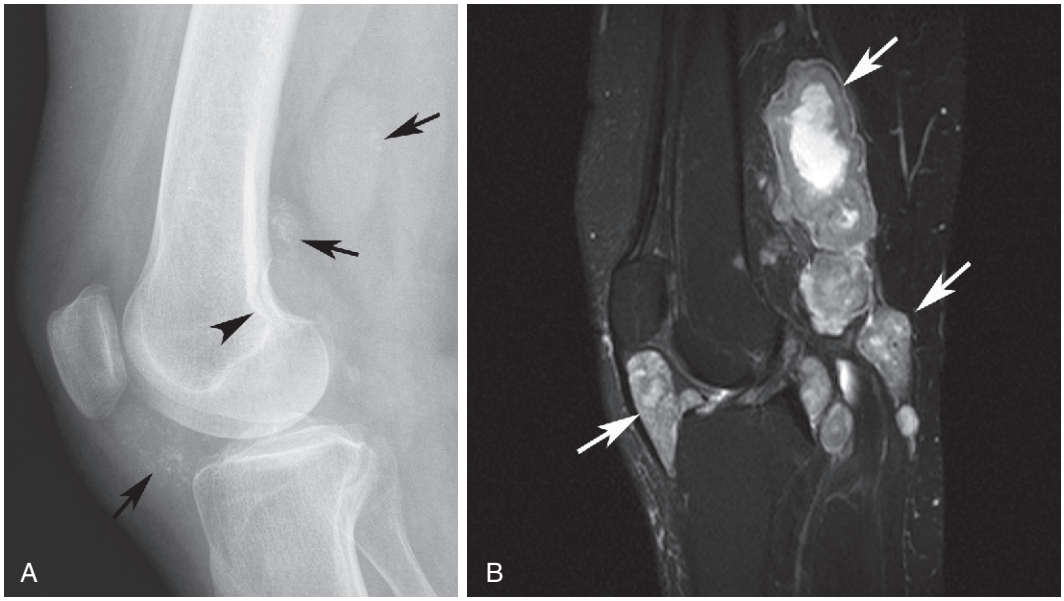

FIGURE 23-5. Knee in synovial chondromatosis. **A,** Lateral view of the knee shows faint calcification in intraarticular and juxta-articular soft tissue masses (*arrows*). There is an erosion of the posterior distal femur (*arrowhead*). **B,** Sagittal fat-suppressed T2-weighted image of the knee shows intermediate and high T2 signal in intraarticular and juxta-articular masses that are typical in synovial chondromatosis.

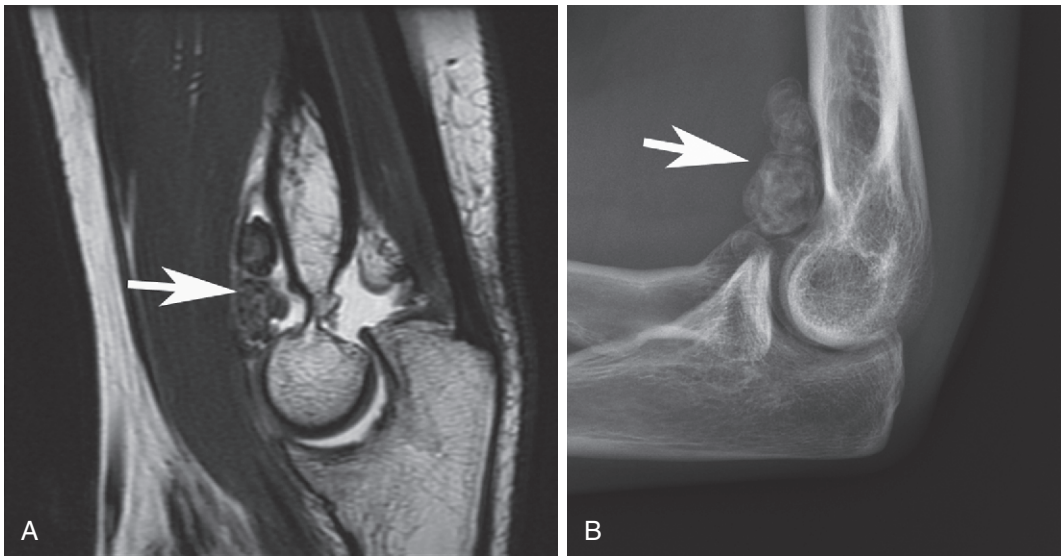

FIGURE 23-6. **A,** Sagittal T2-weighted image of the elbow shows low signal intraarticular masses in the anterior elbow joint (*arrows*) that could be confused with PVNS. **B,** Lateral view of the elbow shows calcified intraarticular masses that confirm the diagnosis of synovial chondromatosis.

AMYLOID ARTHROPATHY

Amyloidosis, regardless of whether primary or secondary to another disease, such as multiple myeloma, may be associated with articular disease. The most common cause of amyloid-related disease is long-term dialysis. The most common complaint in patients with amyloidosis is bilateral carpal tunnel syndrome from deposition of amyloid. Deposition of amyloid in the synovium leads to an arthritis that clinically mimics that of rheumatoid arthritis. The distribution is bilateral and symmetric involvement of the hips, wrists, shoulders, and knees (Fig. 23-7). Prominent soft tissue masses may distinguish amyloidosis from rheumatoid arthritis. The radiographic abnormalities are:

1. Prominent soft tissue masses ("shoulder pads")
2. Erosion
3. Joint space narrowing
4. Subluxation and dislocation
5. Radiolucent lesions in periarticular bone, which may or may not be marginated by a thin sclerotic rim
6. Osseous destruction, articular collapse, and pathological fracture

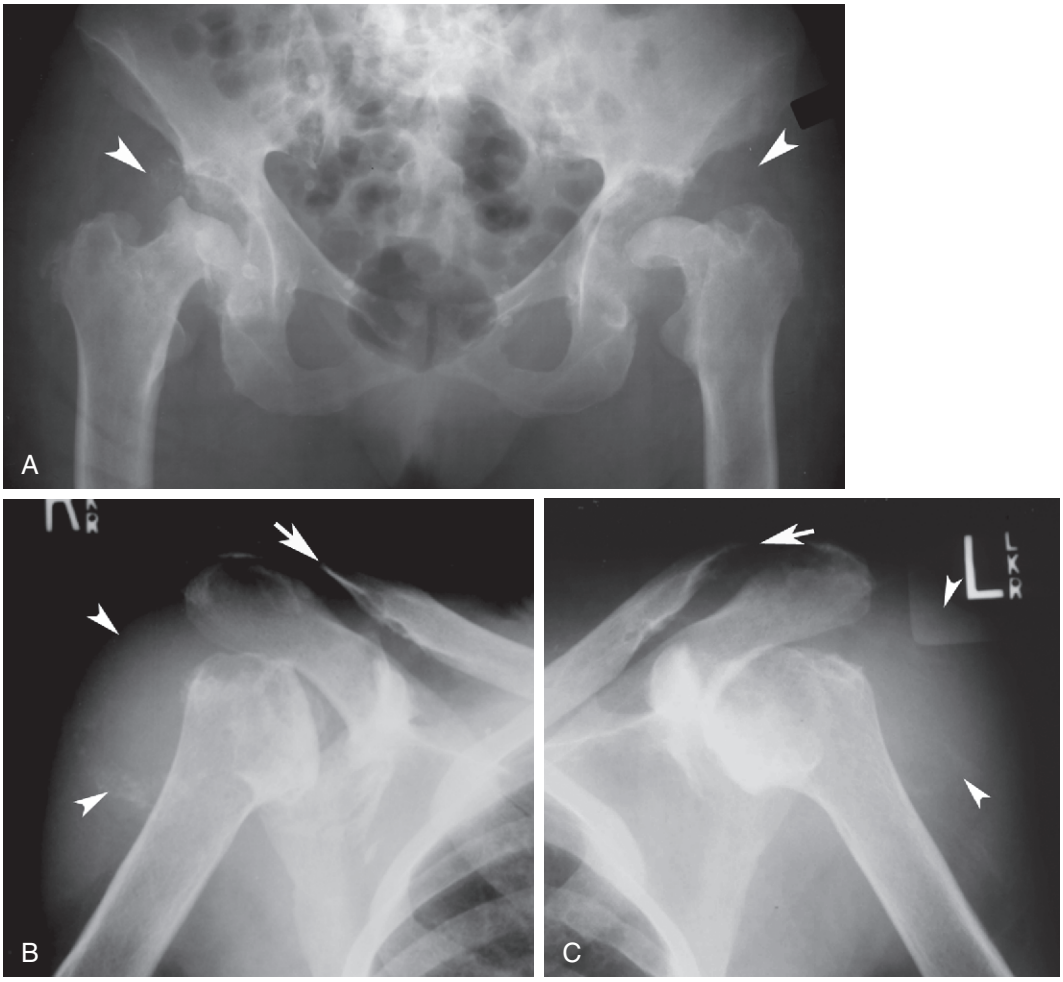

FIGURE 23-7. Hips and shoulders in dialysis-related amyloid arthropathy. **A,** AP view of the pelvis shows erosion and remodelling of the bilateral femoral head and neck. Soft tissue masses are seen (*arrowheads*). AP view of the right (**B**) and left (**C**) shoulders shows extensive glenohumeral and distal clavicular erosions (*arrows*). Large periarticular soft tissue masses are also seen (*arrowheads*).

Amyloid deposition in the spine must not be mistaken for infection. It will lead to erosion of the vertebral bodies, destruction of vertebral end-plates and disc space narrowing. It may lead to vertebral body destruction, vertebral body collapse, and subluxation (Fig. 23-8).

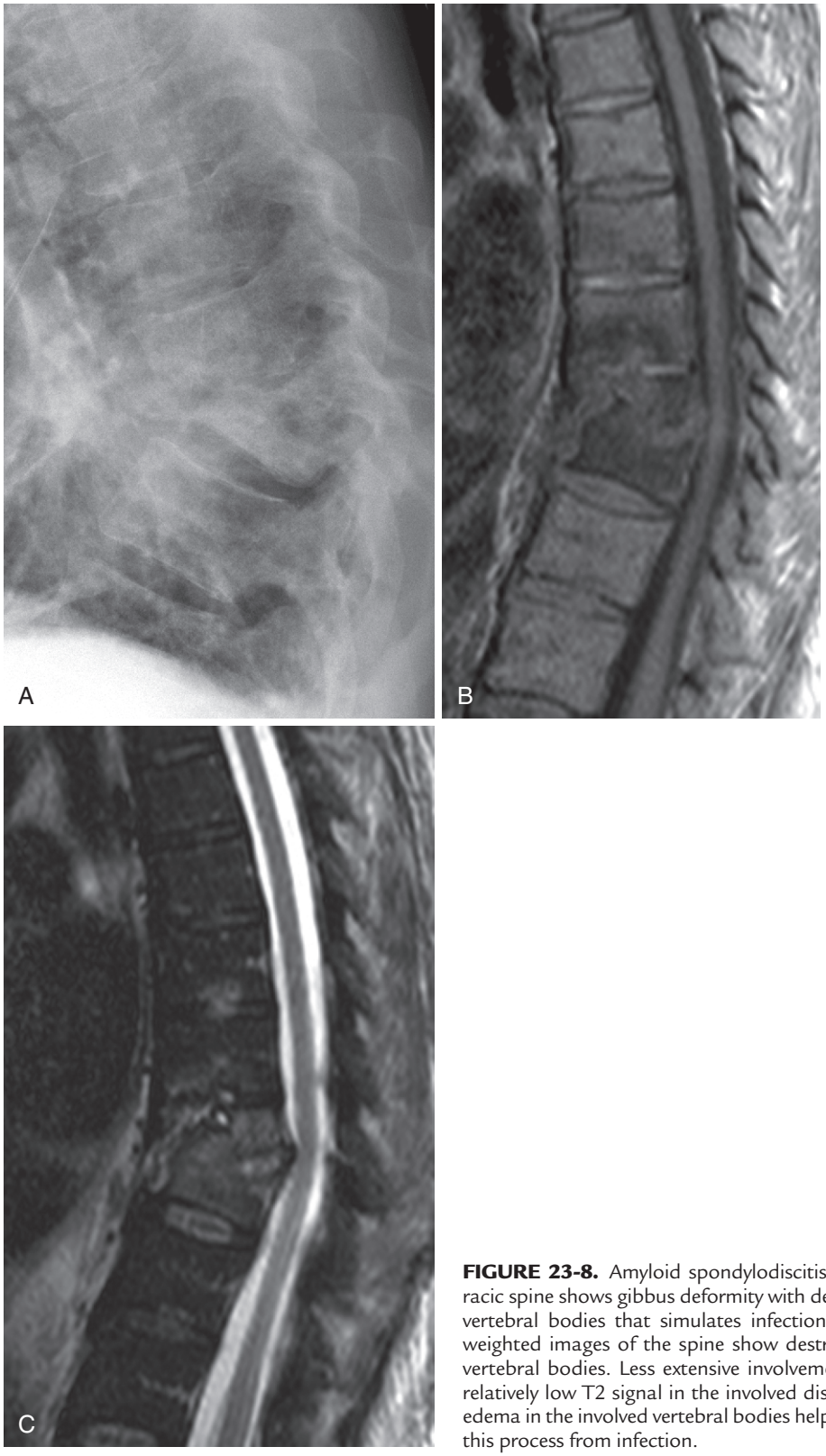

FIGURE 23-8. Amyloid spondylodiscitis in renal dialysis. (**A**) Lateral view of the thoracic spine shows gibbus deformity with destruction of the T8-T9 disk space and adjacent vertebral bodies that simulates infection. (**B**) Sagittal T1 and (**C**) fat suppressed T2 weighted images of the spine show destruction of the T8-T9 disk space and adjacent vertebral bodies. Less extensive involvement of the T7-T8 disk space is also seen. The relatively low T2 signal in the involved disk spaces and lack of significant bone marrow edema in the involved vertebral bodies help establish the correct diagnosis and distinguish this process from infection.

The appearance of amyloid deposition on MR image is distinctive. The amyloid deposits may be mass-like and they tend to be intermediate in signal on T1-weighted images and low in signal on T2-weighted images (Fig. 23-9). However, the polyarticular distribution will clarify any confusion with other entities demonstrating low signal on T2-weighted images.

FIGURE 23-9. Dialysis-associated amyloid arthropathy of the hips. Coronal T1-weighted (**A**) and axial T2-weighted (**B**) images of the hips show low signal intraarticular mass-like deposition of amyloid (*arrows*) with associated femoral neck erosions.

SUMMARY

The mass-like arthopathies are entities that can affect any joint but are more likely to be seen in large articulations. They are characterized by large chronic erosions in many cases and should be considered in monoarticular presentations.

SUGGESTED READINGS

PVNS

Bravo SM, Winalski CS, Weissman BN: Pigmented villonodular synovitis, *Radiol Clin North Am* 34:311, 1996.
Huang GS, Lee CH, Chan WP, et al: Localized nodular synovitis of the knee: MR imaging appearance and clinical correlates in 21 patients, *AJR Am J Roentgenol* 181:539–543, 2003.
Llauger J, Palmer J, Rosón N, et al: Pigmented villonodular synovitis and giant cell tumors of the tendon sheath: Radiologic and pathologic features, *AJR Am J Roentgenol* 172:1087–1091, 1999.
Masih S, Antebi A: Imaging of pigmented villonodular synovitis, *Semin Musculoskelet Radiol* 7:205–216, 2003.
Murphey MD, Rhee JH, Lewis RB, et al: Pigmented villonodular synovitis: Radiologic-pathologic correlation, *Radiographics* 28:1493–1518, 2008.

Synovial Chondromatosis

Crotty JM, Monu JU, Pope TL Jr: Synovial osteochondromatosis, *Radiol Clin North Am* 34:327–342, 1996.
McKenzie G, Raby N, Ritchie D: A pictorial review of primary synovial osteochondromatosis, *Eur Radiol* 18:2662–2669, 2008.
Murphey MD, Vidal JA, Fanburg-Smith JC, Gajewski DA: Imaging of synovial chondromatosis with radiologic-pathologic correlation, *Radiographics* 27:1465–1488, 2007.
Ryan RS, Harris AC, O'Connell JX, et al: Synovial osteochondromatosis: The spectrum of imaging findings, *Australas Radiol* 49:95–100, 2005.

Amyloid Arthropathy

Fukuda K, Yamamoto H: Dialysis-related amyloidosis, *Semin Musculoskelet Radiol* 5:113–119, 2001.
Sheldon PJ, Forrester DM: Imaging of amyloid arthropathy, *Semin Musculoskelet Radiol* 7:195–203, 2003.

INDEX

Note: Page numbers followed by *f* indicate figures.

C

D

E

F

G

H

P

R

S

T

U

V

W